UNIVERSITY OF SOUTHAMPTON

FACULTY OF ENGINEERING, SCIENCE & MATHEMATICS

School of Ocean & Earth Sciences

Towards Deep-Sea Toxicology: Experimental Approaches With Echinoderms

by

Sarah Jane Murty Hughes

Thesis for the degree of Doctor of Philosophy

September 2010

UNIVERSITY OF SOUTHAMPTON

ABSTRACT

FACULTY OF ENGINEERING, SCIENCE & MATHEMATICS
SCHOOL OF OCEAN & EARTH SCIENCES

Doctor of Philosophy

TOWARDS DEEP-SEA TOXICOLOGY: EXPERIMENTAL APPROACHES WITH ECHINODERMS

by Sarah Jane Murty Hughes

As anthropogenic activities expand into the deep sea, it is only recently that the importance of deep-sea ecosystems and processes to global biogeochemical systems has become clear. If the potential impact of human activity upon deep-sea organisms and ecosystems is to be understood and predicted, experimental studies are required to improve our knowledge of their sensitivity to contamination and disturbance. Echinoderms are integral components of deep-sea benthic communities and, by virtue of their abundance, they contribute significantly to deep-sea biogeochemical processes. As such, echinoderms can be considered relevant target organisms for deep-sea experimental studies.

Three approaches to the investigation of deep-sea anthropogenic impact upon echinoderms were undertaken in this study. The first was based on contaminant exposure experiments with two species of shallow-water echinoid, the eurytopic *Psammechinus miliaris* and the stenotopic *Brissopsis lyrifera.* A range of biomarkers was used to assess the responses of the echinoids to contaminant exposure. Compared with the significant cytological and molecular (assess via qPCR) responses in *P. miliaris*, a reduced capacity to respond to contaminant exposure was found in *B. lyrifera* at these levels of biological organisation. Stenotopic species are hence recommended for future experimental studies as proxies for deep-sea echinoderms which, due to their adaptation to the stable environment of the deep sea, are also considered to have a reduced capacity for homeostasis in the face of environmental perturbation.

The second experimental approach involved sediment burial experiments, simulating anthropogenic drilling disturbance, with the deep-water echinoderm species *Echinus acutus*. ROV technology was used to perform the burial experiments *in situ* at 114 m depth. The application of quantitative PCR molecular biomarker methodology revealed a significant increase in the expression of a *stress-70* protein in response to sediment burial. These results demonstrate the sensitivity of the qPCR technique to assess an organism's stress-response, and its relevance to deep-sea experimental studies.

Finally, the development and successful deployment of an *in situ* respirometer, the benthic incubation chamber system (BICS) 2, made possible the acquisition of physiological measurements from deep-sea echinoderms at the abyssal sea floor at 3500 m. The results revealed similarities between the oxygen consumption rates of shallow-water and deep-sea echinoderms. The future performance of *in situ* deep-sea experimentation is dependent on the development of experimental equipment that confers the ability to perform experiments *in situ* with ROV technology and to obtain results without interference from recovery-related side effects.

Table of Contents

List of Figures

List of Tables

DECLARATION OF AUTHORSHIP

I, Sarah Jane Murty Hughes, declare that the thesis entitled

Towards deep-sea toxicology: experimental approaches with echinoderms

and the work presented in the thesis are both my own, and have been generated by me as the result of my own original research. I confirm that:

- this work was done wholly or mainly while in candidature for a research degree at this University;
- where any part of this thesis has previously been submitted for a degree or any other qualification at this University or any other institution, this has been clearly stated;
- where I have consulted the published work of others, this is always clearly attributed;
- where I have quoted from the work of others, the source is always given. With the exception of such quotations, this thesis is entirely my own work;
- I have acknowledged all main sources of help;
- where the thesis is based on work done by myself jointly with others, I have made clear exactly what was done by others and what I have contributed myself;
- none of this work has been published before submission, although at the time of submission of this thesis, the manuscripts listed on the following page and attached as appendices have been submitted to the journals indicated for consideration of suitability for publication:

Signed: ……..

Date:…….

DECLARATION OF AUTHORSHIP (continued)

Manuscripts:

Hughes, S.J.M., Jones, D.O.B., Hauton, C., Gates, A.R., Hawkins, L.E., in press. A systems approach to assessment of drilling disturbance on *Echinus acutus* var. *norvegicus* (Düben & Koren, 1846) based on *in situ* observations and experiments using a Remotely Operated Vehicle (ROV). Journal of Experimental Marine Biology and Ecology.

Please note, that in the above manuscript (attached as an Appendix), the practical and statistical work concerning the assessment of the diversity of the megabenthic community around the Ragnarrok drilling site was carried out by Dr. Andrew Gates and Dr. Daniel Jones. The *in situ* experiments with *Echinus acutus* were also carried out by Dr. Daniel Jones. All molecular related work with regard to the quantitative polymerase chain reaction was performed by myself. The manuscript was written by myself with review by the other authors prior to submission.

Hughes, S.J.M., Amaro, T., Ingels, J., Boorman, B., Hawkins, L.E., Vanreusel, A., Cunha, M.R., submitted. Benthic abyssal research using a remotely operated vehicle (ROV): novel experimentation in the Nazaré Canyon. Deep-Sea Research Part II: Topical Studies in Oceanography.

Submitted to the editor of the HERMES Canyons special edition for Deep-sea Research Part II on 28 January 2010.

Please note that the sections of the above manuscript (attached to this thesis as an Appendix) concerning the Feedex 13C pulse-chase experiment and the 'Poo-Collector' were written by Dr. Jeroen Ingels and Dr. Teresa Amaro. I edited these sections as I deemed to be required, and all other sections of the manuscript are my own work. The manuscript was reviewed by the other authors prior to submission.

Signed: ……..

Date:…….

Graduate School of the

National Oceanography Centre, Southampton

This PhD thesis by

Sarah Jane Murty Hughes

has been produced under the supervision of the following persons

Supervisors

Dr. Lawrence E. Hawkins

Dr. Chris Hauton

Dr. David S.M. Billett

Chair of Advisory Panel

Professor Paul. A. Tyler

Acknowledgements

I would like to thank my supervisors at the National Oceanography Centre, Southampton, Dr. Lawrence E. Hawkins, Dr. Chris Hauton and Dr. David S.M. Billett. Thank you also to my panel chair, Prof. Paul Tyler. I am very grateful for their kindness, help and support during my work on this PhD as well as during my absences from NOCS. I must particularly thank Dr. Chris Hauton for taking me on as one of his students a year into my PhD, teaching me molecular biology from scratch, and then finally turning around the reviews of my draft chapters so quickly, for typing all his comments on my manuscripts and for his patience.

Thank you to Dr. Sam Dupont and Prof. Rutger Rosenberg for their assistance during my visit to the Kristineberg Marine Research Centre in Sweden. I thank Dr. Dan Jones and Dr. Andy Gates for their hard work offshore in performing the *Echinus acutus in situ* experiments and video surveys; Ben Boorman for remaking BICS2 and his work at sea; and the officers and crew of the RRS James Cook and the ROV Isis. I would also like to thank my friends at NOCS, all those in the DEEPSEAS Group and those who have worked in the molecular lab; it has been a pleasure working with so many dedicated professionals.

Lastly, without the support and encouragement of Adrian, particularly during the darkness of the final year, I could not have completed this thesis. Thank you.

This study was supported by NERC studentship NER/S/A/2005/13480. Research cruise JC10 was part of Hotspot Ecosystems in the NE Atlantic, the UK contribution to the HERMES Project (EU contract GOCE-CT-2005-511234). ROV work with *E. acutus* was carried out as part of the SERPENT project.

Chapter 1. General Introduction

The deep sea lies below the continental shelf break, which occurs at approximately 200 m depth, and covers more than 300 x 10^6 km^2 or approximately 65% of the Earth's surface (Sverdrup et al., 1942; Gage and Tyler, 1991). The oceans are the world's largest global habitat and, as sea levels have fluctuated over evolutionary time, a wide variety of organisms have adapted to inhabit the deep-sea environment successfully (Rogers, 2000). For humans, the deep sea is remote and difficult to access, therefore the study of these deep-sea organisms has historically been, and still is, a challenge. As a result, little detail is known about the lifestyles and physiology of deep-sea inhabitants or the functioning of deep-sea ecosystems.

Modern technological improvements are currently increasing scientific access to the deep sea. For example, manned submersibles (also known as human occupied vehicles or HOVs) and remotely operated vehicles (ROVs) have made possible real-time observations in the deep sea, targeted sample collection, instrument deployment and the manipulation of sea floor experiments (Bachmayer et al., 1998; Van Dover and Lutz, 2004; Gage and Bett, 2005; Jones, 2009). The current development of deep-ocean observatories will lead to the ability to continuously monitor the deep-sea environment (Favali and Beranzoli, 2009; ESONET DONET MARS, 2010). Concurrent to scientific advancement into the deep sea, however, other aspects of human activity are also extending further into deep water.

Today, human activities in the deep sea currently include natural resource exploitation (fishing), commercial mining (e.g. polymetallic nodules and crusts), disposal of permitted wastes (e.g. sewage, dredge spoil) and hydrocarbon exploration. In coming years these, and new activities such as CO_2 sequestration and methane hydrate extraction, will continue to expand into deeper water and affect larger areas of the deep-sea floor (Carney, 1997; Glover and Smith, 2003; Thiel, 2003; Tyler, 2003a; Smith et al., 2008b). Whilst some of these activities can be related to natural analogues on a small scale, such as sediment slumps and the chemical input found at hydrothermal vent areas (Tyler, 2003a), other activities impact the deep-sea environment in unnatural ways. These include, for example, the mass deposition of waste matter, the large-scale disturbance of the seafloor by mining operations and the contamination of the deep sea by industrial and agricultural chemicals via atmospheric fall out, riverine input or terrestrial run off (Phillips, 1980; Clark, 1992; Thiel, 2003; Tyler, 2003a).

In order to carry out informed deep-sea environmental impact assessments of human activity and to be able to offer educated options to mitigate possible anthropogenic damage (Angel and Rice, 1996; Smith et al., 2008b), it is therefore important at this time to investigate and understand the

functioning of the deep-sea environment and its inhabitants. Most recently, following the deepwater oil spill in the Gulf of Mexico (which commenced in April 2010), the International Union for Conservation of Nature (IUCN) has called for a global moratorium on oil and gas exploration in ecologically sensitive areas including deepwater ocean sites until our knowledge base regarding the potential impacts is significantly improved (IUCN, 2010). To obtain a greater understanding of the deep-sea biota and their sensitivity to environmental perturbation, there is a need for appropriate laboratory-based and manipulative *in situ* experiments (Glover and Smith, 2003; Guinotte et al., 2006). With well-planned and executed experimentation, our ability to potentially predict the consequences of anthropogenic impacts in the deep sea will improve (Gage, 1996).

1.1. Contamination in the deep sea

The contamination of deep-sea ecosystems by anthropogenic chemicals is an issue of concern because the deep sea acts as a sink and final reservoir for persistent contaminants (Harvey et al., 1974; Barber and Warlen, 1979; Looser et al., 2000). Pollutants reach the deep-sea environment via a number of possible routes. These include seepage from local sources on the sea bed (e.g. dumped materials and drilling operations) and input to surface waters followed by long-range and long-term transportation by sinking water and deep-ocean currents (Thiel, 2003). At the sea floor, pollutants absorb to sediment particles forming an available reservoir for benthic animals (Clark, 1992; Danis et al., 2006). The routes of exposure to anthropogenic contaminants for deep-sea organisms are therefore via the surrounding water and sedimentary environment, which they live in and feed on, followed by associated biomagnification through the food chain (Van Dover et al., 1992; Chapman and Riddle, 2003; Unger et al., 2008).

The presence of contaminants in the deep-sea environment has been proven in different regions of the world's deep oceans. Polycyclic aromatic hydrocarbons (PAH), generated during industrial processes and the processing and combustion of fossil fuels and which have toxic and carcinogenic properties, are efficiently transferred to deep waters in the Mediterranean (Bouloubassi et al., 2006), where the presence of artificial radionuclides has also been demonstrated (Garcia-Orellana et al., 2009). In the northeast Atlantic it has been found that submarine canyons act as conduits for the transportation of anthropogenically-generated lead pollution from coastal waters into the deep sea (Richter et al., 2009). Silver, alkyl benzenes and *Clostridium perfringen* spores, all indicators of sewage pollution, were found in sediment at the deepwater municipal sewage dumpsite DWD 106 off the coast of New Jersey in the northwest Atlantic; where the local echinoderm benthos was found to be processing the sewage-derived organic matter (Van Dover et al., 1992; Rieley et al., 1997). In bathyal (0.2-2 km depth) and abyssal (2-6 km) sediments in the northwest Pacific

persistent organic pollutants (POPs); noted for their toxic, long lived and bioaccumulative characteristics (Clark, 1992; Ritter et al., 1996), have been found including the organotin biocide tributyltin (TBT) which is highly toxic to aquatic organisms (Harino et al., 2005; Harino, 2009).

A body of evidence collected since the late 1970s demonstrates that anthropogenic contaminants accumulate in deep-sea organisms. Lipophilic POPs including organochlorine pesticides (e.g. dichloro-diphenyl-trichloroethane: DDT), polychlorinated biphenyls (PCBs), organotin (OT) and organobromine compounds (e.g. brominated flame retardants: BFRs) have been found in deep-sea organisms throughout the deep oceans. Fish, crustaceans, cephalopods, echinoderms and gastropods from 200 – 3500 m depth in the western north Pacific off Japan were found to contain PCBs, OTs, DDTs and BFRs (Lee et al., 1997; Takahashi et al., 1997; De Brito et al., 2002; Harino et al., 2005; Takahashi et al., 2010). PCBs and DDTs were found in amphipods and fish from 2075 m in the Arctic Ocean (Hargrave et al., 1992), and between 1000 and 2000 m in fish and cephalopods from the western North Atlantic (Barber and Warlen, 1979; Unger et al., 2008). In the Mediterranean Sea fish and shrimp from 300-2500 m have been found to contain OT, DDT, dioxin and PAH contaminants (Escartín and Porte, 1999; Borghi and Porte, 2002; Rotllant et al., 2006; Storelli et al., 2009). In the Rockall Trough, fish contain high levels of POPs, including chlorobiphenyls at levels above those adopted by OSPAR as acceptable (Mormede and Davies, 2001, 2003; Webster et al., 2009).

The levels of contamination found in deep-sea species are often higher than those found in surface-living species. Concentrations of POPs in deep-sea fish from the North and South Atlantic and the Monterey Bay Canyon were found to be 10-17 times higher than in related species from the surface or shallower depths (Froescheis et al., 2000; Looser et al., 2000; Mormede and Davies, 2003). Off Japan, higher concentrations of hexachlorocyclohexanes were found in deep-sea organisms compared with coastal shallow water species (Lee et al., 1997), whilst in the Mediterranean the shrimp *Aristeus antennatus* contained dioxin levels of the same magnitude or higher than a comparable shallow water species (Rotllant et al., 2006).

These studies demonstrate that the long-term spatial and temporal transport of persistent contaminants into deepwater and sediments has occurred, that contaminants have entered deep-sea food chains and that deep-sea organisms have bioaccumulation capacities. Despite the vastness of the deep-sea floor, due to global deep-water circulation and the persistence of these organic pollutants, it can be assumed that no region of the deep sea has escaped anthropogenic impact and that contaminants are ubiquitous throughout the oceans, becoming biomagnified as they move up deep-sea food chains (Thiel, 2003; Smith et al., 2008b).

1.2. Deep-sea ecotoxicology

Due to their proximity to human urbanization and industry, and often due to their economic importance, the effect of anthropogenic contaminants on freshwater and coastal marine organisms has been the subject of intense scientific investigation for many years (Vernberg et al., 1977; Bayne et al., 1985; Calow, 1994). Many different species and chemicals have been studied; for example the US Environmental Protection Agency Ecotox database includes over 220,000 records concerning over 7000 chemicals and over 4000 aquatic species (Chapman and Riddle, 2003).

The body of literature on the impact of anthropogenic contaminants upon deep-sea organisms is, in comparison, limited (Vevers et al., 2010). As summarised above, there is no doubt that anthropogenic contaminants have entered deep-sea ecosystems, but predicting the effects they may have on deep-sea organisms can currently only be based on evidence from terrestrial, freshwater and shallow water organisms. Studies from polar environments, comparable to the deep sea with respect to the low temperatures, indicate that the sensitivity of polar species to contaminants cannot be predicted as it may be reduced, enhanced or similar in comparison to that of tropical and temperate species (Chapman and Riddle, 2005). There have been no toxicological studies involving deep-sea organisms, and we do not know with certainty whether they may be more or less sensitive to contaminants than their shallow water relatives.

Differences between shallow-water and deep-sea species are found in their physiology, behaviour and ecology (Childress, 1995; Siebenaller and Garrett, 2002). The physical environmental factors that influence the biological systems of deep-sea organisms are hydrostatic pressure, temperature, light and productivity (Somero, 1991; Childress, 1995). The deep sea is characterised by ubiquitous high pressure, which increases by one atmosphere (10^5 Pascals) for every 10 m increase in depth (Thistle, 2003). The vast majority of the deep-sea environment is typified by low levels of temperature (below the permanent thermocline the temperature is <4°C), and there is a complete absence of light below 1000 m (Menzies, 1965; Tyler, 1995). Because of the absence of light, primary productivity is absent, apart from at hydrothermal vent and cold seep areas, and the vast majority of deep-sea ecosystems rely on the fall of organic matter from surface waters as their primary source of energy (Tyler, 1995).

As a result of these environmental conditions, many organisms inhabiting the deep sea have low rates of metabolism, growth and reproduction, all of which influence the sensitivity of an organism to a contaminant and the effect it may have (Gage and Tyler, 1991; Glover and Smith, 2003; Chapman and Riddle, 2005). In order to understand the impact of anthropogenic contaminants on deep-sea organisms, there is a need for basic research on the sensitivities of appropriate

representatives of deep-sea fauna to contaminants present in this environment (Davies et al., 2007). It is this research requirement that is the topic of this current thesis.

1.3. Echinoderms – representative deep-sea fauna?

The deep sea is characterised by an abundance of echinoderms (Carney, 2001), members of this phyla being important and integral components of deep-sea benthic communities (Tyler, 1980; Billett, 1991; Gage and Tyler, 1991; Ruhl, 2007) and being found throughout the world's oceans. There are five extant classes of echinoderm; the Ophiuroidea (brittle stars and basket stars), Asteroidea (sea stars), Echinoidea (sea urchins), Holothuroidea (sea cucumbers) and the most primitive class, the Crinoidea (feather stars or sea lilies). Holothurians and ophiuroids are particularly abundant (Carney, 2001), but species from one or more of the five echinoderm classes dominate deep-sea benthic megafaunal communities in terms of abundance and/or biomass in the Arctic Ocean (Piepenburg, 2000), the Atlantic Ocean (Haedrich et al., 1980; Billett et al., 2001; Lavaleye et al., 2002; Hargrave et al., 2004), the Pacific Ocean (Smith and Hamilton, 1983; Lauerman et al., 1996; Bluhm, 2001), the Indian Ocean (Rodrigues et al., 2001), the Arabian Sea (Turnewitsch et al., 2000; Murty et al., 2009) and the Southern Ocean (Sumida et al., 2008). The numerical dominance of echinoderms (holothurians) even extends to the hadal depths of the ocean (Beliaev, 1989; Herring, 2002).

In addition to being important components of deep-sea benthic communities, echinoderms are also present in pelagic ecosystems as a consequence of many species' indirect lifecycles; where one or more life stage(s) occupy the water column before settling to the (adult) benthic habitat (Pearse and Lockhart, 2004; Dupont et al., 2010). Adult benthic echinoderms have important functional roles in structuring the chemical and physical features of their habitats, both in shallow water and in the deep sea. During feeding and locomotion echinoderms bioturbate the sediment (Lohrer et al., 2005; Vardaro et al., 2009) displacing particles, increasing sediment heterogeneity and exposing otherwise anoxic sediments to oxygen. As a result, they contribute to the maintenance of overall sediment biodiversity and total benthic respiration (Smith et al., 2000; Turnewitsch et al., 2000; Vopel et al., 2007; Glud, 2008; Thistle et al., 2008). Benthic echinoderm activity also contributes to inorganic and organic carbon cycling, sediment geochemical flux and deep-sea nutrient regeneration (Piepenburg, 2000; Smith et al., 2008a; Lebrato et al., 2010).

It is clear that, due to their importance within deep-sea communities, and their ubiquitous presence throughout the world's oceans, echinoderms are highly appropriate representatives of deep-sea fauna. The potential impact of anthropogenic activity upon deep-sea echinoderms, however, is not currently known, although evidence that they are sensitive to both environmental change and

anthropogenic contamination has become apparent. Significant alterations in the abundance of Atlantic and Pacific deep-sea echinoderm communities in response to climate-forced fluctuations in food supply indicate that the effects of global climate change reach abyssal depths and influence the deep-sea ecosystems and processes (Smith et al., 2009). Most recently, with large numbers of dead holothurians found on the sea surface in the vicinity of the Gulf of Mexico Deepwater Horizon oil spill (Amon, 2010), the potential detrimental impact of anthropogenic activities upon adult echinoderms (or at the larval stage, irrespective of whether or not the adult is impacted) and their relevance as representative deep-sea species is evident.

1.3.1. Echinoderms as model organisms for toxicological studies

Echinoderm embryos and larvae have been used in several lines of research as model experimental systems for more than a century (Micael et al., 2009). An extensive body of work exists regarding experimental toxicological work on echinoderm embryos and larvae, which have been accepted internationally as appropriate test subjects for toxicological studies, and much is known about the developmental defects caused by various toxicants (Kobayashi, 1984; Bay et al., 1993; ASTM, 2004b).

Although not traditionally used in toxicology studies, a growing body of evidence has led a number of researchers to argue that adult echinoderms are also an excellent choice as shallow water toxicological model organisms (Newton and McKenzie, 1996; Temara et al., 1998; Coteur et al., 2003; Danis et al., 2006; Sugni et al., 2007; Micael et al., 2009). Many of the arguments behind the choice of echinoderms for shallow-water investigations are applicable to deep-sea studies, and correspond to the relevant criteria that a bioindicator species should demonstrate as proposed by previous authors (Phillips, 1980; Widdows, 1985). A number of reasons can therefore be proposed for the use of adult echinoderms as model organisms for the assessment of anthropogenic impact in the deep sea:

1) As discussed above, deep-sea echinoderms are abundant and integral components of their ecosystems, and are a phyla to which a systems level of ecological importance has been proposed (Carney, 2001). The ability to assess to what extent they are affected by anthropogenic contamination and disturbance will provide important evidence for, and an understanding of, anthropogenic impact upon deep-sea communities.

2) Echinoderms have a wide geographic distribution throughout the deep sea. As such, specimens for research should be available in research locations in all oceans.

3) Benthic infaunal and deposit feeding echinoderms (which have the capacity to rework large

quantities of sediment) will have direct contact with, and cannot avoid, sediment-bound contaminants. These can be taken up across external respiratory surfaces, the epidermis, the intestine or via secondary uptake from food assimilation (Sugni et al., 2007; Micael et al., 2009).

4) Echinoderms are relatively sedentary, when compared to highly motile deep-sea fauna such as fish and crustaceans. This means that echinoderms cannot undertake long-range movement to avoid local seafloor contamination and collected specimens will be representative of the local area. At a practical level, if *in situ* experimentation or the controlled collection and retrieval of echinoderms to the surface are to be undertaken, echinoderms will be more easily captured by ROVs or HOVs (R/HOVs) than more motile organisms.

   It should be noted that some holothurian species are capable of active swimming movement; with benthopelagic species swimming for most of their lives (though still depending on seafloor sediments for feeding) and facultative swimming species leaving the seafloor in response to environmental cues, including for dispersal between phytodetrital foodfall patches (Miller and Pawson, 1990; Billett, 1991).

5) Echinoderms are relatively large, giving adequate tissue for analysis, and contributing to their ease of collection by R/HOV.

6) Deep-water studies have demonstrated that adult echinoderms accumulate pollutants without being killed by levels encountered in the environment (Arima et al., 1979; Lee et al., 1997; Moore et al., 1997; Takahashi et al., 1997). These studies are supported by a body of bioaccumulation evidence in shallow-water echinoderms (see below).

In addition, echinoderms are deuterostomes and have a key phylogenetic position as, together with the hemichordates, they are the closest known relatives of the chordates (Sea Urchin Genome Sequencing Consortium, 2006). The genome of the echinoid, *Strongylocentrotus purpuratus,* has been sequenced and, as well as providing an important resource for future research, it has indicated that echinoids have strong similarities with vertebrate gene families, immune responses, biomineralisation and hormonal pathways (Sea Urchin Genome Sequencing Consortium, 2006; Smith et al., 2006). Therefore, as well as echinoderms being suitable research proxies for vertebrate systems, a large body of human and other vertebrate research may be relevant as reference material for echinoderm toxicological research.

1.3.2. Shallow-water echinoderm toxicological studies

Adult echinoderms have not been used as extensively in toxicological investigations as traditional marine invertebrate model organisms such as *Mytilus* spp., *Corophium* spp., *Arcartia tonsa* and *Macoma* spp. (Bayne et al., 1985; ASTM, 2004a; OSPAR Commission, 2005). Despite this, a number of toxicological studies have been carried out with adult echinoderms to assess their response to contaminant-induced stress. Stress has been defined as "a state produced by any environmental or other factor which extends the adaptive responses of an animal beyond the normal range, or which disturbs the normal functioning to such an extent that, in either case, the chances of survival are significantly reduced" (Brett, 1958). Stress can therefore be measured as a deviation from an organism's normal state, which has a detrimental effect on the potential of an organism to survive.The stress response can take many forms (Clark and Peck, 2009), and can correspondingly be assessed at a number of levels of biological organisation using a variety of biomarkers.

A biomarker can be defined as a "biochemical, cellular, physiological, or behavioural variation that can be measured in tissue or body fluid samples or at the level of whole organisms that provides evidence of exposure to and/or effects of, one or more chemical pollutants" (Depledge, 1993 cited in Depledge et al., 1995). A brief review of adult echinoderm biomarkers and toxicology studies is included at Appendix 1.1, and summarised at Figure 1.1. A number of conclusions regarding toxicological testing with adult echinoderms can be drawn from the results of these studies:

1) The effects of anthropogenic contaminants upon adult echinoderms can be detected at the level of the community and via a number of biomarkers assessed at different biological levels ranging from the molecular to the behavioural (Appendix 1.1 and references therein).

2) Adult echinoderms are bioaccumulators of heavy metals and POPs on both spatial and temporal gradients (Temara et al., 1998; Warnau et al., 1998; Den Besten et al., 2001), and can be used as *in situ* indicators of contamination as they accumulate contaminants at levels correlated with those found in the ambient environment (Den Besten et al., 2001; Coteur et al., 2003; Danis et al., 2006). Deposit feeding holothurians (Moore et al., 1997; Laboy-Nieves and Conde, 2001) asteroids (Temara et al., 1998; Coteur et al., 2003; Danis et al., 2006) and grazing echinoids (Warnau et al., 1998) are highlighted as important biomonitoring organisms.

3) Heavy metals, POPs and hydrocarbon contaminants all have measurable deleterious effects on adult echinoderms (Appendix 1.1 and references therein).

4) Evidence for the deleterious effects of anthropogenic contaminants upon echinoderms has been found in temperate (Ordzie and Garofalo, 1981; Temara et al., 1999; Georgiades et al., 2005), tropical (Böttger et al., 2001) and polar (O'Clair and Rice, 1985; Békri and Pelletier, 2004) adult echinoderms including asteroids (Stronkhorst et al., 2003; Ryder et al., 2004), echinoids (Axiak and Saliba, 1981; Lavado et al., 2006b; Schäefer and Köehler, 2009), ophiuroids (Maurer and Nguyen, 1996; Newton and McKenzie, 1998) and crinoids (Barbaglio et al., 2006; Lavado et al., 2006a; Sugni et al., 2008).

5) The responses of adult echinoderms to anthropogenic pollutants are not always consistent, which is attributed to natural intraspecific variation (Coteur *et al.*, 2003; Békri and Pelletier, 2004).

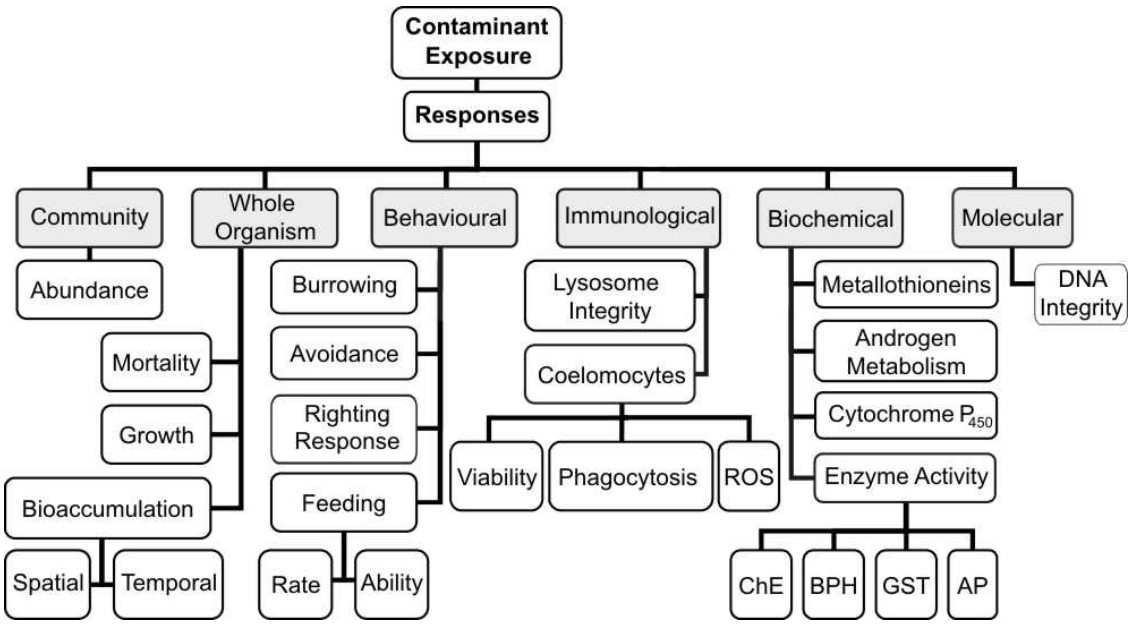

Figure 1.1. Summary of the different levels of biomarker responses which have provided evidence of bioaccumulation and /or the deleterious effects of anthropogenic contaminants upon adult echinoderms (the literature forming the basis of this figure is reviewed at Appendix 1.1 where acronym explanations are also provided).

These studies demonstrate that adult echinoderm toxicology studies can be performed with a variety of echinoderm species using a number of different biomarkers. The challenge for deep-sea toxicology studies is to employ suitable experimental methodologies that account for the limitations associated with the physical conditions of the deep-sea environment.

1.4. Experimental approaches to deep-sea toxicology

There are two approaches to the study of the potential impact of anthropogenic contaminants upon deep-sea organisms:

a) To use shallow-water species as analogues for deep-sea species. Experiments could be

performed at ambient surface conditions, in pressurised vessels or with shallow-water specimens transplanted to deep water.

b) To use deep-sea echinoderm species directly in toxicological exposures. Experiments could be performed on specimens retrieved to the surface or *in situ* at the deep-sea floor.

The advantage of the first, shallow-water species, approach is that experimental methodology and performance under surface laboratory conditions will be simpler and less expensive than operating with deep-sea organisms *in situ* at the sea floor, or recovered and maintained under pressurised conditions. The benefit of using deep-sea species directly in experimental research under deep-sea conditions, however, is that the generated results will be directly applicable to the interpretation of anthropogenic impact in the deep sea - without having to account for any uncertainties associated with the different physiologies of shallow-water and deep-sea species. Additionally, the physicochemical properties of contaminants under deep-sea pressure and temperature conditions may be altered compared with those found under shallow-water conditions, which may influence their availability to biological systems. However, two key factors that will influence the performance of experiments with shallow-water species under deep-sea (elevated pressure) conditions, and influence experiments with deep-sea species that have experienced decompression, are the effects of baro- and/or thermo-trauma, with associated implications for the interpretation of experimental results.

1.4.1. Thermo- and baro-trauma

Physiological and biochemical systems are sensitive to both pressure and temperature change (Somero, 1998), which means deep-sea adapted organisms are detrimentally effected by physical conditions at the surface and shallow-water adapted organisms detrimentally effected by those of the deep sea. Temperature influences the weak chemical bonds that are primarily responsible for maintaining correct protein formation, functioning and subunit aggregation, enzyme-ligand complex integrity and lipid-based physical structures (Somero et al., 1983). Pressure influences the volume of both gas- and water-filled spaces, with alterations in pressure having consequences to biological functioning ranging from the molecular level to that of the whole organism (Somero, 1991). Both pressure and temperature change therefore result in the dissociation of weak acids and bases, denatured proteins and altered lipid fluidity (Somero, 1991; Mozhaev et al., 1996). Enzyme catalytic rate and regulation, osmotic regulation, transmembrane transport and ion flux, nerve resting potentials and synaptic transmission are hence strongly affected by pressure and temperature change (Somero et al., 1983; Somero, 1991, 1992; Siebenaller and Garrett, 2002).

The physical differences between shallow-water and deep-sea environmental conditions therefore

influence the biological systems of organisms moved between the two. Surface water temperatures are typically warmer (Polar Regions excepted) and always at a lower pressure than those found in the deep sea. Early experiments, which attempted to elucidate the effect of pressure on physiological processes, involved the subjection of terrestrial or shallow water organisms, or their excised tissues, to high-pressure conditions. These experiments were carried out either in laboratory-based pressure chambers or by submergence of the organisms to abyssal depths (Brauer, 1972). The animals exhibited a suite of extreme reactions to compression progressing through tetany to paralysis and finally death; a suite of responses termed the "High Pressure Neurological Syndrome" (Brauer, 1972; Hunter and Bennett, 1974).

Deep-sea organisms retrieved to the surface, inadequately protected from decompression and increasing temperature, also experience deleterious side effects. Decompression is well known to affect gas-filled organs of organisms such as fish, which exhibit swim bladder overinflation and exophthalmia (Wilson and Smith, 1985; Rogers et al., 2008). Yet in all deep-sea organisms, volume change at the molecular level alters molecule arrangements, enzyme void volumes, chemical reaction rates, solvent organisation and lipid bilayer structure (Somero et al., 1983; Somero et al., 1991). The decompression of deep-sea organisms has been found to cause molecular change (Dixon et al., 2004), transmembrane ion flux inhibition (Somero, 1991), cardiovascular and nervous system perturbation (Mickel and Childress, 1982; Gibbs, 1997), convulsions (Shillito et al., 2008), oxygen consumption rate change (Bailey et al., 1994; Cottin et al., 2008), paralysis (Macdonald, 1997) and death (Hessler, 1972; Treude et al., 2002). The performance of toxicological studies under environmental conditions, to which the test organisms are not adapted, is therefore problematic.

1.4.2. Shallow-water echinoderms as deep-sea analogues

If the stress-responses of shallow water echinoderms to contaminants were shown to be representative of those that would be exhibited by deep-sea species, the results of such toxicological investigations could be applied to the prediction of the affect of anthropogenic contamination upon deep-sea species. An investigative approach using shallow-water species would mean that the costly and logistically complex use of deep-sea echinoderms in toxicological investigations could be avoided, and the wide range of accurate experimental methodologies available for laboratory-based studies could be utilised. Experimental approaches using shallow-water echinoderms could take one of two forms a) via the performance of experiments under deep-sea physical conditions, or b) using shallow-water species that inhabit an environment, which in terms of a gradient of stress, is analogous to that of the deep-sea.

Shallow-water species and pressurised toxicology studies

A small body of work on the use of shallow-water organisms for deep-sea toxicological studies has been reported. Galgani et al. (2005) transplanted shallow-water mussels (*Mytilus galloprovincialis*) to various depths of up to 1550 m in the Mediterranean Sea, located in the vicinity of an aluminium factory bauxite waste outflow pipe. Two months later, measurements of a general indicator of bivalve health, the condition index, showed no change in the mussels with depth or proximity to the pipe. At the deepest sites, however, mortality was highest and there had been histological damage to the digestive glands. Additionally, during laboratory-based pressurisation tests prior to transplantation, clear signs of mussel stress had been observed (spawning). In a recent laboratory-based larval 'eco-barotoxicological' study, Vevers et al. (2010) exposed gametes from the littoral polychaete *Pomatoceros lamarcki* to oil and oil dispersants at various pressures up to 300 bar (3059 m depth equivalent). It was found that hydrostatic pressure was the key factor influencing larval survivorship, not the oil or dispersant, and Vevers et al. concluded that the use of static pressurisation devices (and the associated compression/decompression process) does not produce a realistic deep-sea simulation that can be applied to toxicological studies.

These studies, together with the body of historical work concerning the effects of pressure on terrestrial and shallow-water organisms (Brauer, 1972), demonstrate that shallow water species are not adapted to the elevated pressure of the deep-sea environment. In toxicological studies, the detrimental side effects caused by pressure are likely to have a greater stress inducing impact than, and will mask any affects of, the test contaminant. As such, experimental approaches that involve subjecting shallow-water organisms to deep-sea pressurised conditions should not be used in studies investigating the impact of anthropogenic contaminants upon deep-sea organisms.

Gradients of environmental stress

An alternative experimental approach with shallow-water organisms is to perform contaminant exposures at ambient surface conditions using species which inhabit environments analogous, to some extent, to that of the deep-sea. Organisms from either stable or pollutant-free environments have a different stress response, and susceptibility to stressful conditions, to those that live in environments that are inherently more stressful due to environmental instability or contamination (Feder and Hofmann, 1999; Maltby, 1999; Patruno et al., 2001a). These differences may be found at the individual level (phenotypic plasticity) for example, organisms with a history of contaminant exposure are less sensitive than those from uncontaminated sites (Maltby, 1999; Bresler et al., 2003). Or differences may be found at the population level (genotypic adaptation), where animals adapted to highly stable environments lack certain stress-response mechanisms,

such as the absence of a constitutive heat shock response in polar species (Pörtner et al., 2007; Clark and Peck, 2009).

The coastal intertidal zone can be considered a highly stressful environment (Hofmann, 1999; Tomanek and Helmuth, 2002). Organisms inhabiting the intertidal zone may be regularly exposed to large and rapid variations in temperature, emersion, salinity, oxygen concentration and wave action. Adaptation and acclimation to stress are therefore particularly important in eurytopic intertidal organisms (Collén et al., 2007). The response by intertidal organisms to environmental or contaminant induced stress could therefore be expected to be different to that which would be exhibited by an organism inhabiting a typically low-stress environment. For example, during arm regeneration following wounding, intertidal specimens of the starfish, *Asterias rubens*, show a greater and longer elevation of the levels of a stress inducible heat shock protein than specimens from a stable benthic environment (Patruno et al., 2001a).

The deep-sea physical environment, highly stable in terms of salinity, pH, oxygen concentration, temperature and pressure (Tyler, 1995), is a habitat where deep-sea animals have evolved in the absence of substantial environmental instability and related stress (Seibel and Walsh, 2003). As a result, stenotopic deep-sea animals are considered to be highly intolerant of stressful situations as they lack the adaptations that would allow regulation of their internal milieu in the face of altered environmental conditions (Angel, 1992; Seibel and Walsh, 2003). With appropriate experimental investigation, it may be found that shallow-water species of echinoderm inhabiting stable (low stress) environments exhibit a contaminant-induced stress response different to that of echinoderms that inhabit highly stressful environments. As such, the stress responses of stenotopic echinoderms from stable environments may more closely reflect those that would be expected by deep-sea species. An investigation of the differences in the contaminant induced stress response in two species of echinoderm from environments differing in terms of variability and stress is reported in this current thesis.

1.4.3. Experimentation with deep-sea echinoderms

Retrieval to the surface

As discussed above, deep-sea organisms retrieved to the surface unprotected from decompression and temperature change experience detrimental side effects (Hessler, 1972; Macdonald, 1997). It has been found, however, that the tolerance of deep-sea organisms to decompression is both depth- and species-dependent, as studies with hydrothermal vent organisms demonstrate. Whilst some crustacean (*Bythograea thermydron*, collected from ~2460 m depth) and polychaete (*Paralvinella sulfincola*, 1800 m) species have been maintained for long periods (up to 18 months) in pressured aquaria, experiencing decompression / recompression cycles for feeding and cleaning (Mickel and

Childress, 1982; Girguis and Lee, 2006), other species show a low tolerance to decompression. Specimens of the shrimp, *Mirocaris fortunata* and mussel *Bathymodiolus azoricus* (collected from ~2300 m collection depth), have a higher mortality rate than those collected from 840m (Dixon et al., 2004; Shillito et al., 2006), and the polychaete *Alvinella pompejana* suffers such traumatisation during collection that subsequent *in-vivo* experimentation is not possible (Cottin et al., 2008).

Although some deep-sea species can be collected in a suitable physiological state to allow experimental investigations to proceed, the decompression and/or recompression process has been found to introduce artefacts into physiological measurements and experimental results. For example, the behaviour and oxygen consumption rates of the polychaete *Paralvinella grasslei* (retrieved from 2600 m, Cottin et al. (2008) and the shrimp *M. fortunata* (Shillito et al., 2006) reflect the deleterious consequences of the collection process from the deep sea, and the oxygen consumption and heart rate of *B. thermydron* is altered by decompression (Mickel and Childress, 1982). In an investigation of the antioxidant defence capacity of the vent mussel *B. azoricus* (840 m collection depth), the same change in enzyme activity and capacity to detoxify reactive oxygen species was found in both the mussels experimentally exposed to copper and the non-exposed control mussels, and it was impossible to distinguish the effects of metal toxicity from those of decompression and maintenance in artificial aquaria (Company et al., 2008). Reliable and accurate toxicological research using deep-sea organisms recovered to the surface hence requires the use of specialist retrieval equipment that enables the organisms to be maintained at *in situ* temperature and pressure at all times (Gibbs, 1997; Shillito et al., 2008), in order to prevent artefacts from the collection process influencing experimental results.

Pressure- and temperature-retaining devices have been used successfully to capture organisms in the deep sea, return them to the surface and to perform simple physiological measurements such as oxygen consumption rates (refer to review in Chapter 7). The application of such retrieval equipment to the collection of deep-sea echinoderms is somewhat restricted though. Retrieval device designs based on autonomous baited traps, which attract scavenging organisms such as fish and amphipods (Brown, 1975; Wilson and Smith, 1985; Drazen et al., 2005), are not suitable for the capture of benthic organisms such as echinoderms (Shillito et al., 2008). This is because of slow echinoderm locomotion and the inaccessibility of the traps (which are elevated above the sea floor on freefall frames or mooring lines) to a benthic organism. Instead, echinoderm specimens would need to be actively captured by R/HOV and placed directly inside a retrieval device.

Basic toxicological experiments with deep-sea echinoderms or other organisms returned to the surface could be performed inside the retrieval device with *in situ* pressure and temperature maintained. However, enclosure inside a pressurised vessel limits direct access to the specimens.

The use of biomarkers for contaminant exposure that require tissue collection, such as enzyme or cellular activities, would hence require decompression of the specimen for sample access. As discussed above, decompression may lead to artefacts that mask stress responses caused by the contaminant itself. The assessment of the effects of a contaminant upon a recovered deep-sea echinoderm would therefore have to be based on either biomarkers that can be assessed within the pressurised device, such as behavioural observations, physiological measurements such as oxygen consumption rate or mortality, or biomarkers that are not altered by decompression. The same principles also apply to the performance of deep-sea toxicology experiments *in situ*.

***In situ* experimentation**

The alternative to the protected retrieval of deep-sea specimens to the surface is the performance of echinoderm contaminant exposures *in situ* at the sea floor. The logistical and technical expertise and expense required to perform research below depths accessible by human divers makes any kind of scientific activity in the deep-sea difficult, but it has already been proved that small-scale *in situ* contaminant exposure experiments are possible. Barry et al. (2004) and Thistle et al. (2005; 2007) have reported the use of R/HOVs at 3000-3600 m depth to fill corrals on the seafloor with liquid CO_2, to deploy monitoring instrumentation and to collect cores or traps for subsequent results analysis. Tamburri et al. (2000) used ROV capability to expose epibenthic organisms to CO_2 plumes and to observe subsequent behavioural responses. These studies demonstrate that *in situ* exposure experiments are feasible, however, the exposure of deep-sea organisms to a contaminant that will disperse quickly into the water column has not been reported. New equipment development is required which will permit the controlled introduction of a contaminant into an *in situ* experimental system, such as the syringe pump system used for *in situ* underwater dosing of shallow-water benthic organisms by Hatay et al. (2005). It is possible that current deep-sea equipment designs, such as those which permit the introduction of labelled diatoms into benthic chambers (Aberle and Witte, 2003; Aspetsberger et al., 2007), could be adapted to deliver contaminants instead. Irrespective of equipment design, the biomarkers, which offer the ability to assess the stress response of a deep-sea organism to contaminant-induced stress *in situ*, are again limited by the effects of decompression or temperature change.

1.4.4. Deep-sea biomarkers

At the community level, assessments of the impact of anthropogenic disturbance in the deep sea are relatively common. Surveys based on photographic analysis and sample collection via core, grab and trawl have been used to assess the impact of disturbance upon deep-sea community faunal diversity and abundance from the meiofauna to megafauna. For example, polymetallic nodule mining (Bluhm, 2001; Borowski, 2001; Rodrigues et al., 2001), hydrocarbon drilling

(Jones et al., 2007; Santos et al., 2009) and trawl fishing (Koslow et al., 2001; Roberts, 2002) have been found to eliminate species from deep-sea communities and reduce diversity. The abundance of echinoderms, as typical members of benthic communities, is commonly found to be affected by such disturbance (Peterson et al., 1996). Indeed, holothurians have been proposed as indicators for deep-sea recolonisation processes in environmental assessments due to their initial elimination from disturbed sites (Bluhm, 1999).

As reviewed in section 1.3.2, a variety of biomarker methodologies have been used in toxicology experiments with shallow-water echinoderms, but not all of these are suitable for use with deep-sea organisms maintained in pressured aquaria or *in situ*. At the level of the individual organism, deep-sea echinoderms have already been found to be representative bioaccumulators of anthropogenic contaminants (Lee et al., 1997; Moore et al., 1997; Harino et al., 2005). Also assessed at the individual level, behaviour, as a visible reaction to a stimulus, is amongst one of the most sensitive indicators of environmental alteration (Gerhardt, 2007). Behavioural change can represent either a response to mitigate potential detrimental effects (e.g. the avoidance of contaminated sediment, Ryder et al. (2004)) or the effects of a toxicant (e.g. righting response or feeding activity (O'Clair and Rice, 1985; Böttger et al., 2001; Canty et al., 2009)). Behavioural observation is possible in the deep sea, as R/HOVs or lander cameras offer live or recorded *in situ* video footage from which behaviour can be monitored and assessed (Tamburri et al., 2000; Jamieson et al., 2006; Raymond and Widder, 2007). As such, the application of behavioural biomarkers to deep-sea toxicology studies is technically feasible. However, the length of time that would be required during a ROV dive for sufficient replicates of, for example a righting response assay to be performed, could be prohibitive.

The use of physiological biomarkers, such as oxygen consumption rate, which represent an interaction of the many cellular and biochemical processes that alter in response to changes in the environment (Bayne et al., 1985; Handy and Depledge, 1999) is possible *in situ*. Over the past thirty years, the oxygen consumption rates of deep-sea echinoderms, fish and crustacea have been obtained from bathyal and abyssal depths (refer to review in Chapter 7). The *in situ* contaminant exposure of an echinoderm enclosed inside a respiratory device, and the use of oxygen consumption as a biomarker of possible contaminant-induced stress is therefore an option for deep-sea toxicology studies. In this regard, the development of an *in situ* respirometer suitable for application to the measurement of deep-sea echinoderm oxygen consumption rates was undertaken during this study.

At the molecular level, biomarkers such as gene expression allow the quantification of sub-lethal effects across a range of functions and are considered best able to predict an organism's

vulnerability to stress (Clark and Peck, 2009). Toxicant exposure alters the gene expression profile of an organism as cells regulate certain genes to protect, repair or remove damaged proteins (Snell et al., 2003). Altered gene expression is an early and sensitive means of detecting an organisms stress response (Williams et al., 2003), with the induction of some proteins being more sensitive to stress than traditional indices such as growth inhibition (Depledge et al., 1995; Feder and Hofmann, 1999; Mukhopadhyay et al., 2003). The stress-induced upregulated expression of a family of proteins called the heat shock proteins has been most investigated in this regard, and it has been found to be a near-universal response to stress in many organisms (Gross, 2004, and refer to section 2.1.1.2). As such, a focus in this current thesis is the development and application of heat shock protein biomarkers to echinoderm studies, due to the high likelihood that deep-sea echinoderms will exhibit such a stress response.

1.5. The current study

There is a need to develop reliable methods to investigate the impact of anthropogenic activities on deep-sea organisms and, as discussed above, various approaches could be taken in this regard. In this current study, three approaches to the investigation of anthropogenic impact on echinoderms have been used and/or developed, primarily using echinoids as representatives of the echinoderm phylum.

In the first approach, the theory was tested that a eurytopic echinoid species (*Psammechinus miliaris*), from a physically variable environment (the intertidal zone), would display a response to contaminant-induced stress different to that of a stenotopic echinoid species from a stable benthic environment (*Brissopsis lyrifera*). A range of biomarker methodologies were employed to detect the echinoid stress responses. Particular attention was paid to the development of the molecular biomarker methodology (quantitative analysis of gene expression), as this investigative technique has the potential to be applied to *in situ* deep-sea investigations by virtue of the near universal alteration in the expression of stress-induced genes (the heat shock proteins) in organisms from all three of the Archaea, Bacteria and Eukarya domains (Gupta and Golding, 1993; Gross, 2004).

As a stenotopic species, the *B. lyrifera* stress response was expected to be reduced compared with that of *P. miliaris*, and hence to be more representative of echinoderm species inhabiting other stable environments such as the deep sea. Due to their adaptation to an environment characterised by an absence of variability, deep-sea organisms are considered to have a reduced capacity for homeostasis in the face of environmental perturbation (Seibel and Walsh, 2003), and to hence have little tolerance to environmental change (Angel, 1992).

In the second experimental approach, the application of *in situ* experimentation to echinoderm

anthropogenic impact research was tested, with the experimental results analysis incorporating the molecular biomarker methodology developed during the previous work with *P. miliaris* and *B. lyrifera*. ROV technology was used to simulate the *in situ* burial of deep-water echinoids (*Echinus acutus*) by drill cuttings and disturbed sediment as a result of offshore hydrocarbon drilling activity disturbance. To test the hypothesis that in-situ induced stress in deeper-water echinoderms could be detected at the molecular level, an assessment of the echinoids' stress response was performed via the quantitative analysis of heat shock protein (*hsp*) gene expression in tissue samples. Additionally, the effect of unprotected retrieval to the surface upon the echinoids was investigated to assess whether decompression and temperature change influenced *hsp* expression.

Finally, the development and first scientific deployments of an *in situ* respirometer, designed to determine the oxygen consumption rates of deep-sea echinoderms (and other megafauna) is discussed. The development of *in situ* deep-sea experimental apparatus is important if our understanding of the physiology of deep-sea organisms is to improve, along with the ability to interpret their sensitivity to anthropogenic impacts. The specific hypothesis that deep-sea echinoderm mass-specific metabolic rates do not differ from those of shallow-water echinoderms was tested using the results obtained from the deployment of the *in situ* respirometer.

The major topics covered in this study, and the format of this thesis, are hence:

1) The isolation of the genetic sequences for three genes of interest from two species of shallow-water echinoid (Chapter 2) inhabiting environments differing in physical stability, and from these sequences the development and optimisation of molecular biomarkers for the quantification of gene expression (Chapter 3) to assess echinoid sublethal stress.
2) The determination of any differences between the biomarker responses to contaminant-induced stress in shallow-water echinoids from two different environments: the variable intertidal (*P. miliaris*, Chapter 4) and the stable benthic (*B. lyrifera*, Chapter 5).
3) The application of the molecular biomarker methodology to a deeper, continental shelf, species of echinoid (*E. acutus*) subjected to *in situ* disturbance stress (Chapter 6).
4) The development of a deep-sea megafaunal respirometer, its deployment and the measurement of *in situ* abyssal echinoderm oxygen consumption rates (Chapter 7).

Through an analysis of the results of these studies, it will be possible to draw conclusions as to the application of experimental investigation relevant to assess the potential impact of anthropogenic activity upon deep-sea echinoderms (Chapter 8).

Chapter 2. Gene Hunting

2.1. The cellular stress response

Stress-inducing environmental conditions or toxic contaminants can perturb the intracellular protein structure of an exposed organism (Sanders, 1993; Goldberg, 2003; Kültz, 2003). In order to defend against stressful conditions, the cell employs a molecular strategy that is referred to as the cellular stress response or defensome (Feder and Hofmann, 1999; Todgham and Hofmann, 2009). This response includes the synthesis of osmotic stress protectants, modifications to membrane lipid saturation (homeoviscous adaptation), metabolic alterations and the up-regulation of radical scavengers (e.g. cytochrome P_{450}) and defensive proteins (Lindquist, 1986; Feder and Hofmann, 1999; Kültz, 2005).

The up-regulated gene expression and the activities of stress-inducible defensive proteins and metabolic enzymes have been used as biomarkers of both environmental and pollutant induced stress for a number of years (Feder and Hofmann, 1999; Bierkens, 2000; Dahlhoff, 2004). Quantifying gene expression by determining the number of mRNA transcripts from a specific gene provides a sensitive indication of the extent to which an organism is stressed and/or the level of an organisms' stress response (Snell et al., 2003; Dahlhoff, 2004; Gupta et al., 2010).

The stress-induced upregulated expression of a family of proteins called the heat shock proteins has been found to be a near-universal response to stress in many organisms (Gross, 2004; Clark and Peck, 2009; and refer to section 2.1). This 'heat shock response', found in response to many stressors not just to thermal stress, has been found in deep-sea organisms such as crustacea (*Rimicaris exoculata* and *Mirocaris fortunata),* bivalvia *(Bathymodiolus thermophilus* and *Bathymodiolus azoricus)* and polychaetes *(Paralvinella pandorae* and *Paralvinella grasslei)* (Pruski and Dixon, 2007; Ravaux et al., 2007; Cottin et al., 2008; Boutet et al., 2009; Ravaux et al., 2009). As such, a focus in this current thesis is the development and application of a gene expression biomarker to echinoderm studies, due to the high likelihood that it will be possible to assess the stress response of deep-sea echinoderms using such a technique.

The current chapter is a methodology chapter reviewing the work carried out to identify and isolate complete cDNA sequences relating to the citrate synthase (*cs*), heat shock protein 70 (*hsp70*) and polyubiquitin (*ubc*) genes in *Psammechinus miliaris* and *Brissopsis lyrifera*. The nucleotide sequence for each of these genes was required in order that species-specific primers for the quantitative real-time polymerase chain reaction (qPCR) assays could be designed. The qPCR assays could then be optimised (section 2.3) in order to subsequently assess the expression of the three genes in each echinoid species during their response to stress.

2.1.1. Genes of interest

In this study, the expression of three genes in response to anthropogenic-contaminant induced stress was investigated. The three genes of interest (GOI) were those coding for the metabolic enzyme citrate synthase and two 'molecular chaperones' involved in the cellular stress response: a stress-70 (hsp70) protein and ubiquitin. The following discussions of these genes and proteins, and subsequent thesis chapters, use abbreviated gene and protein names where appropriate. Abbreviated gene names are listed in lower case italics and abbreviated protein names in uppercase characters. Following the terminology for *Mus musculus* (MGI88529) the citrate synthase gene is referred to as *cs* (protein = CS). The abbreviated terms used for the stress-70 gene are discussed in section 2.1.1.2 and the ubiquitin gene is referred to as *ubi* (protein = UBI).

2.1.1.1. Citrate synthase

Citrate synthase (CS; E.C. 4.1.3.7) was chosen for expression analysis as the protein is an important regulatory enzyme, being one of the 'pace-maker' enzymes in the citric acid cycle (Goldenthal *et al.*, 1998). CS activity is an indicator of aerobic respiration occurring at the mitochondrial level, and hence of an organism's metabolic capacity (Seibel and Childress, 2000). It is one of a number of metabolic enzymes that have been used as indicators of metabolic activity in a variety of organisms. For example, the activities of lactate dehydrogenase (LDH), a glycolytic enzyme and an indicator of anaerobic metabolic capacity, and CS have been shown to be closely linked with depth, metabolic rate and food availability in deep-sea fish (Childress and Somero, 1979; Drazen and Seibel, 2007) and cephalopods (Seibel, 2007). Seasonal changes in both LDH and CS activity in Antarctic krill are linked to changes in physiological status (Cullen *et al.*, 2003), and differences in the activity of CS and malate dehydrogenase (also a citric acid cycle enzyme) in the mussel *Mytilus californianus* are linked with food availability (Dahlhoff and Menge, 1996).

As well as being used as biomarkers of metabolic capacity, these metabolic enzymes have also been used as ecotoxicological biomarkers. Lactate dehydrogenase has been shown to be a biomarker for exposure to petroleum hydrocarbon contamination in Atlantic salmon (*Salmo salar*), bass (*Macquaria novemaculeata*) and rainbowfish (*Melanotaenia fluviatilis*) (Gagnon and Holdway, 1999; Pollino and Holdway, 2003; Cohen et al., 2005). Citrate synthase activity is significantly inhibited during exposure to the water accommodated fraction of crude oil and dispersed crude oil in the gills of Atlantic salmon (Gagnon and Holdway, 1999) and rainbowfish (Pollino and Holdway, 2003), although activity levels increase again after exposure ceases, indicating that it is a short-term biomarker in these species. Copper contamination is associated with reduced CS activities in the muscle of wild yellow perch (*Perca flavescens*) (Couture et al., 2008), whilst cadmium exposure reduces CS activity in the oyster *Crassostrea virginica* (Ivanina

et al., 2008). However, metabolic enzymes are not universal biomarkers of contaminant exposure; in *M. edulis planulatus* neither LDH nor CS were sensitive biomarkers of exposure to petroleum hydrocarbons (Long et al., 2003). Studies concerning CS and echinoderms have focused on the influence of environmental (e.g. salinity) or developmental stage (egg to adult) upon the rate of CS activity (Okabayashi and Nakano, 1978; Marsh and Lawrence, 1985; Meyer et al., 2007).

The citric acid cycle

The citric acid cycle (or tricarboxylic acid cycle or Krebs cycle) which takes place within mitochondria, comprises a series of sequential enzyme-mediated reactions that generate metabolic energy aerobically (Figure 2.1). During the citric acid cycle, carbon compounds are oxidised and carbon dioxide (CO_2), reduced Nicotinamide adenine dinucleotide ($NADH_2$) and reduced flavin adenine dinucleotide ($FADH_2$) are generated as end products. CO_2 is eliminated as waste and the high-energy electrons associated with NADH and $FADH_2$ are transferred to O_2, which is reduced to H_2O during oxidative phosphorylation. The energy released during oxidative phosphorylation is passed along a series of enzymes called the electron-transport chain, which in turn release energy used to generate a proton motive force across the inner mitochondrial membrane. Adenosine triphosphate (ATP) synthases embedded in the membrane then use the energy from the proton gradient to generate ATP from adenosine diphosphate (ADP) and phosphate (Alberts, 1994). Citrate synthase catalyses the first reaction in the citric acid cycle, a condensation reaction between acetyl-coenzyme A and oxaloacetate forming citrate (Wiegand and Remington, 1986).

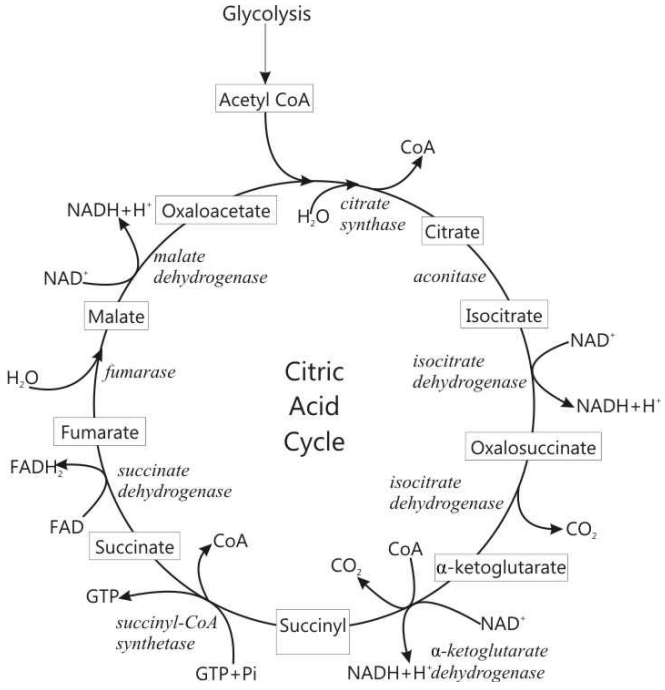

Figure 2.1. The Citric Acid Cycle. CS is the first enzyme involved in the series of sequential enzyme-mediated reactions. CoA = Coenzyme A. Figure modified from Thauer (1988).

2.1.1.2. Stress-70 proteins

Heat shock proteins (HSPs) are termed molecular chaperones because they facilitate the folding or assembly of other proteins but are not part of the final biologically-active structure (Hightower *et al.*, 1994; Ellis, 1996). As chaperones, HSPs stabilize denaturing proteins and refold reversibly denatured proteins (Lindquist, 1986; Feder and Hofmann, 1999). It is thought that HSPs bind to exposed hydrophobic amino acid side chains and unstructured backbone regions in damaged proteins and either shield them to prevent unwanted protein aggregation or inappropriate reactions with other cellular proteins, or refold the damaged proteins (Georgopoulos and Welch, 1993; Parsell and Lindquist, 1994). The expression of some forms of HSP is hence found to be up-regulated during the cellular stress response, and the presence of high amounts of these molecular chaperones can be used as a proxy for cell stress (Dahlhoff, 2004).

The genes encoding HSPs are highly conserved (Lindquist and Craig, 1988; Sørensen et al., 2003) and are assigned to different HSP families on the basis of their sequence homology and typical molecular weight. For example, the following major families are known; *hsp100*, *hsp90*, *hsp70*, *hsp60*, and *hsp27* and each family have a slightly different cellular function (Morimoto et al., 1994; Feder and Hofmann, 1999; Arya et al., 2007; Gupta et al., 2010). The majority of cellular translational activity in response to stress is accounted for by the 70-kDa HSP family (complete size range 68-75 kDa), which has been the most studied HSP family to date (Lewis et al., 1999). There are multiple members of the 70-kDa HSP family, located in different cellular compartments and organelles. The same family members have been assigned different names throughout the literature. To clarify the terminology used in this thesis: the term stress-70 (Gething and Sambrook, 1992) is used to refer collectively to members of the 70-kDa HSP family unless more specific terms are required, in which case the terminology listed in Table 2.1 is followed.

Different degrees of inducibility exist for different stress-70 proteins, including; constitutively expressed, constitutively expressed but increasing during or after stress, and exclusively inducible (Feder and Hofmann, 1999). Included in the stress-70 family are the constitutively expressed heat shock cognate (*hsc*)70 and the stress inducible *hsp70* genes, both code for proteins with extremely similar amino acid sequences and functions. The traditional view is that *hsc70* is constitutively expressed during normal physiological conditions, being the most abundant stress-70 protein found in normal cells, and the HSC70 proteins act as molecular chaperones to assist protein folding, unfolding, translocation across membranes and regulatory protein control (Sharp et al., 1999; Daugaard et al., 2007; Gupta et al., 2010). The *hsp70* gene is traditionally thought to only be expressed in response to protein-denaturing stress, and its synthesis can increase to a point where it is one of the most abundant proteins in a cell (Sharp et al., 1999). The HSP70 proteins are

involved with processes to repair and stabilise cellular proteins, stabilize lysosomal membranes and minimize protein aggregations (Hartl and Hayer-Hartl, 2002; Kirkegaard et al., 2010).

Recent work has, however, indicated that the distinction between the expression of *hsc70* and *hsp70* is not straight forward (Franzellitti and Fabbri, 2005). Both forms are expressed at the same time in *Ostrea edulis* and *Mytilus* spp. (Hofmann and Somero, 1995; Piano et al., 2002; Piano et al., 2005). Elevated expression of both *hsc70* and *hsp70* have also been found in response to heat shock in the prawn *Macrobrachium rosenbergii* (Liu et al., 2004), and during mercury and chromium exposure in *M. galloprovinicalis* (Franzellitti and Fabbri, 2005). Studies with teleost fish which have investigated both genes have found that *hsc70* expression does increase significantly in response to acute heat shock although not to the same extent as the increase found in *hsp70* expression (Deane and Woo, 2005; Ojima et al., 2005). If *hsp70* expression was to be used as a biomarker in the current echinoid study, to reduce possible confusion with the constitutive form, it was important to ensure that its quantification was isolated from that of *hsc70*.

Table 2.1. Different terminology used to refer to members of the stress-70 family of 70kDa heat shock proteins in the literature. The bold terms at the start of each list refer to the official HGNC* symbol for the relevant human gene.

Description	Alternative terms	Terms used in this thesis
Located in the cytosol		
Inducible form	**Eukaryote: HSPA1A**, HSPA1B, HSPA1, HSP70-1, HSP70-2, HSP70, HSP72, HSP70i, HSPA1B, HSP70-1A, HSP70-1B, HSP70A2, HSPAIL **Prokaryote**: DnaK	HSP70
Constitutively expressed form	**Eukaryote: HSPA8**, HSC71, HSC70, HSP73, HSP71, LAP1, HSPA10, Nip71	HSC70
Located in the endoplasmic reticulum	**HSPA5**, GRP78, immunoglobulin heavy chain-binding protein (BiP), MIF2	BiP
Located in the mitochondria	**HSPA9,** mBiP, GRP75, PBP, mortalin, mtHSP70, MTP70, MOT, MOT2, HSPA9, PBP74	mortalin

*HGNC = HUGO Gene Nomenclature Committee. Terminology compiled from the literature, with reference to the 'HSP70 Sequence Database' (http://bioinfo.med.utoronto.ca/HSP70/) and to the NCBI Entrez Gene Database (http://www.ncbi.nlm.nih.gov/gene).

Heat shock protein 70 as a biomarker

The HSP name is derived from the heat stress experiments during which these proteins were first found to be expressed, but it is now known that virtually every type of stress can induce *hsp70* expression (Lindquist and Craig, 1988; Feder and Hofmann, 1999). Due to this inducible response, analyses of *hsp70* expression and the activity of the HSP70 protein have been widely used in

biomonitoring and environmental toxicology, in particular aquatic toxicology (Feder and Hofmann, 1999; Lewis *et al.*, 1999). The *hsp70* gene is viewed as a useful biomarker because its expression is directly linked with cellular damage, and its induction is more sensitive to stress than traditional indices such as growth inhibition (Feder and Hofmann, 1999; Mukhopadhyay et al., 2003; Hamer et al., 2004). It is for these reasons, and in addition because of its highly conserved nature leading to transcripts of the *hsp70* gene being relatively easy to isolate using degenerate PCR (Clark and Peck, 2009), that *hsp70* was chosen for expression analysis in this study.

The vast majority of studies investigating toxicant induced *hsp70* expression in aquatic organisms have been carried out with bivalve and fish species. A wide variety of stressors have been found to induce *hsp70* expression in aquatic organisms, including: heat (Franzellitti and Fabbri, 2005; Cheng et al., 2007), several metals such as mercury, chromium, copper and cadmium (Vedel and Depledge, 1995; Boutet et al., 2003; Franzellitti and Fabbri, 2005; Ivanina et al., 2009); tidal emersion (Hofmann and Somero, 1996) , hypoxia (Cheng et al., 2003; Delaney and Klesius, 2004), hydrocarbons (Boutet et al., 2004) and industrial effluents (Vijayan et al., 1998). A smaller body of work investigating *hsp70* expression in echinoderm embryos and adult echinoderm coelomocytes has demonstrated inducible *hsp70* responses to stress (temperature, acidic pH, heavy metals and trauma) and that *hsp70* expression can be used as an indicator of echinoderm stress (Giudice et al., 1999; Matranga et al., 2000; Schröder et al., 2005; Pinsino et al., 2007; Todgham and Hofmann, 2009).

2.1.1.3. Ubiquitin

Ubiquitin is a small protein only 76 amino acids (228 bp) in size; its name is derived from the fact that it is ubiquitous in all eukaryotic organisms (Varshavsky, 1997). Ubiquitin has a vital role in intracellular protein turnover, being the "tag" that marks proteins for proteolysis (destruction), and it is also referred to as a molecular chaperone (Finley and Chau, 1991). The cell must be able to selectively degrade proteins that are no longer needed and either recycle or destroy their amino acids. Proteins that must be degraded include irreversibly damaged, mutated or denatured proteins as well as obsolete regulatory proteins (Finley and Chau, 1991; Ciechanover, 1998). Extracellular proteins are usually degraded in lysosomes, while intracellular proteins are degraded via the ubiquitin-proteasome pathway in the cytosol (Hershko and Ciechanover, 1992; Glickman and Ciechanover, 2002). During this pathway ubiquitin molecules are attached to damaged proteins in a process called ubiquitination (Jentsch, 1992; Hochstrasser, 1996).

Ubiquitination

A variety of enzymes are needed to catalyse ubiquitination. The free form of ubiquitin must be activated by an E1 enzyme (ubiquitin-activation enzyme) via an ATP-dependent reaction. Once

activated, ubiquitin is transferred to an E2 enzyme (ubiquitin-conjugating enzyme) which catalyzes the covalent attachment of ubiquitin to the target, or substrate, protein. A protein is recognised as a substrate if it is already attached, either directly or indirectly, to a posttranslationally activated E3 enzyme (ubiquitin-protein ligase). Transfer of ubiquitin from the E2 enzyme to the substrate protein is promoted by the E3 enzyme and is either direct in the case of RING (Really Interesting New Gene) domain E3 enzymes, or via an additional step as a E3-ubiquitin intermediate in the case of HECT (Homologous to E6-AP C Terminus) domain E3 enzymes (Hochstrasser, 1996; Ciechanover *et al.*, 2000; Pickart, 2001; Glickman and Ciechanover, 2002). The isopeptide bond between ubiquitin and the target protein occurs between the carboxy-terminal glycine residue at the end of the ubiquitin molecule and the ε-amino group of a lysine residue on the target protein (Jentsch, 1992; Varshavsky, 1997).

Once one ubiquitin molecule is attached to a substrate protein additional free ubiquitins are joined to the original, via one of seven lysine residues, forming a polyubiquitin chain (Varshavsky, 1997). Once a chain of at least 4 ubiquitin monomers exists this polyubiquitin molecule is recognised by the 26S proteasome, a large multisubunit protease complex that carries out proteolysis in the cell (Coux *et al.*, 1996; Dahlmann, 2005). The polyubiquitinated substrate protein is degraded into small peptides by the 26S proteasome. The ubiquitin molecules are not destroyed but, via deubiquitinating enzymes such as ubiquitin C-terminal hydrolases (UCHs) (Johnston et al., 1997), are recycled back into the proteome as free ubiquitins (Amerik and Hochstrasser, 2004). A hierarchical organization of the three enzymes involved in ubiquitination exists in the cell. In humans there are two forms of the E1 enzyme; 37 E2 enzyme forms and over 600 E3 forms (Pickart, 2001; Komander, 2009). Each E3 recognizes a different set of protein substrates and cooperates with one or more E2s.

Ubiquitin is not just involved in proteolysis, but has an important part in many cellular processes where protein activity needs to be modified or proteins relocated. Monoubiquitination, the addition of a single ubiquitin unit to a protein, is an important cellular regulatory signal. Proteins bind to ubiquitin via ubiquitin binding domains such as the ubiquitin-associated domain, the ubiquitin-interacting motif or the CUE motif (Shih et al., 2003; Hicke et al., 2005). Ubiquitination is involved with the regulation of cell cycle and division, differentiation and development, organelle biogenesis, the cellular stress response, neuronal network morphogenesis, cell surface receptor modulation, secretory pathways, transcriptional regulation and silencing, immune and inflammatory response regulation, DNA repair and apoptosis (Finley and Chau, 1991; Jentsch, 1992; Hershko and Ciechanover, 1998; Glickman and Ciechanover, 2002; Broemer and Meier, 2009). Ubiquitin has been found to target cell cycle regulators, tumour suppressors and growth

modulators, transcriptional activators and inhibitors, cell surface receptors and endoplasmic reticulum proteins (Ciechanover et al., 2000). The diverse functioning of ubiquitin is made possible by the large number of possible combinations that can occur between the different E2 and E3 enzymes and the specific pattern of lysine residues polyubiquitin chains are linked at (Pickart, 2001; Glickman and Ciechanover, 2002; Komander, 2009).

Ubiquitin expression

In higher eukaryotes there are two classes of ubiquitin genes, and ubiquitin is not expressed directly as a free ubiquitin monomer by either of these classes. Polyubiquitin genes (which shall be referred to as *ubc*, following *M. musculus* (MGI98889) terminology) are comprised of identical 228 bp repeats which code for a precursor protein comprised of a number of ubiquitin monomers linked in a head-to-tail configuration. The number of ubiquitin monomers coded for by *ubc* varies depending on the species, but can vary from two to more than 50 repeats (Noventa-Jordão et al., 2000). There are estimated to be approximately 10 (±2) ubiquitin repeats in the *S. purpuratus* polyubiquitin precursor (Nemer et al., 1991), and in the painted sea urchin (*Lytechinus pictus*) *ubc* codes for 7 to 10 repeat sequences (Gong et al., 1991).

Ubiquitin fusion genes code for a single ubiquitin monomer fused to one of two carboxyl extension proteins (CEPs): the 40S ribosomal protein S27a or the 60S ribosomal protein L40 (coded by the UBA52 gene in humans) (Özkaynak et al., 1984; Finley et al., 1989; Catic and Ploegh, 2005). Post-translation both inactive forms of protein (polyubiquitin and ubiquitin fusion proteins) are processed by deubiquitinating enzymes to generate free mature ubiquitin molecules (Perelygin et al., 2002; Amerik and Hochstrasser, 2004). Under normal conditions, most ubiquitin is generated from the ubiquitin fusion genes, but *ubc* is the main supplier of ubiquitin during stress (Finley et al., 1989; Catic et al., 2007).

Ubiquitin as a Biomarker

Polyubiquitin is one of the group of proteins whose expression is induced as part of the cellular stress response (Parag et al., 1987; Lewis et al., 1999). Stress generates denatured and damaged proteins in the cell, some of which require degrading via the ubiquitin-proteasome pathway instead of salvaging by heat shock proteins. The ubiquitin system is responsible for much of the turnover of stress-damaged proteins in eukaryotes (Parsell and Lindquist, 1994). Greater numbers of *ubc* transcripts are needed to provide larger numbers of free ubiquitin monomers as the number of permanently damaged proteins increases in the cell. Polyubiquitin gene expression can therefore be used as an indirect measure of protein degradation, and hence of cellular stress (Dahlhoff, 2004).

The *ubc* gene has been found to be induced by several diverse stressors, including: heat (Bond and Schlesinger, 1985; Fornace et al., 1989; Niedzwiecki and Fleming, 1993; Noventa-Jordão et al., 2000), cold (Müller-Taubenberger et al., 1988), cadmium (Müller-Taubenberger et al., 1988; Jungmann et al., 1993), arsenite (Bond et al., 1988), the alkylating agents (DNA damaging) N-Methyl-N′-nitro-N-nitrosoguanidine, methyl methane sulphonate and Bis (2-chloroethyl) methylamine (Treger et al., 1988; Fornace et al., 1989), diammine dichloride (Fornace et al., 1989), starvation (Finley et al., 1987) and isoleucine deficiency (Fornace et al., 1989). The complexity of the *ubc* gene, however, makes the use of ubiquitin as an accurate biomarker for environmental contamination difficult. Due to the repeated ubiquitin monomers in the *ubc* gene absolute quantification of mRNA transcripts by qPCR is complicated (Koenders *et al.*, 2002), and the validity of ubiquitin as a biomarker of marine environmental contamination is yet to be proven.

As for stress-70 investigations, only a small body of work regarding echinoderm ubiquitin expression exists. Nemer et al. (1991) found that heat shock and zinc ions induced an increase in the level of *ubc* RNA in *S. purpuratus* embryos. With regard to ubiquitin activity, Patruno et al. (2001b) found significant changes in patterns of ubiquitin conjugation that corresponded with the early regenerative stages, and the later growth and regeneration, of new tissues in *Asterias rubens* and in the crinoids *Antedon mediterranea* and *A. bifida*. Changes in ubiquitin conjugation following heat stress were also found in these three species and also in the ophiuroid, *Amphiura filiformis* (Patruno et al., 2001b). This pattern of increased ubiquitin conjugate levels during tissue growth is similar to that seen in developing larvae of sea urchins during which embryogenesis is accompanied by significant protein degradation (Pickart *et al.*, 1991).

2.2. Measurement of gene expression

There are a number of techniques with which to investigate gene expression, either via the analysis of specific genes or of the cellular transcriptome (the collection of all RNA transcripts in a cell). These include northern blotting, differential display, serial analysis of gene expression (SAGE), qPCR, suppressive subtractive hybridisation (SSH), DNA microarrays and nucleic acid sequence-based amplification (NASBA) (Table 2.2). The challenge for small research projects intending to compare large numbers of samples from non-model organisms, as is the case in this study, is to use a cost-effective, sensitive, reliably accurate and quantitative technique that is not dependent on the prior knowledge of large numbers of species-specific gene sequences.

DNA microarray analysis is a powerful technique, allowing the expression of large numbers of genes to be analysed simultaneously (Baldwin *et al.*, 1999; Streit *et al.*, 2008). It has primarily been used to detect differential gene expression in model organisms such as humans or yeast whose entire genomes have been sequenced. Although its use is increasing in environmental (Zhou

and Thompson, 2002) and ecotoxicological (Snape *et al.*, 2004) research, the requirement for prior knowledge of, at a minimum, hundreds of gene sequences (Clark *et al.*, 2002) has traditionally prevented its use by small projects working with non-model organisms. Recently, studies have started to use DNA microarrays generated from one species to examine gene expression in a second species via heterologous hybridization. This avoids the time and monetary expense associated microarray design, and makes possible the use of microarray technology with non-model organisms if a suitable comparative library exists (Buckley, 2007; Castilho et al., 2009). It has also been shown to be possible to construct microarrays with normalised cDNA libraries from non-model organisms, permitting the determination of gene identities by comparing different expression profiles (Li et al., 2009). These developments demonstrate that it is possible to use DNA microarrays with non-model organisms. However, as their use is most suited to the analysis of the expression of hundreds of genes, and for a detailed quantitative analysis results must be subsequently validated by qPCR, their use by small research projects will continue to be limited.

Techniques that can identify changes in gene expression without prior knowledge of large numbers of sequences such as northern blotting, differential display, SSH, SAGE and NASBA all have their own advantages and disadvantages. Northern blotting is an inexpensive and straightforward technique (Streit *et al.*, 2008). Its main drawbacks are that it is not sensitive enough to detect low transcript numbers (King and Sinha, 2001) and only a limited number of samples can be quantified simultaneously (Baldwin *et al.*, 1999; Streit *et al.*, 2008). These drawbacks mean that northern blotting is not ideal for the accurate analysis of differential gene expression in numerous samples.

Both SSH and SAGE permit the entire transcriptome of a sample to be analysed for differentially expressed genes (Stollberg *et al.*, 2000; Snell *et al.*, 2003; van Ruissen *et al.*, 2005). However, both are technically difficult (Wan *et al.*, 1996; Yamamoto *et al.*, 2001), time consuming and expensive due to the large amounts of sequencing required (van Ruissen *et al.*, 2005; Distler *et al.*, 2007), and are not suitable for high throughput of numerous samples (Wan *et al.*, 1996; van Ruissen *et al.*, 2005). Differential display, although not as technically difficult as SSH and SAGE, still involves a large amount of sequencing (Baldwin *et al.*, 1999), and it lacks in quantitative strength compared with qPCR (Jurecic and Belmont, 2000; Stollberg *et al.*, 2000). NASBA avoids the reliability issues associated with the reverse transcription step when using PCR based methods for transcript quantification, but is not widely used and hence a wide body of literature relating to its methodology and analysis does not yet exist.

The advent of next generation sequencing technologies, for example massively parallel signature

sequencing (Brenner et al., 2000) and 454 pyrosequencing (Ronaghi et al., 1998), appear to be poised to replace the traditional Sanger method of sequencing (Metzker, 2005; Wall et al., 2009). These new methods make it possible to combine the method of generating large numbers of gene fragments from a transcriptome, in a manner similar to SAGE, with cheaper sequencing costs when performed on a large scale - so removing one of the main disadvantages associated with SSH, SAGE and differential display. The complexities of the data collection and analysis, and continued prohibitive sequencing costs if performed on a small-scale, limit the application of these next generation methods to small projects.

The method selected to quantify gene expression in this study was quantitative PCR, a term which refers to the ability to determine the number of starting copies of mRNA in a sample via a PCR based process. Real time PCR refers to the continuous collection of a fluorescent signal from one or more reactions over a range of cycles (Valasek and Repa, 2005; Shipley, 2006). Together, they form quantitative real time PCR, which shall be referred to as qPCR (Bustin et al., 2009). The qPCR method has a sensitive and wide ($>10^7$-fold) detection range, even permitting the detection of a single transcript copy. Post-amplification manipulation and large amounts of sequencing are not required (Valasek and Repa, 2005; Wong and Medrano, 2005). The important disadvantages of qPCR are that it depends on prior knowledge of the sequences for the GOI, requires extensive optimisation to generate reliable results and the reverse transcription reaction that produces the cDNA to be amplified contributes greatly to qPCR variability and lack of reproducibility (Bustin et al., 2005). Other disadvantages associated with the qPCR method also apply to any technique based on RNA samples and PCR. For example there are natural variations in mRNA expression between individual organisms and cells, extracted mRNA can be unstable and of variable quality, the sensitivity of cDNA synthesis varies with the primers used, and the analysis of qPCR results is subjective (Bustin and Nolan, 2004c; Bustin et al., 2005; Farrell, 2005; Fleige and Pfaffl, 2006).

To generate accurate and comparable qPCR results with these disadvantages, significant amounts of work are required to optimise the methodology of a qPCR reaction to a specific gene (Chuaqui et al., 2002; Valasek and Repa, 2005). It is important to use consistent priming strategies, reaction conditions and analytical processes; all of which are determined during the optimisation process (Nolan et al., 2006). With correct standardisation, qPCR is highly reproducible, reliable and high sample throughput is possible. therefore making possible the accurate detection of the differential expression of a limited number of genes between numerous samples (Bustin, 2004; Wong and Medrano, 2005). It is for these reasons that this technique was selected to investigate differential gene expression during this current study.

Table 2.2 A summary of the main alternative techniques available to quantify gene expression from the transcriptome. Superscript numbers refer to references listed on page 34.

Technique	Basic Methodology	Advantages	Disadvantages
Northern Blotting (NB)[1]	mRNA extracted from samples is separated by agarose gel electrophoresis, transferred onto a nylon membrane, fixed and hybridized to radioactively (^{32}P) labelled probes (RNA, DNA or oligonucleotides) complementary to the target gene sequence. Labelled RNA is then detected by autoradiography. Band intensity indicates mRNA abundance in the original sample [2]	• Inexpensive [2] • Straight forward method allowing the direct comparison of mRNA abundance between samples on a single membrane [2] • Only method that permits the discrimination of alternately sized and spliced transcripts, and RNA quality [2,6] • Relative high specificity [2] • Hybridisation probes with only partial homology can be used [2] • Blots can be stored for years on the membranes [2] • Prior knowledge of EST databases and cDNA libraries not required	• Chemicals used for RNA gel electrophoresis are harmful to humans [2] • Use of radioactive labelling carries risk, although non-radioactive labelling methods are now available [2] • Requires relatively large amounts of starting RNA • Prior knowledge of target gene sequences is required. • Has low analytical sensitivity, i.e. cannot detect low mRNA transcript numbers [3,7] • Only a limited number of genes and samples can be quantified simultaneously [2,4,7] • mRNA sample degradation during electrophoresis is a problem and has a large effect on data quality [2]
Differential Display PCR [5]	RNA is extracted from samples, and reverse transcribed to produce cDNA. PCR is performed with both anchored oligo(dT) and random degenerate primers, or with just random primers [4]. The resulting DNA fragments from each sample are run side by side on a denaturing polyacrylamide gel (has a greater resolving power than agarose gels). Bands present in one lane but not the other are excised, cloned and sequenced to identify the differentially expressed genes. Thus, the relative expression of mRNAs from different samples can be compared [10]	• Technically simple [4] • Prior knowledge of large EST databases and cDNA libraries not required [4,8] • Inexpensive [4] • Sensitive: rare transcripts can be detected [4,9,10] • Relatively small amounts of mRNA transcripts can be detected [4] • Can screen entire transcriptome for differentially expressed genes.	• Lacking in quantitative strength compared with qPCR or NB [8,9] • Prone to false positives via non-specific priming [4,10,11,12] • Excised bands need to be cloned and sequenced to identify differentially expressed genes (i.e. expensive and time consuming)[4] • Sequence length generated from 3'-end may be insufficient to identify a gene [4,8]

Suppressive subtractive hybridisation (SSH) PCR [13]	mRNA extracted from control and experimental samples is reverse transcribed to cDNA. Both cDNA samples are then digested with a restriction enzyme to give shorter blunt ended fragments. The experimental cDNA is divided into two portions, and each is ligated with a different adaptor to form two different populations which are then mixed with each other again. The control cDNA is then hybridised with the mixed experimental cDNA. cDNA of similar abundance in the control and experimental samples are eliminated (subtracted) from amplification during subsequent PCR. During PCR only differentially expressed cDNA with two different adaptors (targeted by SSH primers) are amplified [13,14]. These PCR products can then be gel electrophoresed, cloned, sequenced and identified.	• Can screen the entire transcriptome for differentially expressed genes [14] • Efficient at obtaining low abundance transcripts [12] • The expression levels of genes can be assessed without prior knowledge of the transcripts	• Only two different samples (control and experimental) can be compared at the same time [11,12,15] • Gene redundancy: If a few genes are highly differentially expressed, they may mask transcripts that are differentially expressed at a lower level [10,15] • Technically difficult [11] • Expensive and time intensive to generate a complete expression profile [15]
Serial Analysis of Gene Expression (SAGE) [16]	Extracted mRNA is reverse transcribed into cDNA with biotinylated oligo(dT) primers. Type II restriction enzyme digestion gives short cDNA fragments. The biotinylated 3'-most fragments are isolated with paramagnetic streptaviden beads. The fragments are divided into two portions and ligated to different linkers and tags. The two portions are then mixed, fragments with different linkers ligate, and are then PCR amplified. The fragments are then ligated to form concatemers (a string of multiple copies of the same DNA sequence), cloned and sequenced. The sequenced gene fragments can then be identified with comparison to known EST libraries. The proportion of the tag within the total number of fragments gives a quantitative estimate of the relative transcript abundance in the original mRNA sample[9]	• The expression profile of the complete transcriptome can be mapped [9,17] • The expression levels of thousands of genes can be assessed without prior knowledge of the differentially expressed transcripts [16]	• Expensive and time consuming (large amounts of sequencing required)[17] • Technically difficult [18] • Prone to sequencing errors [17,18] • Identity of gene corresponding to tagged fragment can only be inferred if it is already recorded in a public sequence database [8] • Not suitable for high throughput analyses of numerous samples [17] • Rare transcripts difficult to detect without high depth sequencing [8,19] • Short tag sequences may not be unique to one gene [9,18] • Cannot be directed at a small subset of the transcriptome [19]

Quantitative Real Time PCR (qPCR) [20,21]	Reverse transcribed cDNA from isolated mRNA is used with gene-specific primers in PCR to amplify transcripts corresponding to a specific gene. A linear relationship is established between the amount of starting target DNA and PCR product generated by amplification. Dyes or probes are used to generate a fluorescent signal proportional to the quantity of DNA. The "real-time" description refers to the continuous collection of fluorescent signal from one or more PCRs over a range of cycles. The fluorescent signals from each reaction are then converted into a numerical value relating to the starting number of mRNA transcripts [22, 23]	• Highly sensitive assay with a large dynamic range, and can detect extremely low transcript numbers[2,6,22] • High throughput[2] • Straight forward[2] • Provides accurate and reproducible data on mRNA copy number[7,22] • Less RNA starting template is required in comparison to the other techniques[30] • Post amplification manipulation not required[22,30,]	• Only a limited number of specified genes can be quantified simultaneously [28] • Requires significant up front optimisation to achieve the advantages listed to the left [22,24] • Prior knowledge of target gene sequences required. • The reverse transcription step can be the course of variability and non-reproducibility in a qPCR assay [41]
DNA Microarrays [25]	Effectively a reverse northern blot technique [26], a microarray is a chip covered in tiny immobilised spots (probes) which each hold oligonucleotides or cDNA complementary to a specific gene. Each probe corresponds to a different gene, and thousands of probes can be held by one chip. The mRNA transcripts obtained from an experimental sample are labelled with fluorescence tags, and washed across the chip. When the mRNAs hybridise to their complementary probes their fluorescence can be detected[25]. The luminescent intensity of each probe indicates the relative quantity of the target present. The raw data is analysed by bioinformatics software and databases [27]	• Transcript levels of hundreds or thousands of individual genes can be measured simultaneously [2, 4] • With the use of different fluorescent tags, more than one sample can be run simultaneously [12]	• Requires prior knowledge of many gene sequences[8] • Expensive [12, 27] • Only the genes represented on the microarrays are analysed [17] • Variable quality of quantitative data [24] • Huge quantity of data produced, data analysis and interpretation is difficult [7,26] • Limited availability of DNA microarrays for non-model organisms [27] • Small mRNA samples are insufficient [26] • Microarray data require verification by other methods such as NB and qPCR [7] • Not suitable for high throughput analyses of numerous samples [19]

Nucleic acid sequence-based amplification (NASBA)[31]	NASBA is an alternative method to those based on traditional forms of PCR thermal cycling. It makes possible the direct amplification of low abundance RNA transcripts in an isothermal cycling process. It is based on the concurrent activity at one temperature (41°C) of AMV reverse transcriptase, RNase H and T7 RNA polymerase with two primers to produce amplification, and results in the exponential amplification of RNA and DNA products within 90 min[31,32]. When combined with detection methods such as SYBR green-II single-stranded binding dye or molecular beacon probes (single-stranded oligonucleotides with a stem–loop structure that only fluoresce when hybridised with their target), NASBA is a real-time analysis method faster than qPCR[32,33].	• Faster detection times than qPCR[32] • Contamination risks are reduced by the one tube format[32,33] • The omission of the prior reverse transcription step removes its associated uncertainty • High specificity and sensitivity, detection of extremely low starting RNA numbers is possible[31,32] • Genomic DNA cannot contaminate assay as there is no denaturation[31] • Specialist thermocycler equipment not required[31,33] • High throughput analysis possible[32] • Cloning is not required.	• RNA is unstable, poor RNA integrity is a concern, particularly over extended periods of storage time[33] • Amplified RNA target sequence length needs to be 120–250 bp, otherwise amplification efficiently is compromised[33] • Non-specific amplification is more likely than with thermocycling methods because amplification temperature cannot > 41 °C without risk of enzymatic denaturation[34] • It is impossible to control reaction extent by adjusting the number of cycles because it is isothermal[34]
Next generation sequencing technologies: **Massively parallel signature sequencing (MPSS) analysis**[35] and **Massively parallel (454) pyrosequencing**[40]	cDNA is transcripted from Poly(A) mRNA transcripts, then digested and cloned into plasmid vectors. Each clone contains a different oligonucleotide tag[35]. When linearised these are hybridised to complementary tags covalently linked to microbeads, which are deposited in wells on a high-density plate. Single dNTP washes are passed across the beads in limiting amounts, and DNA polymerase sequences the cDNA from a primer complementary to the tag. The polymerase pauses when it reaches a base noncomplementary to the dNTP wash, starting synthesis again when the next wash is added. When a nucleotide is added to a sequence, inorganic pyrophosphate is released, which is converted into visible light by a series of enzymatic reactions[40]. The light generated, corresponding to the synthesis order of complementary dNTPs, is recorded digitally, so revealing the cDNA sequence. The frequency with which each transcript sequence is detected provides a measure of its abundance.	• No prior knowledge of any of the genome is required[36,42] • In-depth quantification of the entire transcriptome is possible[36,38] • High specificity and analytical sensitivity, detection of extremely low starting RNA numbers is possible[36] • Like SAGE, a very large number of individual ESTs are provided, therefore a robust statistical comparison of gene expression is possible[38] • Cost per base is substantially less than traditional, Sanger, large scale EST sequencing[38]	• Data storage and analysis requirements are extremely large[42] • It is possible to work with non model organisms, but lack of annotation information will remain a problem[36,37,39] • Cost per run is greater than microarray analysis, this will therefore not be the tool of choice for routine transcript analysis[38,42] • Regions of repeated nucleotide bases are difficult to sequence. • Access to these technologies is only through commercial companies[44]

References listed in the preceding Table 2.2: 1. (Alwine *et al.*, 1977), 2. (Streit *et al.*, 2008), 3. (Liu *et al.*, 2004), 4. (Baldwin *et al.*, 1999), 5. (Liang and Pardee, 1992), 6. (Bustin, 2000), 7. (King and Sinha, 2001), 8. (Jurecic and Belmont, 2000), 9. (Stollberg *et al.*, 2000), 10. (Goetz, 2003), 11. (Wan *et al.*, 1996), 12. (Huang *et al.*, 2007), 13. (Diatchenko *et al.*, 1996), 14. (Snell *et al.*, 2003), 15. (Distler *et al.*, 2007), 16 (Velculescu *et al.*, 1995), 17 (van Ruissen *et al.*, 2005), 18. (Yamamoto *et al.*, 2001), 19. (Wang *et al.*, 1999), 20. (Heid *et al.*, 1996), 21. (Higuchi *et al.*, 1993), 22.(Valasek and Repa, 2005), 23. (Shipley, 2006), 24. (Chuaqui *et al.*, 2002), 25. (Schena *et al.*, 1995), 26. (Walker and Hughes, 2008), 27. (Lettieri, 2006), 28. (Etienne et al., 2004) 29. (Clark *et al.*, 2002) 30. (Wong and Medrano, 2005), 31. (Compton, 1991), 32. (Leone et al., 1998), 33. (Loens et al., 2005), 34. (Cools et al., 2006), 35. (Brenner et al., 2000), 36. (Reinartz et al., 2002), 37. (Bellin et al., 2009), 38. (Weber et al., 2007), 39. (Vera et al., 2008), 40. (Ronaghi et al., 1998), 41. (Bustin et al., 2005), 42. (Wall et al., 2009), 43. (Metzker, 2005), 44. (Gracey, 2007).

2.3. Optimisation of the qPCR assay

In order to ensure that a qPCR assay produces reliable, accurate and reproducible results each step of the assay must be optimised before experimental samples can be analysed. It is this aspect of the qPCR technique that is time consuming (Table 2.2). Many components of the assay require optimisation, for example: RNA isolation, reverse transcription, primer design, primer concentrations, PCR cycling conditions and results normalisation (Nolan et al., 2006; Bustin, 2008). Due to the quantity of work required to optimise six qPCR assays (three genes of interest (GOI) in two species of echinoid) for genes not previously sequenced, the molecular methodology for this study is separated into two parts. This chapter reviews the procedures followed to obtain cDNA sequences for each GOI (Figure 2.2). Chapter 3 reviews the procedures followed to optimise the qPCR assay for each gene.

Detailed protocols for each of the experimental processes summarised are not included in these chapters, but are listed in the Appendices where indicated. Specific manufacturer details for the reagents, consumables and equipment used during this study are listed at Appendix 1.2, consequently complete manufacturers details are not listed after every reagent, chemical or consumable in the following pages.

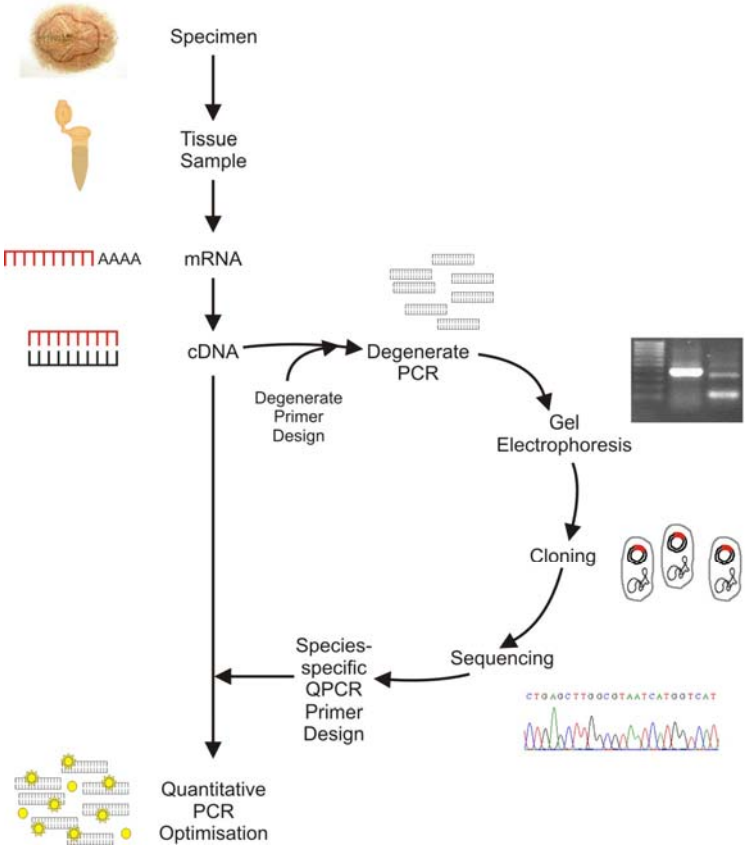

Figure 2.2 Flow chart illustrating the different processes followed in order to obtain species-specific sequences for each of the genes of interest for *P. miliaris* and *B. lyrifera*, in order to allow qPCR primers to be designed for use in the subsequent qPCR assay optimisation.

2.4. The isolation and sequencing of species-specific mRNA transcripts

The high specificity and accuracy of the qPCR technique is derived from the use of species-specific primers complementary to the gene being investigated. This specificity means that only cDNA corresponding to a target GOI should be amplified during a qPCR assay. The design of qPCR primers must be specific to the exact nucleotide sequence of the target gene in the target species; if this sequence is not known, it must first be obtained. In this study, none of the species-specific sequences for the three GOI were previously known for either *P. miliaris* or *B. lyrifera*. Messenger RNA transcripts for the genes of interest therefore had to be first obtained before the primers for qPCR could be designed and the assays optimised.

The isolation of mRNA transcripts coding for the *hsp70* gene required an initial step not necessary for the *cs* and *ubi* transcripts. This initial step is first summarised below, before the processes that applied to the transcripts from all three GOI for both species are discussed.

2.4.1. Induction of heat shock protein 70

As discussed in the general introduction (section 2.1.1.2), *hsp70* expression is upregulated in

response to stress, and when not required its background expression levels are low. In order to isolate *hsp70* transcripts successfully it was therefore necessary to first induce *hsp70* expression. Initial attempts to do so were first carried out with *P. miliaris* based on two published heat shock induction protocols used with the echinoids *Paracentrotus lividus* (Matranga *et al.*, 2000) and *Strongylocentrotus purpuratus* (Osovitz and Hofmann, 2005).

Psammechinus miliaris

Psammechinus miliaris were collected by hand from Corbyn's Head, Torquay (50° 27' 17 N; 3° 32' 38 W) in August 2006. They were held in recirculating aquaria and fed *ad libitum* on *Ulva lactuca*, *Laminaria* sp. and salmon pellets (EWOS Ltd, Westfield, UK) until required.

Following the Matranga et al. (2000) protocol, individual *P. miliaris* were placed in heated seawater (29-33ºC) for 90 minutes, and then returned to ambient seawater (20ºC) for a further 90 minutes. Coelomic fluid was then bled into an ice cold watch glass from an incision in the peristomal membrane, 0.75 ml of coelomic fluid was transferred into a 1.5 ml microcentrifuge tube and mixed with an equal volume of ice cold ISO-EDTA (20 mM Tris, 0.5 M NaCl, 30 mM EDTA acid, pH 7.5) (Matranga et al., 2000). The coelomic fluid was then centrifuged at 3000 g for 3 minutes, the supernatant removed and 1 ml of TRI Reagent™ added to the remaining pellet of coelomocytes, which was then frozen at -80 ºC until required. Subsequent degenerate PCR with cDNA reverse transcribed from the total mRNA extracted from these coelomocyte samples did not isolate *hsp70* transcripts.

Following the Osovitz and Hofman (2005) protocol, multiple tube feet were removed from *P. miliaris* specimens, placed into 1.5 ml microcentrifuge tubes containing 0.5 ml of seawater, incubated at 27ºC for 30 min, transferred to a fresh microcentrifuge tube containing 1 ml of TRI Reagent and frozen at -80ºC until required. Subsequent degenerate PCR on cDNA generated from these samples also did not isolate *hsp70* transcripts.

The final method used to induce heat shock expression was successful, and was based loosely on *hsp70* induction protocols outlined for the European flat oyster *Ostrea edulis* (Piano et al., 2005) and the Pacific abalone *Haliotis discus hannai* (Cheng et al., 2007). Seven echinoids were transferred from ambient seawater (15.3 ºC) to seawater at 24 ºC. An echinoid was removed from the heated seawater at 2, 3, 4, 6, 8, 10 and 12 hours, upon removal the echinoid was transferred to ambient seawater for 30 minutes. The echinoid was then dissected and the compass elevator, compass depressor, protractor and retractor muscles of the Aristotle's Lantern (Figure 2.3) were removed and placed directly into 1 ml of TRI Reagent, then frozen at -80 ºC until further use. An eighth echinoid was exposed to heated seawater for 12 hours, and then placed in ambient seawater

for a further 12 hours before dissection. Subsequent degenerate PCR on cDNA generated from these samples successfully produced evidence of *hsp70* transcripts (section 2.4.6).

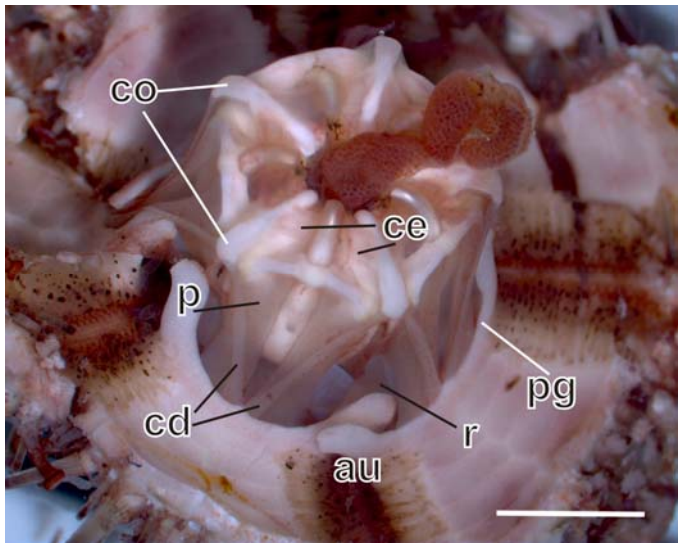

Figure 2.3. Dorsal view of the Aristotle's lantern of *P. miliaris*. au = auricle-like flange (broken) of the perignathic girdle (pg), ce = compass elevator muscles, cd = compass depressor muscles, co = compass ossicles, p = protractor muscle, r = retractor muscle (attached to au). Bar = 7.5 mm. Photograph taken by S. Hughes, labels follow Dolmatov et al. (2007).

Brissopsis lyrifera

Brissopsis lyrifera were collected by trawl in May 2007 from the Gullmar Fjord, Sweden (33-38 m depth; 58º 14. 86 N, 11º 25. 68 E). Four echinoids were transferred from ambient seawater (10.2ºC) to seawater at 16.4-17.2ºC. One echinoid was removed from the heated seawater every two hours and placed in ambient seawater for 30 minutes. All of the tube feet were then removed (Figure 2.4), and a tissue sample from the oesophagus and the intestine dissected out. All tissue samples were placed directly into individual 2.0 ml eppendorf tubes containing 1 ml of RNAlater® (RNA preservative solution) and then frozen at -80ºC until further use. Subsequent degenerate PCR on cDNA generated from these samples did not produce evidence of *hsp70* transcripts. Tissue samples from a repeat heat shock procedure, carried out at higher temperatures of 25-27ºC, resulted in successful degenerate PCR and evidence of *hsp70* transcripts (2.4.6).

2.4.2. Total RNA isolation

Total RNA from the tissue samples was isolated using TRI Reagent, following the manufacturers' instructions (Sigma 1999; Technical Bulletin MB-205). Total RNA is the entire population of RNA found in a cell, comprised of different types of RNA including mRNA. The TRI Reagent isolation technique used is based on the lysis of cells with a monophasic solution of guanidine

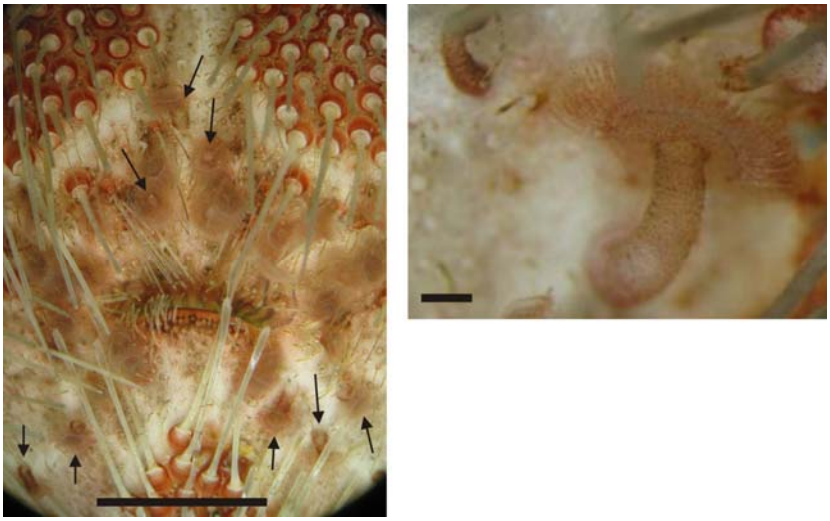

Figure 2.4 Left: Oral view of *B. lyrifera* mouth (centre) and surrounding tube feet (some arrowed) and interambulacral spines, bar = 1 cm. Right: tube foot, bar = 750 µm. Photographs taken with a Leica DC 350F digital camera / microscope system by S. Hughes.

isothiocyanate and phenol, and was originally described by Chomczynski (1993; cited by Sambrook and Russell, 2001). The detailed protocol followed for this method is included in Appendix 1.3.

Approximately 100 mg of tissue was homogenised in 1 ml of TRI Reagent. Once dissociation of the nucleoprotein complexes was complete, chloroform was added to cause phase separation and the samples were centrifuged. The total RNA from the homogenate was subsequently located in the resulting upper aqueous phase, which was transferred to a fresh microcentrifuge tube. Total RNA was recovered from the aqueous phase by 2-propanol precipitation and ethanol wash to produce a pellet of total RNA. An appropriate volume of diethyl pyrocarbonate (DEPC)-treated Milli-Q® water was added to each pellet, which was resuspended by repeated pipetting. A ND-1000 Spectrophotometer (Nanodrop®) was used to determine the quantity and quality of total RNA present in the samples, which were stored at -80ºC until further use. Appendix 1.4 includes further details of the modified Beer-Lambert equation used by the Nanodrop to determine the concentration of nucleic acids in a sample.

2.4.3. Reverse transcription

The manufacturer's instructions (Sigma 2003; Technical Bulletin MB-520) were followed to synthesize cDNA using 1 µl (200 units) of M-MLV RT (Moloney Murine Leukemia Virus Reverse Transcriptase) with 1-5 µg total RNA (exact quantity and hence volume dependant on the concentration of the RNA sample). Oligo deoxythymidine $(dT)_{23}$ primers were used to prime the reverse transcription. Oligo$(dT)_{23}$ primers are oligonucleotides comprised solely of thymine

nucleotides. The use of these primers attempts to ensure that only the mRNA in the total RNA population is reverse transcribed, because the primers anneal by T:A base pairing to the poly(A) tail present at the 3'end of mRNA transcripts. A detailed protocol of the reverse transcription step is included at Appendix 1.7. Once synthesized, the first strand cDNA samples were stored at -20ºC until further use.

2.4.4. Degenerate PCR

QIAGEN *Taq* DNA Polymerase was used to amplify the first strand cDNA via degenerate PCR, a complete protocol is included at Appendix 1.8. The PCR reactions were primed with degenerate primers, manually designed to anneal to cDNA coding for the three genes GOI (section 2.4.5). Only one pair of degenerate primers was used in each separate reaction, so that primers and amplicons relating to different genes did not interfere with each other. A positive control was included during each PCR to provide proof that the reagents were functioning correctly in the event that there was no amplification (and hence to determine whether or not the reason for this was due to primer failure). The positive control consisted of a PCR reaction identical the other reactions apart from the degenerate primers, which were instead complementary to the gene for the protein actin, a highly conserved cytoskeleton protein found in all eukaryotic cells. Degenerate PCR was performed in a thermal cycler (one of two PTC-0200 DNA Engine thermal cyclers or a Primus 96 legal PCR System Thermocycler) according to the cycling parameters listed in Table 2.3.

Table 2.3 Degenerate PCR cycle parameters for the target GOI.

Step	ºC	Time	Number of Cycles
Initial Denaturing	95	5 min	
Denaturing	95	30 sec	x35-40[b]
Annealing	49/54[a]	45 sec	
Extension	72	50 sec	
Final Extension	72	10 min	

[a] *ubi* and *hsp70* = 49ºC annealing temperature, *cs* and actin = 54ºC.

[b] *ubi*, citrate *cs*, actin and *P. miliaris hsp70* cycled 35 times. *B. lyrifera hsp70* cycled 40 times for both initial amplification and subsequent reamplification.

Due to low numbers of *hsp70* transcripts present in the *B. lyrifera* samples, two amplifications were required to produce sufficient *hsp70* PCR product for visualisation and extraction. 1 µl of 10 x diluted PCR product from the first amplification was used as template DNA for the second amplification; the cycling conditions were not changed.

2.4.5. Degenerate primer design

A degenerate primer is an oligonucleotide where certain base locations in its sequence have more than one type of nucleotide associated with them (degeneracy). It is the typical type of primer manually designed when RNA or DNA whose specific sequence is unknown needs to be amplified. A pair of degenerate primers ('forward' and 'reverse') were required for each GOI and the actin positive control, as two primers are needed to prime the amplification of both complementary strands of double stranded template.

The degenerate primer designs were based on previously published sequences for each GOI from a variety of vertebrate and invertebrate species (refer to Appendix 1.16 for more detail on the degenerate primer design). A multiple alignment of these sequences allows regions of the genes that are highly similar to each other in all species (conserved regions) to be identified. Degenerate primers based on the nucleotide sequences found in these conserved regions are likely to anneal to the same regions within the same gene in other species. In this way, mRNA transcripts coding for the three GOI in the two echinoid species could be amplified via PCR despite the species-specific sequences being unknown.

Because primers that are not exactly complementary to a gene may not anneal strongly to the target region, or may anneal to a region on a different gene that they are coincidently complementary to, it is important to design degenerate primers as carefully as possible. The published literature regarding degenerate primer design provided guidelines regarding the characteristics that successful primers exhibit (McPherson et al., 1991; Thomas, 1996; Avison, 2007). These guidelines were followed where possible, with later degenerate primer design adhering to more guidelines as further literature sources were researched:

- Primer length: 12-25 nucleotides
- GC content: 45-55%
- Primer melting temperature (T_m); 50-60°C (refer to Appendix 2.1 for T_m calculation)
- Avoidance of repeating nucleotides
- Avoidance of degeneracy at the 3'-end of the primer
- Avoidance of highly degenerate primers
- The inclusion of a 'GC clamp' – the presence of 2 or 3 G or C bases within the last 5 bases at the primer's 3'end.

The degenerate primers for *hsp70* and *cs* were originally designed based on reverse translated nucleotide sequences from aligned amino acid sequences (McPherson et al., 1991; Metzenberg,

2007). A pair of *hsp70* primers (Appendix 1.16) worked successfully, but none of the *cs* primers did. One more pair of *cs* primers was therefore designed, in order to reduce the primer degeneracy the design was instead based on published mRNA sequences and this primer pair was successful (Appendix 1.17). Two pairs of *ubi* primers (Appendix 1.18) and one pair of actin primers (Appendix 1.19) were also designed based on the conserved regions of aligned mRNA sequences. The sequences of the successful degenerate primer pairs (section 2.4.6) are listed below in Table 2.4. All of the degenerate primers were initially trialled with *P. miliaris* samples. Only the successful primers were subsequently used with *B. lyrifera* samples, immediately producing positive results in this second echinoid species. All primers were synthesized by MWG-Biotech (now Eurofins MWG Operon; Ebersberg, Germany). Upon delivery, the freeze-dried degenerate primers were eluted in nuclease-free water to provide stock primer solutions of 100 µM. Working 25µM aliquots were then made up by further dilutions with nuclease-free water.

Table 2.4 Successful degenerate primers. Details of the melting temperature (T_m) and expected PCR product amplicon length in nucleotide base pairs (bp) are listed.

Gene / Primer Name	Primer Sequence (5' to 3')	T_m °C	Product Size (bp)
Actin			
ACTINFWD	TTCAAYDCVCCCGNCATGTAC	59.8	357
ACTINRVS	TCRTTDGCRATRGTGATRACCTG	59.5	
Citrate Synthase			
CSFWD	TGAYCAYGARGGHGGHAAYGT	59.2	424
CSRVS	TGDGCRTCYACRTTRGGCCA	60.0	
Heat Shock Protein 70			
HSP70dF2	ATHGCNAAYGANCARGGNAA	54.9	399
HSP70dR1	GCRTCYTTNGKNGCYTG	55.2	
Ubiquitin			
UBQFWDb	CHAARATHCARGAYAARGARGG	56.8	113
UBQRVSd	VGAYTCYTTYTGRATRTTRTARTC	56.2	
UBQFWDe	HATGCARATYTTYGTBAARAC	52.0	196
UBQRVSd	VGAYTCYTTYTGRATRTTRTARTC	56.2	

Representations for sequence positions which can have alternative bases are: N = A,C,G,T; V = G,A,C; D = G,A,T; B = G,T,C; H = A,T,C; W = A,T; M = A,C; R = A,G; K = G,T; S = G,C; Y = C,T (International Union of Pure and Applied Chemistry).

All of the *ubi* degenerate primers were successful. The primer pair that resulted in the strongest discrete band of PCR products (section 2.4.6) produced an amplicon 113 bp in length. In order to elongate this sequence and have more options available for subsequent qPCR primer design, further degenerate primers were designed. Once the *P. miliaris ubi* 113 bp **fragment** had been sequenced, homologous *ubi* sequences from other species were found via a BLASTN search on the NCBI database (Zhang et al., 2000). A selection of the most homologous sequences were then aligned using the CLUSTALW program (Combet *et al.*, 2000) and an additional pair of degenerate

primers designed to target the regions outside of the original 113 bp sequence. One of the new degenerate *ubi* primers was successful, and together with one of the original primers, generated a new amplicon of 196 bp.

2.4.6. Visualisation of PCR products

Degenerate PCR samples containing amplified DNA fragments (PCR products) were separated in a 1% agarose gel containing 0.1 mg ml^{-1} ethidium bromide run at 75 V in 1x tris-acetate (TAE) buffer for 25-45 minutes. Gels were visualized with a Gel Doc™ UV transilluminator system (complete protocol included at Appendix 1.10). The results generated from the *P. miliaris* samples are illustrated at Figure 2.5, and from *B. lyrifera* at Figure 2.6. A comparison between the expected amplicon sizes (Table 2.4) and the sizes of the bands in the gel indicated that amplicons of approximately the correct size had been amplified by these primers. However, confirmation that these fragments were from the target mRNA transcripts could not be obtained until the fragments were cloned and sequenced (see below).

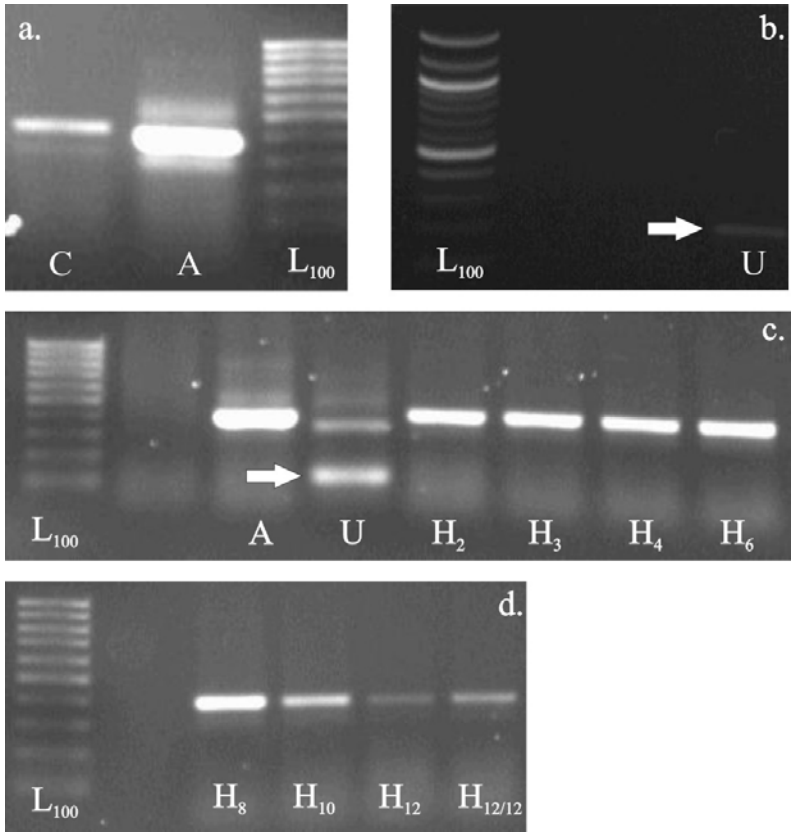

Figure 2.5 Visualized *P. miliaris* PCR products after gel electrophoresis. Figures in brackets refer to expected amplicon size. a) C = *cs* (424 bp), A = Actin (357 bp). b) U = *ubi* (196 bp; arrowed). c) and d) A = Actin (357 bp), U = *ubi* (113bp original sequence length; arrowed). H = *hsp70* (399 bp), subscript numbers indicate number of hours heat shocked ($H_{12/12}$ was heat shocked for 12 hours and recovered for 12 hours). L_{100} = 100 bp ladder.

The *P. miliaris hsp70* PCR products illustrate a progression in the *hsp70* expression over the course of the heat shock-induction. The product bands generated by the *hsp70* degenerate primers (Figure 2.5 c,d) reflect strong expression up until eight hours of heat shock (H_8), after which levels of expression apparently decline progressively (less bright bands) at 10 hours (H_{10}), 12 hours (H_{12}) and 12 hours heat shock/12 hours recovery ($H_{12/12}$). Such variation in the expression of *hsp70* with time of heat shock or time after heat shock has been found in previous studies (Piano et al., 2002; Cheng et al., 2007; Park et al., 2007), and is typical of stress inducible *hsp70*.

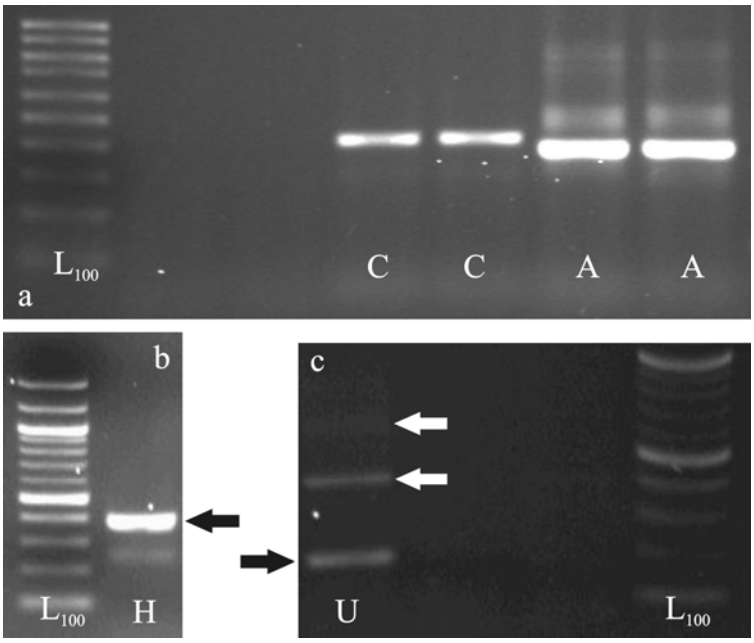

Figure 2.6 *B. lyrifera* PCR Results. Figures in brackets refer to expected amplicon size. a) C = *cs*(424 bp), A = Actin (357 bp). b) H = *hsp70* (399 bp; arrowed) and c) U = *ubi* (196bp; black arrow; 424 & 652 bp white arrows). L_{100} = 100 bp Ladder.

The PCR amplification of the *ubi* cDNA from both echinoids generated more than one discrete product as can be seen in Figure 2.5c and 2.6c. The smallest discrete product in both cases was the size predicted from hybridization of the forward and reverse primers to known locations in the coding sequence for one ubiquitin monomer (section 2.1.1.3). Further larger products are also visible (arrowed in Figure 2.6), each indicating amplicon repeats approximately equal to 228 bp (76 amino acids) apart, which would be expected if the primers annealed to regions on more than one monomer of a *ubi* transcript and fragments spanning more than one monomer were amplified.

2.4.7. Cloning

PCR product bands were excised from the gels using sterile scalpel blades, and extracted from the agarose using QIAquick® Gel Extraction Kits (Appendix 1.11). The purified fragments were then cloned into pCR®4-TOPO® plasmid vectors and propagated in OneShot® TOP10 chemically

competent *Escherichia coli* according to the manufacturer's instructions (Invitrogen Manual 25-0276, Version N). The *E. coli* were grown up overnight on ampicillin selective Luria Bertani (LB) agar plates, then ten of the resulting colonies were re-plated and the presence of a PCR product insert in each colony analysed via PCR with QIAGEN *Taq* Polymerase. The primers used (M13 Forward (-20): GTAAAACGACGGCCAG; M13 Reverse: CAGGAAACAGCTATGAC) annealed to specific priming sites in the vector flanking the PCR product insert. Subsequent gel electrophoresis and visualisation indicated whether the colonies were positive. For each GOI, three of the colonies containing the positive transformants were cultured overnight. The plasmids were then extracted using QIAprep® Miniprep kits and sent for sequencing by Geneservice Ltd. (Department of Biochemistry, University of Oxford) on a 3730xl DNA Analyzer (Applied Biosystems). A complete cloning methodology protocol is included at Appendix 1.12.

2.4.8. Alignment and analysis of sequences

The resulting three mRNA sequences for each of the GOI from *P. miliaris* and *B. lyrifera* were edited to remove clone sequences and reverse transcribed where necessary using the Geneious Basic 3.0.6 freeware program (http://www.geneious.com/; Biomatters Ltd, Auckland, NZ). The nucleotide sequences were then aligned using the CLUSTALW Multiple Alignment program (Combet *et al.*, 2000) and a consensus sequence produced. Each consensus sequence was then translated using Geneious Basic 3.0.6 (Drummond et al., 2010) to give an inferred amino acid sequence for each protein. For each amino acid sequence an internet based NCBI database search using BLASTP (Schäffer *et al.*, 2001), and an ExPASy website PROSITE search (Gasteiger et al., 2003), was carried out to investigate sequence and structure similarity to amino acid sequences for the same proteins from other species. The results from these searches, and evidence that fragments from the GOI had been isolated and sequenced, are discussed for each gene in turn below.

2.5. Degenerate PCR gene sequence results

2.5.1. Citrate synthase

The consensus mRNA sequences from the cloned PCR products produced inferred amino acids 140 aa in length. A CLUSTALW comparison of the *P. miliaris* and *B. lyrifera* amino acid sequences determined that the two sequences shared an 87.9 % identity with each other. The BLASTP database search revealed identities between both of these sequences and citrate synthase protein sequences from other invertebrate and vertebrate species. Figure 2.7 illustrates the multiple alignment of the inferred amino acid sequences for both echinoid species with five other species' CS amino acid sequences. Overall, multiple alignment identity for all seven sequences was 70.7%.

During the BLASTP and PROSITE searches both the *P. miliaris* and *B. lyrifera* amino acid

sequences were identified as containing conserved domains relating to the CS protein (Marchler-Bauer et al., 2009). Included in the sequences were residues corresponding to the binding sites between the CS enzyme and citrate, acetyl coenzyme-A (Co-A) and oxaloacetate. The active acetyl Co-A binding site is located at residues 314-320 (numbers refer to residue positions in a complete CS sequence) (Wiegand and Remington, 1986). The arginine residue Arg-324 is also involved in the active site between acetyl Co-A and CS (Remington, 1992). The histidine residues His-238, His-274, His-320 and Arg-329 and Asp(Aspartic acid)-375 residues are involved with the binding of oxaloacetate, and His-238, His-320 and Arg-329 with the subsequent oxaloacetate/ citrate binding site (Wiegand and Remington, 1986; Karpusas et al., 1990; Russell et al., 1994). Of these residues, His-274, His-320 and Asp-375 are catalytically important (the "catalytic triad") within the functioning of CS (Karpusas et al., 1990). Argine-329 is a highly conserved residue (Daidone et al., 2004), and is the last amino acid in the highly conserved domain of the CS protein: G -[FYAV]-[GA]-H-x -[IV]-x(1,2)-[RKTQ]-x(2)-[DV]-[PS]-R (prosite ID: PS00480), which in the sequence below is represented by GYGHAVLRKTDPR between residue positions 81 to 93.

Further to the sequence and structural evidence summarised above, it was concluded that these sequenced fragments were amplified from within the echinoid genes. Species-specific primers for qPCR analysis of *cs* expression were subsequently designed based on these cDNA sequences.

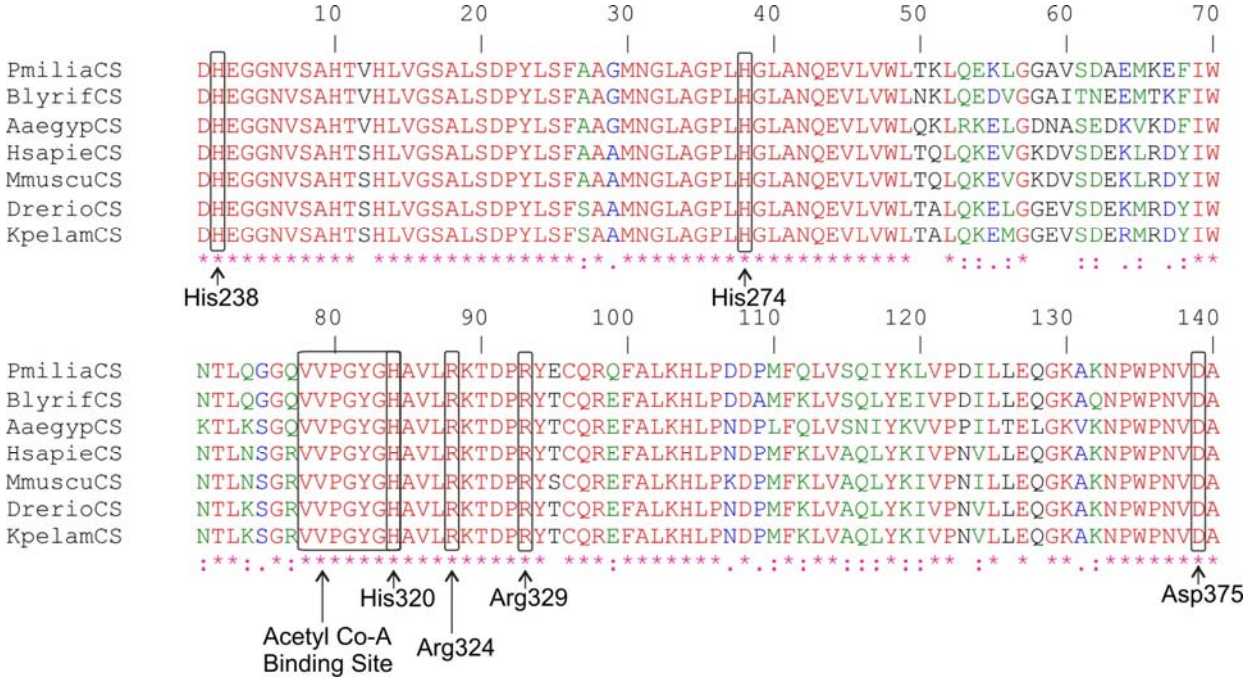

Figure 2.7 CLUSTALW multiple alignment of CS amino acid sequences for *P. miliaris* and *B. lyrifera*. Multiple alignment with CS sequences from the following organisms are shown; zebrafish *Danio rerio* (NP_955892), mouse *Mus musculus* (NP_080720), human *Homo sapiens* (AAC25560), skipjack tuna *Katsuwonus pelamis* (AAR98860) and yellow fever mosquito *Aedes aegypti* (XP_001655738). Multiple alignment identity for these is 70.7%. Amino acid annotations: * = identical, : = strongly similar identity, . = weakly similar identity (Combet et al., 2000). Catalytically important CS residues are labelled.

2.5.2. Heat shock protein 70

The *P. miliaris* and *B. lyrifera* mRNA consensus sequences generated from the *hsp70* degenerate primers produced two inferred amino acid sequences of 127 aa and 129 aa length. A ClustalW comparison determined that these sequences shared an identity of 84.8%. A BLASTP search found similarities with HSP70 protein sequences from the echinoids *P. lividus* (Q06248) and *S. purpuratus* (XP_780151). The overall multiple alignment identity for these four echinoid sequences was 73.5% (Figure 2.8). The BLASTP search also identified the conserved HSP70 domain PTZ00009. Included in the inferred amino acid sequence was one of the signature sequences of the stress-70 family, TVPAYFND (Rensing and Maier, 1994). Also evident in the amino acid sequence is a conserved sequence found in proteins such as HSP70 that bind ATP, the ATP/GTP-binding site motif A (also known as the P-loop); [AG]-x(4)-G-K-[ST] (prosite ID: ATP_GTP_A PS00017; Walker et al., (1982)). The evidence summarised above indicated that a fragment from the stress-70 family of genes had been isolated from both species of echinoid.

Due to the highly conserved nature of the stress-70 protein family (section 2.1.1.2), from the above evidence it was not possible to determine whether the mRNA sequence fragments had been derived from *hsp70* or *hsc70* transcripts. Before species–specific *hsp70* primers for qPCR analysis could be designed, the sequenced cDNA fragment ideally needed to be elongated to provide conclusive evidence as to the identity of the gene. To obtain the complete cDNA sequence, the rapid amplification of cDNA ends (RACE) technique was used, and is discussed in detail in section 2.6. However, due to time constraints, it was not possible to obtain a complete cDNA sequence before it was necessary to design primers and continue with the qPCR assay. Species-specific primers were therefore designed based on these original isolated during degenerate PCR.

```
                    10        20        30        40        50        60        70
                     |         |         |         |         |         |         |
PmiliHSP      -INDQGN---PSYVGFTDTERLIGDAAKNQVAMNPRNTIFDAKRLIGRRFTDATVQSDMKHWPFTVVNQG
SpurpHSP      IANDQGNRTTPSYVAFTDTERLIGDAAKNQVAMNPKNTIFDAKRLIGRRFTDDNVQSDMKHWPFTVINQG
BlyriHSP      --INQGNRTTPSYVAFTDSERLIGDAAKNQVAMNPKNTIFDAKRLIGRRFDDVGVQSDMKHWPFSVVNRG
PliviHSP      IANDQGNRTTPSYVAFTDSERLIGDAAKNQVAMNPTNTIFDAKRLIGRRFNDSSIQADMKHWPFRVINKD
                 :***   ****.***:*************** ************** *  :*:******* *:*:.
Prim.cons.    IANDQGNRTTPSYVAFTD2ERLIGDAAKNQVAMNPKNTIFDAKRLIGRRFTD44VQSDMKHWPFTV2NQG

                    80        90       100       110       120       130
                     |         |         |         |         |         |
PmiliHSP      GKPMLQAEY-GEKKTMAPEEISSMVLTKMKETAEAYLGQKVTDAVVTVPAYFNDAQRQATKD
SpurpHSP      GKPVLQAEYIGEKKTMAPEEISSMVLTKMKETAEAYLGQQITDAVITVPAYFNDAQRQATKD
BlrifHSP      GKPMLQADYMGETKTLAPEEVSSMVLTKMKETAEAYLGQKVTDAVITVPAYFNDSQRQAKD-
PliviHSP      GKPMLQAEYMGETKTLSPEEVSSMVLTKMKETAEAYLGKKVTSAVITVPAYFNDAQRQATKD
              ***:***:* **.**::***:******************::*.**:********:****..
```

Figure 2.8 CLUSTALW multiple alignment of inferred HSP70 amino acid sequences for *P. miliaris* and *B. lyrifera*. Sequence homologies with HSP70 from *P. lividus* (Q06248) and *S. purpuratus* (XP_780151) are included. Multiple alignment identity for these four sequences is 73.5%. The stress-70 family motif TVPAYFND and the ATP/GTP-binding site motif A (P-loop) AEAYLGK are boxed.

2.5.3. Ubiquitin

The *P. miliaris* and *B. lyrifera* consensus mRNA sequences isolated with the *ubi* degenerate primers produced inferred amino acid sequences of 65 aa length that were 100% identical. BLASTP searches determined that they were also 100% identical to ubiquitin sequences from other species. Figure 2.9 illustrates how conserved the ubiquitin protein is in all eukaryotic organisms. The *P. miliaris* and *B. lyrifera* sequences were 100% identical to polyubiquitin (*ubc*) sequences from; *H. sapiens* (NP_066289), the rat *Rattus norvegicus* (NP_620250), *M. musculus* (NP_062613), the sheep *Ovis aries* (NP_001009202), the African clawed frog *Xenopus laevis* (NP_001080865), brine shrimp *Artemia franciscana* (CAA52416), the red flour beetle *Tribolium castaneum* (NP_001034506), the silkworm *Bombyx mori* (NP_001036839), the pacific oyster *Crassostrea gigas* (BAD15290) and the trematode worm *Schistosoma japonicum* (AAP13102)

The BLASTP search also identified the conserved ubiquitin domain cd01803, containing three catalytically active features; the UBQ-E2 interaction site (Hamilton et al., 2001), the UBQ-UCH interaction site (Johnston et al., 1997) and the UBQ-CUE interaction site (Kang et al., 2003) (refer to section 2.1.1.3 for more details). As well as the cd1803 domain being present in the polyubiquitin gene, however, it is also found in the ubiquitin fusion genes which code for a single ubiquitin monomer fused to a carboxy-terminal extension protein (L40 or S27a). This situation arises because ubiquitin is a multigene family of highly similar proteins, and the active proteins are formed after post-translational cleavage (section 2.1.1.3). The *P. miliaris* and *B. lyrifera* ubiquitin amino acid sequences were also identical to the ubiquitin monomers fused to other species' S27a and L40 proteins, as illustrated in Figure 2.9. The basic 76 amino acid ubiquitin monomer sequence starts at the MQIF sequence, finishing at the C-terminal consensus sequence VLRLRGG. Differences in the sequences of polyubiquitin and monomeric fusion genes occur after the C-terminus, and unfortunately, this region was not isolated from *P. miliaris* or *B. lyrifera*.

From the above results, it can be confidentially concluded that mRNA from the ubiquitin multigene family was isolated from *P. miliaris* and *B. lyrifera*. Unfortunately, the BLASTP results indicate that the sequences could not be confirmed as relating to the *ubc* gene because the carboxy-terminus region was not sequenced. However, as discussed in section 2.1.1.3, *ubc* codes for a string of ubiquitin monomers. As can been seen in Figure 2.6, when the PCR products from *B. lyrifera* were visualised, a second larger band was obtained above that corresponding to the expected 196 bp product. If the degenerate primers had annealed to *ubc* mRNA, it would be expected that they would anneal at the same point on each repeat monomer along the entire *ubc* sequence. In which case, the second larger band would relate to an amplified sequence crossing two tandem repeats. The presence of these repeat bands provided some evidence that *ubc*

transcripts had been isolated by the degenerate primers. As explained above for the sequences generated from the *hsp70* degenerate primers, the incomplete ubiquitin cDNA sequences required extending in order to provide positive sequence identifications for *ubc*. However, the RACE technique could not be completed prior to the requirement to design the species–specific primers for qPCR. The cDNA sequences isolated during the degenerate PCR were therefore used as templates for the qPCR primer design.

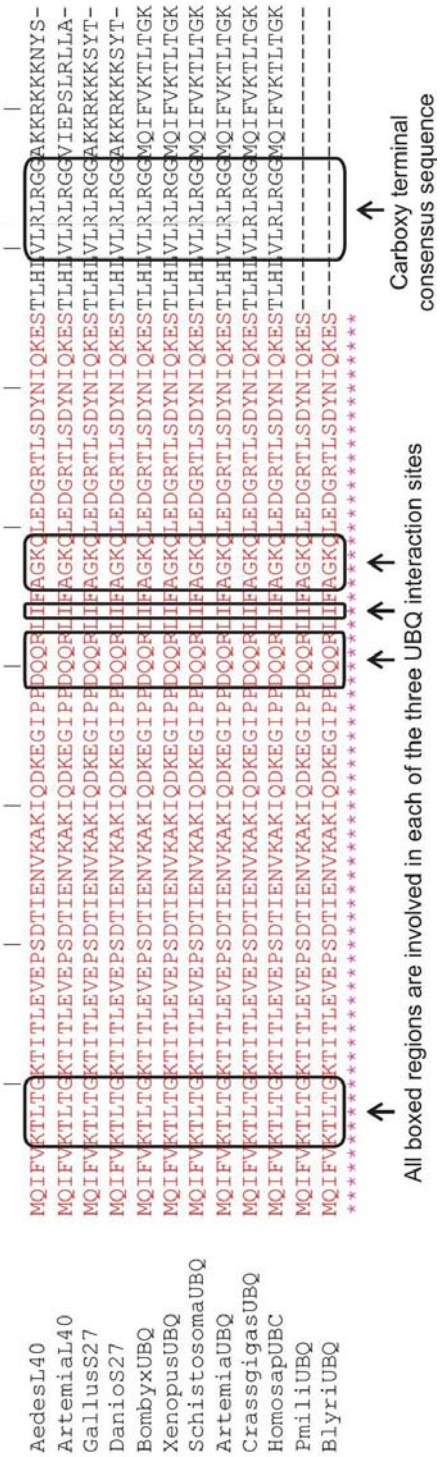

Figure 2.9. CLUSTALW multiple alignment of the inferred amino acid sequences for *P. miliaris* (PmiliUBQ) and *B. lyrifera* (BlyriUBQ); and the polyubiquitin amino acid sequences from *Homo sapiens* (NP_066289), *Xenopus laevis* (NP_001080865), *Artemia franciscana* (CAA52416), *Crassostrea gigas* (BAD15290), *Bombyx mori* (NP_001036839), *Tribolium castaneum* (NP_001034506) and *Schistosoma japonicum* (AAP13102). Also included above are the amino acid sequences for *Danio rerio* ubiquitin ribosomal protein S27a (NP_956796), *Gallus gallus* ribosomal protein S27a (NP_990284), *Aedes aegypti* ubiquitin ribosomal protein L40 (XP_001663729) and *A. franciscana* ribosomal L40 fusion protein (ABS19964). The carboxy-terminal consensus sequence (VLRLRGG) is boxed; unfortunately, this region of the sequence was not isolated from *P. miliaris* or *B. lyrifera*. The conserved domains relating to the ubiquitin interaction sites with E2, UCH and CUE are also boxed. Amino acid position annotations: * = identical identity (Combet et al., 2000).

2.6. Rapid amplification of cDNA ends (RACE)

Rapid amplification of cDNA ends (RACE) is a PCR-based technique which makes it possible to isolate and clone unknown nucleotide sequences flanking a known region, i.e. the 5' and 3'ends, and hence to obtain the complete coding sequence (CDS) and 5' and 3' UTRs of a target transcript (Schaefer, 1995). The RACE technique was originally developed by Frohman et al. (1988), and today a number of manufacturers' kits are available to facilitate its use. In this current study, the Clontech SMART™ RACE cDNA Amplification Kit (PT3269-1) was used to obtain the full-length mRNA sequences corresponding to the GOI from both echinoid species. The Clontech technique replies on the incorporation of a 'SMART (Switching Mechanism At 5'end of RNA Transcript) II™ A Oligonucleotide' sequence into the first strand cDNAs during the reverse transcription step (Clontech user manual PT3269-1).

2.6.1. SMART™ RACE technique

In brief, the Clontech SMART RACE technique is based on the following three steps; the synthesis of first strand 5' and 3'cDNA ends via reverse transcription, the amplification of these cDNA ends via RACE PCR reactions and then the cloning of an appropriately sized PCR fragment for subsequent sequencing. A summary of the RACE procedure is included below (refer to Appendix 1.14 for a complete protocol):

1) **First strand cDNA synthesis: 5'ends.** Reverse transcription of 1 µg total RNA proceeded using anchored oligo d(T) primer (two degenerate nucleotides at the 3'end of a dT oligo) and PowerScript Reverse Transcriptase, an enzyme which adds dC residues to the 3'end of first strand cDNA (corresponding to the 5'end of the mRNA transcript). A SMART II Oligonucleotide (added to the reaction mix), which contains a terminal stretch of G residues, anneals to the dC cDNA tail and acts as an extended template for reverse transcription. The PowerScript RT continues the reverse transcription of the template with the SMART II oligo extension, generating a cDNA copy of the original RNA with the SMART II sequence at the 3'end.

2) **First strand cDNA synthesis: 3'ends.** This reverse transcription procedure with 1 µg total RNA used a modified anchored oligo(dT) primer, which was comprised of an anchored (dT) primer with the SMART II sequence at the 5'end. The PowerScript Reverse Transcriptase generates a cDNA copy of the original RNA sequence with the SMART oligo sequence included at the 5'end of the first strand cDNA.

3) **RACE PCR.** Amplification of the first strand cDNA ends took place via RACE PCR reactions (Table 2.5) primed by gene-specific primers (see next section) manually designed from the cDNA fragments already sequenced (section 2.5) and a Universal Primer

containing the SMART II sequence (which anneals to the corresponding SMART II sequences incorporated into the first strand cDNA templates).

Table 2.5. RACE PCR cycling parameters.

Step	ºC	Time	Number of Cycles
Initial Denaturing	94	7 min	
Denaturing	94	30 sec	x40
Annealing	68/69.5[a]	30 sec	
Extension	72	3 min 30 sec	
Final Extension	72	7 min	

[a] Annealing temperature of 68°C for the *cs* RACE PCR and 69.5°C for the *hsp70* and *ubi* RACE PCR.

4) The RACE PCR products were visualised via gel electrophoresis, and bands of the expected size gel-extracted (Appendix 1.12) and cloned (Appendix 1.13) for sequencing. Only once the RACE PCR products had been sequenced could their identity as a fragment of the target GOI be confirmed.

2.6.2. Gene-specific primers for RACE

Gene-specific primers (GSPs) were designed from the species-specific mRNA sequences obtained following the degenerate PCR for each of the echinoid GOI (section 2.5). The following specifications were incorporated into the GSP design: 23-28 nucleotides in length, a GC% of 50-70%, a T_m greater than 65-70°C and avoidance of self-complementarity and complementarity to the universal primers (Clontech user manual PT3269-1). GSP1s were used in the RACE PCR amplifications to prime the amplification of first strand 5'cDNA, GSP2s were used to prime the amplification of the first strand 3'cDNA. Where required, nested GSPs were also designed to facilitate the isolation of target mRNA in nested RACE PCRs. All GSPs (Table 2.6) were ordered from MWG-Biotech (now Eurofins MWG Operon; Ebersberg, Germany).

2.6.3. RACE PCR results and discussion

2.6.3.1. Citrate synthase

The RACE PCR for both *P. miliaris* and *B. lyrifera* produced bands of strong intensity when visualised via gel electrophoresis (Figure 2.10). These bands were excised and extracted from the gel using QIAquick® Gel Extraction Kits (Appendix 1.11), and cloned directly into pCR®4-TOPO® plasmid vectors and propagated in OneShot® TOP10 chemically competent *E. coli* (see section 2.4.7 and Appendix 9). Resulting colonies containing positive transformants were obtained for all the cDNA ends apart from the *P. miliaris* 3'end. The positive colonies were cultured; the plasmids extracted and sent for sequencing by Geneservice Ltd. The resulting sequences were

edited, consensus sequences generated and aligned using Geneious Basic 3.0.6 and 4.8.3 (Drummond et al., 2010) to give a complete *cs* mRNA sequence for *B. lyrifera* (Appendix 1.23), and the *P. miliaris cs* 5'end.

Table 2.6. Gene specific primers for RACE PCR. Details of the melting temperature (T_m), GC% and length are listed.

Species / Gene / Primer Name	Primer Sequence (5' to 3')	T_m°C	GC%	bp
P. miliaris				
Citrate synthase				
PMCS_GSP1	CAGCATCTGAGACAGCACCACCAAGC	68.0	57.7	26
PMCS_GSP2	CAGTGCTCACACGGTTCATCTTGTAGGC	68.0	53.6	28
Heat shock protein 70				
PmHGSP1	ATGGAGCTGATTTCCTCTGGAGCCATCG	68.0	53.6	28
PmHGSP2	TCAACCAAGGAGGCAAGCCGATGC	66.1	58.3	24
Ubiquitin				
PmUGSP1	CTGCTTGCCAGCGAAGATCAGACGC	67.9	60.0	25
PmUGSP2	GAAGACCCTTACGGGCAAGACCATCACC	69.5	57.1	28
PmNestUGSP1	GCCCGTCAGGGTCTTCACAAAAATCTGC	68.0	53.6	28
B. lyrifera				
Citrate synthase				
BlCS_GSP1	GTCATCTCCTCATTGGTGATGGCTCCTC	68.0	53.6	28
BlCS_GSP2	TGTAGGAGGAGCCATCACCAATGAGGAG	68.0	53.6	28
Heat shock protein 70				
BrHGSP1	AGAACGGCCAGTGCTTCATGTCGGACTG	69.5	57.1	28
BrHGSP2	TGCGAACGACCAGGGTAACAGGACGAC	69.5	59.3	27
BrHGSP2b	CGTAYTTCAACGACAGCCAGCGACAGG	68.8	57.4	27
Ubiquitin				
BrUGSP1	TGGTCGGGTGGGATACCCTCCTTGTC	69.5	61.5	26
BrUGSP2b	GCACACTGTCAGACTACAACATCCAAAAAG	65.4	43.3	30
BrNestUGSP1	ATGGTGTCGCTTGGCTCGACCTCAAGAG	69.5	57.1	28
BrNestUGSP2	GACAAGGAGGGTATCCCACCCGACCAG	71.0	63.0	27

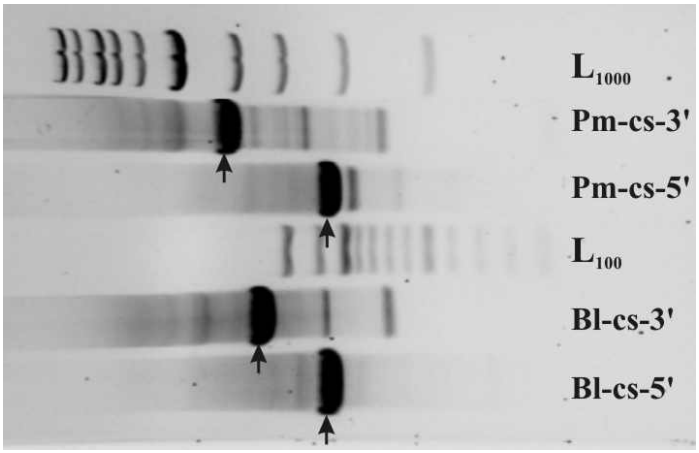

Figure 2.10. Visualised *cs* RACE PCR products after gel electrophoresis. The bright bands (arrowed) were excised for cloning, and correspond to the amplified cDNA ends were generated from RACE PCRs primed by the following GSPs (from top): PmCS_GSP2 (Pm-cs-3'), PmCS_GSP1 (Pm-cs-5'), BlCS_GSP2 (Bl-cs-3'), BlCS_GSP1 (Bl-cs-5').

In order to clone successfully the *P. miliaris* 3'end, the RACE PCR products were column purified with a QIAquick® Gel Extraction Kit, and diluted to give a 1:1 ratio of moles of ends of the insert: moles of ends of the vector. Details of the calculation of the required dilution factor, and the modified protocol to prepare the RACE products for cloning are provided at the end of Appendix1.14. The resulting colonies included positive transformants and the 3'cDNA end was successfully sequenced from these. However, because the 3'cDNA end was approximately 2200 bp in length (Figure 2.10) and sequencing reactions typically only extended to ~1000 bp of good read, internal sequencing primers were designed from the flanking sequence reads and further plasmids were sent for sequencing with the new sequencing primers. The resulting sequences were edited and aligned with the original degenerate PCR sequences, the sequenced 5'cDNA end reads already obtained from the RACE PCR and the initial flanking 3'cDNA end sequence reads (Figure 2.11) to produce a full-length *P. miliaris cs* mRNA sequence (Appendix 1.24)

Citrate synthase cDNA sequence analysis

The 1973 bp *B. lyrifera* mRNA sequence (Accession number: FM865901) included a 99 bp 5' UTR, a 482 bp 3' UTR and a 1392 bp coding sequence which produced a 464 aa protein sequence with a mass of 51.22 kDa (Accession number: CAR98205). The *P. miliaris* mRNA sequence was 3308 bp in length (Accession number: FN677804), including a 148 bp 5' UTR and a 1768 bp 3' UTR. The 1392 bp *P. miliaris* coding sequence was translated to produce a 464 aa protein sequence with a mass of 51.41 kDa (Accession number: CBK39083). These are the only echinoderm citrate synthase sequences yet to be submitted to the online sequence databases.

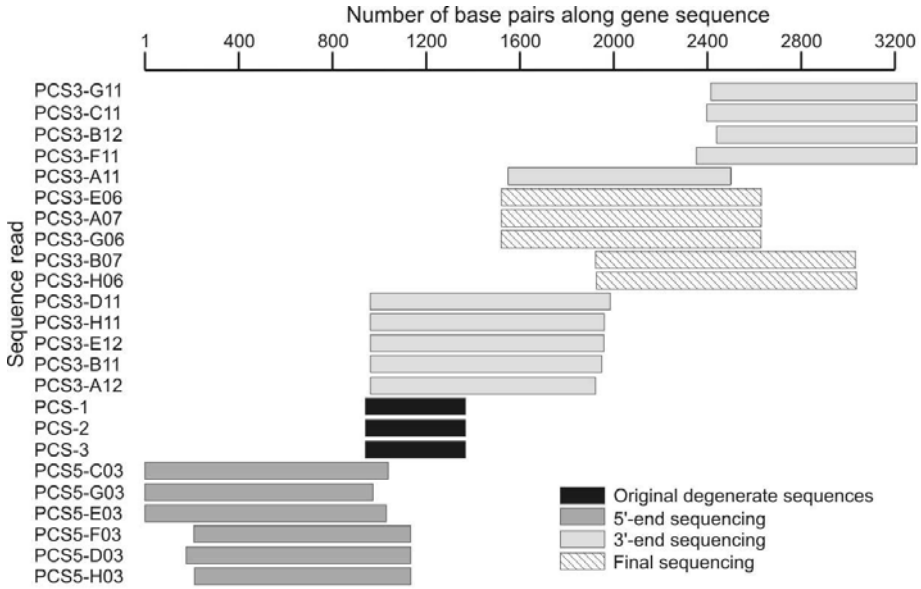

Figure 2.11. Schematic diagram illustrating the alignment of the 24 sequence reads obtained for *P. miliaris cs* from the original degenerate PCR (in black), the sequenced RACE 5' cDNA ends (dark grey), the flanking RACE 3'end cDNA sequences (light grey) and the final bridging RACE 3'ends sequences (hatched).

Close analysis of the *P. miliaris* 3' UTR revealed two putative polyadenylation signals, AATAAA (see Appendix 1.24), which signal the addition of a poly(A) tail to pre-mRNA. In mammals the polyadenylation signal is located 10-30 bp upstream of the start of poly(A) tail (Beaudoing et al., 2000). In the *P. miliaris* 3' UTR one of the polyadenylation signal was located at 22 to 27 bp upstream of the poly(A) tail, indicating that it may be a functional signal. The second polyadenylation signal was located over 1350 bp upstream of the poly(A) tail and therefore is unlikely to be a functional signal.

Citrate synthase protein structure

The echinoid protein sequences were aligned (Figure 2.12) with the CS protein sequences for *S. scrofa* (NP_999441), *B. taurus* (NP_001038186) and *H. sapiens* (NP_004068), three mammalian sequences which have been subject to detailed structural analysis. The citrate synthase enzyme is helical, containing 20 helices per monomer (labelled helix A to T in Figure 2.12 (Remington et al., 1982). Six citrate synthase motifs have been identified (PROSITE ID: PRO0143). The fourth motif encompasses the acetyl Co-A binding site (VVPGYGH) and the citrate synthase signature sequence (GYGHAVLRKTDPR: PROSITE ID: PS00480) (Karpusas et al., 1990).The active sites between amino acid residues 237 and 376 (with reference to the mammalian sequence numbering in Figure 2.12) have already been discussed in section 2.5.1. The additional active residues labelled in Figure 2.12 are binding sites for citrate / oxaloacetate and acetyl Co-A.

Citrate synthase is synthesised in the cytoplasm in an immature precursor form, and is post-translationally transported into mitochondrial organelles. The citrate synthase precursor protein contains a N-terminal mitochondrial transit peptide, or mitochondrial targeting signal, that mediates its transport into mitochondria (Douglas et al., 1986). The precursor protein binds to receptor proteins on the mitochondrial outer surface and then penetrates across the mitochondrial membranes (Attardi and Schatz, 1988). As the CS protein penetrates the membrane, the transit peptide is cleaved by proteases, and the mature protein released. The precursor protein must be prevented from being misfolded in the cytosol in order to keep the transit peptide signal exposed, and members of the stress-70 family take part in this process (Hartl and Neupert, 1990).

The two echinoid 29 aa mitochondrial transit peptide sequences, which are 93.1% identical to each other, lack any acidic amino acid residues (D and E) and contain the basic amino acid residues H, K and R, which is typical of mitochondrial transit peptide sequences (Douglas et al., 1986), although a consensus transit peptide signal has not been identified (Pfanner, 2000). They share only a 40% identity with the mammalian sequences illustrated in Figure 2.12, although notably all five CS sequences contain a TAA(A/R)R(RL)L sequence at the N-terminal end of the peptide.

The complete echinoid CS amino acid sequences (including the transit peptide) share an 89% identity with each other. BLASTP analysis indicates that they both share a 74-75% identity with the actinopterygid fishes and amphibians included in Figure 2.13, a 72-74% identity with the mammalian and reptilian sequences and a 69-72% similarly with the diptera sequences. The echinoid sequences form their own cluster in the dendrogram at Figure 2.13, but are part of the larger cluster containing the vertebrate deuterostome sequences, rather than being more closely related to the diptera protostome sequences. The inclusion in this phylogenetic analysis of sequences from other invertebrates such as bivalvia species is prevented restricted by a lack of complete CS sequences submitted to the online sequence databases.

Figure 2.12 (figure overleaf). CLUSTALW multiple alignment of the *P. miliaris* and *B. lyrifera* CS protein sequences with those from *S. scrofa*, *B. taurus* and *H. sapiens* (Accession numbers NP_999441, NP_001038186, NP_004068). Characteristic structural regions and active residues are highlighted as follows: mitochondrial transit peptide = grey text and solid box; start of the mature citrate synthase peptide = star; helix sites = arrowed bars at the top of the peptide sequences labelled A through T; citrate synthase motifs (PRO0143) = dotted boxes; citrate synthase signature sequence = yellow highlighted box; acetyl Co-A binding site = solid box (residues 314-320); citrate / oxaloacetate binding residues =black arrows; coenzyme A binding residues = white arrows, catalytic triad = red highlighted boxes and numbered. Numbers on the right hand side of each sequence indicate the last amino acid number of that line, with numbering starting at the first amino acid of the mature protein (starred).

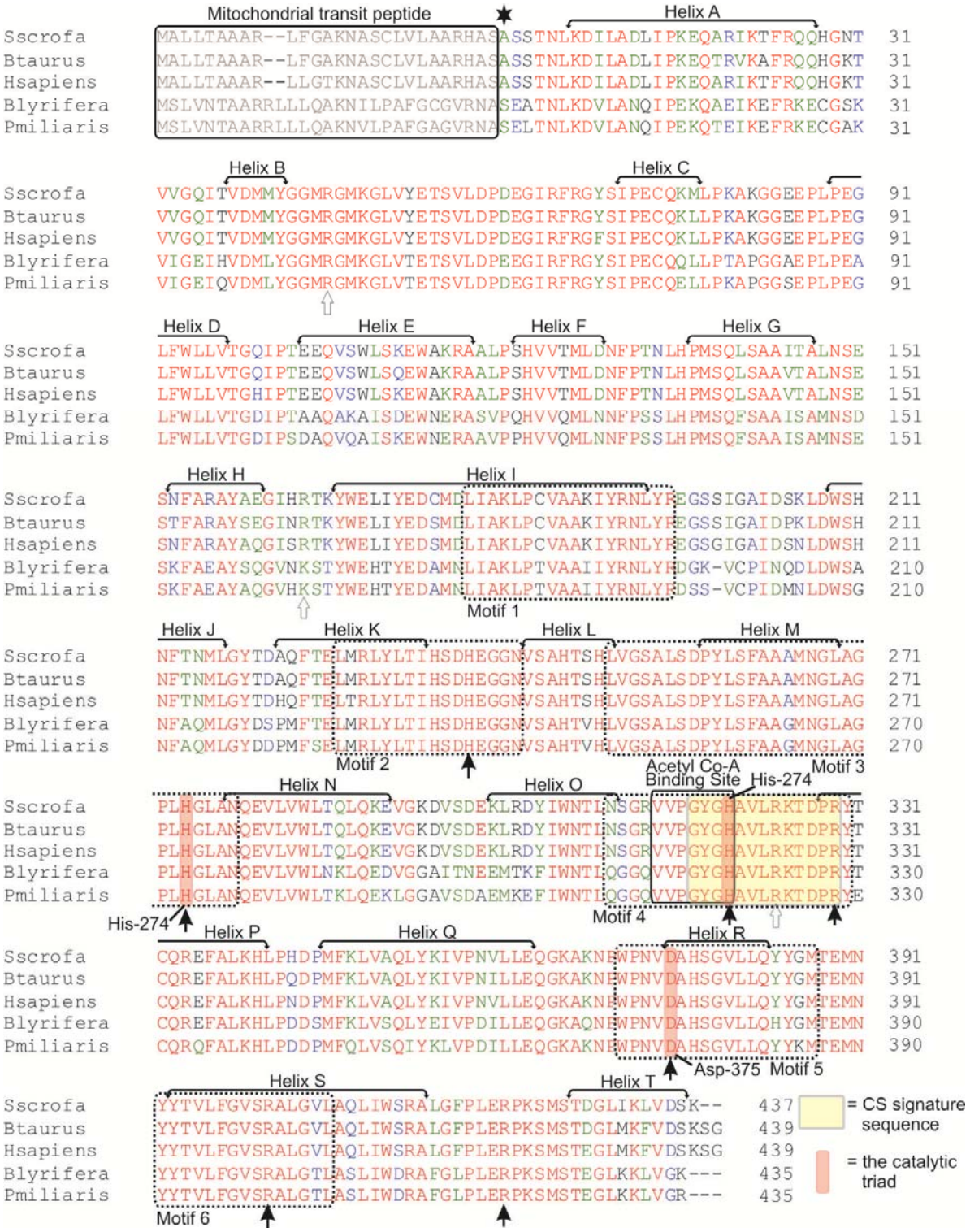

Figure 2.12. Refer to figure caption on previous page.

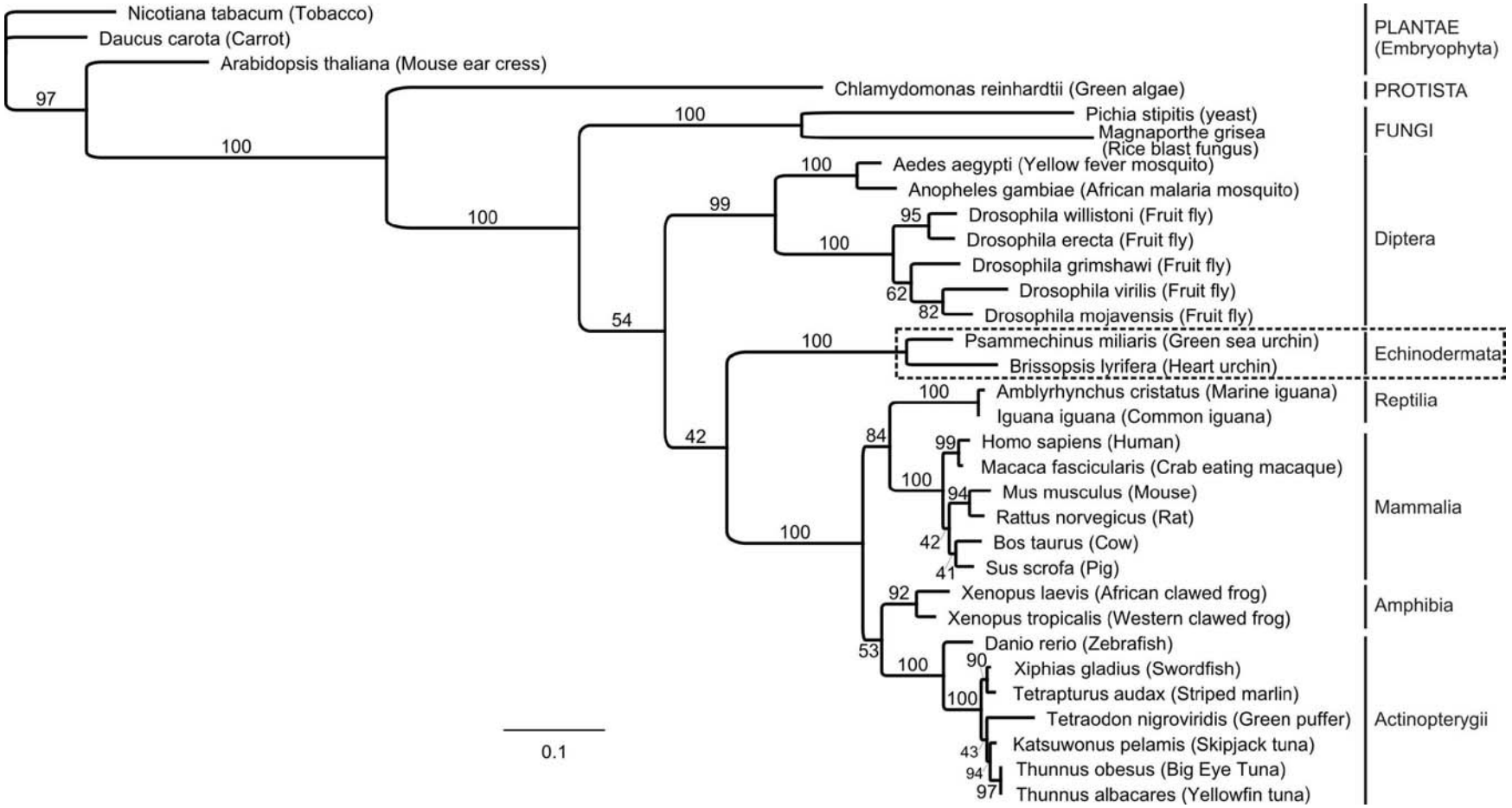

Figure 2.13. Phylogenetic relationship of the *P. miliaris* and *B. lyrifera* citrate synthase amino acid sequences (dashed box) with those from other organisms. The tree was constructed using the PHYML MtREV substitution model using the Geneious Basic 4.8.3 program package (Guindon and Gascuel, 2003). Bootstrap consensus support % for the sequence grouping are indicated in the tree (n=100). The scale bar represents the proportion of amino acid sites at which two sequences are different. GenBank accession numbers for the above sequences are listed at appendix 1.28. Refer to main body of text for further discussion.

2.6.3.2. Heat shock protein 70

The RACE PCR for the echinoid *hsp70* cDNA ends produced three bands of strong intensity when visualised via gel electrophoresis (Figure 2.14a), the *B. lyrifera* 5'cDNA end did not produce a strong band. All four bands, however, were excised, gel extracted, cloned directly into pCR®4-TOPO® plasmid vectors and propagated in OneShot® TOP10 chemically competent *Escherichia coli* (see section 2.4.7 and Appendix 9). Only the two 5'cDNA end fragments resulted in colonies containing positive transformants. These were cultured and the plasmids extracted and sent for sequencing by Geneservice Ltd. (Department of Biochemistry, University of Oxford).

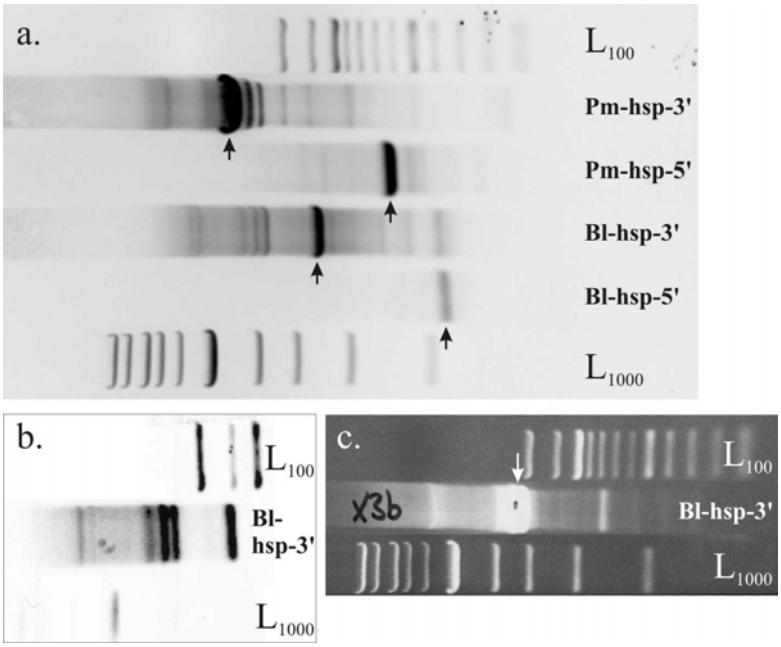

Figure 2.14. Visualised *hsp70* RACE PCR products after gel electrophoresis, arrowed bands were excised for cloning. a) Initial RACE primed by the universal primer and GSPs 1 and 2 listed in Table 2.6. b) A repeat RACE of the *B. lyrifera* 3'cDNA end, primed by the universal primer and BrHGSP2. c) Nested RACE PCR with diluted product from the *B. lyrifera* RACE PCR visualised in b, this time primed by the nested universal primer and BrHGSP2b.

The inserts corresponding to the two 3'cDNA ends did not successfully clone initially. The *B. lyrifera* 3'cDNA ends were subjected to a second RACE PCR with the same primers as originally used (Figure 2.14b), the products from which were diluted and subjected to nested RACE PCR in an attempt to isolate the intended 3'cDNA end, the concentrated band of fragments generated (Figure 2.14c) however, also did not clone successfully.

The 3'cDNA RACE PCR for the two echinoids was repeated under the same initial reaction conditions, and as for the *P. miliaris cs* 3'cDNA end, the gel extracts were column purified with a QIAquick® Gel Extraction Kit, then diluted to give a 1:1 ratio of moles of ends of the insert: moles of ends of the vector. The resulting colonies included positive transformants and the outstanding

3'cDNA ends were successfully sequenced from these. The complete mRNA sequence for the *B. lyrifera hsp70* gene is listed at Appendix 1.25. For the *P. miliaris* 3' cDNA end, because it was approximately 2500 bp in length (Figure 2.14), internal sequencing primers were designed from the flanking sequence reads and further plasmids sent for sequencing with the new sequencing primers. The resulting sequences were edited and aligned with the original degenerate PCR sequences, the sequenced 5'cDNA end reads already obtained and the flanking 3'cDNA end sequence reads (Figure 2.15) to produce a full-length mRNA sequence (Appendix 1.26)

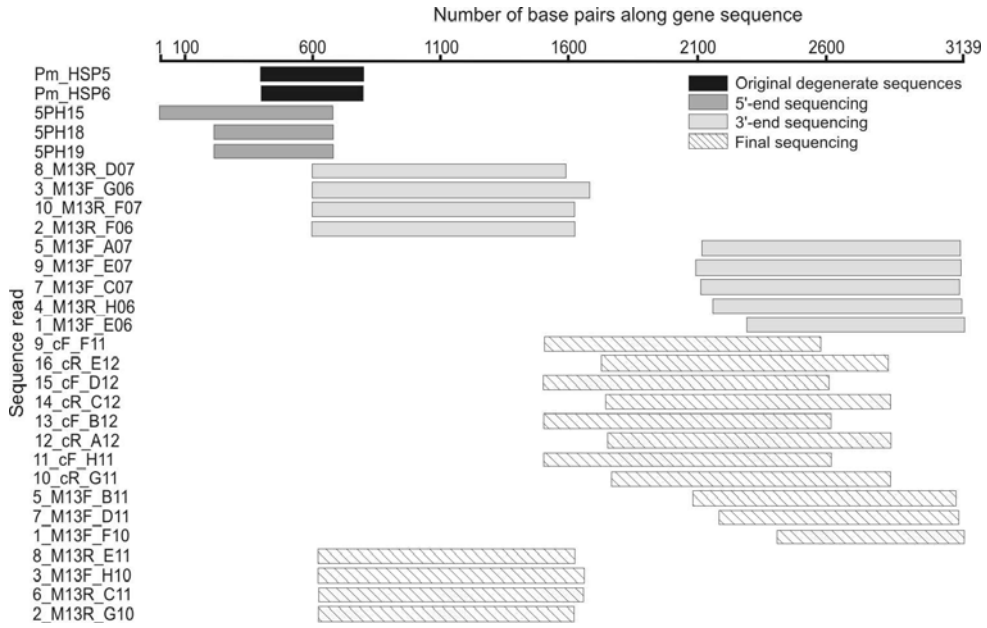

Figure 2.15. Schematic diagram illustrating the alignment of the 29 sequence reads obtained for *P. miliaris hsp70* from the original degenerate PCR (in black), the sequenced 5'RACE cDNA ends (dark grey), the flanking RACE 3'end cDNA sequences (light grey) and the final bridging RACE 3'end ends sequences (hatched).

Heat shock protein70 cDNA sequence analysis

The 2085 bp *B. lyrifera hsp70* mRNA sequence (Accession number: FN667017) included a 117 bp 5' UTR, a 51 bp 3' UTR and a 1917 bp coding sequence which produced a 639 aa protein sequence with a mass of 69.78 kDa (Accession number: CBJ55211). The *P. miliaris* mRNA sequence was 3139 bp in length (Accession number: FN796462), including a 321 bp 5' UTR, a 913 bp 3' UTR, and a 1905 bp coding sequence which produced a 635 aa protein sequence with a mass of 69.34 kDa (Accession number: CBL53159). Analysis of the two nucleotide sequences revealed the presence in the 5' UTRs of putative TATA boxes and heat-shock elements. The 3'UTRs both ended in a poly(A) tail, and the *P. miliaris* 3' UTR contained putative polyadenylation sites.

The TATA box is a core promoter element in eukaryotic protein-coding genes, although not all genes have a TATA box (Smale and Kadonaga, 2003). A promoter element is a region of DNA

that indicates the start site and direction for transcription of a gene. In higher eukaryotes, the TATA box is usually found 25-30 bp upstream of the transcription initiation site but in yeast, the location varies between 40 and 120 bp. There is no single consensus sequence for a TATA promoter element and a wide variety of A/T-rich sequences can function as TATA boxes. The TATA box is the binding site for TATA-binding protein (TBP), a protein that is part of the TFIID transcription factor, which starts the transcription process. In the *B. lyrifera* nucleotide sequence, an AT rich region ('TAAAATAA') is located at 14 to 7 bp upstream fromo the 'ATG' transcription initiation site. This location is closer to the initiation site than expected for a TATA box, although no other A/T rich region in the sequenced 5' UTR is present. In the *P. miliaris* 5' UTR, a number of sites are AT rich, including two which could be putative TATA boxes located at 83 to 92 bp (TATTATTAAA) and 96 to 102 bp (TAATAAA) upstream of the start of the coding sequence.

Heat shock protein induction is regulated at the transcriptional level via the activation of heat shock transcription factor (HSF), which binds to heat shock promoter elements (HSEs) located in the 5' UTR region of heat shock genes (Morimoto, 1993). HSEs are characterized as multiple adjacent and inverse iterations of the pentameric motif 5'-nGAAn-3' (n = any nucleotide). The number of pentameric units in HSEs varies, three units are thought to be the minimum required (nGAAnnTTCnnGAAn) (Fernandes et al., 1994). Functional HSEs can differ from this consensus, with 'gapped' HSEs frequently observed that contain a number of bases between the pentameric units, for example the *Saccharomyces cerevisiae* promoter has an insertion of 11 bp between the first and the second repetition [nTTCn-(11 bp)-nGAAn-(5 bp)-nGAAn] (Tachibana et al., 2002). In *Tetrahymena thermophila*, there are two HSEs, the second being a gapped-HSE containing an insertion of 15 bp between the second and the third units (Barchetta et al., 2008). In the *P. miliaris* 5' UTR, there are three putative HSEs each consisting of three pentameric repetitions, whilst the *B. lyrifera* 5' UTR contains one putative HSE consisting of a possible maximum of five pentameric units. In the echinoid *Paracentrotus lividus*, three HSEs were found in the hsp70IV gene (Sconzo et al., 1992) and four HSEs in the hsp70II gene (La Rosa et al., 1990).

Heat shock protein 70 protein structure

A stress-70 protein is comprised of two main structures. The first is a highly conserved N-terminal nucleotide binding domain (NBD), also referred to as the ATPase domain, which binds and hydrolyses ATP (Flaherty et al., 1990; McKay et al., 1994). The second is a C-terminal substrate-binding domain (SBD) which binds peptides and folds non-native polypeptides, and has a more variable amino acid sequence (Gething and Sambrook, 1992; Hightower et al., 1994; Zhu et al., 1996). The binding process between HSP70 and a substrate protein is ATP regulated; ATP binds

to the N-terminal domain causing a change in the configuration of the C-terminal domain which subsequently increases its affinity for substrate proteins.

Analysis of the deduced amino acid sequences for the two echinoids revealed that they contained the stress-70 family signatures (Gupta and Golding, 1993; Boorstein et al., 1994; Rensing and Maier, 1994): IDLGTTYSC (signature 1; PROSITE ID: PS00297), IFDLGGGTFDVSIL (signature 2: PROSITE ID: PS00329), and VVLVGGSTRIPKVIQK (signature 3: PROSITE ID: PS01036). Additionally, the stress-70 sequences TVPAYFND and NEPTAA are present in the sequences, together with the eukaryotic non-organelle stress-70 motif, RARFEEL (Rensing and Maier, 1994). As originally identified from the sequences isolated during degenerate PCR (section 2.5.2), the amino acid sequence also contains the ATP/GTP-binding site motif A (P-loop), AEAYLGK (Walker et al., 1982). All of these motifs are located within the conserved N-terminal NBD (Figure 2.16). The *P. miliaris* protein sequence has one major feature distinguishing it from most other eukaryotic HSP70s: the substitution of an M for a V in the terminal tetrapeptide of the cytosolic stress-70 C-terminal motif (EEMD instead of EEVD). This is a situation not commonly found, although four bivalve sequences have been reported with this same sequence (Piano et al., 2005).

The alignment of the *P. miliaris* and *B. lyrifera* protein sequences with other echinoderm stress-70 sequences (the two *P. lividus* HSP70 sequences already mentioned, together with the *S. purpuratus* HSP70 and HSC70 sequences and the holothurian *Apostichopus japonicas* HSP70 sequence (Meng et al., 2009), is illustrated at Figure 2.16. It can be seen that the *S. purpuratus* HSC70 sequence contains GGMP repeats within the extreme C-terminus. Whilst the function of these repeats has not yet been determined (Wang et al., 2009), it has previously been found that GGMP repeats are present in the *Ostrea edulis* HSC70 but are absent in *O. edulis* HSP70 (Piano et al., 2005). Neither of the *P. miliaris* and *B. lyrifera* sequences contain GGMP repeats.

The two echinoid amino acid sequences shared an 86% identity with each other. BLAST analysis of the *B. lyrifera* amino acid sequence indicated sequence identities with *P. lividus* HSP70IV (83%), *S. purpuratus* HSP70 (81%), *S. japonicus* HSP70 (77%) and *H. sapiens* HSP1A (75%). The *P. miliaris* amino acid sequence BLAST sequence results indicated sequence identities with *P. lividus* HSP70IV (84%), *S. purpuratus* HSP70 (81%), *S. japonicus* HSP70 (76%) and *H. sapiens* HSP1A/1B (74%). The six published echinoderm HSP70 sequences form an independent cluster on a phylogenetic dendrogram of stress-70 amino acid sequences (Figure 2.17), adjacent to the mammalian amphibian and actinopterygid HSP70 cluster. In this dendrogram, the *S. purpuratus* HSC70 sequence is separate from the echinoderm HSP70 sequence, instead being included in a large cluster that includes crustacean, mammalian, amphibian and actinopterygid HSC70 sequences and bivalve HSP70 and HSC70 sequences.

Figure 2.16. Multiple alignment of echinoderm stress-70 sequences. Boundary between N-terminal ATPase domain and C-terminal domain, as determined by an alignment of the sequences with that for *H. sapiens* (NP_005518) and reference to Flaherty et al. (1990) and Zhu et al. (1996), is indicated by the black line between the 390 and 391 amino acid residues Sequence identity is 56.13%. Accession numbers (top to bottom): CAA43653, Q06248, CBL53159, CBJ55211, XP_780020, ACJ54702, XP_802129.

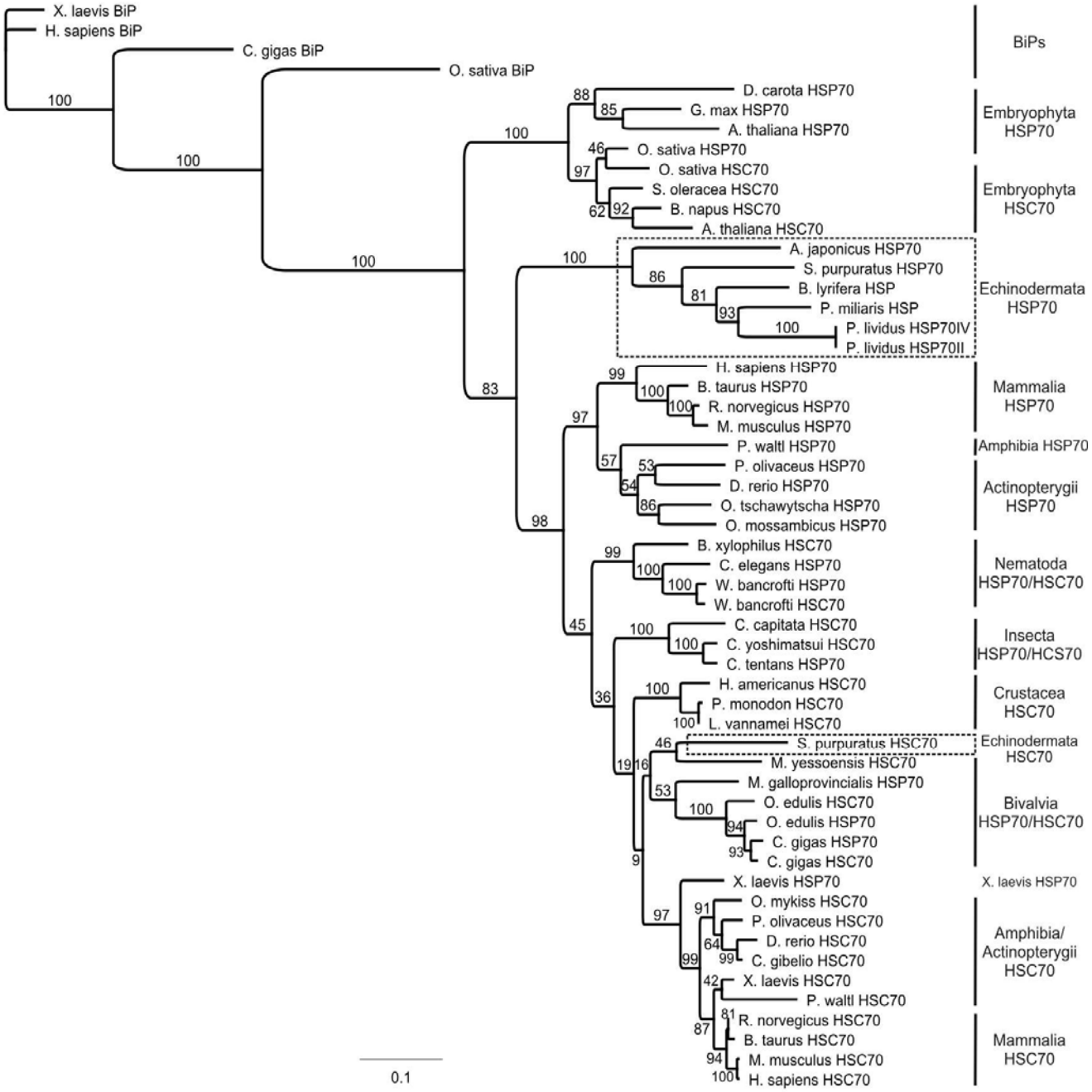

Figure 2.17. Phylogenetic relationship of the *P. miliaris* and *B. lyrifera* HSP70 amino acid sequences with the sequences for the cytoplasmic forms of HSP70 and HSC70 from other organisms, including other species of echinoderm (dashed boxes). Examples of the endoplasmic reticulum stress-70 protein (BiP) were also included to provide an outgroup. The tree was constructed using the PHYML MtREV substitution model with the Geneious Basic 4.8.3 program package (Guindon and Gascuel, 2003). Bootstrap consensus support % for the sequence grouping are indicated in the tree (n=100). The scale bar represents the proportion of amino acid sites at which two sequences are different. GenBank accession numbers for the above sequences are listed at appendix 1.28. Refer to main body of text for further discussion.

2.6.3.3. Ubiquitin

The RACE technique was not applied successfully to the *ubi* gene for either of the echinoids. The initial RACE PCR (Figure 2.18a), primed by the universal primer and the GSP1s and 2s listed in Table 2.6 produced weak bands for all the cDNA ends apart from the *P. miliaris* 3'cDNA end. The strong band that resulted from the *P. miliaris* 3'cDNA RACE PCR (universal primer and PmUGSP2) was successfully cloned. For the remaining ubiquitin cDNA ends, nested RACE PCRs with diluted products from the initial RACE reaction and the nested universal primer (NUP) produced multiple bands of fragments (Figure 2.18b). Repeated nested RACE with PCRs primed by both the NUP and by nested GSPs (BrNestUGSP1, BrNestUGSP2, PmNestUGSP1) again produced multiple bands of fragments and extensive smearing (Figure 2.18c and d). No further attempt was made to improve the RACE PCR results for these 3'cDNA ends, due to the cost of running each reaction, and the known complexity of the *ubc* gene.

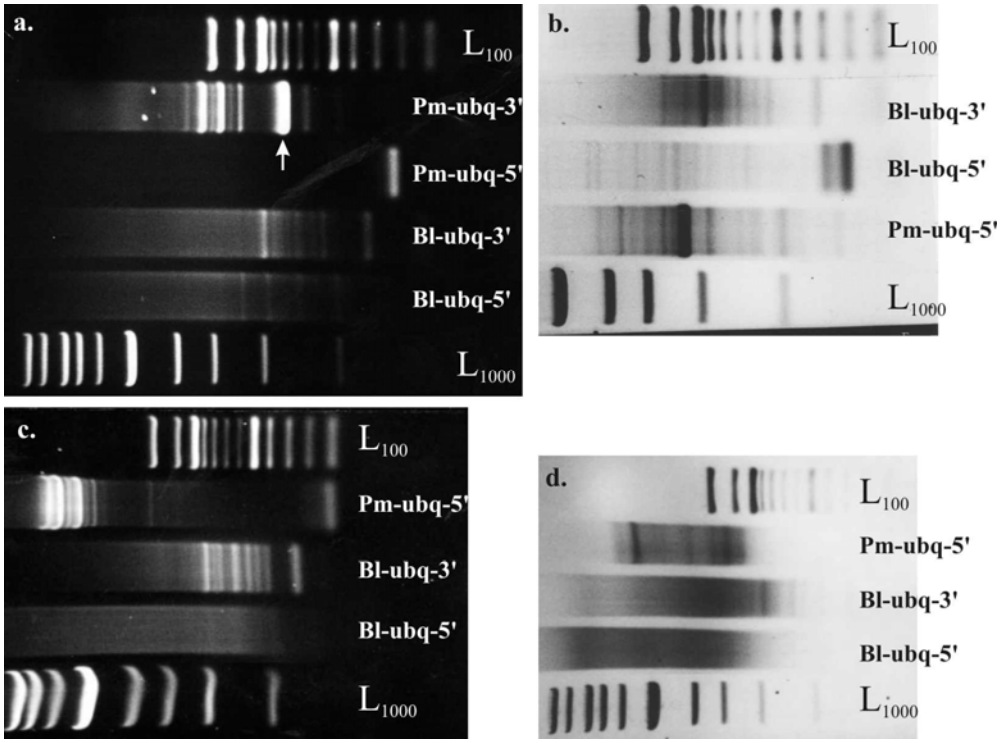

Figure 2.18. Visualised *ubi* RACE PCR products after gel electrophoresis, the arrowed band was excised for cloning. a) Initial RACE primed by the universal primer and the GSPs 1 and 2 listed in Table 2.6. b) Nested RACE primed by the nested universal primer and the GSP1s and 2s. c & d) Nested RACE PCR, this time primed by the nested universal primer and the nested ubiquitin GSPs listed in Table 2.6.

***P. miliaris* ubiquitin sequence analysis**

As already discussed (section 2.1.1.3), ubiquitin is not expressed directly as free ubiquitin but in a precursor form, either as a string of ubiquitin monomers linked in a head-to-tail configuration

(polyubiquitin; *ubc*) or as a single ubiquitin monomer fused to a carboxyl extension protein which is either ribosomal protein L40 or S27a (Özkaynak *et al.*, 1984; Finley *et al.*, 1989; Catic and Ploegh, 2005). During the gel electrophoresis visualisation of both the degenerate and RACE PCR products, the multiple bands of fragments observed were interpreted as being generated from the amplification of *ubc* transcripts (section 2.5.3). However, the final *P. miliaris* mRNA sequence obtained from the RACE PCR does not code for *ubc* (Appendix 1.27).

The alignment of the *P. miliaris* sequences obtained from the degenerate and RACE PCR produced a 788 bp consensus mRNA sequence (accession number: FN796463), incorporating a coding sequence of 384 bp and a 401 bp 3' UTR ending in a poly(A) tail. The 128 amino acid sequence (accession number: CBL53160) coded for by the nucleotide sequence was found to contain both the ubiquitin (cl00155) and the ribosomal L40e superfamilies (cl00671). The *P. miliaris* sequence was found to be 96% identical to the *S. purpuratus* ubiquitin sequence, which also included the ribosomal L40 protein sequence. Other sequence identities with numerous organisms were all in excess of 90%, and all included the ubiquitin monomers associated with the 60S ribosomal protein L40 (coded for by the UBA52 gene in humans). A multiple alignment of a selection of these sequences illustrates the highly conserved nature of the ubiquitin and ribosomal protein sequences (Figure 2.19).

Phylogenetic analysis (Figure 2.20) of the ubiquitin sequences clustered the two echinoderm ubiquitin and L40 sequences with those from insects rather than closer to the mammalian and actinopterygid sequences as found in the citrate synthase and stress-70 phylogenies. The reason for these relationships would appear to be due to the replacement of the I residue at position 77 in the echinoid sequences, and the L or I residue at position 84 rather than the mammalian Q (Figure 2.19).

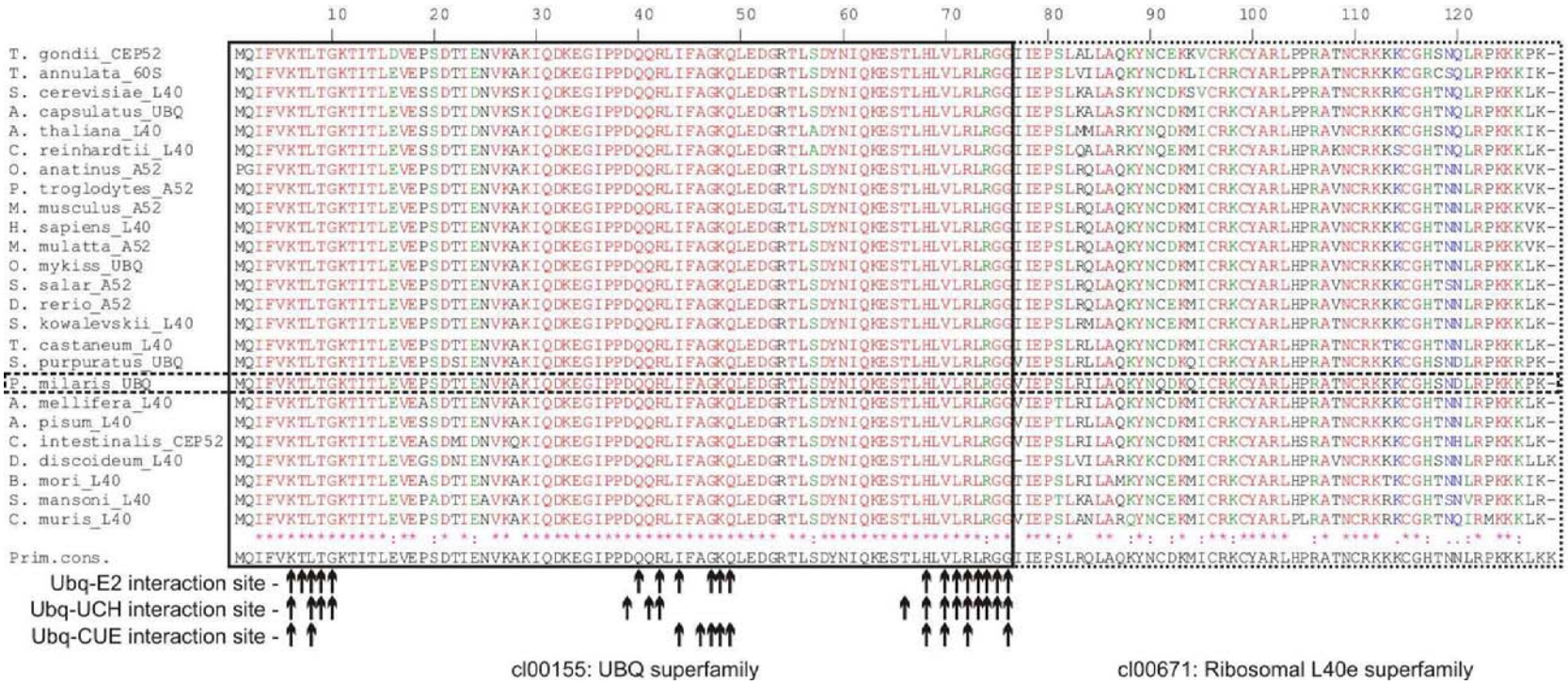

Figure 2.19. CLUSTALW multiple alignment of ubiquitin and ribosomal L40 protein sequences. The *P. miliaris* sequence is highlighted in a dashed box. The active interaction sites on the ubiquitin monomer are arrowed. Refer to main body of text for further discussion. Accession numbers are listed at Appendix 1.28 in accordance with the order of sequences in Figure 2.20.

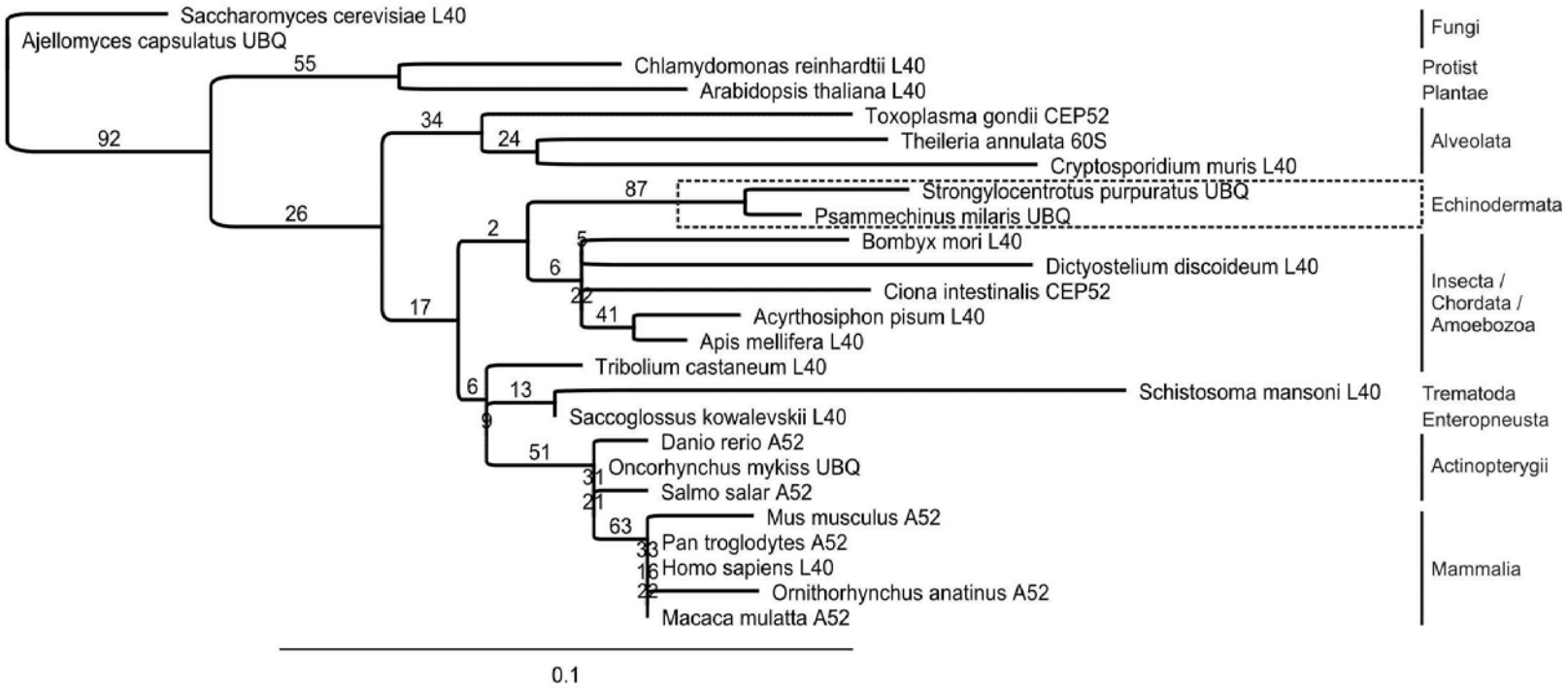

Figure 2.20. Phylogenetic relationship of the *P. miliaris* ubiquitin and ribosomal L40 amino acid sequences with those from other organisms, including the echinoid *S. purpuratus* (dashed box). The tree was constructed using the PHLYM MtREV substitution model using the Geneious Basic 4.8.3 program package (Guindon and Gascuel, 2003). Bootstrap consensus support % for the sequence grouping are indicated in the tree (n=100). The scale bar represents the proportion of amino acid sites at which two sequences are different. GenBank accession numbers for the above sequences are listed at appendix 1.28. Refer to main body of text for further discussion.

2.7. Gene hunting: conclusions

It is with high confidence that the mRNA sequences, isolated from total RNA with the degenerate *cs* primers, and subsequently extended via RACE PCR to full-length sequences, are identified as derived from the echinoid citrate synthase genes. Although, because of time constraints, the primers for qPCR analysis of *cs* expression had to be designed from the original cDNA fragment isolated during the degenerate PCR, this should have no impact on the qPCR assay results because citrate synthase is not part of a multigene family.

Despite the highly conserved nature of the stress-70 family, based on the primary structure of the translated sequences and the BLASTP and phylogenetic results, the mRNA sequences isolated from *P. miliaris* and *B. lyrifera* using degenerate *hsp70* primers have been putatively identified as corresponding to the *hsp70* gene. It is with added confidence that the *P. miliaris* sequence is confirmed as that from the *hsp70* gene, rather than the constitutively expressed *hsc70* gene, as evidence of its upregulated expression was obtained from the original heat shock treatment which induced its expression (Figure 2.5). No such visual confirmation was obtained from the *B. lyrifera* tissue samples, and although the same *hsp70* degenerate primers were used to isolate the cDNA fragments from this species, there was no evidence of enhanced expression as the degenerate PCR required a second amplification to produce sufficient product for cloning and sequencing. The results from the *hsp70* qPCR assays will need to be interpreted taking into account these points.

The results of the *ubi* gene hunting process are complex. The complete mRNA sequence for the *P. miliaris* gene coding for a ubiquitin monomer fused to the 60S ribosomal protein L40 has been isolated, and identified with high confidence (due to the high similarity found with other species homologous genes). However, the target mRNA sequence was that coding for polyubiquitin and was not isolated from either *P. miliaris* or *B. lyrifera*. The *ubi* qPCR primers were designed from the cDNA fragments for a single ubiquitin monomer isolated during degenerate PCR, and as these do not extend to the C-terminal region of polyubiquitin, the primers may amplify mRNA transcripts from any gene of the ubiquitin multigene family, as all will contain the same sequences. Additionally, any amplification of polyubiquitin mRNA transcripts may involve the amplification of more than one product from a single transcript due to the string of monomer repeats (which would have been avoided had the C-terminal sequence containing the non-repeating 3'UTR been isolated and a primer designed in this region). The results from the ubiquitin qPCR assays will need to be interpreted taking into account these points.

Chapter 3. Quantitative PCR Optimisation

The aim of optimising a qPCR assay is to minimise the variation possible at each step of the assay from tissue sample preservation to the manipulation of raw data for statistical analysis. RNA isolation, reverse transcription, primer selection and the qPCR reaction are all important steps that require attention (Bustin, 2008). The optimisation of a qPCR assay is essential if unwanted variability is to be minimised and assay reproducibility maximised (Nolan et al., 2006). In comparison to the previous degenerate PCR process, there are additional steps to take during the preparation of samples prior qPCR analysis (Figure 3.1). Once an optimal methodology has been developed, all samples must be subject to it in order to minimise inter-sample results variation occurring for reasons other than differential gene expression. The following sections provide detail regarding the optimisation of the qPCR assays for the echinoid genes of interest (GOI), only once this process was complete could experimental samples be analysed.

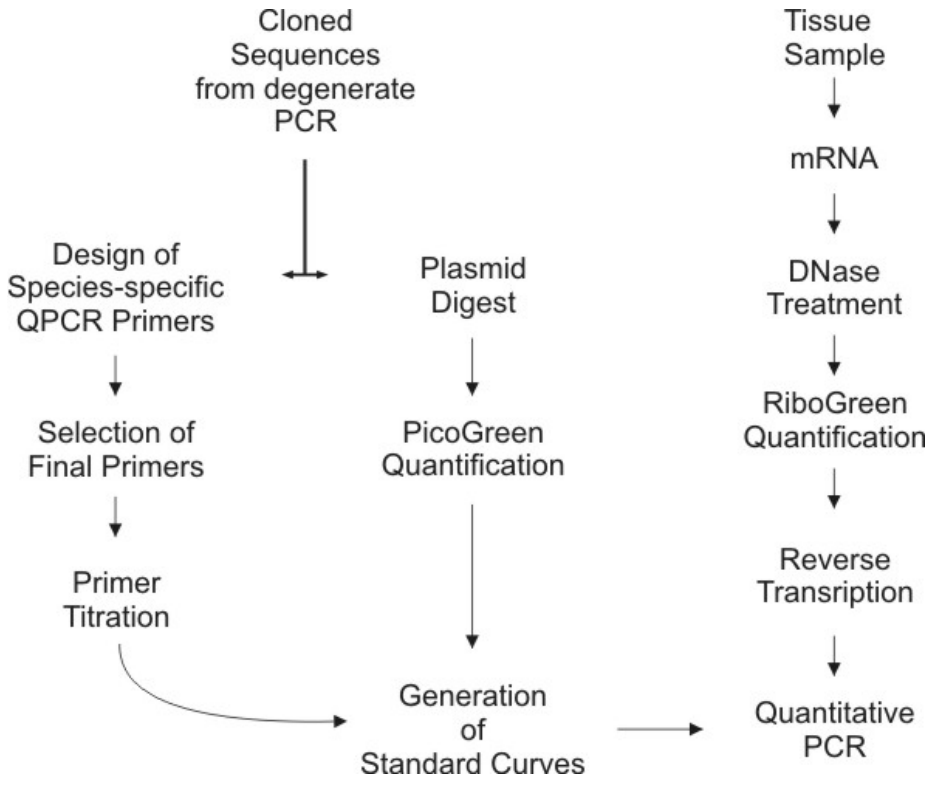

Figure 3.1. Flow chart illustrating the different processes followed in order to optimise the qPCR assays for each of the genes of interest for *P. miliaris* and *B.lyrifera*.

3.1. Quantification of differential gene expression

There are two main approaches to the quantification of target mRNA transcripts via qPCR: relative or absolute (Bustin, 2000). Relative quantification analyses the differential expression of a GOI in

relation to one or more endogenous reference genes (commonly referred to as 'housekeeping' genes). Because the absolute quantity of a reference gene is not known, only relative changes in gene expression can be determined by this method. Reference genes are involved in basic cellular functions (e.g., Histone H3, glyceraldehyde-3-phosphate dehydrogenase (GAPDH) or β-actin), and as such are assumed to be constitutively expressed and to not change under experimental conditions (Bustin and Nolan, 2004b; Kubista et al., 2006). However, this has been found not to be the case with all reference genes, and natural or experimentally induced expression differences are found between samples (Bustin, 2002; Huggett et al., 2005; Arukwe, 2006).

The most recent relative quantification method is to evaluate the expression stability of 10-12 candidate endogenous reference genes, and then from these to select the 3-5 genes that optimally remove most technical variation from the experimental results (Vandesompele et al., 2002; Derveaux et al., 2010). For this current study, however, the requirement to isolate and sequence multiple additional reference genes and then design and optimise multiple pairs of species-specific primers for qPCR represented prohibitive additional expenditure of time and funds. Therefore, the absolute quantification method was used during this study.

Absolute quantification permits the number of mRNA transcripts for a GOI in a given sample to be calculated, which is normalised to a unit such as amount of total RNA or mass of tissue (Bustin, 2000). The linear regression of a standard curve is used to calculate the number of mRNA transcripts in an experimental sample (Bustin, 2000). The standard curve is prepared from the qPCR of a serial dilution of a template that has the same sequence as that of the target cDNA in experimental samples. This ensures that both the standard template and the experimental samples are amplified with equal efficiencies, essential for absolute quantification. The qPCR results from the dilution series are plotted to form a standard curve that gives a log linear relationship between the C_q value and the concentration of starting template in each sample. The C_q value refers to the PCR cycle number at which the generated fluorescence (see next section) crosses a pre-determined background threshold (Figure 3.2), a point commonly referred to as the threshold cycle point (C_t), but now correctly termed the quantification cycle point (Bustin et al., 2009). The C_q value is inversely correlated to the logarithm of the initial cDNA copy number, and so the linear regression of the standard curve can be used to determine the quantity of the GOI in an unknown experimental sample based on its C_q value (Bustin, 2000; Tevfik Dorak, 2006). In this study, the standard curves were generated by serial dilutions of recombinant DNA from plasmid vectors carrying a fragment of the GOI.

The assumptions made whilst using the absolute quantification method (Bustin, 2000; Valasek and

Repa, 2005; Wong and Medrano, 2005) are that a) the amplification efficiency is approximately equal in all samples and standards, and b) The kinetics of the amplification are independent of the initial target concentration. These assumptions can only be made with confidence if the qPCR reaction has been appropriately optimised.

Figure 3.2. (overleaf) qPCR Amplification plots, melt curve and standard curve from the *P. miliaris* recombinant DNA dilution series with ubiquitin species-specific primers (see section 3.3). a) Linear scale qPCR results from a dilution series of recombinant DNA run in triplicate, which illustrate typical sigmoidal-shaped PCR amplification plots. Fluorescence is plotted against cycle number. An amplification curve has four phases (refer to figure inset, taken from Sigma-Aldrich Ltd. (2008)). 1) An early background phase which lasts until PCR product fluorescence is greater than background (baseline) fluorescence. 2) An exponential growth phase, or log linear phase, then begins. The threshold is set above the baseline and within this exponential phase. 3) Once product inhibition and/or reagent limitation is reached amplification is limited, causing a linear phase of amplification. 4) The final plateau phase, where no further amplification is possible. b) The same qPCR amplification plot in semi-logarithmic scale, enabling easy identification of the exponential log linear phase of the qPCR. The threshold setting illustrated here is at the same value as that illustrated in the linear scale plot. Quantification of transcript numbers is determined during the exponential phase because here the amount of PCR product is directly proportional to initial numbers of target sequence. The samples producing curves further to the left contain highest amounts of starting template and have lower C_q values. c) Melt curve of the same qPCR amplification. d) Standard curve generated from the plasmid dilution series. Triplicate C_q values are plotted against the logarithm of starting recombinant DNA template concentration (starting from an arbitrary concentration of 1) ($R^2 = 0.986$, $p < 0.05$).

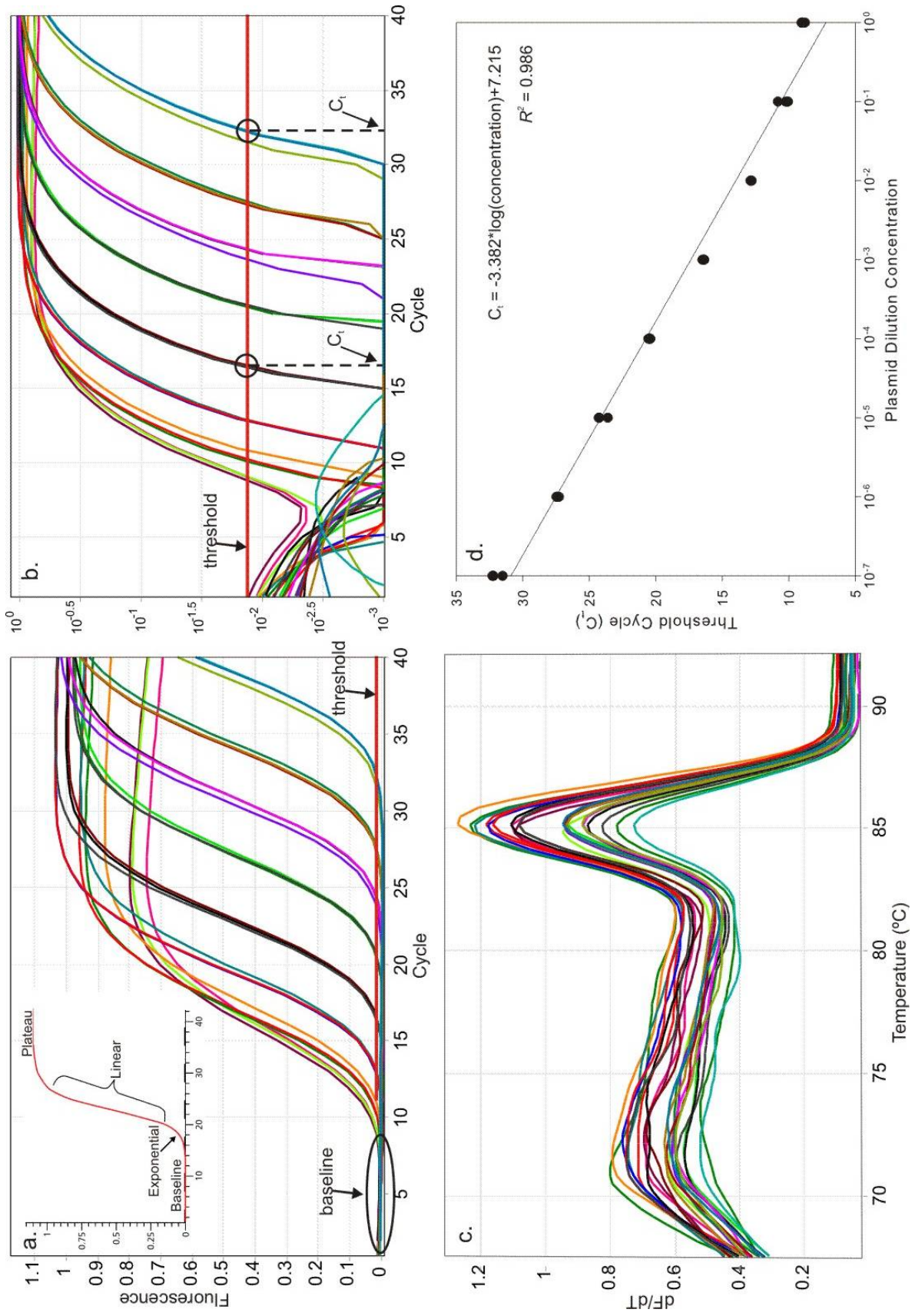

Figure 3.2 (caption previous page).

3.1.1. qPCR detection chemistry

The fluorescence emitted by a dye or probe is used to visualise the increase in template copy numbers during each qPCR cycle. The fluorescence is emitted in proportion to the amount of double stranded DNA present in a sample. As each extension step of the PCR cycle is completed, the increase in the amount of amplified DNA in a sample is reflected by a corresponding increase in fluorescence (Bustin, 2000). The fluorescence signal can be monitored in "real-time" throughout the cycles of a PCR (Bustin and Nolan, 2004a; Ponchel, 2006) and from the resulting amplification curve the C_q can be determined (Figure 3.2). It is therefore important that the detection chemistry selected for a qPCR assay is appropriate to the target, is sensitive and is reliable.

SYBR green dye is the most popular detection system for qPCR (Shipley, 2006). SYBR green fluoresces whilst bound to double stranded DNA. It is inexpensive compared with other detection chemistries (Bustin, 2000; Wong and Medrano, 2005), has low background fluorescence in solution and hence good analytical sensitivity when primer dimers are absent (Hawkes, 2007a). Its limitations are that it cannot be used for multiplexing, can inhibit PCR in high concentrations and most importantly that it binds non-specifically to any fragment of double stranded DNA and hence is prone to false positives (Wong and Medrano, 2005). Thus, fluorescence from specific and non-specific PCR products cannot be differentiated. Alternative detection chemistries to SYBR Green include: single or dual labelled fluorescent probes, molecular beacons, scorpions and Locked Nucleic Acids (LNA) (Shipley, 2006). These chemistries can increase assay sensitivity, specificity and stability, as well as provide the ability to detect single nucleotide polymorphisms (SNPs) and facilitate multiplexing (quantifying more than one gene per qPCR reaction). Their disadvantages are that they can be difficult to design and optimise, they introduce additional complications to the qPCR assay and are more expensive than SYBR green (Hawkes, 2007b).

For this study the fluorescent dye SYBR® Green I was used. The choice was made to use this detection chemistry because of its simplicity (no probes to be designed), cost (inexpensive) and appropriateness to the assay (simple quantification of mRNA transcripts without multiplexing). As mentioned above, SYBR Green does not only bind to target DNA. In a qPCR reaction, it will also bind to contaminating genomic DNA, incorrectly primed non-specific PCR product or primer dimers. This reduces qPCR assay specificity and can lead to the inaccurate quantification of the transcript of interest. The specificity of the SYBR Green qPCR assay is hence derived primarily from the design of the species-specific primers (Bustin, 2000). Reaction specificity is determined after a qPCR is complete via gel electrophoresis to review PCR product size, and by melt curve analysis (Wang and Seed, 2006).

A melt curve is generated by slowly raising the temperature of a post-qPCR sample and tracking the fluorescence profile emitted at increasing temperatures (Bustin, 2000). The progressive application of increased temperature to the double-stranded DNA results in a sharp reduction in the fluorescence signal around the melting temperature (T_m) of the PCR product, resulting in a clear peak in the plotted negative derivative of a melting curve (Figure 3.2c). Different sized DNA fragments from the intended PCR product will have different melting temperatures and will appear as separate peaks on a melt curve (Ririe et al., 1997). Non-specific PCR product and primer dimers generate broad peaks at temperatures different to that expected from the target DNA, and hence their presence can be determined. In this way, the specificity of the manually designed species-specific primers was tested during the optimisation process in order to ensure qPCR specificity using the SYBR Green detection chemistry (see below).

3.1.2. qPCR instrumentation

The instrument used for all the qPCR assays was the Corbett Research Rotor-Gene™ 3000 real time thermal cycler. In this thermal cycler sample are centrifugally rotated in a changing thermal environment that produces a uniform temperature between reactions (Shipley, 2006). A maximum of up to 36 or 72 samples can be run at the same time. Fluorescence readings are taken at the end of every extension step and can be reviewed as the reaction progresses in 'real-time'.

3.2. Species-specific qPCR primers

3.2.1. Primer design

As has been discussed above, the species-specific primer design for a qPCR assay is a critical component of a reproducible and accurate qPCR assay. The species-specific qPCR primers used during this study were designed from the cDNA sequences obtained from degenerate PCR for each GOI (section 2.3). As well as following the guidelines suggested for degenerate primer design (section 2.4.5), additional guidelines for species-specific qPCR primer design were followed where possible in order to achieve maximal reaction efficiency:

1) **Avoid complex regions of mRNA.** Some RNA transcripts can have highly complex secondary structures (Bustin, 2000). qPCR primers should be designed to anneal to an open region of the mRNA molecule at 60°C. If primers are instead targeted to a location that remains tightly or convolutedly folded during the annealing step of the qPCR cycle, primer annealing is compromised and the ability of the polymerase to synthesise cDNA copies can be impaired, so reducing qPCR reaction efficiency (Bustin, 2008). The predicted folding at 60°C of the transcript fragments were visualised using the Mfold web server (Mathews et al., 1999;

Zuker, 2003), and where possible open regions used for primer design.

2) **Amplicon length should be <100bp**. RNA degradation effects the efficiency of the reverse transcription reaction (Fleige et al., 2006), but this has least effect on subsequent qPCR if the amplicons are less than 200 bp long (Pfaffl, 2007). Additionally, smaller amplicons improve PCR efficiency as they are less likely to form secondary structures themselves and reduce qPCR reaction efficiency (Wang and Seed, 2006; Hawkes, 2007b). The optimal amplicon length is recommended to be less than 100 bp (Bustin, 2000).

3) **Melting temperature, T_m**. qPCR primer melting temperatures should be between 58-60°C, and not differ by more than 1-2°C (Bustin, 2000).

4) **Primer Length**. Recommendations on qPCR primer length vary, from 15-20 bp (Bustin, 2000), 15-25 bp (Nolan et al., 2006) to 16-28 bp (Wang and Seed, 2006). The successful primers designed during this study were all between 20 and 25 bp long.

5) **Limit 3'-end stability**. The 3'end of the primer is most important, as it is from here that the DNA polymerase will start cDNA synthesis. There should be low 3'end stability to ensure that should the 3'end bind to a non-target sequence it is too unstable for the DNA polymerase to commence cDNA synthesis (Bustin, 2000). This is why the last five bases should not contain more than 2 or 3 G/C nucleotides. More specifically, stability can be determined from the ΔG value (Gibbs Free Energy) for the five 3'end bases (Appendix 1.20). The more negative the ΔG the more stable the primer's 3'end is, and the ΔG should be no more negative than -9 kcal/mol (Rychlik, 2000; Wang and Seed, 2006).

6) **Avoid primer dimers**. Primer dimer formation should be prevented by ensuring that the primers do not form stable hybrids with either themselves (homodimers) or to the second primer (heterodimers) (Wang and Seed, 2006). Stability can be determined from the ΔG value for any dimers formed, the ΔG value representing the energy required to break primer dimer structure. If primer dimers are capable of being formed they should not have a ΔG value more negative than -10 kcal/mol (Nolan et al., 2006).

7) **Ensure primer specificity**. A BLAST search using the primer sequences should be performed to check that they are specific to the gene of interest and will not also anneal to regions on alternative genes (Nolan et al., 2006; Derveaux et al., 2010).

A variety of software was used to assist with primer design and to provide information regarding the properties of the primers. The freeware software, Primer 3 (http://bioinfo.ebc.ee/mprimer3/; Rozen and Skaletsky (2000)) and the software package Primer Express® (Applied Biosystems) were used to design primers from the mRNA sequences. The freeware program NetPrimer

(http://www.premierbiosoft.com/netprimer/; Premier Biosoft International) was used to calculate the physical properties of each primer including the ΔG values for the stability of primer dimers and the primers' 3'end. To select the primers most likely to be optimal, the qualities of each primer were reviewed, and where required, manually amended or new primers were designed by hand. Once individual primers had been designed, homo- and hetero-dimer creation between possible primer pairs was checked with NetPrimer. Once all primer options had been investigated, three forward and three reverse species-specific primers were selected for each GOI (Appendix 1.21) and synthesized by MWG-Biotech now Eurofins MWG Operon.

3.2.2. Primer selection

The freeze-dried qPCR species-specific primers were eluted in TE Buffer to provide a stock primer solution of 100 µM. Working 5 µM aliquots of primers were then made up by dilutions of the stock primer solutions with nuclease free water. Trial qPCR assays were then run with all suitable primer pair combinations (1.5 µl of each primer used in each qPCR reaction giving a final concentration of 300 nM each) for each GOI. Precision 2x qPCR master mix (10 µl), pre-mixed with SYBR green I, *Taq* DNA polymerase, dNTPs and buffer (Primer Design Ltd.), was used for all qPCR assays to standardise reaction reagents. Further to the Precision master mix protocol, the cycling conditions listed in Table 3.1 were followed. Duplicate cDNA template (1 µl) and non-template controls (NTCs) were run in each reaction (total volume 20 µl), to provide initial information regarding the efficiency of the qPCR assay primer by each primer pair and the possible formation of primer dimers or non-specifically primed targets. The cDNA templates used for all trial qPCR assays were the same as those used successfully in the degenerate PCR (section 2.4.4); this ensured that the cDNA samples had already been confirmed as containing templates for the GOI. Refer to appendix 1.10 for a summary of the qPCR protocol.

Table 3.1 Cycling conditions for qPCR assays.

PCR Step	Temperature (ºC)	Time	
Initial denaturation	95	10 min	
Denaturation	95	15 sec	x 25-45* cycles
Annealing	60	40 sec	
Extension and data collection	60	20 sec	
Melt Curve Analysis	67-95	Hold 45 sec on 1st step Hold 5 sec on next steps	

*Although 45 cycles were run for the assays included as illustrations in this thesis, this large number of cycles was only performed to enable the complete qPCR cycle to be imaged and interpreted during optimisation. Actual qPCR assays only require 25 cycles to be run.

The results obtained from two of the *B. lyrifera* trial primer pairs, *hsp70* (BLHQPF2 and BLHQPR2) and *cs* (BLCQPF2 and BLCQPR2) are illustrated at Figure 3.3. These reactions were selected for illustration as they provide examples of one of the worst and one of the best primer pair results. The trial qPCR with the *hsp70* primer pair produced amplification curves for the duplicate template reactions (C_q = 28.00 & 28.22) very close to the amplification curves of the NTCs (C_q = 33.25 & 34.30) (Figure 3.3a). The melt curve profiles illustrate a peak at ~85°C for the template reactions, but there is also a second peak at ~80°C. The NTC melt curves also show a broad peak at ~80°C (Figure 3.3b). These results indicate that, whilst the cDNA template used probably contained low numbers of *hsp70* transcripts, the trialled primer pair would be unlikely to prime qPCR reactions from which it would be possible to confidently differentiate between low transcript copy number in experimental samples and the NTC reactions. The NTC melt curve peaks at ~80°C also indicate that the primer pair was likely to have been forming primer dimers. The fluorescence generated from these may interfere with experimental sample results, as evidenced by the ~80°C peak found within the template melt curve. This pair of primers was unacceptable for selection as final primer pairs.

In comparison, the amplification cycles for the trial *cs* primer pair (BLCQPF2 and BLCQPR2) reflected a better result. The duplicate template reactions generated amplification curves (C_q = 22.93 & 22.50) much earlier than those associated with the NTCs (C_q = 44.61 & 39.06; Figure 3.3c). The associated melt curve (Figure 3.3d) illustrates a strong clear peak at ~87°C within the template reactions, indicating the presence of specifically primed DNA fragments. The NTC melt curves, whilst indicating a small peak at ~88°C from one of the NTC reactions (which is not found in the template melt curves), illustrate a lack of primer dimers. This primer pair was selected for use in the final qPCR assay.

The qPCR and melt curve results for all primer pairs for all GOI were reviewed for qPCR assay suitability. A pair of most optimal primers were selected for each GOI, apart from those for the *B. lyrifera hsp70* assay. None of the originally designed *B. lyrifera hsp70* primer pair combinations proved to be suitable for qPCR assay, and so a further two forward and two reverse primers were designed, ordered and then tested as above. From a review of the results generated from the additional primer pairs, a final primer pair was selected for use in the *B. lyrifera hsp70* qPCR assay (Table 3.3).

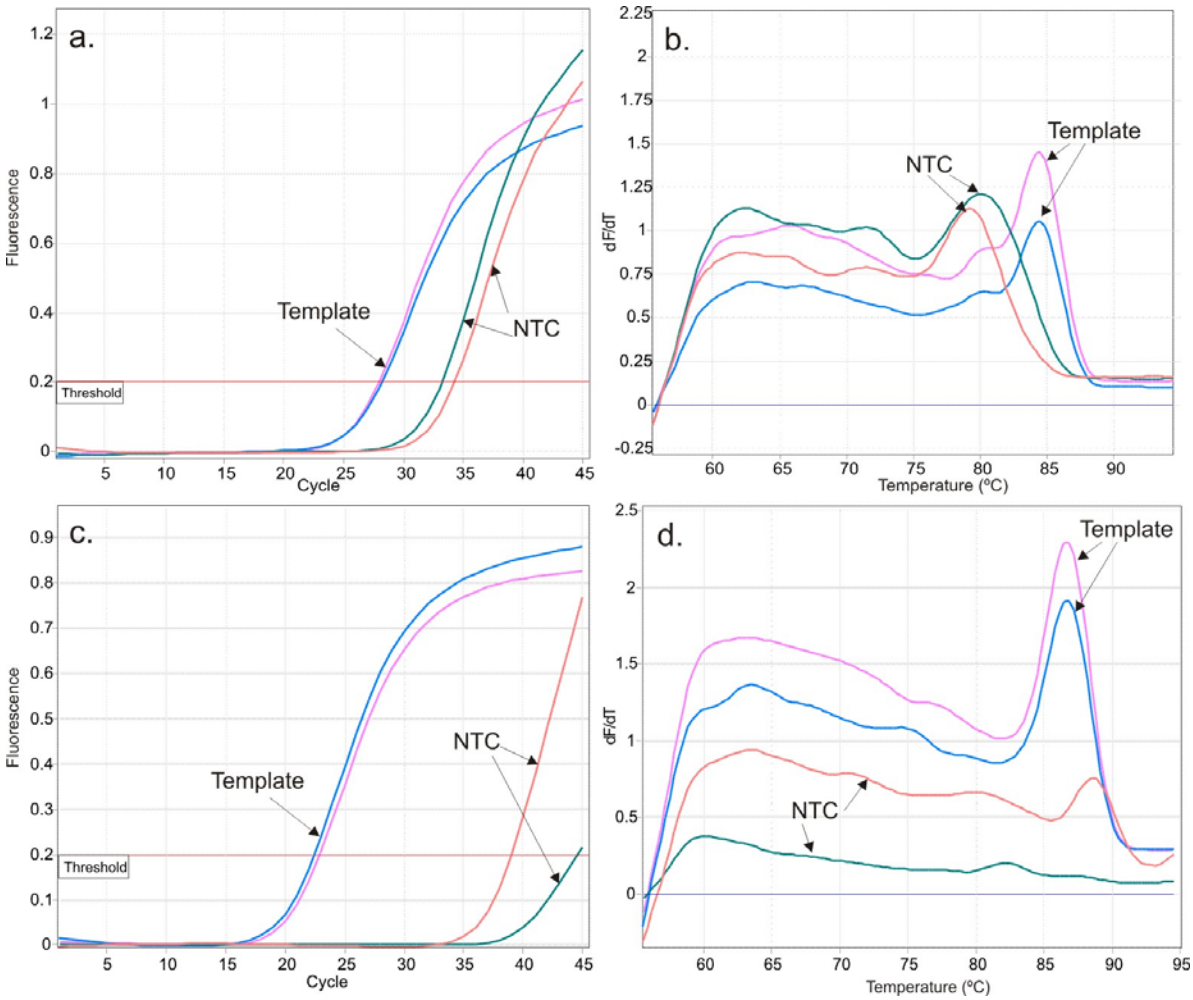

Figure 3.3 qPCR and melt curve profiles from two different qPCR reactions using *B. lyrifera* cDNA template and no template controls (NTC). a) qPCR profile from trial *hsp70* primer pairs BLHQPF2 and BLHQPR2 and their associated b) melt curve. This was a poor qPCR reaction. c) qPCR profile from trial *cs* primer pairs BLCQPF2 and BLCQPR2 and their associated d) melt curve. This was an acceptable qPCR reaction. These qPCR reactions were run for 45 cycles in order to demonstrate how late NTC reactions reach the C_q point.

3.2.3. Primer titrations

qPCR reaction efficiency varies depending on the concentration of each primer, which must be optimised (Ponchel, 2006). Once the optimal primer pair combinations had been selected, the optimal primer concentrations to use for each qPCR assay was therefore determined by 'primer titration'. A primer titration for each primer pair consisted of duplicate template and NTC qPCR reactions being run for each primer concentration combination listed in Table 3.2. The cDNA templates (1 µl) and other reagents were the same as those used during the primer-pair selection process (above), apart from the varying primer concentrations and hence added water volume (appendix 1.10). The qPCR cycling conditions listed in Table 3.1 were used.

Table 3.2 Primer titration concentration combinations.

Reverse Primer (nM)	Forward Primer (nM)		
	50	**300**	**900**
50	50/50	50/300	50/900
300	300/50	300/300	300/900
900	900/50	900/300	900/900

Taking the results of the primer titration for the *P. miliaris ubi* primer pair (PMUQPF2 and PMUQPR3) as an example, average C_q values for each duplicate cDNA template qPCR reaction ranged from 12.80 to 15.24 (Figure 3.4a). Average C_q values for each NTC qPCR reaction ranged from 24.79 to 35.79. As the C_q values for the template qPCR reactions fell within only 2.44 cycles of each other, so a concentration combination resulting in highly efficient amplification was not obvious. The final selection of the best possible primer concentrations was hence based on those that produced the largest C_q difference between the template and NTC qPCR assays. As illustrated at Figure 3.4b, the primer concentrations producing the largest difference were forward primer 50 nM and reverse primer 300 nM.

The final optimal primer pair and concentration combinations are listed at Table 3.3. Following their selection, a standard curve was constructed for each qPCR assay to test for reaction efficiency and to determine the limits of the assay sensitivity.

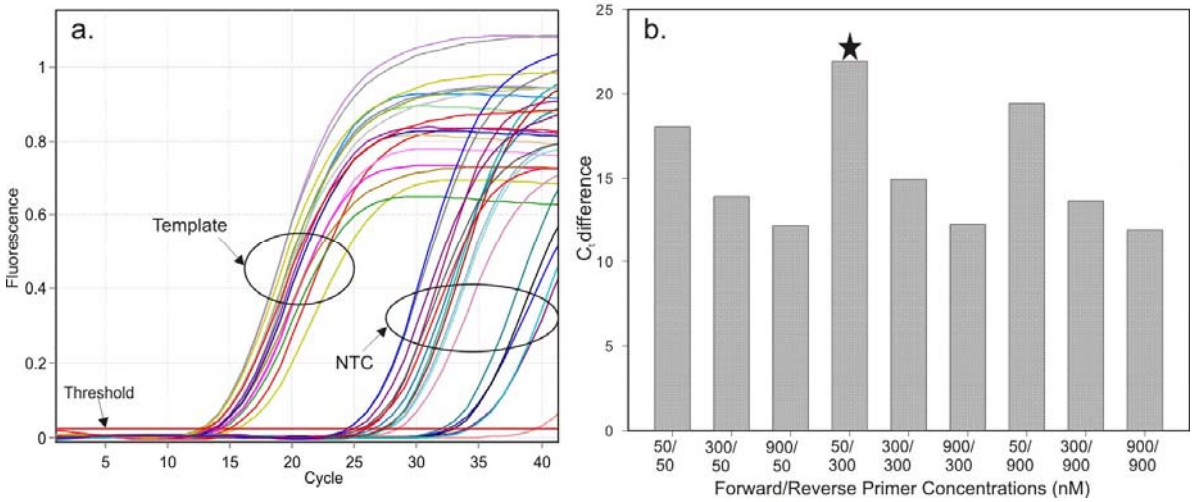

Figure 3.4. Primer titration results for *P. miliaris* primer pair PMUQPF2 and PMUQPR3. a) All qPCR profiles from the nine cDNA template reactions and the no-template control (NTC) reactions. b) The differences in C_q values between the template qPCR reactions and corresponding NTC qPCR reactions, largest difference is starred.

3.3. Standard curves

A standard curve provides information on the sensitivity and efficiency of a qPCR assay (Ponchel, 2006), and therefore the accuracy of the absolute quantification method depends on the accuracy of the standard template and curve (Bustin, 2010). A well optimised assay with a serial dilution of a template will give a linear relationship between the C_q and $\log_{10}$(concentration). The equation for the linear slope is $y=mx+c$ where:

m = the gradient of the linear regression (slope), from which can be determined the efficiency of a reaction. The slope is calculated from the change in C_q divided by the change in $\log_{10}$ (concentration).

Reaction efficiency = $(10^{\frac{-1}{m}}) - 1$

x = $\log_{10}$(concentration)

c = the intercept on the y-axis, which is the theoretical C_q if there was only a single copy of the target in the sample.

If the amplification of the qPCR reactions is 100% efficient (i.e. the amount of PCR product doubles each cycle), m will be -3.322. Different sources offer different guidelines as to acceptable values of m and hence acceptable qPCR reaction efficiencies. QIAGEN (2006) advises acceptable values for m range from -3.3 to -3.8, whilst Sigma-Aldrich (2008) advise 3.0 to -3.9. Most recently, Taylor et al. (2010) have recommended that the goal for reaction efficiency is 90-110%. For this study, the aim was to achieve reaction efficiencies of 80-105%, for which m = -3.2 to -3.5, based on the guidelines given by Nolan et al. (2006).

In addition, the R^2 value for a standard curve gives an indication of the amount of variability in the dataset that can be explained by the fitted linear regression (Grafen and Hails, 2008). The closest the value is to 1, the higher the reliability of the PCR assay. If R^2 is ≤ 0.98, the assay may not give reliable results (Taylor et al., 2010), but operator error from poor pipetting accuracy may also be at fault if low R^2 values are obtained (Nolan et al., 2006).

The serial dilution of a cloned plasmid containing the GOI's target sequence has been shown to be robust and reliable standard, and was used to maximise accuracy in this regard (Dhanasekaran et al., 2010). Two standard curves were generated from two different templates for each qPCR assay for each GOI. The templates were comprised of recombinant DNA derived from the degenerate PCR fragments cloned in plasmid vectors during the post-degenerate PCR cloning and sequencing process (section 2.4.7), and also the cDNA templates used for the qPCR primer titrations (section 3.2.3). The cDNA template standard curve was prepared to compare with the recombinant cDNA

curve to check for similar amplification efficiencies, in order to determine whether the recombinant DNA would be a valid standard for the quantification of experimental samples.

Prior to qPCR, the recombinant DNA in each standard dilution was linearised with 1 unit of the restriction endonuclease Not I at the cleavage site within the pCR4-TOPO vector (Appendix 9). The linearised plasmid vectors were immediately diluted in tenfold steps with nuclease free water to produce a dilution series ranging from a default concentration value of 1 to $1x10^{-7}$. The cDNA templates were also diluted tenfold producing a dilution series ranging from 1 to $1x10^{-5}$. Each dilution was run in triplicate qPCR reactions based on the cycling conditions in Table 3.1 and the primer concentrations in Table 3.3. No template controls were also run in triplicate. The standard curves generated from all dilution series are illustrated at Figure 3.5, and details of the calculated slope (m), reaction efficiency, R^2 and limits of reaction sensitivity are summarised at Table 3.4.

It was not possible to produce linear regressions with a slope, *m*, of -3.2 to -3.5 from the initial cDNA standard curves produced with the *P. miliaris ubi* primers under Table 3.1 cycling conditions. The cycling temperatures were therefore changed to an annealing temperature of 61°C and extension temperature of 65°C. The qPCR of the cDNA dilution series under these cycling conditions did generated a linear regression with acceptable results (Figure 3.5f). These cycling parameters for the *P. miliaris ubi* primers were used for the final experimental qPCR assays.

Table 3.3. Species-specific qPCR primers selected for use in final qPCR assays, their physical characteristics and concentrations for use.

Species/ Gene/ Primer Name	Primer sequence 5' to 3'	Length (bp)	GC %	Tm (°C)	3' end stability (ΔG kcal/mol)	Homodimer stability (ΔG kcal/mol)	Net Primer Score	Concentration (nM)	Amplicon Size (bp)	Heterodimer stability (ΔG kcal/mol)
P. miliaris										
Citrate synthase										
PMCQPF1	TCTCTCAGATCCTTACCTCTCG	22	50	60.3	-8.36	-4.62	91	50	82	-4.54
PMCQPR1	CACTTCCTGGTTAGCAAGTCC	21	52	59.8	-7.58	-5.88	87	50		
Heat shock protein 70										
PMHQPF2	AGTACCTCGGAGAAAAGAAGACG	23	48	60.6	-8.13	-3.65	93	50	78	-7.06
PMHQPR2	CGGCTGTCTCTTTCATTTTGGTC	23	48	60.6	-7.94	none formed	100	50		
Ubiquitin										
PMUQPF2	AAGATCCAAGACAAAGAAGGTATCC	25	40	59.7	-7.08	-4.62	91	50	99	-7.12
PMUQPR3	GATGTTGTAGTCTGACAGAGTGC	23	48	60.6	-8.03	-5.13	90	300		
B. lyrifera										
Citrate synthase										
BLCQPF2	CGTTTGCAGCTGGTATGAACG	21	50	59.8	-8.47	-10.24	81	50	67	-5.74
BLCQPR2	ACAAGCACCTCCTGGTTAGC	20	55	59.4	-7.64	none formed	100	50		
Heat shock protein 70										
BLHQPF4	GGTTCAGTCCGACATGAAGC	20	55	59.4	-8.26	-6.47	85	300	78	-8.26
BLHQPR1	ATGTAATCGGCCTGTAGCATCG	22	50	60.3	-8.61	-4.43	92	50		
Ubiquitin										
BLUQPF2	CAAAGCCAAAATCCAGGACAAGG	23	48	60.6	-8.57	none formed	100	50	106	-5.24
BLUQPR3	GATGTTGTAGTCTGACAGTGTGC	23	48	60.6	-8.39	-4.3	92	50		

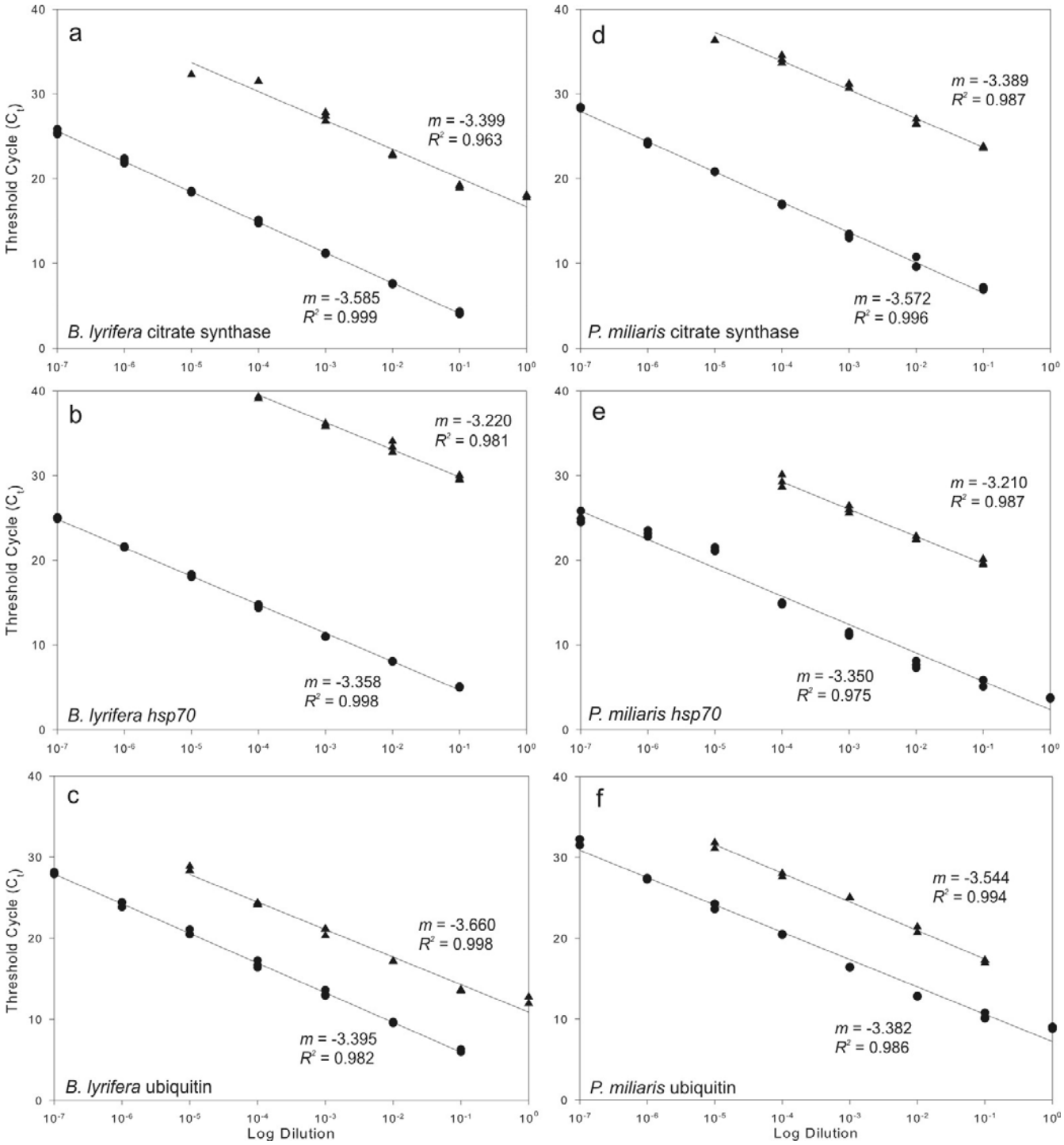

Figure 3.5 Plasmid (●) and cDNA (▲) standard curves for each gene of interest. qPCR reactions were run according to the cycling conditions listed at Table 3.1 for all primer pairs apart from the *P. miliaris ubi* primers (see main body of text). Primer pair concentrations were as listed in Table 3.3. The slope of each linear regression (*m*) is listed, as is the R^2 value (all R^2 values at $p < 0.05$).

Table 3.4. Summary of the attributes for the plasmid and cDNA standard curves for each primed qPCR assay for gene of interest illustrated at Figure 3.5.

Species / Gene	Template	*m*	Efficiency (%)	R^2 (p<0.05)	Sensitivity
P. miliaris					
Citrate synthase	Plasmid	-3.572	91	0.996	10^{-1} to 10^{-7}
	cDNA	-3.389	97	0.987	10^{-1} to 10^{-4}
Heat shock protein 70	Plasmid	-3.350	99	0.975	10^{-1} to 10^{-7}
	cDNA	-3.210	105	0.987	10^{-1} to 10^{-4}
ubiquitin	Plasmid	-3.382	98	0.986	10^{-1} to 10^{-7}
	cDNA	-3.544	92	0.994	10^{-1} to 10^{-5}
B. lyrifera					
Citrate synthase	Plasmid	-3.585	90	0.999	10^{-1} to 10^{-7}
	cDNA	-3.399	97	0.963	1 to 10^{-5}
Heat shock protein 70	Plasmid	-3.358	99	0.998	10^{-1} to 10^{-7}
	cDNA	-3.220	104	0.981	10^{-1} to 10^{-4}
ubiquitin	Plasmid	-3.660	88	0.998	10^{-1} to 10^{-7}
	cDNA	-3.395	97	0.982	10^{-1} to 10^{-5}

3.3.1. qPCR specificity

Whilst the efficiency and sensitivity of the qPCR assays could be determined from the linear regressions, specificity could not. Instead, gel electrophoresis to check the size of the products amplified during the qPCR was performed and the melt curves from the qPCR assays were inspected for indications of whether non-specific products or primer dimers were generated in the reactions (Nolan, 2007). It can be seen from the gel electrophoresis results (Figure 3.6) that amplicons corresponding to the expected size of PCR product were generated in each of the qPCR assays, with no evidence of a second band that would represent misprimed amplicons. The qPCR melt curves also did not suggest the presence of non-specific priming.

3.4. Experimental samples: from tissue collection to transcript copy number

3.4.1. Tissue collection

The isolation of mRNA transcripts from experimental tissue samples is a crucial process, as the RNA quality influences subsequent qPCR results (Fleige et al., 2006). Ribonucleases (RNases) are enzymes that degrade RNA, and are found in nearly all cells as they have an important role in nucleic acid metabolism. To limit the degradation of experimental RNA samples by RNases, steps

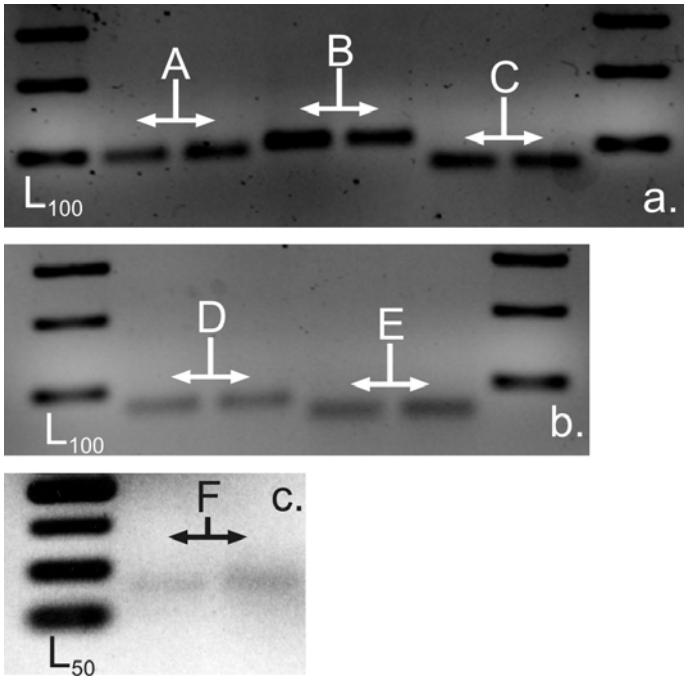

Figure 3.6 Gel electrophoresis of qPCR products to check amplicon size against that expected, which is included in brackets below. L_{100} = 100 bp ladder, bottom most band in figures a and b is 100 bp in size. L_{50} = 50 bp ladder, bottom most band in figure c is 50 bp in size. a) A = *P. miliaris ubi* (99 bp), B = *B. lyrifera ubi* (106 bp), C = *P. miliaris hsp70* (78 bp), b) D = *P. miliaris cs* (82 bp), E = *B. lyrifera cs* (67 bp), c) F= *B. lyrifera hsp70* (78 bp).

were taken to limit RNase contamination. In additional to good laboratory working practices, these included the use of RNase decontamination solution (RNase Away®), RNase-free filter barrier pipette tips and the use of previously unopened (hence uncontaminated) certified RNase-free chemicals, reagents and consumables.

Tissue samples dissected from *P. miliaris* were immediately placed in RNA*later*® Solution, frozen in liquid nitrogen (N_2) and stored at -80°C until processed. RNA*later* Solution is a stabilisation solution that prevents RNA degradation by released cellular RNases before the RNA can be extracted and isolated (Ambion, 2008). Although immediate freezing of tissue samples is not required when RNA*later* Solution is used for tissue storage, as this additional process was readily available when processing the *P. miliaris* tissues it was used to further protect samples from RNA degradation. Tissue samples from *B. lyrifera* were dissected and placed immediately into RNA*later* Solution, stored at 4°C overnight and then stored at -80°C until required.

3.4.2. RNA isolation

The tissue samples in the RNA*later* Solution were defrosted immediately prior to the TRI Reagent extraction process. The samples were removed from the RNA*later* Solution with sterile forceps, excess solution carefully blotted from the sample, placed immediately in TRI Reagent and

promptly homogenized. The RNase inhibitory function of RNA*later* Solution was hence taken up by the TRI Reagent as soon as the cells were disrupted. RNA isolation was based on the TRI Reagent protocol (Appendix 1.3). An appropriate volume of nuclease-free water (QIAGEN) was used to resuspend the resulting pellets of total RNA. The approximate quantity and quality of the RNA present in the samples was determined via Nanodrop spectrophotometry (Appendix 1.4).

3.4.3. DNase treatment and RiboGreen® quantification

Prior to reverse transcription, 2 µg of each total RNA sample was treated with 1 unit of deoxyribonuclease (DNase) I (Appendix 1.6). Deoxyribonuclease is an endonuclease that digests double and single stranded DNA. Purified DNase, free of residual RNases, is used to eliminate contaminating genomic DNA from RNA samples prior to use in applications sensitive to DNA contamination such as qPCR (Bustin, 2002). The quantity of total RNA in each DNase I treated sample was then determined using Quant-iT™ RiboGreen® RNA reagent (Appendix 1.5), an ultrasensitive (detecting as little as 25 pg ml^{-1}) fluorescent nucleic acid stain which binds to single stranded RNA and fluoresces in proportion to the quantity of RNA present. The use of this fluorescent nucleic acid dye is a preferential method for determining the quantity of RNA in a sample in comparison to Nanodrop spectrophotometry because contaminant interference from proteins, DNA and free nucleotides is minimised (Bustin, 2000). It is also the most accurate and convenient technique for quantitating large numbers of RNA samples (Nolan et al., 2006). The quantity of total RNA in each experimental sample was determined from comparison with the linear gradient of a standard curve generated from a series of diluted stock RNA standard of known concentration (provided with the RiboGreen Kit). The RNA standard was quantified using the same working solution of RiboGreen as that used to quantify the experimental samples. Each RNA sample (2 µl) was quantified in duplicate to determine the concentration of RNA in ng μl^{-1}.

3.4.4. Reverse transcription

The reverse transcription step is extremely important within an optimised qPCR assay (Bustin, 2008), as the synthesised cDNA must accurately reflect the input number of mRNA transcripts (Kubista et al., 2006) and the reverse transcription step has been found to contribute greatly to unwanted inter-sample qPCR results variation (Ståhlberg et al., 2004). The reverse transcriptase SuperScript™ III (200 units) was used to synthesise first strand cDNA from 300 ng total RNA (Appendix 1.7). This enzyme was selected for use because it was considered to have the best efficiency of commercially available reverse transcriptases (Ståhlberg et al., 2004; Pfaffl, 2007).

Oligo$(dT)_{23}$ priming is not suitable for qPCR reverse transcription because it does adequately prime degraded RNA samples, and the transcription process may not reach the target sequence if

this is not located near to the 3'-end (Kubista et al., 2006). The reverse transcription process is less affected by degraded RNA if random primers are used, as they anneal to any part of an RNA transcript, not just to the 3'-poly(A) tail. The use of random primers does, however, result in the priming of the total RNA in the sample not just mRNA transcripts. It is possible to minimise this background priming by instead using mRNA sequence-specific primers, a strategy which has been found to generate optimal results for qPCR (Bustin, 2000). Following the sequence-specific priming strategy in this study, however, would have required each RNA sample to be reverse transcribed three times in order to generate first strand cDNA for each GOI, and hence involve additional expenditure on reagents and time. Therefore, random nonamers (9-base oligodeoxy-nucleotides; 2 µM final concentration) were used to prime the RNA for cDNA synthesis.

The reverse transcription reactions were performed in as few batches as possible in order to limit reverse transcription variability and hence limit unwanted inter-sample cDNA variation. A common reference 'calibrator' sample was included in all batches to provide the ability to subsequently normalise qPCR results for reverse transcription inter-batch variation (Nolan et al., 2006). Once synthesized, the first strand cDNA samples were stored at -20ºC until they were used in the final qPCR assays (Appendix 1.9).

3.4.5. Final qPCR assays

All qPCR assays were performed using the Rotorgene-3000 real time thermal cycler. The thermal cycling conditions, primers and primer concentrations optimised for each GOI, as discussed above, were used. Experimental cDNA samples were run in duplicate, together with duplicate no template controls. In each run of the thermal cycler duplicate calibrator cDNA samples, corresponding to the cDNA sample reverse transcription batch, were also run with the same reaction mix as the experimental cDNA samples. The qPCR reaction mix contained 1 µl of experimental cDNA sample, each qPCR primer (final concentrations as listed in Table 3.3), 10 µl Precision Master mix with SYBRgreen (PrimerDesign Ltd.) and nuclease-free water to a total volume of 20 µl (refer to appendix 1.10 for a summary of the qPCR protocol).

3.4.6. Calculation of starting transcript numbers

Standard curves, required to calculate the number of mRNA transcript copies originally present in the starting total RNA experimental samples, were generated from new qPCR assays of serial dilutions of NotI linearised pCR4-TOPO plasmid vectors containing inserts for the GOI (section 2.4.7). Calibrator cDNA samples from the reverse transcription batches were also run at the same time in order to provide normalisation values with which to correct the experimental cDNA samples for reverse transcription batch variation (see below). The number of copies of standard

curve plasmid vector in each diluted sample was determined using the following equations, where the concentration of the plasmid vector in g μl^{-1} was determined from optical fluorescence measurements using the PicoGreen® dsDNA Quantitation Reagent (Appendix 1.6):

$$\text{Number of plasmid vector copies } \mu l^{-1} = \frac{6.022 \times 10^{23}\left[copies/mol\right] \times concentration\ \left[g/\mu l\right]}{Plasmid\ molecular\ weight\ (MW)\ \left[g/mol\right]}$$

Where

Plasmid molecular weight (MW) (g/mol) = (plasmid bp + insert bp) x 660 Da

6.022×10^{23} (copies/mol) = Avogadro's number

660 Da = Average weight of a single base pair.

For example, the number of plasmid vector copies in the *B. lyrifera cs* plasmid sample standard (which had been diluted 10 fold) was calculated as follows:

$$\text{plasmid copy number (copies } \mu l^{-1}) = \frac{6.022 \times 10^{23}\left[copies/mol\right] \times (8.1 \times 10^{-12}\left[g/\mu l\right])}{(3956+424) \times 660\ \left[g/mol\right]}$$

$$= 1.686 \text{ x } 10^{6}$$

The plasmid copy numbers in each of the other diluted samples used to generate the plasmid qPCR serial dilution could then be calculated and the standard curve plotted (C_q against $\log_{10}$(copies μl^{-1})). The equation for the linear regression of the standard curve was then rearranged and used to calculate the number of starting copies of mRNA transcripts from which the cDNA experimental samples were reverse transcribed. For example, the linear regression equation for the *B. lyrifera cs* standard curve was rearranged as follows:

$$C_q = \left(-3.315 \times \log\left(copy\ number\right)\right) + 25.375$$

$$\text{transcript copy number} = 10^{\frac{C_q - 25.375}{-3.315}}$$

The rearranged equation was then applied to the mean C_q values for the duplicate experimental cDNA samples once they had been normalized to that of the corresponding cDNA calibrator sample included in each qPCR assay (Wong and Medrano, 2005). To normalise the mean C_q values of the experimental samples, they were multiplied by the ratio found between the mean C_q values for the calibrator samples when run with the experimental cDNA samples and also when run with the standard curve plasmid serial dilutions.

The experimental cDNA samples included in the qPCR assays (1 µl) had been taken from 20 µl cDNA samples, reverse transcribed from 300 ng of total RNA. To standardise the copy number results to transcript copies per µg total RNA the calculated copy number was then multiplied by the following factor: 20/(300 x 10^{-3}). The following worked example, based on a *B. lyrifera* cDNA

sample run with a *cs* qPCR assay, is provided to illustrate the above calculations:

Experimental cDNA C_q results: 20.82 and 20.66, mean C_q = 20.74
Calibrator sample, run with experimental cDNA samples, C_q: 19.91 and 19.96; mean C_q =19.94
Calibrator sample, run with plasmid dilution series, C_q: 21.96 and 21.96; mean C_q = 21.96
Ratio of calibrator samples: 21.96 /19.94 = 1.101
Adjusted Experimental cDNA C_q = 20.74 x 1.101 = 22.84
Transcript copy number in cDNA sample subject to qPCR = $10^{((22.83-25.375)/-3.315)}$ = 5.82
Transcript copy number per µg total RNA = 5.82 x (20/(300 x 10^{-3}) = 387.80

3.5. Final qPCR assay: conclusions

Optimisation of the qPCR methodology

By virtue of its accuracy, sensitivity and fast results, qPCR is now a routine technique and considered the 'gold standard' for medium throughput gene expression analysis (Bustin, 2010; Derveaux et al., 2010). However, it is easy to produce inaccurate results from an inadequately standardised qPCR assay (Huggett et al., 2005; Bustin, 2010). Whilst every effort was made to optimise the qPCR assays used in this study and to ensure assay specificity, sensitivity and accuracy, there are areas of the qPCR methodology followed that can introduce sources of potential error, but actions were taken to minimise these as discussed in the above chapter.

As can be seen from the summary of the standard curve results (Table 3.4), the recombinant DNA and cDNA standard curve qPCRs displayed highly similar efficiencies and R^2 values. This indicated that the recombinant DNA provided a valid standard for experimental sample quantification. The sensitivity ranges and efficiencies of the qPCR assays (80-105%) were also all acceptable according to the guidelines give by Nolan et al. (2006), indicating that the qPCR assays were satisfactorily optimised and would produce reliable results with experimental samples.

Based on the melt curve and gel electrophoresis results, the selected primer pairs in the concentrations listed in Table 3.3 showed no evidence of mispriming and the amplification of non-target products. These primers and concentrations were used for the final optimised qPCR assays for the *P. miliaris* and *B. lyrifera* experimental samples.

The final qPCR assays for each GOI for each echinoid species therefore appeared to be well optimised, and capable of producing reliable quantitative results. The methodology listed in this chapter to process all experimental samples was followed for all *P. miliaris* and *B. lyrifera* experimental cDNA samples, and the calculations detailed above were used to obtain transcript copy numbers per µg total RNA.

Chapter 4. The stress response of the intertidal echinoid, *Psammechinus miliaris*

4.1. Introduction

As discussed in Chapter 1, it has been found that differences occur in the stress responses exhibited by organisms which inhabit environments that differ in terms of their physical variability. This leads to the theory that a eurytopic organism (or population) inhabiting a highly variable, and hence physiologically demanding and stressful, environment may be more able to cope with another encountered stress due to the adaptive response(s) that can be induced as a result of their historical experiences (Hoffmann and Parsons, 1991; Minois, 2000; Badyaev, 2005). Conversely, stenotopic organisms inhabiting more stable environments have a reduced requirement to cope with environmental variability and are hence more sensitive to stressful conditions due to a reduced adaptive capacity to respond accordingly (Angel, 1992; Seibel and Walsh, 2003; Timofeyev and Steinberg, 2006). This theory is extended to contaminant-induced stress, where an organism which has evolved in, and is adapted to, a physically variable environment is better able to tolerate stress caused by a contaminant than an organism adapted to a stable environment (Fisher, 1977).

In this current study, the responses of two species of echinoid to challenge by an anthropogenic contaminant were investigated. The species were selected to represent echinoderms inhabiting environments typified by inherently different levels of physical stress. *Psammechinus miliaris*, an intertidal epibenthic sea urchin, was considered to represent a eurytopic echinoderm adapted to a physically variable, and hence stressful, environment. *Brissopsis lyrifera,* an infaunal sea urchin with a preference for stable benthic environments was considered to represent a stenotopic echinoderm adapted to a typically low stress environment. As such, it was predicted that *P. miliaris* would readily exhibit a response to contaminant exposure, whilst *B. lyrifera*, by virtue of a reduced adaptive capacity to respond to environmental perturbation, would not. Due to their adaptation to an environment characterised by an absence of variability, deep-sea organisms are also considered to lack the capacity adaptations to facilitate homeostatic regulation in the face of environmental perturbation (Seibel and Walsh, 2003), and to hence have little tolerance to environmental change (Angel, 1992). The *B. lyrifera* stress response could hence be expected to be representative of that which would be expected from stenotopic deep-sea echinoderm species. In this regard, should differences between the *P. miliaris* and *B. lyrifera* stress responses be apparent, a recommendation could be made that future experimental work investigating the impact of anthropogenic activity on deep-sea echinoderms using shallow water proxies should ensure stenotopic species were used in preference to eurytopic species.

The variation in stress response between organisms inhabiting different environments has been demonstrated in studies with amphipods from supralittoral to deeper water habitats. In response to oxidative stress immediate changes in the activities of antioxidant enzymes were found in amphipod species inhabiting the upper littoral zone of the freshwater Lake Baikal, but in the deeper living species collected from 50-100 m depth no change in these enzyme activities was evident until after 6 days of exposure (Timofeyev and Steinberg, 2006). It was noted that the deepest living species (with a delayed stress response) was generally regarded as a very sensitive organism when exposed to any significant environmental stress other than pressure (Timofeyev and Steinberg, 2006). Similar differences in the immediacy of antioxidant enzyme change were also found in response to acute heat stress between amphipod species inhabiting the more variable supralittoral zone (in which a rapid oxidative enzyme response was found) and the comparatively more stable sublittoral zone in which a delayed response was found (Bedulina et al., 2010).

The work presented in the current chapter introduces and discusses exposure experiments performed with *P. miliaris*, whilst the subsequent Chapter 5 presents the results of the *B. lyrifera* exposure experiments and a comparison between the stress responses of the two species. In order to detect possible variation in the stress response of the two echinoids at different biological levels of investigation (Depledge, 1998; Dalziel et al., 2009), a suite of biomarkers were selected for the investigation of their stress responses. The contaminant was a water based drilling fluid used by the offshore drilling industry, and one that would be expected to enter the deep-sea environment (discussed in the next section).

4.1.1. Deep-sea hydrocarbon exploration

As the worldwide demand for oil continues, existing hydrocarbon fields continue to age and drilling technologies advance, the oil industry is being pushed into ever deeper waters to feed global oil consumption. The offshore drilling industry has advanced from exploratory drilling in 185 m water depth in 1956 to a record 3051 m in the Gulf of Mexico in 2003 (Brandt et al., 1998; Transocean, 2003). Today in the Atlantic, developments to the west of the Hebrides and Rockall in waters in excess of 2000 m are being considered (OSPAR Commission, 2009). The drilling industry generally defines ‘deepwater’ as greater than 500 m, and waters in excess of 2000 m as ‘ultradeep’ for drilling purposes (Pettingill and Weimer, 2002). It has been estimated that 95% of unexplored offshore oil fields lie in water deeper than 915 m (Brandt et al., 1998) and with the construction of ultra-deepwater drilling vessels, capable of operating in water depths of up to 3650 m (Chevron Inc, 2010; Transocean, 2010), it is clear that the bathyal and abyssal deep-sea is not out of reach for the oil and gas exploration industry.

Benthic impacts of deepwater hydrocarbon exploration

Most deepwater drilling operations and activities are substantially the same as those associated with operations on the shallower continental shelves, and the general impacts on the environment will be similar to those in shallow water (Carney, 1998). Large scale incidents at deepwater platforms are considered to only pose an occasional hazard to marine life, instead likely to be just a temporary ecological incident (Glover and Smith, 2003); a view that will be tested by the release of hundreds of thousands of barrels of oil at the seafloor at 1522 m in the Gulf of Mexico (GOM) following the Deepwater Horizon underwater blowout in April 2010.

The primary impacts of offshore drilling upon the local benthic environment come from the release of drilling fluids (see below) and drill cuttings (particles of crushed rock produced as the drill bit grinds against formation rock) from the drilling platform into the sea. The major pollution sources from offshore drilling installations arise from the discharge of such waste products, including produced-water (water injected into the reservoir to maintain pressure or water naturally associated with the oil), drilling fluids and cuttings, and crude oil from the extraction process (Holdway, 2002). Although discharge of drill cuttings occurs after separation from the majority of drilling fluids, the cuttings which accumulate on the seabed when water currents are insufficient to cause dispersal are usually contaminated with drilling fluids (Figure 4.1); an issue of concern in areas with sensitive benthic fauna (Glover and Smith, 2003; OSPAR Commission, 2009).

The accumulation of cuttings contaminated with drilling muds at the seafloor, together with a constant low level release of hydrocarbons around drilling platforms, cause a chronic level of environmental pollution. Biological exposure to these contaminants continues over long periods of time and over wide shelf areas, causing substantial ecological change (Gray et al., 1990; Olsgard and Gray, 1995; Peterson et al., 1996). The primary changes that occur to sediments close to drilling platforms are alterations in sediment texture, increased hydrocarbon and trace metal concentrations, and organic enrichment (Kingston, 1992; Peterson et al., 1996). These sedimentary changes result in local benthic community diversity changing due to toxicity and organic enrichment, typically with an increase in polychaetes and a decrease in crustacea and echinoderms (Kingston, 1992; Peterson et al., 1996). The extent of the benthic disturbance around a platform is dependent on the type of drilling fluid used, with that caused by oil based fluids being detectable up to 10 km from a drilling platform (Gray et al., 1990; Kingston, 1992; Olsgard and Gray, 1995). The disturbance associated with water based fluids is reported to only extend to 200 m (Peterson et al., 1996).

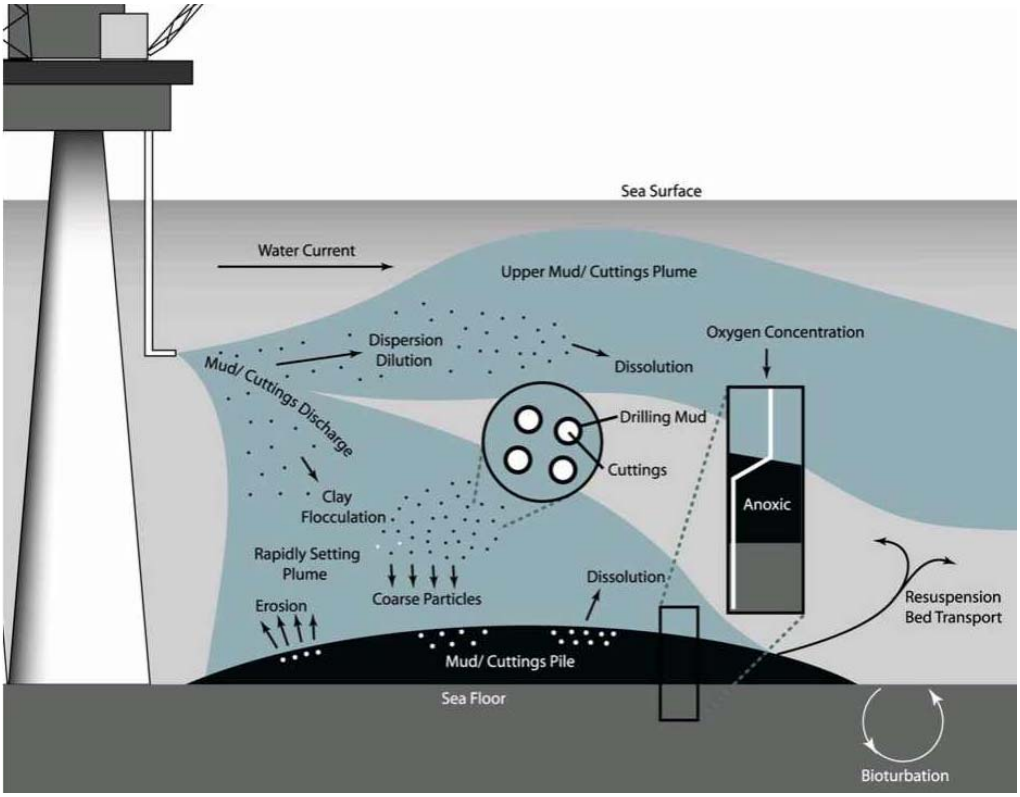

Figure 4.1. Dispersal and fate of water based drilling mud (WBM) following discharge. The WBM forms two plumes; the upper contains fine-grained unflocculated solids and dissolved components of the mud, the lower rapidly settles to the seabed and contains dense larger-grained particles, including cuttings. The WBM solids undergo dispersion, dilution, dissolution, flocculation, and settling in the water column. If the WBM contains a high concentration of organic matter, the cuttings pile may become anaerobic near the surface. The cuttings pile is altered by redox cycling, bioturbation, and seabed transport. Figure taken from Neff (2005).

Drilling fluids and chemicals

The successful drilling of an oil well depends to a large extent on drilling fluids, or drilling muds as they are also called. Drilling fluids are used for a variety of reasons, including (OSPAR Commission, 2001; Holdway, 2002; Neff, 2005):

a) to control well pressure to prevent blowouts or to prevent the well collapsing during drilling,

b) to wash drill cuttings from the drill bit and then lift them to the surface,

c) to lubricate, cool and clean the drill bit,

d) to support the weight of the drill pipe, and

e) to provide information about what is happening downhole by monitoring the behaviour, flow-rate, pressure and composition of the drilling fluid.

The base fluid of a drilling mud determines its classification; water for water based muds (WBM),

oil for oil-based muds (OBM) and a number of different hydrocarbons for synthetic-based muds (SBM). The discharge of OBM and SBM is banned or restricted in various regulatory regimes around the world due to their toxicity and enrichment in organic matter (Neff, 2005). Because of this, WBM are commonly used as drilling fluids as they are permitted to be discharged directly to the seafloor, and WBM cuttings are discharged continuously during actual drilling (Holdway, 2002; Continental Shelf Associates Inc., 2006; OSPAR Commission, 2009). WBMs consist of fresh or salt water containing a weighting agent, clay or organic polymers, various inorganic salts, inert solids or organic additives (Neff, 2005). The WBMs are customised via the addition of other substances in order to meet the demands of the well to be drilled. These include weighting agents, viscosifers, pH control additives, corrosion inhibitors, dispersants, flocculants, surfactants, biocides, fluid loss reducers and calcium reducers. While many of these additives are readily water soluble and will be removed during the separation of the drilling mud from drill cuttings prior to cuttings discharge into the sea, some will inevitably contaminate the cuttings (Boehm et al., 2001; Neff, 2005). The impact of WBM on benthic communities have been documented to be less severe than those from OBM and SBM (Daan and Mulder, 1996; Sayle et al., 2002; Neff, 2005). However, WBM-cuttings represent the most common discharge from drilling operations and detrimental effects of WBM have been observed in field and experimental studies (Peterson et al., 1996; Cranford et al., 1999; Schaanning et al., 2008; Trannum et al., 2010).

In deep water it is anticipated that an increased need for the chemical components that improve the flow of oil and gas will be required due to the cold temperatures and high ambient pressures encountered (Boehm et al., 2001). The average deepwater well uses approximately 14 times more drilling fluid chemicals than the shallow water well. Most of this is weighting agent (barite) but higher amounts of hydrate inhibitors and defoamers are also needed due to the deepwater environment and the nature of the produced fluids (Boehm et al., 2001). These chemicals often enter the waste stream which is discharged into the ocean following treatment. As such, a WBM was used for the echinoid exposure experiments during this current study as representative of an anthropogenic contaminant likely to enter the deep-sea environment.

The deep-sea ecosystem and deepwater hydrocarbon exploration

The following characteristics of deep-sea ecosystems have been identified as relevant to the determination of the environmental impact of deepwater hydrocarbon exploration activities, and are also relevant to other anthropogenic activities in the deep sea (Carney, 1998; Boehm et al., 2001; Carney, 2001; Glover and Smith, 2003):

1) Vertical zonation: the benthic fauna changes progressively with depth. Species in the deep

sea are different to those found in shallow water and, as discussed in Chapter 1, the direct application of the results of shallow-water toxicology studies to the deep sea is problematic. Until large scale deep-sea experimentation is possible, however, shallow-water based studies are the best option available to explore and understand the impacts of contaminants in the deep sea.

2) Biodiversity: deep-sea biodiversity is high, but the reasons behind this are poorly understood. Some explanations suggest that the stable deep-sea environment is a factor in generating high biodiversity but, as already discussed, stability also means that deep-sea communities may have a low resistance to environmental perturbations.

3) A predominance of soft bottom and deposit feeding organisms: with the consequence that any chemical input or disturbance activity that causes a change in food availability at the seafloor would be potentially significant to deep-sea organisms.

These characteristics demonstrate that the sensitivity of deep fauna to drilling impacts must be known before accurate environmental assessments of hydrocarbon exploration can be made. Additionally, before appropriate deep-sea monitoring regimes and regulations can be developed and applied to the deep-sea oil and gas industry, the nature of faunal gradients and the processes behind species diversity in deep water must be understood (Carney, 2001).

4.1.2. Biomarkers for the assessment of the effects of exposure to WBM

A suite of biomarkers was selected for the analysis of the effects of WBM exposure upon *P. miliaris*, into order to assess the stress response at more than one level of biological organisation (Depledge, 1998). Biomarker responses that were indicators of the general, or non-specific, stress-response of *P. miliaris* were selected for application to the exposure experiments (Depledge, 1998), as opposed to those that show some degree of specificity (e.g. metallothionein induction in response to metal exposure), because any specific action of the WBM and the possible reaction by *P. miliaris* was not known.

Behavioural (whole organism) biomarker

A variety of echinoderm behavioural assays have been reported in the published literature, including responses to mitigate the potential effects of a contaminant stressor and those demonstrating the effects of a toxicant at the whole organism level (Appendix 1.1). Many of these assays have indicated a dose-dependent sensitivity including: burrowing behaviour, avoidance of contaminated sediment, righting response time, feeding rate and foraging behaviour (Ordzie and Garofalo, 1981; O'Clair and Rice, 1985; Newton and McKenzie, 1998; Temara et al., 1999; Georgiades et al., 2003; Ryder et al., 2004; Canty et al., 2009). The behavioural biomarker used

during the *P. miliaris* experiments was righting response – i.e. the time required for an inverted echinoid to return to its normal orientation. This behavioural assay has been used previously with echinoids and it has been found to be sensitive to sublethal stress (Lawrence and Cowell, 1996; cited in Ubaldo et al., 2007) with a concentration- and time-dependent response (Lawrence, 1975; Axiak and Saliba, 1981; Davies et al., 1998; Böttger et al., 2001; Canty et al., 2009).

Physiological biomarker

An organism's oxygen consumption rate is an important physiological measurement. It is used as a practical measure of the metabolic rate of an organism (Schmidt-Nielsen, 1981; Burggren and Roberts, 1991) as it can be precisely quantified and represents the overall metabolic demand being made upon an individual at the time of measurement (Bayne et al., 1985; Dahlhoff, 2004). In response to pollutant stress, oxygen consumption rates show a clear dose-response in many organisms (Handy and Depledge, 1999), but the direction of the response is not consistent. It has been demonstrated that echinoderm oxygen consumption rates alter in response to sub-optimal environmental conditions including decreasing in response to altered salinity (Talbot and Lawrence, 2002), increased in response to elevated pH (Farmanfarmaian, 1966), and increased following hydrogen sulphide exposure (Christensen and Colacino, 2000).

Cytological biomarker

Echinoderm coelomocytes

Echinoderms have large body cavities, filled with coelomic fluid that contains free cells called coelomocytes. The coelomocytes are part of the echinoderm immune defence system, being the main effectors of the defence response and capable of chemotaxis, phagocytosis and cytotoxic metabolite production (Chia and Xing, 1996; Matranga et al., 2005; Smith et al., 2006). It is currently agreed that four types of echinoid coelomocyte exist: phagocytes (seen in either a petaloid or philopodial form), spherule cells (also referred to as amoebocytes) in either a red or colourless form, and vibratile cells that have a long flagellum (Smith, 1981; Matranga et al., 2005). The proportions of each cell type in echinoderm coelomic fluid varies interspecifically, and also intraspecifically depending on an individual's size or physiological condition (Matranga et al., 2005). Three other echinoderm coelomocyte types are also reported in the literature: crystal cells, progenitor cells and haemocytes (containing haemoglobin), but these have not been reported as present in echinoid coelomic fluid (Smith, 1981; Chia and Xing, 1996).

Cytological related investigations of echinoderm stress which have detected detrimental effects of pollutants have included assessments of lysosomal integrity (Békri and Pelletier, 2004), phagocytic activity (Békri and Pelletier, 2004) and changes in the populations of circulating

coelomocytes (Pinsino et al., 2008). The total number of coelomocytes in echinoderm coelomic fluid has been found to increase in response to hypoxia and wounding stress (Holm et al., 2008) and manganese exposure (Oweson et al., 2008). Within the echinoid coelomocyte population, red spherule cells are found to increase in number in response to injury or pollution (Matranga et al., 2000; Pinsino et al., 2008). Further to this evidence of echinoderm coelomocyte variation in response to stress, during the current *P. miliaris* study, total and differential coelomocyte counts were used as cellular level biomarkers.

Biochemical biomarker

Biochemical assays involve the measurement of molecular components of cells, tissues or extracellular fluids (Bayne et al., 1985). Within the variety of biochemical assays, metabolic enzyme activities have been used as indices of an organism's physiological condition, being useful where accurate determination of field metabolic rate is difficult (Dahlhoff, 2004). Whilst metabolic enzyme activities have also been successfully used as ecotoxicological biomarkers in a number of fish and invertebrate studies (section 2.1.1.1), published data on echinoderm toxicological investigations with metabolic enzyme activities are scarce. Despite this, in order to investigate its application as a biomarker and possible interaction with the expression of the citrate synthase gene (see below) and the oxygen consumption rate of the *P. miliaris* specimens, an assessment of citrate synthase (CS) enzyme activity was included in this study. CS is an important regulatory enzyme, being one of the 'pace-maker' enzymes in the citric acid cycle (Goldenthal et al., 1998). The activity of CS is an indicator of aerobic metabolism occurring at the mitochondrial level, and hence of an organism's metabolic capacity (Seibel and Childress, 2000).

Molecular biomarker

Quantification of the expression of certain genes in an organism can provide a sensitive indicator of an organism's exposure to toxicants (Calzolai et al., 2007), and altered gene expression has been used as a biomarker of both environmental- and pollutant-induced stress in aquatic invertebrates for a number of years (Feder and Hofmann, 1999; Bierkens, 2000; Dahlhoff, 2004). In this current study quantitative PCR (qPCR) was used to assess the level of expression of the genes coding for citrate synthase (*cs*), heat shock protein 70 (*hsp70*) and ubiquitin (*ubi*) in *P. miliaris*. The relevance of the expression of these genes, and the activity of the associated proteins, to toxicological studies has been discussed at length in chapter 2 (section 2.1.1.1 to 2.1.1.3).

In summary, as an indicator of aerobic metabolism, and to compliment the assessment of the activity of the enzyme, the expression of the *cs* gene was selected for quantification. The other two genes, *hsp70* and *ubi,* code for two proteins whose expression is up-regulated during a cellular

stress response. Heat shock protein 70 stabilizes denaturing proteins and refolds reversibly denatured proteins (Lindquist, 1986; Feder and Hofmann, 1999). Ubiquitin is a protein that 'tags' irreversibly damaged molecules for destruction (Finley and Chau, 1991). In studies of an organisms stress response, *hsp70* expression can be viewed as a measure of reversible protein damage; *ubi* expression as a measure of irreversible protein damage. The presence of high amounts of these two proteins can therefore be used as a proxy for cell stress (Dahlhoff, 2004).

4.1.3. The ecology of *Psammechinus miliaris* (Müller, 1771)

P. miliaris is an epifaunal regular echinoid (Figure 4.2) found throughout the British Isles from the intertidal zone to a depth of 100 m (Ellis and Rogers, 2000; Southward and Campbell, 2006). Intertidally it is found on rocky shores under stones, boulders and seaweeds, whilst subtidally it is found in seagrass beds or on mixed coarse bottoms such as muddy sand and gravel and also on artificial structures such as those associated with bivalve and fish culture (Kelly et al., 2007; Jackson, 2008). It is commonly known as the 'green' or 'purple tipped' sea urchin.

P. miliaris can reach up to 75 mm test diameter, but British populations more typically range in size from 5 to 35 mm (Bedford and Moore, 1985; Jackson, 2008). It is an omnivore, feeding on a wide range of food types including algae and associated epizoic animals, fresh plant material and a variety of benthic invertebrate fauna including other echinoderms (Kelly et al., 2007). *P. miliaris* may have a key ecosystem role, its grazing pressure being sufficient to control macro-epiphytic biomass, intertidal encrusting communities and fouling organisms on bivalve cultivation and salmon cage nets (Guillou et al., 2002; Ross et al., 2004; Kelly et al., 2007), but conclusive studies demonstrating its importance within its ecosystems have not been reported (Jackson, 2008).

The most recent research involving *P. miliaris* has been concentrated on the development of this species as an edible sea urchin (Kelly et al., 2007) and the impact of increased CO_2 and reduced pH conditions, which are predicted to have major impacts on the biomineralisation process in echinoderms (Miles et al., 2007; Dupont et al., 2010). Other studies have demonstrated that *P. miliaris* is a suitable organism for toxicological investigations. Adults of the species are found to bioaccumulate contaminants such as the antibiotic oxytetracycline, which reduces gonadal growth and sub-cuticular bacteria (Campbell et al., 2001). Developmental implications are found from exposure to the polycyclic aromatic hydrocarbon phenanthrene which causes gonadal lesions in female specimens (Schäefer and Köehler, 2009), whilst the diatom aldehyde 2E,4E-decadienal caused dose- and time-dependent decreases in sperm motility (Caldwell et al., 2004). In the field, *P. miliaris* demonstrates extreme sensitivity to oil, with 100 % mortalities recorded after oil spills on the coast of Cornwall and France (Smith, 1968; Barille-Boyer et al., 2004).

4.1.4. The Western Channel environment

The Western English Channel environment is considered to be an important biogeographic boundary between cold-temperature (Boreo-arctic) and warm-temperature (Lusitanian) provinces (Herbert et al., 2009). The Great West Bay, in which the Tor Bay collection site for the *P. miliaris* specimens was situated (Figure 4.3), is located within the warm temperature zone (Hiscock et al., 2004). There are large areas of intertidal rock in the Great West Bay, where the maximum tidal range is 4.0 to 4.5 m. Average winter sea surface (not intertidal) temperatures are ~8.5 °C, whilst summer temperatures are ~16 °C (Lee and Ramster, 1981 cited in Herbert et al. (2009)). In Tor Bay mean tidal range is 3.1 m, and whilst mean wave height is 0.5 m the maximum wave height extends to 3.0 m (SCOPAC, 2003).

The *P. miliaris* specimens were collected from underneath boulders or ledges in rock pools exposed during low tide. The rock pool environment is known to be extremely variable, with marked changes in physicochemical parameters (salinity, pH, temperature, oxygen tension) occurring over diurnal and seasonal time spans (Daniel and Boyden, 1975; Morris and Taylor, 1983). As such, the intertidal zone is considered to be a highly stressful physical environment (Hofmann, 1999; Tomanek and Helmuth, 2002).

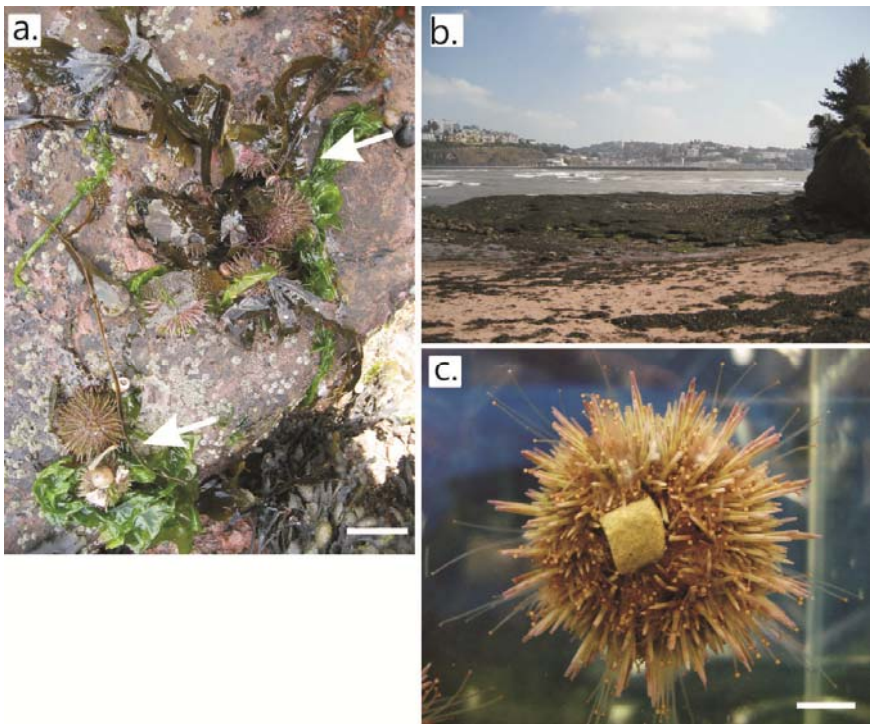

Figure 4.2. a. *Psammechinus miliaris* attached to the underside of a rock prior to collection in the field. White arrows indicate two groups of *P. miliaris*, which are hidden by algae and shell fragments attached to their tube feet, bar indicates 3 cm. b. Corbyn's Head, Torquay, UK, *P. miliaris* were collected from the intertidal zone, pictured here at low tide. c. Specimen of *P. miliaris* (oral view) feeding on a salmon feed pellet, bar indicates 0.75 cm.

4.1.5. Aims of the *P. miliaris* exposure experiments

The primary aim of the exposure experiments was to investigate whether a stress-response caused by exposure to a water based drilling fluid could be detected throughout a suite of biomarkers ranging from the behavioural to the molecular level of biological organisation in *P. miliaris*. For each biomarker, the specific null-hypothesis being tested was that WBM exposure would not cause a deviation in the observed biomarker response compared with that found in control specimens.

4.2. Materials and methods

4.2.1. Experimental procedure

Echinoids

Psammechinus miliaris were collected by hand from Corbyn's Head, a sandstone outcrop in Torquay in April 2008 (50° 27' 17 N; 3° 32' 38 W: Figure 4.3). They were held in recirculating aquaria, in which the original seawater supply had been sourced from Southampton Water, UK. The echinoids were fed *ad libitum* on *Ulva lactuca*, *Laminaria* sp. and salmon pellets (EWOS Ltd, Westfield, UK) until required for the exposure experiments, approximately eight weeks later.

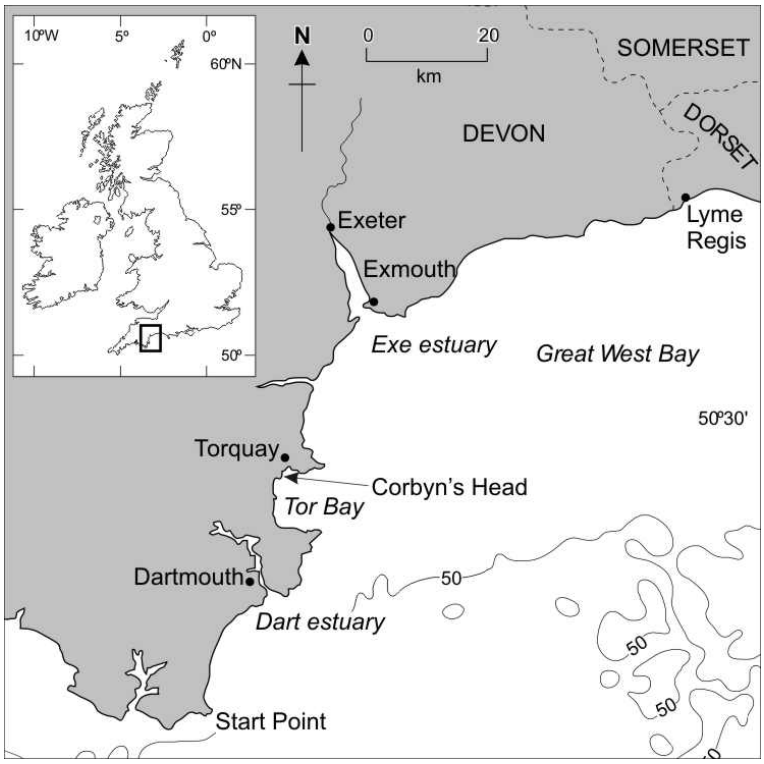

Figure 4.3. Region of the Western English Channel featuring Corbyn's Head located in Tor Bay, where the *P. miliaris* specimens were collected. Figure adapted from Davies (1998).

WBM Drilling fluid

Samples of a WBM called Water Based Spud Mud (WBSM), a water based drilling fluid manufactured by Baker Hughes (trade name not provided), were provided by BP p.l.c. WBSM is

used during the early stages of drilling at shallow depths in the upper section of the well to move large quantities of drill cuttings away from the hole (Mr. Rory Somerset, Baker Hughes Ltd., Aberdeen, pers. comm). Per the accompanying safety data sheets, the WBSM used in the experiments was comprised of 92.8 wt% water, 7 wt% Milben (bentonite), 0.1 wt% sodium hydroxide (NaOH, CAS No.: 1310-73-2) and 0.1 wt% sodium carbonate (Na_2CO_3, CAS No.: 497-19-8).

Bentonite, an absorbent silicate mineral (clay), is used in drilling muds to increase fluid viscosity and maintain the gel strength needed to suspend and carry drill cuttings to the surface and also to coat the borehole wall to prevent loss of fluids into permeable rock formations (Boehm et al., 2001; Neff, 2005). Sodium hydroxide is a strong base used to control the pH of the fluid and to cause clays to hydrate and thicken, so creating the viscosity needed to lift drill cuttings. Sodium carbonate is also used to control the fluid pH and its viscosity (Boehm et al., 2001).

Exposure experiments

In a range finding preliminary experiment, *P. miliaris* were exposed to concentrations of 1, 5, 10, 20, 50 or 100 ml L^{-1} WBSM, which was mixed with 120 µm-filtered seawater and remained in suspension at all times without further mixing required. The seawater was filtered to remove debris and / or plankton present in the recirculating seawater and maintained at 8°C. Each treatment consisted of aerated tanks (glass vessels with a volume of 1 L) containing three echinoids of approximately 35 - 40 mm diameter. The outcome of the range finding experiment is detailed in Table 4.1. Since no mortality occurred with the lowest concentration, 1 ml L^{-1} WBSM was chosen as the test concentration for the subsequent exposure experiments.

Table 4.1. Outcomes of the preliminary WBSM range-finding experiment. Echinoids non-responsive to touch (i.e. no tube feet movement upon physical stimulation) were defined as moribund.

WBSM ml L^{-1}	Observations and outcome
1	No apparent reaction upon entry to solution. Gut contents were ejected during the following 18 hours. After 5 days, two echinoids were unable to right themselves after being inverted.
5	No apparent reaction upon entry to solution. Gut contents were ejected during the following 18 hours. After 5 days, all echinoids were dead.
10	Spines depressed upon entry to solution, all moribund after 18 hours. All echinoids dead after 5 days.
20	Immediate rigidity of spines. After 1.5 hours spawning had occurred, all dead after 18 hours.
50	Immediate paralysis, removed from experiment after two hours
100	Immediate paralysis, removed from experiment after two hours

Echinoids of a minimum size of 20 mm horizontal test diameter were selected for the WBSM exposure experiments. Echinoids were exposed to 1 ml L^{-1} WBSM mixed with 120 µm-filtered seawater or in the control groups to 120 µm-filtered seawater only (total volume 8.5 L). Each treatment consisted of eight echinoids, held in a 17 °C temperature-controlled room (the temperature to which the echinoids were already acclimatised) in aerated static aquaria on a 12 hour light: 12 hour dark cycle. The experimental periods were 24, 48, 72 or 96 hours, after each time period had elapsed one experimental and one control group of echinoids was processed for biomarker responses. Every day, the temperature, pH and salinity of each remaining aquarium were checked with a hand held multi parameter instrument (L323-B conductivity meter, WTW, Weilheim, Germany) and 1 L of 120 µm filtered seawater or the WBSM-seawater mix renewed in each aquaria. The average temperature of all aquaria throughout the experimental period was 16.82 °C (± 0.07 SD). The mean pH and salinity for the control aquaria was 7.73 (±0.04 SD) and 35.29 (±0.14 SD), and for the experimental aquaria 7.81 (±0.05 SD) and 34.95 (±0.44 SD).

4.2.2. Experimental biomarkers

4.2.2.1. Righting response (behavioural biomarker)

Self-righting times were calculated as described by other authors (Axiak and Saliba, 1981; Böttger et al., 2001). Each echinoid was placed on its aboral surface on the base of an aquarium tank containing WBSM-free seawater. The time taken for the animal to right itself onto its oral side, visually assessed as the point when the test base was horizontal with the bottom of the aquarium, was measured. Once an echinoid had self-righted, it was transferred into a respirometer as soon as possible (see next section). Had an echinoid not made any movement to right itself within 30 minutes the trial period was ended and the urchin was placed into a respirometer.

4.2.2.2. Oxygen consumption rate (physiological biomarker)

Oxygen consumption rates were measured using closed-system respirometry in 500 ml clear glass Kilner jars. Oxygen concentration in the respirometers was measured using a Fibox 3 single-channel oxygen meter with accompanying oxygen probe on a 2 mm optical fibre (Pre-Sens Gmbh, Regensburg, Germany). Oxygen sensor spots, consisting of an oxygen-sensitive foil (diameter 5 mm with optical isolation, PreSens), were glued inside the Kilner jars using silicone rubber sealant (RS Components). Each sensor spot was calibrated prior to starting the experiments with 0% and 100 % oxygen in seawater. A saturated solution of sodium dithionite ($Na_2S_2O_4$) at a concentration of 25 mg ml^{-1} was used to remove all oxygen from seawater for the 0% calibration. Seawater saturated with oxygen was achieved via vigorous aeration for two hours.

An echinoid was transferred to a respirometer as soon as possible after the righting time had been

determined. WBSM-free seawater was used in the respirometer in order to remove the possibility of chemical interference with the oxygen sensor spots. The individual Kilner jars contained platforms consisting of a Perspex disc drilled with multiple holes and mounted on top of two Perspex blocks, which provided sufficient room for the movement of a magnetic stir bar underneath the platform. During placement of an echinoid inside a respirometer, both the Kilner jar and echinoid were held underwater at all times to avoid the introduction of air bubbles into the closed system. The closed respirometer was placed in an aquarium tank of water in order to maintain a stable temperature, and sited above an electronic stirrer positioned underneath the aquaria. The stirrer drove a stir bar underneath the platform to circulate gently the water enclosed in the respirometer to prevent an oxygen concentration gradient forming around the echinoid (Kamler, 1969; Irwin and Davenport, 2006). The entire aquarium was covered with black plastic sheeting in order to limit desensitisation of the oxygen sensor spot by ambient light.

The phase angle of the fluorescing chemical surface of the oxygen sensor was measured in the respirometer at the start of the incubation period, then again two hours later and then at hourly intervals. Measurements were recorded until the earlier of a) a reduction by 20% of the raw oxygen saturation value given by the Fibox unit, or b) six hours had elapsed. The measurements of phase angle readings from a control respirometer just containing filtered seawater were also taken. A custom designed MS Excel spreadsheet program from Christian Huber (Pre-Sens Gmbh) was used to calculate the oxygen concentration in μmol O_2 h^{-1}, with corrections for temperature (from the Fibox data) and air pressure (from www.sotonmet.co.uk), from the raw Fibox phase angle data.

The wet mass-specific oxygen consumption rate of an individual echinoid was then calculated from the change in the oxygen concentration of the seawater in the respirometer (with correction for the oxygen consumption in the control respirometer) during the incubation period according to the following equation:

$$\dot{M}O_2 = \frac{(Cwo_2(A) - Cwo_2(B))V}{T} * \frac{1}{M} \qquad [4.1] \quad \text{(Cech, 1990)}$$

Where,

$\dot{M}O_2$	= oxygen consumption rate (μmol O_2 g^{-1} $hour^{-1}$)
$Cwo_2(A)$	= oxygen concentration (μmol O_2 L^{-1}) at start of incubation
$Cwo_2(B)$	= oxygen concentration (μmol O_2 L^{-1}) at end of incubation
V	= volume of respirometer minus echinoderm volume (L)
T	= duration of incubation period (hours)
M	= wet weight mass of echinoid (g)

Echinoid volume was calculated by the hydrostatic balance method (Scherle, 1970), based on the Archimedes principle, where an object submerged in a liquid will lose weight quantitatively equal to the weight of liquid displaced by the body. In practice, this was performed by placing the echinoid upon a small plastic mesh platform that was attached to a laboratory stand by fine cotton thread. The echinoid and platform were completely submerged in seawater held inside a 2 L plastic beaker, ensuring that there was no direct contact between the organism and the beaker walls. The beaker was stood on a balance, and the increase in the measured weight (g) after the echinoid was submerged in the seawater (accounting for the weight of the platform) multiplied by the specific gravity of seawater (1.025 kg m^{-2}) corresponded to the volume of liquid (ml) displaced by the echinoid and hence its volume.

4.2.2.3. Total and differential coelomocyte counts (cellular biomarker)

After the behavioural and physiological measurements had been taken, 0.75 ml coelomic fluid was drawn from the coelomic cavity of each echinoid into an equal volume of anticoagulant solution using a sterile 5 ml syringe with 0.8 mm hypodermic needle, the latter being used to pierce the peristomal membrane. The anti-coagulant was as described by Matranga et al. (2000): 30 mM ethylenediaminetetraacetic acid, 0.5 M sodium chloride and 20 mM Tris, pH 7.5 (ISO-EDTA) and previously tested for its anticoagulant properties with *P. miliaris* coelomocytes. The diluted coelomic fluid was then placed in an ice-cold watch glass, and an aliquot carefully transferred to a Neubauer haemocytometer. Differential cell counts were then performed under Nomarski contrast interference optics using an Olympus BH2 microscope. Identification of the cells was based on the images and descriptions provided by Smith (1981) and Matranga et al. (2005). Counts of phagocytes, red or colourless spherule cells and vibratile cells were observed, recorded and calculated as cells ml^{-1} for all control and exposed echinoids. Triplicate counts were made from each sample of coelomic fluid from an echinoid, and the mean number of each type of coelomocyte for an individual echinoid was calculated from the three counts. Each mean number was used as a single replicate for statistical analysis. The total coelomocyte count (TCC) was calculated from the sum of the mean differential cell counts.

4.2.2.4. Citrate synthase activity (biochemical biomarker)

Protein extraction

Tissue samples (from the gut and, where possible, lantern musculature) were dissected from the echinoids and placed into individual pre-weighed 2.0 ml microcentrifuge tubes. The tissue sample was then weighed, frozen immediately in liquid nitrogen and transferred to a -80ºC freezer. When required the tissue samples were ground directly from frozen into a powder in a liquid nitrogen

cooled ceramic pestle and mortar. Powdered tissue samples were then transferred into a microcentrifuge tube containing an appropriate volume (2 ml per 100 mg tissue) of CelLytic™ MT Tissue Lysis / Extraction Reagent (C3228: Sigma-Aldrich® Company Ltd., Dorset, UK). Protease Inhibitor Cocktail (P8340: Sigma-Aldrich) had already been added to the CelLytic MT at 200 µl per 50 ml. The ground tissue samples were then vortexed and centrifuged at 4ºC at 14,000 *g* for 10 minutes to pellet the tissue debris. The protein-containing supernatant was then transferred to a fresh microcentrifuge tube and stored at -80 ºC until required.

Protein quantification

The quantity of protein present in each sample was determined using the Bicinchoninic Acid (BCA) Protein Assay Kit (BCA1: Sigma-Aldrich). The principle of the BCA assay is based on the formation of a Cu^{2+}-protein complex under alkaline conditions, followed by reduction of the Cu^{2+} to $Cu^{1+.}$ The reduction is in proportion to the protein present, and is measured by absorbance because BCA forms a purple-blue complex with Cu^{1+} in alkaline environments (BCA1 Technical Bulletin, Sigma-Aldrich).

The BCA assays were performed in 96 well plates, and absorbance read at 562 nm with a Dynex microplate reader using Dynex Revelation v 3.2 software (Dynex Technologies, Chantilly, VA, USA). Following manufacturer advice (personal communication), prior to performing the BCA assay each protein sample was diluted 50% with distilled water in order to dilute the Bicine concentration of the CelLytic MT lysis reagent. A standard protein concentration curve was prepared with a stock solution of 10 mg Bovine Serum Albumin (A7906: Sigma-Aldrich) in 1 ml 50% diluted CelLytic MT lysis reagent, and a series of solutions ranging in concentration from 0.1 mg ml^{-1} to 1 mg ml^{-1}. A separate standard curve was included on each 96 well plate.

Twenty µl of each protein sample was added to duplicate wells on a 96 well plate. 200 µl of BCA working reagent was then added to each well, the solution mixed with the pipette and the plates left to stand for 30 minutes at room temperature. In order to ensure protein samples were within the range of the standard curve in addition to running the 50% diluted protein samples a further duplicate 1 in 10 dilution was prepared and assayed for each sample. The protein concentration in each sample was then calculated from the measured absorbance with reference to the standard protein concentration curve generated from each plate with adjustment for the corresponding sample dilution.

Citrate synthase enzyme activity analysis

The activity of the CS enzyme was carried out in 96 well plates using a CS assay kit (CS0720:

Sigma-Aldrich). Following the manufacturer's protocol, 2 µl of 10 mM 5,5'-dithio-bis(2-nitrobenzoic acid) (DTNB) solution and 2 µl of 30 mM acetyl coenzyme A (CoA) solution was added to each well. To this was added 2-8 µl of protein sample (>8 µg whole protein extract) and sufficient Assay Buffer to make the total volume to 190 µl.

The baseline absorbance of this reaction mixture was then monitored for 1.5 minutes at 410 nm on a Multiscan RC 96-well plate reader (Lab System, Franklin, MA). Ten µl of 10 mM oxaloacetate solution was then added to each well to initiate the CS catalysed reaction between acetyl CoA and oxaloacetic acid. During this reaction, the acetyl CoA thioester is hydrolysed and CoA with a thiol group is formed. The thiol reacts with the DTNB in the reaction mixture forming 5-thio-2-nitrobenzoic acid (TNB); a yellow product that can be quantified by measuring absorbance at 412 nm (Technical Bulletin, Sigma-Aldrich). The plate was shaken for 10 seconds before the absorbance of the catalysed reaction was followed at 410 nm for 1.5 minutes. The activity in the sample was calculated using the following equation (given in the Sigma Aldrich CS assay kit technical bulletin):

$$Units\ \ (\mu mole/ml/\min) = \frac{(\Delta A_{410}) \times V \times dilution\ \ factor}{\varepsilon^{mM} \times L \times V_{enz}}$$

Where,

ΔA_{410} = The maximum linear change in the absorbance of the reaction solution after the addition of 10 mM OAA, minus the baseline change in absorbance prior to OAA addition.

V (ml) = the reaction volume (200 µl)

V_{enz} (ml) = the volume of the enzyme sample in ml

ε^{mM} (mM^{-1} cm^{-1}) = extinction coefficient of TNB at 410 nm = 13.6

L (cm) = 0.255 cm (the path length for absorbance measurement (see below))

Path length (L) was computed according to Copeland (2000). The following solution was prepared: 0.04g of potassium chromate (K_2CrO_4) and 3.2 g of potassium hydroxide (KOH) dissolved in 1 L of distilled water. The absorbance of this solution at 363 nm was measured in a 1cm cuvette on a spectrophotometer and at 363 nm in the same 96 well plates that the CS measurements were performed in. The path length of the 96 well plate was then computed from: $A_{96\ well\ plate} / A_{1\ cm}$.

4.2.2.5. Gene expression (molecular biomarker)

Tissue samples (from the Aristotle's lantern, oesophagus and gut) were dissected from the

echinoids at the same time as the tissue samples for CS activity were collected. The tissue samples for gene expression analysis were immediately placed in RNA*later*® Solution, frozen in liquid nitrogen (N_2) and stored at -80°C until processed. The tissue samples were subsequently processed and subject to qPCR assays as explained previously in detail from section 3.4.1 to 3.4.6. All gene expression results were standardised to transcript copy number per µg total RNA.

4.3. Statistical analysis

For analysis of the righting response biomarker results, a 'righting index' was calculated (1000 / righting response time in seconds), as per Lawrence (1975). Statistical analyses were performed on these indexed results. For the differential coelomocyte analysis, the numbers of each coelomocyte type within the total coelomocyte population were converted into proportions and then arcsine transformed prior to statistical analysis. For these and the other biomarker results, the Kolmogorov-Smirnov test was used to test for a normally distributed underlying population. Where required, data were log transformed (if not already arcsine transformed) to meet the assumptions of parametric significance testing (a normal distribution and equal variances). Where transformation did not result in these assumptions being met, nonparametric tests were employed on untransformed data.

Differences in biomarker responses were analysed using a two-way analysis of variance (2-way ANOVA) with 'treatment' (exposure and control) and 'time' (24, 48, 72, 96 hours) as fixed factors. Where a parametric 2-way ANOVA was possible, and significant differences were found for a factor, *post-hoc* Holm-Sidak (HS) tests were performed to investigate which groups differed significantly from each other. Where the assumptions of normality failed, a non-parametric 2-way ANOVA on ranks was performed and *post-hoc* tests were performed with the Dunn's test method. Where required, a one-way analysis of variance (1-way ANOVA) on normally distributed data was performed with *post-hoc* Tukey tests. For data not normally distributed, Kruskall-Wallis (KW) 1-way ANOVA on ranks was employed with *post-hoc* Dunn's tests. Correlations between different biomarker responses were investigated with Spearman rank correlation tests. Regression analysis was performed with ANOVA, and the determination of a significant difference from a slope other than zero was calculated from the ANOVA coefficients (Grafen and Hails, 2008). All significance tests were performed at the 5% significance level. All statistical tests were performed with the statistical software SigmaPlot for Windows Version 11.0, apart from the calculation of the deviation of the slope from 1 of the linear regression for echinoid oxygen consumption and wet weight, which was calculated manually from instructions in Grafen and Hails (2008).

4.4. Results

Experimental set up

A two-way ANOVA indicated that there was no significant difference between the mean temperatures recorded in the aquaria over time or between treatments ($F_{3,12} = 0.600$ and $F_{1,12} = 0.411$ respectively, $p > 0.05$). A significant difference between the mean pH values of the control and exposed aquaria was found ($F_{1,12} = 18.574$, $p = 0.001$), but no difference in the mean pH values of the aquaria with time ($F_{3,12} = 1.505$, $p > 0.05$). The pH of the seawater in the exposed aquaria was higher (mean pH = 7.81 ± 0.04 SD) than the control aquaria (mean pH = 7.73 ± 0.05 SD), which would be expected as the WBSM contained the strong base sodium hydroxide and the weaker base sodium carbonate (Lister and Renshaw, 1991). A significant interaction between treatment and time was found for the aquarium salinities ($F_{3,12} = 5.355$, $p < 0.001$), with mean salinities being significantly higher in the control (35.29 ± 0.15 SD) than the exposure (34.95 ± 0.44 SD) tanks at 24, 48 and 72 hours. With regard to the echinoids, there was no significant difference in the mean wet weights of the specimens in each aquaria with time ($F_{3,56} = 0.007$, $p > 0.05$) or between treatments ($F_{1,56} = 2.737$, $p > 0.05$). No echinoids died during the course of the experiments in either the control or exposed aquaria.

Righting response

Despite the mean righting response indices of the echinoids in the exposed aquaria being lower than those of the control aquaria (and hence the righting response times in the exposed groups being longer) (Figure 4.4a), there were no significant differences between the mean righting index of the echinoids with treatment ($F_{1,56} = 0.876$, $p > 0.05$) or time ($F_{3,56} = 2.079$, $p > 0.05$). This result indicates that neither exposure to WBSM nor the duration of the experiment had an effect on the ability of the echinoids to right themselves. As the locomotory capacity of the echinoids may have been expected to be associated with their metabolism (as movement requires energy), the relationships between the righting response and the biomarker indicators related to aerobic metabolism were also investigated. However, no significant correlation was found between the righting response of the echinoids and their oxygen consumption rate ($r_s = -0.038$, $p > 0.05$). The activity of the CS enzyme in the gut ($r_s = -0.002$, $p > 0.05$) and the lantern tissue ($r_s = -0.246$, $p > 0.05$) were also not correlated with the echinoid righting response.

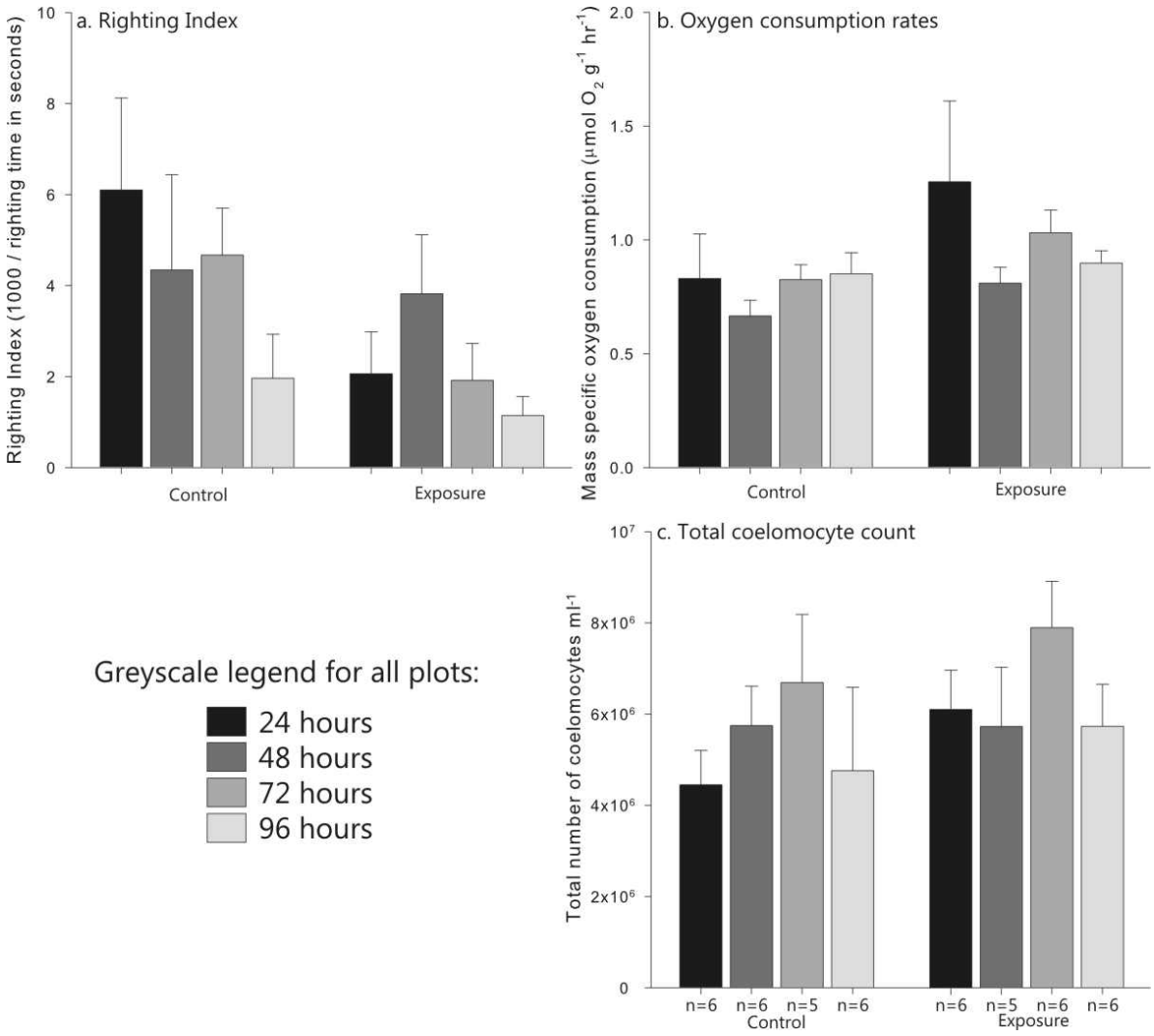

Figure 4.4. The mean (± SE) biomarker responses of the *P. miliaris* specimens in the control and exposed treatments with time are illustrated. Unless specified otherwise, n = 8 for all mean values. a). Righting response; as the righting index is the reciprocal of the righting time, the smallest righting index represents the longest righting time. b). Variation in echinoid mass specific oxygen consumption rate. c). Total coelomocyte numbers, no significant differences were found with treatment or time.

Oxygen consumption rate

The mean mass specific oxygen consumption rates ($\dot{M}O_2$) of the echinoids did not vary significantly with treatment ($F_{1,56} = 3.336$, $p > 0.05$) or time ($F_{3,56} = 1.158$, $p > 0.05$) (Figure 4.4b). The overall mean $\dot{M}O_2$ for all echinoids (control and exposed) was 0.896 (±0.45 SD) µmol O_2 g wet weight^{-1} hr^{-1}. As expected for the normal relationship between metabolic rate (for which oxygen consumption rate is a proxy) and mass in ectothermic organisms, the echinoid's $\dot{M}O_2$ was found to vary highly significantly with wet weight mass ($F_{1,62} = 40.02$, $p < 0.001$). The slope of the linear regression (data plotted on logarithmic coordinates) between these two variables was -0.611, significantly steeper than -0.25 (ANOVA, $F_{1,62} = 40.02$, $p < 0.001$), the slope which is typically

found for this relationship (Schmidt-Nielsen, 1981). This indicates that the oxygen consumption rates of the echinoids decreased faster with increasing mass than would normally be expected from a usual relationship between mass and metabolic rate (Figure 4.5). There was no significant difference between the slope of the linear regression between echinoid $\dot{M}O_2$ and wet weight mass with either treatment (ANCOVA, $F_{1,61} = 3.15$, $p > 0.05$) or time (ANCOVA, $F_{3,59} = 0.21$, $p > 0.05$).

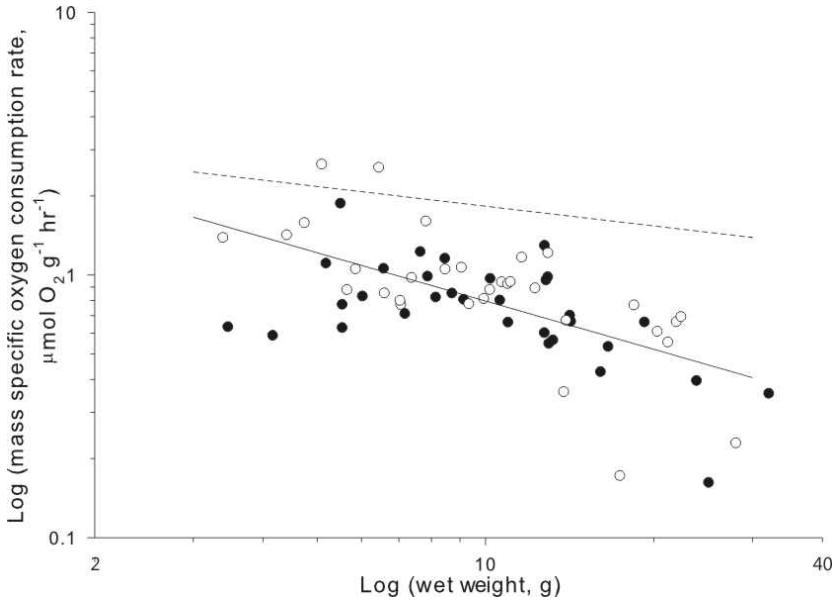

Figure 4.5. The mass specific oxygen consumption rates ($\dot{M}O_2$) of the echinoids from control (filled circles) and exposed (open circles) treatments. The solid line indicates the linear regression of the echinoid $\dot{M}O_2$ with wet weight ($\dot{M}O_2 = 3.2497$ wet weight$^{-0.611}$, $F = 40.02$, $p < 0.001$). Also illustrated is the hypothetical regression line (dashed) representing the more typical scaling coefficient for the linear regression of these two variables (-0.25).

Total and differential coelomocyte counts

Total and differential cell counts were only taken from six echinoid individuals from each group, and in two instances it was not possible to take cell counts due to the coelomic fluid clotting after collection. The overall mean total number of coelomocyte cells was 5.88×10^6 ($\pm 2.77 \times 10^6$ SD) per ml coelomic fluid. There was no difference between the total number of coelomocyte cells with treatment ($F_{1,38} = 2.095$, $p > 0.05$) or time ($F_{3,38} = 1.611$, $p > 0.05$) (Figure 4.4c). A significantly greater proportion of phagocytes ($F_{1,38} = 4.782$, $p < 0.05$) and a smaller proportion of vibratile cells ($F_{1,38} = 7.213$, $p < 0.05$) were found in the exposed than the control echinoids (Figure 4.6). No differences were found between the treatments for the proportions of either of the two types of spherule cells. As the experimental period progressed, the proportion of phagocytes changed significantly in both control and exposed treatment groups ($F_{3,38} = 4.590$, $p < 0.05$), with

the 72 hour phagocyte proportions being significantly greater than those at 24 (HS, t= 3.408, $p < 0.05$) and 48 (HS, t= 2.836, $p < 0.05$) hours. The proportion of colourless spherule cells decreased significantly as the experiment progressed ($F_{3,38} = 8.135$, $p < 0.001$), with the proportion of colourless spherule cells at 24 hours highly significantly greater than that found at 72 ($t = 4.444$, $p < 0.001$) and 96 hours ($t = 4.044$, $p < 0.001$).

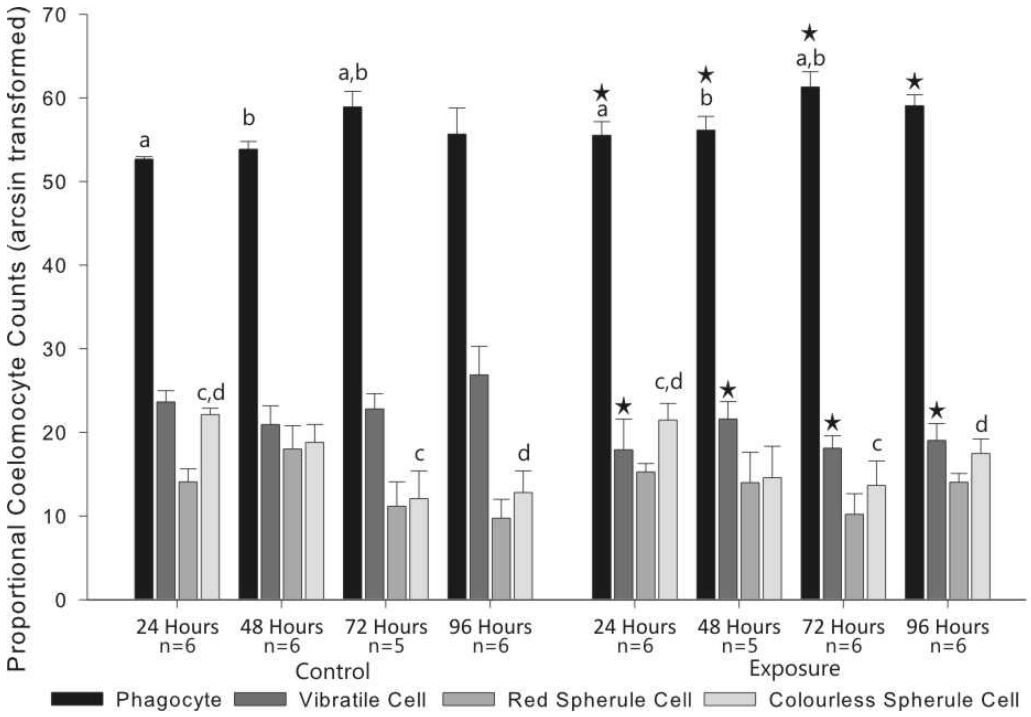

Figure 4.6. Proportional counts of the four different coelomocyte cell types from the control and exposed treatments during the course of the experiment. Lower case letters indicate the experimental times at which phagocyte proportions were significantly different to each other, and stars indicate the coelomocyte types which were present in significantly different numbers in the exposed treatments compared with the controls.

Citrate synthase activity

The mean CS activities in the gut tissue samples did not vary with treatment, but did vary significantly with time ($F_{3,54} = 5.519$, $p < 0.05$), with the 72 ($t = 3.793$, $p < 0.05$) and 96 ($t = 3.100$, $p < 0.05$) hour groups being significantly greater than the 24 hour groups (Figure 4.7a). Due to the small size of some Aristotle's lanterns, and the collection of lantern muscle tissue for both gene expression analysis and for CS activity determination, it was not possible to obtain lantern samples from each echinoid for both of these biomarkers. However, despite the small number of replicates, with regard to the tissue samples from the Aristotle's lantern musculature, no difference was found between the two treatments, but a significant difference was found between the mean activities of CS with time ($F_{3,25} = 5.670$, $p < 0.05$). The 96 ($t = 3.719$, $p < 0.05$) and 48 hour ($t = 3.072$, $p < 0.05$) mean CS activities were both significantly greater than those of the 24 hour group (Figure

4.7b). A comparison between the activity of the CS enzyme in the gut and lantern tissues with the expression of the *cs* gene in these tissues indicated that there was no correlation between the two. The mean CS activity in the gut (0.086 units ug protein^{-1}) was significantly greater than that of the lantern tissue (0.042 units ug protein^{-1}) ($H = 13.040$, $p < 0.001$)).

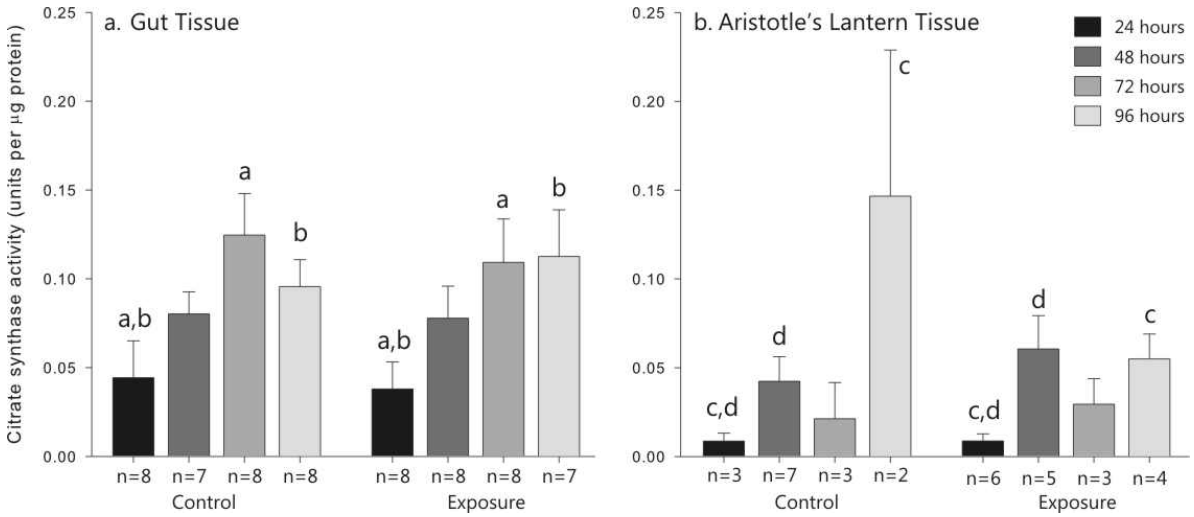

Figure 4.7. Mean (± SE) citrate synthase activities of the *P. miliaris* a) gut and b) Aristotle's lantern tissue samples from the control and exposed treatments with time. Lower case letters above vertical bars indicate groups with significant differences between time.

Gene expression

The expression in the gut tissue of the *cs* and *hsp* genes did not differ significantly with either treatment or time (Figure 4.8a). Whilst the expression of *ubi* in the gut tissue also did not differ significantly with treatment, it did differ highly significantly with time ($F_{3,54} = 6.833$, $p < 0.001$). The level of *ubi* expression at 48 hours was significantly lower than that found in each of the other time periods, at 24 (Dunn's test $q = 3.040$, $p < 0.05$), 72 ($q = 3.874$, $p < 0.001$) and 96 ($q = 3.886$, $p < 0.001$) hours. For the gene expression levels from the oesophagus tissue (Figure 4.8b), whilst there were no significant differences between treatment or time for the *cs* and *hsp70* levels of expression, *ubi* gene expression was significantly greater in exposed than control echinoids ($F_{1,22} = 5.054$, $p < 0.05$). The fold increase in the expression of ubiquitin in the oesophagus tissue between each control and exposed groups ranged from 3.32 to 9.87, with a mean fold increase of 5.81.

Due to the small quantities of muscle tissue obtained from the Aristotle's lantern from some of the echinoids, the total RNA extraction procedure was only able to generate samples suitable for the generation of cDNA for qPCR analysis in a small number of replicate samples. It was therefore not possible to perform two-way ANOVAs on the gene expression data generated from the lantern muscle tissue samples. One-way ANOVAs were performed on the data with respect to the two

different treatment groups (control and exposed), but no significant difference in any of the three genes in the lantern tissue samples was found.

Correlated gene expressions

The *cs* expression was highly significantly correlated with that of *ubi* in both the gut ($r_s = 0.501$, $p < 0.001$) and oesophagus ($r_s = 0.856$, $p < 0.001$) tissue (Figure 4.9a). Additionally, the expression of the *cs* gene in the lantern and gut tissue were significantly positively correlated ($r_s = 0.718$, $p < 0.05$), as was that of the *hsp70* gene ($r_s = 0.783$, $p < 0.05$). Whilst investigating the alteration of gene expression between treatment and time, it was also found that within each tissue type the expression of *ubi* was significantly correlated with the expression of *hsp70* (Figure 4.9b): lantern musculature ($r_s = 0.833$, $p < 0.05$), gut ($r_s = 0.385$, $p < 0.001$) and oesophagus ($r_s = 0.612$, $p < 0.05$).

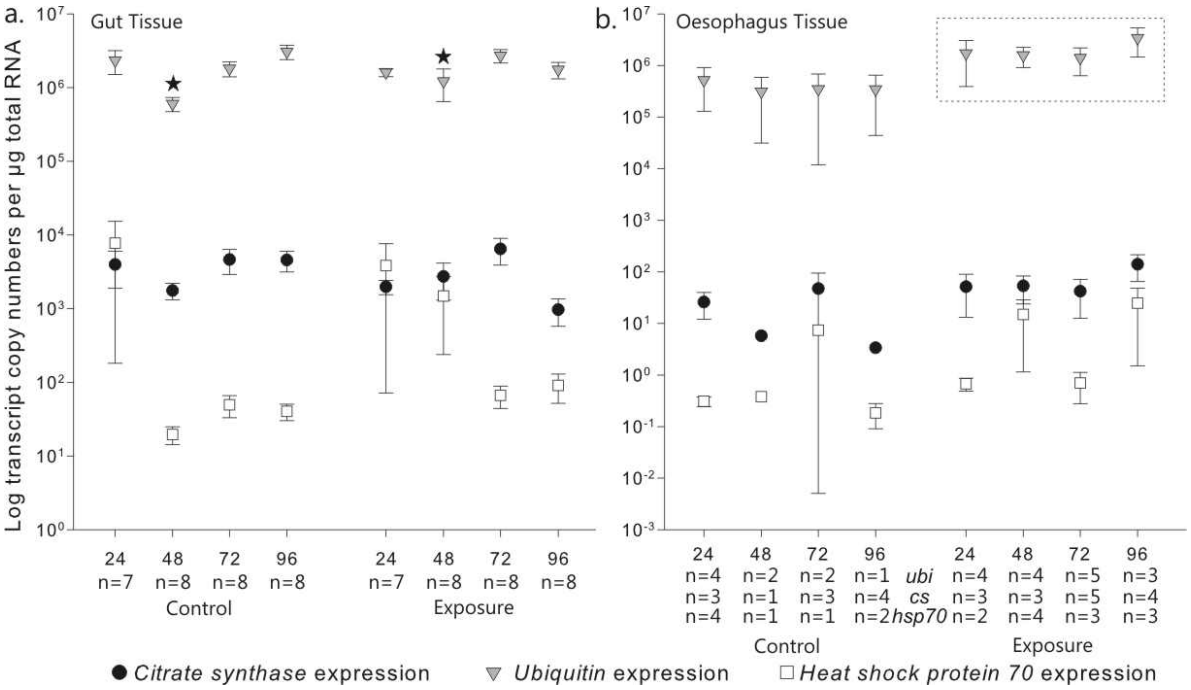

Figure 4.8. Mean (±SE) gene expression of *cs* (filled circles), *hsp70* (open squares) and *ubi* (filled triangles) with time and treatment in a) the gut tissue samples and b) the oesophagus tissue samples. The box indicates gene expression differing significantly between treatments, whilst the starred data points are significantly lower than those for the same gene at the three other time points. The number of replicates for each mean value is listed below the *x*-axis.

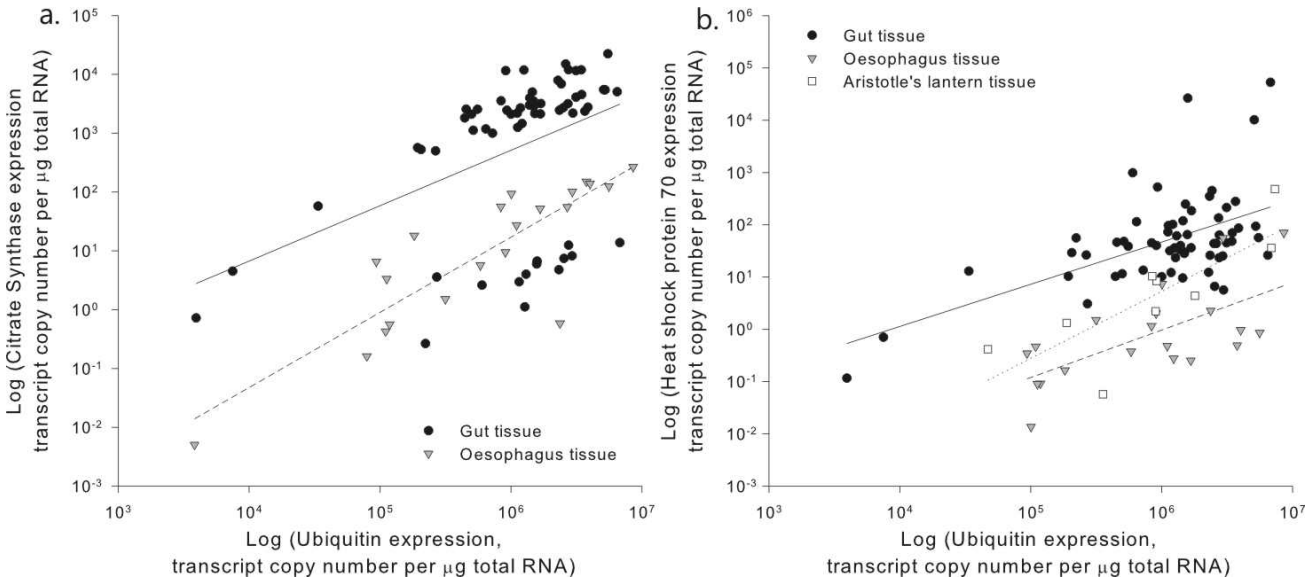

Figure 4.9. Correlation of gene expression levels in *P. miliaris* tissue samples. a). *cs* and *ubi* expression in the gut (solid trend line) and oesophagus (dashed trend line) tissue samples. b). Correlated *ubi* and *hsp70* expression in the gut (solid trend line), oesophagus (dashed trend line) and lantern muscle (dotted trend line) tissue samples.

4.5. Discussion

4.5.1. Biomarker responses

Behaviour

A dose-dependent response has been reported in previous studies using echinoderm righting response times as a behavioural biomarker. Compounds such as the antiparasitic Ivermectin (Davies et al., 1998), the neurotoxicant cyclophosphamide (Canty et al., 2009) and inorganic and organic phosphate compounds (Böttger et al., 2001) have been found to cause dose-dependent decreases in righting response, where low doses had no effect on the ability of echinoids or asteroids to right themselves after inversion. Although there is an indication that the WBSM exposure had a negative effect on the ability of *P. miliaris* to right itself (Figure 4.4a), no significant change in the righting time taken by the exposed *P. miliaris* specimens was found. It can be concluded that the WBSM did not cause a response in *P. miliaris* that was evident at the behavioural level of organisation.

Oxygen consumption

The oxygen consumption rate of echinoderms is known to vary in response to a variety of environmental parameters, including salinity, pH and oxygen tension. Talbot and Lawrence (2002) found that the oxygen consumption rate of *Ophiophragmus filograneus* decreased in salinity conditions which were both lower and higher than that to which the ophiuroid was acclimatised. The decrease in the oxygen consumption rate of *O. filograneus* under the lower salinity conditions was accompanied by reduced ammonia excretion, arm regeneration and growth, indicating that the

altered oxygen consumption rate reflected salinity-stress induced metabolic depression at the level of the whole organism. It has been reported that echinoderm oxygen consumption rate is elevated under pH conditions higher than a pH of ~8, which is typically experienced by echinoderms in the marine environment, and is inhibited at lower pH (Farmanfarmaian, 1966). Many echinoderms are oxyconformers and their rate of oxygen consumption is subject to the oxygen tension of the surrounding water (Spicer, 1995; Christensen and Colacino, 2000). With regard to the influence of anthropogenic pollutants upon echinoderm oxygen consumption there is, however, a paucity of published data.

The effect of WBMs and bentonite, which is a principal component of many WBMs, on an organism's physiology has been previously demonstrated. The clearance and respiration rates of adult *Placopecten magellanicus* are detrimentally affected by both acute and chronic exposure to 2 mg l^{-1} bentonite. Chronic exposure of the adult scallops to WBM resulted in significantly increased respiration rates, but acute exposure had no apparent effect (Cranford et al., 1999). No previous reports have documented the response of adult echinoderms to a WBM and in this study, no effect of exposure to the WBSM was found in the *P. miliaris* oxygen consumption rates. It is possible that, as found in the study with *P. magellanicus,* the length of exposure time was insufficient for an alteration in the oxygen consumption rate to result, or the dose of WBSM was insufficient to induce a physiological level response.

Coelomocytes

In the current study, a mean number of total coelomocyte cells of 5.88 x 10^6 ml^{-1} (± 2.77 x 10^6 SD) was found in *P. miliaris*, a number typical to that found in other echinoderms. In echinoids, total coelomocyte concentrations ranging from 4.25 to 10 x 10^6 ml^{-1} were recorded from *Strongylocentrotus droebachiensis* and *Arbacia puntulata* (Chia and Xing, 1996), and in the asteroid *A. rubens* coelomocyte numbers range from ~1.8 to 4 x 10^6 ml^{-1} (Pinsino et al., 2007; Holm et al., 2008). Typically though, as well as varying interspecifically, echinoderm coelomocyte concentrations vary intraspecifically, as found in *P. miliaris* (Smith, 1981; Chia and Xing, 1996).

Whilst phagocyte cells in *Lytechinus pictus* account for 15% of the total coelomocyte cell population, in *S. droebachiensis, S. purpuratus* and *Echinometra lucunter* they account for 64-77%, and in *Paracentrotus lividus* 80-85%. Correspondingly, the percentages of the other cell types also varies, with spherule and vibratile cells respectively reported as accounting for 4-70% and 5-22% of the total coelomocyte populations (Smith, 1981; Chia and Xing, 1996; Matranga et al., 2005; Matranga et al., 2006; de Faria and da Silva, 2008). In *P. miliaris* the percentages of each coelomocyte cell also varied between individuals, with cell proportions ranging as follows:

phagocytes: 56-86%, vibratile cells 0–33%, red spherule cells 0-18% and colourless spherule cells 0–25%; a range of percentages comparable to those reported in other echinoid species.

An increased proportion of phagocytes, which accounted for the majority of the total coelomocyte population, was found in the WBSM exposed *P. miliaris*. The number of phagocytes also increased with time in both the control and exposed groups of echinoids. Phagocytes have a functional defensive role in echinoderms being actively phagocytic, capable of encapsulating foreign bodies, important in cell clotting and are the major cell type to express immune genes including complement homologues (Smith, 1981; Matranga et al., 2005; Smith et al., 2006). Vibratile cells, the second most common form of coelomocyte in the *P. miliaris* specimens, were present in exposed individuals in reduced proportions compared with those in control individuals. Vibratile cells are thought to be involved with the immobilisation of invading microbes and in the clotting process, although their exact function is still not clear (Smith, 1981; Matranga et al., 2005; Smith et al., 2006). The proportion of colourless spherule cells, considered by Matranga et al. (2000; 2006) to be the primary coelomocytes affected by pollution and temperature stress, decreased with experimental length.

These changes indicate that the coelomocyte population is responsive to either the WBSM exposure or the overall experimental environment. An increase in the phagocyte population of the coelomic fluid may indicate an elevation in the immunological functioning of the exposed echinoid specimens, perhaps caused by an attempt to defend against an increased susceptibility to infectious disease due to stress (Coteur et al., 2005b). However, in the absence of further investigation into the immunological capability of these cells (for example by investigating phagocytic activity during bacterial challenge (Silva and Peck, 2000; Coteur et al., 2002) it cannot be assumed that the phagocytes had maintained normal functioning as a result of WBSM exposure. If phagocyte functioning had been inhibited by the WBSM exposure, a greater proportion of phagocytes may just have been required to maintain normal immunological functioning.

Citrate synthase activity

Citrate synthase is a regulatory enzyme of the citric acid cycle and is used an indicator of an organism's aerobic metabolism (Goldenthal et al., 1998; Seibel and Childress, 2000). The investigation of CS activity in echinoderms has not been extensive, as is the case for most enzymes involved with the citric acid cycle in echinoderms, and the small numbers of studies that have investigated its activity have shown that it varies with development, season and salinity. Okabayashi and Nakano (1978) followed the change in CS activity during *Hemicentrotus*

pulcherrimus and *Anthocidaris crassispina* embryo development and determined that it increased gradually up to the pluteus stage. Meyer et al. (2007) demonstrated that the increase in CS activity in developing *S. purpuratus* larvae was in direct proportion to their DNA content. In female adult *Asterias rubens*, CS activity in the pyloric caeca was reduced in the autumn/winter period compared with the summer, but generally CS activity varied considerably in both the pyloric caeca and ovaries throughout the year (van der Plas and Oudejans, 1982). Salinity has been reported to alter CS activity in the pyloric caeca of *Luidia clathrata* (Marsh and Lawrence, 1985).

The CS activity in the *P. miliaris* lantern muscle tissue was lower than that found in the gut (Figure 4.4 d,e), suggesting that the gut tissue was more metabolically active than the lantern muscle. These conclusions were also drawn by Ellington (1982) who, when reporting the activity of CS in the muscles of *Echinus esculentus* and *Thyone* sp., commented that it was, '*...so low as to place in doubt the quantitative importance of aerobic energy metabolism in these tissues*'. The correlation between CS activity and metabolic rate (typically measured as oxygen consumption rate) in echinoderms is not clear. Meyer et al. (2007) found a positive relationship between these two variables during the growth of fed larvae (but not unfed larvae), but Marsh et al. (1999) instead reported a correlation between the two in unfed larvae (but not fed larvae). In *P. miliaris,* no correlation was found between the rate of CS activity and the rate of oxygen consumption.

In *P. miliaris* an alteration in CS activity in the gut and lantern tissue was not found in response to exposure to WBSM, but was found as the time course of the experiment progressed. In both tissue types in both the control and exposed echinoids, a progression towards greater CS activity with time was evident. This indicates that, rather than exposure to the WBSM, the actual experimental conditions may have altered CS activity in *P. miliaris.* A greater demand for energy derived from the citric acid cycle could have been caused by increasing attempts to maintain homeostasis, with associated requirements for ATP, under inadequate environmental conditions as the experimental period progressed. However, the absence of a corresponding increase in the oxygen consumption rates of the echinoids does not provide support for an increased supply of ATP, which is generated using the energy released during oxidative phosphorylation (section 2.1.1.1).

Gene expression

Ubiquitin

The only gene to indicate a significant difference in expression between the exposed and control groups of *P. miliaris* was the *ubi* gene in the oesophagus tissue, which on average demonstrated a 5.8 fold increase in exposed individuals. Altered expression of the *ubi* gene has recently been found to significantly vary in the larvae of *S. purpuratus* grown in conditions of high elevated CO_2

(1020 ppm) and reduced pH (7.88), where its fold change increase ranged from 1.15 to 1.38 (Todgham and Hofmann, 2009). The ubiquitin gene is important in echinoid larvae due to the significant amount of protein degradation that occurs during embryogenesis (Pickart et al., 1991), and the significant increase in the expression of the *ubi* gene in the WBSM exposed *P. miliaris* would suggest that there is an increase in the quantity of damaged proteins requiring degradation in these echinoids.

As discussed in Chapter 2 (section 2.6.3.3), because of the lack of specificity of the qPCR primers used to quantify *ubi* gene expression, the increase in expression found in WBSM-exposed echinoids does not differentiate between different members of the ubiquitin multigene family (polyubiquitin and the ubiquitin fusions genes). The mRNA transcripts for each member contain the same nucleotide sequence and could have been amplified during the PCR. Additionally, with the structure of the polyubiquitin gene being comprised of identical repeating monomer units (section 2.1.1.3), there is a possibility that one polyubiquitin mRNA transcript could generate ~ 7-10 amplified fragments of the same size. Due to the absence of multiple sized peaks in the qPCR melt curves, however, the possible amplification of fragments spanning more than one of these monomers did not occur. The combination of more than one ubiquitin family gene member being amplified is likely to be the reason that the quantified expression of '*ubi'* in *P. miliaris* was 4 to 5 orders of magnitude greater than that of the *cs* and *hsp70* genes.

Heat shock protein 70

The expression of the *hsp70* gene, and levels of the HSP70 protein, in both larvae and adult echinoderms have been found to be induced by heat shock, with individual thermal history determining the temperature at which elevated *hsp70* expression is initiated (Giudice et al., 1999; Matranga et al., 2000; Osovitz and Hofmann, 2005; Meng et al., 2009). Wounding of adult echinoderms has also been shown to cause a stress response with elevated HSP70 levels found in coelomocytes or in tissue from wounded echinoderms (Patruno et al., 2001a; Pinsino et al., 2007; Holm et al., 2008). The coelomocytes of echinoids stressed by metal pollution and UV-B radiation also respond with elevated amounts of HSP70 (Matranga et al., 2006; Oweson et al., 2008; Pinsino et al., 2008). In *P. miliaris*, exposure to WBSM did not result in significant differences in *hsp70* expression indicating that this treatment did not cause sufficient stress to induce this near-universal molecular stress response. However, it has been found that not all toxicants stimulate hsp expression, and some authors have raised doubts about the use of hsps as unequivocal signatures for the presence of contaminants (Sanders, 1993; Gupta et al., 2010). It is therefore possible that *hsp70* was not an appropriate indicator to use as a tool to assess exposure to WBSM.

Citrate synthase

A differential expression of the *cs* gene in response to stressful conditions had not been reported in echinoderms until its reduced expression was found in *L. pictus* larvae raised under simulated high CO_2 conditions (O'Donnell et al., 2010). Although the changes reported by O'Donnell et al. were not significant, interestingly they were reported alongside similar fold changes of the ubiquitin gene. In *P. miliaris*, the expression of *cs* in individuals exposed to WBSM compared with controls was variable but not significant. The expression of the *cs* gene was correlated in the gut and lantern tissue, perhaps indicating that similar demands on the metabolism of these tissues were being made. However, the expression of the *cs* gene was not correlated with CS enzyme activity in these tissues, highlighting a problem associated with using the quantification of gene expression as a direct indicator of an organism's physiological state. There is no certainty that a mRNA transcript will be translated, and the resulting polypeptide chain post-translationally modified to form an active protein, as there are cellular translation and post-translational controls over protein formation (Greenbaum et al., 2003). Studies which have tried to link mRNA and corresponding protein levels (mostly in human and yeast models) indicate a wide variation in correlation strengths according to the protein studied and the level of mRNA expression (Greenbaum et al., 2003; Maier et al., 2009).

Correlation of the expression of different genes

The correlated increase in the expression of *hsp70* and *ubi* in all three *P. miliaris* tissue types (Figure 4.9b) reflects a pattern of change in the expression of these molecular chaperones that has been found in a variety of organisms. During heat shock, free swimming *Xenopus laevis* tadpoles accumulate *hsp70* and *ubi* mRNA in a coordinated manner (Krone and Heikkila, 1988), a pattern also found during mosaic virus invasion in infected pea embryos (Aranda et al., 1996). Halpin et al. (2002) and Hofmann and Somero (1995) found that increased levels of ubiquitin conjugates in *Mytilus californianus* and *M. trossulus*, collected in summer from areas high in the intertidal zone (associated with high thermal and desiccation stress), were also correlated with increased quantities of the HSP70 protein.

These studies demonstrate that high levels of the HSP70 protein may not be sufficient to prevent irreversible protein denaturation in the cell because of stressful conditions, and hence increased quantities of ubiquitin are required to direct denatured proteins to the proteolytic 26S proteasome for destruction. It has additionally been found that the HSP70 protein is also involved in the protein degradation process (Goldberg, 2003). As well as refolding denatured proteins, the binding of HSP70 to damaged protein substrates can also tag them for degradation. An E3 enzyme (section 2.1.1.3) called CHIP (carboxy terminus of HSP70-interacting protein) interacts with HSP70 by

binding to their C-terminus when they are bound to an unfolded or hydrophobic domain of a damaged protein. The CHIP then promotes the ubiquitination of the damaged substrate protein, followed by degradation by the 26S proteasome (Goldberg, 2003; Arndt et al., 2007). Although there is no direct evidence that the increased levels of *hsp70* transcripts in the *P. miliaris* samples correspond to increased quantities of HSP70 protein in the cell, the correlated increase in *ubi* transcripts suggest a coordinated increase in the activity of the pathways that protect the cell against misfolded or damaged proteins.

Both the processes of ubiquitin directed protein degradation and the refolding of proteins by HSP70 require energy in the form of adenosine 5'triphosphate (ATP). ATP hydrolysis is essential for the chaperone activity of HSP70 proteins; ATP energy induces conformational change in the HSP70 protein and drives the substrate binding/release cycle (Mayer and Bukau, 2005). The activation of an ubiquitin monomer by a E1 enzyme is also an ATP-dependent reaction (Hershko and Ciechanover, 1998). As such, the energy costs associated with replacing damaged and destroyed proteins can contribute substantially to cellular energy demands (Hofmann and Somero, 1995). This demand for energy may also explain the correlation found between the expression levels of the *ubi* and *cs* genes in the gut and oesophagus tissues of *P. miliaris* (Figure 4.9a). As previously discussed (section 2.1.1.1), CS is a key enzyme in the citric acid cycle which operates in conjunction with oxidative phosphorylation to produce ATP. In eukaryotic cells, CS is inhibited by ATP, i.e. if ATP levels fall substrate catabolism by the citric acid cycle will increase (Plaxton, 2004). I speculate that the correlated increase in *cs* and *ubi* transcript numbers may be related to a demand for ATP to fuel increased protein degradation, and hence an increased demand for the CS enzyme. However, the lack of correlation between the expression of the *cs* gene and the measured activity of the CS enzyme prevents any firm conclusions being made in this regard.

4.5.2. The effect of WBSM

As a species from a variable environment, adapted to maintain homeostatic functioning under changing physical conditions in the intertidal zone, it was predicted that *P. miliaris* would demonstrate a measureable response to stress caused by exposure to WBSM. Significant changes were found in the cytological (coelomocyte populations) and molecular biomarkers (*ubi* expression) in response to WBSM exposure. An inspection of the environmental conditions in the control and exposure aquaria indicated that these might have been induced by the WBSM altering in the water quality in the exposure tanks.

There was a significantly higher pH and lower salinity in the exposed (respective means 7.81 and 35.29) than the control aquaria (means 7.73 and 34.95). An increased pH is typically found to

occur if sodium hydroxide and sodium carbonate (both components of the WBSM) are released to an aquatic environment which has insufficient buffering capacity (OECS, 2002a, 2002b; European Commission, 2008). The pH in Southampton Water, from where the water in the experimental aquaria was derived, has been recorded to range from 7.94 to 6.76 (Al-Rasheid and Sleigh, 1995). The water in the aquaria therefore exhibited a pH typical of the Southampton Water environment. However, because it was obtained from the recirculating system to which the echinoids had been acclimatised to, the increased pH of the seawater in the exposed aquaria (as opposed to that of the control aquaria) may therefore have been stressful to *P. miliaris*.

As the pH of echinoderm coelomic fluid varies with that of the surrounding seawater (Farmanfarmaian, 1966), the reduced pH in the WBSM exposure tanks could have caused the observed changes in the coelomocytes (phagocytes and vibratile cells) and *ubi* expression. As the coelomic fluid altered in exposed echinoids in response to the pH of the surrounding water, the coelomocytes (directly exposed to the coelomic fluid) may have lost normal functioning. As ubiquitin tags proteins for destruction, the increase in *ubi* expression could indicate an increase in the number of damaged proteins requiring processing, but without an assessment of the level of actual ubiquitin conjugates in the tissue samples this can only be assumed.

It is possible that the absence of a significant response to the WBSM exposure at the physiological and behavioural levels of organisation occurred because the wrong biomarker responses were selected for study. However, sufficient time may not have elapsed for more significant effects of WBSM exposure to have become apparent. In a study assessing the impact of seawater acidification on *P. miliaris*, Miles et al. (2007) reported that significant alterations in the coelomic fluid pH of echinoids maintained in seawater of pH 7.44 (control pH 7.96) did not significantly differ from that of controls until 7 days of exposure had elapsed. This result, combined with Cranford et al.'s (1999) report that acute exposure to WBM had no apparent effect on scallops but chronic exposure did cause significant physiological effects, points towards the *P. miliaris* WBSM experiments, at 4 days total length, being of insufficient length to elicit a greater stress response in the echinoids.

It is possible that the *P. miliaris* individuals used for the experiments, in both control and exposed treatments, were already stressed because of the temperature of the recirculating water system in which they had been maintained. As a non-temperature controlled system, the hot weather experienced in the weeks prior to the experiments had resulted in the water being ~ 17°C. Although such a temperature would be experienced by intertidal organisms during summer diurnal fluctuations, the continuous exposure to water of elevated temperatures may have resulted in *P.*

miliaris having been under continuous thermal stress for a number of days. The evidence that all echinoids were exhibiting metabolic rates (as measured via oxygen consumption rate) which were lower than expected with increasing echinoid mass indicates that their metabolism was suppressed. This may have led to the echinoids exposed to the WBSM being unable to respond significantly to any additional stress associated with the drilling fluid. Alternatively, the lack of a more severe stress response to the WBSM may have been because the concentration used was not at a dose sufficient to have a more significant effect on the echinoids at all levels of organisation. The range finding experiments conducted before the final exposure experiments did indicate that some of the echinoids could not right themselves after inversion at 1 ml l^{-1} WBSM, but an assessment of the other biomarker responses was not carried out at the same time, which was an omission.

4.6. Conclusions

With significant differences found at the cytological and molecular levels of biomarker assessment, effects of WBSM exposure in *P. miliaris* were evident at lower levels of biological organisation as opposed to higher level behavioural and physiological functioning. With regard to the original null hypotheses, that WBSM exposure would not cause deviations in the observed biomarker responses compared with those found in control specimens, it has been proved that this hypothesis is false as assessed by the differential gene expression and coelomocyte variation. However, with regard to the assessment of citrate synthase enzyme activity, oxygen consumption and behavioural activity, the null hypothesis has not been rejected.

In general though, there was insufficient evidence to prove that *P. miliaris* was severely affected by the WBSM, which would have been indicated by highly significant responses at all levels of organisation. It is possible that, as the WBSM was found to cause only a small increase in aquarium pH and a small reduction in salinity, as *P. miliaris* is a robust organism accustomed to variations in these parameters in the intertidal environment, the scale of the variation was insufficient to cause significant stress to the echinoids. It is also possible that the biomarker assays selected to assess the possible stress response were insufficiently sensitive, or that other biomarker assays, for example: feeding rate, lysosomal integrity, antioxidant enzyme activity or DNA integrity may instead have revealed additional significant responses to WBSM exposure.

With regard to the development of a shallow-water based experimental approach to the investigation of anthropogenic impact on deep-sea echinoderms, and the predicted differences in the stress responses of eurytopic and stenotopic echinoids, the results of the *P. miliaris* exposure experiments must be compared with those found with *B. lyrifera*, and this is discussed in the next chapter.

Chapter 5. The stress response of *Brissopsis lyrifera* and a comparison with that of *P. miliaris*

5.1. Introduction

Stenotopic species inhabiting stable environments are considered by some to be more vulnerable to novel perturbation than eurytopic species inhabiting physically variable environments (Fisher, 1977; Angel, 1992; Seibel and Walsh, 2003; Timofeyev and Steinberg, 2006). For example, organisms from either cold or warm stenothermal environments have been found to lack the otherwise near-universal heat shock protein response to thermal shock (Clark and Peck, 2009; Tomanek, 2010), and wounded specimens of *Asterias rubens* from stable benthic environments show reduced levels of HSP70 protein in regenerating tissue than specimens from the intertidal environment (Patruno et al., 2001a). As discussed in the previous chapter, in response to oxidative stress amphipods from more stable environments had a delayed increase in the activity of antioxidant enzymes in comparison to species from the more variable littoral zone, and were considered to be highly sensitive to the significant alteration of physical variables other than pressure (Timofeyev and Steinberg, 2006).

In species from the deep sea, the total oxyradical scavenging capacity of the amphipod *Eurythenes gryllus* was found to be lower than that of a surface living species, *Anonyx nugax* (Camus and Gulliksen, 2005), and Janssens et al. (2000) found reduced enzymatic antioxidant defence levels in deep-sea fish compared with those in shallower water species. These last two studies did introduce the theory that these reduced enzyme activities were related to the reduced metabolic rate of the deep-sea species in comparison to those from shallower depths. However, as reduced metabolic rates are themselves an adaptation to the deep-sea environment in visually sighted organisms (see manuscript at Appendix 1.30), it would appear that the physical environment of the deep-sea influences the responsive capacities of organisms to stress both directly and indirectly.

As discussed in the general introduction, the cost and logistical complexity of performing experiments with shallow-water species under shallow-water physical conditions are reduced compared with those associated with deep-sea experimentation. A wide range of experimental approaches is possible with shallow-water experimentation, and the effects of decompression and temperature change can be controlled to not influence experimental results. A restriction to applying the results of shallow-water experiments to the prediction of anthropogenic impact in the deep sea is, however, the difference found between the physiology and ecology of organisms from the two environments (section 1.4.2). If shallow-water species with life histories similar to that of deep-sea organisms (benthic deposit feeders) were used as experimental subjects, it is possible that

the influence of these differences could be limited. Therefore, further to the water based spud mud (WBSM) exposure experiments reported in Chapter 4, which were carried out with the intertidal echinoid species *Psammechinus miliaris*, this chapter reports the results of similar experiments performed with a fjord-dwelling infaunal echinoid species, *Brissopsis lyrifera*. As *B. lyrifera* inhabits an environment which is physically more stable than that of the intertidal *P. miliaris* it was predicted that the responses to WBSM would differ between the two species, with that of *B. lyrifera* being reduced in comparison to *P. miliaris*.

5.2. The ecology of *Brissopsis lyrifera* (Forbes, 1841)

Brissopsis lyrifera is an infaunal spatangoid echinoid, commonly known as a heart urchin (Figure 5.1), distributed from Scandinavia to South Africa (Budd, 2004; Southward and Campbell, 2006). Although Southward and Campbell (2006) record its depth distribution as ranging from 5 to more than 200 m, Féral et al. (1990) recorded collecting specimens of *B. lyrifera* from up to 930 m depth and Harvey et al. (1988) record its distribution as 5 to 1400 m depth. In comparison to the 0-100 m depth range of *P. miliaris* (section 4.1.3), *B. lyrifera's* depth distribution extends to bathyal depths, and in this regard it can be considered a deeper water species than *P. miliaris*. Living buried in fine mud or muddy sands offshore or in stable nearshore environments (Southward and Campbell, 2006), *B. lyrifera* burrows to ~2 – 5 cm depth, where it ingests sediment in bulk and feeds on the associated organic matter. *B. lyrifera* is capable of reworking relatively large volumes of sediment and is an active bioturbator, its activity affecting sediment species diversity (Austen and Widdicombe, 1998) and increasing sediment oxygen concentrations, so stimulating microorganism growth and organic material decomposition and influencing biogeochemical processes (Widdicombe and Austen, 1998; Hollertz and Duchêne, 2001).

Very few ecotoxicological studies have been carried out with *B. lyrifera*. As part of sediment communities exposed to water based drill cuttings, numbers of *B. lyrifera* were found to be not significantly reduced in exposed sediments (Schaanning et al., 2008) , though in a separate experiment dead individuals were found in drill cutting contaminated sediments (Trannum et al., 2010). In regions of enhanced organic matter (fish farm waste), *B. lyrifera* densities are enhanced and the echinoids are found feeding on the sediment surface, being significant contributors to the decomposition of carbon (Kutti et al., 2007).

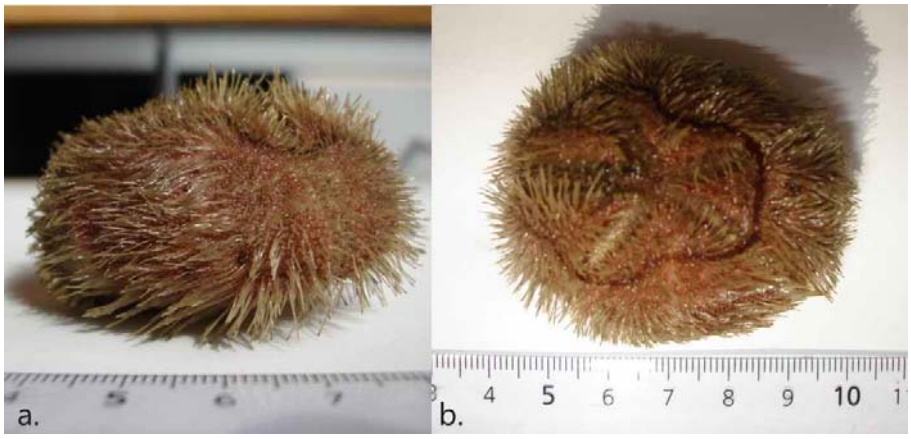

Figure 5.1. *Brissopsis lyrifera* specimens collected from the Gullmar Fjord. a. Lateral view, b. Aboral view in which a lyre-shaped band of ciliated dark spines ringing the five ambulacra petals, which gives the species its name, can be seen. Scale bars in the photographs are in cm.

5.2.1. The Gullmar Fjord environment

The Gullmar Fjord, from which the experimental specimens used in this study were collected (Figure 5.2), is one of a series of sill fjords along the west coast of Sweden. The fjord is ~30 km long and 1-3 km wide and has a maximum depth of 120 m. It is orientated in a NE/SW direction and opens into the Skagerrak across a sill at 42 m depth (Svansson, 1984). Tides are weak in the area with a tidal amplitude of 0.15 m (Erlandsson et al., 2006). The fjord is strongly stratified with a halocline occurring at depths of between 15 and 20 m, where upper low-salinity Baltic water (24–27 psu) is separated from more saline intermediate water (32-33 psu). A second interface occurs between 50 and 60 m where highly saline deep basin water (34–35 psu) is separated from the intermediate water. The residence time of the surface water is 20-38 days, and 29-62 days for the intermediate water (Arneborg, 2004).

Like most sill fjords, the Gullmar Fjord is subject to periods of stagnation. The deeper, more saline, waters are relatively stagnant and have little seasonal variation in temperature or salinity. The Gullmar Fjord has not been subject to any major source of water pollution from either sewage or industry since the late 1960s and early mid 1970s. However, eutrophication is still considered as ongoing (Harland et al., 2006). The reasons behind this are still not completely understood, but it has been demonstrated that variations in climate have influenced water renewal in the fjord, which is thought to have caused the establishment of stagnant bottom water, oxygen deficiency and benthic mortality (Nordberg et al., 2000).

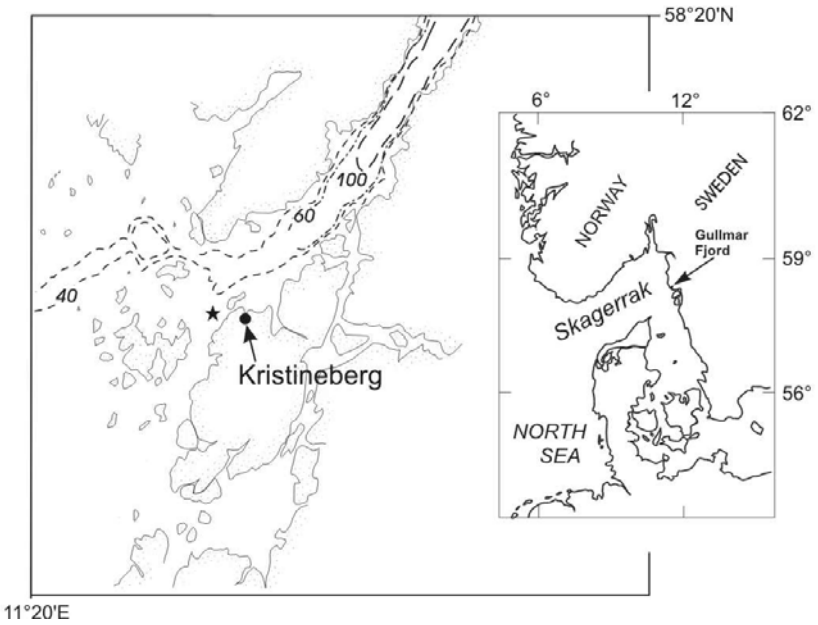

Figure 5.2. Map of the Gullmar Fjord, Sweden, showing the location of the *B. lyrifera* sampling sites (starred) and Kristineberg marine research station. Figure adapted from Arneborg (2004).

The Gullmar Fjord is an environment where the phenomenon of deep-water emergence occurs, where species normally found in the deep sea are present in comparatively shallow fjord waters (Häusserman, 2006). For example, *Stichopus tremulus* and *Mesothuria intestinalis* are two important and numerically abundant species of holothurian that are globally distributed at depths of ~1000 m (Billett, 1991), but they also occur in the Gullmar Fjord at ~100 m (Hudson, 2004). The presence of these deep-water species in the Gullmar Fjord indicates that its stable environment can be considered as more analogous to that of the deep sea.

B. lyrifera is distributed throughout the entire fjord where the depth is greater than ~23-30 m and the bottom consists of mud-like clay and silt (Brattström, 1946). The physical characteristics of the deepest parts of the fjord where some of the largest (7 – 8 cm length) specimens of *B. lyrifera* are found are generally of high and constant salinity (34.02 – 35.01) and low and constant temperature (4 – 7°C) (Brattström, 1946). It is known that the water from the intermediate water mass of the fjord (from which the *B. lyrifera* specimens were collected, see section 5.3.1) experiences seasonal fluctuations in temperature (5.4-12.5°C), salinity (32.7-34.8), oxygen content (3.6-6.4 ml l^{-1}) and primary productivity flux to the seabed (Majoran et al., 2000; Hollertz, 2001). However, in comparison to *P. miliaris* from the highly variable intertidal zone, the *B. lyrifera* specimens from the Gullmar Fjord can be considered representative of echinoids inhabiting a stable benthic environment.

5.2.2. Aims of the *B. lyrifera* exposure experiments

The primary aim of the *B. lyrifera* experiments was to investigate whether exposure to the water based drilling fluid, WBSM (section 4.2.1), elicited a detectable stress response in one or more biomarkers ranging from the behavioural to the molecular level of biological organisation. For each biomarker, the specific null hypothesis tested was that WBSM exposure would not cause a deviation in response compared with that found in control specimens.

With regard to the overall approach towards deep-sea impact assessments, a reduced response to contaminant induced stress in a stenotopic species may indicate a reduced capacity to maintain homeostatic regulation when subject to environmental perturbation, as is expected in deep-sea organisms (Angel, 1992; Seibel and Walsh, 2003). The biomarker results from *B. lyrifera* are therefore compared with those obtained from *P. miliaris* (Chapter 4) in order to determine whether there are any differences or similarities between these species from two different environments, and whether the *B. lyrifera* stress response was indeed reduced in comparison to that of *P. miliaris*.

5.3. Materials and methods

5.3.1. Experimental procedure

Echinoids

Brissopsis lyrifera were collected using a 1.5 m Agassiz trawl from four locations (Table 5.1) in May 2007 in the Gullmar Fjord, Sweden (Figure 5.2). The echinoids were then maintained at Kristineberg Marine Research Station in 20 L polyethylene aquaria filled with muddy sediment collected from the Agassiz trawls to a depth of 8 cm. A continuous flow (20 L per hour) of seawater from 30 m depth in the fjord was maintained in each aquarium, with a constant water depth of 3 cm above the sediment surface. The echinoids were acclimated to this aquaria system for 9 days prior to the exposure experiments.

Table 5.1. Agassiz trawl locations for the collection of *B. lyrifera* in the Gullmar Fjord.

Trawl No.		Latitude (°N)	Longitude (°E)	Depth (m)
1.	Start	58°14.86	11°25.68	36
	End	58°14.69	11°25.50	33
2.	Start	58°14.72	11°25.55	36
	End	58°14.04	11°25.76	37
3.	Start	58°14.75	11°25.54	37
	End	58°15.67	11°25.70	38
4.	Start	58°14.78	11°25.56	35
	End	58°15.00	11°25.85	37

Exposure experiments

Muddy sediment, collected from the Agassiz trawls, was sieved (1 cm) to remove large macrobenthos and then mixed with WBSM to give a concentration of 10 ml per L sediment. The contaminated sediment was placed in four aquaria, clean sediment was placed in a fifth aquarium to serve as a control (all to depths of 8 cm), and the sediment was allowed to settle overnight. Flow through seawater was then started and eight echinoids of a minimum size of 35 mm test length were placed on the sediment surface of each aquarium at which point the behavioural biomarker observation commenced (see next section). Exposure to the WBSM/sediment mix proceeded for 24, 48, 72 or 96 hours. A single group of control echinoids were processed after 24 hours had elapsed. Covers were placed over each aquaria to maintain constant darkness (as would be experienced by the burrowing echinoids *in situ*). Due to the common flow-through water circulation, all aquaria experienced the same environmental conditions during the experimental period: mean salinity = 33.94 ± 0.68 SD, mean temperature = 8.66 °C ± 0.40 SD (pH measurements were not taken).

5.3.2. Experimental assays

Burrowing time (behavioural biomarker)

Rather than the righting time assay used for the *P. miliaris* experiments, the behavioural biomarker used with *B. lyrifera* was burrowing time as described in the National Institute for Coastal and Marine Management (Netherlands) *Echinocardium cordatum* sediment toxicity test (RIKZ, 1999). Each echinoid was placed at regular intervals on the sediment surface of each aquarium. Burrowing time was determined with a stopwatch starting from the moment the last echinoid was placed on the sediment surface. An echinoid was considered to have completely reburrowed when the upper side of the echinoid's aboral test was level with the sediment surface.

However, due to the lack of a burrowing response in the majority of the echinoids over the first 12 hours of the experimental period, any attempt to assess burrowing behaviour over time was abandoned. Instead, when each aquarium reached the end of the exposure period, a 'burrowing index' was allocated to each echinoid as follows: A = fully burrowed, B = partially burrowed (part of echinoid below sediment surface), C = no evidence of burrowing activity. In addition, during processing of the echinoids, it was noticed that some had 'lesions' where the test was blackened and spines were absent (Figure 5.3), and which had not been present at the start of the experimental period. A 'lesion index' was therefore also allocated to each echinoid as follows: A = no lesions, B = one lesion, C = more than one lesion.

Figure 5.3. A specimen of *B. lyrifera* illustrating the presence of a 'lesion', comprised of darkened test with an absence of spines. Scale bar = 1cm.

Total and differential coelomocyte counts (cellular biomarker)

After the exposure time had lapsed for each aquarium (24, 48, 74, 96 hours) the cellular biomarker assay proceeded as described for the *P. miliaris* assay (section 4.2.2.3); 0.75 ml coelomic fluid was drawn from the coelomic cavity of each echinoid into an equal volume of anticoagulant solution (ISO-EDTA). Once tissue samples had been taken for gene expression analysis (see next section) differential cell counts, following the Smith (1981) and Matranga et al. (2005) coelomocyte descriptions, were performed with a Neubauer haemocytometer under Nomarski contrast interference optics using a Leica^{TM} LEITZ DMRB microscope. Counts of phagocytes, red or colourless spherule cells and vibratile cells (Figure 5.4) were recorded and calculated as cells ml^{-1} for all live control and exposed echinoids. Triplicate counts were made from each sample of coelomic fluid from an echinoid, and the mean number of each type of coelomocyte calculated from the three counts. These mean numbers were used as a single replicate for subsequent statistical analysis. The total coelomocyte count (TCC) was calculated from the sum of the mean differential cell counts for each echinoid.

Oxygen consumption and citrate synthase activity

Due to equipment failure the determination of *B. lyrifera* oxygen consumption rates was not possible. At the time the exposure experiments were performed, a decision to assess echinoid tissue samples for CS activity had not been made, and so this biomarker was not incorporated into the *B. lyrifera* experiments.

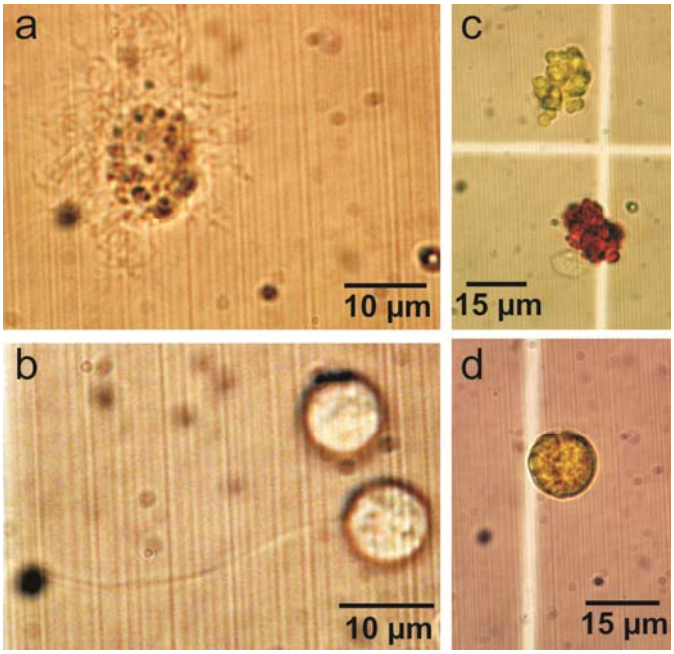

Figure 5.4. *B. lyrifera* coelomocyte cells. a) Phagocyte in filipodial form, b) two vibratile cells, the lower cell with flagellum in focus, c) colourless spherule cell (above) and red spherule cell (below), d) spherical colourless spherule cell. All images taken with a Leica LEITZ DMRB microscope under Nomarski optics with fitted Leica IC D Camera.

Gene expression (molecular biomarker)

Tissue samples (from the gut and oesophagus) were dissected from each echinoid, and as many tube feet as possible were removed, and placed into 2.0 ml microcentrifuge tubes containing 1.5 ml RNA*later* Solution. The tissue samples were stored at 4°C overnight and then stored at -80°C until required. The tissue samples were subsequently processed for gene expression analysis and qPCR assays as explained previously in detail from section 3.4.1. to 3.4.6. All gene expression results were standardised to transcript copy number per µg total RNA.

5.3.3. Statistical analysis

The Kolmogorov-Smirnov test was used to test the biomarker results for a normally distributed population. Where required, data were log transformed to meet the assumptions of parametric significance testing (a normal distribution and equal variances). Where transformation did not result in these assumptions being met, nonparametric tests were employed on untransformed data. Because a control group of echinoids was not included at each time point to accompany the exposed groups of echinoids, it was not possible to perform two-way ANOVAs on the biomarker results data with regard to treatment and time. Instead, for the statistical analysis of the biomarker responses one-way analysis of variance (ANOVA) was performed on the experimental data using the treatment conditions of each aquaria as the factor, i.e. the different levels of the treatment factor were 24, 48, 72, 96 hours and the control. Statistical analysis of the burrowing and general

health indices (examples of categorical data), proceeded with Fishers exact test of independence, as it is considered more accurate than the chi-squared test when expected numbers are small (McDonald, 2009). All statistical tests were performed at the 5% significance level and with the statistical software SigmaPlot for Windows Version 11.0, apart from the Fisher's test which was performed via the website: http://udel.edu/~mcdonald/statfishers.html (McDonald, 2009).

5.4. Results

Experimental setup

There was a significant difference in the mean wet weight of the echinoids between the treatment groups ($F_{4,35} = 3.637$, $p < 0.05$) with the 96 hour group being significantly heavier than the 24 hour group ($q = 4.547$, $p < 0.05$). It was therefore necessary to check any significant differences that were subsequently found between biomarker responses for the 96 and 24 hours groups were not caused by the variations in the wet weight of the echinoids, which was found to not be the case. During the experiment, two echinoids died in the 72-hour group.

Burrowing and lesion indices

The burrowing and lesion indices of the *B. lyrifera* in each of the experimental aquaria are recorded in Table 5.2. Two echinoids were found to be dead in the 72 hour exposure tank, neither of these individuals had attempted to burrow into the sediment and were allocated a non-burrowed index (C). An assessment of the presence of lesions on the tests of the deceased individuals was not recorded, as it was not known whether lesions had formed pre- or post-death (due to decomposition). Significance tests indicated that there were no differences between the lesion index with treatment (Fishers = 3.8×10^{-5}, $p > 0.05$), and there were no significant differences in the burrowing index (Fishers = 2.9×10^{-6}, $p > 0.05$).

Table 5.2. Details of the numbers of *B. lyrifera* allocated a specific category of burrowing index or general health index and found dead in the experimental aquaria. Burrowing index: A = fully burrowed, B = partially burrowed, C = no evidence of burrowing activity. Lesion index: A = no lesions, B = one lesion, C = more than one lesion. Dead *B. lyrifera* were allocated a burrowing index, but not a general health index. n = 8 for each aquaria.

Experimental Aquaria	Number of dead *B. lyrifera*	Burrowing Index			Lesion Index		
		A	B	C	A	B	C
24 hours	0	3	4	1	4	3	1
48 hours	0	2	4	2	2	4	2
72 hours	2	1	3	4	1	3	2
96 hours	0	4	3	1	5	1	2
Control (24 hours)	0	5	0	3	3	2	3

Total and differential cell counts

The determination of total and differential cell counts were made on every live echinoid specimen where the coelomic fluid did not immediately clot (which occurred in one echinoid from both the 48 and 96-hour treatment groups). The mean total number of coelomocyte cells was 1.34 x 10^6 ml^{-1} (± 1.1 x 10^6 SD), although the counts from individual echinoids ranged widely from 0.1 x 10^6 ml^{-1} to 5.7 x 10^6 ml^{-1}. There were no significant differences in the total number of coelomocyte cells with treatment ($F_{4,31} = 0.701$, $p > 0.05$) (Figure 5.5a). The only significant difference within the coelomocyte types was found between the mean number of colourless spherule cells in the 48 hour group which had a greater proportion of cells than the 96 hour group (Dunn's test $q = 6.184$, $p < 0.001$) (Figure 5.5b)

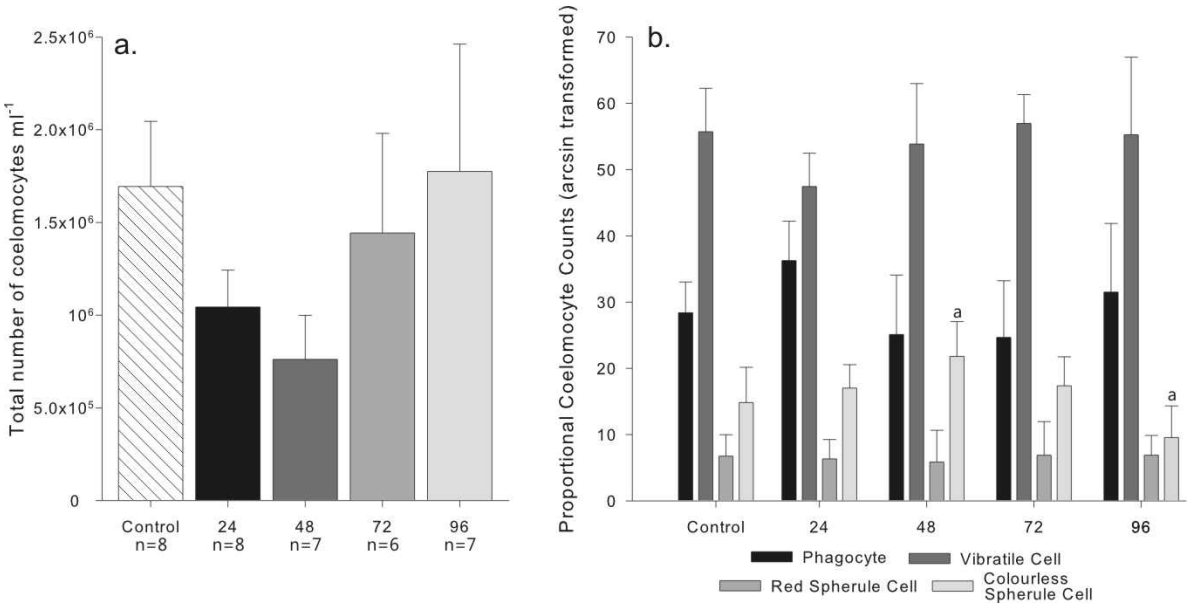

Figure 5.5. a. Mean (±SE) number of total coelomocyte cells. b. Mean (± SE) proportion of differential cell counts, lower case letters indicate the significant difference in the number of colourless spherule cells between the 96 and 48 hours groups. Number of replicates for each treatment group is the same as for figure a.

Gene expression

In the gut tissue samples there were no significant differences in the expression of the *ubi* and *hsp70* genes between the echinoids in different treatment groups. However, the expression of *cs* in the gut tissue was found to be significantly different between groups ($H = 12.104$, $p < 0.05$, Figure 5.6a), with the level of *cs* expression in the 72 hour group greater than that of the 96 hour group (Dunns test $q = 3.124$, $p < 0.05$). There was no significant difference in any of the three genes with treatment group in the oesophagus or tube feet tissue samples (Figure 5.6 b and c).

During analysis of the gene expression results, it was determined that the level of *cs* expression was correlated with that of the *ubi* gene in each of the three different tissue types (Figure 5.7). In

addition, the expression of *ubi* in each of the three tissue types was also significantly correlated with each other.

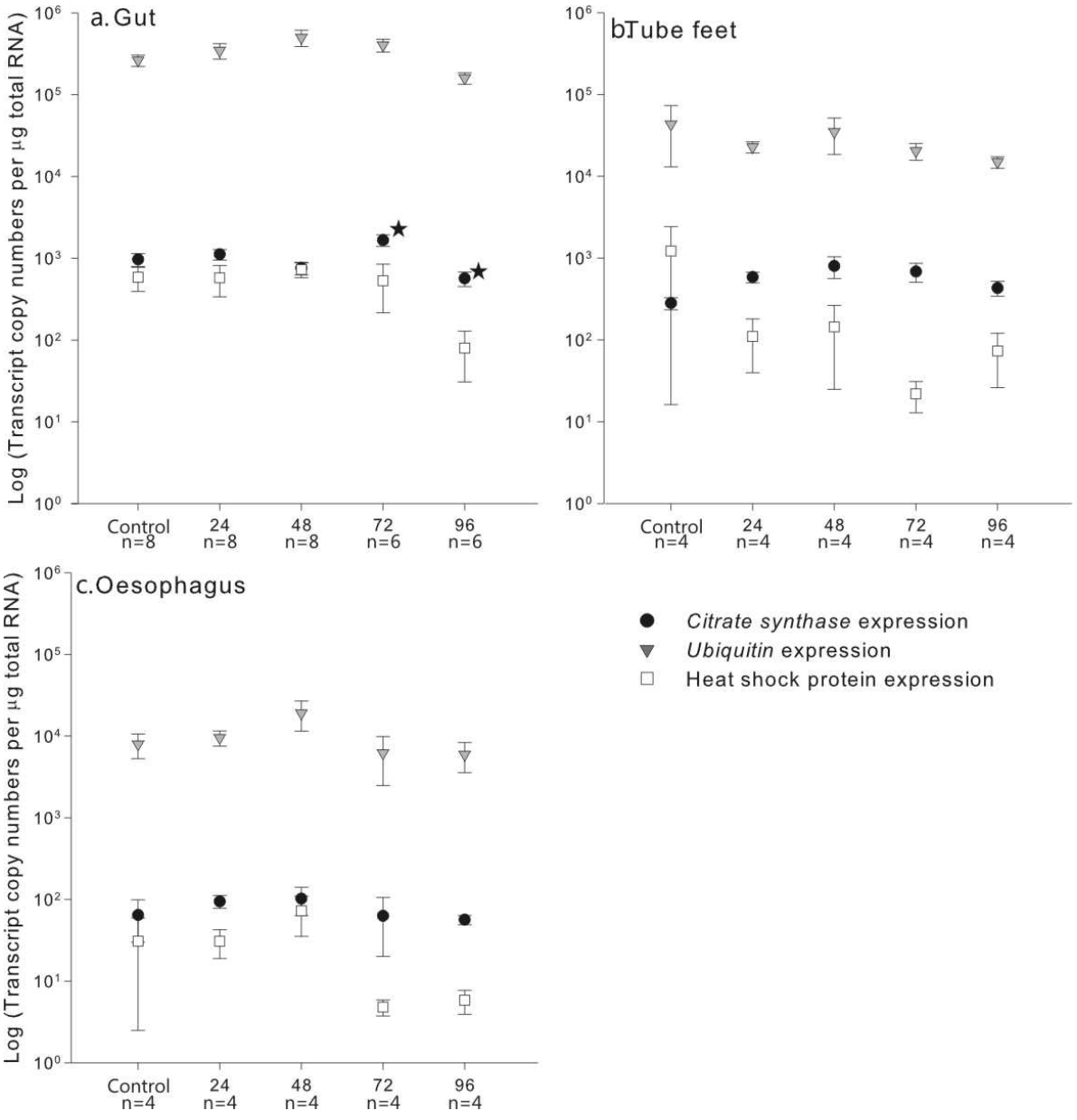

Figure 5.6. Mean (±SE) gene expression of *cs, hsp70* and *ubi* in a) the gut tissue samples b) the tube feet, and c) oesophagus tissue. Starred data points are significantly different from each other.

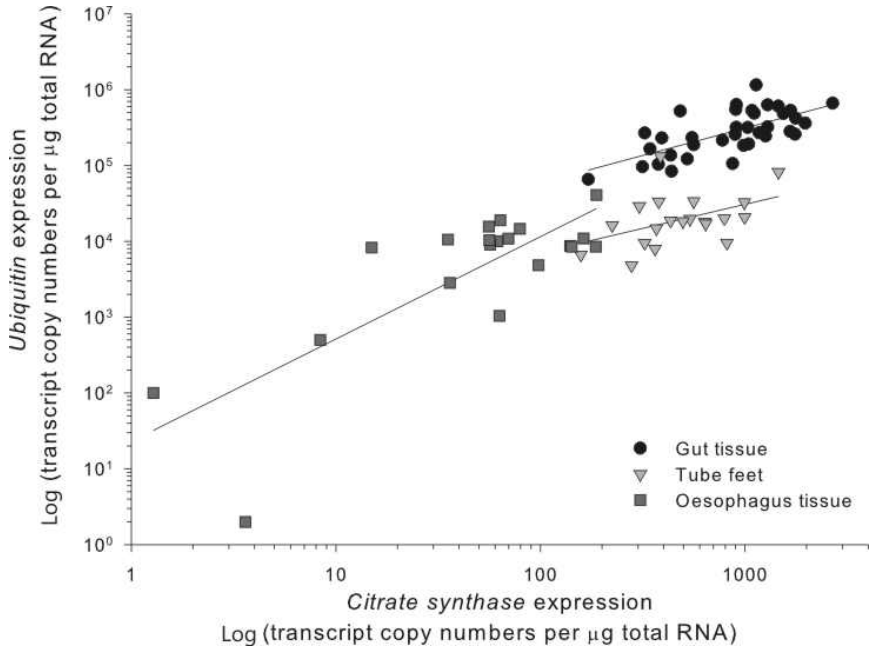

Figure 5.7. Correlation between the citrate synthase and ubiquitin levels of gene expression for gut ($r_s = 0.675$, $p < 0.001$), tube feet ($r_s = 0.504$, $p < 0.05$) and oesophagus ($r_s = 0.501$, $p < 0.05$) tissue samples from *B. lyrifera*.

5.5. Discussion

No previous reported studies have utilised *B. lyrifera* as a toxicological test organism, other than as part of the assessment of alterations in the diversity of benthic communities following drill cutting exposure or organic enrichment (Kutti et al., 2007; Schaanning et al., 2008; Trannum et al., 2010). The assessment of reduced reburial activity and mortality in heart urchins (*E. cordatum*) in response to contaminated marine sediments is routinely used in European studies though, and a standardised experimental procedure has been developed for use with the burrowing echinoid *E. cordatum*, which has been demonstrated to have good reliability in inter-laboratory comparisons (RIKZ, 1999; Stronkhorst et al., 2004).

In this current study, the behaviour of *B. lyrifera* appeared to be abnormal. Previous reports of *B. lyrifera* burrowing activity indicate that it starts immediately following placement onto sediment, with the time taken to be covered completely by sediment ranging between 49 and 86 minutes (Hollertz and Duchêne, 2001). Despite the experimental conditions used with *B. lyrifera* in this study being similar to those used by Hollertz and Duchêne (Gullmar Fjord specimens, sieved sediment, flow through water, ~7-8 cm sediment with a smooth surface), none of the *B. lyrifera* had reburrowed within five hours in either the WBSM mixed sediment or the control clean sediment. In the first 12 hours only four (out of 40) echinoids had completely burrowed underneath the sediment, and only a further eleven completed burrowing over the total course of

their experimental period.

In general the burrowing response of the population of *B. lyrifera* was poor. The possiblity that the echinoids avoided burrowing into the sediment because of the WBSM contamination is not supported due to the lack of a significant difference between burrowing activities in the exposed and control aquaria. One consequence of the poor burrowing activity is that the echinoids which remained on or within the sediment surface may have had a reduced exposure to the WBSM, which was mixed with the sediment, than the echinoids which had completely burrowed under the surface. It is therefore unlikely that all echinoids received a similar exposure dose of WBSM, and this may have influenced the results of the subsequent biomarker assays.

It has been noted that the responses of *E. cordatum* collected from the field can be affected by trauma caused to the echinoids during collection, which in turn influences experimental results (Schipper et al., 2008). It is possible that the specimens of *B. lyrifera* had been internally damaged (no external damage was visible) during field collection by the Agassiz trawl and that either this, their exposure to the air during transfer to holding tanks or their subsequent transport and acclimatisation to the test conditions, detrimentally affecting their burrowing capability (Hauton et al., 2003; Stronkhorst et al., 2004). These results, in conjunction with those of the *P. miliaris* righting response indicate that behavioural biomarkers were not reliable indicators of echinoid exposure to WBSM.

The mean number of *B. lyrifera* coelomocyte cells (1.34×10^6 ml^{-1} $\pm$ 1.1×10^6 SD) was lower than that of *P. miliaris* ($5.88 \times 10^6 \pm 2.77 \times 10^6$ SD), but as also found for the *P. miliaris* coelomocyte counts, there was no difference in the total number of coelomocyte cells with exposure treatment. The vibratile cells comprised the largest group of coelomocytes whilst the phagocytes accounted for the second highest proportion. Only the colourless spherule cells varied under the different treatment conditions, although significant differences only occurred between the 48 and 96 hours exposed treatment groups. This result is in contrast to the *P. miliaris* coelomocytes and responses, where the phagocytes comprised the biggest proportion of cells, followed by the vibratile cells, and both of these cells types varied significantly in the exposed and control groups of echinoids.

The dominance of the *B. lyrifera* vibratile cells amongst the coelomocyte population of an echinoid has not been reported previously, although no accounts of spatangoid echinoid coelomocyte numbers were found in the published literature. Deposit feeding echinoderms, like *B. lyrifera*, are known to suffer from a number of different protozoan infestations, and a report by Coulon and Jangoux (1987) details 'aciculate' (having needle like parts) coelomocytes covering invading microbes and rendering them motionless. An inspection of images of these aciculate

coelomocytes indicates that the needle like parts resemble the flagella of vibratile cells (image 19; Coulon and Jangoux, 1987). As vibratile cells are thought to be involved with the active immobilisation of invading microbes (Matranga et al., 2005), the great proportion of vibratile cells in *B. lyrifera* are indicative of the echinoids suffering from protozoan infestation for which the defensive vibratile cells are required. Alternatively, vibratile cells may play a greater role than phagocytes in the immune response of *B. lyrifera* (and other spatangoid echinoids), and hence are always present in greater proportions than found in *P. miliaris*.

Unlike the results of the *P. miliaris* gene expression biomarkers, in *B. lyrifera* no significant difference in the expression of any of the three genes of interest was found in response to WBSM exposure. As also found in *P. miliaris*, the expression of the *cs* and *ubi* gene were significantly correlated in each of the three *B. lyrifera* tissue types indicating that, as discussed previously (section 4.5.1), a correlated adjustment in citrate synthase and ubiquitin transcript numbers may be related to the demand for ATP to fuel increased protein degradation.

With regard to the determination of whether the WBSM-induced stress responses in *B. lyrifera* and *P. miliaris* differed, it was found that whilst the molecular and cytological biomarkers in *P. miliaris* did display significant changes in response to WBSM exposure, no change in either of these biomarkers was evident in *B. lyrifera.* At the biochemical (CS activity) and physiological levels (oxygen consumption) of organisation, no change was found following WBSM exposure in *P. miliaris*, and at the behavioural level no change was found in either of the echinoid species. Therefore, a response to WBSM exposure was evident at the lower levels of biological organisation in *P. miliaris* and absent from all biomarker assessments in *B. lyrifera*. The lack of response to WBSM in *B. lyrifera* does support the prediction that, as a stenotopic species unaccustomed to significant environmental perturbation, it would lack an adaptive capacity to respond to stress caused by contaminant exposure.

In both the experiments with *P. miliaris* and with *B. lyrifera*, there was evidence that the overall experimental conditions and/or collection process were detrimental to the field-collected echinoids. The significant change in coelomocytes (greater phagocyte, reduced colourless spherule cell, proportions) with overall experimental time in both exposed and control *P. miliaris* suggests that the experimental treatment of *P. miliaris* caused an overall deterioration in condition. This, in addition to the behavioural evidence that the *B. lyrifera* were adversely affected by the field collection process, shows that adult echinoderms are sensitive to artificial experimental conditions. It is therefore likely that the laboratory based experimental conditions had a greater impact on the echinoids than the WBSM exposure. Schipper et al. (2008) found that the use of cultured *E.*

cordatum in sediment toxicity tests resulted in improved test reproducibility and lower statistical variation, with multiple environmental stressors reducing the toxicity test performance of field specimens. Therefore, whilst in comparison to *in situ* field studies, shallow water laboratory based studies are cheaper and have greater flexibility in methodology, great care must be taken in ensuring the collection process and quality of the aquarium environment does not detrimentally affect the echinoid specimens.

The use of WBM in the offshore drilling industry and its discharge to the environment is permitted because of its reduced toxicity in comparison to oil based- and synthetic-based drilling fluids (Holdway, 2002; OSPAR Commission, 2009). There is a general paucity of published studies which have reported the effects of WBM on marine organisms in detail though, and what has been published does not illustrate a clear picture of WBM toxicity. Whilst some studies have indicated extremely low toxicities of the components of WBM, or concluded that, whilst finding high toxicity in some WBM components, following dilution in the seawater after discharge their environmental toxicity will be negligible (Terzaghi et al., 1998; Melton et al., 2000; Neff, 2005). Other studies alternatively indicate that even low-toxicity WBM at environmentally realistic test concentrations (0.002 to 200 mg l^{-1}) can have significant impacts on adult mortality and processes such as larval settlement (Raimondi et al., 1997). The impact of bentonite (which comprised 7% of the WBM used in this study) on organisms is related to its suspension in sea water as opposed to any direct toxic effects, with related burial and clogging of gills causing death in oysters and its shading effect reducing sunlight penetration and hence photosynthesis of microalgae (Cabrera, 1971 and Sprague and Lugan, 1979, cited in Neff, 2005).

The effects of WBM fluid and WBM cuttings on benthic fauna also depend on the hydrodynamic character of the seafloor environment (Dalmazzone et al., 2004). In low energy situations, the smothering, burial and physical effects of solid drill cuttings are an important determinant of community change (Schaanning et al., 2008) , although these physical effects are localised to the vicinity of the source of the drill spoil (Neff et al., 2000; Jones et al., 2007; Netto et al., 2009; Santos et al., 2009). Studies investigating the physical impact of WBM cuttings have found evidence that factors other than burial, such as oxygen depletion, primarily affect impacted benthic communities (Trannum et al., 2010), and potential toxicological effects are highly dependent on the composition of the drilling fluids (Holdway, 2002; Dalmazzone et al., 2004; Neff, 2005). Trannum et al. (2010) comment that despite the fact that the effects of WBM are less severe that those of OBM and SBM, WBM cuttings still have a significant impact on faunal communities and their preferential use should be supported by scientific evidence.

5.6. Conclusions

The results of the *B. lyrifera* experiments indicate that WBSM exposure did not cause a deviation in the echinoid biomarker responses compared with the control specimens. The null hypothesis (section 5.2.2) is accepted in the case of each biomarker. With regard to the differences between the *P. miliaris* and *B. lyrifera* WBSM responses, whilst significant differences were found in the molecular and cytological biomarker results between the exposed and control *P. miliaris* specimens, there were no significant differences in the *B. lyrifera* biomarker results. These results indicate that in comparison to *P. miliaris*, *B. lyrifera* did not demonstrate a response to the WBSM. In light of this outcome, it can be determined that the stenotopic species *B. lyrifera* has a reduced capacity to respond to WBSM contaminant exposure in comparison to the eurytopic species *P. miliaris*.

The work with *P. miliaris* and *B. lyrifera* also demonstrated that any future laboratory-based experimental investigations with field-collected echinoderms must minimise the potential effects of the collection process, or that experiments should be carried out with *in situ* echinoderm populations. In this regard, the next chapter concerns the second approach used in this study to investigate anthropogenic impact on echinoderms. An *in situ* approach was undertaken to investigate the stress response of echinoids inhabiting deeper waters to disturbance caused by offshore hydrocarbon drilling activity. The *hsp70* expression biomarker, developed during the *P. miliaris* and *B. lyrifera* experiments, was applied to a third species of echinoid in order to determine whether the quantitative gene expression methodology could easily be applied to a novel species.

Chapter 6. *In situ* disturbance and decompression experiments with *Echinus acutus*

6.1. Introduction

As found during the experiments with *Brissopsis lyrifera,* the process of collecting echinoderms from their habitats may result in trauma being caused to the specimens. This in turn may alter their natural activity (e.g. burrowing) during experimental investigations. The collection of megafaunal specimens from the deep sea, via trawls, sled or dredge, does not protect the organisms from physical damage or the effects of decompression and temperature change (section 1.4.1) (Hessler, 1972; Macdonald, 1975) and it is difficult to obtain accurate experimental results with deep-sea specimens retrieved to the surface, as they may be influenced by artefacts introduced during the recovery process (Theron and Sebert, 2003; Dixon et al., 2004). In order to obtain reliable experimental results, investigations with deep-sea organisms should therefore either use specimens retrieved to the surface protected from damage and decompression, or be performed *in situ* at the sea floor. This latter approach is developed in this chapter and the following Chapter 7.

In this current chapter, the performance of *in situ* disturbance and decompression experiments with a remotely operated vehicle (ROV) is described. ROVs are used extensively by the offshore drilling industry to support deep-water activities (Jones, 2009), and are increasingly being used by the international scientific community for enhanced deep-sea observation, fine scale mapping, sampling, instrument deployment and interactive experimentation (Bachmayer et al., 1998; Favali and Beranzoli, 2006; Yoerger et al., 2007). The opportunity to perform *in situ* experimentation and to test the application of the molecular biomarker methodology, developed during the previous *Psammechinus miliaris* and *B. lyrifera* experiments, to echinoderms subject to experimental manipulation in deep waters was made possible by the SERPENT project[1].

The epifaunal echinoid *Echinus acutus* var. *norvegicus* (referred to as *E. acutus*) was abundant around the drilling site of a hydrocarbon exploration well in the North Sea off Norway at 114 m water depth. The ROV associated with the drilling rig was used to carry out *in situ* experiments to assess the effect of drilling disturbance (via sediment burial) on the expression of a stress-70 gene in *E. acutus* and, in addition, to determine any effect of retrieval to the surface on its expression (due to decompression and temperature change). The use of the ROV allowed the experiments to

[1] The "Scientific and Environmental ROV Partnership using Existing iNdustrial Technology" (SERPENT) project aims to make cutting-edge industrial ROV technology and data more accessible to the world's science community by collaborating closely with key companies in the oil and gas industry. It is hosted by the NOC.

proceed without physical damage being caused to the echinoids either during the experiments or during retrieval. It should be noted that all offshore experimental and observational work was performed by Drs D. Jones and A. Gates of the SERPENT project. I subsequently developed the molecular biomarker and quantified the changes in the expression of an inducible stress-70 protein in the Aristotle's lantern muscle and intestine of the echinoids using quantitative PCR (qPCR).

The aim of these experiments was to apply the quantitative gene expression technique to samples from the *in situ* experiments, and to determine whether stress caused by simulated anthropogenic disturbance and/or the collection process could be detected via altered gene expression. This work has been published in the Journal of Experimental Marine Biology and Ecology entitled Hughes et al. (in press) '*A systems approach to assessment of drilling disturbance on* Echinus acutus *var.* norvegicus *(Düben & Koren, 1846) based on* in situ *observations and experiments using a Remotely Operated Vehicle (ROV)*' (Appendix 1.31). A summary of the methods, results and discussion reported in the manuscript is included in this chapter, together with an expanded discussion of the stress-70 gene expression results.

6.1.1. The ecology of *Echinus acutus* (Düben and Koren, 1846)

Echinus acutus is a regular epifaunal echinoid, distributed from Iceland to northwest Africa. Three varieties comprise the *E. acutus* species: *flemingii*, *norvegicus* and *mediterraneus*, the first two being found in the North Sea (Cranmer, 1985). Test colour is variable, but generally consists of reddish brown or green vertical stripes separated by pinkish-white ambulacral areas. The *norvegicus* variety, the subject of the *in situ* ROV experiments, is recognisable by its slightly flattened test (not larger than 70 mm diameter) and long slender spines (Figure 6.1) (Southward and Campbell, 2006). A continental shelf and bathyal species, *E. acutus* var. *norvegicus* is reported to occur below 100 m depth and has been reported as collected off the coast of Scotland in trawls from up to 1075 m depth (Gage et al., 1986; Southward and Campbell, 2006).

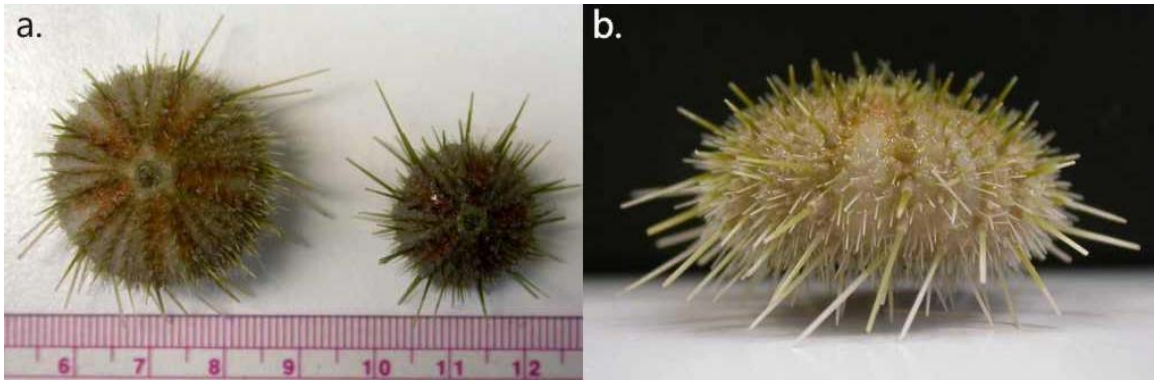

Figure 6.1. *Echinus acutus* var. *norvegicus* collected from the Ragnarokk Field in the North Sea off Norway. a). Aboral view of two specimens of differing size, scale bar in cm. b). lateral view of test, illustrating the flattened form.

6.1.2. *In situ* experimentation

As already discussed (section 4.1.1), drilling activities cause physical changes to the seafloor as drill cuttings comprised of drilling mud, chemicals, and fragments of rock are discharged to the seabed (Breuer et al., 2004). Solid cuttings physically affect benthic fauna by burial, altering sediment particle size, generating anoxic conditions and changing chemical fluxes in the sediment-water interface (Neff et al., 2000; Trannum et al., 2010). Burial by sediment can have sublethal effects on affected organisms (Rogers, 1990) caused by changes in food supply, feeding inhibition and physical injury (Hall, 1994), as well as directly causing mortality (Chandrasekara and Frid, 1998; Hinchey et al., 2006). In this study, to simulate the impact on *E. acutus* of physical disturbance caused by sedimentary burial during the initial phases of a potential tophole drilling programme, an experiment was carried out involving the burial of echinoids with sediment collected by an ROV. A surface retrieval manipulation experiment was also performed with the ROV to provide a preliminary indication of whether or not the retrieval of *E. acutus* individuals from the seabed to deck, with associated decompression and temperature change, could alter stress-70 expression.

6.2. Materials and Methods

6.2.1. Study site

The experimental work was carried out in summer 2007 at the Ragnarokk hydrocarbon exploration area located west of Stavanger, Norway in the North Sea (058º 53 N, 002º 22 E). All work was carried out from the M.V. *West Epsilon*, a three-legged cantilever jack-up drilling unit, using a work-class Oceaneering Hydra Magnum 034 ROV. The water depth at the drill site was 114 m and the water temperature recorded at the seabed with the ROV's parascientific temperature sensor was 8.4°C. The sea surface temperature was not recorded during the time of deployment by the ROV, but CTD data collected previously at this location indicate a surface temperature of ~14°C during July and August (BODC, 2009). The ROV-facilitated sediment burial and surface retrieval experiments were performed with specimens of the abundant echinoid *E. acutus* between 30/08/2007 and 05/09/2007.

6.2.2. ROV experimentation

Echinoids were collected by being scooped up into a push core by the ROV with minimal disturbance and no damage caused. Once collected, the echinoids were transferred directly into experimental chambers or immediately brought to the surface in upturned push cores for further experimentation or preservation as detailed below. The time taken to transport the echinoids from the seabed to the deck of the rig was 14 minutes. Tissue samples dissected from the intestine and

Aristotle's lantern musculature of the echinoids were immediately transferred into separate 2.5 ml sterile microcentrifuge tubes that contained 1.5 ml RNAlater® Solution (Ambion). The tissue samples were transferred to a freezer (-20°C) within 1 hour of dissection.

Experiment 1: The effects of surface retrieval on stress-70 gene expression

On one dive, two echinoids were collected and immediately brought to the surface in a push core, dissected and preserved. From collection at the seafloor to final preservation took approximately 50 minutes. On the next ROV dive another two echinoids were collected in the core and brought up to a depth of 10 m. These two echinoids were then returned to the seabed and then immediately brought back up through the water column and recovered onto the deck of the rig. The echinoids were then dissected and preserved (within 70 minutes of collection at the seafloor). Temperature difference between the seafloor and sea surface was approximately 5.6°C and the pressure change was approximately 1054 kPa.

Experiment 2: The effects of sedimentation on stress-70 gene expression

To investigate the impact of physical disturbance by sedimentary burial on stress-70 expression, an experiment was carried out subjecting *E. acutus* individuals to three treatments: a procedural control (C), a single sedimentation event (S) and multiple sedimentation events (MS), designed to simulate the discharge of sediment during the initial phases of a potential tophole drilling programme. Experimental chambers were constructed using 5 L plastic buckets. A lid was placed on the bucket with hole cut in it to allow for video inspection and the introduction of echinoid specimens and sediment.

Three experimental treatment chambers were deployed by the ROV next to each other on the seabed 5 m from one of the drilling rig legs. Six echinoids were carefully added to each experimental chamber using a push core sampler. Immediately after echinoid introduction, approximately 1000 cm^3 of sediment was collected from the immediate seabed using the push core sampler, and introduced to both the S and MS experimental chambers. No sediment was added to the control treatment chamber. A sediment volume of 1000 cm^3 produced an approximate level sediment depth of 3 cm at the base of the experimental chambers, and just covered the echinoids. The echinoids were observed in all chambers using a small camera on an ROV manipulator arm. One hour after the first sediment treatment, and after the echinoids had all repositioned themselves on the sediment surface, another ~1000 cm^3 of sediment was added to the MS treatment. Twenty-four hours after initial deployment another ~1000 cm^3 of sediment was added to the MS treatment. All experimental chambers were retrieved simultaneously 48 hours after the start of the experiment. Three echinoids were found to remain in each of the experimental chambers (the missing echinoids were presumed to have escaped from the chambers via the lid observational

hole); each remaining echinoid was processed and preserved within 80 minutes of leaving the seafloor.

Experiment 3: preliminary induction of a stress-70 HSP

To ensure the collection of tissue samples which contained sufficient numbers of stress-70 transcripts to allow the mRNA to be isolated with degenerate primers (see below), individual echinoids were heat shocked (section 2.4.1). Twenty echinoids were collected on the seafloor with a push core and brought immediately to the surface, where they were transferred to gently aerated aquaria maintained at 25±1°C on the rig. One echinoid was removed from the aquaria hourly from the start of the experiment, dissected and preserved immediately.

6.2.3. Gene expression analysis

Isolation of a stress-70 fragment

As with the *P. miliaris* and *B. lyrifera* studies, the application of qPCR analysis of gene expression to tissue samples from *E. acutus* first required the isolation of the nucleotide sequence of a stress-70 gene. Total RNA was extracted from the preserved Aristotle's lantern muscle tissue from a 10-hour heat shocked echinoid using TRI Reagent™ (Sigma-Aldrich) according to the manufacturer's protocol, and quantified by measuring the absorbance at 260 nm. Total RNA (~2 µg) was reverse transcripted into complementary DNA (cDNA) in a 20 µl reaction which included 200 units SuperScript II Reverse Transcriptase with accompanying First Strand Buffer and 0.1 M DTT (Invitrogen), 40 units RNase Inhibitor (Sigma-Aldrich), random nonamers (2.5 µM final concentration; Sigma-Aldrich) and 10 mM dNTP mix (New England Biolabs). The cDNA obtained was used for degenerate polymerase chain reaction (PCR) cycling with the HSP70dF2 and HSP70dR1 degenerate oligonucleotide primers (section 2.4.4).

A single band of approximately 400-bp was obtained and gel-purified on a TAE 1% agarose gel, extracted using a QIAquick gel extraction kit (QIAGEN) and cloned using an Invitrogen TOPO TA Cloning® Kit for sequencing (pCR®4-TOPO® vector and One Shot® TOP10 *Escherichia coli*; Invitrogen, Appendix 9). The plasmids were extracted from the *E. coli* cultures using a QIAprep® Miniprep Kit (QIAGEN). The fragment was sequenced (three random clones; both strands) using M13 primers by Geneservice Ltd. (Department of Biochemistry, University of Oxford). The obtained nucleotide sequences were aligned and translated using Geneious Basic trial software 4.8.3 (Drummond et al., 2010). A similarity analysis of the deduced protein sequence was carried out using BLAST 2.2.19+ at NCBI (Altschul et al., 1997).

Quantitative PCR assay

Quantification of mRNA transcript abundance required a pair of species-specific primers to be

designed for the *E. acutus* stress-70 gene. Two qPCR primers, 5′-GAGTTCAAGGGAGAAACCAAGAC-3′ (forward) and 5′-GCAGTTTCTTTCATCTTGAGCAG-3′ (reverse) were designed targeting a 77-bp region of the sequenced *E. acutus* gene fragment. The primers were designed manually according to the qPCR primer design requirements detailed previously (section 3.2.1). The optimal primer concentration used in the qPCR was determined from a primer concentration matrix (section 3.2.3), and the products from these optimisation tests run out on an agarose gel and visualised to confirm the product was the expected size. The efficiency and sensitivity of the qPCR assay was tested using a qPCR standard curve produced from a dilution series of the extracted and linearised (*Not I* restriction enzyme) pCR4-TOPO vectors containing the target amplicon (section 3.3). The relationship between concentration and C_q value was linear for seven orders of magnitude for the plasmid dilution series and calculated assay efficiency was 95% ($C_T = 31.525 – 3.447$ x Log Dilution; $r^2 = 0.995$).

Total RNA was isolated from the Aristotle's lantern muscle and intestine tissue taken from each echinoid with TRI Reagent. To remove genomic DNA contamination, the total RNA samples were treated with DNase Amplification Grade I (Sigma-Aldrich). The total RNA was then quantified with Quant-iT™ RiboGreen® RNA Quantitation Reagent (Invitrogen). For cDNA synthesis, 300 ng of DNase-treated total RNA was reverse-transcripted using SuperScript Reverse Transcriptase III (Invitrogen) with random nonamer primers (Invitrogen). The qPCR assay was performed using a Rotorgene-3000 (Corbett Research Ltd.) in reactions containing 1 µl of cDNA, each qPCR primer (50 nM final concentration), 10 µl Precision Master mix with SYBRgreen (PrimerDesign Ltd.) and nuclease-free water to a total volume of 20 µl. The qPCR was run with the following cycle parameters: 1 cycle of 95 ºC for 10 min; 35 cycles of 95 ºC for 10 s, 60 ºC for 40 s, 60 ºC for 20 s. Each experimental cDNA sample was run in duplicate, three times (in order to control for qPCR reproducibility), together with no template controls and a cDNA calibrator sample (see below). Melt curve analysis was performed following each qPCR to confirm that only a single product was amplified.

The number of gene mRNA transcript copies were determined using the absolute quantification approach (section 3.1). To correct for inter-run variations, the C_q value of every sample was normalized to that of a cDNA calibrator sample included in each qPCR assay (Wong and Medrano, 2005). The mean C_q value of each duplicate sample was then compared with a standard curve produced from a serial dilution of the Not I linearised pCR4-TOPO vector. The numbers of mRNA transcripts in each qPCR reaction were then calculated from the standard curve regression equation, and converted to transcript numbers per µg of starting total RNA (section 3.4.6).

6.2.4. Statistical analysis

For statistical analysis, the mean transcript copy number for each echinoid tissue sample (i.e. average transcript number derived from all runs of duplicate cDNA samples) was used as a replicate. Therefore, the sedimentation experiment consisted of three biological replicates per treatment and the surface retrieval experiment two biological replicates per treatment. As the two experiments were conducted independently of each other, the results of each experiment were analysed for statistical significance as separate tests but with the same methods. The results from the intestine and Aristotle's lantern muscle tissue were tested separately for each experiment. Prior to analysis, results were tested for homogeneity of variance and normality. Where these assumptions did not hold, data were log transformed prior to statistical analysis. Student's t-test or one-way analysis of variance was carried out on the mean transcript numbers. When log transformation did not achieve a normal distribution, the Kruskal-Wallis test was used to test for significance. Subsequent multiple comparison procedures to identify significant relationships followed the Student-Newman-Keuls method. All transformations and statistical analyses were conducted using the software package Sigmaplot Version 11.0.

6.3. Results

Isolation of a stress-70 gene fragment from *E. acutus*

A 398-bp mRNA nucleotide fragment was obtained and sequenced from *E. acutus*, from which a 129 amino acid peptide was inferred. A sequence homology search using BLASTP (Altschul et al., 1997) did not prove whether the *E. acutus* sequence had been isolated from the *hsp70* or *hsc70* gene. Phylogenetic analysis indicated that the fragment was most likely to relate to the *hsc70* gene (Figure 6.2). The *E. acutus* fragment clustered clearly with the HSC70 amino acids from the echinoid *Strongylocentrotus purpuratus* and those from other vertebrate and invertebrate species. However, only a short fragment of the amino acid sequence was included in this phylogeny, and it did not include the carboxy terminus end where differences between the HSP70 and HSC70 proteins are most obvious (section 2.6.3.2). Without a comparison of full-length amino acid sequences, ideally accompanied by functional studies regarding the expression of the gene (Leignel et al., 2007), a definitive identification of this gene fragment could not be made. The *E. acutus* fragment was submitted to the online databases as a putative *hsc70*, and was the first nucleotide sequence to be registered for this species (Accession no. FM877470). The gene quantification facilitated with primers designed from this fragment is hereafter referred to that relating to a *stress-70* gene.

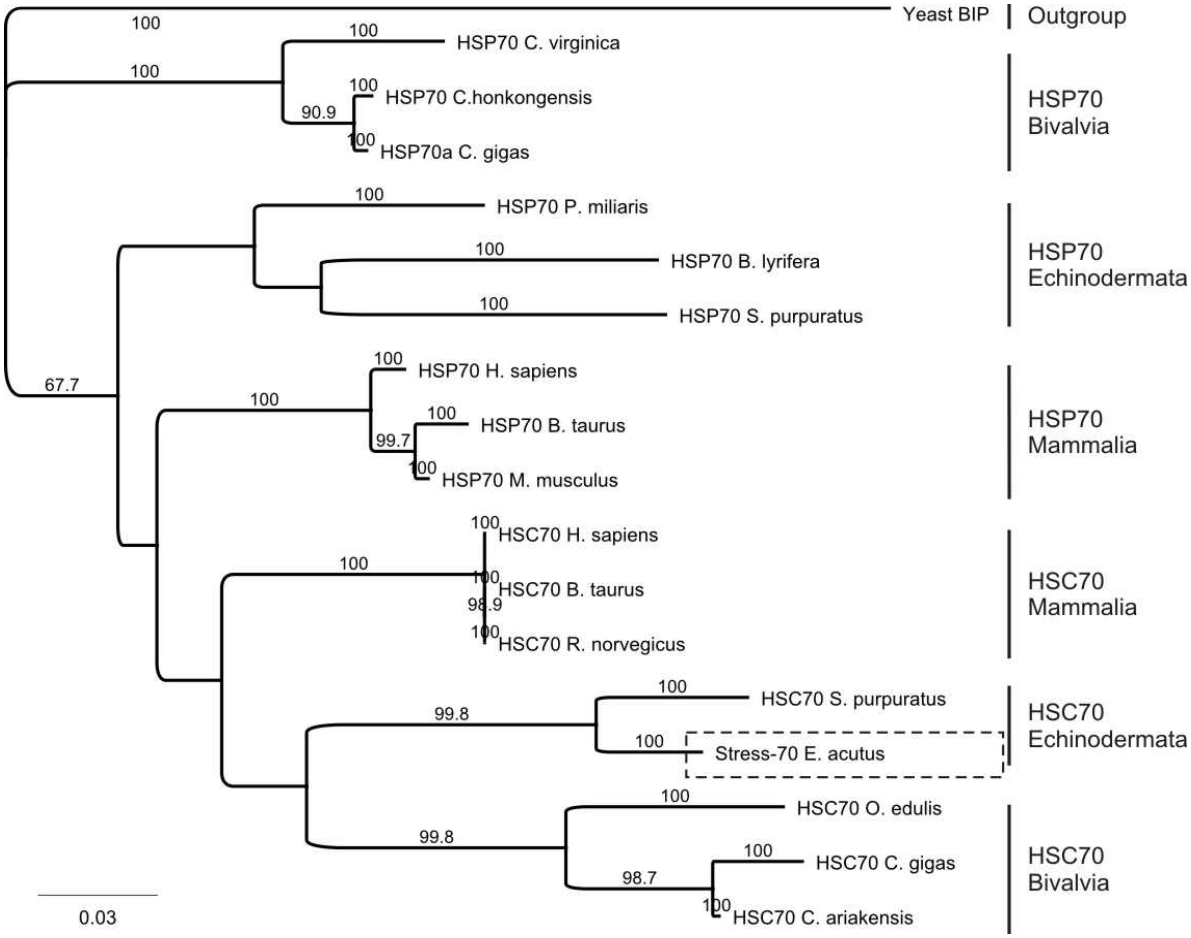

Figure 6.2. Phylogenetic relationship among stress-70 amino acid sequences (129 aa in length) from mammals, bivalves and echinoderms. Yeast binding protein (BIP) was included as an outgroup. The *E. acutus* sequence is highlighted by a dashed box. The tree was constructed using the Jukes Cantor genetic distance model with the neighbour joining algorithm using Geneious Basic 4.8.3. Bootstrap consensus support % for the sequence grouping are indicated (n=1000). The scale bar represents the proportion of amino acid sites at which two sequences are different. GenBank accession numbers for the sequences are as follows (top to bottom): AAA08536, CAB89802, ACH95805, BAD15286, CBL53159, CBJ55211, XP_780020, AAH36107, NP_776769, AAH04714, CAA68265, CAA68445, P19120, XP_802129, CAT00003, CAC83684, CAC83683 and AAO41703.

In situ experimental results

No significant effect of repeated surface retrieval events on the expression of the *stress-70* gene was found in either the intestine ($H = 0.00$, d.f. = 1, p = n.s.) or the Aristotle's lantern muscle tissue ($H = 0.00$, d.f. = 1, p = n.s.) of *E. acutus* (Figure 6.3). Of the six echinoids placed inside each experimental chamber for the sediment burial experiments, after recovery to deck only three echinoids remained in each chamber. The number of individual echinoids providing tissue samples for determination of the *stress-70* expression results was therefore only three per treatment (total nine echinoids).

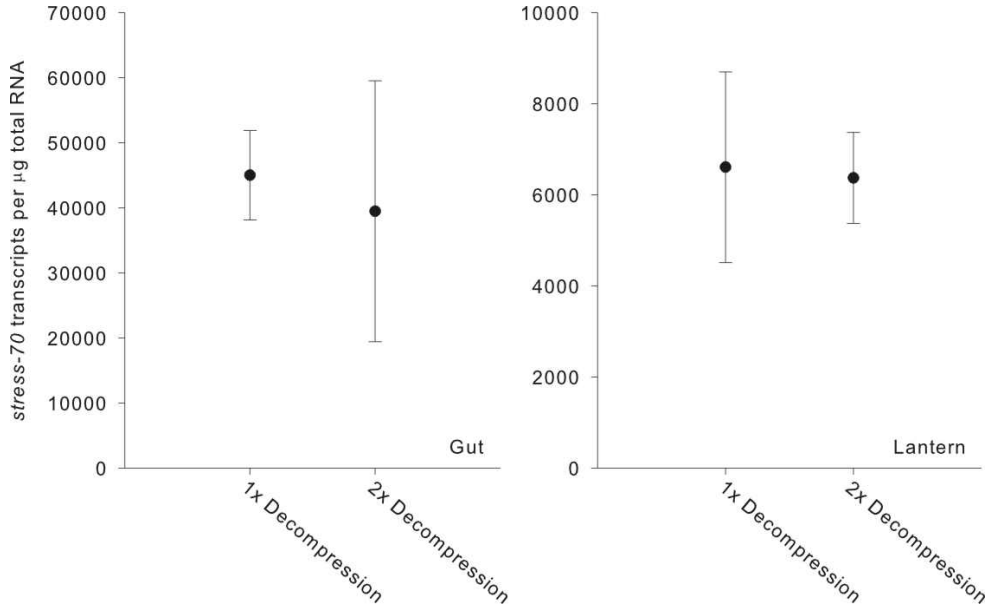

Figure 6.3. The effects of repeated decompression on *hsc70* expression in intestine tissue (left) and Aristotle's lantern muscle tissue (right) of *E. acutus*. Error bars represent ±1 standard deviation. Note different y-axis scales.

The intestinal tissue of *E. acutus* showed no change in *stress-70* expression in response to the sediment burial treatments ($F_{2,8} = 1.85$, p = n.s., Figure 6.4). In comparison, a significant increase in *stress-70* expression following sediment burial treatment was found in the Aristotle's lantern muscle tissue ($F_{2,8} = 5.67$, $p < 0.05$, Figure 6.4). Pairwise tests revealed significant differences in the Aristotle's lantern muscle tissue *stress-70* expression between both the control and the S ($q = 4.532$, $p < 0.05$) and MS ($q = 3.527$, $p < 0.05$) treatments. Although the mean Aristotle's lantern muscle tissue *stress-70* expression was higher in the MS than the S treatment, the difference between these two sediment burial treatments was not significant ($q = 1.005$, p = n.s.).

6.4. Discussion

In situ experimentation and observations

The surface retrieval manipulation experiment was performed to provide a preliminary indication of whether or not the retrieval of *E. acutus* individuals from the seabed to deck could alter *stress-70* expression. Retrieval to the surface involved changes in two physical variables that have been shown to alter gene expression: pressure (via decompression) and temperature (an increase). Decompression causes a reduction in pressure which effects biological systems by altering molecular volume, which together with increased temperature, destabilizes the structure of proteins and membranes and their functioning (Somero, 1992, 1998). The echinoids' retrieval to

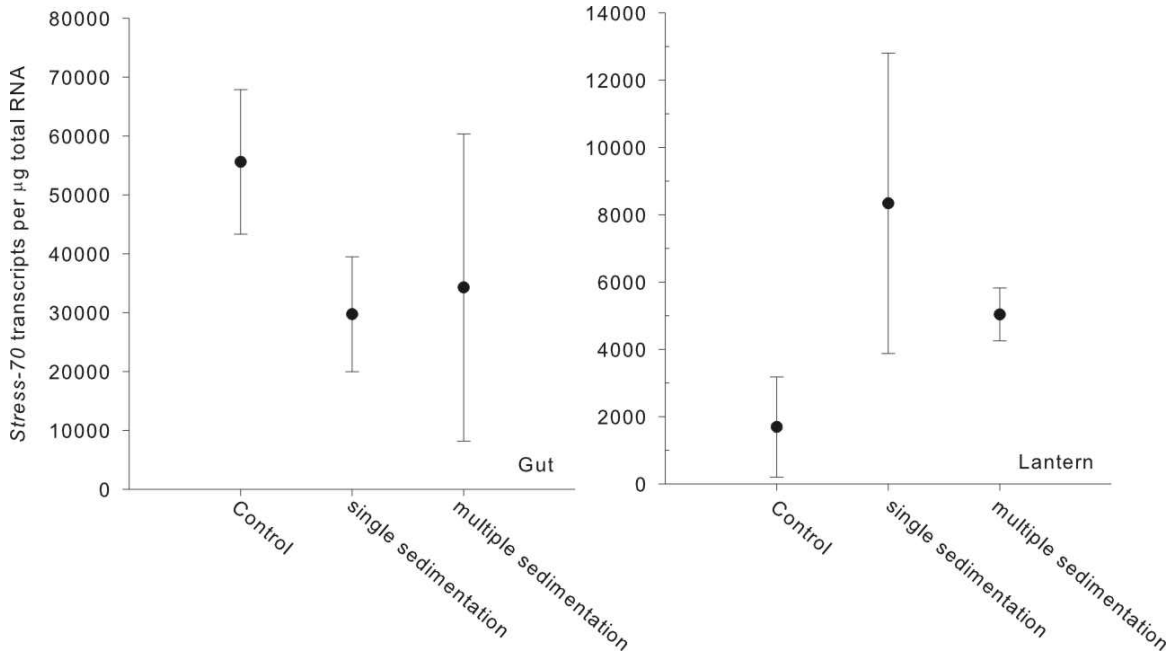

Figure 6.4. The effects of sediment burial treatments on *stress-70* mRNA transcript expression in intestine tissue (left) and Aristotle's lantern muscle tissue (right) of *E. acutus*. Error bars represent ±1 standard deviation (n=3). Note different y-axis scales.

the sea surface may therefore cause the induction of *stress-70* protein expression (Su et al., 2004; Ravaux et al., 2007) on account of deleterious effects on protein integrity (Mosholder et al., 1979; Dixon et al., 2004). Any such change may consequently mask alterations in *stress-70* expression caused by the stress of sedimentary burial at the sea floor. It is this unintended molecular artefact of retrieval to the surface that is a limiting factor in the successful performance of *in situ* experiments which aim to investigate gene expression in deep-sea species.

The surface retrieval manipulations with *E. acutus* did not cause differences in *stress-70* expression between the single or double retrieval events in either tissue type. There is a limit to the conclusions that can be drawn from this result because of the low number of individual echinoid replicates used (two per manipulation), but there are four possible explanations: 1) the echinoids' expression of *stress-70* was not affected by decompression or temperature change. 2) The echinoids were not decompressed from a depth, or experienced a temperature increase, sufficient to elicit the expression of *stress-70* during surface retrieval. 3) The time taken for recovery from the seafloor to final preservation of tissue samples was rapid (50-70 minutes), which was insufficient time for changes in *stress-70* expression owing to decompression and/or temperature change to become apparent in the transcriptomes. 4) As the relative change in pressure for each unit change in depth is greatest near the sea surface, and the echinoids subject to the two surface retrieval events were only brought to a depth of 10 m below surface between dives, they were not sufficiently decompressed twice to cause a difference in *stress-70* expression compared with the

echinoids subject to the single decompression event. If one of the first three possible explanations is correct, it can therefore be assumed that the surface retrieval of the echinoids did not cause any changes to the altered *stress-70* expression caused by the burial experiments.

In addition to the *in situ* experimentation, the ROV had also been used to perform video transect surveys of the seabed megafaunal community before and after the drilling of a hydrocarbon exploration well (refer to Appendix 1.31 for more details). It was found that the disturbance caused by drilling the well had a significant effect on the visible megabenthic community, with density one month after drilling being lower than that found prior to the drilling event. Compared with its abundance prior to drilling, a significant reduction in the abundance of *E. acutus* after drilling was also found in a 50 m zone around the drilling site.

In some situations the smothering, burial and physical effects of solid drill cuttings are thought to be a more important determinant of community change than the potentially toxic action of the associated drilling fluid chemicals (Schaanning et al., 2008) , although these physical effects are localised to the vicinity of the source of the drill spoil (Neff et al., 2000; Jones et al., 2007; Netto et al., 2009; Santos et al., 2009). Other studies investigating the physical impact of cuttings have found evidence that factors other than the burial effects of drill cuttings, for example hypoxia, primarily affect the benthic community (Trannum et al., 2010), and any potential toxicological effects are highly dependent on the composition of the drilling fluids (Holdway, 2002; Dalmazzone et al., 2004; Neff, 2005).

Whilst no direct correlation could be made between the reduction in *E. acutus* numbers around the drilling site and the elevation found in the inducible *stress-70* gene during the sedimentary burial experiments, the elevation in expression indicates that burial caused sublethal stress detectable at the molecular level in *E. acutus*. This indicates that burial by drill cuttings and disturbed sediment may be detrimental to impacted benthic organisms such as *E. acutus*, as elevated levels of a molecular chaperone (and associated energy demands) are required to maintain cellular homeostasis during possible exposure to drilling fluids associated with the drill cuttings and escape from underneath a cuttings or disturbed sediment pile (section 4.1.1).

***Stress-70* expression**

Stress-70 proteins act as molecular chaperones to assist protein folding, unfolding, translocation across membranes and regulatory protein control (Daugaard et al., 2007). As already discussed (section 2.1.1.2) two stress-70 proteins, HSC70 and HSP70, have extremely similar amino acid sequences and functions. The *hsc70* gene is traditionally viewed as being constitutively expressed during normal physiological conditions, with its expression not changing in response to stress. In

comparison, the expression of *hsp70* is traditionally viewed as being upregulated in response to protein-denaturing stress, as it assists with the repair and stabilisation of cellular proteins and minimizes protein aggregations (Hartl and Hayer-Hartl, 2002).

Based on these generalizations, it was expected that the heat shock exposures performed with *E. acutus* would enhance expression of the stress-inducible *hsp70* gene. Degenerate PCR should then have amplified mRNA transcripts coding for the HSP70 protein, as they would have made up a higher proportion of stress-70 mRNA transcripts within the total mRNA isolated from the *E. acutus* tissue samples. Instead, transcripts from a, putative, highly similar HSC70 protein were isolated from the heat-stressed echinoids, and from these the qPCR primers were designed.

It has been suggested that early one-dimensional gel electrophoresis work on the stress-70 family failed to discriminate amongst closely related heat shock proteins and that altered gene expression or protein levels may have been incorrectly attributed to HSP70 instead of HSC70 (Miller et al., 1991; Fangue et al., 2006). Both Liu et al. (2004) and Ojima et al. (2005) have found that northern blot analysis (section 2.2) failed to detect upregulated *hsc70* expression which was revealed by analysis using the the more sensitive and quantitative qPCR technique. It is therefore possible that, of the many studies which report the stress-inducible expression of *hsp70*, in some of these a possible increase in *hsc70* expression was not reported as it was attributed to, or masked by, a greater increase in *hsp70* expression (Miller et al., 1991).

Different degrees of inducibility exist for individual heat shock proteins, including; constitutively expressed, constitutively expressed but increasing during or after stress, and exclusively inducible (Feder and Hofmann, 1999). Some authors argue that the *hsp70* and *hsc70* genes can only be differentiated by studies that indicate which gene is induced in response to stress (Leignel et al., 2007). However, other authors have found that the distinction between the expression of these two stress-70 family members is not straight forward (Franzellitti and Fabbri, 2005).

Gene expression studies with teleost fish which have investigated both *hsc70* and *hsp70* have found that *hsc70* expression does increase significantly in response to acute heat shock, although not to the same extent as the increase found in *hsp70* expression (Deane and Woo, 2005; Ojima et al., 2005). The elevated expression of both *hsc70* and *hsp70* has also been found in response to heat shock in the Chinese shrimp *Fenneropenaeus chinensis* (Luan et al., 2010) and the prawn *Macrobrachium rosenbergii* (Liu et al., 2004), although in the latter the combined increase was only detected in muscle tissue. As well as *hsp70* expression increasing in the brains of heat shocked or hyperthermic rats, *hsc70* expression also increased two- to threefold; although there were marked differences in the regional expression of these two genes (Miller et al., 1991). The

above studies demonstrate that in some cases, it is not just the expression of the *hsp70* gene which is induced in response to stress, the *hsc70* gene is also induced and it is not a gene which only displays constitutive expression.

In this current study, a significant increase in *stress-70* expression was found in the *E. acutus* Aristotle's lantern muscle tissue, but not in intestinal tissue. There are two possible explanations for this result. First, that these results provide further evidence that *hsc70* expression is upregulated in response to acute stress, and that in *E. acutus* this response is specific to muscle tissue. In this regard, there is sufficient scope to review the traditional view of *hsc70* only being a constitutively expressed gene as this study, and the others summarized above, indicate that it is a stress-inducible gene. Alternatively, as already discussed, the putative identification of the isolated *E. acutus* stress-70 fragment as derived from the *hsc70* gene could be wrong. Due to the short length of the sequence, the phylogenetic analysis which placed the fragment with other HSC70 amino acids may be inaccurate. Without a complete analysis of the full length of the gene from which the fragment was isolated, the identification of this gene can only remain putative.

In view of the possible misidentifications which may have historically taken place when techniques used for the analysis of *stress-70* gene expression did not definitively differentiate between different genes; it is clear that there is scope for the prevailing understanding of the inducibility of the various *stress-70* genes to be clarified via functional gene expression studies. However, irrespective of whether the fragment isolated from *E. acutus* was correctly identified as derived from the *hsc70* gene, it can be confirmed that it was derived from an inducible *stress-70* gene which was induced in response to heat shock and sediment burial stress.

6.5. Conclusions

This study has shown that it is possible to apply the qPCR technique to samples recovered from *in situ* experimental investigation of anthropogenic impact at continental shelf depths, and the stress-70 molecular biomarker reflects burial induced stress in echinoids. The isolation of a fragment from a stress-70 gene indicates that the degenerate primers used during the *P. miliaris* and *B. lyrifera* investigations can be successfully applied to other echinoid species and used during the development of future echinoid qPCR assays.

The recovery of the specimens from 114 m depth was presumed to have not caused an alteration in the expression of the *stress-70* gene, as there was no difference in the expression profiles of the echinoids subjected to either one or two retrieval events. One limit to this conclusion is related to the fact that it was not possible to include a control in this study (i.e. no decompression or temperature change), as the echinoids had to be returned to the surface for processing. Given the

range of depths over which *E. acutus* is reported to occur (below 100 m depth and up to 1075 m), it can only be assumed that no alteration occurred in the expression of the *stress*-70 gene in the retrieved echinoids (subjected to pressure conditions outside of their normal range) in comparison to the transcriptome of specimens that had not been subject to any pressure or temperature change.

The decompression (a change of ~1054 kPa) and temperature change (~5.6°C) experienced by the echinoids during recovery from 114 m depth is not as extreme as that which would be experienced by organisms during collection from bathyal or abyssal depths. The issue of decompression and temperature change altering the transcriptome profiles of organisms collected from depths below the continental shelf remains an obstacle to accurate and conclusive deep-sea experimental research that utilises modern quantitative molecular techniques. Ravaux et al. (2007) have already reported that there was evidence of inducible stress-70 gene expression in *Mirocaris fortunata* specimens recovered from 2300 m depth and immediately frozen (i.e. not subject to any stress inducing conditions other than the retrieval process). It would therefore not be appropriate to assume that no change in gene expression and transcriptome profiles would occur in echinoderm specimens retrieved from below continental shelf depths during an unprotected retrieval process. In this regard, the future development of experimental devices that eliminate the effects of decompression and temperature on molecular profiles, and permit modern quantitative molecular techniques to be incorporated within deep-sea experimental research, are required.

The successful performance of the *in situ* experiments described in this chapter demonstrate the usefulness of ROV technology to deep-sea research, and the potential importance of the application of molecular techniques to collected experimental samples. This application of ROV technology to abyssal depth experimentation is further demonstrated in the next chapter, which introduces a purpose built *in situ* respirometer designed for operation by ROV and used to obtain information on the metabolic rates of bathyal and abyssal echinoderms.

Chapter 7. Physiological Investigation of Deep-Sea Echinoderms

7.1. Introduction

Below 1000 m water depth, the physical environment is cold (the temperature below the permanent thermocline is <4 °C, although with notable exceptions such as hydrothermal vent areas, the Red Sea and the Mediterranean), dark and highly pressurized (Menzies, 1965; Tyler, 1995, 2003b). Recovering organisms unharmed from this environment for physiological investigations and experimentation is difficult. Any organism brought to the surface without adequate protection suffers both thermo- and baro-trauma during the transition through the water column to surface ambient temperature and pressure (Hessler, 1972; Macdonald, 1975). However, as deep-sea retrieval and experimental technology has developed over the past 40 years, researchers have started to investigate how deep-sea organisms differ physiologically from their shallow-water counterparts using organisms recovered from depth and via *in situ* experimentation.

This chapter briefly considers the historical development of deep-sea megafaunal experimental equipment. Then follows a review of the development of the Benthic Incubation Chamber System 2 (BICS2), a respirometer designed for the *in situ* measurement of deep-sea megafaunal oxygen consumption rates (a practical measurement of metabolic rates). Details of the practical aspects of the first scientific deployments of BICS2, including a consideration of using ROVs for *in situ* experimentation, have been submitted to Deep-Sea Research Part II as part of Hughes et al. (submitted) "*Benthic abyssal research using a remotely operated vehicle (ROV): novel experimentation in the Nazaré Canyon*" (Appendix 1.29). The deep-sea echinoderm metabolic rates obtained with BICS2, together with a comparison of deep-sea and shallow-water echinoderm metabolic rates, have been included in a manuscript that will be submitted for review shortly after submission of this thesis: Hughes et al. (in prep) "*Abyssal echinoderm oxygen consumption and an interclass comparison of echinoderm metabolic rates*" (Appendix 1.30). Please note the BICS3 deployment was managed by Dr. H. A. Ruhl, the data analysis concerning the BICS3 oxygen consumption rate results included in the draft manuscript was carried out by myself.

7.1.1. Historical deep-sea biological sampling

Early research voyages collected samples of deep-sea fauna via the deployment of a variety of gear from surface vessels. The first deep-sea biological research expeditions included dredging work from H.M.S. *Beacon* in the Aegean by Edward Forbes (1841-1842), from which he developed his "azoic zone" hypothesis (Gage and Tyler, 1991), and expeditions led by Charles Wyville Thomson and William Carpenter on H.M.S. *Lightning* (1868) and H.M.S. *Porcupine*

(1869-1870). These two latter expeditions led directly to the first circumnavigating voyage of H.M.S. *Challenger* (1872-1876) led by Thomson. During these expeditions, samples were systemically collected for the first time from more than 1000 fathoms (1800 m) depth (Menzies, 1965).

Even today, the same methods of the 19th Century are used during research cruises to collect deep-sea organisms. Traditional biological deep-sea sampling techniques are based on the deployment of trawls, sleds, dredges, grabs, box and tube corers attached to a wire several kilometres long. These techniques are still in extensive use because they are relatively inexpensive and efficient (Bachmayer et al., 1998; Gage and Bett, 2005) and lend themselves to the collection of descriptive data with considerable statistical quantitative power. However, these techniques do not facilitate the collection of organisms in a suitable state for physiological investigation.

The collection of typically fragile organisms from depth without specialised protection results in the retrieval of dead or moribund organisms as a result of mechanical damage, temperature increase or pressure decrease suffered during the transit to the surface (Hessler, 1972; Macdonald, 1975). The detrimental effects of decompression on deep-sea organisms, and of pressurisation on shallow-water organisms (Brauer, 1972; Hunter and Bennett, 1974), indicate that deep-sea organisms are adapted to the deep-sea environment to the extent that they are obligate barophiles and restricted to life at high pressures (Somero, 1992). What form these adaptations take is slowly being investigated, with the majority of studies using teleost fish species as model organisms.

7.1.2. Deep-sea adaptations

Pressure and temperature exert different effects and selective forces on organisms (Gibbs, 1997), and it has been found that cold adapted shallow-water organisms are not pre-adapted to the deep-sea environment (Siebenaller and Somero, 1989). Hence, in addition to cold-temperature adaptations it is thought that deep-sea organisms have specific adaptations to high pressure (Somero, 1998), and depth as a physical variable has great influence on the vertical distribution of deep-sea organisms (Somero, 1992). The adaptations discovered to date can be broadly divided into those applying to either protein or membrane structure.

Similar to cold-adapted membranes, deep-sea adapted membrane phospholipids contain increased quantities of unsaturated fatty acids with low melting points (Somero et al., 1983; Somero, 1998). In deep-sea teleost fish the membrane saturation ratio (i.e. proportion of saturated to unsaturated fatty acids) decreases linearly with depth (Somero, 1991), and obligate barophilic bacteria contain

high amounts of both mono- and poly-unsaturated fatty acids (Simonato et al., 2006). These structural alterations, termed 'homeoviscous adaptation', conserve the fluid membrane physical state under high pressure and cold temperature, and hence enable membrane-based processes and the functioning of embedded proteins to continue (Somero, 1992). Homeoviscous adaption also confers a membrane fluidity which is maintained not just at high pressure but also during pressure change - an advantage to species that move vertically in the water column (Somero, 1998).

Substitutions in amino acids and altered protein primary structure, including Na^+-K^+ ATPase (Gibbs, 1997), lactate dehydrogenase (Somero, 2003; Brindley et al., 2008), α-actin (Morita, 2003) and myosin (Morita, 2008), have been found between confamilial and congeneric deep-sea and shallow-water teleost fish. The structural adaptations make these proteins in deep-sea fish more rigid than homologs found in related shallow-water fish, and hence able to maintain their tertiary and quaternary structure at high pressure (Brindley et al., 2008). This structural stability enables protein functioning to continue over a range of high pressures (Somero et al., 1991; Gibbs, 1997). In addition to increased protein structural stability, it has been found that the thermodynamics of some reactions, such as ligand binding and subunit polymerisation, are altered in deep-sea species. The reaction entropy, enthalpy and volume changes are lower, an adaptation that enables reactions to proceed in the low temperature and high pressure deep-sea conditions (Somero, 1992).

The inhibitory effect of hydrostatic pressure on the functioning of incompletely depth-adapted proteins is thought to be countered in part by some species via an increase in cellular osmotic pressure. For example, a correlation between the content of the organic osmolyte trimethylamine N-oxide (TMAO) and habitat depth has been found in deep-sea teleost fish (Samerotte et al., 2007). TMAO is a protein stabilizer, and it may function to decrease the inhibitory formation under high pressure of water around ligands and proteins. Similar increases, or high levels, of organic osmolytes with depth have also been found in deep-sea bacteria, elasmobranchs, crustacea, echinoderms, gastropods, polychaetes and pycnogonids (Yancey et al., 2002; Simonato et al., 2006), indicating that a number of unrelated organisms regulate osmotic pressure in this manner.

7.1.3. Experimental equipment for deep-sea organisms

Due to the effects of baro- and thermo-trauma (section 1.4.1) the physiological study of deep-sea organisms requires the use of specialist retrieval and/or experimental equipment which enable the organisms to be maintained at *in situ* temperature and pressure (Gibbs, 1997). The manufacture of equipment which facilitates physiological measurements and/or experimentation with deep-sea organisms is expensive and technically difficult (Gibbs, 1997; Sébert, 2002). Due to the

inaccessibility of the deep-sea environment, which is remote both in terms of distance from shore and water depth, the deployment of such equipment is also expensive and the ability to obtain replicate samples and measurements difficult to incorporate within the scope of a research cruise (Smith and Baldwin, 1983). Despite these complications, a number of different equipment designs have been developed by different researchers. Experimental approach, and hence equipment design, has taken one of two forms: the protected collection of the organisms at depth followed by laboratory based investigations, or the performance of experiments *in situ* on the sea floor.

Protected recovery from the deep sea

The mechanical damage and thermal trauma problems associated with recovery of organisms from the deep sea were initially avoided by incorporating a thermally insulated 'cod end' into trawls. Cod ends protect organisms from elevated temperatures and minimise physical damage during surface recovery, and were first used to successfully recover living animals from depths greater than 400 m off Southern California (Childress et al., 1978). In addition to cod-ends, other thermally insulated devices such as traps attached to free fall vehicles or landers (Treude et al., 2002) have been used to retrieve organisms from depth. These methods of deep-sea organism recovery have proved effective in capturing bathypelagic (0.2 – 2 km depth) species and bringing them to the surface in good physiological condition for subsequent experimentation, either at ambient pressure or in a re-pressurising vessel (Childress et al., 1990; Cowles and Childress, 1995). Thermally insulated equipment has been used to successfully recover a variety of deep-sea organisms for physiological investigation including crustaceans (Cowles et al., 1991; Thuesen et al., 1998), fish (Cowles and Childress, 1995), medusae (Thuesen and Childress, 1994), polychaetes (Thuesen and Childress, 1993) and benthic crustaceans (Childress et al., 1990; Treude et al., 2002).

Whilst some deep-sea crustaceans can be brought to the surface, even from an extreme depth of 4420 m (Treude et al., 2002), in an adequate physiological state with only thermal protection (Childress et al., 1990; Macdonald, 1997), organisms from other phyla cannot and some authors view 1000 m depth as a working limit for successful retrieval of deep-sea organisms (Pradillon and Gaill, 2007). The development of equipment that can be used to capture an organism at depth and recover it to the surface at maintained temperature and *in situ* pressure has enabled the recovery of deep-sea organisms from depths which extend to the hadal zone (> 6 km) of the Marianas Trench (Yayanos, 2009).

A summary of the various pressure-retaining equipment designs that have been used to retrieve

deep-sea organisms to the surface is provided at Table 7.1. The most advanced pressure-retaining retrieval equipment designs are the pressure-stat aquarium system from JAMSTEC[2] (Koyama et al., 2002), the autonomous hyperbaric fish trap aquaria respirometer from MBARI[3] (Drazen et al., 2005) and the French PERISCOP device (Shillito et al., 2008). These three equipment designs enable the collection of an organism at depth, maintenance of *in situ* pressure during recovery and for a prolonged period thereafter, observation of the organism's behaviour through a viewing port and a final controlled decompression in an attempt to acclimatise the organism to surface ambient pressure slowly. The JAMSTEC and MBARI designs also permit the determination of the organisms' oxygen (O_2) consumption whilst inside the device. Despite the technological advancement displayed by the most recent retrieval devices, the recovery of animals from depth involves artificial constraints which must be considered when interpreting the results of physiological measurements (Cech, 1990; Smith and Baldwin, 1997):

a) The capture and recovery process is stressful for the organism.

b) The visual pigments of organisms accustomed to low or no light in the deep sea are adversely affected by solar or artificial light, which may cause stress.

c) Organisms transferred to research ships are exposed to abnormal movements from the ships' rolling and pitching, so affecting 'resting' physiological measurements.

d) Maintenance in a confined container places physical and biological constraints on organisms, which may cause stress.

e) Retrieved organisms are usually maintained in surface seawater, which may have a different chemistry to that found at depth.

***In situ* experimentation**

The *in situ* approach to physiological measurements and/or experimentation with deep-sea organisms is based on the capture of an organism at depth, and subsequent investigations are performed at the location of capture with *in situ* equipment. This approach is preferred by some researchers as experiments can be performed, and measurements taken, under natural environmental conditions so avoiding artefacts from the recovery process (Smith and Baldwin, 1983; Kaufman et al., 1989; Tengberg et al., 1995; Theron and Sebert, 2003). There are still artificial constraints associated with the *in situ* approach, which again must be considered when

[2] Japan Agency for Marine-Earth Science and Technology
[3] Monterey Bay Aquarium Research Institute

interpreting results (Kamler, 1969; Smith and Baldwin, 1983; Cech, 1990):

a) The capture process is stressful for the organism, and sufficient time may be required to allow the organism's recovery.

b) The visual pigments of organisms accustomed to low or no light in the deep sea may be adversely affected by artificial light if manned submersibles (human occupied vehicles or HOVs) or remotely operated vehicles (ROVs) are required to capture the organisms and/or operate the *in situ* equipment.

c) Restriction to a confined container places physical and biological constraints on the organism, which may influence 'resting' measurements.

In situ equipment is designed as a free-fall vehicle that operates autonomously once deployed, or as a unit deployed and/or operated by human intervention via R/HOV (Table 7.1). The advantage of completely autonomous *in situ* equipment is that it can be quickly deployed by a research vessel and then takes up no further time within a research cruise timetable until recovery (Bailey et al., 2002). Such equipment can also be deployed by all research vessels, not just by those carrying HOV or ROV capability which, given the limited number of HOV and ROVs in use, means a greater number of potential deployment opportunities. The disadvantage of autonomous equipment is that, by the nature of the baited trapping mechanisms which attract and capture organisms, the target organisms are generally limited to the motile scavenging fish and crustacea. The alternative to autonomous equipment, *in situ* equipment that requires some form of human intervention, has the disadvantage that it can only be deployed from vessels with R/HOV capability. Therefore, there are a smaller number of research cruises suitable for *in situ* equipment deployment, and the equipment's deployment and operation requires allocated time in a cruise schedule. The advantage of such equipment is that specific organisms can be selected for physiological investigation by virtue of the R/HOV being able to collect a target organism and transport it to the equipment.

To date, the majority of *in situ* measurements of megafaunal O_2 consumption have studied pelagic and benthopelagic fish and shrimp attracted to baited respirometer traps (Smith and Baldwin, 1983; Bailey et al., 2002; Bailey et al., 2005a), or gelatinous organisms such as medusa, ctenophores or pelagic holothurians captured via "slurp gun" suction or caught directly into a respirometer by an ROV (Smith, 1982; Bailey et al., 1994; Bailey et al., 1995). Studies that have investigated the *in situ* O_2 consumption rates of epibenthic megafauna are limited. Smith (1983) obtained echinoderm O_2 consumption rates with a HOV-operated epibenthic megafaunal respirometer at bathyal depths in the North East Pacific, but since then, there has been little new work published on *in situ* megafaunal physiological investigations.

Table 7.1. Summary of a) equipment used to recover deep-sea megafauna from depth at a maintained pressure and temperature, and b) equipment used for *in situ* megafaunal physiological measurements. The depths at which the equipment has been recorded in the published literature as being operated at is listed. The theoretical maximum operating depth (m) is listed in brackets where such information was available.

Name	Brief Description	Deployment Method	Depth (m)	Target Organisms	Purpose	Oxygen Sensor	References
a) Equipment for recovery from depth at both maintained pressure and temperature							
Pressure fish trap	Baited hook trap comprised of a 2 m by 30 am diameter tube.	Autonomous free fall vehicle	(1200)	Fish	Capture, pressurised recovery	n/a	Brown (1975)
Deep-sea Benthic Trap	Steel holding chamber with view port, globe valve maintains pressure. 600 ml volume	Attached to mooring line	1200 - 2700	Amphipods	Capture, pressurised recovery, and maintenance	n/a	Macdonald and Gilchrist (1978)
Pressure retaining animal trap (PRAT)	Baited titanium trap, sealed by O-rings and piston. Pressure loss compensation system. Post-recovery water flow through system.	Autonomous free fall vehicle	5700 - 10900	Amphipods	Capture, pressurised recovery, and maintenance	n/a	Yayanos (1978, 2009)
Hyperbaric fish trap	Spring mounted baited hook trap comprised of an aluminium tube with internal hinged door	Autonomous free fall vehicle	750 (1200)	Fish	Capture, pressurised recovery, and maintenance	n/a	Phleger et al. (1979)
Hyperbaric fish trap / aquarium	Baited hook trap comprised of an insulated aluminium pipe with viewing window. A gas accumulator system restores pressure after thermal expansion. 41.7 L volume.	Autonomous free fall vehicle	1115 - 1314 (1400)	Fish	Capture, pressurised recovery, and maintenance	n/a	Wilson and Smith (1985)

Pressure-stat aquarium system	Suction capture of organism into stainless steel oval aquarium. 20 L volume.	HOV	1157 - 1171 (2000)	Fish and shrimp	Capture, recovery, O_2 consumption analysis and controlled decompression	Dissolved O_2 sensor (Toa Electronics DO-21P)	Koyama et al. (2002; 2003; 2005)
Hyperbaric fish trap aquaria respirometer	External baited fish hook, fish drawn inside stainless steel cylinder by spring-loaded reel. 89.1 L volume.	Autonomous free fall vehicle	1400 - 4000 (4200)	Fish	Capture, recovery, O_2 consumption analysis and controlled decompression	Aanderra 3830 Optode	Drazen et al. (2005), Bird et al. (2004)
PERISCOP	Two parts: suction capture of organism into a PVC and polycarbonate sampling cell, which is transferred to a pressurized recovery device	HOV	1700 - 2300 (3000)	Hydrothermal fish and Shrimp	Capture and recovery at maintained pressure	n/a	Shillito et al. (2008)
***b) In situ* equipment**							
Fish Trap Respirometer (FTR)	Retractably baited, dual acrylic chambers with a spring loaded box trap and stirring motors. 53.7 L volume.	HOV	1230 - 3650 (6000)	Fish and other midwater scavengers	O_2 consumption analysis	Polarographic	Smith (1978), Smith & Hessler (1974)
Slurp Gun Respirometer (SGR) or Plankton/ Nekton Respirometer (PNR)	3 or 4-chambered (acrylic cylinders) unit initially attached to front of HOV. Organisms collected by HOV suction, unit closed and then tethered to mooring line for incubation. Variable volume 0.25 – 1.5 L.	HOV	1300 - 3650	Pelagic animals not attracted to bait: bathyal macro- and mega-zooplankton and nekton	O_2 consumption analysis and excretory products.	Polarographic	Smith (1982), Smith & Baldwin (1982; 1983), Smith & Laver (1981), Smith & White (1997), Smith (1985a)

Megafauna Respirometer	Dual plexiglass cylinders with stirring motors and withdrawal syringes for excretory product analysis. Organism captured by HOV.	HOV	1300 - 3600	Epibenthic megafauna	O_2 consumption analysis	Polarographic	Smith (1983)
Free vehicle amphipod respirometer (FVAR)	4 baited acrylic chambers mounted between two discs with stirring motors and withdrawal syringes.	Autonomous, attached to mooring line or placed on seafloor	2490	Amphipods or other small scavengers, vent mussels	O_2 consumption analysis	Polarographic	Smith & Baldwin (1983), Smith (1985b)
Submersible mounted respirometers	8 acrylic respirometer chambers. Organisms collected inside chambers with HOV. Attached to mooring line for incubation.	Johnson Sea Link (HOV)	735 - 900	Zooplankton and micronekton	O_2 consumption analysis	Nester (Leeds and Northrup Corp.)	Bailey et al. (1994; 1995)
FRESP 1,2,3	Baited-trap respirometer constructed from PVC and polycarbonate. Stirrer mechanism included. 225 L volume.	Autonomous free fall vehicle	1500 - 4200 (6000)	Fish and Shrimp	O_2 consumption analysis	Beckman polarographic electrode (Sea Bird Electronics, Inc.)	Bailey et al. (2002), Jamieson et al. (2006)
SPRINT	Baited aluminium tripod frame with lighting and digital video camera systems	Autonomous free fall vehicle	2500	Fish and Shrimp	Burst swimming and muscle performance	n/a	Bailey et al. (2003; 2005a; 2005b)

7.2. BICS equipment development

The Benthic Incubation Chamber System (BICS) is a respirometer system designed for the *in situ* measurement of the oxygen consumption rate of deep-sea megafauna. BICS is a 6000 m rated, elevator-deployed and ROV-operated system comprised of two watertight respirometry chambers within a protective frame. The oxygen concentration and temperature of seawater enclosed inside the chambers are measured with 6000 m rated oxygen optodes (Aanderaa Instruments Oxygen Optode 3975). BICS is a 'closed system' respirometer, where the oxygen consumption rate of an organism is calculated from the decrease in O_2 concentration, the chamber volume and the experimental period (Lampert, 1984; Cech, 1990).

7.2.1. The original BICS design

The original BICS equipment was designed and manufactured by Oceanlab (Aberdeen). The two respirometry chambers were cylindrical transparent acrylic chambers 300 mm internal diameter x 300 mm height with internal volume of ~28 litres (Figure 7.1 a,b). The chambers were sealed at the bottom to 20mm thick acetal plates with butyl rubber compound. Removable stainless steel lids sealed the top. One optode entered each chamber through a port in the base plate (Figure 7.1 c). A mini-submersible pump (SBE-5M; Seabird Electronics, USA) connected to one of the chambers added the facility to pump liquid substances into the chamber at a pre-programmed time.

A custom-built TT8 controller for the optodes and pump was housed within a 6000m rated 6Al-4V titanium cylindrical housing. The O_2 and temperature measurements were recorded via an RS232 link in text file format onto a flash card held within the controller. Measurement details, such as logging interval and logging duration were pre-programmed with text file command generator software and loaded onto the flash card prior to deployment. The program was placed into 'sleep' function prior to deployment, and subsequently activated once BICS was deployed on the seafloor by the ROV pressing a custom-built push-switch. The switch was a moving tensioned shaft containing a magnet that activates a static reed switch as it travelled past. The chambers and controller unit were contained and protected within an aluminium 6082 frame (1125 mm x 500 mm x 600 mm). In air, BICS weighed 77 kg with empty chambers and 133 kg when the chambers were full of water. In water, the system weighed 40 kg.

Following trial deployments during the R.V. *Thomas G. Thompson* cruise TN187 (Jamieson et al., 2005), BICS was delivered to NOCS in autumn 2005 and laboratory testing of its functioning by the current author commenced. Laboratory testing revealed two serious design faults in its design as a respirometer: the omission of a stirring mechanism and poor lid sealing.

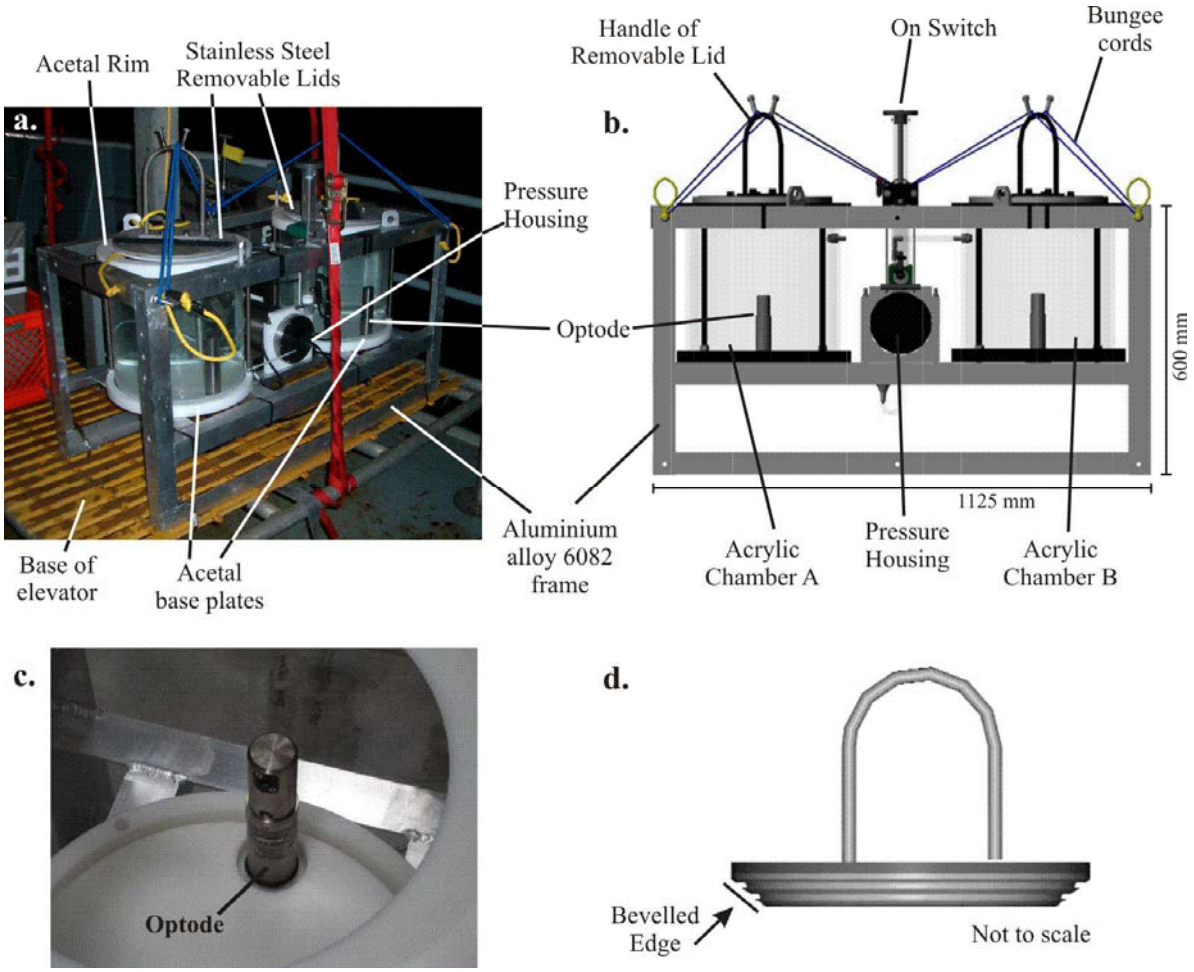

Figure 7.1. a). BICS attached to an elevator system prior to deployment during the 2005 R.V. *Thomas G. Thompson* TN187 cruise. b). Schematic diagram illustrating the design of BICS. c). An optode positioned in the chamber, projecting through a port in the acetal base plate. d). Illustration of the stainless steel lid design.

Stirring requirement

Closed system respirometers normally include stirring mechanisms to mix the enclosed water (Steffensen, 1989; Cech, 1990). Early polarographic sensors such as Clark oxygen electrodes, which were used to measure O_2 concentrations in respirometer systems, consumed O_2 as it was reduced at the electrode surface (Lampert, 1984). A depleted O_2 concentration gradient could therefore develop in the boundary layer at the electrode surface if the water enclosed in the respirometer was not mixed. Modern optical sensors, or optodes, are based on a luminescence quenching principle and do not consume O_2 as they operate. As such, stirring is not required in order to eliminate an O_2 gradient at the sensor surface. The Aanderaa operating manual for the oxygen optodes used in the chambers specifically states that they are not stirring sensitive. It is understood that it is for this reason, as well as budgetary constraints, that the original BICS respirometer was constructed without stirrer capability. However, irrespective of the optode

stirring requirements, an O_2 gradient can also be formed around a weakly ventilating organism inside a closed system respirometer due to stagnation of water at the body surface (Kamler, 1969; Irwin and Davenport, 2006), which may restrict oxygen consumption (Lawrence, 1987). For this reason, a stirrer is required inside a closed respirometer system to remove possible water stratification around the organism.

Laboratory trials with the chambers illustrated the impact including a stirrer had on the measurement of the depleting O_2 concentration during the incubation of an organism. Four trials were performed with the same specimen of an asteroid, *Asterias rubens* (Linnaeus, 1758). The asteroid was placed inside one of the BICS chambers, the lid closed and the oxygen concentration of the enclosed water measured for up to 8 hours. The data recorded from unstirred chambers (Figure 7.2 a) illustrate an erratic decrease in oxygen concentration whilst the data from chambers stirred by a temporary magnetic stir bar instead illustrate a steady decrease (Figure 7.2 b). These results demonstrated that a stirring mechanism was required within the BICS chambers to improve the accurate determination of oxygen concentration rates.

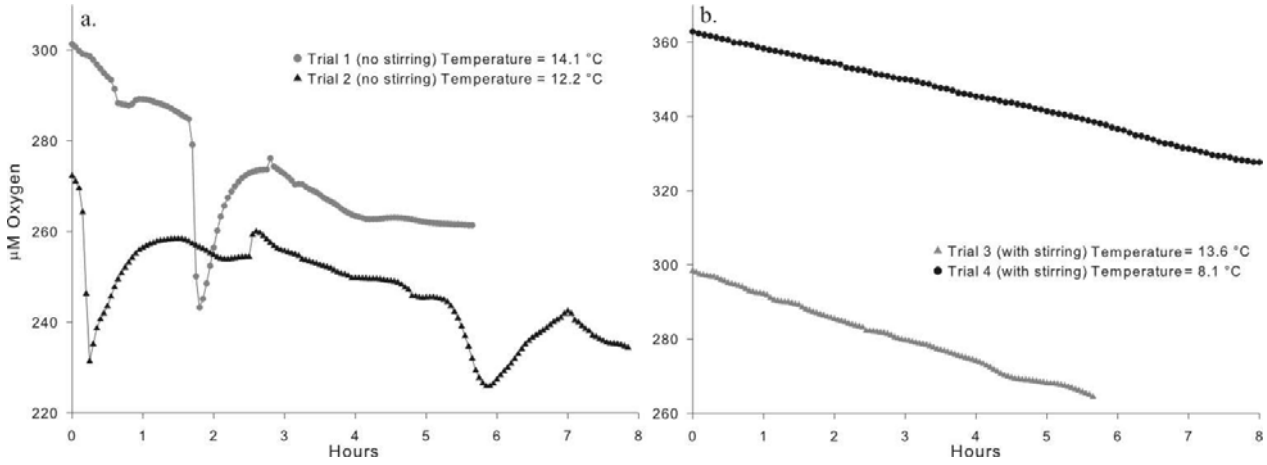

Figure 7.2. Results of trials to investigate the effect of a stirring mechanism upon the measured decrease in O_2 concentration due to the O_2 consumption of a specimen of *Asterias rubens*. Only one of the chambers was used during the trials. a) two trials without stirring, b) two trials with stirring. Variation in O_2 concentration between trials is due to calibration differences between optodes, which do not affect the recorded decline in O_2 concentration.

Lid design

The lids to the BICS chambers were designed to be placed onto the acetal rim around the top of the chambers by an ROV. The underside of the lids was formed of bevelled acetal plates embedded with two nitrile N70 o-rings (Figure 7.1d). The lids were intended to seal the chamber as the o-rings were compressed against the rim by the weight of the stainless steel lid (7.8 kg) and downward force of a securing bungee cord. During the trial deployments, the ROV pilots who

manipulated BICS had commented it was difficult to align the lids accurately onto the chambers. Design modifications to improve lid alignment had therefore already been suggested (Jamieson et al., 2005). In addition to the alignment difficulties, close observation of the lids in the laboratory environment revealed that the weight of the lids was inadequate to form a complete seal, as it was possible to see daylight between the bevelled lid base and the chamber's upper acetal rim (personal observations). The chambers could therefore not be confidently isolated from the external atmosphere when the lids were in place, unless sealed shut with an adhesive, a solution that would not be possible when deployed *in situ*. A new lid design was therefore also required.

7.2.2. Benthic Incubation Chamber System 2

Further to the recommendations to include a stirring mechanism in each chamber and to improve the fit of the lids, a redesign of BICS was undertaken. Due to budgetary constraints, the redesign incorporated as many of the original components as possible, the optodes and the TT8 controller and programming system were therefore retained. Whilst the new design was being drawn up, the opportunity was also taken to change the frame construction and reduce the respirometry chambers volume. The new design, BICS2 (Figure 7.3), differed from the original in the following ways:

- A hinged lid closure mechanism was incorporated that sealed the chambers without the ROV pilot needing to manipulate and align a free moving lid. Personal communication with the pilots of commercial work class ROVs (via the SERPENT[4] project) revealed that the pilots found rotational movements with ROV manipulators were the easiest to perform. The new lid mechanism was therefore designed to incorporate a geared lid, which would open and close when the ROV manipulator rotated a T-handle. A circular rubber V-seal attached to the underside of each lid formed a close seal to the chambers.
- The chambers' frame was reconstructed to incorporate the lid closing mechanism whilst enabling easy access to the chambers by a ROV. The frame was constructed from glass reinforced plastic (GRP) with dimensions 1000 mm x 580 mm x 642 mm. GRP was used instead of the original aluminium because it is lighter and more corrosion resistant. In air, BICS2 weighed 78 kg with empty chambers and 113 kg when the chambers were full of water, in water it weighed 33 kg.

[4] SERPENT (Scientific and Environmental ROV Partnership using Existing iNdustrial Technology), based at NOCS.

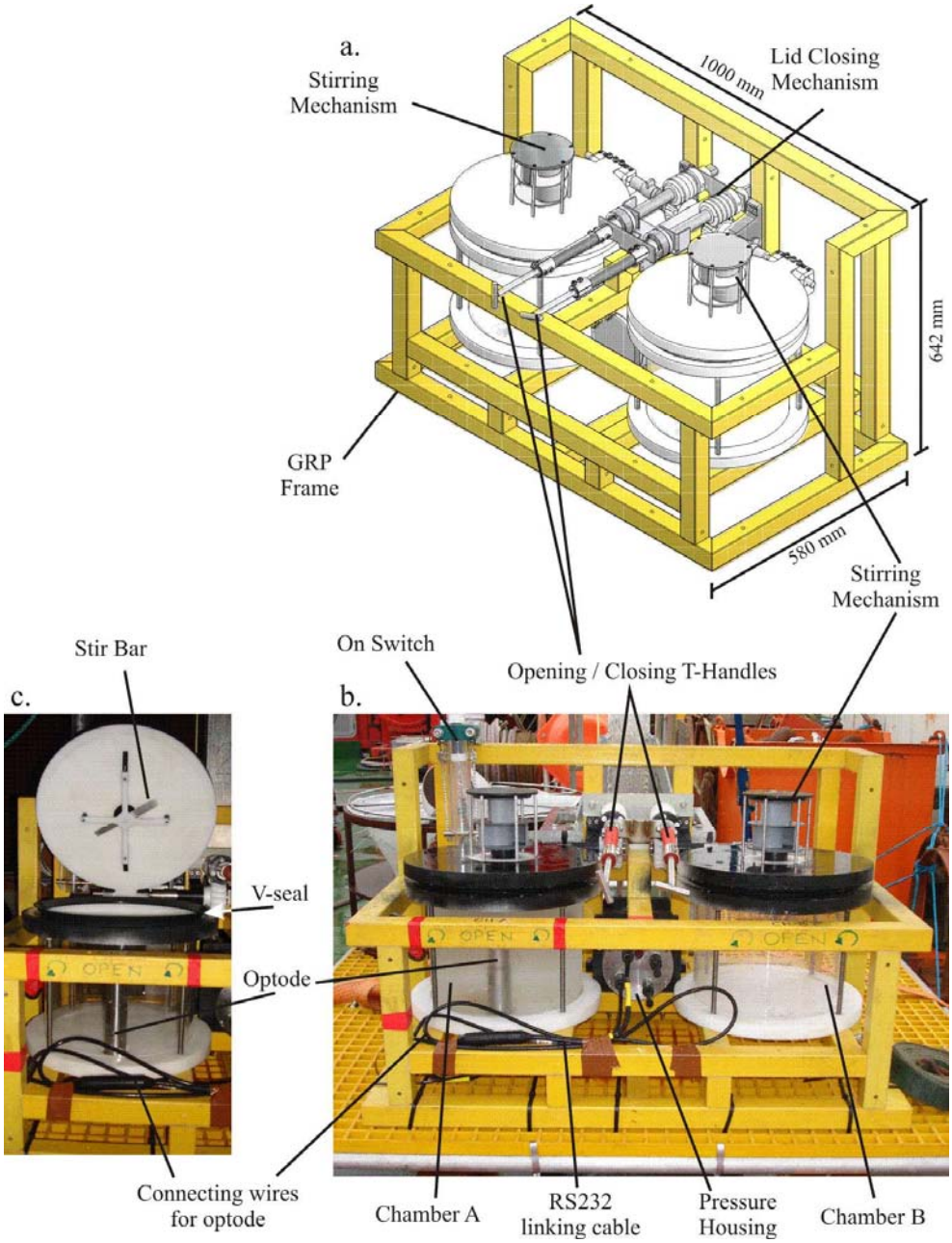

Figure 7.3. Redesigned BICS2 respirometry system a). Aerial view, illustrating the lid closing mechanism and the position of the stirring mechanism on top of the chamber lids. b). Frontal view, illustrating the positioning of the titanium pressure housing within the redesigned frame. c).Frontal chamber view, illustrating the stirring mechanism inside the open lid.

- The two respirometry chambers were reduced to a volume of 15.285 L. The volume reduction was carried out to limit the weight of the system when both chambers were full of water, and to reduce the operating volume of the respirometry system in order to improve the sensitivity of the respirometer system to organisms with low rates of O_2 consumption.
- A stirring mechanism was incorporated into the inside of each chamber's lid. Because of restricted available battery power, limited to that held inside the titanium pressure housing and

only intended to power optode data recording, it was not possible to incorporate a motor powered stirrer into the new BICS design. The stirrer was instead connected by magnets to an adapted current meter paddle mechanism located on the outside of the lids which, powered by ambient water movement, moved the internal stir bar.

7.3. BICS2 field deployment

7.3.1. Study Site

The first scientific deployments of BICS2 in the deep sea took place between the 6th and 28th June 2007 during the R.R.S. *James Cook* (JC) cruise 10. BICS2 was deployed at bathyal and abyssal depths in two different canyon systems, both of which intersect the Western Iberian Margin in the North East Atlantic (Figure 7.4). This region is characterised by a narrow and steep continental shelf, along which intense seasonal upwelling occurs (Schmidt et al., 2001).

The Nazaré Canyon is one of the world's largest submarine canyon systems, and intersects the entire Iberian continental shelf at ~39º30' N (Vitorino et al., 2005) . Starting at just 50 m depth the canyon extends to ~5000 m depth at the Iberian Abyssal Plain (Arzola et al., 2008). The Nazaré Canyon acts as an active trap for sediment and organic matter being transported laterally along the Iberian Shelf, which is then temporarily held in the upper and middle reaches of the canyon. Episodically large amounts of this sediment is released from the canyon to the deep sea (Epping et al., 2002; van Weering et al., 2002), resulting in the Nazaré Canyon being an important route of organic carbon to the Iberia Abyssal Plain. The Setúbal Canyon, located between 38°N and 38°30'N, extends seawards across the shelf from the mouth of the Sado River, and downslope to the Tagus Abyssal Plain at ~4840 m. Unlike the neighbouring Nazaré Canyon the Setúbal Canyon is inactive in terms of sediment transport, and sedimentation rates are lower (Arzola et al., 2008).

7.3.2. BICS2 deployments

Immediately prior to cruise JC10 a trials cruise took place to test the deployment and operation of the ROV *Isis* from the R.R.S. *James Cook* for the first time (Griffiths, 2007). During this cruise (JC09T), BICS2 was deployed to 4850 m to enable the ROV pilots to practice its operation. During preparation for the first scientific deployment of the subsequent JC10 cruise, it was discovered that one of the optodes had failed during the JC09T deployment and had been irreversibly damaged. Five deployments of BICS2 were carried out during cruise JC10 (Table 7.2). For deployments 1 and 5 a second optode was loaned from other equipment being deployed during JC10, but for deployments 2, 3 and 4 only one optode was available and hence only one respirometer chamber could be used.

Following deployment 5, it was discovered that the titanium pressure housing holding the electronic systems had failed. Initial inspections revealed that one of the o-rings in an end cap had been forced up into the chamber. The data recorded from both of the optodes during the deployment had been corrupted, and data from only one of the optodes was subsequently recovered. Further deployments of BICS2 during JC10 were not made due to safety concerns.

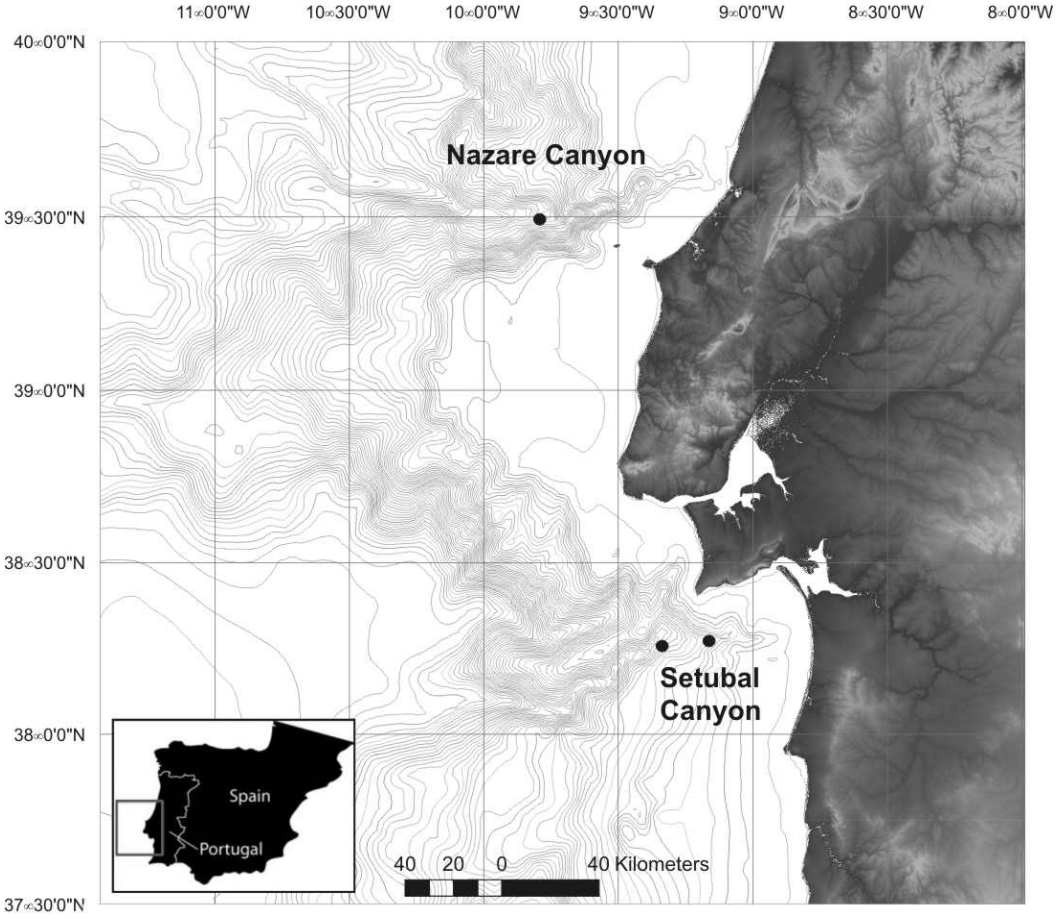

Figure 7.4. Map of the Nazare and Setubal Canyons off the coast of Portugal. Station positions for the BICS2 deployments are indicated. Adapted from Weaver et al. (2005).

Table 7.2. BICS2 deployments. Incubation time refers to the total number of hours *in situ* data was recorded from commencement of data logging to the start of elevator recovery to the surface. The species listed refers to the echinoderm species used inside the respirometry chambers during each deployment (see section 7.3.4).

Deployment	Date	Depth (m)	Latitude (N)	Longitude (W)	Incubation time (hrs)	Species
1. JC10-083	06/06/07	1440	38º16.017	09º09.936	9.9	*Psilaster cassiope*
2. JC10-090	09/06/07	3534	39º29.821	09º55.984	100.6	*Ophiura irrorata concreta*
3. JC10-106	15/06/07	3497	39º29.809	09º55.753	55.2	*Ophiura irrorata concreta*
4. JC10-119	19/06/07	3507	39º29.831	09º55.820	105.7	*Ophiura irrorata concreta*
5. JC10-143	28/06/07	2226	38º14.362	09º23.629	13.1	*Zygothuria lactea*

7.3.3. BICS2 operation

BICS2 was deployed to the seafloor securely attached to an elevator with cable ties, and remained attached to the elevator throughout the deployment. The lids of the two respiration chambers were held open during descent in order to prevent implosion (Figure 7.5a). At the seafloor either prior to, or following, elevator location the ROV searched for suitable echinoderms for use in BICS2. The echinoderms were picked up by collection scoop (Figure 7.5b) and "sieved" from any sediment that was collected at the same time (Figure 7.5c), before being transported to the location of the elevator (Figure 7.5d) and deposited into the chambers (Figure 7.5e). The lids were closed by the ROV turning the T-handles connected to the lid mechanism in an anticlockwise direction (Figure 7.5f). The TT8 controller was activated when the "on switch" (Figure 7.5g) was pressed and confirmed as activated by a flashing LED.

Deployment length was determined by the cruise schedule, although battery life determined the length of time the optode readings could be recorded to the memory disk. Once a deployment was complete, the elevator was released acoustically from its anchoring weights for return to the sea surface (Figure 7.5h), and after recovery to deck, the echinoderms were collected and the data saved to the memory card retrieved (Figure 7.5i).

7.3.4. Echinoderm species

Five specimens from three classes of echinoderm were used in BICS2 during cruise JC10 (Table 7.2, above). These were identified after the cruise as detailed below.

Asteroidea

Psilaster cassiope (Sladen, 1889)

Two specimens of this asteroid species were examined for identification purposes; the specimen used in BICS2 (Figure 7.6 d,e) and a second that was collected from the same location in the biobox on the R.O.V. Isis (JC10_082). Identification was determined to be *P. cassiope* as opposed to the extremely similar *P. andromeda andromeda* based on the characteristic jaw morphology. Each jaw had four spatulate apical oral spines, forming a horizontal "scoop", with the two median spines projecting beyond the two outermost spines. The apical oral spines were not broadened, as found in *P. andromeda andromeda*, and resembled identically the illustration of the ventral jaw of *P. cassiope* by Clark & Downey (1992). Although this identification extended the stated geographical range of *P. cassiope* north of Cap Blanc, as Clark & Downey (1992) point out, there is a gap in the geographical distribution between the southernmost area for *P. andromeda andromeda* (Bay of Biscay) and the northern most area for *P. cassiope* (the vicinity of Cap Blanc).

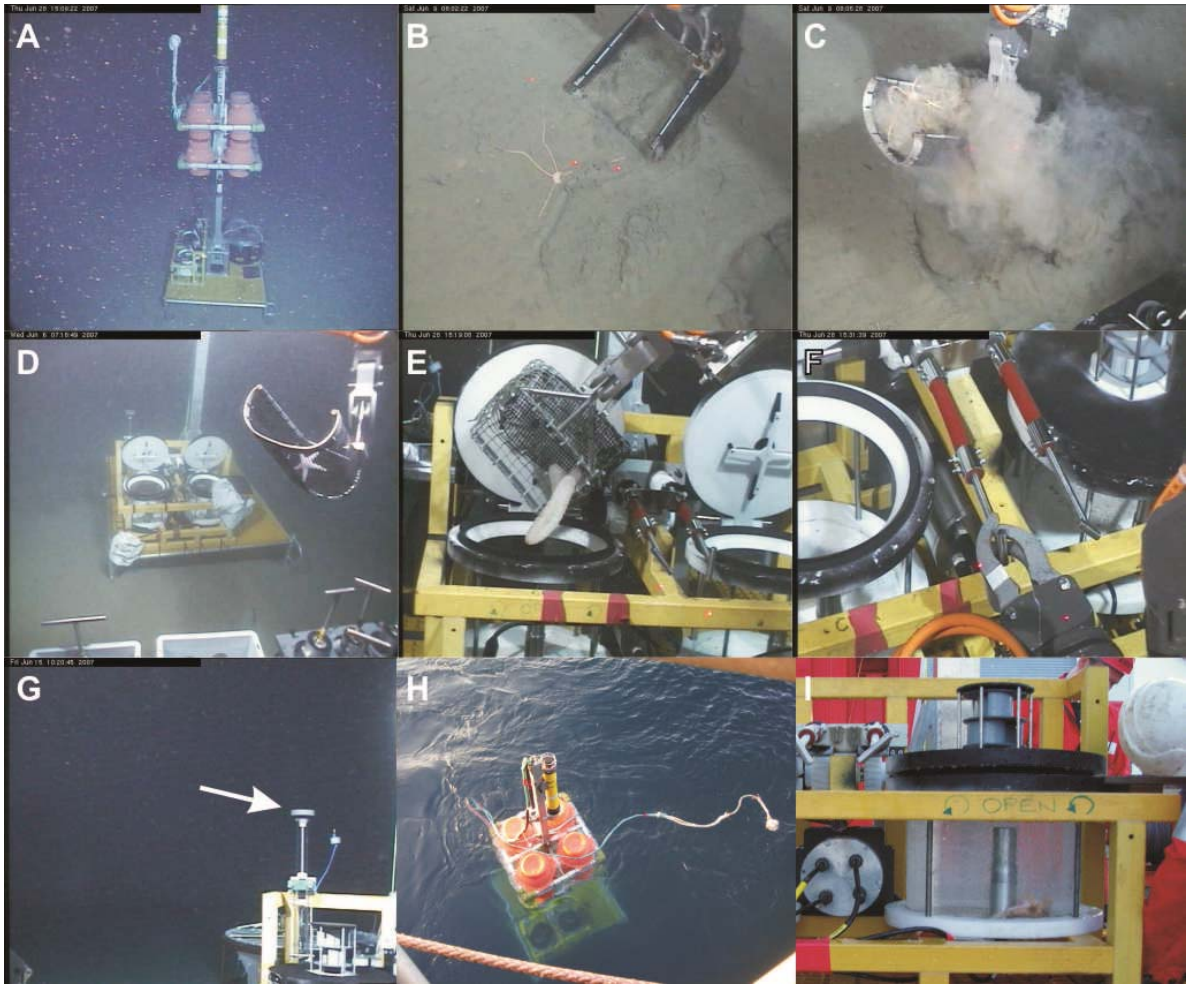

Figure 7.5. BICS2 Operation during JC10. Photographs are compiled from images taken during all five deployments. Refer to text for detailed commentary. a) BICS2 deployed to the seafloor attached to (the left hand side) of an elevator, b) specimen collection, c) sieving, d) approaching BICS2 (plastic rubbish trapped against the BICS2 frame having drifted there in the current can be seen), e) specimen introduction to a chamber, f) lid closure by T-handle rotation, g) on switch (arrowed), h) surface recovery, i) specimen retrieval.

Ophiuroidea

Ophiura (Ophiuroglypha) irrorata concreta (Koehler, 1901)

The three ophiuroid specimens used with BICS2 (Figure 7.6 a,b,c) were each identified as *Ophiura irrorata concreta* (Koehler, 1901), a species which is part of the *O. irrorata* group (Paterson, 1985), and now accepted as *Ophiura (Ophiuroglypha) irrorata concreta* (Stöhr, 2009). The BICS2 specimens had several characteristics strongly indicative of *O. irrorata concreta*: a) the arrangement of the 3 arm spines; with a clear separation between the single dorsal most arm spine and the two ventral spines, b) the large second oral tentacle pore opened into the mouth slit via a furrow, c) subsequent to the first ventral arm plate the arm plates were axe shaped, and d) the plate between the radial shields and the arm combs extended to almost the entire width of the radial shield's distal edge (Paterson, 1985). There were also characteristics that mitigated against

the identification as *O. irrorata concreta* including, the disk diameters in the BICS2 specimens being 26-29 mm, rather than less than the 20 mm description; the arms in the BICS2 specimens ranged from 4.85 – 5.46 times the disk diameter as opposed to 3 – 4 times in the described species, and the radial shields did not extend to 1/3 the disk radius (Paterson, 1985). However, the strength of the morphological characteristics summarised a) to d) above confirmed the identification as *O. irrorata concreta*. These specimens therefore represented an extension to the reported depth distribution of *O. irrorata concreta* from 2250 – 2743 m (Paterson, 1985) to 2250 - 3534 m. Assistance with the ophiuroid identification was provided by Prof. P. Tyler (NOCS).

Holothuroidea

Zygothuria lactea (Théel, 1886)

This species belongs to the Synallactidae holothurian family, members of which are found almost exclusively in the deep sea (Billett, 1991). A cosmopolitan epibenthic species, *Z. lactea* feeds on organic matter found in the uppermost layer of the sediment and has been found at depths of 694-2102 m (Solís-Marín, 2003). Identification of the specimen used in BICS2 (Figure 7.6 f) was confirmed based on the structure of the calcareous spicules located in the epidermis. Assistance with the identification of this holothurian was provided by Ian Cross (NOCS) and Antonina Rogacheva (visiting scientist from the P.P. Shirshov Institute of Oceanology, Moscow).

7.3.5. Calculation of oxygen consumption rate

Depth and salinity compensation

The optode expresses the absolute oxygen content of the water contained inside a chamber in µmole (µM), and records temperature in ºC. The response of the optode's sensing foil decreases with ambient water pressure (3.2% lower response per 1000 m of water depth). This effect is completely reversible but a depth compensation is not performed to the data automatically within the optode. This is compensated for by applying the following equation to the recorded data, where d is depth in metres, O_{2c} is compensated O_2 concentration in µM and O_2 is the oxygen concentration recorded by the optode in µM:

$$O_{2c} = O_2 \times \left(1 + \frac{0.032 \times d}{1000}\right) \qquad [1] \text{ (Aanderra Instruments AS, 2004)}$$

A compensation for salinity is also required. The O_2 concentration measured is the O_2 concentration behind the sensing foil, which is only gas permeable, not water permeable. Therefore, the optode measurements do not account for the effect of dissolved salt. A salinity value can be set within the optode programming, but if the salinity varies significantly *in situ*, the following correction can be applied to the data after it has been collected:

$$O_{2c} = (O_2) \times e^{S\left(B_0 + B_1 T_S + B_1 T_S^2 + B_1 T_S^3\right) + C_0 S^2}$$ [2] (Aanderra Instruments AS, 2004)

Where: (all from Aanderra Instruments AS, 2004)

O_{2c} = compensated O_2 concentration (µM)

O_2 = depth compensated oxygen concentration (µM)

e = 2.71828 (the mathematical constant, listed here to 5 decimal places)

S = *in situ* salinity (ppt)

T_s = scaled temperature = $\ln\left[\frac{298.15 - t}{273.15 + t}\right]$ t = temperature in ºC

B_0 = -6.24097e^{-3} B_1 = -6.93498e^{-3} B_2 = -6.90358e^{-3}

B_3 = -4.29155e^{-3} C_0 = -3.11680e^{-7}

If a salinity value has been set within the optode programming, the compensated O_2 concentration must then also be divided by the following expression, where all terms are the same as above, apart from S_1, which is the optode's programmed salinity value (ppt):

$$e^{S_1\left(B_0 + B_1 T_S + B_1 T_S^2 + B_1 T_S^3\right) + C_0 S_1^2}$$ [3] (Aanderra Instruments AS, 2004)

Oxygen consumption rate

The individual echinoderm oxygen consumption rates were calculated according to the difference in oxygen concentration at the start and the end of the trial period (see next section for details of the trial period):

$$\dot{V}O_2 = \frac{(Cwo_2(A) - Cwo_2(B))V}{T}$$ [4] (Cech, 1990)

Where,

$\dot{V}O_2$ = oxygen consumption rate (µmol O_2 hour^{-1})

$Cwo_2(A)$ = oxygen concentration (µmol O_2 L^{-1}) at start of trial

$Cwo_2(B)$ = oxygen concentration (µmol O_2 L^{-1}) at end of trial

V = volume of respirometer minus echinoderm volume (L)

T = duration of incubation period (hours)

The echinoderm volumes were calculated according to the same Archimedes principle method outlined in section 4.2.2.2. Once $\dot{V}O_2$ was calculated, the mass specific rate of oxygen consumption ($\dot{M}O_2$) was calculated by dividing by the echinoderm wet weight (g) determined by weighing on a motion compensated balance (POLS S-182 onboard marine scale).

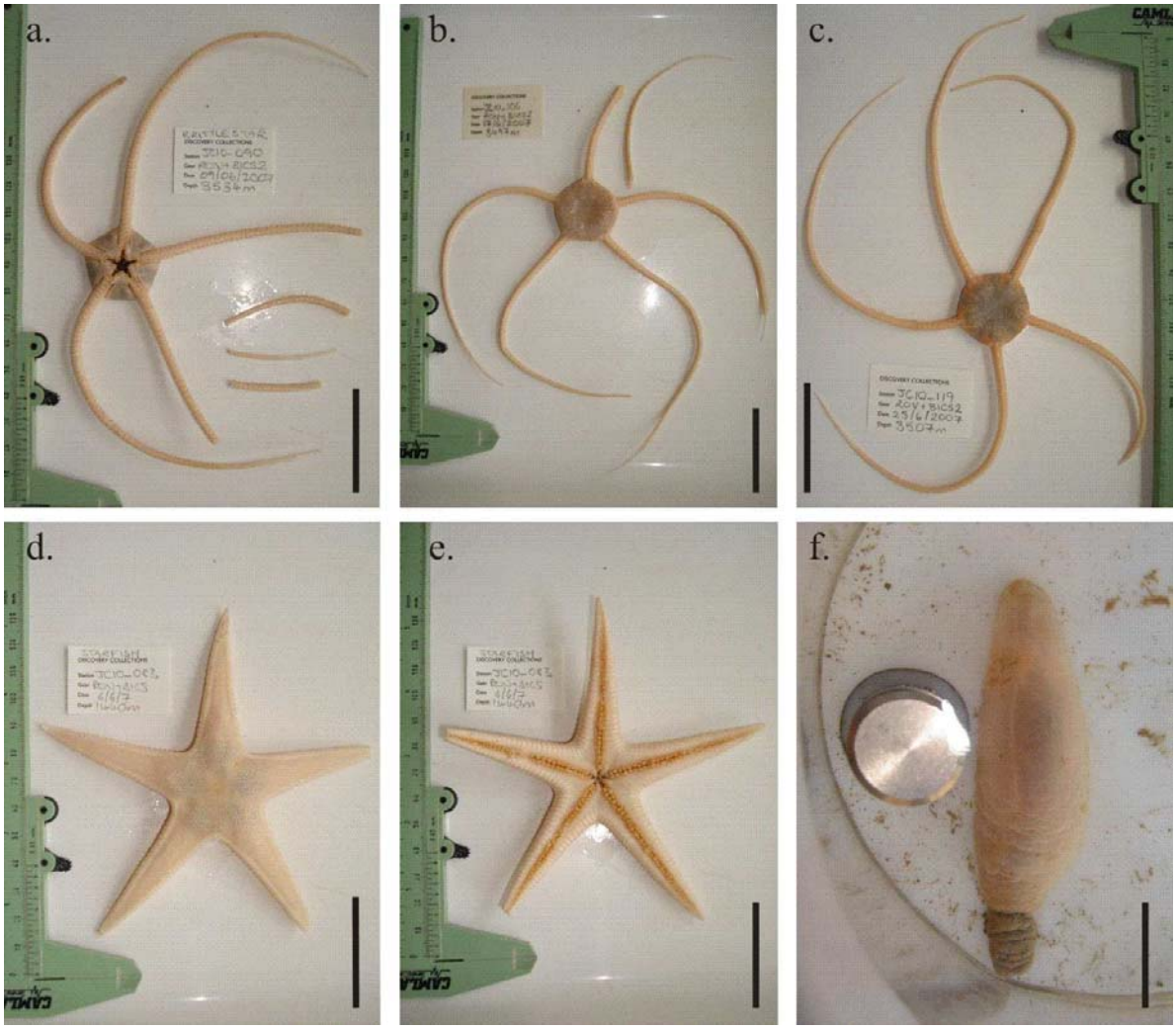

Figure 7.6. Echinoderm specimens used in BICS2 during JC10, all scale bars = 40 mm. a). Deployment 2: *Ophiura irrorata concreta* (oral view), b). Deployment 3: *O. irrorata concreta* (aboral view), c). Deployment 4: *O. irrorata concreta* (aboral view), d). Deployment 1: *Psilaster cassiope* (aboral view), and e). oral view, f). Deployment 5: *Zygothuria lactea*, image taken whilst holothurian inside respirometry chamber immediately following retrieval.

7.3.6. Results

Deployment 1. *Psilaster cassiope*

The first BICS2 deployment, at 1440 m depth in the Setúbal Canyon, included two optodes and hence two operating respirometry chambers. One chamber was used as a control chamber, intended to assess the background oxygen consumption of the microbial community in the seawater. A specimen of the asteroid *P. cassiope*, present in the upper Setúbal Canyon at 5-13 individuals per hectare (Pattenden, 2009), was placed inside the second chamber. An incubation time, from lid closure to commencement of elevator recovery to the surface, of 9.93 hours was possible (Figure 7.7a). It can be seen from the figure that the oxygen profiles recorded from the two respirometry chambers (experimental and control) are erratic. There appears to be an influence

of ROV proximity to BICS2 upon the readings, with the profile from the asteroid indicating changes in readings corresponding to ROV movement. Whether the ROV influenced the optodes directly via electrical interference, or the measurements were influenced by ROV-stimulated asteroid activity is not known. Due to the lack of a clear trend in the change of oxygen concentration that would be indicative of oxygen consumption by the asteroid or by a microbial community in the control chamber, no attempt to calculate oxygen consumption was made from the results of this first deployment.

Deployments 2, 3 and 4. *Ophiura irrorata concreta*

The next three BICS deployments, at 3497-3534 m depth in the Nazaré Canyon, were all performed with only one functioning respirometry chamber. One specimen of *O. irrorata concreta* was used in each deployment, an abundant ophiuroid in this middle section of the canyon (585 individuals per hectare (Pattenden, 2009)), total incubation times ranged from 55.2 to 105.7 hours. The recorded oxygen concentration profiles demonstrated that the presence of the ROV near to BICS2 possibly interfered with the optode measurements, though it is unknown is this was physical or electronic interference or due to ophiuroid movement. Therefore, in order to standardise results, the 'trial period' over which oxygen consumption rate calculations were made was deemed to have started 24 hours after commencement of data logging and ended at the earliest of a) 48 hours later or b) commencement of elevator recovery to deck. The initial, disregarded, 24-hour period was selected to remove any ROV influence upon readings, and for any stress caused to the ophiuroids during handling to subside. Due to fluctuations observed in the seawater oxygen concentrations recorded from the respiration chambers, the oxygen consumption of the ophiuroid specimens collected during each deployment (Table 7.3) were computed from the average linear gradient of the decrease in oxygen concentration (Figure 7.8).

Figure 7.7 caption (figure next page). Recorded oxygen concentration profiles for each BICS2 deployment. The oxygen concentration (µM) within the respirometers is plotted as a function of incubation time (hours), beginning at time zero where the on switch was pressed by the ROV and ending either at the time of battery expiration or during the surface transit period. a). Deployment: 1 *P. cassiope* (black plot) and control (grey plot), b). Deployment 2: *O. irrorata concreta*, c). Deployment 3: *O. irrorata concreta*, d). Deployment 4: *O. irrorata concreta*, e) Deployment 5: *Z. lactea*, f). Deployment 5: *Z. lactea*, incubation time from to 9.13 to 13.06 hours (see text for more details). Labels: A = time ROV departed vicinity of BICS2, B = time anchoring weights released from elevator, C = time ROV returned to vicinity of BICS, D = battery power expired and optode recording ceased. Bars on figures b, c and d refer to the trial periods used to calculate the oxygen consumption rate of the three *O. irrorata concreta* specimens (see text for more details).

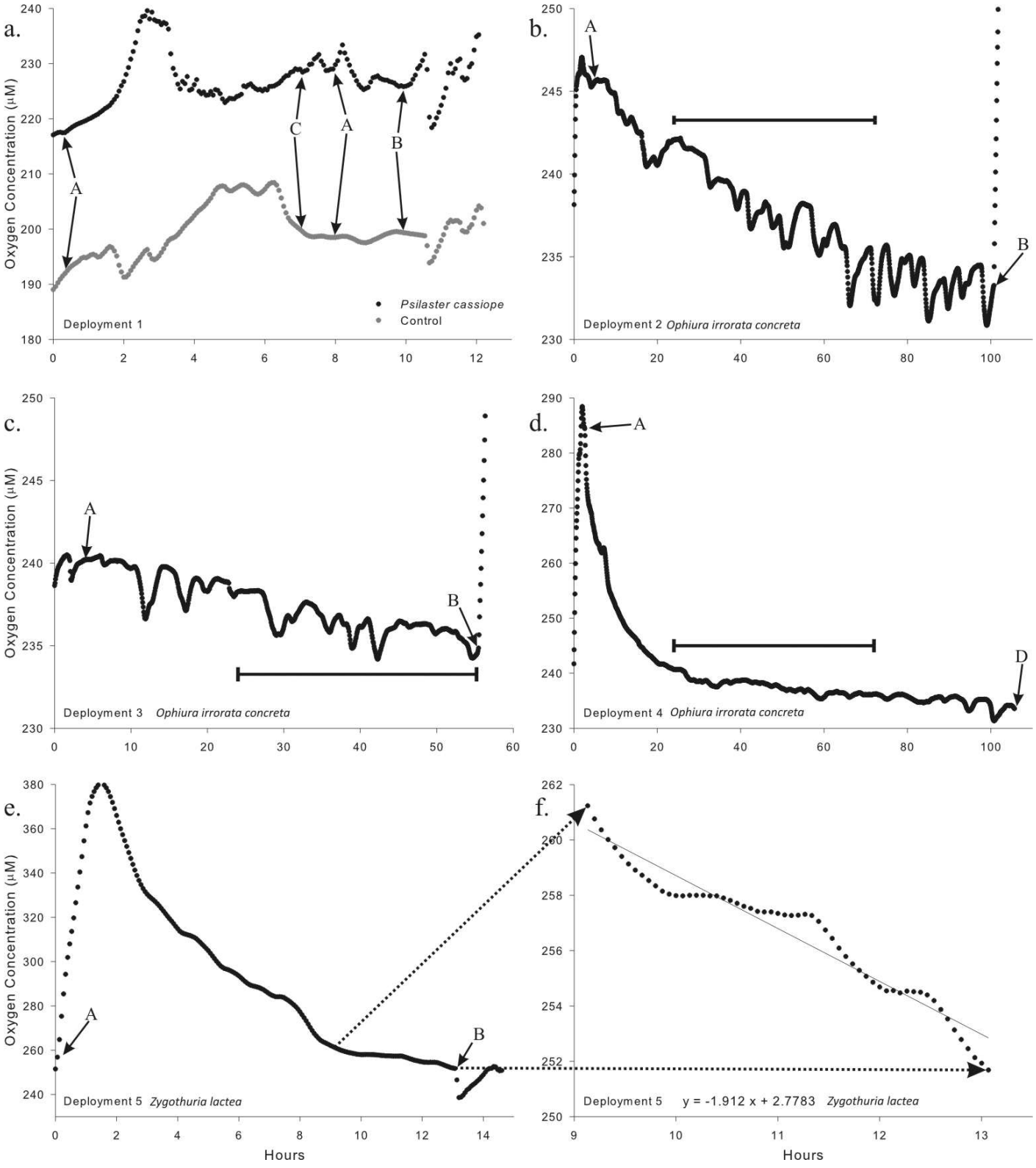

Figure 7.7. caption on previous page.

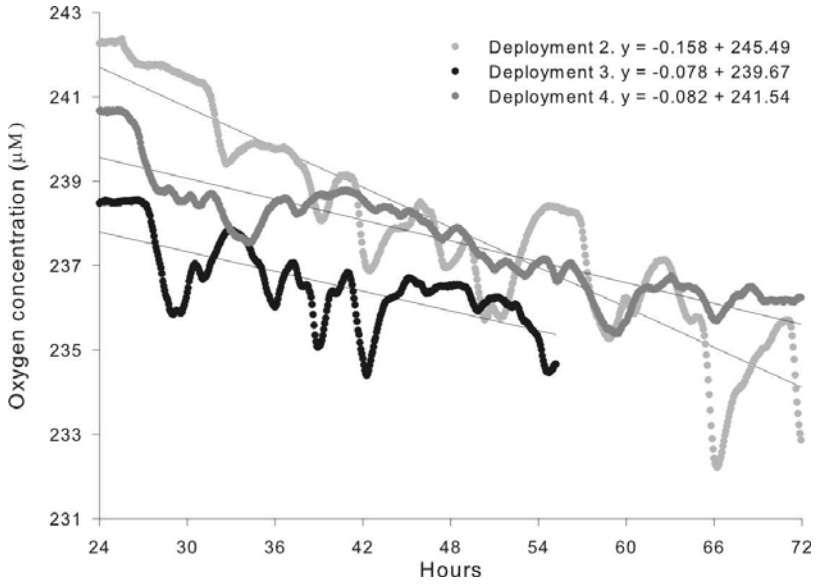

Figure 7.8. Oxygen concentration (µM) of the seawater inside the experimental BICS2 respiration chamber during the trial periods for deployments 2 (light grey), 3 (black) and 4 (dark grey). All echinoderm specimens were *O. irrorata concreta* individuals. Hours represents the time elapsed from 24 hours after commencement of the incubation to either 72 hours after incubation commencement (a 48 hour trial period), or commencement of elevator recovery. Equations for the linear regressions of the oxygen concentration profiles with time are listed, from which the average oxygen consumption rate of the ophiuroids were calculated.

A closer analysis of the fluctuations observed in the oxygen concentrations via Fourier analysis (assisted by Matthew Thomas, UEA), indicated that the fluctuations varied in the ophiuroid deployments with a frequency of 6 to 8 hours and 23 to 26 hours. It is hypothesised that that the observed fluctuations could have been caused by tidal flux in the canyon, which caused the current power stirrer to function at times of optimal current velocity. There is circumstantial evidence to support this hypothesis – the final deployment of BICS2 in the Setúbal Canyon did not demonstrate similar fluctuations in oxygen concentration (Figure 7.7e). It was noted during this deployment by the ROV pilots that the current velocity was notably greater in this canyon system at the time of deployment than had been found in the Nazaré Canyon, which may have caused the stirrer mechanism to function throughout the last deployment as opposed to intermittently during the three previous deployments.

Deployment 5. *Zygothuria lactea*

The final BICS deployment, at 2226 m depth in the Setúbal Canyon, was performed with both respirometry chambers, but due to equipment failure the measurements from only one respirometer chamber were recovered. Oxygen consumption measurements were obtained from an individual holothurian specimen of *Z. lactea*, present in the middle Setúbal Canyon at

67 individuals per hectare (Pattenden, 2009)). The total incubation period was only 13 hours in length (due to cruise scheduling); the trial period was therefore selected as the last 4 hours of incubation prior to elevator retrieval (Figure 7.7f), eliminating the first 9 hours during which the rate of oxygen depletion could have been influenced by organism stress and ROV interference. The oxygen consumption of the holothurian was computed from the average linear gradient of the decrease in oxygen concentration over these 4 hours (Table 7.3).

Table 7.3. Oxygen consumption rates of the echinoderm individuals.

Deployment	Temperature (ºC)	$\dot{V}O_2$ (µmol hr^{-1})	Wet Weight (g)	$\dot{M}O_2$ (µmol hr^{-1} g^{-1})
2. JC10-090	2.55	2.415	9.2	0.263
3. JC10-106	2.54	1.190	8.8	0.135
4. JC10-119	2.51	1.259	7.0	0.180
5. JC10-143	4.23	28.933	130.2	0.222

7.3.7. Discussion

BICS2 performance

During JC10, although the ROV pilots could manipulate the new lid closing mechanism and it functioned well, it became apparent that the new mechanism for closing the lids was somewhat 'over engineered' and should be simplified in future designs. The current-powered stirrer bars appeared to be moved by tidal fluxes in the canyon so that, although they stirred the internal chamber water, the stirring was intermittent and introduced fluctuations in measurements from the optode. A battery-powered stirrer is required in future designs. The chamber size was determined by the requirement for BICS2 to be operated, and the placement of an organism into the chambers to be carried out, by an ROV. Whilst not suitable for short term respiration measurements, the large volume (15.29 L) provided for measurements of oxygen consumption to be taken from an organism over the course of all five deployments (up to 106 hours), the length of which were determined by the research cruise requirements. These long periods of measurements also enabled 24 hours of readings after experiment commencement to be discarded from analysis in order to remove data interference from ROV proximity and organism stress following handling. Overall, the design of BICS2 made possible the measurement of the first readings of the oxygen consumption rates of abyssal ophiuroids, and the equipment was easily manipulated at the seafloor by the ROV.

Investigations after return to shore revealed that the end caps to the titanium pressure housing were too narrow for the housing cylinder and incorrectly sized o-rings had been used. The electronic

control systems located inside the pressure housing were irretrievably damaged, following failure of the pressure housing during deployment 5, and BICS2 could not be used again without repair. A third design was therefore commissioned, incorporating the lid closure and motor-powered stirrer improvements that were recommended following the JC10 deployments. The first scientific deployment of BICS3 is discussed in the manuscript at Appendix 1.29.

Echinoderm oxygen consumption rates

In order to assess the biological relevance of the data obtained with the BICS2 *in situ* respirometry chamber, the oxygen consumption rates obtained from *O. irrorata concreta* and *Z. lactea* were compared against selected published data from ophiuroids and holothurians obtained at comparable temperatures (Figure 7.9). For comparative purposes the data were temperature normalised via Q_{10} adjustment (refer to manuscript at Appendix 1.30 for a complete description of methodology). Following adjustment for background seawater oxygen consumption rates (obtained during the first deployments of BICS3), the three *O. irrorata concreta* oxygen consumption rates ranged from 0.61 to 1.76 μmol O_2 hr^{-1}. The highest rate was comparable to those obtained from *Ophioscolex glacialis* (Schmid, 1996) and also to those obtained via *in situ* respirometry at 1300 m from specimens of the holothurian *Scotoplanes globosa* with similar mass (Smith, 1983). The *Z. lactea* oxygen consumption rate (0.217 μmol O_2 hr^{-1}) is in line with those obtained from the holothurian species *Cucumaria frondosa, Psolus* spp. (Hargrave et al., 2004) and *Heterocucumis steineni* (Fraser et al., 2004).

The results obtained with BICS2 were also included in a data set incorporating the oxygen consumption rates of 84 species of echinoderm, which was analysed in order to determine whether there was any variation in echinoderm metabolic rate with depth. Detailed investigations of the effect of depth on metabolic rate have previously been carried out on data sets relating to deep-sea cephalopod molluscs (Seibel, 2007), crustacea (Childress, 1995) and fish (Drazen and Seibel, 2007). With regard to visually dependent deep-sea pelagic organisms, it has been found that metabolic rate declines with water depth, in a manner that is independent of mass or temperature (Seibel, 2007) and is instead attributed to light availability. According to the visual interactions hypothesis (Childress and Mickel, 1985), light availability determines the locomotory requirements of visually sighted pelagic organisms that participate in predator-prey interactions. As light decreases through the water column so does locomotory requirement and the associated metabolic rate of an organism (Childress, 1995; Seibel and Drazen, 2007).

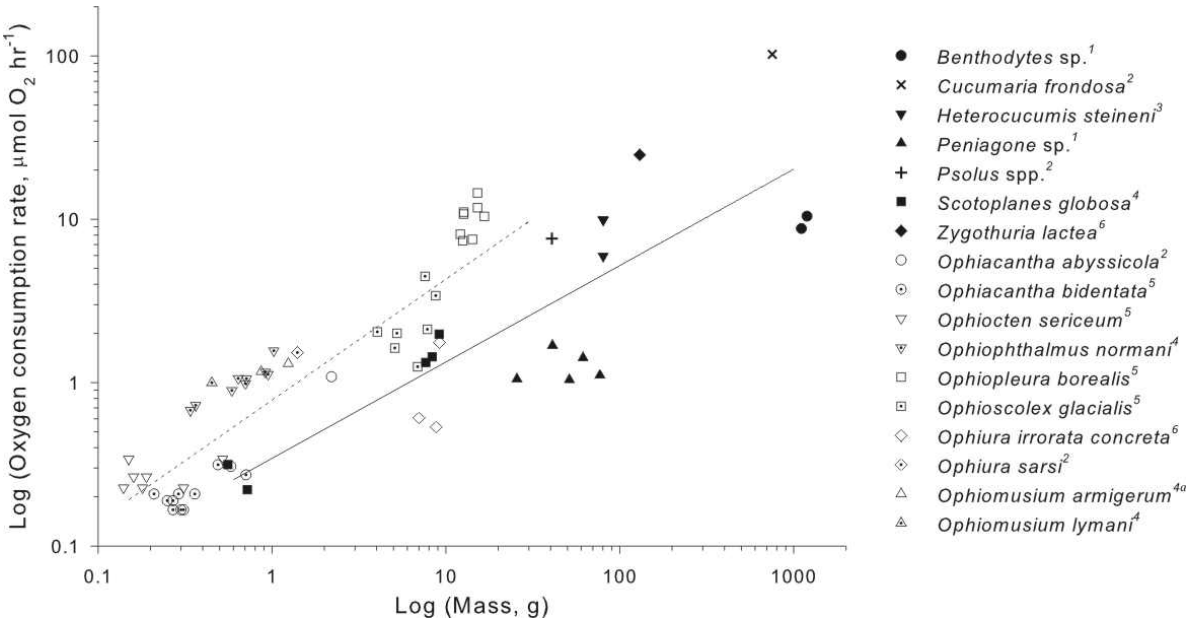

Figure 7.9. Comparison of individual metabolic rates ($\dot{V}O_2$) as a function of wet weight mass (M) of ophiuroid and holothurian species, obtained at their normal habitat temperature between -1.8 and 4.0 °C, including those obtained from the deep-sea species investigated in this study using the *in situ* BICS2 respirometer (2.51 – 4.23 °C). All individual metabolic rates have been Q_{10} adjusted to 2.5 °C using a Q_{10} of 2.154 (see Hughes et al., in prep). The solid line indicates the linear regression for the holothurian metabolic rates ($\dot{V}O_2 = 0.344\ M^{0.5901}$, $R^2 = 0.6485$, $p < 0.001$), the dashed line indicates the linear regression for the ophiuroid metabolic rates ($\dot{V}O_2 = 0.7808\ M^{0.6559}$, $R^2 = 0.7403$, $p < 0.001$). Superscript indicators: Data from [1]Hughes et al. (in prep), [2]Hargrave et al (2004), [3]Fraser et al (2004), [4]Smith (1983), [5]Schmid (1996) and [6]this study. [a]*Ophiomusium armigerum* is now accepted as *Ophiosphalma armigerum* (Stöhr and Hansson, 2009).

No decline in metabolic rate with depth was found within the echinoderm dataset, as would be predicted by the visual interactions hypothesis given that the echinoderm lifestyle, at any depth, is not dependent on visual-locomotor interactions with prey or predators. A lack of a depth related trend in metabolism has also been found in other deep-sea non-visual pelagic organisms, or benthic visual taxa that can find refuge from predation on the sea floor, including crustacea, cephalopods, medusae and fish (Childress et al., 1990; Thuesen and Childress, 1994; Thuesen et al., 1998; Seibel and Childress, 2000; Seibel and Drazen, 2007). The result of the echinoderm metabolic rate review confirms those of previous studies that have used smaller echinoderm data sets. Smith (1983) found that the metabolic rates of two species of deep-sea ophiuroids were comparable to those of shallow living species at comparable temperatures, and Seibel and Drazen (2007) found no difference between shallow water and deep-sea echinoderm metabolic rates.

The database of metabolic rates from 84 species of echinoderm was also used to generate allometric scaling relationships between metabolic rate and body mass for each echinoderm class.

These figures represent updated values for weight dependant deep-sea echinoderm respiration rates since those published for general deep-sea invertebrate organisms by Mahaut et al. (1995). These scaling coefficients are relevant for use within models relating to the contribution of echinoderms to ecosystem food web analysis and carbon cycling in both shallow water and deep-sea systems. Their relevance to deep-sea benthic boundary layer communities is high, and as interest in the impacts of climate change upon deep-sea ecosystems increases, will contribute to the estimation of future change in these systems.

7.3.8. Conclusions

The BICS2 respirometer was a successful design for the collection of data regarding the metabolic rate of deep-sea echinoderms. As discussed above, the oxygen consumption (metabolic) rates obtained from *O. irrorata concreta* and *Z. lactea* were broadly comparable to those obtained from other echinoderm species. From a large comparison of the metabolic rates of 84 species of echinoderm, no significant change in echinoderm metabolic rate with depth is evident. It is likely that the maintenance of metabolic rate with depth is made possible by the enzymes involved with aerobic metabolism in deep-sea species being structurally adapted to function optimally under the high pressure and low temperature conditions of the deep sea.

The original BICS design included the functionality to pump liquid substances into one of the respirometry chambers at a pre-programmed time. Whilst this ability was not included in the BICS2 design in order to concentrate on its development as a fully functional respirometer, only basic modifications are required to reintroduce the pumping mechanism. In this regard, by virtue of its successful operation as a deep-sea respirometer, there is clear potential to take the BICS design forward to function as an experimental device to assess the impact of contaminant-induced stress upon deep-sea echinoderms *in situ.*

Chapter 8. Conclusions

Traditionally, the deep sea has been viewed as a remote environment, one where human waste can be disposed of and from which natural resources can be exploited without significant consequence (Carney, 2001). It is only recently that the importance of deep-sea ecosystems and processes to global biogeochemical systems has become clear. Whilst attempts are now being made to estimate the economic value of the goods and services provided by deep-sea ecosystems, to develop deep-sea governance and management regimes and to research deep-sea processes, the expansion of anthropogenic activities into the deep sea continues (Cochonat, 2007; UNEP, 2007; Pfannkuche et al., 2009). If the potential impact of human activity upon deep-sea organisms and ecosystems is to be understood and predicted, experimental studies are required to increase our knowledge of representative deep-sea biota and their sensitivity to environmental perturbation.

Echinoderms, as a group of organisms, can serve as 'diagnostic indicators' for the deep sea. They are distributed over the wide geographical and depth ranges of the oceans, are key components of deep-sea communities, show variation in physiological responses to abiotic factors and, via the sequenced genome of *Strongylocentrotus purpuratus*, transcriptomics tools have been developed (Mykles et al., 2010). Although inferences as to the sensitivity of deep-sea echinoderms to anthropogenic impact can be made from shallow-water studies, the suitability of using shallow-water species as proxies for deep-sea echinoderms is not known. However, using specimens of deep-sea echinoderms directly in experiments is logistically complex and expensive. Therefore, the challenge for future research is to adopt an experimental methodology, and to employ experimental specimens, which will produce reliable results that can be used to understand and predict the sensitivity of deep-sea echinoderms to anthropogenic impact.

8.1. Experimental approaches with echinoderms

To test different experimental approaches to the investigation of deep-sea echinoderm sensitivity to anthropogenic impact, this study used the following methods:

1) The use of eurytopic and stenotopic shallow-water echinoid species in contaminant exposure experiments in order to determine whether stenotopic species are an appropriate proxy for deep-sea echinoderms. These experiments were performed under surface laboratory conditions.
2) The performance of *in situ* disturbance experiments with a deep-water echinoid species. The collection of tissue samples for molecular analysis was, however, performed at the sea surface once the echinoids were retrieved.

3) The acquisition of physiological measurements from deep-sea echinoderms *in situ* at the abyssal sea floor using a novel deep-sea *in situ* respirometer.

8.1.1. Shallow-water proxies

The theory tested in Chapters 4 and 5 related to the differences in homeostatic regulation between different species of shallow-water echinoid. *Psammechinus miliaris,* as a eurytopic species, is adapted to respond to a fluctuating physical environment and can readily respond to environmental perturbation. This response capacity was predicted to extend to a ready response to contaminant exposure. Conversely, *Brissopsis lyrifera*, a stenotopic species adapted to a stable environment, was predicted to be unable to respond readily to contaminant exposure. With regard to relevance to the deep sea, the response of *B. lyrifera* (if found to be different to that of *P. miliaris*) could be considered representative of deep-sea echinoderms which, due to their adaptation to an environment also characterised by an absence of variability, are considered to be unable to maintain homeostatic regulation in the face of environmental perturbation (Seibel and Walsh, 2003).

The stress responses of the two species of shallow-water echinoid to water based spud mud (WBSM), a chemical used by the offshore hydrocarbon drilling industry and expected to enter the deep-sea environment, were assessed using a number of biomarker assays each focused on a different level of biological organisation. At the behavioural level of organisation, the self-righting and burrowing biomarker approaches were considered insufficiently sensitive to detect a stress response. The physiological and biochemical biomarkers in *P. miliaris* also did not reflect any variation in response to WBSM exposure, but it was not possible to make any comparison with *B. lyrifera* at these levels of organisation. In *P. miliaris* both the cytological and molecular biomarkers indicated significant differences in response to WBSM exposure, a pattern that was not repeated in *B. lyrifera*.

These differences could have arisen from differential degrees of exposure between the two species, with the non-burrowed *B. lyrifera* potentially not exposed to the WBSM. However, with no evidence of a response to the WBSM occurring in any of the biomarker assays applied to *B. lyrifera*, it is possible that this had resulted from a lack of an ability to readily respond to environmental perturbation and maintain homeostasis. This result demonstrates that future laboratory-based experiments, from which the outcomes will be applied to predicting the impact of contaminants on deep-sea echinoderms, should use a stenotopic species as an experimental proxy species. Due to similar lifestyles and habitats, a benthic deposit feeding species from a stable environment like *B. lyrifera* is likely to produce experimental results more applicable to deep-sea

species than would species from the intertidal environment.

In addition to the differences found between the *P. miliaris* and *B. lyrifera* responses at the lower levels of biological organisation, evidence was found that collection from the field and maintenance in aquarium conditions were detrimental to the echinoid specimens, which influenced the biomarker assessments of WBSM response. With regard to the investigation of anthropogenic impact on deep-sea organisms, the benefits of the methodological flexibility and control available with laboratory-based investigations on shallow-water proxies must be considered against *in situ* experimentation that avoids the requirement to collect and maintain specimens under artificial conditions.

8.1.2. *In situ* deep-sea experimentation

***In situ* anthropogenic disturbance**

With significant differences in responses to WBSM exposure only being found via the cytological and molecular biomarkers in the shallow-water echinoid experiments, the ability to detect a stress response at these levels of biological organisation indicates potential as early warning systems for sublethal effects of contamination (Depledge et al., 1995). With the qPCR technique enabling the accurate quantitation of gene transcripts in a tissue sample, it is possible to investigate differential gene expression in any organism once a fragment of the target gene sequence has been identified (Chapter 3). The application of the qPCR methodology developed for the *P. miliaris* and *B. lyrifera* experiments to samples obtained from echinoids subject to *in situ* experimentation formed part of the second experimental approach to the investigation of deep-sea echinoderm sensitivity to anthropogenic impact.

The *in situ* experiments performed by ROV with *Echinus acutus* (Chapter 6) investigated the echinoid stress response to sedimentary burial associated with drilling disturbance. Using a molecular biomarker approach, the burial experiments were found to cause a significant stress response in *E. acutus*. An increase in the expression of an inducible member of the *stress-70* family of genes was found in specimens subject to multiple sedimentation events. Additional manipulation of *E. acutus* specimens indicated that recovery of the echinoids from the depth at which the experiments were performed (114 m) did not alter the expression of the *stress-70* gene. The *in situ* experiments demonstrated that ROV technology could be used successfully to collect and manipulate echinoids, and that stress caused by anthropogenic disturbance could be detected at the molecular level in the echinoids. The isolation of a *stress-70* fragment from the *E. acutus* species also demonstrated that the degenerate primers designed for application to the *P. miliaris* and *B. lyrifera* samples can be successfully applied to new species of echinoid.

The possible ecological relevance of the stress caused by the sediment burial was indicated by the significant reduction of the abundance of *E. acutus* after drilling in a 50 m zone around the central drilling site (Appendix 1.31). Whilst no direct correlation could be made between the elevation in gene expression following sedimentary burial and the reduction in *E. acutus* numbers following drilling disturbance, both demonstrate the detrimental impact anthropogenic disturbance has on benthic organisms and communities.

The application of biomarkers successfully used with shallow-water species to deep-sea organisms is restricted. With the adaptation of deep-sea organisms to the high pressure and low temperature found at depth, the effects of pressure and temperature change on biological systems during recovery to the surface make it exceedingly difficult to carry out sensitivity testing of species with a traditional bioassay (Carney, 2001). The effects of the surface retrieval process on proteins, physiological processes and the whole organism may not be distinguishable from those caused by the experimental treatment if the results are obtained once the specimen has been retrieved to the surface (Ravaux et al., 2007; Company et al., 2008; Vevers et al., 2010). The *in situ* experiments performed with *E. acutus* occurred at a depth that did not cause experimental artefacts related to decompression and temperature change. However, with 1000 m considered by some authors as a working limit for the successful retrieval of deep-sea organisms (Pradillon and Gaill, 2007), the collection of results from *in situ* bathyal and abyssal experiments should be isolated from the effects of surface recovery. To achieve this, tissues could instead be fixed or results obtained whilst the experimental specimens are still *in situ.* In this regard, the development of the *in situ* benthic incubation chamber system (BICS) represented the third experimental approach in this study.

***In situ* physiological measurements**

The application of *in situ* deep-sea experimental approaches and equipment is restricted by the accessibility of specimens present at depths below those accessible by humans. Technology such as remotely operated or human occupied vehicles (R/HOVs) is required to capture specific target specimens and to operate experiments *in situ* at the sea floor (Van Dover and Lutz, 2004). However, whilst making *in situ* experimentation possible, the use of R/HOVs within research cruise timetables is typically limited; deployment is weather dependent and dive time is shared with other researchers. Any *in situ* experimentation should therefore require minimal R/HOV time (Shillito et al., 2008) and involve simple tasks tailored to the basic dexterity of R/HOV manipulators (Gallucci et al., 2008). These requirements limit the possible complexity of *in situ* experimentation and the number of experimental replicates that can be obtained during any one dive.

The BICS2 respirometer is highly suitable for use during deep-sea research cruises because ROV time is required only for its initial operation (Chapter 7), and its operation is simple and designed for ROV manipulators. Once the target specimens have been collected and BICS2 activated, it can be left to operate autonomously. When required, the elevator it is attached to can be remotely triggered to return to the surface. With regard to the collection of biomarker results *in situ*, all data concerning the oxygen consumption rate of the deep-sea echinoderm specimens was successfully recorded at the sea floor - so avoiding the potential influence of decompression and/or temperature change on data obtained from the specimens had they been retrieved to the surface first. The data obtained with BICS2 represent the first *in situ* measurements of benthic echinoderm oxygen consumption rates for over 25 years. The results obtained, and the operation of BICS2, also demonstrate that it should be possible to perform contaminant exposures at depth (via the pre-programmed introduction of substances into the respirometry chamber when closed), and to monitor any subsequent variation in an organism's oxygen consumption rate *in situ*.

The comparison of the abyssal echinoderm oxygen consumption rates (a proxy for metabolic rates) obtained with BICS2 with those published from other deep-sea and shallow-water echinoderm species, indicated no decline in metabolic rate with depth. According to the visual interactions hypothesis (Childress and Mickel, 1985), this result was expected as echinoderms are a group of organisms that are not dependent on visual-locomotor interactions with prey or predators. Whilst this result appears to support the suitability of shallow-water echinoderms as proxies for deep-sea organisms, due to the similarity in physiological processes, the structural adaptations that will be present in the proteins and membranes of deep-sea echinoderms to maintain metabolic functioning mean that the effects of contaminants upon shallow-water and deep-sea species may be different. In addition, rates of toxic effect of contaminants may be different in the high pressure and cold temperature conditions of the deep sea. In this regard, the structural differences that must exist in deep-sea echinoderm metabolic enzymes to make possible levels of metabolic activity similar to those of shallow-water species require elucidation by further research, as undertaken to investigate the differences found in teleost fish (Somero, 1992; Somero, 2003).

8.2. qPCR as a biomarker and its application to *in situ* experimentation

Future quantification of gene expression

It has become evident that two new techniques will replace qPCR as the mRNA quantification method of choice for projects that can afford to do so. Next generation sequencing (NGS) technologies are becoming increasingly prevalent and can simultaneously detect thousands of mRNA transcripts including those in low-abundance (Asmann et al., 2008; Ozsolak et al., 2009; Bustin, 2010). Meanwhile, the use of microarray technology, a method which also makes possible

the simultaneous quantification of thousands of gene transcripts (Hofmann et al., 2005; Wilson et al., 2005), has gradually been expanding in echinoderm (and other marine organism) transcriptomics research. Most recently in echinoderm studies microarray technology has been applied to the investigation of the cellular mechanisms involved in the biomineralisation pathways of sea urchin larvae (Hofmann et al., 2008; Todgham and Hofmann, 2009; O'Donnell et al., 2010), revealing the altered expression of hundreds of genes in larvae cultured under reduced pH conditions.

Microarray data still require verification via qPCR analysis though, and qPCR is a more targeted approach for the investigation of a particular physiological pathway of interest (Hofmann et al., 2008). The relative accessibility of the qPCR technique to a researcher with access to a real time thermal cycler, means that small research projects will continue to use the qPCR assay for the foreseeable future. As such, the addition to the online databases of the complete transcript sequences isolated during this study (Chapter 2) for the *citrate synthase* (Accession numbers: FN677804 and FM865901) and *hsp70* (FN796462 and FN667017) genes from *P. miliaris* and *B. lyrifera*, the *P. miliaris* ubiquitin ribosomal protein L40 (FN796463) and the *stress-70* fragment (FM877470) from *E. acutus* will contribute to the future development of species-specific primers in other echinoderm qPCR based studies.

Irrespective of the method used to quantify mRNA levels, the underlying assumption which accompanies the identification of genes that are up- or down-regulated during experimental studies is that there is a direct relationship between transcript and protein levels (Gry et al., 2009; Nikinmaa and Schlenk, 2010). Numerous studies have assessed the correlation between the differential expression of specific mRNAs and corresponding proteins, resulting in the overall conclusion that whilst significant correlations exist they vary considerably, and in some cases suggest that mRNA abundance is a poor indicator of levels of the corresponding protein (Pradet-Balade et al., 2001; Gry et al., 2009).

The variations in correlation coefficients between different genes, organisms and methods of quantification indicate that typically less than 50% of the variation in protein levels can be explained by mRNA transcript changes. The remaining variation is explained by posttranscriptional and posttranslational regulation and measurement errors (Greenbaum et al., 2003; Abreu et al., 2009). In this regard, it has been argued that, unless the relationship between the mRNA and protein levels in an organism has been studied, the discussion of an organism's physiological status on the basis of transcript quantification is premature (Nikinmaa and Schlenk, 2010). The lack of a significant correlation between the citrate synthase enzyme activity and the

expression of the *citrate synthase* gene in *P. miliaris* found in this study demonstrates this point (Chapter 4).

One of the major challenges facing the field of comparative physiology today is the integration of the processes found across the different levels of biological organisation within an organism, and to align an organism's physiology with its transcriptome (Mykles et al., 2010). For example, whilst the determination of differences in the *stress-70* gene expression in *E. acutus* demonstrated a stress response to disturbance, it is not known how this response related to physiological changes at the level of the whole organism. If gene expression analysis is therefore to be applied to echinoderm research, in order to determine the physiological relevance of the results, a large-scale investigation of the mRNA/protein correlation in an echinoderm (most probably in *S. purpuratus*) is required.

qPCR and *in situ* deep-sea experimentation

As demonstrated in the *P. miliaris* and *E. acutus* experiments, quantifying gene expression provides a sensitive indication of an organism's stress response, and changes are found at this level of organization before physiological and behavioral stress responses. As such, the application of molecular biomarkers to *in situ* deep-sea experimentation is recommended, if they can be combined with accompanying assessments of an organism's physiological state.

Due to the near universal nature of the heat shock protein response to stressful conditions (Sanders, 1993; Gross, 2004), the expression levels of inducible hsps are typically considered a useful tool to indicate the detrimental action of stressful events upon an organism. However, marked differences have been found in the ability of toxicants to induce hsp expression, leading some authors to argue that hsp levels are not an unequivocal signature for the presence of pollutants (Gupta et al., 2010). The results of the *P. miliaris* and *B. lyrifera* experiments support this viewpoint, with WBSM exposure not causing a significant alteration in *hsp70* expression, whereas the *E. acutus in situ* disturbance experiments did cause a significant increase in the expression of an inducible hsp. With regard to future deep-sea experimentation, hsp levels should be considered a potential biomarker of a stress response, but will require validation for each experimental specimen targeted.

In addition to validating the selection of a specific gene as a biomarker of stress, it's possible induction by decompression and temperature change requires preventing, and the results of an *in situ* experimental manipulation isolating from the effects of surface recovery. If an organism's transcriptome could be fixed at depth these requirements could be met. The ability to stabilise and protect RNA from degradation already exists. Reagents such as RNA*later*® solution (Ambion,

2008), which inactivates RNases and stabilises RNA in tissue samples, could be used to preserve samples prior to surface recovery - provided that the organism's tissues can be disrupted and bathed in the preservation solution *in situ.* With the development of suitable equipment that could achieve this level of *in situ* sample processing, an organism's transcriptome could be preserved at depth.

8.3. Future deep-sea experimentation

The three approaches used in this study all demonstrated different routes to obtaining a greater understanding of the potential impact of anthropogenic activity on deep-sea organisms. The results of the biomarker assays applied to the two shallow-water echinoid species indicated that, as predicted, stenotopic echinoids (*B. lyrifera*) do not demonstrate a readily inducible stress response, in comparison to the eurytopic *P. miliaris*. The *P. miliaris* and *B. lyrifera* experiments also demonstrated that working with field-collected specimens can result in unwanted experimental artefacts caused by the collection process and maintenance in artificial aquaria. Whilst appropriate action can be taken to minimise such side effects, the performance of *in situ* experimentation, which avoids the removal of experimental animals from their habitat, has particular relevance for the investigation of anthropogenic impact in the deep sea.

The application of molecular biomarkers to assess the results of *in situ* experimentation has potential, although the development of equipment to allow an organism's transcriptome to be fixed at depth is required to remove any influence of recovery related artefacts upon experimental results. The demonstration of the relevance of altered gene expression to physiological changes at the whole organism level is also required. The combination of molecular approaches with the collection of physiological data, such as the measurement of oxygen consumption rates with equipment such as *in situ* respirometers, would make the investigation of such a link between different levels of biological organisation possible.

Going forward, the more accessible and cost-effective shallow-water approach to echinoderm experimentation cannot be replaced completely by expensive and logistically demanding deep-sea studies, and so shallow-water based studies are needed to improve our understanding of how echinoderms will response to anthropogenic impact. However, the results of shallow-water studies require validation before being confidently applied to deep-sea echinoderms. In this regard, deep-sea *in situ* experimentation is required, and the development of new experimental apparatus which confers the ability to perform experiments *in situ*, and to obtain results without interference from recovery-related side effects is necessary.

References

Aanderra Instruments AS, 2004. TD218 Operating Manual. Oxygen Optode 3830, 3930, 3975, 3835, 4130 and 4175., Bergen, Norway.

Aberle, N., Witte, U., 2003. Deep-sea macrofauna exposed to a simulated sedimentation event in the abyssal NE Atlantic: *in situ* pulse-chase experiments using 13C-labelled phytodetritus. Marine Ecology Progress Series 251, 37-47.

Abreu, R.D., Penalva, L.O., Marcotte, E.M., Vogel, C., 2009. Global signatures of protein and mRNA expression levels. Molecular Biosystems 5 (12), 1512-1526.

Al-Rasheid, K.A.S., Sleigh, M.A., 1995. Distribution and abundance of interstitial ciliates in southampton water in relation to physicochemical conditions, metal pollution and the availability of food organisms. Estuarine, Coastal and Shelf Science 41 (1), 61-80.

Alberts, B., Bray, D., Lewis, J., Raff, M., Roberts, K., Watson, J.D., 1994. Molecular Biology of the Cell. New York & London, Garland Publishing, Inc. pp. 1291.

Altschul, S.F., Madden, T.L., Schäffer, A.A., Zhang, J., Zhang, Z., Miller, W., Lipman, D.J., 1997. Gapped BLAST and PSI-BLAST: a new generation of protein database search programs. Nucleic Acids Research 25, 3389-3402.

Alwine, J.C., Kemp, D.J., Stark, G.R., 1977. Method for detection of specific RNAs in agarose gels by transfer to diazobenzyloxymethyl-paper and hybridization with DNA probes. Proceedings of the National Academy of Sciences of the United States of America 74 (12), 5350-5354.

Ambion, 2008. RNA*later*® Tissue Collection: RNA Stabilization Solution. RNA*later* Protocol bp_7020., Applied Biosystems, Ambion.

Amerik, A.Y., Hochstrasser, M., 2004. Mechanism and function of deubiquitinating enzymes. Biochimica et Biophysica Acta - Molecular Cell Research 1695 (1-3), 189-207.

Amon, R.M.W., 2010. Deepwater spill survey: contaminated Gulf kills thousands of sea cucumbers [Online]. Scientific American, 15 June 2010, Available: http://www.scientificamerican.com/blog/post.cfm?id=deepwater-spill-survey-contaminated-2010-06-15 [accessed 2010, June 20].

Angel, M., 1992. Managing biodiversity in the oceans. In: Peterson, M. (Ed.), diversity of oceanic life: an evaluative review. The Center for Strategic and International Studies, Washington, DC, USA, pp. 23-62.

Angel, M.V., Rice, T.L., 1996. The ecology of the deep ocean and its relevance to global waste management. Journal of Applied Ecology 33 (5), 915-926.

Aranda, M.A., Escaler, M., Wang, D., Maule, A.J., 1996. Induction of HSP70 and polyubiquitin expression associated with plant virus replication. Proceedings of the National Academy of Sciences of the United States of America 93 (26), 15289-15293.

Arima, S., Marchand, M., Martin, J.-L.M., 1979. Pollutants in deep-sea organisms and sediments. Ambio Special Report, No. 6, The Deep Sea: Ecology and Exploitation, 97-100.

Arndt, V., Rogon, C., Höhfeld, J., 2007. To be, or not to be - molecular chaperones in protein degradation. Cellular and Molecular Life Sciences 64 (19-20), 2525-2541.

Arneborg, L., 2004. Turnover times for the water above sill level in Gullmar Fjord. Continental Shelf Research 24 (4-5), 443-460.

Arukwe, A., 2006. Toxicological housekeeping genes: do they really keep the house? Environmental Science and Technology 40, 7944-7949.

Arya, R., Arid, M.M., Lakhotia, S.C., 2007. Heat shock genes - integrating cell survival and death. Journal of biosciences 32 (3), 595-610.

Arzola, R.G., Wynn, R.B., Lastras, G., Masson, D.G., Weaver, P.P.E., 2008. Sedimentary features and

processes in submarine canyons: a case study from the Nazaré and Setúbal Canyons, west Iberian margin. Marine Geology 250, 64-88.

Asmann, Y.W., Wallace, M.B., Thompson, E.A., 2008. Transcriptome profiling using next generation sequencing. Gastroenterology 135 (5), 1466-1468.

Aspetsberger, F., Zabel, M., Ferdelman, T., Struck, U., Mackensen, A., Ahke, A., Witte, U., 2007. Instantaneous benthic response to different organic matter quality: in situ experiments in the Benguela upwelling system. Marine Biology Research 3 (5), 342 - 356.

ASTM, 2004a. Standard guide for determination of the bioaccumulation of sediment-associated contaminants by benthic invertebrates. Annual book of ASTM standards: Water and Environmental Technology. ASTM International, West Conshohocken, PA, USA, pp. 1077-1131.

ASTM, 2004b. Standard guide for conducting static acute toxicity tests with echinoid embryos. Annual book of ASTM standards: Water and Environmental Technology. ASTM International, West Conshohocken, PA, USA, pp. 957-978.

Attardi, G., Schatz, G., 1988. Biogenesis of mitochondria. Annual Review of Cell Biology 4, 289-333.

Austen, M.C., Widdicombe, S., 1998. Experimental evidence of effects of the heart urchin *Brissopsis lyrifera* on associated subtidal meiobenthic nematode communities. Journal of Experimental Marine Biology and Ecology 222 (1-2), 219-238.

Avison, M.B., 2007. PCR-based methods for measuring transcript levels. Measuring Gene Expression. Taylor & Francis Group, Abingdon, pp. 167-216.

Axiak, V., Saliba, L.J., 1981. Effects of surface and sunken crude oil on the behaviour of a sea urchin. Marine Pollution Bulletin 12 (1), 14-19.

Bachmayer, R., Humphris, S., Fornari, D., Dover, C.V., Howland, J., Bowen, A., Elder, R., Crook, T., Gleason, D., Sellers, W., et al., 1998. Oceanographic research using remotely operated underwater robotic vehicles: exploration of hydrothermal vent sites on the Mid-Atlantic Ridge at 37°North 32°West. Marine Technology Society Journal 32 (3), 37-47.

Badyaev, A.V., 2005. Stress-induced variation in evolution: from behavioural plasticity to genetic assimilation. Proceedings of the Royal Society B-Biological Sciences 272 (1566), 877-886.

Bailey, D.M., Bagley, P.M., Jamieson, A.J., Collins, M.A., Priede, I.G., 2003. In situ investigation of burst swimming and muscle performance in the deep-sea fish *Antimora rostrata* (Günther, 1878). Journal of Experimental Marine Biology and Ecology 285-286, 295-311.

Bailey, D.M., Bagley, P.M., Jamieson, A.J., Cromarty, A., Collins, M.A., Tselepidis, A., Priede, I.G., 2005a. Life in a warm deep sea: routine activity and burst swimming performance of the shrimp *Acanthephyra eximia* in the abyssal Mediterranean. Marine Biology 146, 1199–1206.

Bailey, D.M., Genard, B., Collins, M.A., Rees, J.-F., Unsworth, S.K., Battle, E.J.V., Bagley, P.M., Jamieson, A.J., Priede, I.G., 2005b. High swimming and metabolic activity in the deep-sea eel *Synaphobranchus kaupii* revealed by integrated in situ and in vitro measurements. Physiological and Biochemical Zoology 78 (3), 335-346.

Bailey, D.M., Jamieson, A.J., Bagley, P.M., Collins, M.A., Priede, I.G., 2002. Measurement of in situ oxygen consumption of deep-sea fish using an autonomous lander vehicle. Deep-Sea Research Part I: Oceanographic Research Papers 49, 1519–1529.

Bailey, T.G., Torres, J.J., Youngbluth, M.J., Owen, G.P., 1994. Effect of decompression on mesopelagic gelatinous zooplankton - a comparison of in-situ and shipboard measurements of metabolism. Marine Ecology-Progress Series 113 (1-2), 13-27.

Bailey, T.G., Youngbluth, M.J., Owen, G.P., 1995. Chemical composition and metabolic rates of gelatinous zooplankton from midwater and benthic boundary layer environments off Cape Hatteras, North Carolina, USA. Marine Ecology Progress Series 122, 121-134.

Baldwin, D., Crane, V., Rice, D., 1999. A comparison of gel-based, nylon filter and microarray techniques

to detect differential RNA expression in plants. Current Opinion in Plant Biology 2 (2), 96-103.

Barbaglio, A., Mozzi, D., Sugni, M., Tremolada, P., Bonasoro, F., Lavado, R., Porte, C., Carnevali, M., 2006. Effects of exposure to ED contaminants on crinoid echinoderms: comparative analysis of regenerative development and correlated steroid levels. Marine Biology 149, 65-77.

Barber, R.T., Warlen, S.M., 1979. Organochlorine insecticide residues in deep sea fish from 2500 m in the Atlantic Ocean. Environmental Science & Technology 13 (9), 1146-1148.

Barchetta, S., La Terza, A., Ballarini, P., Pucciarelli, S., Miceli, C., 2008. Combination of two regulatory elements in the *Tetrahymena thermophila* HSP70-1 gene controls heat shock activation. Eukaryotic Cell 7 (2), 379-386.

Barille-Boyer, A.L., Gruet, Y., Barille, A., Harin, N., 2004. Temporal changes in community structure of tide pools following the "Erika" oil spill. Aquatic Living Resources 17 (3), 323-328.

Barry, J., Buck, K., Lovera, C., Kuhnz, L., Whaling, P., Peltzer, E., Walz, P., Brewer, P., 2004. Effects of direct ocean CO_2 injection on deep-sea meiofauna. Journal of Oceanography 60 (4), 759-766.

Bay, S., Burgess, R., Nacci, D., 1993. Status and applications of Echinoid (phylum Echinodermata) toxicity test methods. In: Landis, W.G., Hughes, J.S., Lewis, M.A. (Eds.), Environmental toxicology and risk assessment. ASTM, Philapdelphia, USA, pp. 281-302.

Bayne, B.L., Brown, D.A., Burns, K., Dixon, D.R., Ivanovici, A., Livingstone, D.R., Lowe, D.M., Moore, M.N., Stebbing, A.R.D., Widdows, J., 1985. The effects of stress and pollution on marine animals. Praeger Publishers, New York.

Beaudoing, E., Freier, S., Wyatt, J.R., Claverie, J.-M., Gautheret, D., 2000. Patterns of variant polyadenylation signal usage in human genes. Genome Research 10 (7), 1001-1010.

Bedford, A.P., Moore, P.G., 1985. Macrofaunal involvement in the sublittoral decay of kelp debris: the sea urchin *Psammechinus miliaris* (Gmelin) (Echinodermata: Echinoidea). Estuarine, Coastal and Shelf Science 20 (1), 19-40.

Bedulina, D.S., Zimmer, M., Timofeyev, M.A., 2010. Sub-littoral and supra-littoral amphipods respond differently to acute thermal stress. Comparative Biochemistry and Physiology Part B: Biochemistry and Molecular Biology 155 (4), 413-418.

Békri, K., Pelletier, E., 2004. Trophic transfer and in vivo immunotoxicological effects of tributyltin (TBT) in polar seastar *Leptasterias polaris*. Aquatic Toxicology 66 (1), 39-53.

Beliaev, G.M., 1989. Deep Sea Ocean Trenches and their Fauna. Translated by Mira Beerbaum 2004. originally published: Nauka Publishing House, Moscow, accessed from Scripps Institution of Oceanography Library, San Diego.

Bellin, D., Ferrarini, A., Chimento, A., Kaiser, O., Levenkova, N., Bouffard, P., Delledonne, M., 2009. Combining next-generation pyrosequencing with microarray for large scale expression analysis in non-model species. BMC Genomics 10 (1), 555.

Bierkens, J., 2000. Applications and pitfalls of stress-proteins in biomonitoring. Toxicology 153, 61-72.

Billett, D.S.M., 1991. Deep-sea holothurians. Oceanography and marine biology: an annual review 29, 259-317.

Billett, D.S.M., Bett, B.J., Rice, A.L., Thurston, M.H., Galeron, J., Sibuet, M., Wolff, G.A., 2001. Long-term change in the megabenthos of the Porcupine Abyssal Plain (NE Atlantic). Progress in Oceanography 50, 325-348.

Bird, L.E., Drazen, J.C., Barry, J.P., 2004. 4,000 meter hyperbaric fish trap aquaria respirometer. Ocean '04 - MTS/IEEE Techno-Ocean '04: Bridges across the Oceans - Conference Proceedings, pp. 972-976.

Bluhm, H., 1999. Holothurians as indicators for recolonisation processes in environmental assessment. In: Chung, J.S., Sharma, R. (Eds.), The proceedings of the third (1999) ISOPE ocean mining symposium: deep-ocean mining, exploration and survey, environment, mining systems and technology, and

processing., NIO, Goa, India, pp. 177-184.

Bluhm, H., 2001. Re-establishment of an abyssal megabenthic community after experimental physical disturbance of the seafloor. Deep-Sea Research Part II: Topical Studies in Oceanography 48, 3841-3868.

BODC, 2009. British Oceanographic Data Centre, http://www.bodc.ac.uk/. http://www.bodc.ac.uk/.

Boehm, P., Turton, D., Raval, A., Caudle, D., French, D., Rabalais, N., Spies, R., Johnson, J., 2001. Deepwater program: literature review, environmental risks of chemical products used in gulf of mexico deepwater oil and gas operations. Volume I: Technical Report. OCS Study MMS 2001-011. U.S. Department of the Interior, Minerals Management Service, GOM OCS Region, New Orleans, LA. 326 pp.

Bond, U., Agell, N., Haas, A.L., Redman, K., Schlesinger, M.J., 1988. Ubiquitin in stressed chicken-embryo fibroblasts. Journal of Biological Chemistry 263 (5), 2384-2388.

Bond, U., Schlesinger, M.J., 1985. Ubiquitin is a heat shock protein in chicken embryo fibroblasts. Molecular and Cellular Biology 5 (5), 949-956.

Boorstein, W.R., Ziegelhoffer, T., Craig, E.A., 1994. Molecular evolution of the HSP70 multigene family. Journal of Molecular Evolution 38 (1), 1-17.

Borghi, V., Porte, C., 2002. Organotin pollution in deep-sea fish from the Northwestern Mediterranean. Environmental Science and Technology 36 (20), 4224-4228.

Borowski, C., 2001. Physically disturbed deep-sea macrofauna in the Peru Basin, southeast Pacific, revisited 7 years after the experimental impact. Deep-Sea Research Part II: Topical Studies in Oceanography 48 (17-18), 3809-3839.

Böttger, S.A., McClintock, J.B., Klinger, T.S., 2001. Effects of inorganic and organic phosphates on feeding, feeding absorption, nutrient allocation, growth and righting responses of the sea urchin *Lytechinus variegatus*. Marine Biology 138, 741-751.

Bouloubassi, I., Méjanelle, L., Pete, R., Fillaux, J., Lorre, A., Point, V., 2006. PAH transport by sinking particles in the open Mediterranean Sea: a 1 year sediment trap study. Marine Pollution Bulletin 52 (5), 560-571.

Boutet, I., Jollivet, D., Shillito, B., Moraga, D., Tanguy, A., 2009. Molecular identification of differentially regulated genes in the hydrothermal-vent species *Bathymodiolus thermophilus* and *Paralvinella pandorae* in response to temperature. BMC Genomics 10 (222).

Boutet, I., Tanguy, A., Auffret, M., Mujdzic, N., Moraga, D., 2003. Expression of Hsp70 in experimentally metal-exposed European flat oysters *Ostrea edulis*. Journal of Shellfish Research 22 (3), 763-766.

Boutet, I., Tanguy, A., Moraga, D., 2004. Response of the Pacific oyster *Crassostrea gigas* to hydrocarbon contamination under experimental conditions. Gene 329 (1-2), 147-157.

Brandt, W., Dang, A., Magne, E., Crowley, D., Houston, K., Rennie, A., Hodder, M., Stringer, R., Juiniti, R., Ohara, S., et al., 1998. Deepening the search for offshore hydrocarbons. Oilfield Review 10 (1), 2-21.

Brattström, H., 1946. Observations on *Brissopsis lyrifera* (Forbes) in the Gullmar Fjord. Arkiv För Zoologi 37A (18), 1-27.

Brauer, R.W. (Ed.), 1972. Barobiology and the Experimental Biology of the Deep Sea. North Carolina Sea Grant Program, Chapel Hill, N.C., USA. pp 428.

Brenner, S., Johnson, M., Bridgham, J., Golda, G., Lloyd, D.H., Johnson, D., Luo, S., McCurdy, S., Foy, M., Ewan, M., et al., 2000. Gene expression analysis by massively parallel signature sequencing (MPSS) on microbead arrays. Nature Biotechnology 18 (6), 630-634.

Bresler, V., Mokady, O., Fishelson, L., Feldstein, T., Abelson, A., 2003. Marine molluscs in environmental monitoring II. Experimental exposure to selected pollutants. Helgoland marine research 57 (3), 206-211.

Brett, J.R., 1958. Implications and assessments of environmental stress. In: Larkin, P.A. (Ed.), The

Investigation of Fish-power Problems. University of BC, Institute of Fisheries, pp. 69-93.

Breuer, E., Stevenson, A.G., Howe, J.A., Carroll, J., Shimmield, G.B., 2004. Drill cutting accumulations in the Northern and Central North Sea: a review of environmental interactions and chemical fate. Marine Pollution Bulletin 48 (1-2), 12-25.

Brindley, A.A., Pickersgill, R.W., Partridge, J.C., Dunstan, D.J., Hunt, D.M., Warren, M.J., 2008. Enzyme sequence and its relationship to hyperbaric stability of artificial and natural fish lactate dehydrogenases. Plos One 3 (4), e2042. doi:2010.1371/journal.pone.0002042.

Broemer, M., Meier, P., 2009. Ubiquitin-mediated regulation of apoptosis. Trends in Cell Biology 19 (3), 130-140.

Brown, D.M., 1975. Four biological samplers: opening-closing midwater trawl, closing vertical tow net, pressure fish trap, free vehicle drop camera. Deep Sea Research & Oceanographic Abstracts 22, 565-567.

Buckley, B.A., 2007. Comparative environmental genomics in non-model species: using heterologous hybridization to DNA-based microarrays. Journal of Experimental Biology 210 (9), 1602-1606.

Budd, G., 2004. *Brissopsis lyrifera*. A heart urchin. Marine Life Information Network: Biology and Sensitivity Key Information Sub-programme [Online]. Plymouth: Marine Biological Association of the United Kingdom. Available: http://www.marlin.ac.uk/speciesfullreview.php?speciesID=2801 [accessed 2010, May 25].

Burggren, W., Roberts, J., 1991. Respiration and metabolism. In: Prosser, C.L. (Ed.), Environmental and Metabolic Animal Physiology. Wiley-Liss, Inc., New York, pp. 353-435.

Bustin, S., 2008. Essential considerations for generating reliable RT–qPCR data. Bio-Rad Laboratories Seminar: Rethink the Way You do Real-Time PCR, London, UK.

Bustin, S.A., 2000. Absolute quantification of mRNA using real-time reverse transcription polymerase chain reaction assays. Journal of Molecular Endocrinology 25 (2), 169-193.

Bustin, S.A., 2002. Quantification of mRNA using real-time reverse transcription PCR (RT-PCR): trends and problems. Journal of Molecular Endocrinology 29 (1), 23-39.

Bustin, S.A., 2004. Quantification of Nucleic Acids by PCR. In: Bustin, S.A. (Ed.), A-Z of Quantitative PCR. International University Line, La Jolla, CA, pp. 3-46.

Bustin, S.A., 2010. Why the need for qPCR publication guidelines? The case for MIQE. Methods 50 (4), 217-226.

Bustin, S.A., Benes, V., Garson, J.A., Hellemans, J., Huggett, J., Kubista, M., Mueller, R., Nolan, T., Pfaffl, M.W., Shipley, G.L., et al., 2009. The MIQE guidelines: Minimum Information for Publication of Quantitative Real-Time PCR Experiments. Clinical Chemistry 55 (4), 611-622.

Bustin, S.A., Benes, V., Nolan, T., Pfaffl, M.W., 2005. Quantitative real-time RT-PCR - a perspective. Journal of Molecular Endocrinology 34 (3), 597-601.

Bustin, S.A., Nolan, T., 2004a. Chemistries. In: Bustin, S.A. (Ed.), A-Z of Quantitative PCR. International University Line, La Jolla, CA, pp. 271-278.

Bustin, S.A., Nolan, T., 2004b. Data Analysis and Interpretation. In: Bustin, S.A. (Ed.), A-Z of Quantitative PCR. International University Line, La Jolla, CA, pp. 439-492.

Bustin, S.A., Nolan, T., 2004c. Pitfalls of quantitative real-time reverse-transcription polymerase chain reaction. Journal of Biomolecular Techniques 15 (3), 155-166.

Caldwell, G.S., Bentley, M.G., Olive, P.J.W., 2004. First evidence of sperm motility inhibition by the diatom aldehyde 2E,4E-decadienal. Marine Ecology-Progress Series 273, 97-108.

Calow, P., 1994. Handbook of Ecotoxicology. Blackwell Science, Oxford.

Calzolai, L., Ansorge, W., Calabrese, E., Denslow, N., Part, P., Lettieri, T., 2007. Transcriptomics and proteomics. Applications to ecotoxicology. Comparative Biochemistry and Physiology - Part D: Genomics

and Proteomics 2 (3), 245-249.

Campbell, D.A., Pantazis, P., Kelly, M.S., 2001. Impact and residence time of oxytetracycline in the sea urchin, *Psammechinus miliaris*, a potential aquaculture species. Aquaculture 202 (1-2), 73-87.

Camus, L., Gulliksen, B., 2005. Antioxidant defence properties of Arctic amphipods: comparison between deep-, sublittoral and surface-water species. Marine Biology 146 (2), 355-362.

Canty, M.N., Hutchinson, T.H., Brown, R.J., Jones, M.B., Jha, A.N., 2009. Linking genotoxic responses with cytotoxic and behavioural or physiological consequences: differential sensitivity of echinoderms (*Asterias rubens*) and marine molluscs (*Mytilus edulis*). Aquatic Toxicology 94 (1), 68-76.

Carney, R.S., 1997. Basing conservation policies for the deep-sea floor on current-diversity concepts: a consideration of rarity. Biodiversity and Conservation 6 (11), 1463-1485.

Carney, R.S. (Ed.), 1998. Workshop on environmental issues surrounding deepwater oil and gas development. Final Report. OCS Study MMS 98-0022. U.S. Dept. of the Interior, Minerals Management Service, Gulf of Mexico OCS Region. New Orleans, LA., 163 pp.

Carney, R.S., 2001. Management applicability of contemporary deep-sea ecology and reevaluation of Gulf of Mexico studies. Final Report. OCS Study MMS2001-095. U.S. Department of the Interior Minerals Management Service, Gulf of Mexico OCS Region Office, New Orleans, LA. 174 pp.

Castilho, P.C., Buckley, B.A., Somero, G., Block, B.A., 2009. Heterologous hybridization to a complementary DNA microarray reveals the effect of thermal acclimation in the endothermic bluefin tuna (*Thunnus orientalis*). Molecular Ecology 18 (10), 2092-2102.

Catic, A., Ploegh, H.L., 2005. Ubiquitin - conserved protein or selfish gene? Trends in Biochemical Sciences 30 (11), 600-604.

Catic, A., Sun, Z.Y.J., Ratner, D.M., Misaghi, S., Spooner, E., Samuelson, J., Wagner, G., Ploegh, H.L., 2007. Sequence and structure evolved separately in a ribosomal ubiquitin variant. The European Molecular Biology Organisation Journal 26 (14), 3474-3483.

Cech, J.J., 1990. Respirometry. In: Schreck, C.B., Moyle, P.B. (Eds.), Methods for Fish Biology. American Fisheries Society, Bethesda, MA, pp. 335-362.

Chandrasekara, W.U., Frid, C.L.J., 1998. A laboratory assessment of the survival and vertical movement of two epibenthic gastropod species, *Hydrobia ulvae* (Pennant) and *Littorina littorea* (Linnaeus), after burial in sediment. Journal of Experimental Marine Biology and Ecology 221 (2), 191-207.

Chapman, P.M., Riddle, M.J., 2003. Missing and needed: polar marine ecotoxicology. Marine Pollution Bulletin 46 (8), 927-928.

Chapman, P.M., Riddle, M.J., 2005. Toxic effects of contaminants in polar marine environments. Environmental Science and Technology 39 (9), 201A-207A.

Cheng, P., Liu, X., Zhang, G., He, J., 2007. Cloning and expression analysis of a HSP70 gene from Pacific abalone (*Haliotis discus hannai*). Fish and Shellfish Immunology 22, 77-87.

Cheng, S.H., So, C.H., Chan, P.K., Cheng, C.W., Wu, R.S.S., 2003. Cloning of the HSP70 gene in barnacle larvae and its expression under hypoxic conditions. Marine Pollution Bulletin 46 (5), 665-671.

Chevron Inc, 2010. Chevron deploys a second ultra-deepwater drillship [Online]. Press release, March 11, 2010. http://www.chevron.com/news/press/release/?id=2010-03-11 [accessed 2010, May 12].

Chia, F.-S., Xing, J., 1996. Echinoderm coelomocytes. Zoological Studies 35 (4), 231-254.

Childress, J.J., 1995. Are there physiological and biochemical adaptations of metabolism in deep-sea animals? Trends in Ecology and Evolution 10 (1), 30-36.

Childress, J.J., Barnes, A.T., Quetin, L.B., Robison, B.H., 1978. Thermally protecting cod ends for the recovery of living deep-sea animals. Deep-Sea Research 25 (4), 419-420.

Childress, J.J., Cowles, D.L., Favuzzi, J.A., Mickel, T.J., 1990. Metabolic rates of benthic deep-sea

decapod crustaceans decline with increasing depth primarily due to the decline in temperature. Deep-Sea Research 37 (6), 929-949.

Childress, J.J., Mickel, T.J., 1985. Metabolic rates of animals from the hydrothermal vents and other deep-sea habitats. Bulletin of the Biological Society of Washington 6, 249-260.

Childress, J.J., Somero, G.N., 1979. Depth-related enzymic activities in muscle, brain and heart of deep-living pelagic marine teleosts. Marine Biology 52, 273-283.

Chomczynski, P., 1993. A reagent for the single-step simultaneous isolation of RNA, DNA and proteins from cell and tissue samples. BioTechniques 15 (3), 532-534, 536-537.

Christensen, A., Colacino, J., 2000. Respiration in the burrowing brittlestar, *Hemipholis elongata* Say (Echinodermata, Ophiuroidea): a study of the effects of environmental variables on oxygen uptake. Comparative Biochemistry and Physiology Part A: Molecular and Integrative Physiology 127, 201-213.

Chuaqui, R.F., Bonner, R.F., Best, C.J.M., Gillespie, J.W., Flaig, M.J., Hewitt, S.M., Phillips, J.L., Krizman, D.B., Tangrea, M.A., Ahram, M., et al., 2002. Post-analysis follow-up and validation of microarray experiments. Nature Genetics 32, 509 - 514.

Ciechanover, A., 1998. The ubiquitin–proteasome pathway: on protein death and cell life. The European Molecular Biology Organisation Journal 17, 7151–7160.

Ciechanover, A., Orian, A., Schwartz, A.L., 2000. Ubiquitin-mediated proteolysis: biological regulation via destruction. Bioessays 22 (5), 442-451.

Clark, A.M., Downey, M.E., 1992. Starfishes of the Atlantic. Chapman & Hall, London.

Clark, M.S., Peck, L.S., 2009. HSP70 heat shock proteins and environmental stress in Antarctic marine organisms: a mini-review. Marine Genomics 2 (1), 11-18.

Clark, R.B., 1992. Marine Pollution. Oxford University Press., Oxford, UK. pp 172.

Clark, T., Lee, S., Scott, L.R., Wang, S.M., 2002. Computational analysis of gene identification with SAGE. Journal of Computational Biology 9 (3), 513-526.

Cochonat, P., Dürr, S., Gunn, V., Herzig, P., Mevel, C., Mienert, J., Schneider, R., Weaver, P., Winkler, A., 2007. The deep-sea frontier: science challenges for a sustainable future. Office for Official Publications of the European Communities, Luxembourg, 53 pp.

Cohen, A., Gagnon, M.M., Nugegoda, D., 2005. Alterations of metabolic enzymes in Australian bass, *Macquaria novemaculeata*, after exposure to petroleum hydrocarbons. Archives of Environmental Contamination and Toxicology 49 (2), 200-205.

Collén, J., Guisle-Marsollier, I., Léger, J., Boyen, C., 2007. Response of the transcriptome of the intertidal red seaweed *Chondrus crispus* to controlled and natural stresses. New Phytologist 176 (1), 45-55.

Combet, C., Blanchet, C., Geourjon, C., Deléage, G., 2000. NPS@: Network protein sequence analysis. Trends in Biochemical Sciences 25 (3), 147-150.

Company, R., Serafim, A., Cosson, R.P., Fiala-Médioni, A., Camus, L., Colaço, A., Serrão-Santos, R., Bebianno, M.J., 2008. Antioxidant biochemical responses to long-term copper exposure in *Bathymodiolus azoricus* from Menez-Gwen hydrothermal vent. Science of the Total Environment 389 (2-3), 407-417.

Compton, J., 1991. Nucleic acid sequence-based amplification. Nature 350 (6313), 91-92.

Continental Shelf Associates Inc., 2006. Effects of oil and gas exploration and development at selected continental slope sites in the Gulf of Mexico, Volume II: Technical report. U.S. Department of the Interior. Minerals Management Service, Gulf of Mexico OCS Region, New Orleans, LA. OCS Study MMS 2006-045. 636 pp.

Cools, I., Uyttendaele, M., D'Haese, E., Nelis, H.J., Debevere, J., 2006. Development of a real-time NASBA assay for the detection of *Campylobacter jejuni* cells. Journal of Microbiological Methods 66 (2), 313-320.

Copeland, R.A., 2000. Enzymes: A Practical Introduction to Structure, Mechanism, and Data Analysis. Wiley-VCH, New York. pp. 397.

Coteur, G., Danis, B., Wantier, P., Pernet, P., Dubois, P., 2005a. Increased phagocytic activity in contaminated seastars (*Asterias rubens*) collected in the Southern Bight of the North Sea. Marine Pollution Bulletin 50 (11), 1295-1302.

Coteur, G., DeBecker, G., Warnau, M., Jangoux, M., Dubois, P., 2002. Differentiation of immune cells challenged by bacteria in the common European starfish, *Asterias rubens* (Echinoderma). European Journal of Cell Biology 81 (7), 413-418.

Coteur, G., Gillan, D., Pernet, P., Dubois, P., 2005b. Alteration of cellular immune responses in the seastar *Asterias rubens* following dietary exposure to cadmium. Aquatic Toxicology 73 (4), 418-421.

Coteur, G., Gosselin, P., Wantier, P., Chambost-Manciet, Y., Danis, B., Pernet, P., Warnau, M., Dubois, P., 2003. Echinoderms as bioindicators, bioassays, and impact assessment tools of sediment-associated metals and PCBs in the North Sea. Archives of Environmental Contamination & Toxicology 45, 190-202.

Cottin, D., Ravaux, J., Leger, N., Halary, S., Toullec, J.-Y., Sarradin, P.-M., Gaill, F., Shillito, B., 2008. Thermal biology of the deep-sea vent annelid *Paralvinella grasslei*: in vivo studies. Journal of Experimental Biology 211 (14), 2196-2204.

Coulon, P., Jangoux, M., 1987. Gregarine species (Apicomplexa) parasitic in the burrowing echinoid *Echinocardium cordatum* - occurrence and host-reaction. Diseases of Aquatic Organisms 2 (2), 135-145.

Couture, P., Rajotte, J., Pyle, G., 2008. Seasonal and regional variations in metal contamination and condition indicators in yellow perch (*Perca flavescens*) along two polymetallic gradients. III. Energetic and physiological indicators. Human and Ecological Risk Assessment 14 (1), 146-165.

Coux, O., Tanaka, K., Goldberg, A.L., 1996. Structure and functions of the 20S and 26S proteasomes. Annual Review of Biochemistry 65, 801-847.

Cowles, D.L., Childress, J.J., 1995. Aerobic metabolism of the anglerfish *Melanocetus johnsoni*, a deep-pelagic marine sit-and-weight predator. Deep-Sea Research Part I: Oceanographic Research Papers 42 (9), 1631-1638.

Cowles, D.L., Childress, J.J., Wells, M.E., 1991. Metabolic rates of midwater crustaceans as a function of depth of occurrence off the Hawaiian Islands: food availability as a selective factor? Marine Biology 110, 75-83.

Cranenburgh, R.M., 2004. An equation for calculating the volumetric ratios required in a ligation reaction. Applied Microbiology and Biotechnology 65 (2), 200-202.

Cranford, P.J., Gordon Jr., D.C., Armsworthy, S.L., Lee, K., Tremblay, G.-H., 1999. Chronic toxicity and physical disturbance effects of water- and oil-based drilling fluids and some major constituents on adult sea scallops (*Placopecten magellanicus*). Marine Environmental Research 48 (3), 225-256.

Cranmer, G.J., 1985. Recent investigations into the distribution of regular echinoids in the North Sea. Journal of the Marine Biological Association of the UK 65 (02), 351-357.

Cullen, M., Kaufmann, R.S., Lowery, M.S., 2003. Seasonal variation in biochemical indicators of physiological status in *Euphausia superba* from Port Foster, Deception Island, Antarctica. Deep-Sea Research Part II: Topical Studies in Oceanography 50 (10-11), 1787-1798.

Cunha, I., García, L.M., Guilhermino, L., 2005. Sea-urchin (*Paracentrotus lividus*) glutathione S-transferases and cholinesterase activities as biomarkers of environmental contamination. Journal of Environmental Monitoring 7 (4), 288-294.

Daan, R., Mulder, M., 1996. On the short-term and long-term impact of drilling activities in the Dutch sector of the North Sea. ICES Journal of Marine Science 53 (6), 1036-1044.

Dahlhoff, E.P., 2004. Biochemical indicators of stress and metabolism: applications for marine ecological studies. Annual Review of Physiology 66, 183-207.

Dahlhoff, E.P., Menge, B.A., 1996. Influence of phytoplankton concentration and wave exposure on the ecophysiology of *Mytilus californianus*. Marine Ecology Progress Series 144 (1-3), 97-107.

Dahlmann, B., 2005. Proteasomes. Essays in Biochemistry 41, 31-48.

Daidone, I., Roccatano, D., Hayward, S., 2004. Investigating the accessibility of the closed domain conformation of citrate synthase using essential dynamics sampling. Journal of Molecular Biology 339 (3), 515-525.

Dalmazzone, C., Blanchet, D., Lamoureux, S., Dutrieux, E., Durrieu, J., Camps, R., Galgani, F., 2004. Impact of drilling activities in warm sea: recolonization capacities of seabed. Oil and Gas Science and Technology 59 (6), 625-647.

Dalziel, A.C., Rogers, S.M., Schulte, P.M., 2009. Linking genotypes to phenotypes and fitness: how mechanistic biology can inform molecular ecology. Molecular Ecology 18 (24), 4997-5017.

Daniel, M.J., Boyden, C.R., 1975. Diurnal variations in physico-chemical conditions within intertidal rockpools. Field Studies 4, 161-176.

Danis, B., Cotret, O., Teyssie, J., Fowler, S., Warnau, M., 2004. Coplanar PCB 77 uptake kinetics in the sea star *Asterias rubens* and subsequent effects on reactive oxygen species (ROS) production and levels of cytochrome P450 immunopositive proteins (CYP1A-IPP). Marine Ecology Progress Series 279, 117-128.

Danis, B., Wantier, P., Flammang, R., Pernet, P., Chambost-Manciet, Y., Coteur, G., Warnau, M., Dubois, P., 2006. Bioaccumulation and effects of PCBs and heavy metals in sea stars (*Asterias rubens*, L.) from the North Sea: a small scale perspective. Science of the Total Environment 356 (1-3), 275-289.

Daugaard, M., Rohde, M., Jäättelä, M., 2007. The heat shock protein 70 family: highly homologous proteins with overlapping and distinct functions. Federation of European Biochemical Societies Letters 581 (19), 3702-3710.

Davies, A.J., Roberts, J.M., Hall-Spencer, J., 2007. Preserving deep-sea natural heritage: emerging issues in offshore conservation and management. Biological Conservation 138 (3-4), 299-312.

Davies, I.M., Gillibrand, P.A., McHenery, J.G., Rae, G.H., 1998. Environmental risk of ivermectin to sediment dwelling organisms. Aquaculture 163 (1-2), 29-46.

Davies, J., 1998. Western Channel (Durlston Head to Cape Cornwall, including the Isles of Scilly) (MNCR Sector 8). In: Hiscock, K. (Ed.), Marine Nature Conservation Review. Benthic marine ecosystems of Great Britain and the north-east Atlantic. Peterborough, Joint Nature Conservation Committee (Coasts and seas of the United Kingdom. MNCR series), pp. 219-253.

De Brito, A.P.X., Takahashi, S., Ueno, D., Iwata, H., Tanabe, S., Kubodera, T., 2002. Organochlorine and butyltin residues in deep-sea organisms collected from the western North Pacific, off-Tohoku, Japan. Marine Pollution Bulletin 45 (1-12), 348-361.

de Faria, M.T., da Silva, J.R.M.C., 2008. Innate immune response in the sea urchin *Echinometra lucunter* (Echinodermata). Journal of Invertebrate Pathology 98 (1), 58-62.

Deane, E.E., Woo, N.Y.S., 2005. Cloning and characterization of the hsp70 multigene family from silver sea bream: modulated gene expression between warm and cold temperature acclimation. Biochemical and Biophysical Research Communications 330 (3), 776-783.

Delaney, M.A., Klesius, P.H., 2004. Hypoxic conditions induce Hsp70 production in blood, brain and head kidney of juvenile Nile tilapia *Oreochromis niloticus* (L.). Aquaculture 236 (1-4), 633-644.

Den Besten, P.J., Valk, S., Van Weerlee, E., Nolting, R.F., Postma, J.F., Everaarts, J.M., 2001. Bioaccumulation and biomarkers in the sea star *Asterias rubens* (Echinodermata: Asteroidea): a North Sea field study. Marine Environmental Research 51 (4), 365-387.

Depledge, M.H., 1993. The rational basis for the use of biomarkers as ecotoxicological tools. In: Fossi, M.C., Leonzio, C. (Eds.), Nondestructive Biomarkers in Vertebrates. Lewis Publishers, Boca Raton, FL, USA, pp. 261-285.

Depledge, M.H., 1998. Recovery of ecosystems and their components following exposure to pollution. Journal of Aquatic Ecosystem Stress and Recovery 6 (3), 199-206.

Depledge, M.H., Aagaard, A., Györkös, P., 1995. Assessment of trace metal toxicity using molecular, physiological and behavioural biomarkes. Marine Pollution Bulletin 31 (1-3), 19-27.

Derveaux, S., Vandesompele, J., Hellemans, J., 2010. How to do successful gene expression analysis using real-time PCR. Methods 50 (4), 227-230.

Dhanasekaran, S., Doherty, T.M., Kenneth, J., 2010. Comparison of different standards for real-time PCR-based absolute quantification. Journal of Immunological Methods 354 (1-2), 34-39.

Diatchenko, L., Lau, Y.F., Campbell, A.P., Chenchik, A., Moqadam, F., Huang, B., Lukyanov, S., Lukyanov, K., Gurskaya, N., Sverdlov, E.D., et al., 1996. Suppression subtractive hybridization: a method for generating differentially regulated or tissue-specific cDNA probes and libraries. Proceedings of the National Academy of Sciences of the United States of America 93 (12), 6025-6030.

Distler, J.H.W., Distler, O., Neidhart, M., Gay, S., 2007. Subtractive Hybridization. In: Cope, A.P. (Ed.), Arthritis Research: Methods and Protocols Volume 1 Human Press, pp. 77-90.

Dixon, D., Pruski, A., Dixon, L., 2004. The effects of hydrostatic pressure change on DNA integrity in the hydrothermal-vent mussel *Bathymodiolus azoricus*: implications for future deep-sea mutagenicity studies. Mutation Research - Fundamental and Molecular Mechanisms of Mutagenesis 552 (1-2), 235-246.

Dolmatov, I.Y., Mashanov, V.S., Zueva, O.R., 2007. Derivation of muscles of the Aristotle's lantern from coelomic epithelia. Cell and Tissue Research 327 (2), 371-384.

Douglas, M.G., McCammon, M.T., Vassarotti, A., 1986. Targeting proteins into mitochondria. Microbiological Reviews 50 (2), 166-178.

Drazen, J.C., Bird, L.E., Barry, J.P., 2005. Development of a hyperbaric trap-respirometer for the capture and maintenance of live deep-sea organisms. Limnology and Oceanography: Methods 3, 488-498.

Drazen, J.C., Seibel, B.A., 2007. Depth-related trends in metabolism of benthic and benthopelagic deep-sea fishes. Limnology and Oceanography 52 (5), 2306-2316.

Drummond, A.J., Ashton, B., Buxton, S., Cheung, M., Heled, J., Kearse, M., Moir, R., Stones-Havas, S., Thierer, T., Wilson, A., 2010. Geneious v4.8.

Düben, M.W.v., Koren, J., 1846. Öfversigt af Skandinaviens Echinodermer [Overview of Scandinavian Echinodermata]. Kungl. Svenska Vetenskapsakademiens Handlingar 1844.

Dupont, S., Ortega-Martínez, O., Thorndyke, M., 2010. Impact of near-future ocean acidification on echinoderms. Ecotoxicology 19 (3), 449-462.

Ellington, W.R., 1982. Intermediary Metabolism. In: Jangoux, M., Lawrence, J.M. (Eds.), Echinoderm Nutrition. A.A. Balkema, Rotterdam, pp. 395-415.

Ellis, J.R., Rogers, S.I., 2000. The distribution, relative abundance and diversity of echinoderms in the eastern English Channel, Bristol Channel, and Irish Sea. Journal of the Marine Biological Association of the United Kingdom 80 (1), 127-138.

Ellis, R.J., 1996. Chaperonins: introductory perspective. In: Ellis, R.J. (Ed.), The Chaperonins. Academic Press, San Diego, pp. 1-25.

Epping, E., van der Zee, C., Soetaert, K., Helder, W., 2002. On the oxidation and burial of organic carbon in sediments of the Iberian margin and Nazaré Canyon (NE Atlantic). Progress in Oceanography 52 (2-4), 399-431.

Erlandsson, C.P., Stigebrandt, A., Arneborg, L., 2006. The sensitivity of minimum oxygen concentrations in a fjord to changes in biotic and abiotic external forcing. Limnology and Oceanography 51 (1), 631-638.

Escartín, E., Porte, C., 1999. Hydroxylated PAHs in bile of deep-sea fish. Relationship with xenobiotic metabolizing enzymes. Environmental Science and Technology 33 (16), 2710-2714.

ESONET DONET MARS, 2010. European Seas Observatory NETwork, http://wwz.ifremer.fr/esonet_emso, Dense Oceanfloor Network System for Earthquakes and Tsunamis (DONET), http://www.jamstec.go.jp/jamstec-e/maritec/donet/index.html, The Monterey Accelerated Research System, http://www.mbari.org/mars/

Etienne, W., Meyer, M.H., Peppers, J., Meyer, R.A., 2004. Comparison of mRNA gene expression by RT-PCR and DNA microarray. BioTechniques 36 (4), 618-626.

European Commission, 2008. Sodium Hydroxide. Summary Risk Assessment Report. Final report. Institute for Health and Consumer Protection, Toxicology and Chemical Substance (TCS). EUR 23040 EN/2. pp. 30.

Fangue, N.A., Hofmeister, M., Schulte, P.M., 2006. Intraspecific variation in thermal tolerance and heat shock protein gene expression in common killifish, *Fundulus heteroclitus*. Journal of Experimental Biology 209 (15), 2859-2872.

Farmanfarmaian, A., 1966. The respiratory physiology of echinoderms. In: Boolootian, R.A. (Ed.), Physiology of Echinodermata. Interscience Publishers, New York, pp. 245-300.

Farrell, R.E., Jr., 2005. RT-PCR. In: Farrell, R.E., Jr. (Ed.), RNA Methodologies. Academic Press, Burlington, pp. 439-489.

Favali, P., Beranzoli, L., 2006. Seafloor observatory science: a review. Annals of Geophysics 49 (2-3), 515-567.

Favali, P., Beranzoli, L., 2009. EMSO: European multidisciplinary seafloor observatory. Nuclear Instruments and Methods in Physics Research Section A: Accelerators, Spectrometers, Detectors and Associated Equipment 602 (1), 21-27.

Feder, M.E., Hofmann, G.E., 1999. Heat-shock proteins, molecular chaperones, and the stress response: evolutionary and ecological physiology. Annual Review of Physiology 61, 243-282.

Féral, J.P., Ferrand, J.G., Guille, A., 1990. Macrobenthic physiological responses to environmental fluctuations: the reproductive cycle and enzymatic polymorphism of a eurybathic sea urchin on the northwestern Mediterranean continental shelf and slope. Continental Shelf Research 10, 1147-1155.

Fernandes, M., Xiao, H., Lis, J.T., 1994. Fine structure analyses of the *Drosophila* and *Saccharomyces* heat shock factor - heat shock element interactions. Nucleic Acids Research 22 (2), 167-173.

Finley, D., Bartel, B., Varshavsky, A., 1989. The tails of ubiquitin precursors are ribosomal proteins whose fusion to ubiquitin facilitates ribosome biogenesis. Nature 338, 394–401.

Finley, D., Chau, V., 1991. Ubiquitination. Annual Review of Cell Biology 7, 25-69.

Finley, D., Özkaynak, E., Varshavsky, A., 1987. The yeast polyubiquitin gene is essential for resistance to high-temperatures, starvation, and other stresses. Cell 48 (6), 1035-1046.

Fisher, N.S., 1977. On the differential sensitivity of estuarine and open-ocean diatoms to exotic chemical stress. The American Naturalist 111 (981), 871-895.

Flaherty, K.M., DeLuca-Flaherty, C., McKay, D.B., 1990. Three-dimensional structure of the ATPase fragment of a 70K heat-shock cognate protein. Nature 346 (6285), 623-628.

Fleige, S., Pfaffl, M.W., 2006. RNA integrity and the effect on the real-time qRT-PCR performance. Molecular Aspects of Medicine 27 (2-3), 126-139.

Fleige, S., Walf, V., Huch, S., Prgomet, C., Sehm, J., Pfaffl, M.W., 2006. Comparison of relative mRNA quantification models and the impact of RNA integrity in quantitative real-time RT-PCR. Biotechnology Letters 28, 1601–1613.

Fornace, A.J., Alamo, I., Hollander, M.C., Lamoreaux, E., 1989. Ubiquitin messenger RNA is a major stress-induced transcript in mammalian cells. Nucleic Acids Research 17 (3), 1215-1230.

Franzellitti, S., Fabbri, E., 2005. Differential HSP70 gene expression in the Mediterranean mussel exposed to various stressors. Biochemical and Biophysical Research Communications 336 (4), 1157-1163.

Fraser, K.P.P., Peck, L.S., Clarke, A., 2004. Protein synthesis, RNA concentrations, nitrogen excretion, and metabolism vary seasonally in the Antarctic holothurian *Heterocucumis steineni* (Ludwig 1898). Physiological and Biochemical Zoology 77 (4), 556-569.

Froescheis, O., Looser, R., Cailliet, G., Jarman, W., Ballschmiter, K., 2000. The deep-sea as a final global sink of semivolatile persistent organic pollutants? Part I: PCBs in surface and deep-sea dwelling fish of the North and South Atlantic and the Monterey Bay Canyon (California). Chemosphere 40 (6), 651-660.

Frohman, M.A., Dush, M.K., Martin, G.R., 1988. Rapid production of full-length cDNAs from rare transcripts - amplification using a single gene-specific oligonucleotide primer

Proceedings of the National Academy of Sciences of the United States of America 85 (23), 8998-9002.

Gage, J.D., 1996. Why are there so many species in deep-sea sediments? Journal of Experimental Marine Biology and Ecology 200 (1-2), 257-286.

Gage, J.D., Bett, B.J., 2005. Deep-sea benthic sampling. In: McIntyre, A.D., Eleftheriou, A. (Eds.), Methods for the Study of Marine Benthos. Blackwell Science Publishing, Oxford, pp. 273-325.

Gage, J.D., Tyler, P.A., 1991. Deep-sea biology: a natural history of organisms at the deep-sea floor. Cambridge University Press, Cambridge.

Gage, J.D., Tyler, P.A., Nichols, D., 1986. Reproduction and growth of *Echinus acutus* var. *norvegicus* Düben & Koren and *E. elegans* Düben & Koren on the continental slope off Scotland Journal of Experimental Marine Biology and Ecology 101 (1-2), 61-83.

Gagnon, M.M., Holdway, D.A., 1999. Metabolic enzyme activities in fish gills as biomarkers of exposure to petroleum hydrocarbons. Ecotoxicology and Environmental Safety 44, 92-99.

Galgani, F., Chiffoleau, J.F., Gall, P.L., Pichot, Y., Andral, B., Martin, C., 2005. Deep-sea caging of the mussel *Mytilus galloprovincialis*: potential application in ecotoxicological studies. Chemistry and Ecology 21 (2), 133-141.

Gallucci, F., Fonseca, G., Soltwedel, T., 2008. Effects of megafauna exclusion on nematode assemblages at a deep-sea site. Deep-Sea Research Part I: Oceanographic Research Papers 55 (3), 332-349.

Garcia-Orellana, J., Pates, J.M., Masqué, P., Bruach, J.M., Sanchez-Cabeza, J.A., 2009. Distribution of artificial radionuclides in deep sediments of the Mediterranean Sea. Science of the Total Environment 407 (2), 887-898.

Gasteiger, E., Gattiker, A., Hoogland, C., Ivanyi, I., Appel, R.D., Bairoch, A., 2003. ExPASy: the proteomics server for in-depth protein knowledge and analysis. Nucleic Acids Research 31, 3784-3788.

Georgiades, E.T., Holdway, D.A., Brennan, S.E., Butty, J.S., Temara, A., 2003. The impact of oil-derived products on the behaviour and biochemistry of the eleven-armed asteroid *Coscinasterias muricata* (Echinodermata). Marine Environmental Research 55, 257-276.

Georgiades, E.T., Temara, A., Holdway, D.A., 2005. Influence of the reproductive cycle on cytochrome P450 levels in the sea star *Coscinasterias muricata.* Marine Pollution Bulletin 50 (9), 1007-1014.

Georgopoulos, C., Welch, W.J., 1993. Role of the major heat shock proteins as molecular chaperones. Annual Review of Cell Biology 9 (1), 601-634.

Gerhardt, A., 2007. Aquatic behavioral ecotoxicology - prospects and limitations. Human and Ecological Risk Assessment: An International Journal 13 (3), 481 - 491.

Gething, M.-J., Sambrook, J., 1992. Protein folding in the cell. Nature 355 (6355), 33-45.

Gibbs, A.G., 1997. Biochemistry at depth. In: Randall, D.J., Farrell, A.P. (Eds.), Deep-Sea Fishes. Academic Press Ltd., London, pp. 239-278.

Girguis, P.R., Lee, R.W., 2006. Thermal preference and tolerance of alvinellids. Science 312 (5771), 231-.

Giudice, G., Sconzo, G., Roccheri, M.C., 1999. Studies on heat shock proteins in sea urchin development. Development, Growth & Differentiation 41 (4), 375-380.

Glickman, M.H., Ciechanover, A., 2002. The ubiquitin-proteasome proteolytic pathway: destruction for the sake of construction. Physiological Reviews 82 (2), 373-428.

Glover, A.G., Smith, C.R., 2003. The deep-sea floor ecosystem: current status and prospects of anthropogenic change by the year 2025. Environmental Conservation 30 (3), 219-241.

Glud, R.N., 2008. Oxygen dynamics of marine sediments. Marine Biology Research 4 (4), 243-289.

Goetz, F.W., 2003. The "ups" and "downs" in using subtractive cloning techniques to isolate regulated genes in fish. Integrative and Comparative Biology 43 (6), 786-793.

Goldberg, A.L., 2003. Protein degradation and protection against misfolded or damaged proteins. Nature 426 (6968), 895-899.

Goldenthal, M.J., Marin-Garcia, J., Ananthakrishnan, R., 1998. Cloning and molecular analysis of the human citrate synthase gene. Genome 41 (5), 733-738.

Gong, Z., Cserjesi, P., Wessel, G.M., Brandhorst, B.P., 1991. Structure and expression of the polyubiquitin gene in sea urchin embryos. Molecular Reproduction and Development 28 (2), 111-118.

Gracey, A.Y., 2007. Interpreting physiological responses to environmental change through gene expression profiling. Journal of Experimental Biology 210 (9), 1584-1592.

Grafen, A., Hails, R., 2008. Modern Statistics for the Life Sciences. Oxford University Press, Oxford.

Gray, J.S., Clarke, K.R., Warwick, R.M., Hobbs, G., 1990. Detection of initial effects of pollution on marine benthos: an example from the Ekofisk and Eldfisk oilfields, North Sea. Marine Ecology Progress Series 66, 285-299.

Greenbaum, D., Colangelo, C., Williams, K., Gerstein, M., 2003. Comparing protein abundance and mRNA expression levels on a genomic scale. Genome Biology 4 (9), 117.

Griffiths, 2007. RRS James Cook Cruise JC009T, 01 May - 11 May 2007. Trials of the Isis Remotely Operated Vehicle. National Oceanography Centre, Southampton. UK. Cruise Report No. 18, p. 42.

Gross, M., 2004. Emergency services: a bird's eye perspective on the many different functions of stress proteins. Current Protein & Peptide Science 5 (4), 213-223.

Gry, M., Rimini, R., Stromberg, S., Asplund, A., Ponten, F., Uhlen, M., Nilsson, P., 2009. Correlations between RNA and protein expression profiles in 23 human cell lines. BMC Genomics 10.

Guillou, M., Grall, J., Connan, S., 2002. Can low sea urchin densities control macro-epiphytic biomass in a north-east Atlantic maerl bed ecosystem (Bay of Brest, Brittany, France)? Journal of the Marine Biological Association of the UK 82 (5), 867-876.

Guindon, S., Gascuel, O., 2003. A simple, fast, and accurate algorithm to estimate large phylogenies by maximum likelihood. Systematic Biology 52 (5), 696-704.

Guinotte, J.M., Orr, J., Cairns, S., Freiwald, A., Morgan, L., George, R., 2006. Will human-induced changes in seawater chemistry alter the distribution of deep-sea scleractinian corals? Frontiers in Ecology and the Environment 4 (3), 141-146.

Gupta, R.S., Golding, G.B., 1993. Evolution of HSP70 gene and its implications regarding relationships between archaebacteria, eubacteria, and eukaryotes. Journal of Molecular Evolution 37 (6), 573-582.

Gupta, S.C., Sharma, A., Mishra, M., Mishra, R.K., Chowdhuri, D.K., 2010. Heat shock proteins in toxicology: how close and how far? Life Sciences 86 (11-12), 377-384.

Haedrich, R.L., Rowe, G.T., Polloni, P.T., 1980. The megabenthic fauna in the deep sea south of New England, USA. Marine Biology 57 (3), 165-179.

Hall, S.J., 1994. Physical disturbance and marine benthic communities: life in unconsolidated sediments. Oceanography and marine biology: an annual review 32, 179-239.

Halpin, P., Sorte, C., Hofmann, G., Menge, B., 2002. Patterns of variation in levels of Hsp70 in natural rocky shore populations from microscales to mesoscales. Integrative & Comparative Biology 42, 815-824.

Hamer, B., Hamer, D.P., Muller, W.E.G., Batel, R., 2004. Stress-70 proteins in marine mussel *Mytilus galloprovincialis* as biomarkers of environmental pollution: a field study. Environment International 30 (7), 873-882.

Hamilton, K.S., Ellison, M.J., Barber, K.R., Williams, R.S., Huzil, J.T., McKenna, S., Ptak, C., Glover, M., Shaw, G.S., 2001. Structure of a conjugating enzyme-ubiquitin thiolester intermediate reveals a novel role for the ubiquitin tail. Structure 9 (10), 897-904.

Handy, R.D., Depledge, M.H., 1999. Physiological responses: their measurement and use as environmental biomarkers in ecotoxicology. Ecotoxicology 8 (5), 329-349.

Hargrave, B.T., Harding, G.C., Vass, W.P., Erickson, P.E., Fowler, B.R., Scott, V., 1992. Organochlorine pesticides and polychlorinated biphenyls in the Arctic Ocean food web. Archives of Environmental Contamination and Toxicology 22 (1), 41-54.

Hargrave, B.T., Kostylev, V.E., Hawkins, C.M., 2004. Benthic epifauna assemblages, biomass and respiration in The Gully region on the Scotian Shelf, NW Atlantic Ocean. Marine Ecology Progress Series 270, 55-70.

Harino, H., Iwasaki, N., Arai, T., Ohji, M., Miyazaki, N., 2005. Accumulation of organotin compounds in the deep-sea environment of Nankai Trough, Japan. Archives of Environmental Contamination and Toxicology 49, 497-503.

Harino, H., Iwasaki, N., Arai, T., Ohji, M., Miyazaki, N. , 2009. Occurrence of antifouling biocides and fluorinated alkyl compounds in sediment core from deep sea: Suruga Bay, Tosa Bay, and Nankai Tough, Japan. Archives of Environmental Contamination and Toxicology 57 (4), 661-669.

Harland, R., Nordberg, K., Filipsson, H.L., 2006. Dinoflagellate cysts and hydrographical change in Gullmar Fjord, west coast of Sweden. Science of the Total Environment 355 (1-3), 204-231.

Hartl, F.U., Hayer-Hartl, M., 2002. Molecular chaperones in the cytosol: from nascent chain to folded protein. Science 295 (5561), 1852-1858.

Hartl, F.U., Neupert, W., 1990. Protein sorting to mitochondria - evolutionary conservations of folding and assembly. Science 247 (4945), 930-938.

Harvey, G.R., Miklas, H.P., Bowen, V.T., Steinhauer, W.G., 1974. Observations on the distribution of chlorinated hydrocarbons in Atlantic Ocean organisms. Journal of Marine Research 32 (2), 103-118.

Harvey, R., Gage, J.D., Billett, D.S.M., Clark, A.M., Paterson, G.L.J., 1988. Echinoderms of the Rockall Trough and adjacent areas. 3. Additional records. Bulletin of the British Museum (Natural History) Zoology Series 54(4), 153-198.

Hatay, M., Kuntz, N.M., Rohwer, F., 2005. SPIDERS: a syringe pump system for in situ underwater dosing of benthic organisms. Limnology and Oceanography: Methods 3, 38-45.

Häusserman, V., 2006. Biodiversity of Chilean sea anemones (Cnidaria: Anthozoa): distribution patterns and zoogeographic implications, including new records for the fjord region. Investigaciones marinas 34 (2), 23-35.

Hauton, C., Atkinson, R.J.A., Moore, P.G., 2003. The impact of hydraulic blade dredging on a benthic megafaunal community in the Clyde Sea area, Scotland. Journal of Sea Research 50 (1), 45-56.

Hawkes, V., 2007a. Selecting appropriate qPCR detection chemistries. Sigma-Aldrich QPCR Total Solution Seminar Series.

Hawkes, V., 2007b. Assay design and optimisation. Sigma-Aldrich QPCR Total Solution Seminar Series.

Heid, C., Stevens, J., Livak, K., Williams, P., 1996. Real time quantitative PCR. Genome Research 6, 986-994.

Herbert, R., Southward, A., Clarke, R., Sheader, M., Hawkins, S., 2009. Persistent border: an analysis of the geographic boundary of an intertidal species. Marine Ecology Progress Series 379, 135-150.

Herring, P., 2002. The biology of the deep ocean. Oxford University Press, Oxford.

Hershko, A., Ciechanover, A., 1992. The ubiquitin system for protein degradation. Annual Review of Biochemistry 61, 761-807.

Hershko, A., Ciechanover, A., 1998. The ubiquitin system. Annual Review of Biochemistry 67, 425-479.

Hessler, R.R., 1972. Deep water organisms for high pressure aquarium studies. In: Brauer, R.W. (Ed.), Barobiology and the Experimental Biology of the Deep Sea. North Carolina Sea Grant Program, Chapel Hill, N.C., USA, pp. 151-163.

Hicke, L., Schubert, H.L., Hill, C.P., 2005. Ubiquitin-binding domains. Nature Reviews Molecular Cell Biology 6 (8), 610-621.

Hightower, L., Sadis, S., Takenaka, I., 1994. Interactions of vertebrate hsc70 and hsp70 with unfolded proteins and peptides. In: Morimoto, R., Tissières, A., Georgopoulos, C. (Eds.), The Biology of Heat Shock Proteins & Molecular Chaperones. Cold Spring Harbor Laboratory Press, New York, pp. 179-207.

Higuchi, R., Fockler, C., Dollinger, G., Watson, R., 1993. Kinetic PCR analysis - real-time monitoring of DNA amplification reactions. Bio-Technology 11 (9), 1026-1030.

Hinchey, E.K., Schaffner, L.C., Hoar, C.C., Vogt, B.W., Batte, L.P., 2006. Responses of estuarine benthic invertebrates to sediment burial: the importance of mobility and adaptation. Hydrobiologia 556 (1), 85-98.

Hiscock, K., Southward, A., Tittley, I., Hawkins, S., 2004. Effects of changing temperature on benthic marine life in Britain and Ireland. Aquatic Conservation: Marine and Freshwater Ecosystems 14, 333-362.

Hochstrasser, M., 1996. Ubiquitin-dependent protein degradation. Annual Review of Genetics 30, 405-439.

Hoffmann, A.A., Parsons, P.A., 1991. Evolutionary Genetics and Environmental Stress. Oxford University Press, Oxford. Accessed from http://books.google.co.uk/.

Hofmann, G.E., 1999. Ecologically relevant variation in induction and function of heat shock proteins in marine organisms. American Zoologist 39 (6), 889-900.

Hofmann, G.E., Burnaford, J.L., Fielman, K.T., 2005. Genomics-fueled approaches to current challenges in marine ecology. Trends in Ecology and Evolution 20 (6 SPEC. ISS.), 305-311.

Hofmann, G.E., O'Donnell, M.J., Todgham, A.E., 2008. Using functional genomics to explore the effects of ocean acidification on calcifying marine organisms. Marine Ecology-Progress Series 373, 219-225.

Hofmann, G.E., Somero, G.N., 1995. Evidence for protein damage at environmental temperatures: seasonal changes in levels of ubiquitin conjugates and Hsp70 in the intertidal mussel *Mytilus trossulus*. Journal of Experimental Biology 198, 1509-1518.

Hofmann, G.E., Somero, G.N., 1996. Protein ubiquitination and stress protein synthesis in *Mytilus trossulus* occurs during recovery from tidal emersion. Molecular Marine Biology and Biotechnology 5 (3), 175-184.

Holdway, D.A., 2002. The acute and chronic effects of wastes associated with offshore oil and gas production on temperate and tropical marine ecological processes. Marine Pollution Bulletin 44, 185-203.

Hollertz, K., 2001. On the ecology of the sediment burrowing heart urchin *Brissopsis lyrifera* (Echinoidea: Spatangoida). PhD Thesis., Department of Marine Ecology, Göteborg University, pp. 295.

Hollertz, K., Duchêne, J.C., 2001. Burrowing behaviour and sediment reworking in the heart urchin *Brissopsis lyrifera* Forbes (Spatangoida). Marine Biology 139 (5), 951-957.

Holm, K., Hernroth, B., Thorndyke, M., 2008. Coelomocyte numbers and expression of HSP70 in wounded sea stars during hypoxia. Cell and Tissue Research 334, 319-325.

Huang, X., Li, Y., Niu, Q., Zhang, K., 2007. Suppression Subtractive Hybridization (SSH) and its modifications in microbiological research. Applied Microbiology and Biotechnology 76 (4), 753-760.

Hudson, I.R., 2004. Deep-sea biology food for thought? Examining dietary selection and resource allocation in deep-sea holothurians. PhD Thesis, School of Ocean and Earth Science, University of

Southampton, Southampton, UK. pp. 300.

Huggett, J., Dheda, K., Bustin, S., Zumla, A., 2005. Real-time RT-PCR normalisation; strategies and considerations. Genes and Immunity 6 (4), 279-284.

Hughes, S.J.M., Amaro, T., Ingels, J., Boorman, B., Hawkins, L.E., Vanreusel, A., Cunha, M.R., submitted. Benthic abyssal research using a remotely operated vehicle (ROV): novel experimentation in the Nazaré Canyon. Deep-Sea Research Part II: Topical Studies in Oceanography.

Hughes, S.J.M., Jones, D.O.B., Hauton, C., Gates, A.R., Hawkins, L.E., in press. An assessment of drilling disturbance on *Echinus acutus* var. *norvegicus* based on in situ observations and experiments using a Remotely Operated Vehicle (ROV). Journal of Experimental Marine Biology and Ecology.

Hughes, S.J.M., Ruhl, H.A., Hawkins, L.E., Hauton, C., Boorman, B., Billett, D.S.M., in prep. Abyssal echinoderm oxygen consumption and an interclass comparison of echinoderm metabolic rates.

Hunter, W.L., Jr., Bennett, P.B., 1974. The causes, mechanisms and prevention of the high pressure nervous syndrome. Undersea Biomedical Research 1 (1), 1-28.

Irwin, S., Davenport, J., 2006. Implications of water flow and oxygen gradients for molluscan oxygen uptake and respirometric measurements. Journal of the Marine Biological Association of the United Kingdom 86 (2), 401-402.

IUCN, 2010. International Union for Conservation of Nature (IUCN) statement on the Gulf of Mexico oil spill, 7 June 2010. http://cmsdata.iucn.org/downloads/iucn_statement_on_the_gulf_of_mexico_oil_spill.pdf.

Ivanina, A.V., Habinck, E., Sokolova, I.M., 2008. Differential sensitivity to cadmium of key mitochondrial enzymes in the eastern oyster, *Crassostrea virginica* Gmelin (Bivalvia: Ostreidae). Comparative Biochemistry and Physiology Part C: Toxicology & Pharmacology 148 (1), 72-79.

Ivanina, A., Taylor, C., Sokolova, I., 2009. Effects of elevated temperature & cadmium exposure on stress protein response in eastern oysters *Crassostrea virginica* (Gmelin). Aquatic Toxicology 91, 245-254.

Jackson, A., 2008. *Psammechinus miliaris*. Green sea urchin. Marine Life Information Network: Biology and Sensitivity Key Information Sub-programme [Online]. Plymouth: Marine Biological Association of the United Kingdom. Available from: http://www.marlin.ac.uk/speciesinformation.php?speciesID=4216 [accessed 2010, May 25].

Jamieson, A., Jones, D., Bailey, D., 2005. Benthic Incubation Chamber System (BICS) Cruise Report. TN-187 (Pulse 48) R/V Thomas G. Thompson w/ JASON 2 ROV 2nd Nov–18th Nov 2005. p. 39.

Jamieson, A.J., Bailey, D.M., Wagner, H.J., Bagley, P.M., Priede, I.G., 2006. Behavioural responses to structures on the seafloor by the deep-sea fish *Coryphaenoides armatus*: implications for the use of baited landers. Deep-Sea Research Part I: Oceanographic Research Papers 53 (7), 1157-1166.

Janssens, B.J., Childress, J.J., Baguet, F., Rees, J.F., 2000. Reduced enzymatic antioxidative defense in deep-sea fish. Journal of Experimental Biology 203 (24), 3717-3725.

Jentsch, S., 1992. The ubiquitin-conjugation system. Annual Review of Genetics 26 (1), 179-207.

Johnston, S.C., Larsen, C.N., Cook, W.J., Wilkinson, K.D., Hill, C.P., 1997. Crystal structure of a deubiquitinating enzyme (human UCH-L3) at 1.8 Å resolution. EMBO J 16 (13), 3787-3796.

Jones, D.O.B., 2009. Using existing industrial remotely operated vehicles for deep-sea science. Zoologica Scripta 38, 41-47.

Jones, D.O.B., Wigham, B.D., Hudson, I.R., Bett, B.J., 2007. Anthropogenic disturbance of deep-sea megabenthic assemblages: a study with remotely operated vehicles in the Faroe-Shetland Channel, NE Atlantic. Marine Biology 151 (5), 1731-1741.

Jungmann, J., Reins, H.-A., Schobert, C., Jentsch, S., 1993. Resistance to cadmium mediated by ubiquitin-dependent proteolysis. Nature 361, 369-371.

Jurecic, R., Belmont, J.W., 2000. Long-distance DD-PCR and cDNA microarrays. Current Opinion in Microbiology 3 (3), 316-321.

Kamler, E., 1969. A comparison of the closed-bottle and flowing-water methods for measurement of respiration in aquatic invertebrates. Polskie Archiwum Hydrobiologii 16 (29), 31-49.

Kang, R., Daniels, C., Francis, S., Shih, S., Salerno, W., Hicke, L., Radhakrishnan, I., 2003. Solution structure of a CUE-ubiquitin complex reveals a conserved mode of ubiquitin binding. Cell 113, 621-630.

Karpusas, M., Branchaud, B., Remington, S.J., 1990. Proposed mechanism for the condensation reaction of citrate synthase: 1.9-Å structure of the ternary complex with oxaloacetate and carboxymethyl coenzyme A. Biochemistry 29 (9), 2213-2219.

Kaufman, R., Forstner, H., Wieser, W., 1989. Respirometry - methods and approaches. In: Bridges, C.R., Butler, P.J. (Eds.), Techniques in Comparative Respiratory Physiology, An Experimental Approach. Cambridge University Press, Cambridge, pp. 51-76.

Kelly, M.S., Hughes, A.D., Cook, E.J., 2007. Ecology of *Psammechinus miliaris*. In: Lawrence, J.M. (Ed.), Edible sea urchins: biology and ecology. Elsevier, Amsterdam, pp. 287-295.

King, H.C., Sinha, A.A., 2001. Gene expression profile analysis by DNA microarrays: promise and pitfalls. Journal of the American Medical Association 286 (18), 2280-2288.

Kingston, P.F., 1992. Impact of offshore oil production installations on the benthos of the North Sea. ICES Journal of Marine Science 49 (1), 45-53.

Kirkegaard, T., Roth, A.G., Petersen, N.H.T., Mahalka, A.K., Olsen, O.D., Moilanen, I., Zylicz, A., Knudsen, J., Sandhoff, K., Arenz, C., et al., 2010. Hsp70 stabilizes lysosomes and reverts Niemann–Pick disease-associated lysosomal pathology. Nature 463, 549-553.

Kobayashi, N., 1984. Marine Ecotoxicological Testing with Echinoderms. In: Persoone, G., Jaspers, E., Claus, C. (Eds.), Ecotoxicological Testing for the Marine Environment. State University of Ghent and Institute for Marine Scientific Research, Ghent, pp. 341-405.

Koehler, R., 1901. Note preliminaire sur quelques Ophiures nouvelles provenant des compagnes de la *Princess Alice*. Bulletin de la Societe Zoologique de France 26, 222-231.

Koenders, A., Yu, X., Chang, E.S., Mykles, D.L., 2002. Ubiquitin and actin expression in claw muscles of land crab, *Gecarcinus lateralis*, and American lobster, *Homarus americanus*: differential expression of ubiquitin in two slow muscle fiber types during molt-induced atrophy. Journal of Experimental Zoology 292 (7), 618-632.

Komander, D., 2009. The emerging complexity of protein ubiquitination. Biochemical Society Transactions 37 (5), 937-953.

Koslow, J.A., Gowlett-Holmes, K., Lowry, J.K., O'Hara, T., Poore, G.C.B., Williams, A., 2001. Seamount benthic macrofauna off southern Tasmania: community structure and impacts of trawling. Marine Ecology Progress Series 213, 111-125.

Koyama, S., Horii, M., Miwa, T., Aizawa, M., 2003. Tissue culture of the deep-sea eel *Simenchelys parasiticus* collected at 1,162 m. Extremophiles 7 (3), 245-248.

Koyama, S., Miwa, T., Horii, M., Ishikawa, Y., Horikoshi, K., Aizawa, M., 2002. Pressure-stat aquarium system designed for capturing and maintaining deep-sea organisms. Deep-Sea Research Part I: Oceanographic Research Papers 49, 2095–2102.

Koyama, S., Nagahama, T., Ootsu, N., Takayama, T., Horii, M., Konishi, S., Miwa, T., Ishikawa, Y., Aizawa, M., 2005. Survival of deep-sea shrimp (*Alvinocaris* sp.) during decompression and larval hatching at atmospheric pressure. Marine Biotechnology 7 (4), 272-278.

Krone, P.H., Heikkila, J.J., 1988. Analysis of hsp 30, hsp 70 and ubiquitin gene-expression in *Xenopus laevis* tadpoles. Development 103 (1), 59-67.

Kubista, M., Andrade, J.M., Bengtsson, M., Forootan, A., Jonák, J., Lind, K., Sindelka, R., Sjöback, R., Sjögreen, B., Strömbom, L., et al., 2006. The real-time polymerase chain reaction. Molecular Aspects of Medicine 27, 95-125.

Kültz, D., 2003. Evolution of the cellular stress proteome: from monophyletic origin to ubiquitous function. Journal of Experimental Biology 206 (18), 3119-3124.

Kültz, D., 2005. Molecular and evolutionary basis of the cellular stress response. Annual Review of Physiology 67, 225–257.

Kutti, T., Hansen, P.K., Ervik, A., Høisæter, T., Johannessen, P., 2007. Effects of organic effluents from a salmon farm on a fjord system. II. Temporal and spatial patterns in infauna community composition. Aquaculture 262 (2-4), 355-366.

La Rosa, M., Sconzo, G., Guidice, G., Roccheri, M.C., Di Carlo, M., 1990. Sequence of a sea urchin hsp70 gene and its 5' flanking region. Gene 96 (2), 295-300.

Laboy-Nieves, E.N., Conde, J.E., 2001. Metal levels in eviscerated tissue of shallow-water deposit-feeding holothurians. Hydrobiologia 459 (1), 19-26.

Lampert, W., 1984. The measurement of respiration. In: Downing, J.A., Rigler, F.H. (Eds.), A Manual on Methods for the Assessment of Secondary Productivity in Fresh Waters. Blackwell Scientific Publications, Oxford, pp. 413-468.

Lauerman, L.M.L., Kaufmann, R.S., Smith, K.L., 1996. Distribution and abundance of epibenthic megafauna at a long time-series station in the abyssal northeast Pacific. Deep-Sea Research Part I: Oceanographic Research Papers 43 (7), 1075-1103.

Lavado, R., Barbaglio, A., Carnevali, M.D.C., Porte, C., 2006a. Steroid levels in crinoid echinoderms are altered by exposure to model endocrine disruptors. Steroids 71 (6), 489-497.

Lavado, R., Sugni, M., Candia Carnevali, M.D., Porte, C., 2006b. Triphenyltin alters androgen metabolism in the sea urchin *Paracentrotus lividus*. Aquatic Toxicology 79 (3), 247-256.

Lavaleye, M.S.S., Duineveld, G.C.A., Berghuis, E.M., Kok, A., Witbaard, R., 2002. A comparison between the megafauna communities on the N.W. Iberian and Celtic continental margins - effects of coastal upwelling? Progress in Oceanography 52 (2-4), 459-476.

Lawrence, J.M., 1975. The effect of temperature salinity combinations on the functional well being of adult *Lytechinus variegatus* (Lamarck) (Echlnodermata, Echinoldea). Journal of Experimental Marine Biology and Ecology 18 (3), 271-275.

Lawrence, J.M., 1987. Echinodermata. In: Pandian, T.J., Vernberg, F.J. (Eds.), Animal Energetics. Volume 2. Bivalvia through Reptilia. Academic Press, Inc. (London) Ltd., San Diego, pp. 229-321.

Lawrence, J.M., Cowell, B.C., 1996. The righting response as an indication of stress in *Stichaster striatus* (Echinodermata, Asteroidea). Marine and Freshwater Behaviour and Physiology 27 (4), 239-248.

Lebrato, M., Iglesias-Rodriguez, D., Feely, R., Greeley, D., Jones, D., Suarez-Bosche, N., Lampitt, R., Cartes, J., Green, D., Alker, B., 2010. Global contribution of echinoderms to the marine carbon cycle: a re-assessment of the oceanic $CaCO_3$ budget and the benthic compartments. Ecological Monographs 80 (3), 441-467.

Lee, A.J., Ramster, J.W., 1981. Atlas of the seas around the British Isles. Ministry of Agriculture, Fisheries and Food, Lowestoft.

Lee, J.S., Tanabe, S., Takemoto, N., Kubodera, T., 1997. Organochlorine residues in deep-sea organisms from Suruga Bay, Japan. Marine Pollution Bulletin 34 (4), 250-258.

Leignel, V., Cibois, M., Moreau, B., Chenais, B., 2007. Identification of new subgroup of HSP70 in Bythograeidae (hydrothermal crabs) and Xanthidae. Gene 396 (1), 84-92.

Leone, G., van Schijndel, H., van Gemen, B., Kramer, F., Schoen, C., 1998. Molecular beacon probes combined with amplification by NASBA enable homogeneous, real-time detection of RNA. Nucleic Acids Research 26 (9), 2150-2155.

Lettieri, T., 2006. Recent applications of DNA microarray technology to toxicology and ecotoxicology. Environmental Health Perspectives 114 (1), 4-9.

Lewis, S., Handy, R.D., Cordi, B., Billinghurst, Z., Depledge, M.H., 1999. Stress proteins (HSPs): methods of detection and their use as an environmental biomarker. Ecotoxicology 8 (5), 351-368.

Li, W., Gracey, A., Mello, L., Brass, A., Cossins, A., 2009. ExprAlign - the identification of ESTs in non-model species by alignment of cDNA microarray expression profiles. BMC Genomics 10, 560.

Liang, P., Pardee, A.B., 1992. Differential display of eukaryotic messenger-RNA by means of the polymerase chain-reaction. Science 257 (5072), 967-971.

Lindquist, S., 1986. The heat-shock response. Annual Review of Biochemistry 55, 1151-1191.

Lindquist, S., Craig, E.A., 1988. The heat-shock proteins. Annual Review of Genetics 22 (1), 631-677.

Linnaeus, C., 1758. Systema Naturae per regna tria naturae, secundum classes, ordines, genera, species cum characteribus, differentiis, synonymis, locis. Editio decima, reformata. Laurentius Salvius: Holmiae. ii, 824 pp.

Lister, T., Renshaw, J., 1991. Understanding chemistry for advanced level. Stanley Thornes (Publishers) Ltd., Cheltenham, UK. pp. 602.

Liu, J., Yang, W.J., Zhu, X.J., Karouna-Renier, N.K., Rao, R.K., 2004. Molecular cloning and expression of two HSP70 genes in the prawn, *Macrobrachium rosenbergii*. Cell Stress and Chaperones 9 (3), 313-323.

Loens, K., Ursi, D., Goossens, H., Ieven, M., 2005. Nucleic Acid Sequence-Based Amplification. Medical Biomethods Handbook, pp. 273-291.

Lohrer, A.M., Thrush, S.F., Hunt, L., Hancock, N., Lundquist, C., 2005. Rapid reworking of subtidal sediments by burrowing spatangoid urchins. Journal of Experimental Marine Biology and Ecology 321 (2), 155-169.

Long, S.M., Ryder, K.J., Holdway, D.A., 2003. The use of respiratory enzymes as biomarkers of petroleum hydrocarbon exposure in *Mytilus edulis planulatus.* Ecotoxicology and Environmental Safety 55 (3), 261-270.

Looser, R., Froescheis, O., Cailliet, G.M., Jarman, W.M., Ballschmiter, K., 2000. The deep-sea as a final global sink of semivolatile persistent organic pollutants? Part II: Organochlorine pesticides in surface and deep-sea dwelling fish of the North and South Atlantic and the Monterey Bay Canyon (California). Chemosphere 40 (6), 661-670.

Luan, W., Li, F.H., Zhang, J.Q., Wen, R., Li, Y.T., Xiang, J.H., 2010. Identification of a novel inducible cytosolic Hsp70 gene in Chinese shrimp *Fenneropenaeus chinensis* and comparison of its expression with the cognate Hsc70 under different stresses. Cell Stress & Chaperones 15 (1), 83-93.

Macdonald, A.G., 1975. Physiological Aspects of Deep-Sea Biology. Cambridge University Press, Cambridge. pp. 450.

Macdonald, A.G., 1997. Hydrostatic pressure as an environmental factor in life processes. Comparative Biochemistry and Physiology - A Physiology 116 (4), 291-297.

Macdonald, A.G., Gilchrist, I., 1978. Further studies on the pressure tolerance of deep-sea crustacea, with observations using a new high-pressure trap. Marine Biology 45 (1), 9-21.

Mahaut, M.-L., Sibuet, M., Shirayama, Y., 1995. Weight-dependent respiration rates in deep-sea organisms. Deep-Sea Research Part I: Oceanographic Research Papers 42 (9), 1575-1582.

Maier, T., Güell, M., Serrano, L., 2009. Correlation of mRNA and protein in complex biological samples. FEBS Letters 583 (24), 3966-3973.

Majoran, S., Agrenius, S., Kucera, M., 2000. The effect of temperature on shell size and growth rate in *Krithe praetexta praetexta* (Sars). Hydrobiologia 419 (1), 141-148.

Maltby, L., 1999. Studying stress: the importance of organism-level responses. Ecological Applications 9 (2), 431-440.

Marchler-Bauer, A., Anderson, J.B., Chitsaz, F., Derbyshire, M.K., DeWeese-Scott, C., Fong, J.H., Geer, L.Y., Geer, R.C., Gonzales, N.R., Gwadz, M., et al., 2009. CDD: specific functional annotation with the Conserved Domain Database. Nucleic Acids Research 37 (suppl_1), D205-210.

Marsh, A., Lawrence, J., 1985. The effects of cations on the activity of citrate synthase (EC 4.1.3.7) in *Luidia clathrata* (Say) (Echinodermata: Asteroidea). Comparative Biochemistry and Physiology Part B: Biochemistry and Molecular Biology 81 (3), 767-770.

Marsh, A.G., Leong, P.K.K., Manahan, D.T., 1999. Energy metabolism during embryonic development and larval growth of an Antarctic sea urchin. Journal of Experimental Biology 202 (15), 2041-2050.

Mathews, D.H., Sabina, J., Zuker, M., Turner, D.H., 1999. Expanded sequence dependence of thermodynamic parameters improves prediction of RNA secondary structure. Journal of Molecular Biology 288, 911-940.

Matranga, V., Pinsino, A., Celi, M., Di Bella, G., Natoli, A., 2006. Impacts of UV-B radiation on short-term cultures of sea urchin coelomocytes. Marine Biology 149 (1), 25-34.

Matranga, V., Pinsino, A., Celi, M., Natoli, A., Bonaventura, R., Schröder, H.C., Müller, W.E.G., 2005. Monitoring chemical and physical stress using sea urchin immune cells. In: Matranga, V. (Ed.), Echinodermata. Springer-Verlag, Berlin, pp. 85-110.

Matranga, V., Toia, G., Bonaventura, R., Müller, W.E.G., 2000. Cellular and biochemical responses to environmental and experimentally induced stress in sea urchin coelomocytes. Cell Stress and Chaperones 5 (2), 113-120.

Maurer, D., Nguyen, H., 1996. The brittlestar *Amphiodia urtica*: a candidate bioindicator? Marine Ecology 17 (4), 617-636.

Mayer, M., Bukau, B., 2005. Hsp70 chaperones: cellular functions and molecular mechanism. Cellular and Molecular Life Sciences 62 (6), 670-684.

McDonald, J.H., 2009. Handbook of Biological Statistics (2nd ed.). Sparky House Publishing, Baltimore, Maryland.

McKay, D.B., Wilbanks, S.M., Flaherty, K.M., Ha, J.-H., O'Brien, M.C., Shirvanee, L.L., 1994. Stress-70 proteins and their interaction with nucleotides. In: Morimoto, R.I., Tissières, A., Georgopoulos, C. (Eds.), The Biology of Heat Shock Proteins and Molecular Chaperones. Cold Spring Harbor Laboratory Press, New York, pp. 153-177.

McPherson, M.J., Jones, K.M., Gurr, S.J., 1991. PCR with highly degenerate primers. In: McPherson, M.J., Quirke, P., Taylor, G.R. (Eds.), PCR: A Practical Approach. Oxford University Press, Oxford.

Melton, H.R., Smith, J.P., Martin, C.R., Nedwed, T.J., Mairs, H.L., Raught, D.L., 2000. Offshore discharge of drilling fluids and cuttings - a scientific perspective on public policy. Rio Oil and Gas Expo and Conference, Rio De Janeiro, Brazil.

Meng, X.., Ji, T.., Dong, Y., Wang, Q., Dong, S., 2009. Thermal resistance in sea cucumbers (*Apostichopus japonicus*) with differing thermal history: The role of Hsp70. Aquaculture 294, 314-318.

Menzies, R.J., 1965. Conditions for the existence of life on the abyssal sea floor. Oceanography and marine biology: an annual review 3, 195-210.

Metzenberg, S., 2007. The polymerase chain reaction. In: Metzenberg, S. (Ed.), Working with DNA. Taylor and Francis Group, Abingdon, pp. 291-374.

Metzker, M.L., 2005. Emerging technologies in DNA sequencing. Genome Research 15 (12), 1767-1776.

Meyer, E., Green, A.J., Moore, M., Manahan, D.T., 2007. Food availability and physiological state of sea urchin larvae (*Strongylocentrotus purpuratus*). Marine Biology 152 (1), 179-191.

Micael, J., Alves, M.J., Costa, A.C., Jones, M.B., 2009. Exploitation and conservation of echinoderms. Oceanography and marine biology: an annual review 47, 191-208.

Mickel, T.J., Childress, J.J., 1982. Effects of pressure and temperature on the EKG and heart rate of the

hydrothermal vent crab *Bythograea thermydron* (Brachyura). Biological Bulletin 162 (1), 70-82.

Miles, H., Widdicombe, S., Spicer, J.I., Hall-Spencer, J., 2007. Effects of anthropogenic seawater acidification on acid-base balance in the sea urchin *Psammechinus miliaris*. Marine Pollution Bulletin 54 (1), 89-96.

Miller, E.K., Raese, J.D., Morrison-Bogorad, M., 1991. Expression of heat shock protein 70 and heat shock cognate 70 messenger RNAs in rat cortex and cerebellum after heat shock or amphetamine treatment. Journal of Neurochemistry 56 (6), 2060-2071.

Miller, J.E., Pawson, D.L., 1990. Swimming sea cucumbers (Echinodermata: Holothuroidea); a survey with analysis of swimming behavior in four bathyal species. Smithsonian Contributions to the Marine Sciences (35), 1-18.

Minois, N., 2000. Longevity and aging: beneficial effects of exposure to mild stress. Biogerontology 1 (1), 15-29.

Moore, H.M., Roberts, D., Harriott, M., Burns, D.T., 1997. Holothurians - potential biomonitors for metal levels in deep-sea sediments. Fresenius' Journal of Analytical Chemistry 358 (5), 652-655.

Morimoto, R.I., 1993. Cells in stress: transcriptional activation of heat shock genes. Science 259 (5100), 1409-1410.

Morimoto, R.I., Tissières, A., Georgopoulos, C., 1994. Progress and perspectives on the biology of heat shock proteins and molecular chaperones. In: Morimoto, R.I., Tissières, A., Georgopoulos, C. (Eds.), The Biology of Heat Shock Proteins and Molecular Chaperones. Cold Spring Harbor Laboratory Press, New York, pp. 1-30.

Morita, T., 2003. Structure-based analysis of high pressure adaptation of α-actin. Journal of Biological Chemistry 278 (30), 28060-28066.

Morita, T., 2008. Comparative sequence analysis of myosin heavy chain proteins from congeneric shallow- and deep-living rattail fish (genus *Coryphaenoides*). Journal of Experimental Biology 211 (9), 1362-1367.

Mormede, S., Davies, I.M., 2001. Polychlorobiphenyl and pesticide residues in monkfish *Lophius piscatorius* and black scabbard *Aphanopus carbo* from the Rockall Trough. ICES Journal of Marine Science 58 (3), 725-736.

Mormede, S., Davies, I.M., 2003. Horizontal and vertical distribution of organic contaminants in deep-sea fish species. Chemosphere 50 (4), 563-574.

Morris, S., Taylor, A.C., 1983. Diurnal and seasonal variation in physico-chemical conditions within intertidal rock pools. Estuarine, Coastal and Shelf Science 17 (3), 339-355.

Mosholder, R., RV, J., Phleger, C., 1979. Swimbladder membrane protein of an abyssal fish, *Coryphaenoides acrolepis*. Physiological Chemistry and Physics 11 (1), 37-47.

Mozhaev, V.V., Balny, C., Heremans, K., Frank, J., Masson, P., 1996. High pressure effects on protein structure and function. Proteins: Structure, Function and Genetics 24 (1), 81-91.

Mukhopadhyay, I., Nazir, A., Saxena, D.K., Kar Chowdhuri, D., 2003. Heat shock response: hsp70 in environmental monitoring. Journal of Biochemical and Molecular Toxicology 17 (5), 249-254.

Müller-Taubenberger, A., Hagmann, J., Noegel, A., Gerisch, G., 1988. Ubiquitin gene expression in D*ictyostelium* is induced by heat and cold shock, cadmium, and inhibitors of protein synthesis. Journal of Cell Science 90, 51-58.

Murty, S.J., Bett, B., Gooday, A., 2009. Megafaunal responses to strong oxygen gradients on the Pakistan margin of the Arabian Sea. Deep-Sea Research Part II: Topical Studies in Oceanography 56, 472-487.

Mykles, D.L., Ghalambor, C.K., Stillman, J.H., Tomanek, L., 2010. Grand challenges in comparative physiology: integration across disciplines and across levels of biological organization. Integrative and Comparative Biology icq015 1-11.

Neff, J.M., 2005. Composition, environmental fates, and biological effects of water based drilling muds and cuttings discharged to the marine environment: a synthesis and annotated bibliography. Prepared for the Petroleum Environmental Research Forum (PERF) and American Petroleum Institute. pp 73.

Neff, J.M., McKelvie, S., Ayers, R., 2000. Environmental impacts of synthetic based drilling fluids. U.S. Department of the Interior Minerals Management Service GOM OCS Region New Orleans, LA., p. 118.

Nemer, M., Rondinelli, E., Infante, D., Infante, A.A., 1991. Polyubiquitin RNA characteristics and conditional induction in sea-urchin embryos. Developmental Biology 145 (2), 255-265.

Netto, S.A., Gallucci, F., Fonseca, G., 2009. Deep-sea meiofauna response to synthetic-based drilling mud discharge off SE Brazil. Deep-Sea Research Part II: Topical Studies in Oceanography 56 (1-2), 41-49.

Newton, L.C., McKenzie, J.D., 1995. Echinoderms and oil pollution: a potential stress assay using bacterial symbionts. Marine Pollution Bulletin 31 (4-12), 453-456.

Newton, L.C., McKenzie, J.D., 1996. Development and evaluation of echinoderm pollution assays. In: Mooi, R., Telford, M. (Eds.), Proceedings of the Ninth International Echinoderm Conference. A.A. Balkema, San Francisco, California, USA, pp. 405-410.

Newton, L.C., McKenzie, J.D., 1998. Brittlestars, biomarkers and beryl: assessing the toxicity of oil-based drill cuttings using laboratory, mesocosm and field studies. Chemistry and Ecology 14-15 (1-4), 533-545.

Niedzwiecki, A., Fleming, J.E., 1993. Heat shock induces changes in the expression and binding of ubiquitin in senescent *Drosophila melanogaster*. Developmental Genetics 14 (1), 78-86.

Nikinmaa, M., Schlenk, D., 2010. Genomics in aquatic toxicology. Aquatic Toxicology 97 (3), 173-173.

Nolan, T., 2007. Deriving a troubleshooting protocol. Sigma-Aldrich QPCR Total Solution Seminar Series.

Nolan, T., Hands, R.E., Bustin, S.A., 2006. Quantification of mRNA using real-time RT-PCR. Nature Protocols 1 (3), 1559-1582.

Nordberg, K., Gustafsson, M., Krantz, A.-L., 2000. Decreasing oxygen concentrations in the Gullmar Fjord, Sweden, as confirmed by benthic foraminifera, and the possible association with NAO. Journal of Marine Systems 23 (4), 303-316.

Noventa-Jordão, M., do Nascimento, A., Goldman, M., Terenzi, H., Goldman, G., 2000. Molecular characterization of ubiquitin genes from *Aspergillus nidulans*: mRNA expression on different stress and growth conditions. Biochimica et Biophysica Acta - Gene Structure and Expression 1490 (3), 237-244.

O'Clair, C.E., Rice, S.D., 1985. Depression of feeding and growth rates of the seastar *Evasterias troshelii* during long-term exposure to the water-soluble fraction of crude oil. Marine Biology 84, 331-340.

O'Donnell, M.J., Todgham, A.E., Sewell, M.A., Hammond, L.M., Ruggiero, K., Fangue, N.A., Zippay, M.L., Hofmann, G.E., 2010. Ocean acidification alters skeletogenesis and gene expression in larval sea urchins. Marine Ecology-Progress Series 398, 157-171.

OECS, 2002a. OECS Safety Information Data Sheet. Initial Assessment Report. Sodium hydroxide. CAS 1310-73-2. Organisation for Economic Co-operation and Development. UNEP. pp. 112.

OECS, 2002b. OECS Safety Information Data Sheet. Initial Assessment Report. Sodium carbonate. CAS 497-19-8. Organisation for Economic Co-operation and Development. UNEP. pp. 112.

Ojima, N., Yamashita, M., Watabe, S., 2005. Quantitative mRNA expression profiling of heat-shock protein families in rainbow trout cells. Biochemical & Biophysical Research Communications 329, 51-57.

Okabayashi, K., Nakano, E., 1978. Enzymes of the tricarboxylic acid cycle in sea urchin eggs and embryos. Development Growth & Differentiation 20 (2), 115-123.

Olsgard, F., Gray, J.S., 1995. A comprehensive analysis of the effects of offshore oil and gas exploration and production on the benthic communities of the Norwegian continental shelf. Marine Ecology Progress Series 122 (1-3), 277-306.

Ordzie, C.J., Garofalo, G.C., 1981. Lethal and sublethal effects of short term acute doses of Kuwait crude oil and a dispersant Corexit 9527 on bay scallops, *Argopecten irradians* (Lamarck) and two predators at different temperatures. Marine Environmental Research 5, 195-210.

Osovitz, C.J., Hofmann, G.E., 2005. Thermal history-dependent expression of the hsp70 gene in purple sea urchins: biogeographic patterns and the effect of temperature acclimation. Journal of Experimental Marine Biology and Ecology 327 (2), 134-143.

OSPAR Commission, 2001. Environmental aspects of on and off-site injection of drill cuttings and produced water. Best Available Techniques (BAT) and Best Environmental Practice (BEP) Series. Oslo–Paris Commission. pp. 33.

OSPAR Commission, 2005. Protocols on Methods for the Testing of Chemicals Used in the Offshore Oil Industry. Offshore Industry Series. Publication Number: 2005/237. Oslo–Paris Commission, pp 26.

OSPAR Commission, 2009. Assessment of impacts of offshore oil and gas activities in the North-East Atlantic. Offshore Industry Series Report No. 453. pp 40.

Oweson, C., Skold, H., Pinsino, A., Matranga, V., Hernroth, B., 2008. Manganese effects on haematopoietic cells and circulating coelomocytes of *Asterias rubens* (Linnaeus). Aquatic Toxicology 89 (2), 75-81.

Özkaynak, E., Finley, D., Varshavsky, A., 1984. The yeast ubiquitin gene: head-to-tail repeats encoding a polyubiquitin precursor protein. Nature 312, 663-666.

Ozsolak, F., Platt, A.R., Jones, D.R., Reifenberger, J.G., Sass, L.E., McInerney, P., Thompson, J.F., Bowers, J., Jarosz, M., Milos, P.M., 2009. Direct RNA sequencing. Nature 461 (7265), 814-818.

Parag, H., Raboy, B., Kulka, R., 1987. Effect of heat shock on protein degradation in mammalian cells: involvement of the ubiquitin system. The European Molecular Biology Organisation Journal 6 (1), 55–61.

Park, H., Ahn, I.-Y., Lee, H.E., 2007. Expression of heat shock protein 70 in the thermally stressed Antarctic clam *Laternula elliptica*. Cell Stress & Chaperones 12 (3), 275–282.

Parsell, D.A., Lindquist, S., 1994. Heat shock proteins and stress tolerance. In: Morimoto, R.I., Tissières, A., Georgopoulos, C. (Eds.), The Biology of Heat Shock Proteins and Molecular Chaperones. Cold Spring Harbor Laboratory Press, New York, pp. 457-494.

Paterson, G.L.J., 1985. The deep-sea Ophiuroidea of the North Atlantic Ocean. Bulletin of the British Museum (Natural History) Zoology Series 49 (1), 1-162.

Patruno, M., Thorndyke, M., Candia Carnevali, M., Bonasoro, F., Beesley, P., 2001a. Growth factors, heat-shock proteins and regeneration in echinoderms. Journal of Experimental Biology 204 (5), 843-848.

Patruno, M., Thorndyke, M.C., Carnevali, M.D., Bonasoro, F., Beesley, P., 2001b. Changes in ubiquitin conjugates and Hsp72 levels during arm regeneration in echinoderms. Marine Biotechnology 3 (1), 4-15.

Pattenden, A.C.D., 2009. The influence of submarine canyons on the structure and dynamics of megafaunal communities. PhD Thesis, School of Ocean and Earth Science, University of Southampton, Southampton, UK. pp. 184.

Pearse, J., Lockhart, S., 2004. Reproduction in cold water: paradigm changes in the 20th century and a role for cidaroid sea urchins. Deep Sea Research Part II: Topical Studies in Oceanography 51, 1533-1549.

Perelygin, A.A., Kondrashov, F.A., Rogozin, I.B., Brinton, M.A., 2002. Evolution of the mouse polyubiquitin-C gene. Journal of Molecular Evolution 55 (2), 202-210.

Peterson, C.H., Kennicutt II, M.C., Green, R.H., Montagna, P., Harper Jr., D.E., Powell, E.N., Roscigno, P.F., 1996. Ecological consequences of environmental perturbations associated with offshore hydrocarbon production: a perspective on long-term exposures in the Gulf of Mexico. Canadian Journal of Fisheries and Aquatic Sciences 53 (11), 2637-2654.

Pettingill, H.S., Weimer, P., 2002. Worlwide deepwater exploration and production: past, present, and future. The Leading Edge 21 (4), 371-376.

Pfaffl, M.W., 2007. Influence of RNA integrity on real-time RT-PCR quantification data., Sigma-Aldrich QPCR Total Solution Seminar Series.

Pfanner, N., 2000. Protein sorting: recognizing mitochondrial presequences. Current Biology 10 (11), R412-R415.

Pfannkuche, O., Camerlenghi, A., Canals, M., Cochonat, P., Diepenbroek, M., Grand, P., Heip, C., Kopf, A., Lampitt, R., et al., 2009. The deep-sea frontier: sustainable use of Europe´s deep-sea resources. Scientific needs and strategies. Foresight document DSF Workshop 25 May 2009 Brussels. pp. 20.

Phillips, D., 1980. Quantitative aquatic biological indicators. Applied Science Publishers Ltd., London.

Phleger, C.F., McConnaughey, R.R., Crill, P., 1979. Hyperbaric fish trap operation and deployment in the deep sea. Deep-Sea Research Part A. Oceanographic Research Papers 26 (12), 1405-1409.

Piano, A., Asirelli, C., Caselli, F., Fabbri, E., 2002. Hsp70 expression in thermally stressed *Ostrea edulis*, a commercially important oyster in Europe. Cell Stress and Chaperones 7 (3), 250-257.

Piano, A., Franzellitti, S., Tinti, F., Fabbri, E., 2005. Sequencing and expression pattern of inducible heat shock gene products in the European flat oyster, *Ostrea edulis*. Gene 361, 119-126.

Pickart, C.M., 2001. Mechanisms underlying ubiquitination. Annual Review of Biochemistry 70, 503-533.

Pickart, C.M., Summers, R.G., Shim, H., Kasperek, E.M., 1991. Dynamics of ubiquitin pools in developing sea urchin embryos. Development, Growth & Differentiation 33 (6), 587-598.

Piepenburg, D., 2000. Arctic brittle stars (Echinodermata: Ophiuroidea). Oceanography and marine biology: an annual review 38, 189-256.

Pinsino, A., Della Torre, C., Sammarini, V., Bonaventura, R., Amato, E., Matranga, V., 2008. Sea urchin coelomocytes as a novel cellular biosensor of environmental stress: a field study in the Tremiti Island Marine Protected Area, Southern Adriatic Sea, Italy. Cell Biology and Toxicology.

Pinsino, A., Thorndyke, M.C., Matranga, V., 2007. Coelomocytes and post-traumatic response in the common sea star *Asterias rubens*. Cell Stress & Chaperones 12 (4), 331-341.

Plaxton, W.C., 2004. Principles of metabolic control. In: Storey, K.B. (Ed.), Functional Metabolism. Regulation and Adaptation. Wiley-Liss, Inc., Hoboken, NJ, USA., pp. 1-24.Accessed at http://books.google.co.uk/.

Pollino, C.A., Holdway, D.A., 2003. Hydrocarbon-induced changes to metabolic and detoxification enzymes of the Australian crimson-spotted rainbowfish (*Melanotaenia fluviatilis*). Environmental Toxicology 18 (1), 21-28.

Ponchel, F., 2006. Real-time PCR using SYBR® Green. In: Tevfik Dorak, M. (Ed.), Real-time PCR. Taylor and Francis, Abingdon, pp. 139-154.

Pörtner, H., Peck, L., Somero, G., 2007. Thermal limits and adaptation in marine Antarctic ectotherms: an integrative view. Philosophical Transactions of the Royal Society B: Biological Sciences 362, 2233-2258.

Pradet-Balade, B., Boulmé, F., Beug, H., Müllner, E.W., Garcia-Sanz, J.A., 2001. Translation control: bridging the gap between genomics and proteomics? Trends in Biochemical Sciences 26 (4), 225-229.

Pradillon, F., Gaill, F., 2007. Pressure and life: some biological strategies. Reviews in Environmental Science and Biotechnology 6 (1), 181-195.

Pruski, A.M., Dixon, D.R., 2007. Heat shock protein expression pattern (HSP70) in the hydrothermal vent mussel *Bathymodiolus azoricus*. Marine Environmental Research 64 (2), 209-224.

QIAGEN, 2006. Critical factors for successful RT PCR [Online]. Available from: http://www1.qiagen.com/literature/render.aspx?id=23490 [accessed 2007, July 1].

Raimondi, P.T., Barnett, A.M., Krause, P.R., 1997. The effects of drilling muds on marine invertebrate larvae and adults. Environmental Toxicology and Chemistry 16 (6), 1218-1228.

Ravaux, J., Cottin, D., Chertemps, T., Hamel, G., Shillito, B., 2009. Hydrothermal vent shrimps display

low expression of the heat-inducible hsp70 gene in nature. Marine Ecology Progress Series 396, 153-156.

Ravaux, J., Toullec, J.Y., Léger, N., Lopez, P., Gaill, F., Shillito, B., 2007. First hsp70 from two hydrothermal vent shrimps, *Mirocaris fortunata* and *Rimicaris exoculata*: characterization and sequence analysis. Gene 386 (1-2), 162-172.

Raymond, E.H., Widder, E.A., 2007. Behavioral responses of two deep-sea fish species to red, far-red, and white light. Marine Ecology Progress Series 350, 291-298.

Reinartz, J., Bruyns, E., Lin, J.-Z., Burcham, T., Brenner, S., Bowen, B., Kramer, M., Woychik, R., 2002. Massively parallel signature sequencing (MPSS) as a tool for in-depth quantitative gene expression profiling in all organisms. Briefings in Functional Genomics and Proteomics 1 (1), 95-104.

Remington, S., Wiegand, G., Huber, R., 1982. Crystallographic refinement and atomic models of two different forms of citrate synthase at 2·7 & 1·7 Å resolution. Journal of Molecular Biology 158, 111-152.

Remington, S.J., 1992. Structure and mechanism of citrate synthase. Current topics in cellular regulation 33, 209-229.

Rensing, S.A., Maier, U.G., 1994. Phylogenetic analysis of the stress-70 protein family. Journal of Molecular Evolution 39 (1), 80-86.

Richter, T.O., de Stigter, H.C., Boer, W., Jesus, C.C., van Weering, T.C.E., 2009. Dispersal of natural and anthropogenic lead through submarine canyons at the Portuguese margin. Deep Sea Research Part I: Oceanographic Research Papers 56 (2), 267-282.

Rieley, G., Van Dover, C.L., Eglinton, G., 1997. Fatty acids as sensitive tracers of sewage sludge carbon in a deep-sea ecosystem. Environmental Science & Technology 31 (4), 1018-1023.

RIKZ, 1999. The 14d Marine Urchin *Echinocardium cordatum* Mortality and Behaviour Sediment Toxicity Test. National Institute for Coastal and Marine Management/RIKZ. Standard Operating Procedures Nr: SPECIE-03.

Ririe, K.M., Rasmussen, R.P., Wittwer, C.T., 1997. Product differentiation by analysis of DNA melting curves during the polymerase chain reaction. Analytical Biochemistry 245 (2), 154-160.

Ritter, L., Solomon, K.R., Forget, J., Stemeroff, M., O'Leary, C., 1996. Persistent organic pollutants. The International Programme on Chemical Safety (IPCS) within the framework of the Inter-Organization Programme for the Sound Management of Chemicals (IOMC). pp 43.

Roberts, C.M., 2002. Deep impact: the rising toll of fishing in the deep sea. Trends in Ecology & Evolution 17 (5), 242-245.

Rodrigues, N., Sharma, R., Nagender Nath, B., 2001. Impact of benthic disturbance on megafauna in Central Indian Basin. Deep-Sea Research Part II: Topical Studies in Oceanography 48 (16), 3411-3426.

Rogers, A., 2000. The role of the oceanic oxygen minima in generating biodiversity in the deep sea. Deep-Sea Research Part II: Topical Studies in Oceanography 47, 119-148.

Rogers, B.L., Lowe, C.G., Fernández-Juricic, E., Frank, L.R., 2008. Utilizing magnetic resonance imaging (MRI) to assess the effects of angling-induced barotrauma on rockfish (*Sebastes*). Canadian Journal of Fisheries and Aquatic Sciences 65 (7), 1245-1249.

Rogers, C.S., 1990. Responses of coral reefs and reef organisms to sedimentation. Marine Ecology Progress Series 62 (1-2), 185-202.

Ronaghi, M., Uhlen, M., Nyren, P., 1998. A sequencing method based on real-time pyrophosphate. Science 281 (5375), 363-365.

Ross, K.A., Thorpe, J.P., Brand, A.R., 2004. Biological control of fouling in suspended scallop cultivation. Aquaculture 229 (1-4), 99-116.

Rotllant, G., Abad, E., Sardà, F., Ábalos, M., Company, J.B., Rivera, J., 2006. Dioxin compounds in the deep-sea rose shrimp *Aristeus antennatus* (Risso, 1816) throughout the Mediterranean Sea. Deep-Sea Research Part I: Oceanographic Research Papers 53 (12), 1895-1906.

Rozen, S., Skaletsky, H.J., 2000. Primer3 on the WWW for general users and for biologist programmers. In: Krawetz, S., Misener, S. (Eds.), Bioinformatics Methods and Protocols: Methods in Molecular Biology. Humana Press, Totowa, NJ, pp. 365-386.

Ruhl, H.A., 2007. Abundance and size distribution dynamics of abyssal epibenthic megafauna in the northeast Pacific. Ecology 88 (5), 1250-1262.

Russell, R.J.M., Hough, D.W., Danson, M.J., Taylor, G.L., 1994. The crystal structure of citrate synthase from the thermophilic Archaeon, *Thermoplasma acidophilum*. Structure 2 (12), 1157-1167.

Rychlik, W., 2000. Primer selection and design for polymerase chain reaction. In: Rapley, R. (Ed.), The Nucleic Acid Protocols Handbook. Humana Press, Totowa, NJ, pp. 581-588.

Ryder, K., Temara, A., Holdway, D.A., 2004. Avoidance of crude-oil contaminated sediment by the Australian seastar, *Patiriella exigua* (Echinodermata: Asteroidea). Marine Pollution Bulletin 49, 900-909.

Sambrook, J., Russell, D.W., 2001. Molecular Cloning: A Laboratory Manual. Third Edition. Cold Spring Harbor Laboratory Press, Cold Spring Harbour, New York.

Samerotte, A.L., Drazen, J.C., Brand, G.L., Seibel, B.A., Yancey, P.H., 2007. Correlation of trimethylamine oxide and habitat depth within and among species of teleost fish: an analysis of causation. Physiological and Biochemical Zoology 80 (2), 197-208.

Sanders, B.M., 1993. Stress proteins in aquatic organisms: an environmental perspective. Critical Reviews in Toxicology 23 (1), 49-75.

Santos, M.F.L., Lana, P.C., Silva, J., Fachel, J.G., Pulgati, F.H., 2009. Effects of non-aqueous fluids cuttings discharge from exploratory drilling activities on the deep-sea macrobenthic communities. Deep-Sea Research Part II: Topical Studies in Oceanography 56 (1-2), 32-40.

Sayle, S., Seymour, M., Hickey, E., 2002. Assessment of Environmental Impacts from Drilling Muds and Cuttings Disposal, Offshore Brunei. International Conference on Health, Safety and Environment in Oil and Gas Exploration and Production, Kuala Lumpur, pp. 477-489.

Schaanning, M.T., Trannum, H.C., Øxnevad, S., Carroll, J., Bakke, T., 2008. Effects of drill cuttings on biogeochemical fluxes and macrobenthos of marine sediments. Journal of Experimental Marine Biology and Ecology 361 (1), 49-57.

Schaefer, B.C., 1995. Revolutions in rapid amplification of cDNA ends: new strategies for polymerase chain reaction cloning of full-length cDNA ends. Analytical Biochemistry 227 (2), 255-273.

Schäefer, S., Köehler, A., 2009. Gonadal lesions of female sea urchin (*Psammechinus miliaris*) after exposure to the polycyclic aromatic hydrocarbon phenanthrene. Marine Environmental Research 68 (3), 128-136.

Schäffer, A.A., Aravind, L., Madden, T.L., Shavirin, S., Spouge, J.L., Wolf, Y.I., Koonin, E.V., Altschul, S.F., 2001. Improving the accuracy of PSI-BLAST protein database searches with composition-based statistics and other refinements. Nucleic Acids Research 29 (14), 2994-3005.

Schena, M., Shalon, D., Davis, R.W., Brown, P.O., 1995. Quantitative monitoring of gene-expression patterns with a complementary-DNA microarray. Science 270 (5235), 467-470.

Scherle, W., 1970. A simple method for volumetry of organs in quantitative stereology. Mikroskopic 26, 57-60.

Schipper, C.A., Dubbeldam, M., Feist, S.W., Rietjens, I.M.C.M., Murk, A.T., 2008. Cultivation of the heart urchin *Echinocardium cordatum* and validation of its use in marine toxicity testing for environmental risk assessment. Journal of Experimental Marine Biology and Ecology 364 (1), 11-18.

Schmid, M.K., 1996. On the distribution and oxygen consumption of ecologically important benthic animals in the waters around Svalbard (Arctic). Berichte zur Polarforschung 202, 1-93.

Schmidt-Nielsen, K., 1981. Animal physiology: adaptation and environment. Cambridge University Press, Cambridge. pp. 560.

Schmidt, S., de Stigter, H.C., van Weering, T.C.E., 2001. Enhanced short-term sediment deposition within the Nazaré Canyon, North-East Atlantic. Marine Geology 173 (1-4), 55-67.

Schröder, H.C., Di Bella, G., Janipour, N., Bonaventura, R., Russo, R., Müller, W.E.G., Matranga, V., 2005. DNA damage and developmental defects after exposure to UV and heavy metals in sea urchin cells and embryos compared to other invertebrates. Progress in Molecular and Subcellular Biology 39, 111-137.

Sconzo, G., Scardina, G., Grazia Ferraro, M., 1992. Characterization of a new member of the sea urchin *Paracentrotus lividus* hsp70 gene family and its expression. Gene 121 (2), 353-358.

SCOPAC, 2003. SCOPAC Standing Conference on Problems Associated with the Coastline. Sediment Transport Database. Lyme Bay and SE Devon Sediment Transport Study, Berry Head to Hope's Nose, Tor Bay.

Sea Urchin Genome Sequencing Consortium, 2006. The genome of the sea urchin *Strongylocentrotus purpuratus*. Science 314 (5801), 941-952.

Sébert, P., 2002. Fish at high pressure: a hundred year history. Comparative Biochemistry and Physiology - A Molecular and Integrative Physiology 131 (3), 575-585.

Seibel, B.A., 2007. On the depth and scale of metabolic rate variation: scaling of oxygen consumption rates and enzymatic activity in the Class Cephalopoda (Mollusca). Journal of Experimental Biology 210 (1), 1-11.

Seibel, B.A., Childress, J.J., 2000. Metabolism of benthic octopods (Cephalopoda) as a function of habitat depth and oxygen concentration. Deep-Sea Research Part I: Oceanographic Research Papers 47 (7), 1247-1260.

Seibel, B.A., Drazen, J.C., 2007. The rate of metabolism in marine animals: environmental constraints, ecological demands and energetic opportunities. Philosophical Transactions of the Royal Society B: Biological Sciences 362 (1487), 2061-2078.

Seibel, B.A., Walsh, P.J., 2003. Biological impacts of deep-sea carbon dioxide injection inferred from indices of physiological performance. Journal of Experimental Biology 206, 641-650.

Sharp, F.R., Massa, S.M., Swanson, R.A., 1999. Heat-shock protein protection. Trends in Neurosciences 22 (3), 97-99.

Shih, S., Prag, G., Francis, S., Sutanto, M., Hurley, J., Hicke, L., 2003. A ubiquitin-binding motif required for intramolecular monoubiquitylation, the CUE domain. The EMBO Journal 22 (6), 1273-1281.

Shillito, B., Hamel, G., Duchi, C., Cottin, D., Sarrazin, J., Sarradin, P.M., Ravaux, J., Gaill, F., 2008. Live capture of megafauna from 2300 m depth, using a newly designed Pressurized Recovery Device. Deep-Sea Research Part I. Oceanographic Research Papers 55 (7), 881-889.

Shillito, B., Le Bris, N., Hourdez, S., Ravaux, J., Cottin, D., Caprais, J-C., Jollivet, D., Gaill, F., 2006. Temperature resistance studies on the deep-sea vent shrimp *Mirocaris fortunata*. J Exp Biol 209, 945-955.

Shipley, G.L., 2006. An introduction to real-time PCR. In: Tevfik Dorak, M. (Ed.), Real-time PCR. Taylor and Francis, Abingdon, pp. 1-37.

Siebenaller, J.F., Garrett, D., 2002. The effects of the deep-sea environment on transmembrane signaling. Comparative Biochemistry and Physiology - B Biochemistry and Molecular Biology 131 (4), 675-694.

Siebenaller, J.F., Somero, G.N., 1989. Biochemical adaptation to the deep sea. Reviews in Aquatic Sciences, pp. 1-27.

Sigma-Aldrich Inc., 2008. qPCR Technical Guide. http://www.sigmaaldrich.com/etc/medialib/docs/Sigma/General_Information/qpcr_technical_guide.pdf.

Silva, J.R.M.C., Peck, L., 2000. Induced in vitro phagocytosis of the Antarctic starfish *Odontaster validus* (Koehler 1906) at 0°C. Polar Biology 23, 225-230.

Simonato, F., Campanaro, S., Lauro, F.M., Vezzi, A., D'Angelo, M., Vitulo, N., Valle, G., Bartlett, D.H., 2006. Piezophilic adaptation: a genomic point of view. Journal of Biotechnology 126 (1), 11-25.

Sladen, W.P., 1889. Zoology LI. Report on the Asteroidea (Starfish) collected by H.M.S. *Challenger* during the years 1873-1876. Report on the scientific results of the voyage of H.M.S. *Challenger* during the years 1873-76. 30, 1-935.

Smale, S.T., Kadonaga, J.T., 2003. The RNA polymerase II core promoter. Annual Review of Biochemistry 72 (1), 449-479.

Smith, C.R., De Leo, F.C., Bernardino, A.F., Sweetman, A.K., Arbizu, P.M., 2008a. Abyssal food limitation, ecosystem structure and climate change. Trends in Ecology & Evolution 23 (9), 518-528.

Smith, C.R., Hamilton, S.C., 1983. Epibenthic megafauna of a bathyal basin off southern California: patterns of abundance, biomass, and dispersion. Deep-Sea Research 30, 907–928.

Smith, C.R., Levin, L.A., Hoover, D.J., McMurtry, G., Gage, J.D., 2000. Variations in bioturbation across the oxygen minimum zone in the northwest Arabian Sea. Deep-Sea Research Part II: Topical Studies in Oceanography 47 (1-2), 227-257.

Smith, C.R., Levin, L.A., Koslow, A., Tyler, P.A., Glover, A.G., 2008b. The near future of the deep seafloor ecosystems. In: Polunin, N. (Ed.), Aquatic Ecosystems: Trends and Global Prospects. Cambridge University Press, pp. 334-351.

Smith, J.E., et al,, 1968. Shore surveys - rocky shores. In: Smith, J.E. (Ed.), 'Torrey Canyon' pollution and marine life. A report by the Plymouth Laboratory of the Marine Biological Association of the United Kingdom. Cambridge University Press, Cambridge (UK), pp. 36-74.

Smith, K.L., 1985b. Deep-sea hydrothermal vent mussels: nutritional state and distribution at the Galapagos Rift. Ecology 66 (3), 1067-1080.

Smith, K.L., Jr., 1978. Metabolism of the abyssopelagic rattail *Coryphaenoides armatus* measured in situ. Nature 274 (5669), 362-364.

Smith, K.L., Jr., 1982. Zooplankton of a bathyal benthic boundary layer: in situ rates of oxygen consumption and ammonium excretion. Limnology and Oceanography 27 (3), 461-471.

Smith, K.L., Jr., 1983. Metabolism of two dominant epibenthic echinoderms measured at bathyal depths on the Santa Catalina Basin. Marine Biology 72, 249-256.

Smith, K.L., Jr., 1985a. Macrozooplankton of a deep sea hydrothermal vent: in situ rates of oxygen consumption. Limnology and Oceanography 30 (1), 102-110.

Smith, K.L., Jr., Baldwin, R.J., 1982. Scavenging deep-sea amphipods: effects of food odor on oxygen consumption and a proposed metabolic strategy. Marine Biology 68 (3), 287-298.

Smith, K.L., Jr., Baldwin, R.J., 1983. Deep-sea respirometry: in situ techniques. In: Gnaiger, E., Forstner, H. (Eds.), Polarographic Oxygen Sensors. Springer-Verlag, Berlin, pp. 298-320.

Smith, K.L., Jr., Baldwin, R.J., 1997. Laboratory and *in situ* methods for studying deep-sea fishes. In: Randall, D.J., Farrell, A.P. (Eds.), Fish Physiology (Volume 16), Deep Sea Fishes. Academic Press, San Diego, CA pp. 351-378.

Smith, K.L., Jr., Hessler, R.R., 1974. Respiration of benthopelagic fishes: in situ measurements at 1230 meters. Science 184 (4132), 72-73.

Smith, K.L., Jr., Laver, M.B., 1981. Respiration of the bathypelagic fish *Cyclothone acclinidens.* Marine Biology 61 (4), 261-266.

Smith, K.L., Jr., Ruhl, H., Bett, B., Billett, D., Lampitt, R., Kaufmann, R., 2009. Climate, carbon cycling, and deep-ocean ecosystems. Proceedings of the National Academy of Sciences 106 (46), 19211-19218.

Smith, K.L., Jr., White, G.A., 1997. Ecological energetic studies in the deep-sea benthic boundary layer: in situ respiration studies. In: Randall, D.J., Farrell, A.P. (Eds.), Deep-sea Fishes. Academic Press Limited, London, pp. 351-378.

Smith, L.C., Rast, J.P., Brockton, V., Terwilliger, D.P., Nair, S.V., Buckley, K.M., Majeske, A.J., 2006. The sea urchin immune system. Invertebrate Survival Journal 3, 25-39.

Smith, V.J., 1981. The echinoderms. In: Ratcliffe, N.A., Rowley, A.T. (Eds.), Invertebrate blood cells. Academic Press, London, pp. 513-562.

Snape, J.R., Maund, S.J., Pickford, D.B., Hutchinson, T.H., 2004. Ecotoxicogenomics: the challenge of integrating genomics into aquatic and terrestrial ecotoxicology. Aquatic Toxicology 67 (2), 143-154.

Snell, T.W., Brogdon, S.E., Morgan, M.B., 2003. Gene expression profiling in ecotoxicology. Ecotoxicology 12 (6), 475-483.

Solís-Marín, F.A., 2003. Systematics and phylogeny of the holothurian family Synallactidae. PhD Thesis, School of Ocean and Earth Science, University of Southampton, Southampton. pp. 356.

Somero, G.N., 1991. Hydrostatic pressure and adaptations to the deep sea. In: Prosser, C.L. (Ed.), Environmental and Metabolic Animal Physiology. Wiley-Liss, Inc., New York, pp. 167-204.

Somero, G.N., 1992. Adaptations to high hydrostatic pressure. Annual Review of Physiology 54, 557-577.

Somero, G.N., 1998. Adaptation to cold and depth: contrasts between polar and deep-sea animals. In: Portner, H., Playle, R.(Eds.), Cold Ocean Physiology. Cambridge University Press, Cambridge, pp. 33-57.

Somero, G.N., 2003. Protein adaptations to temperature and pressure: complementary roles of adaptive changes in amino acid sequence and internal milieu. Comparative Biochemistry and Physiology - B Biochemistry and Molecular Biology 136 (4), 577-591.

Somero, G.N., Dahlhoff, E., Gibbs, A.G., 1991. Biochemical adaptations of deep-sea animals: insights into biogeography and ecological energetics. In: Mauchline, J., Nemoto, T. (Eds.), Marine Biology: Its accomplishment and future prospect. Elsevier Science Publishers B.V., Amsterdam., pp. 39-57.

Somero, G.N., Siebenaller, J.F., Hochachka, P.W., 1983. Biochemical and physiological adaptations of deep-sea animals. In: Rowe, G.T. (Ed.), Deep-sea Biology. John Wiley & Sons, New York, pp. 261-330.

Sørensen, J.G., Kristensen, T.N., Loeschcke, V., 2003. The evolutionary and ecological role of heat shock proteins. Ecology Letters 6 (11), 1025-1037.

Sørensen, M., Bjerregaard, P., 1991. Interactive accumulation of mercury and selenium in the sea star *Asterias rubens*. Marine Biology 108 (2), 269-276.

Southward, E.C., Campbell, A.C. (Eds.), 2006. Echinoderms: keys and notes for the identification of British species. FSC Publications, Shrewsbury.

Spicer, J.I., 1995. Oxygen and acid-base status of the sea urchin *Psammechinus miliaris* during environmental hypoxia. Marine Biology 124 (1), 71-76.

Ståhlberg, A., Kubista, M., Pfaffl, M., 2004. Comparison of reverse transcriptases in gene expression analysis. Clinical Chemistry 50 (9), 1678-1680.

Steffensen, J.F., 1989. Some errors in respirometry of aquatic breathers: how to avoid and correct for them. J. Fish. Physiol. Biochem. 6, 49-59.

Stöhr, S., 2009. *Ophiura (Ophiuroglypha) irrorata concreta* (Koehler, 1901). In: Stöhr, S., O'Hara, T. (Eds.), World Ophiuroidea database [Online]. Available: World Register of Marine Species at http://www.marinespecies.org/aphia.php?p=taxdetails&id=244408 [accessed 2010, April 27].

Stöhr, S., Hansson, H., 2009. *Ophiosphalma armigerum* (Lyman, 1878). In: Stöhr, S., O'Hara, T. (Eds.), World Ophiuroidea database [Online]. Available: World Register of Marine Species at http://www.marinespecies.org/aphia.php?p=taxdetails&id=124901 [accessed 2010, April 25].

Stollberg, J., Urschitz, J., Urban, Z., Boyd, C.D., 2000. A quantitative evaluation of SAGE. Genome Research 10 (8), 1241-1248.

Storelli, M.M., Losada, S., Marcotrigiano, G.O., Roosens, L., Barone, G., Neels, H., Covaci, A., 2009. Polychlorinated biphenyl and organochlorine pesticide contamination signatures in deep-sea fish from the Mediterranean Sea. Environmental Research 109 (7), 851-856.

Storelli, M.M., Storelli, A., Marcotrigiano, G.O., 2001. Heavy metals in the aquatic environment of the

Southern Adriatic Sea, Italy: macroalgae, sediments and benthic species. Environment International 26 (7-8), 505-509.

Streit, S., Michalski, C.W., Erkan, M., Kleeff, J., Friess, H., 2008. Northern blot analysis for detection and quantification of RNA in pancreatic cancer cells and tissues. Nature Protocols 4 (1), 37-43.

Stronkhorst, J., Ariese, F., Van Hattum, B., Postma, J.F., De Kluijver, M., Den Besten, P.J., Bergman, M.J.N., Daan, R., Murk, A.J., Vethaak, A.D., 2003. Environmental impact and recovery at two dumping sites for dredged material in the North Sea. Environmental Pollution 124 (1), 17-31.

Stronkhorst, J., Ciarelli, S., Schipper, C.A., Postma, J.F., Dubbeldam, M., Vangheluwe, M., Brils, J.M., Hooftman, R., 2004. Inter-laboratory comparison of five marine bioassays for evaluating the toxicity of dredged material. Aquatic Ecosystem Health and Management 7 (1), 147-159.

Su, C.-L., Wu, C.-P., Chen, S.-Y., Kang, B.-H., Huang, K.-L., Lin, Y.-C., 2004. Acclimatization to neurological decompression sickness in rabbits. American Journal of Physiology - Regulatory Integrative and Comparative Physiology 287 (5), R1214-1218.

Sugni, M., Manno, V., Barbaglio, A., Mozzi, D., Bonasoro, F., Tremolada, P., Candia Carnevali, M., 2008. Echinoderm regenerative response as a sensitive ecotoxicological test for the exposure to endocrine disrupters: effects of p,p′DDE and CPA on crinoid arm regeneration. Cell Biology and Toxicology.

Sugni, M., Mozzi, D., Barbaglio, A., Bonasoro, F., Candia Carnevali, M.D., 2007. Endocrine disrupting compounds and echinoderms: new ecotoxicological sentinels for the marine ecosystem. Ecotoxicology 16 (1), 95-108.

Sumida, P.Y.G., Bernardino, A.F., Stedall, V.P., Glover, A.G., Smith, C.R., 2008. Temporal changes in benthic megafaunal abundance and composition across the West Antarctic Peninsula shelf: results from video surveys. Deep-Sea Research Part II: Topical Studies in Oceanography 55 (22-23), 2465-2477.

Svansson, A., 1984. Hydrography of the Gullmar Fjord., Institute of Hydrographic Research Göteborg Series.

Sverdrup, H.U., Johnson, M.W., Fleming, R.H., 1942. The oceans: their physics, chemistry and general biology. Prentice-Hall, New York.

Taban, I.C., Bechmann, R.K., Torgrimsen, S., Baussant, T., Sanni, S., 2004. Detection of DNA damage in mussels and sea urchins exposed to crude oil using comet assay. Marine Environmental Research 58 (2-5), 701-705.

Takahashi, S., Oshihoi, T., Ramu, K., Isobe, T., Ohmori, K., Kubodera, T., Tanabe, S., 2010. Organohalogen compounds in deep-sea fishes from the western North Pacific, off-Tohoku, Japan: contamination status and bioaccumulation profiles. Marine Pollution Bulletin 60 (2), 187-196.

Takahashi, S., Tanabe, S., Kubodera, T., 1997. Butyltin residues in deep-sea organisms collected from Suruga Bay, Japan. Environmental Science and Technology 31 (11), 3103-3109.

Talbot, T.D., Lawrence, J.M., 2002. The effect of salinity on respiration, excretion, regeneration and production in *Ophiophragmus filograneus* (Echinodermata: Ophiuroidea). Journal of Experimental Marine Biology and Ecology 275 (1), 1-14.

Tamburri, M.N., Peltzer, E.T., Friederich, G.E., Aya, I., Yamane, K., Brewer, P.G., 2000. A field study of the effects of CO_2 ocean disposal on mobile deep-sea animals. Marine Chemistry 72 (2-4), 95-101.

Taylor, S., Wakem, M., Dijkman, G., Alsarraj, M., Nguyen, M., 2010. A practical approach to RT-qPCR - publishing data that conform to the MIQE guidelines. Methods 50 (4), S1-S5.

Temara, A., Gulec, I., Holdway, D.A., 1999. Oil-induced disruption of the foraging behaviour of the asteroid keystone predator, *Cosinasterias muricata* (Echinodermata). Marine Biology 133 (3), 501-507.

Temara, A., Skei, J.M., Gillan, D., Warnau, M., Jangoux, M., Dubois, P., 1998. Validation of the asteroid *Asterias rubens* (Echinodermata) as a bioindicator of spatial and temporal trends of Pb, Cd, and Zn contamination in the field. Marine Environmental Research 45 (4-5), 341-356.

Temara, A., Warnau, M., Dubois, P., Langston, W.J., 1997. Quantification of metallothioneins in the common asteroid *Asterias rubens* (Echinodermata) exposed experimentally or naturally to cadmium. Aquatic Toxicology 38, 17-34.

Tengberg, A., De Bovee, F., Hall, P., Berelson, W., Chadwick, D., Ciceri, G., Crassous, P., Devol, A., Emerson, S., Gage, J., et al., 1995. Benthic chamber and profiling landers in oceanography - a review of design, technical solutions and functioning. Progress in Oceanography 35 (3), 253-294.

Terzaghi, C., Buffagni, M., Cantelli, D., Bonfanti, P., Camatini, M., 1998. Physical-chemical and ecotoxicological evaluation of water based drilling fluids used in Italian off-shore. Chemosphere 37 (14-15), 2859-2871.

Tevfik Dorak, M. (Ed.), 2006. Real-time PCR. Taylor and Francis, Abingdon.

Thauer, R.K., 1988. Citric-acid cycle, 50 years on. Modifications and an alternative pathway in anaerobic bacteria. European Journal of Biochemistry 176 (3), 497-508.

Théel, H., 1886. Report on the Holothuroidea dredged by H.M.S. *Challenger* during the years 1873–1876 Part II. Report on the Scientific Results of the Voyage of H.M.S. *Challenger* 1873-1876, Zoology. 14 (39), 1-290.

Theron, M., Sebert, P., 2003. Hydrostatic pressure and cellular respiration: are the values observed post-decompression representative of the reality under pressure? Mitochondrion 3 (2), 75-81.

Thiel, H., 2003. Anthropogenic impacts on the deep sea. In: Tyler, P. (Ed.), Ecosystems of the deep oceans. Elsevier, Amsterdam, pp. 427-471.

Thistle, D., 2003. The deep-sea floor: an overview. In: Tyler, P. (Ed.), Ecosystems of the deep oceans. Elsevier, Amsterdam, pp. 5-37.

Thistle, D., Eckman, J.E., Paterson, G.L.J., 2008. Large, motile epifauna interact strongly with harpacticoid copepods and polychaetes at a bathyal site. Deep-Sea Research Part I-Oceanographic Research Papers 55 (3), 324-331.

Thistle, D., Sedlacek, L., Carman, K., Fleeger, J., Brewer, P., Barry, J., 2005. Deep-ocean, sediment-dwelling animals are sensitive to sequestered carbon dioxide. Marine Ecology Progress Series 289, 1-4.

Thistle, D., Sedlacek, L., Carman, K.R., Fleeger, J.W., Brewer, P.G., Barry, J.P., 2007. Exposure to carbon dioxide-rich seawater is stressful for some deep-sea species: an in situ, behavioral study. Marine Ecology Progress Series 340, 9–16.

Thomas, C., 1996. PCR techniques. In: Foster, G.D., Twell, D. (Eds.), Plant Gene Isolation: Principles and Practice. John Wiley & Sons Ltd., Chichester, pp. 331-368.

Thuesen, E.V., Childress, J.J., 1993. Metabolic rates, enzyme activities and chemical compositions of some deep-sea pelagic worms, particularly *Nectonemertes mirabilis* (Nemertea; Hoplonemertinea) and *Poeobius meseres* (Annelida; Polychaeta). Deep-Sea Research Part I: Oceanographic Research Papers 40 (5), 937-951.

Thuesen, E.V., Childress, J.J., 1994. Oxygen consumption rates and metabolic enzyme activities of oceanic California Medusae in relation to body size and habitat depth. Biological Bulletin 187 (1), 84-98.

Thuesen, E.V., Miller, C.B., Childress, J.J., 1998. Ecophysiological interpretation of oxygen consumption rates and enzymatic activities of deep-sea copepods. Marine Ecology Progress Series 168, 95-107.

Timofeyev, M.A., Steinberg, C.E.W., 2006. Antioxidant response to natural organic matter (NOM) exposure in three Baikalean amphipod species from contrasting habitats. Comparative Biochemistry and Physiology Part B: Biochemistry and Molecular Biology 145 (2), 197-203.

Todgham, A.E., Hofmann, G.E., 2009. Transcriptomic response of sea urchin larvae *Strongylocentrotus purpuratus* to CO_2-driven seawater acidification. Journal of Experimental Biology 212 (16), 2579-2594.

Tomanek, L., 2010. Variation in the heat shock response and its implication for predicting the effect of global climate change on species' biogeographical distribution ranges and metabolic costs. Journal of

Experimental Biology 213 (6), 971-979.

Tomanek, L., Helmuth, B., 2002. Physiological ecology of rocky intertidal organisms: a synergy of concepts. Integrative and Comparative Biology 42 (4), 771-775.

Trannum, H.C., Nilsson, H.C., Schaanning, M.T., Øxnevad, S., 2010. Effects of sedimentation from water-based drill cuttings and natural sediment on benthic macrofaunal community structure and ecosystem processes. Journal of Experimental Marine Biology and Ecology 383 (2), 111-121.

Transocean, 2003. Transocean Inc. and ChevronTexaco Announce New World Water-Depth Drilling Record in 10,011 Feet of Water [Online]. Press release, November 17, 2003. Available: http://www.deepwater.com/fw/main/Transocean-Inc-and-ChevronTexaco-Announce-New-World-Water-Depth-Drilling-Record-in-10-011-Feet-of-Water-20C4.html [accessed 2010, April 22].

Transocean, 2010. The Fleet, Our Rigs, List by Water Depth [Online]. Available: http://www.deepwater.com/fw/main/List-by-Water-Depth-77.html [accessed 2010, April 22].

Treger, J.M., Heichman, K.A., McEntee, K., 1988. Expression of the yeast UB14 gene increases in response to DNA-damaging agents and in meiosis. Molecular and Cellular Biology 8 (3), 1132-1136.

Treude, T., Janßen, F., Queisser, W., Witte, U., 2002. Metabolism and decompression tolerance of scavenging lysianassoid deep-sea amphipods. Deep-Sea Research Part I: Oceanographic Research Papers 49 (7), 1281-1289.

Turnewitsch, R., Witte, U., Graf, G., 2000. Bioturbation in the abyssal Arabian Sea: influence of fauna and food supply. Deep-Sea Research Part II: Topical Studies in Oceanography 47, 2877-2911.

Tyler, P.A., 1980. Deep-sea ophiuroids. Oceanography and marine biology: an annual review 18, 125-153.

Tyler, P.A., 1995. Conditions for the existence of life at the deep-sea floor: an update. Oceanography and marine biology: an annual review 33, 221-244.

Tyler, P.A., 2003a. Disposal in the deep sea: analogue of nature or *faux ami*? Environmental Conservation 30, 26-39.

Tyler, P.A., 2003b. The peripheral deep seas. In: Tyler, P. (Ed.), Ecosystems of the deep oceans. Elsevier, Amsterdam, pp. 261-293.

Ubaldo, J.P., Uy, F.A., Dy, D.T., 2007. Temperature tolerance of some species of Philippine intertidal echinoderms. Philippine Scientist 44, 105-119.

UNEP, 2007. Deep-sea biodiversity and ecosystems: A scoping report on their socio-economy, management and governance., Biodiversity Series 28.

Unger, M.A., Harvey, E., Vadas, G.G., Vecchione, M., 2008. Persistent pollutants in nine species of deep-sea cephalopods. Marine Pollution Bulletin 56 (8), 1498-1500.

Valasek, M.A., Repa, J.J., 2005. The power of real-time PCR. American Journal of Physiology - Advances in Physiology Education 29 (3), 151-159.

van der Plas, A.J., Oudejans, R.C., 1982. Changes in the activities of selected enzymes of intermediary metabolism in the pyloric caeca and ovaries of *Asterias rubens* during the annual reproductive cycle. Comparative Biochemistry and Physiology - B Comparative biochemistry 71 (3), 379-385.

Van Dover, C.L., Grassle, J.F., Fry, B., Garritt, R.H., Starczak, V.R., 1992. Stable isotope evidence for entry of sewage-derived organic material into a deep-sea food web. Nature 360 (6400), 153-156.

Van Dover, C.L., Lutz, R.A., 2004. Experimental ecology at deep-sea hydrothermal vents: a perspective. Journal of Experimental Marine Biology and Ecology 300 (1-2), 273-307.

van Ruissen, F., Ruijter, J.M., Schaaf, G.J., Asgharnegad, L., Zwijnenburg, D.A., Kool, M., Baas, F., 2005. Evaluation of the similarity of gene expression data estimated with SAGE and Affymetrix GeneChips. BMC Genomics 6, 16.

van Weering, T.C.E., de Stigter, H.C., Boer, W., de Haas, H., 2002. Recent sediment transport and

accumulation on the NW Iberian margin. Progress in Oceanography 52 (2-4), 349-371.

Vandesompele, J., De Preter, K., Pattyn, F., Poppe, B., Van Roy, N., De Paepe, A., Speleman, F., 2002. Accurate normalization of real-time quantitative RT-PCR data by geometric averaging of multiple internal control genes. Genome Biology 3 (7), R34.

Vardaro, M.F., Ruhl, H.A., Smith, K.L., 2009. Climate variation, carbon flux, and bioturbation in the abyssal North Pacific. Limnology and Oceanography 54 (6), 2081-2088.

Varshavsky, A., 1997. The ubiquitin system. Trends in Biochemical Sciences 22, 383-387.

Vedel, G.R., Depledge, M.H., 1995. Stress-70 levels in the gills of *Carcinus maenas* exposed to copper. Marine Pollution Bulletin 31 (1-3), 84-86.

Velculescu, V.E., Zhang, L., Vogelstein, B., Kinzler, K.W., 1995. Serial Analysis of Gene Expression. Science 270 (5235), 484-487.

Vera, J.C., Wheat, C.W., Fescemyer, H.W., Frilander, M.J., Crawford, D.L., Hanski, I., Marden, J.H., 2008. Rapid transcriptome characterization for a nonmodel organism using 454 pyrosequencing. Molecular Ecology 17 (7), 1636-1647.

Vernberg, F., Calabrese, A., Thurberg, F., Vernberg, W., 1977. Physiological responses of marine biota to pollutants. Proceedings of Symposium held Connecticut, November 1975. Academic Press, New York.

Vevers, W.F., Dixon, D.R., Dixon, L.R.J., 2010. The role of hydrostatic pressure on developmental stages of *Pomatoceros lamarcki* (Polychaeta: Serpulidae) exposed to water accommodated fractions of crude oil and positive genotoxins at simulated depths of 1000-3000 m. Environmental Pollution 158, 1702-1709.

Vijayan, M., Pereira, C., Kruzynski, G., Iwama, G., 1998. Sublethal concentrations of contaminant induce the expression of hepatic heat shock protein 70 in two salmonids. Aquatic Toxicology 40 (2-3), 101-108.

Vitorino, J., Oliveira, A., Beja, J., 2005. The Nazaré Canyon (W Portugal): physical processes and sedimentary impacts. European Geosciences Union 2005, Vienna, Austria, 24-29 April, 2005.

Vopel, K., Vopel, A., Thistle, D., Hancock, N., 2007. Effects of spatangoid heart urchins on O_2 supply into coastal sediment. Marine Ecology-Progress Series 333, 161-171.

Walker, J.E., Saraste, M., Runswick, M.J., Gay, N.J., 1982. Distantly related sequences in the alpha- and beta-subunits of ATP synthase, myosin, kinases and other ATP-requiring enzymes and a common nucleotide binding fold. The EMBO Journal 1 (8), 945-951.

Walker, M.S., Hughes, T.A., 2008. Messenger RNA expression profiling using DNA microarray technology: diagnostic tool, scientific analysis or un-interpretable data? International Journal of Molecular Medicine 21 (1), 13-17.

Wall, P.K., Leebens-Mack, J., Chanderbali, A., Barakat, A., Wolcott, E., Liang, H., Landherr, L., Tomsho, L., Hu, Y., Carlson, J., et al., 2009. Comparison of next generation sequencing technologies for transcriptome characterization. BMC Genomics 10 (1), 347.

Wan, J., Sharp, S., Poirier, G., Wagaman, P., Chambers, J., Pyati, J., Hom, Y., Galindo, J., Huvar, A., Peterson, P., et al., 1996. Cloning differentially expressed mRNAs. Nature Biotechnology 14, 1685-1691.

Wang, A., Pierce, A., Judson-Kremer, K., Gaddis, S., Aldaz, C., Johnson, D., MacLeod, M., 1999. Rapid analysis of gene expression (RAGE) facilitates universal expression profiling. Nucleic Acids Research 27 (23), 4609-4618.

Wang, X., Seed, B., 2006. High-throughput primer and probe design. In: Tevfik Dorak, M. (Ed.), Real-time PCR. Taylor and Francis, Abingdon, pp. 93-106.

Wang, Z., Wu, Z., Jian, J., Lu, Y., 2009. Cloning and expression of heat shock protein 70 gene in the haemocytes of pearl oyster (*Pinctada fucata*, Gould 1850) responding to bacterial challenge. Fish & Shellfish Immunology 26 (4), 639-645.

Warnau, M., Biondo, R., Temara, A., Bouquegneau, J.-M., Jangoux, M., Dubois, P., 1998. Distribution of heavy metals in the echinoid *Paracentrotus lividus* from the Mediterranean *Posidonia oceanica*

ecosystem: seasonal and geographical variations. Journal of Sea Research 39 (3-4), 267-280.

Weaver, P.P.E., et al., 2005. The geobiology of the Nazaré and Setúbal canyons, Portuguese Continental Margin. RRS *Discovery cruise* D297 27 Jul - 16 Aug 2005. National Oceanography Centre, Southampton. Cruise Report No. 1, p. 41.

Weber, A.P.M., Weber, K.L., Carr, K., Wilkerson, C., Ohlrogge, J.B., 2007. Sampling the Arabidopsis transcriptome with massively parallel pyrosequencing. Plant Physiology 144 (1), 32-42.

Webster, L., Walsham, P., Russell, M., Neat, F., Phillips, L., Dalgarno, E., Packer, G., Scurfield, J.A., Moffat, C.F., 2009. Halogenated persistent organic pollutants in Scottish deep water fish. Journal of Environmental Monitoring 11 (2), 406-417.

Widdicombe, S., Austen, M.C., 1998. Experimental evidence for the role of *Brissopsis lyrifera* (Forbes, 1841) as a critical species in the maintenance of benthic diversity and the modification of sediment chemistry. Journal of Experimental Marine Biology and Ecology 228 (2), 241-255.

Widdows, J., 1985. Physiological responses to pollution. Marine Pollution Bulletin 16 (4), 129-134.

Wiegand, G., Remington, S.J., 1986. Citrate Synthase: structure, control, and mechanism. Annual Review of Biophysics and Biophysical Biochemistry 15, 97-117.

Williams, T.D., Gensberg, K., Minchin, S.D., Chipman, J.K., 2003. A DNA expression array to detect toxic stress response in European flounder (*Platichthys flesus*). Aquatic Toxicology 65 (2), 141-157.

Wilson, K., Thorndyke, M., Nilsen, F., Rogers, A., Martinez, P., 2005. Marine systems: moving into the genomics era. Marine Ecology 26, 3-16.

Wilson, R., Smith, K., 1985. Live capture, maintenance and partial decompression of a deep-sea grenadier fish (*Coryphaenoides acrolepis*) in a hyperbaric trap-aquarium. Deep-Sea Research 32 (12 A), 1571-1582.

Wong, M.L., Medrano, J.F., 2005. Real-time PCR for mRNA quantitation. BioTechniques 39 (1), 1-11.

Yamamoto, M., Wakatsuki, T., Hada, A., Ryo, A., 2001. Use of serial analysis of gene expression (SAGE) technology. Journal of Immunological Methods 250 (1-2), 45-66.

Yancey, P.H., Blake, W.R., Conley, J., 2002. Unusual organic osmolytes in deep-sea animals: adaptations to hydrostatic pressure and other perturbants. Comparative Biochemistry and Physiology - A Molecular and Integrative Physiology 133 (3), 667-676.

Yayanos, A.A., 1978. Recovery and maintenance of live amphipods at a pressure of 580 bars from an ocean depth of 5700 meters. Science 200 (4345), 1056-1059.

Yayanos, A.A., 2009. Recovery of live amphipods at over 102 MPa from the Challenger Deep. Marine Technology Society Journal 43 (5), 132-136.

Yoerger, D.R., Bradley, A.M., Jakuba, M., German, C.R., Shank, T., Tivey, M., 2007. Autonomous and remotely operated vehicle technology for hydrothermal vent discovery, exploration, and sampling. Oceanography 20 (1), 152-161.

Zhang, Z., Schwartz, S., Wagner, L., Miller, W., 2000. A greedy algorithm for aligning DNA sequences. Journal of Computational Biology 7 (1-2), 203-214.

Zhou, J., Thompson, D.K., 2002. Challenges in applying microarrays to environmental studies. Current Opinion in Biotechnology 13 (3), 204-207.

Zhu, X., Zhao, X., Burkholder, W., Gragerov, A., Ogata, C., Gottesman, M., Hendrickson, W., 1996. Structural analysis of substrate binding by the molecular chaperone DnaK. Science 272, 1606-1614.

Zuker, M., 2003. Mfold web server for nucleic acid folding and hybridization prediction. Nucleic Acids Research 31 (13), 3406-3415.

Appendices

1.1. Summary of anthropogenic toxicology studies carried out with adult echinoderms

List of acronyms and abbreviations at bottom of table.

Assay / Biomarker	Species	Contaminant / Stressor	Results / Conclusions	Reference
Community Level				
In situ abundance	*Ophiura albida* (North Sea)	Contaminated port sediment (metals, PAH, TBT, PCB)	Average abundance at dumping site was 1 individual per m^2, compared with 129 individuals per m^2 at control sites.	Stronkhorst et al. (2003)
	Amphiura chiajei, Amphiura filiformis (North Sea)	Proximity to oil platforms	*Amphiura* excluded from sediments proximal to oil platforms, concluded drill cuttings have high chronic toxicity.	Newton and McKenzie (1998)
	Amphiodia urtica (East Pacific)	Treated wastewater and suspended solids	*A. urtica* abundance responded to wastewater ocean outfall proximity. No clear relationship though, authors stress multi-species review needed.	Maurer and Nguyen (1996)
	Paracentrotus lividus, Psammechinus miliaris	*Erika* oil spill (NE Atlantic)	100% absence of echinoids from tidal rock pool communities 3 weeks after spill. Echinoids returned after 2 years absence, took 3 years to reach original densities.	Barille-Boyer et al. (2004)
Whole Organism				
Mortality	*Evasterias troschelii*	Crude Oil WSF (Alaska)	Day 19 LC_{50} = 0.82 ppm TAH	O'Clair and Rice (1985)
	A. chiajei, A. filiformis	Oil based drill cuttings (North Sea)	96 hr LC_{50} = 52000 ppm THC, concluded low acute toxicity.	Newton and McKenzie (1998)
	Echinocardium cordatum (N. Sea)	Contaminated port sediment (metals, PAH, TBT, PCB)	14 day Whole Sediment Bioassay. Mortality rates in contaminated sediment significantly higher than control.	Stronkhorst et al. (2003)
	Antedon mediterranea	TPT-Cl (Mediterranean Sea)	72 hr LC_{50} = 1000 ng l^{-1}	Barbaglio et al. (2006)

In situ bioaccumulation	*Asterias rubens*	*In situ* sediment metal contamination: Pb, Cd, Zn (Norwegian Fjord)	Asteroid metal concentration decreases with spatial & temporal distance from contaminant source. Smaller individuals found nearer to contamination. Pyloric caeca accumulates metals over short term; body wall & skeleton accumulate metals long term.	Temera et al., (1998)
	A. rubens	Sediment heavy metals, PCB, PAH and pesticide contamination (North Sea)	Starfish contaminant (metals, PCBs, DBTs) tissue levels reflect *in situ* spatial pollution gradients and sediment concentrations. Body wall PCB concentration has significant correlation with sediment PCB concentrations.	Den Besten et al. (2001), Coteur et al. (2003)
	A. rubens	Sediment metals, PAH, TBT, PCB, derived from dredged port material (North Sea)	Starfish tissues from dumping site had double Hg, Zn, & PCB levels compared with control site. Cd levels lowest at dumping site. BTs, Ni, Cr, Pb, Cu levels no difference between dumping and control sites. PAH tissue levels not detectable. DBT tissue levels 4x higher than TBT.	Stronkhorst et al. (2003)
	Holothuria polii, P. lividus	Sediment metals: Hg, Cd, Pb, Cu, Zn, Fe (Mediterranean Sea)	*P. lividus* gonad metal concentrations reflect those found in algal food. *H. polii* tissue concentrations reflect sediment. The holothurian is a suitable bioaccumulator organism.	Storelli et al. (2001)
	H. mexicana, Isostichopus badionutus	Sediment metals: Al, Zn, Cu, Mn, Pb, Ni (Caribbean Sea)	Differential uptakes and accumulation processes are found for different metals. Larger holothurians have a higher concentration of metal contaminants in their tissues. Conclude that holothurians are representative bioaccumulator organisms.	Laboy-Nieves and Conde (2001)
	P. lividus	Metals: Zn, Pb, Cd, Fe, Cr, Cu, Ti (Mediterranean Sea)	Seasonally and spatially influenced concentrations of metals were selectively distributed amongst body compartments. Digestive wall primarily recommended for bioaccumulation assessment.	Warnau et al. (1998)
Experimental Bioaccumulation	*Leptasterias polaris*	Experimental TBT exposure (Gulf of St. Lawrence, NE Canada)	Pyloric caeca accumulated TBT, carried out active debutylation & TBT and DBT elimination. BTs primarily bioaccumulated in pyloric caeca, to a limited extent in gonads.	Békri and Pelletier (2004)

	A. rubens	Experimentally PCB contaminated sediments, seawater and food (N. Sea)	PCBs readily accumulated in body wall and pyloric caeca. Accumulation is correlated with ROS production, indicating immunotoxic effects.	Danis et al. (2006)
	A. rubens	Experimentally exposed to Se and Hg contaminated seawater (Kattegat)	Hg accumulated in external tissue and pyloric caeca, although subsequently eliminated. Hg accumulation increases with co-exposure to Se.	Sørensen & Bjerregaard, (1991)
Subcuticular bacteria abundance (SCB)	*A. filiformis, A. chiajei, Ophiothrix fragilis*	Oil based drill cuttings: lab controlled, semi-controlled microcosm & *in situ* studies	Drill cutting exposure decreased SCB abundance. Concluded drill cuttings have low-level acute toxicity but medium to high level chronic toxicity (North Sea)	Newton and McKenzie (1995, 1998)
Behaviour				
Burrowing behaviour	*A. chiajei*	Oil based drill cuttings (North Sea)	96 hr experimental exposure to drill cuttings caused a decrease in burrowing activity	Newton and McKenzie (1998)
Avoidance of contaminated sediment	*Patiriella exigua*	Crude oil (South Australia)	Significant dose dependent avoidance of oil contaminated sediment found. Narcotic effect of exposure was observed.	Ryder et al. (2004)
Feeding Rate	*E. troschelii*	Crude Oil WSF (Alaska)	WSF dose dependent decline in feeding rate. Asteroids exposed to ≥0.2 ppm WSF ate significantly less than control individuals.	O'Clair and Rice (1985)
Foraging behaviour	*Coscinasterias muricata*	Crude Oil WAF (Norwegian Fjord)	Perception and localisation of food significantly affected. Concluded foraging behaviour is reversibly disrupted by oil-derived contaminants.	Temera et al. (1999)
Posturing reflex	*A. forbesi*	Crude oil, dispersant and oil & dispersant. (NW Atlantic)	Posturing reflex in all exposed starfish was significantly affected in comparison to control individuals.	Ordzie and Garofalo (1981)
Prey localisation	*C. muricata*	Crude oil WSF, dispersed oil, burnt oil (South Australia)	Prey localisation significantly disrupted by crude oil WAF and dispersed oil.	Georgiades et al. (2003)
Righting Response	*A. rubens*	Ivermectin (North Sea)	20 mg kg^{-1} sediment dose caused a significant increase in	Davies et al.

			righting times compared with control.	(1998)
	A. rubens	Methyl methane sulfonate and Cyclophosphamide (English Channel)	Righting time increased following MMS exposure but high levels of mortality meant a dose-dependent response could not be determined. Time- & concentration-dependent response in righting time found with CP exposure.	Canty et al. (2009)
	Lytechinus variegatus	Phosphate treatment (Gulf of Mexico)	A dose-dependent change in righting times was found.	Böttger et al. (2001)
	P. lividus	Fresh and 'weathered' crude oil (Mediterranean)	Delay in righting time in individuals exposed to fresh crude oil but not to weathered oil.	Axiak and Saliba (1981)
	E. troschelii	Crude Oil WSF (Alaska)	Starfish were unable to right themselves.	O'Clair & Rice (1985)
Gonad development, growth and regeneration				
Egg diameter and gonad maturation	*P. lividus*	Endocrine disrupters (Mediterranean)	TPT & MET reduced egg diameter, FEN increased egg diameter. Nutritive phagocytes were stimulated in testis, but oocyte maturation halted.	Sugni et al. (2007)
Gonad development	*P. miliaris*	PAH (North Sea)	Gonad weight reduced, severe ovarian lesions observed, growth and maturation of pre-vitellogenic oocytes inhibited and they were degenerating.	Schäefer and Köehler (2009)
Regenerative Growth	*A. mediterranea*	Endocrine disrupters (Mediterranean)	TPT, FEN & MET stimulated regeneration. But reduced blastema cell density and abnormal cell growth was found.	Sugni et al. (2007)
	A. mediterranea	TPT-Cl, Fenarimol (Mediterranean)	Both induce malformations in internal anatomy during regeneration.	Barbaglio et al. (2006)
Growth Rate	*E. troschelii*	Crude Oil WSF (Alaska)	Mean growth rate positively correlated with WSF concentration	O'Clair and Rice (1985)
Cellular/Immune				
Cell viability (Trypan blue exclusion test)	*L. polaris*	*In vivo* TBT (Gulf of St. Lawrence, NE Canada)	No significant loss of amoebocyte viability found.	Békri and Pelletier (2004)
Coelomic	*A. rubens,*	*In situ* sediment associated	No response found (North Sea)	Coteur et al.

amoebocyte concentration		PCBs & metals (Cd, Cu, Pd, Zn)		(2003)
	L. polaris	*In vivo* TBT	No response found.	Békri and Pelletier (2004)
Lysosomal integrity (via NRR)	*L. polaris*	*In vivo* TBT	Accumulated BTs adversely affect lysosomal integrity.	Békri and Pelletier (2004)
Phagocytic activity	*L. polaris*	*In vivo* TBT	BT pre-exposure decreases phagocytic activity significantly	Békri and Pelletier (2004)
	A. rubens	*In situ* metal and PCB contamination (North Sea)	Phagocytic activity reproducibly positively correlated with asteroid metal contamination but not PCB contamination.	Coteur et al. (2005a)
Amoebocyte Reactive Oxygen Species (ROS)	*A. rubens*	*In situ* sediment associated PCBs and metals (Cd, Cu, Pd, Zn) in coastal areas.	Significant inhibition of ROS production linked with sediment and asteroid organ metal concentrations. PCBs enhanced ROS production (North Sea)	Coteur et al. (2003)
	A. rubens	Experimentally PCB contaminated sediments, seawater and food.	PCB exposure increased ROS production although production then decreased with time of exposure (North Sea)	Danis et al. (2004; 2006)
Biochemical				
Androgen Metabolism	*P. lividus*	Triphenyltin (TPT) (Mediterranean)	TPT modulates androgen metabolism and circulating steroid levels in the coelomic fluid.	Lavado et al (2006b)
Microsomal cytochrome P_{450}	*A. rubens*	*In situ* sediment heavy metals, PCB, PAH and pesticide contamination	P_{450} pyloric caeca content was higher in coastal than offshore specimens (North Sea)	Den Besten et al. (2001),
	C. muricata	Dispersed oil (South Australia)	Significantly lower pyloric caeca total cytochrome P_{450} content in asteroids exposed to dispersed oil.	Georgiades et al. (2005)
	A. rubens	*In situ* sediment metals, PAH, TBT, PCB from dredged port material.	No significant change in cytochrome P_{450} content at dump site found compared with control site (North Sea)	Stronkhorst et al. (2003)
	A. rubens	Experimentally PCB contaminated sediments,	CYP1A-IPP (the protein responsible for P_{450} activity) was	Danis et al.

		seawater and food.	significantly induced (North Sea)	(2004)
Alkaline phosphatase (AP) activity	*C. muricata*	Crude Oil WAF, dispersed oil, burnt oil	No significant differences to control found (South Australia)	Georgiades et al. (2003)
	A. rubens	*In situ* Cd contaminated sediments, and experimentally Cd contaminated seawater	Pyloric caeca AP activity was not changed during experimental exposure, however in the most heavily polluted *in situ* sites, AP activity was lowest (Norwegian Fjord)	Temera et al. (1997)
Cholinesterase (ChE) activity	*A. rubens*	*In situ* sediment heavy metals, PCB, PAH and pesticide contamination	Pyloric caeca microsome AChE activity lower in coastal than offshore specimens (North Sea)	Den Besten et al. (2001),
	A. rubens	*In situ* sediment metals, PAH, TBT, PCB from dredged port material.	Insignificant inhibition in pyloric caeca AChE activity found at the dumping site in comparison to the control site. (North Sea)	Stronkhorst et al. (2003)
	P. lividus	Experimental fuel oil WAF, Benzo(a)pyrene exposure, *in situ* hydrocarbon & heavy metal contamination.	Cholinesterase activity is a suitable biomarker for coastal contaminated sites (NE Atlantic, Portugal)	Cunha et al. (2005)
Benzo(a)pyrene hydroxylase (BPH) activity	*A. rubens*	*In situ* sediment heavy metals, PCB, PAH and pesticide contamination	Pyloric caeca microsome BPH activity lower in coastal than offshore specimens (North Sea)	Den Besten et al. (2001),
	A. rubens	*In situ* sediment metals, PAH, TBT, PCB, derived from contaminated dredged port material.	No significant elevation in pyloric caeca BPH activity at the dumping site was found compared with the control site (North Sea)	Stronkhorst et al. (2003)
Metallothionein production	*A. rubens*	*In situ* Cd contaminated sediments, and experimentally Cd contaminated seawater	Experimental exposure to Cd induced metallothionein production. Asteroids present in heavily polluted study sites had significantly higher metallothionein content (Norwegian Fjord)	Temera et al. (1997)
Glutathione S-transferases (GST)	*P. lividus*	Experimental fuel oil WAF, Benzo(a)pyrene exposure, *in*	GST is sensitive to both WAF and benzo(a)pyrene, and is a suitable *in situ* biomarker (NE Atlantic, Portugal)	Cunha et al. (2005)

		situ hydrocarbon & heavy metal contamination.		
Molecular				
DNA integrity via strand break analysis (Comet Assay)	*Strongylocentrotus droebachiensis*	Mechanically dispersed North Sea crude oil	A significant concentration-related increase in DNA damage found in coelomocytes (Norway)	Taban et al. (2004)
	A. rubens	MMS and CP (English channel)	DNA strand breaks increased following MMS exposure, but high mortality levels meant dose-dependent response could not be determined. Time- & concentration-dependent response in DNA strand breaks found with CP exposure.	Canty et al. (2009)
	A. rubens	*In situ* sediment heavy metals, PCB, PAH, TBT and pesticide contamination	No clear relationship between pollutant concentration or dumping site and DNA integrity (North Sea)	Den Besten et al. (2001), Stronkhorst et al. (2003)

Acronyms: AChE = acetylcholinesterase, AP = Alkaline phosphatase, BPH = benzo(a)pyrene hydroxylase, BT = butyltins, CP = cyclophosphamide, DBT = dibutyltin, DDE = DDT metabolite, DDT = Dichloro-Diphenyl-Trichloroethane, FEN = fenarimol, DNA = Deoxyribonucleic acid, GST = Glutathione S-transferase, HSP = heat shock protein, MET = methyltestosterone, MMS = methyl methane sulfonate, NRR = neutral red retention, PA = phagocytic activity, PAH = polycyclic aromatic hydrocarbons, PCB = polychlorinated biphenyl, ROS = Reactive Oxygen Species, SCB = subcuticular bacteria abundance, TAH = total aromatic hydrocarbon, TBT = tributyltin, THC = total hydrocarbon content, TPT = triphenyltin, TPT-Cl = triphenyltin chloride, UV =ultra violet, WAF = water accommodated fraction, WSF = water-soluble fraction.

Chemical Symbols: Al = aluminium, Cd = cadmium, $CdCl_2$ = cadmium chloride, Cr = chromium, Cu = copper, Fe = iron, Hg = mercury, Mn = manganese, Ni = nickel, Pb = lead, Se = Selinium, Ti = titanium, Zn = zinc.

Molecular Protocols

The following protocols relate to the molecular techniques used during experimental work carried out for the preparation of this thesis.

1.2. Notes on protocols

A detailed list of reagents and equipment used during the molecular protocols is first provided in order to assist with their identification and acquisition for any interested parties. From Appendices 1.4 onwards manufacturer's details with regard to specified chemicals, equipment or trademarks will not be included, as full details are provided in Appendix1.3.

All equipment and reagents used for these protocols should be nuclease-free.

Where reference is made to the use of nuclease-free water in the protocols; either nuclease-free water (QIAGEN) or DEPC-treated Milli-Q water was used. Prepare DEPC treated Milli-Q water by making up a 0.1% solution of DEPC using Milli-Q water, stand in a fume cupboard overnight (loosely covered) and then autoclave to degrade the DEPC.

Although not specified in each protocol, where it is appropriate to do so, all reagents should be completely thawed, mixed thoroughly and then briefly centrifuged (~3 seconds) before use. This ensures that each reagent is homogenous prior to use as separation of reagent components can occur during storage and / or thawing.

1.3. List of equipment, reagents, kits and instruments

Equipment

1.5 ml sterile microcentrifuge tubes (TUL-918-016C; Molecular BioProducts (MBP), Fisher Scientific, Loughborough, UK)

200 µl PCR microtubes (AB-0620; ABgene, Fisher Scientific)

50 ml centrifuge tubes (FB55958; Fisher Scientific)

96 well clear microplates (DIS-210-070J; Sterilin Ltd., Fisher Scientific)

96 well microplates (9502867; Thermo Scientific, Fisher Scientific)

Parafilm M® (SEL-400-030P; Fisher Scientific)

Pellet Pestles (Z359947; Sigma-Aldrich® Company Ltd., Dorset, UK)

Petri Dishes (Sterilin Ltd, Fisher Scientific)

Pipette tips low retention with filter (10 µl, 20 µl, 200 µl, 1000 µl; MBP, Fisher Scientific)

Pipettes (various sizes; Gilson Pipetman® P, Gilson Inc., Middleton, USA)

Reagents

100 bp Low Ladder (P1473; Sigma-Aldrich)

100 bp DNA Ladder (N3231S; New England Biolabs (UK) Ltd., Hitchin, UK)

1 kb DNA Ladder (N3232S; New England Biolabs (UK) Ltd.)

2-Propanol for molecular biology ≥99% (I9516; Sigma-Aldrich)

Agarose DNase and RNase free (BPE160; Fisher Scientific)

Ampicillin sodium salt (A9518; Sigma-Aldrich)

CelLytic™ MT Cell Lysis Reagent (C3228; Sigma-Aldrich)

Chloroform ≥ 99% (C2432; Sigma-Aldrich)

Deoxynucleotide Solution Mix (N0447; New England Biolabs (UK) Ltd.)

Deoxynucleotide Mix (D7295; Sigma-Aldrich)

Deoxyribonuclease I (DNase I) amplification grade (AMP-D1; Sigma-Aldrich)

Diethyl pyrocarbonate (DEPC) ≥97.0% (32490; Sigma-Aldrich)

Ethanol for molecular biology 190 proof (E7148; Sigma-Aldrich)

Ethidium bromide (E4391; Sigma-Aldrich)

Luria Agar (L3147; Sigma-Aldrich)

Luria Broth (L3522; Sigma-Aldrich)

Milli-Q® Water (Milli-Q® Integral Water Purification System, Millipore (U.K.) Ltd.)

M-MLV Reverse Transcriptase (M1302; Sigma-Aldrich)

Nuclease-Free Water (129115; QIAGEN®, Crawley, UK)

Precision™ 2X qPCR Mastermix with SYBRgreen (PrimerDesign Ltd., Southampton, UK)

Protease Inhibitor Cocktail (P8340; Sigma-Aldrich)

Random Nonamers (R7647; Sigma-Aldrich)

REDTaq® DNA Polymerase (D4309; Sigma-Aldrich)

Restriction Endonuclease Not I (R8506; Sigma-Aldrich)

Ribonuclease Inhibitor human (R2520; Sigma-Aldrich)

RNAlater® Solution (AM7024; Applied Biosystems, Warrington, UK)

RNase Away® (D/0048/08; MBP, Fisher Scientific)

RNaseOUT™ Recombinant Ribonuclease Inhibitor (10777-019; Invitrogen™, Paisley, UK)

SuperScript™ III Reverse Transcriptase (18080-044; Invitrogen)

Taq PCR Core Kit (201225: QIAGEN)

TE buffer RNAse free (20x, T11493; Invitrogen)

Taq DNA Polymerase (201203; QIAGEN)

TRI Reagent® (T9424; Sigma-Aldrich)

Kits

Citrate Synthase Assay Kit (CS0720; Sigma-Aldrich)

QIAquick® Gel Extraction Kit (28704; QIAGEN)

QIAprep® Miniprep Kit (27104; QIAGEN)

Quant-iT™ Picogreen® dsDNA Reagent and Kit (P7589; Invitrogen)

Quant-iT™ Ribogreen® RNA Reagent and Kit (R11490; Invitrogen)

SMART™ RACE cDNA Amplification Kit (PT3269-1; Takara Bio Europe/Clontech, France)

TOPO TA Cloning® Kit for Sequencing (K4530-20; Invitrogen)

Instruments

FLUOstar Optima multidetection plate reader (BMG LABTECH Ltd., Aylesbury, UK)

Gel Doc™ UV transilluminator system (Bio-Rad Laboratories Ltd., Hemel Hempstead, UK)

Horizon® 58 Horizontal Gel Electrophoresis Apparatus (Life Technologies, Rockville, USA)

ND-1000 Spectrophotometer (Nanodrop®, Wilmington, USA)

Power Pac 300 (Bio-Rad Laboratories Ltd.)

Primus 96 Legal PCR System Thermocycler (MWG Biotech, Eurofins MWG Operon, UK)

PTC-0200 DNA Engine thermal cycler (Bio-Rad Laboratories Ltd.)

PTC-0200 DNA Engine thermal cycler (MJ Research Inc., Waltham, USA)

Rotor-Gene™ 3000 (Corbett Research (UK) Ltd., St. Neots, UK)

Made-up Reagents

1 x Tris-Acetate-EDTA (TAE) buffer (recipe: page A1.17 in Sambrook and Russell, 2001)

TE Buffer (recipe: page A1.7 in Sambrook and Russell, 2001)

Loading Dye (if not supplied with Taq, see recipe: page A1.18 in Sambrook and Russell, 2001)

1.4. Total RNA isolation protocol

This protocol was used to isolate total ribonucleic acid (RNA) from tissue samples that had been preserved in RNAlater solution and stored at -80 ºC. It is based on the Sigma-Aldrich TRI Reagent protocol (Sigma 1999; Technical Bulletin MB-205).

Method

1. Defrost tissue in RNAlater solution, and place approximately 100 mg of tissue in a sterile 1.5 ml microcentrifuge tube containing 500 µl of TRI Reagent.
2. Homogenize tissue in TRI Reagent with an autoclaved pellet pestle. If required, add a small number of autoclaved sand grains to tube to facilitate tissue homogenisation. Once there are no visible tissue fragments, add a further 500 µl TRI Reagent to give a total volume of 1 ml.
3. Leave sample to stand for 5 minutes at room temperature to ensure complete dissociation of nucleoprotein complexes.
4. Add 200 µl of chloroform and mix vigorously for approximately 15 seconds. Then leave sample to stand at room temperature for 15 minutes.
5. Centrifuge at 12,000 x g for 15 minutes at 4 ºC.
6. Without disturbing the resulting middle interphase or lower red organic phase, transfer as much of the upper aqueous phase as possible to a new sterile 1.5 ml microcentrifuge tube. Either appropriately dispose of the lower phases as phenol waste, or store at -80 ºC for subsequent DNA isolation within one month of homogenisation.
7. Add 500 µl of 2-propanol (isopropanol) to the transferred aqueous phase and mix by inverting several times. Stand samples for 10 minutes at room temperature.
8. Centrifuge at 12,000 x g for 10 minutes at 4 ºC. A precipitated pellet of total RNA will adhere to the inside of the tube. Carefully decant off the supernatant, briefly centrifuge the tube again and remove any remaining supernatant with a pipette.
9. Add 1 ml of 75% ethanol (25% nuclease-free water; 75% molecular grade ethanol) to the tube and briefly vortex.
10. Centrifuge sample at 7,500 x g for 5 minutes at 4 ºC. Carefully decant off the 75% ethanol, briefly centrifuge and remove any remaining ethanol from the tube with a pipette. Perform a second brief centrifuge and again remove any remaining ethanol with a pipette.
11. Stand the tube containing the RNA pellet on ice to air dry until the edges of the pellet are opaque (2-15 minutes, depending on pellet size). Add an appropriate volume of nuclease-free water to the pellet (10 – 80 µl, depending on pellet size), and resuspend by repeated pipetting.
12. Assess the quantity and quality of total RNA present in the suspended sample with the ND-1000 Spectrophotometer (Appendix 1.5). Store the RNA sample at -80 ºC until required.

1.5. Nucleic acid quantification with the ND-1000 Spectrophotometer

This protocol was used to determine the amount of RNA or DNA held in suspension following either RNA extraction (Appendix 1.4), DNA extraction from a gel (Appendix 7) or plasmid DNA extraction from a bacterial culture (Appendix 9; Day 4)

Method

1. Blank the ND-1000 spectrophotometer with 1.5 µl nuclease-free water (or other buffer solution that the nucleic acid sample is suspended in). Set the spectrophotometer to either the RNA-40 or the DNA-50 absorbance setting as appropriate.
2. Pipette a 1.5 µl sample aliquot onto the spectrophotometer and measure the absorbance.
3. The quantity of nucleic acid in the sample is given in ng μl^{-1}; the quality of nucleic acid in the sample is indicated by the Abs_{260} / Abs_{280} and Abs_{260} / Abs_{230} ratios. Poor quality samples (see below) indicate the presence of contaminants that may interfere with subsequent processes such as expression analysis.

Background Information

Nucleic Acid Quantity. The ND-1000 spectrophotometer software calculates the concentration of nucleic acids in a sample via a manipulated Beer-Lambert equation (A = E * b * c);

$$c = \left(\frac{A * E}{b} \right)$$

Where c = Concentration of the nucleic acid in ng μl^{-1}

E = Extinction coefficient (ng μl^{-1} cm^{-1})

b = Optical path length (cm)

$$A = \text{absorbance} = -\log\left(\frac{Intensity_{sample}}{Intensity_{blank}} \right)$$

Nucleic acid quality, 260/280 ratio: this ratio provides an indication of the nucleic acid sample purity. For RNA samples a ratio of approximately 2.0 indicates pure RNA, for DNA samples a ratio of approximately 1.8 indicates pure DNA. If the ratio is considerably lower than these values, the nucleic acid sample may have been contaminated with protein or phenol (Sambrook and Russell, 2001).
Nucleic acid quality, 260/230 ratio: this ratio provides a second measure of the nucleic acid sample purity. A pure nucleic acid reading will give a 260/230 ratio of approximately 1.8 – 2.0. If the ratio is lower, the sample may also contain organic contaminants such as carbohydrates, peptides, phenols or aromatic compounds (Luebbehusen, 2004)[5].

[5] Luebbehusen, H., 2004. The Significance of the 260/230 Ratio in Determining Nucleic Acid Purity. http://www.bcm.edu/mcfweb/?PMID=3100. Bayor College of Medicine, Microarray Core Facility.

1.6. Nucleic acid quantification with Ribogreen or Picogreen

This protocol was used for the accurate determination of nucleic acids in a sample, using the fluorescent dyes RiboGreen® (for single-stranded nucleic acid (RNA) quantification) and PicoGreen® (for double stranded nucleic acid (DNA) quantification). It is based on the Invitrogen instructions (Quant-iT™ PicoGreen® dsDNA Reagent and Kits; Manual MP 07581 and Quant-iT™ RiboGreen® RNA Reagent and Kits MP 11490). The details below apply to the 'high-range' standard curves for the Ribo- / Pico-Green quantification of 20 ng/ml to 1 µg/ml RNA or 1 ng/mL to 1 µg/mL DNA respectively. The standard curves are specific only to the batch of Ribo- / Pico-Green that is used to generate the curve. Therefore, in order to avoid the preparation of multiple standard curves, a sufficient quantity of Ribo- or Pico-Green should be made up at the start of the protocol to cover all samples and blanks to be quantified.

Method

1. Calculate the total solution volumes that will be required for the quantification of all nucleic acid samples, blanks and standard curve samples, based on the guideline calculations listed in Table A0.1:

Table A0.1. Guideline calculations for the volumes of components needed to perform the Ribo- / Pico-Green nucleic acid quantifications.

Components	TE Buffer (µl)	Ribo- / Pico-Green (µl)	Notes
1 x nucleic acid sample	198	200	Volumes refer to duplicate readings for 1 sample/blank
1 x blank	200	200	
Standard Curve	1089	1800	For a 6 point standard curve
Nucleic Acid Standard	700	-	For dilution of the nucleic acid
Total Ribo-/Pico-Green	**-**	**2200**	
TE to dilute 200 x Ribo-/Pico-Green (from above)	2189	-	TE to dilute Ribo-/Pico-Green sub-total
Total TE Buffer	**4376**	**-**	

2. Round up the calculated volumes of TE buffer and RiboGreen needed (from Table A0.1) to ensure that excess volumes are available for sample dilutions that may be subsequently required at the end of the initial quantification process.
3. Prepare a 20-fold dilution of 20 x TE buffer with nuclease-free water, a 50 fold dilution of the RNA or DNA standard with the resulting 1 x TE buffer and a 200 fold dilution of the Ribo- / Pico-Green stock solution with the 1 x TE buffer. The Ribo- / Pico-Green solutions are light sensitive therefore shielding from light (foil wrapping) is required.
4. Prepare the RNA or DNA dilutions required for the generation of a standard curve according to the volumes and concentrations listed in Table A0.2.

Table A0.2. Volumes required for the preparation of a standard dilution series for the RNA or DNA standard curve. Volumes listed are sufficient volumes for triplicate (150 µl) readings.

Final RNA/DNA concentration	1 x TE Buffer (µl)	Volume 1 x RNA Standard (µl)	Volume 1 x Ribo-/ Pico-Green (µl)	Total Volume (µl)
1 µg / ml	0	300	300	600
750 ng / ml	75	225	300	600
500 ng / ml	150	150	300	600
100 ng / ml	270	30	300	600
20 ng / ml	294	6	300	600
0 ng / ml	300	0	300	600

5. Prepare sufficient labelled 1.5 ml sterile microcentrifuge tubes for each nucleic acid sample to be quantified. To each tube, add 198 1 x TE buffer and 200 µl 1 x Ribo- / Pico-Green (total volume 398 µl). These volumes are sufficient to produce a duplicate quantification reading (150 µl) for each nucleic acid sample.
6. Prepare sufficient blank solutions (200 µl 1 x TE buffer and 200 µl 1 x Ribo-/Pico-Green) to provide duplicate 150 µl blank readings on each 96-well black microplate which will be run.
7. Add 2 µl of nucleic acid sample to the 398 µl in a correctly labelled 1.5 ml microcentrifuge tube. Mix thoroughly by vortexing and centrifuge briefly to collect contents to the bottom of the tube. Take steps to limit the tube's exposure to light.
8. Using a 96-well black microplate, transfer to wells of known location triplicate 150µl aliquots of each RNA/DNA standard dilution, duplicate 150 µl blank readings and duplicate 150 µl nucleic acid samples.
9. Using the FLUOstar Optima multidetection plate reader, measure the absorbance of all solutions included in the 96-well black microplate.
10. Ensure the gain used to measure the first 96-well black microplate is the same for all subsequent 96-well microplates.
11. Calculate the nucleic acid concentrations contained in each sample (in ng μl^{-1}) with reference to the standard curve generated by the RNA/DNA standards dilution series. Please note that the initial calculated nucleic acid concentrations are 100 x diluted from the original nucleic acid sample.

1.7. DNase treatment of RNA samples

This protocol was used for the Deoxyribonuclease I (DNase I) treatment of total RNA samples (Appendix 1.4), which were then used to synthesise cDNA for use in quantitative polymerase chain reaction (QPCR) gene expression analysis (Appendix 1.10). It is based on the Sigma-Aldrich protocol provided with the DNase I with some modifications. DNase I treatment of the RNA samples is required in order to prevent false positive QPCR results being generated from possible contaminating genomic DNA. DNase I is an endonuclease that digests the double stranded DNA.

Method

1. From the Nanodrop® nucleic acid quantity results (Appendix 1.5), calculate the volume of sample that will contain 2 µg of RNA.
2. To a 200 µl PCR tube add the components listed in Table A0.3, and mix gently:

Table A0.3. List of components for DNase I treatment of total RNA samples.

Component	Volume (µl)
2 µg RNA in 16 µl nuclease-free water	16.0
10 x Reaction Buffer	2.0
Amplification Grade DNase I (1 unit/µl)	2.0
Final Volume	**20.0**

3. Incubate for 15 minutes at room temperature.
4. To denature the DNase I, add 2 µl of STOP Solution (50 nM EDTA) and incubate at 70ºC for 10 minutes.
5. Store samples at -20 ºC until subsequent use.

1.8. First strand cDNA synthesis (reverse transcription)

This protocol was followed for the synthesis of cDNA from isolated total RNA (Appendix 1.4). Differences in synthesis protocol as determined by the use of different reverse transcriptases (RT) are indicated where appropriate. M-MLV RT (Moloney Murine Leukaemia Virus Reverse Transcriptase) was used for non-QPCR applications, whilst SuperScript III RT was used to generate cDNA for QPCR (see section 3.4.4 for more information)

If the cDNA is to be used for QPCR expression analysis, the total RNA should be first treated with DNase I (Appendix 1.7) in order to remove genomic DNA contamination before reverse transcription is performed.

The 5x First-Strand Buffer and 0.1 M DTT listed in Table A0.5 are provided with the SuperScript III RT by Invitrogen. The 10x M-MLV Buffer is provided with the M-MLV RT by Sigma-Aldrich. All

other components listed must be purchased separately.

Method

1. Add the components listed in Table A0.4 to a 200 µl PCR tube. A master mix consisting of the dNTP mix and appropriate primers can be made if multiple reverse transcription reactions are to be performed:

Table A0.4. Components required for the first step of cDNA synthesis**.**

Reverse transcriptase with M-MLV RT (Sigma)		**Reverse transcriptase with SuperScript III RT (Invitrogen)**	
Components	**Volume (µl)**	**Components**	**Volume (µl)**
dNTP mix (10mM)	1.0	dNTP mix (10mM)	1.0
Oligo$(dT)_{23}$ Primer	1.0	Random nonamers (50-250 ng)	1.0
RNA Sample (1-5 µg)	*	RNA Sample (10 pg -5 µg)	*
Nuclease-free water	↓	Nuclease-free water	↓
Total Volume	**10.0**	**Total Volume**	**13.0**

Component volumes indicated * should be calculated according to the required concentration listed. An appropriate volume of nuclease-free water (↓) should be added to make up the total

2. Mix gently and briefly centrifuge tube to collect contents to the bottom.
3. a. For M-MLV RT, incubate at 70ºC for 10 minutes, then place on ice.

   b. For SuperScript III RT, incubate at 65ºC for 5 minutes then place on ice for at least 1 minute.
4. Add the components in the order listed in Table A0.5 to the tube. A master mix comprised of all reagents can be made if multiple reverse transcription reactions are being performed:

Table A0.5. List of components used in the fourth step of cDNA synthesis

Reverse transcriptase with M-MLV RT		**Reverse transcriptase with SuperScript III RT**	
Components	**Volume (µl)**	**Components**	**Volume (µl)**
10x M-MLV RT Buffer	2.0	5x First-Strand Buffer	4.0
RNase Inhibitor (40 units μl^{-1})	0.5	DTT (0.1 M)	1.0
Nuclease-free water	6.5	RNaseOUT (40 units μl^{-1})	1.0
M-MLV RT (200 units μl^{-1})	1.0	SuperScript III RT (200 units μl^{-1})	1.0
Volume	**10.0**	**Volume**	**7.0**

5. Mix gently, centrifuge briefly to collect all components and incubate at room temperature for 5 minutes.
6. a. For M-MLV RT, incubate at 37ºC for 50 minutes.

   b. For SuperScript III RT, incubate at 50ºC for 50 minutes.
7. cDNA has now been reverse transcribed,

   a. For M-MLV RT, denature RT by incubating at 94ºC for 10 minutes.

   b. For SuperScript III RT, denature RT by incubating at 70ºC for 15 minutes.
8. Store cDNA sample at -20ºC until subsequent use. If original RNA sample was very

concentrated, and the cDNA will not be used for QPCR, the cDNA sample can be diluted 2- or 3- fold with nuclease-free water.

1.9. Polymerase chain reaction

This protocol was used for the amplification of cDNA (Appendix 5) or plasmid DNA samples (Appendix 9) via polymerase chain reactions (PCR). Whilst the first PCRs performed during this study were catalysed by REDTaq® DNA Polymerase (Sigma-Aldrich), the performance of this *Taq* was found to be poor. Subsequent to this discovery, all PCRs were performed with QIAGEN *Taq* DNA Polymerase (QIAGEN *Taq* PCR handbook). The 10x CoralLoad PCR Buffer listed in Table A0.6 is provided with the *Taq* DNA Polymerase by QIAGEN, all other components must be purchased separately.

Method

1. Add the reagents listed in Table A0.6 to a 200 µl PCR tube. Keep the *Taq* Polymerase at -20 ºC until just before addition to the tube. For multiple PCR reactions, make a master mix with all components apart from those that are reaction specific (i.e. primers and / or cDNA templates). Keep all components and master mix on ice at all times.

Table A0.6. List of components required for one PCR reaction using QIAGEN *Taq* and degenerate primers.

Component	Volume (µl)	Final Concentration
10x CoralLoad PCR Buffer	2.5	1x
dNTP mix (10 mM each)	0.5	200 µM of each dNTP
Forward Primer (20 µM stock solution)	1.0[a]	1 µM
Reverse Primer (20 µM stock solution)	1.0[a]	1 µM
Taq DNA Polymerase (5 units ul^{-1})	0.1	0.5 units[b]
Nuclease-free water	*	
Template cDNA	*	≤1 µg / reaction
Total Volume	**20.0**	

Component volumes indicated * should be added to make up to concentration listed and a final volume of 20 µl. [a] The degenerate primer concentration in the final reagent mix should be between 0.5-5.0 µM, the concentrations used may require variation subject to degenerate PCR results. If species-specific primers are used, final degenerate primer concentration should range between 0.1 to 0.5 µM. [b] Based on the use of 2.5 units per 100 µl reaction in QIAGEN handbook.

2. If using a master mix, transfer appropriate volumes to 200 µl PCR tubes, and add primers and/or DNA template to each tube as required.
3. Mix all components gently and centrifuge to collect to the bottom of the tube
4. Move tubes quickly from ice into a pre-heated (94 ºC) thermal cycler.
5. Run the PCR thermal cycle program using a suitable cycling program, an example of which is provided in Table A0.7 (see chapter 2 for cycling programs used during experimental work).

Table A0.7. Example cycling conditions for PCR.

PCR Step	Temperature (ºC)	Time	
Initial denaturation	95	5 min	
Denaturation	95	30 sec	x 30 cycles
Annealing	*	30 sec	
Extension	72	80 sec	
Final Extension	72	8 min	

*Annealing temperature used is primer dependant (refer to Chapter 2)

6. When the PCR cycle is complete, gel electrophorese the PCR products in order to visualise the resulting DNA bands (Appendix 0). Store remaining sample in PCR tube at -20 ºC if it will be required for later use.

1.10. Quantitative polymerase chain reaction (qPCR)

This protocol concerns the use of the quantitative polymerase chain reaction (qPCR) to determine differences in the expression levels of genes in experimental samples. Before following the below protocol, the following aspects of the protocol must be optimised: primer design, primer concentrations, cycling conditions (refer to Chapter 3).

The precision 2x qPCR master mix listed in Table A0.8 is a commercial pre-mixed master mix containing the following reagents: 2x reaction buffer, 0.025 µl *Taq* Polymerase, 5 mM $MgCl_2$, dNTP Mix (200µM each dNTP) and SYBR Green I. This should be kept on ice at all times and, because SYBR Green is light sensitive, protected from exposure to light at all times.

Method

1. For each pair of qPCR primers calculate the number of individual qPCR reactions that will be performed for each experimental and calibrator cDNA sample (see Chapter 2). Note that all samples are run in duplicate. Make up a master mix based on the list of components for one QPCR reaction in Table A0.8:

Table A0.8. List of components for one qPCR reaction.

Component	Volume (µl)	Final Concentration
Precision 2x qPCR Mastermix	10.0	1 x
Forward qPCR Primer	*	As optimised
Reverse qPCR Primer	*	As optimised
Nuclease-free water	*	
Total Volume	**19.0**	

Component volumes indicated * should be added per optimised concentration (see Chapter 2) and to a final volume of 19 µl.

2. Transfer 19 µl of the master mix to a 200 µl PCR tube (flat capped) for each reaction to be performed and then add 1 µl of each cDNA to the appropriate tubes.

3. Transfer the PCR tubes to the 36 well rotor inside the Rotor-Gene 3000 thermal cycling machine. Place empty PCR tubes in any unused wells. Place locking ring over tubes and run the qPCR cycle according to the program listed in Table A0.9 below.

Table A0.9. Cycling conditions for qPCR using Precision 2x qPCR Mastermix.

PCR Step	Temperature (ºC)	Time	
Initial denaturation	95	10 min	
Denaturation	95	15 sec	x 25 cycles (or as required)
Annealing and extension	60[a]	40 sec	
Extension and data collection	60	20 sec	
Melt Curve Analysis[b] (see chapter 3)	67-95	Hold 45 sec on 1st step Hold 5 sec on next steps	

[a] 60 °C is the recommended annealing temperature to use with the precision master mix. If this temperature requires adjustment, this should be determined during the qPCR optimisation process. [b]see chapter 3

4. Once cycling has completed, if required gel electrophorese the qPCR products in order to confirm product size, or dispose of samples.
5. Calculate starting transcript copy number from qPCR results, see section3.4.6.

1.11. DNA gel electrophoresis and visualisation

This protocol was used for the electrophoresis of DNA through an agarose gel in order to separate, identify and, if required, purify the DNA fragments generated during PCR (Appendices 8 and 1.10). The DNA is visualised by staining with a fluorescent intercalating dye, ethidium bromide, which is a known carcinogen. Therefore appropriate safety precautions should be taken during ethidium bromide use (e.g. fume cupboard use, and correct disposal of ethidium bromide contaminated materials).

Method

1. Prepare required percentage of agarose with 1 x Tris-acetate and EDTA (TAE) buffer (Table A0.10) in a conical flask. Microwave until agarose has melted and solution is clear & transparent.

Table A0.10. Required agarose gel components based on the use of 30 ml gel trays**.**

		Required for 1 Gel	
Expected PCR Product Size	**% Gel**	**1 x TAE (ml)**	**Agarose (g)**
> 1000 bp	0.8	30	0.24
300 – 1000 bp	1	30	0.30
< 300 bp	2	30	0.60

2. Allow melted agarose to cool, and then add ethidium bromide to give a final concentration of

0.1 mg ml^{-1} and swirl to mix. Pour agarose into a prepared gel tray (open ends closed with tape), insert an appropriate comb and leave for 20-30 minutes to solidify.

3. Once solid, remove comb and tape and place gel and gel tray into an electrophoresis chamber, which contains sufficient 1 x TAE buffer to just cover the gel.
4. Load into each well a 5 – 6 µl aliquot of the DNA sample to be visualised. If a loading buffer was not already included in the DNA sample (e.g. QIAGEN CoralLoad PCR Buffer), mix 1 µl loading buffer with the DNA sample aliquot prior to loading.
5. Include an appropriate sized DNA ladder (Appendix1.15) in at least one of the wells (e.g. 1 µl loading buffer and 5 µl ladder).
6. Close the lid of the electrophoresis chamber, and attach the electrical leads to the chamber and to the Power Pac 300. Run gel at 75 V for a period suitable to separate PCR products (50 to 80 minutes). Do not allow the migrating DNA to run off the end of the gel.
7. Remove gel from electrophoresis chamber and visualize DNA bands with the Gel Doc UV transilluminator system. This step should be performed quickly, and UV exposure limited, because UV light damages DNA.

1.12. Extraction of DNA from an agarose gel

This protocol was used to extract DNA from an agarose gel after electrophoresis and was based on the QIAquick® Gel Extraction Kit. The manufacturers' instructions (QIAquick Spin Handbook) were followed, with modifications highlighted in bold below. The resulting eluted DNA is used for subsequent cloning (Appendix 9) or direct sequencing. All centrifugation is performed at 17,900 x g at room temperature.

Method

1. Wearing a UV-protective visor, identify the migrated DNA bands in the agarose gel with UV light and remove the target DNA band from the gel using a sterile scalpel. This step should be performed quickly, and UV exposure limited, because UV light damages DNA.
2. Place excised gel containing target DNA band in a sterile 1.5 ml microcentrifuge tube and add **500 µl** of Buffer QG.
3. Incubate at 50°C for 10 minutes. To ensure gel dissolution invert the tube every 2–3 minutes during the incubation. After the gel slice has dissolved completely the colour of the mixture should be yellow (pH ≤ 7.5). If it is not yellow, add 10 µl of 3 M Sodium acetate (pH 5.0).
4. Add **200 µl** of 2-propanol and mix by inverting.
5. Transfer the sample to a QIAquick column which has been placed in a 2 ml collection tube

(provided in the kit), and centrifuge for 1 minute. Discard flow-through and place QIAquick column back in the same collection tube.

6. Add 500 µl of Buffer QG to QIAquick column and centrifuge for 1 minute. Discard the flow through and continue to use the same collection tube.
7. Add 750 µl of Buffer PE to QIAquick column, stand for 5 minutes then centrifuge for 1 min.
8. Discard the flow-through and centrifuge the QIAquick column for an additional 1 minute. Then place QIAquick column into a clean 1.5 ml microcentrifuge tube and dispose of used collection tube.
9. To elute the DNA, add 30 µl nuclease-free water to the centre of the QIAquick membrane, stand for 1 minute and then centrifuge for 1 minute. Store eluted DNA at -20ºC.

1.13. Cloning PCR products

This protocol was used to produce sufficient good quality DNA for sequencing and was based on the TOPO TA Cloning® Kit for Sequencing (Invitrogen TOPO TA Cloning® Kit for Sequencing, Version O, 30pp). This cloning protocol is based on the insertion of *Taq* polymerase-amplified PCR products into a plasmid vector (pCR®4TOPO®), which is then transformed into One Shot® TOP10 Chemically Competent *Escherichia coli* for subsequent culture (Invitrogen manual 25-0276). The manufacturer's protocol has been modified from the given instructions for PCR products < 1 kilobase (kb) in length. Difference in the protocol for products of different sizes (< or > 1 kb) are included where appropriate.

The manufacturer's instructions indicate that the PCR products used for the TOPO® Cloning reaction should have a string of single deoxyadenosines (As) at the 3' end to ensure the PCR product ligates efficiently with the TOPO® vector. If the PCR products have been synthesized with a proofreading polymerase which does not add 3' A-overhangs, (for example the Clontech Advantage TAQ used during the SMART RACE protocol), they can be added before cloning is started (see below).

n.b. Waste that has been in contact with E. coli must be disposed of as biohazard waste.

Method

Post amplification addition of 3' A-overhangs

1. Immediately after amplification with a proofreading polymerase, add 0.7 – 1.0 unit of *Taq* polymerase (e.g. QIAGEN *Taq* DNA Polymerase, 1 unit = 0.2 µl) per tube and mix.
2. Incubate at 72 ºC for 8 to 30 minutes.
3. To remove possible contaminants from the DNA products generated during the PCR, electrophorese as much of the PCR product as possible on a gel (Appendix 0) and extract the correct DNA band using the QIAquick Gel Extraction Kit (Appendix 7).

4. Place on ice, and use immediately in the following TOPO cloning reaction.

TOPO cloning reaction (Day 1)

5. Add the components in the order listed in Table A0.11 to a sterile 200 µl PCR tube (> 1 kb) or 1.5 ml microcentrifuge tube (< 1 kb). The TOPO vector should be kept on ice at all times.

6. Mix very gently (vector is fragile) and incubate at room temperature for
   a. 20 minutes for PCR products < 1 kb
   b. 30 minutes for PCR products > 1 kb.
   Then place reaction on ice.

Table A0.11. Components required for the TOPO cloning reaction**.**

Components	PCR Product <1 kb Volume (µl)	PCR Product >1 kb Volume (µl)
Gel-extracted PCR Product	2.0	0.5 – 4.0
Salt Solution (1.2 M NaCl, 0.06 M $MgCl_2$)	0.5	1.0
Sterile Water	none	*
TOPO vector	0.5	1.0
Final Volume	**3.0**	**6.0**

Component volumes indicated * should be added to make a final volume of 6 µl.

Transformation of One Shot TOP10 chemically competent E. coli

7. Remove a vial of One Shot TOP10 chemically competent *E. coli* from -80 ºC storage and thaw on ice.
8. a. If PCR product < 1 kb, add 25 µl of thawed *E. coli* to the 3 µl TOPO Cloning reaction (Table A0.11) and mix gently. Incubate on ice for 20 minutes.
   b. If PCR product > 1 kb, add 2 µl of the TOPO Cloning reaction (Table A10) into a vial of *E. coli* (50 µl) and mix gently. Incubate on ice for 30 minutes.
9. Heat shock *E. coli* for 30 seconds at 42 ºC. Place tube on ice immediately after heat shock treatment.
10. a. If PCR product < 1 kb, add 125 µl room temperature Super Optimal broth with Catabolite repression (SOC) medium, provided with the cloning kit, to the *E. coli*.
    b. If PCR product > 1 kb, add 250 µl room temperature SOC medium to *E. coli*.
11. Secure tube caps firmly and place into a 37 ºC incubator. Rotate or shake horizontally (200 rpm) for 1 hour.
12. Spread 30 µl of *E. coli* onto a pre-warmed selective plate (Luria agar treated with ampicillin sodium salts to give a final concentration of 100 µg ml^{-1}), and 50 µl of *E. coli* onto a second pre-warmed selective plate. Seal plates with parafilm M and incubate at 37 ºC overnight with the plate inverted so that condensation does not collect on the agar.

Selection of positive E. coli transformants (Day 2)

13. After the plates have been incubated overnight, identify 8 to 10 isolated individual *E. coli* colonies of 2-3 mm diameter for further analysis. Blue/white screening is not required because the ligation of a PCR product into a vector disrupts a lethal E. coli gene (*ccdB*) contained in the vector, therefore ensuring that only positive transformants are permitted to grow.
14. Prepare a colony PCR master mix according to the reagents listed in Table A0.12 (based on the use of QIAGEN *Taq* DNA Polymerase). Prepare sufficient reaction volumes for the number of *E. coli* colonies selected for further analysis;

Table A0.12. Master Mix for colony PCR**.**

Reagent	Volume (µl) for 1 PCR reaction
Water	19.0
10x CoralLoad PCR Buffer	2.5
dNTP mix (10 mM stock solution)	1.0
M13 Forward (5'-GTAAAACGACGGCCAG-3')	1.0
M13 Reverse (5'-CAGGAAACAGCTATGAC-3')	1.0
Taq DNA polymerase	0.5
Final Volume	**25.0**

15. Transfer 20 µl of colony PCR master mix to a 200 µl PCR tube. Scrape one *E. coli* colony from the selective plate with a sterile pipette tip or cocktail stick, drop into the master mix in a 200 µl PCR tube and swirl gently. Then, remove the pipette tip or cocktail stick and streak the remaining colony onto an identifiable position on an ampicillin-selective master Luria agar plate.
16. Repeat for all colonies selected for further analysis. Perform the PCR reaction in a thermal cycler using the cycling conditions listed in Table A0.13. Wrap the new selective plates with Parafilm M and incubate overnight at 37 ºC.

Table A0.13. Cycling conditions for colony PCR**.**

PCR Step	Temperature (ºC)	Time
Initial denaturation	95	5 min
3- step cycling for 30 cycles		
Denaturation	95	30 sec
Annealing	55	30 sec
Extension	72	* sec
Final extension period not required		

*Subject to amplicon size and polymerase efficiency. QIAGEN Taq has an extension rate of 2-4 kb per minute at 72°C

17. Upon completion of the colony PCR, follow the instructions listed at Appendix 0 for gel electrophoresis of DNA in order to identify the colonies that have been positively transformed.

A band will be visible at a location equivalent to the size of the PCR product + 166 bp (the length of sequence contained between the M13 forward and reverse priming sites in the TOPO10 vector).

18. From the gel electrophoresis results, select 3 to 5 positively transformed *E. coli* colonies for subsequent culture after overnight growth of the master plate colonies.

Growth of positively transformed E. coli cultures (Day 3)

19. Make up sufficient Luria Broth (also known as Luria Bertani medium) to give a 5 ml volume for each positively transformed *E. coli* colony selected for subsequent culture.
20. Add ampicillin sodium salts to the Luria Broth to give a final concentration of 100 μg ml^{-1}.
21. For each *E. coli* colony selected for culture, add 5 ml of ampicillin-treated broth to a 50 ml centrifuge tube.
22. Take a sterile pipette tip or cocktail stick; select one positively transformed *E. coli* colony from its identifiable location on the selective ampicillin master plate. Inoculate the broth with the transformed *E. coli* colony by placing the entire tip or stick into one of the 50 ml centrifuge tubes. Repeat for all required colonies.
23. Wrap selective plates with Parafilm M and store at 4 ºC.
24. Incubate the *E. coli* inoculated broth overnight at 37 ºC with 200 rpm shaking.

Extraction of plasmid DNA from E. coli cultures (Day 4)

Plasmid DNA was extracted from the E. coli cultures using QIAprep Miniprep Kits. The manufacturers' instructions (QIAprep Miniprep Handbook) were followed:

25. Remove tip or cocktail stick from the, now cloudy, Luria broth. Centrifuge at 3,000 x g for 10 minutes at room temperature.
26. A pellet of bacterial cells will be present following centrifugation. Decant the supernatant slowly and then remove any remaining supernatant carefully using a pipette.
27. Add 250 μl Buffer P1 (from the QIAprep Miniprep Kit) to the pelleted bacterial cells and gently resuspend by repeated pipetting. Transfer bacterial suspension to a sterile 1.5 ml microcentrifuge tube.
28. Add 250 μl Buffer P2 and mix thoroughly, but for no more than 5 minutes, by inverting the tube until there are no visible cell clumps and the suspension is a homogenous blue colour.
29. Add 350 μl Buffer N3 and mix immediately and thoroughly by inverting the tube until the suspension becomes colourless. A precipitate comprised of cellular debris complexed with the detergent sodium dodecyl sulphate (SDS) will form.
30. Centrifuge at 17,900 x g for 10 minutes at room temperature. Then by decanting and pipetting, apply the supernatant to a QIAprep spin column, which is placed inside of a 2 ml collection tube (provided in the QIAprep Miniprep Kit).
31. Centrifuge at 17,900 x g for 1 minute, discard the flow-through. Retain same collection tube.

32. Add 500 µl Buffer PB and centrifuge for 1 minute. Discard the flow-through.
33. Add 750 µl Buffer PE and centrifuge for 1 minute. Discard flow-through and centrifuge for a further 1 minute.
34. To elute the plasmid DNA from the QIAprep spin column membrane, place the spin column in a sterile 1.5 ml microcentrifuge tube. Then add 50 µl Buffer EB to the centre of the spin column membrane, stand for 1 minute and then centrifuge for 1 minute.
35. Assess quantity of eluted plasmid DNA using the ND-1000 Spectrophotometer (Appendix 1.5). To assess plasmid DNA visually, electrophorese a the plasmid DNA sample aliquot (1 µl DNA sample, 1 µl loading buffer & 4 µl distilled water) in an agarose gel. Plasmid DNA appears as a large sized band at the top of the gel. Store the remaining DNA sample at -20 ºC until required.

1.14. Rapid Amplification of cDNA Ends (RACE)

This protocol was followed in order to obtain the 5'- and 3'- ends of the mRNA transcripts from the three genes of interest (see Chapter 2). It was based on the Invitrogen manufacturer's instructions for the SMART RACE cDNA Amplification kit (Clontech user manual PT3269-1), with some modifications. All components required for this protocol are provided in the SMART RACE cDNA Amplification Kit, apart from the nuclease-free water, RNA template and the Gene-Specific Primers (GSPs). Please refer to chapter 2 for more details on the design of the GSPs.

Method

First strand cDNA synthesis

1. Place the components listed in Table A0.14 below into two separate 200 µl PCR tubes, mix together gently, and then briefly centrifuge to collect all components at the tube base:
2. Incubate tubes at 70ºC for 2 minutes, and then place on ice for 2 minutes.
3. Add the following components (Table A0.15) to each tube, and mix gently: Then briefly centrifuge to collect tube contents at the bottom.

Table A0.14. Components required for first-strand RACE-ready cDNA synthesis.

5'-RACE-ready cDNA		**3'-RACE-ready cDNA**	
Components	**Volume (µl)**	**Components**	**Volume (µl)**
1 µg total RNA template	*	1 µg total RNA template	*
5'-CDS primer A	1.0	**3'**-CDS primer A	1.0
SMART II A oligo	1.0	-	-
Nuclease-free water	↓	Nuclease-free water	↓
Total Volume	**5.0**	**Total Volume**	**5.0**

Component volumes indicated * should be calculated according to the required concentration listed. Nuclease-free water (↓) should be added at an appropriate volume to make up a final volume of 5 µl.

Table A0.15. Components required for reverse transcriptase of first-strand RACE cDNA synthesis.

Component	Volume (µl)
5x First Strand Buffer	2.0
DTT (20 mM)	1.0
dNTP mix (10mM)	1.0
Powerscript RT	1.0
Final Volume	**5.0**

4. Incubate tubes at 42 ºC for 1.5 hours.
5. Add 100 µl Tricine-EDTA Buffer, incubate at 72 ºC for 7 minutes. Store cDNA at -20 ºC.

Rapid Amplification of cDNA Ends (RACE)

6. Place components listed in Table A0.16 into two separate tubes, mix gently. If required a master mix can be made of all components apart from gene specific primers (GSP) and cDNA.

Table A0.16. List of components required for primary RACE PCR.

For 5'-RACE		For 3'-RACE	
Components	**Volume (µl)**	**Components**	**Volume (µl)**
10 x Advantage 2 PCR Buffer	2.5	10 x Advantage 2 PCR Buffer	2.5
dNTP mix (10mM)	0.5	dNTP mix (10mM)	0.5
50 x Advantage 2 Polymerase Mix	0.5	50 x Advantage 2 Polymerase Mix	0.5
Nuclease-free water	17.25	Nuclease-free water	17.25
Universal Primer Mix	2.5	Universal Primer Mix	2.5
5'-RACE-Ready cDNA	1.25	3'-RACE-Ready cDNA	1.25
Gene Specific Primer **1**	0.5	Gene Specific Primer **2**	0.5
Total Volume	**25.0**	**Total Volume**	**25.0**

7. Place tubes into a pre-heated (94 ºC) thermal cycler, and perform a PCR cycle according to the conditions listed in Table A0.17.

Table A0.17. Thermal cycling conditions for RACE PCR.

PCR Step	Temperature (ºC)	Time	
Initial denaturation	95	7 min	
Denaturation	95	30 sec	**x 40 cycles**
Annealing	*	30 sec	
Extension	72	3 min 30 sec	
Final Extension	72	7 min	

*Annealing temperature (T_m) specific to each GSP.

8. Once cycling has been completed, perform a gel electrophoresis (Appendix 0) to visualise the RACE products generated. If one bright band of DNA is found of the size expected, this could be a correctly primed PCR product from the mRNA transcript of interest. To confirm that this

fragment is correct, the band should be extracted from the gel (Appendix 7) and cloned (Appendix 9 or below) for subsequent sequencing.

Nested RACE

If multiple bands are observed in the gel, it may be necessary to perform a nested RACE PCR in order to identify the correct target PCR product.

9. Dilute 2.5 µl of the primary RACE PCR product in 122.5 µl Tricine-EDTA Buffer to produce a "Nested RACE template".
10. To perform a nested RACE PCR, add the components listed in Table A0.18 to a 200 µl PCR tube, and mix gently.
11. Place tubes into a pre-heated (94 ºC) thermal cycler, and perform a PCR cycle according to the conditions listed in Table A0.18.
12. Once cycling has been completed, perform a gel electrophoresis (Appendix 0) to visualise the RACE products generated. If one bright band of DNA is found of the size expected, this could be a correctly primed PCR product from the mRNA transcript of interest. To confirm that this fragment is correct, the band should be extracted from the gel (Appendix 7) and cloned (Appendix 9 or below) for subsequent sequencing.

Table A0.18. List of components required for nested RACE PCR.

For nested 5'-RACE		**For nested 3'-RACE**	
Components	**µl**	**Components**	**µl**
10 x Advantage 2 PCR Buffer	2.5	10 x Advantage 2 PCR Buffer	2.5
dNTP mix (10mM)	0.5	dNTP mix (10mM)	0.5
50 x Advantage 2 Polymerase Mix	0.5	50 x Advantage 2 Polymerase Mix	0.5
Nuclease-free water	20.0	Nuclease-free water	20.0
Nested Universal Primer Mix	2.5	Nested Universal Primer Mix	2.5
Nested 5'-RACE template	1.25	Nested 3'-RACE template	1.25
Nested GSP **1**	0.5	Nested GSP **2**	0.5
Total Volume	**25.0**	**Total Volume**	**25.0**

Amended cloning protocol for RACE PCR fragments

The following method can be followed when the standard cloning protocol (Appendix 9) does not result in successful cloning of RACE PCR fragments.

13. Column purify the RACE PCR products according to the procedure described in the QIAGEN protocol (purification of PCR products – not the gel extraction protocol). Final elution volume is 30µl (use Milli-Q® Water for elution)

Addition of 3'-A overhangs:

14. prepare a reaction containing 28µl of the purified PCR products eluted in MQ water, 0.2µl of QIAGEN Taq (1 unit), 1µl of dATP (10mM), 3.2µl of QIAGEN Coral Load buffer. Incubate at 72°C for 30 minutes.

15. Immediately purify the PCR reaction using the QIAGEN gel extraction method (Appendix 7), eluting with 30µl of MQ water.

16. Quantify the gel extract using the NanoDrop (Appendix 1.5), and run 1 µl of the gel extract out on a gel to check for correct sized band.

17. Dilute the gel extract to give a 1:1 ratio of moles of ends of insert: moles of ends of vector. The required dilution was calculated according to the following equations (Cranenburgh, 2004):

$$V_v = \frac{T}{\left(\frac{V_c \times I_l \times I_r}{I_c \times V_l}\right)+1} \quad Dilution\_factor = \frac{V_v}{T - V_v}$$

Where I_l = insert length, V_l = vector length, I_c = insert concentration, V_c = vector concentration, I_r = required insert-to-vector ratio, T=volume of total DNA solution component V_v = vector volume.

e.g. for *B. lyrifera* HSP 3'-end: vector was 3956 bp at 10ng µl^{-1} and the gel extract was ~1700 bp at 37.2 ng µl^{-1}. Therefore, insert needed to be at a concentration of 4.3 ng µl^{-1} to give a 1:1 ratio of mole ends; the gel extract was therefore diluted eight fold. E.g. for *P. miliaris* CS 3': vector was 3956 bp at 10ng µl^{-1}, the gel extract was ~ 2500 bp long at 7.2 ng µl^{-1}. Therefore needed the insert to be at 6.32 ng µl^{-1} to give a 1:1 ratio of mole ends; therefore did not dilute the gel extract.

18. Proceed immediately to cloning by setting up the cloning reaction as listed in Table A0.19:

Table A0.19. Components required for the TOPO cloning reaction with RACE fragments.

Components	Volume (µl)
Diluted gel-extracted RACE PCR Product	1.0
Salt Solution (1.2 M NaCl, 0.06 M $MgCl_2$)	3.2
Sterile Water	14.3
TOPO vector	1.0
Final Volume	**19.5**

Incubate the cloning reaction at room temperature for 2 hours, take 3 µl of the cloning reaction and add to 50 µl of *E. coli*. Follow steps 10b and 11 above. Plate the complete reaction over three LB-AMP plates (AMP at 100 µg ml-1); plated volumes 100 µl, 100 µl and 50 µl. Follow steps 13 onwards in Appendix 9 above

1.15. PCR ladders

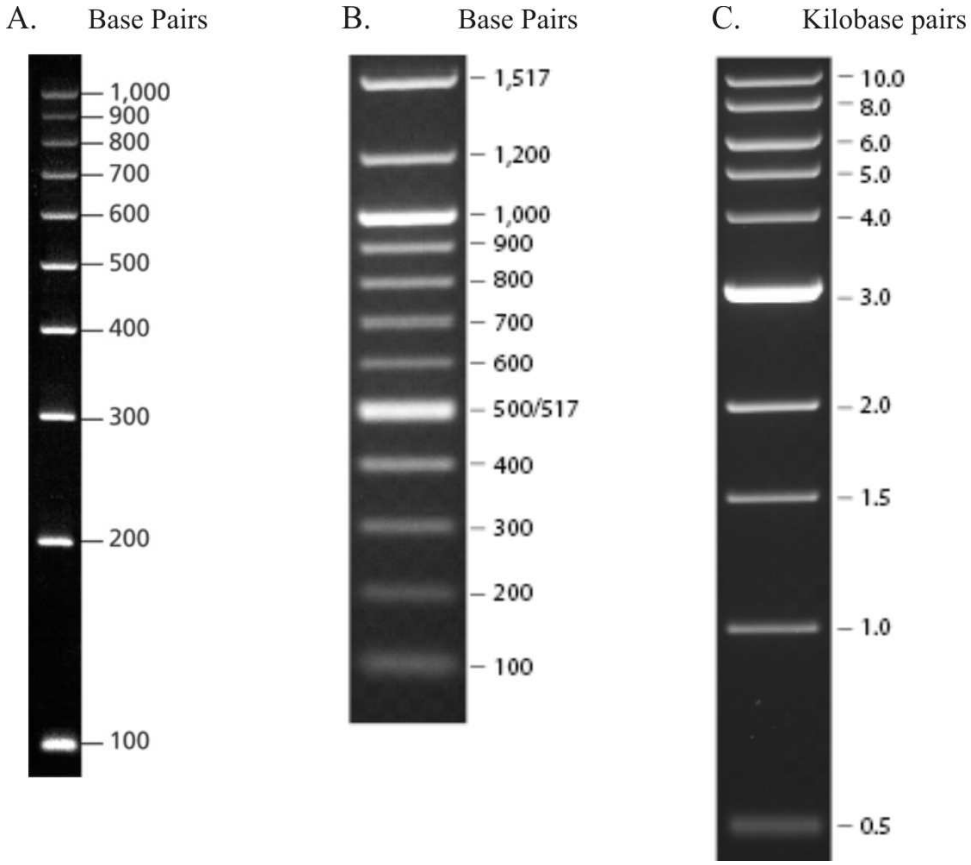

Figure A0.1. PCR ladders used as nucleic acid size markers during gel electrophoresis. From left: A. Sigma-Aldrich 100 bp ladder, B. New England Biolabs 100 bp ladder, C. New England Biolabs 1 kb ladder.

Primer Design

1.16. Degenerate primer design: heat shock protein 70 gene

The design of the *hsp70* primers was based on protein sequences from 13 different metazoan species (Table A0.1). Protein sequences were aligned using CLUSTALW (Combet et al., 2000), and homologous regions of the sequence identified. Forward and reverse primers were designed where possible in these homologous regions, whilst trying to avoid the highly degenerate amino acids leucine (L), arginine (R) and serine (S). The amino acid sequences were then reverse translated to corresponding nucleotide sequences, and primers designed manually (refer to next page and to Table A0.2) according to the following characteristics where possible; length 12-25 nucleotides, GC content (45-55%, melting temperature (Tm) 50-60 ºC, avoidance of repeating nucleotides and the 3' primer end having no degenerate nucleotides.

The T_m values for the primers were calculated by the MWG-Biotech (Germany; now Eurofins MWG Operon) primer ordering service. The basic equation used to estimate the primer melting temperature was as follows:

$$T_m = 69.3 + 41\left(\frac{n_G + n_C}{L}\right) - \frac{650}{L}$$

(Chester and Marshak (1993)[6] cited by von Ahsen (2001)[7]:

Where,

L = the nucleotide length of the primer,

n_X = the number of nucleotides of the base indicated,

and standard conditions of 50 nM primer, 50 mM Na+, and pH 7.0 are assumed

Examples of manual primer design:

[6] Chester, N., Marshak, D.R., 1993. Dimethyl sulfoxide-mediated primer T_m Reduction: A method for analyzing the role of renaturation temperature in the polymerase chain reaction. Analytical Biochemistry 209 (2), 284-290

[7] von Ahsen, N., Wittwer, C.T., Schutz, E., 2001. Oligonucleotide melting temperatures under PCR conditions: nearest-neighbor corrections for Mg^{2+}, deoxynucleotide triphosphate, and dimethyl sulfoxide concentrations with comparison to alternative empirical formulas. Clinical Chemistry 47 (11), 1956-1961.

HSPFWD2 Primer Design

Amino Acid Sequence	I	A	N	D/E	Q	G	N
Nucleotide Sequences	ATC	GCA	AAC	GAA	CAA	GGA	AAC
	A	C	T	C	G	C	T
	T	G		G		G	
		T		T		T	
Final Primer:	ATHGCNAAYGANCARGGNAA						

HSPRVS1 Primer Design, required to be designed from the revese complement of the nucleotide sequence

Amino Acid Sequence	Q	A	T/P	K	D	A
Nucleotide Sequence	GTY	CGN	KGN	TTY	CTR	CGN
Reversed Nucleotide Sequence	NGC	RTC	YTT	NGK	NGC	YTG

Final Primer: GCRTCYTTNGKNGCYTG

Table A0.1. Summary of HSP70 protein sequences used for multiple alignments.

Accession Number	Source Organism	Common Name
Q53IQ6	*Mytilus galloprovincialis*	Mediterranean mussel
Q86GI6	*Manduca sexta*	Tobacco hornworm
Q3S348	*Homarus americanus*	American lobster
Q6GUA8	*Litopenaeus vannamei*	Pacific white shrimp
O93240	*Paralichthys olivaceus*	Japanese flounder
Q91233	*Oncorhynchus tshawytscha*	Chinook salmon
P02827	*Xenopus laevis*	African clawed frog
Q91291	*Pleurodeles waltl*	Iberian ribbed newt
Q6TDU0	*Dicentrarchus labrax*	European sea bass
P08106	*Gallus gallus*	Chicken
Q24952	*Geodia cydonium*	Marine sponge
Q93147	*Botryllus schlosseri*	Star ascidian
Q5FB18	*Pocillopora damicornis*	Lace coral

Table A0.2. List of designed degenerate primers and their basic physical properties for *hsp70*. The success or failure of each primer to amplify a fragment during degenerate PCR is listed.

Primer Name	Sequence	Length	GC%	T_m°C	Result
HSP70dF1	GCNAAYAAYCARGGNAAYMG	20	47.5	56.3	Success
HSP70dF2	ATHGCNAAYGANCARGGNAA	20	44.2	54.9	Fail
HSP70dF3	GGNATHGAYYTNGGNAC	17	52.0	52.4	Fail
HSP70dR1	GCRTCYTTNGKNGCYTG	17	58.8	55.2	Success
HSP70dR2	NGCRTCYTTNGTNGCNA	17	52.9	52.8	Fail
HSP70dR3	WNACRTCRAANGTNCCNC	18	50.0	53.7	Fail

1.17. Degenerate primer design: citrate synthase gene

Following the failure of all citrate synthase degenerate primers designed from conserved regions of aligned protein sequences, two further primers were designed from aligned mRNA sequences (Table A0.3). A CLUSTALW multiple alignment from 11 published citrate synthase mRNA sequences from 11 different organisms (Table A0.4) was constructed. Design of the two further citrate synthase primers were based on the homologous regions of these mRNA sequences. In addition to the primer characteristic suggestions followed for the HSP70 primers (Appendix 1.16), three additional characteristic were a) to have ≤2 GC nucleotides in the last five nucleotides at the 3' end of the primer, b) to ensure that the ΔG of the homodimer and heterodimer forms were lower (less negative) than -10 kcal/mol, and c) to have least calculated degeneracy.

Primers with the lowest possible degeneracy were selected. The "degeneracy" of each primer was calculated according to the total number of oligonucleotides with different base combinations possible (Metzenberg, 2007)[8]. For example, primer CSRVS (Table A0.3), had a degeneracy of 48, calculated as follows:

CSRVS = TG**D**GC**R**TC**Y**AC**R**TT**R**GGCCA

D = G,A,T; R = A,G; Y = C,T (International Union of Pure and Applied Chemistry)

Assign the degenerate bases values according to their degeneracy: D = 3; R & Y = 2.

Degeneracy of CSRVS = D * R * Y * R * R = 48 different oligonucleotides

(= 3 x 2 x 2 x 2 x 2 = 48)

Table A0.3. List of designed degenerate primers and their physical properties for citrate synthase. The success or failure of each primer to amplify a fragment during degenerate PCR is listed, figures in brackets were calculated after the primers had been tested and are listed for comparative purposes.

Primer Name	Sequence	Length (bp)	GC%	T_m°C	Degeneracy	Result
CSfwd1	CAYGARGGNGGNAAYGT	17	55.9	54.0	(128)	Fail
CSfwd2	CAYGAYGGNGGNAAYGT	17	55.9	54.0	(128)	Fail
CSfwd3	ATGAAYGGNYTNGCNGG	17	55.9	54.0	(256)	Fail
CSrvs1	NCKNGGRTCNGTYTTNC	17	55.9	54.0	(1536)	Fail
CSrvs2	GCRAAYTCNCKYTGRCA	17	52.9	52.8	(192)	Fail
CSrvs3	TGNGCRTCNACRTTNGG	17	55.9	54.0	(256)	Fail
CSFWD	TGAYCAYGARGGHGGHAAYGT	21	50.8	59.2	144	Success
CSRVS	TGDGCRTCYACRTTRGGCCA	20	56.7	60.0	48	Success

[8] Metzenberg, S., 2007. The polymerase chain reaction. In: Metzenberg, S. (Ed.), Working with DNA. Taylor and Francis Group, Abingdon, pp. 291-374.

Table A0.4. Summary of citrate synthase mRNA sequences used for multiple alignments.

Accession	Source Organism	Common Name
DQ829807	*Amblyrhynchus cristatus*	Galapagos marine iguana
BC127380	*Xenopus tropicalis*	Western clawed frog
BC114138	*Bos taurus*	Cow
M21197	*Sus scrofa*	Pig
AF047042	*Homo sapiens*	Human
AB056479	*Mus musculus*	House mouse
BC045362	*Danio rerio*	Zebrafish
AY461849	*Thunnus obesus*	Bigeye tuna
XR_026166	*Strongylocentrotus purpuratus*	Purple sea urchin
AY816050	*Schistosoma japonicum*	trematode worm
DQ374006	*Glossina morsitans morsitans*	Tsetse Fly

1.18. Degenerate primer design: ubiquitin gene

Four degenerate primers were originally designed from aligned mRNA sequences; all were successful. Design characteristics were the same as those listed for citrate synthase degenerate primer design (Appendix 1.17). In order to elongate the length of the originally sequenced mRNA fragment, a NCBI BLASTN search with the *P. miliaris* consensus mRNA sequence was carried out. Sequences with maximum identity homologies of 89% or more were then aligned with the *P. miliaris* ubiquitin sequence and additional primers were designed from the sequences extending either side of the consensus *P. miliaris* ubiquitin sequence.

Table A0.5. Summary of ubiquitin nucleic acid sequences used for multiple alignments for degenerate primer design to elongate the *P. miliaris* ubiquitin fragment.

Sequence Name	Sequence Description		
	Species	Common Name	Definition
SUSUBIQ2	*Strongylocentrotus purpuratus*	Purple Sea Urchin	similar to ubiquitin, mRNA
SUSUBIQ3	*S.purpuratus*	Purple Sea Urchin	similar to ubiquitin, mRNA
TETRUBIQ	*Tetraodon nigroviridis*	Green Spotted pufferfish	Full-length cDNA
BIGEUBIQ	*Bigelowiella natans*	Chlorarachniophyte	ubiquitin/ribosomal protein mRNA
SUSUBIQ4	*S. purpuratus*	Purple Sea Urchin	similar to polyubiquitin with 3 Ub domains, mRNA
SUSUBIQ5	*S. purpuratus*	Purple Sea Urchin	similar to polyubiquitin with 3 Ub domains, mRNA
SUSUBIQ1	*S. purpuratus*	Purple Sea Urchin	ubiquitin (polyubiquitin) mRNA
GRACUBIQ	*Gracilaria lemaneiformis*	Rhodophyta (Red algae)	polyubiquitin mRNA

Table A0.6. Designed degenerate primers and their basic physical properties for ubiquitin transcripts.

Primer Name	Sequence	Length	GC%	T_m°C	Degeneracy	Result
UBQFWDa	GGNAARACBATYACHYTNGAG	21	45.2	56.9	1152	Success
UBQFWDb	CHAARATHCARGAYAARGARGG	22	41.7	56.8	288	Success
UBQFWDe	HATGCARATYTTYGTBAARAC	21	33.3	52.0	144	Success
UBQRVSc	TCYTCHARYTGYTTNCCNGC	20	51.7	58.0	768	Success
UBQRVSd	VGAYTCYTTYTGRATRTTRTARTC	24	34.0	56.2	384	Success
UBQRVSf	AGDCGSAGVACVAGRTG	17	59.7	55.5	108	Success

1.19. Degenerate primer design: actin gene (positive control)

A CLUSTALW multiple alignment of 26 nucleic acid sequences for the actin protein from 6 species of echinoderm was generated (Table A0.7). One pair of degenerate primers was designed (Table A0.8) from the conserved regions of the aligned sequences. The primer pair was successful.

Table A0.7. Summary of echinoderm actin nucleic acid sequences used for multiple alignments for degenerate primer design.

Accession	Gene Description	Source Organism	Common Name
M26501	cytoplasmic actin gene, complete cds	*Pisaster ochraceus*	Purple Ochre Sea Star
M26500	muscle actin gene, complete cds	*P. ochraceus*	Purple Ochre Sea Star
U32352	cytoskeletal actin (HeM) gene, exon 5 and complete	*Heliocidaris*	Purple sea urchin
U32357	cytoskeletal actin (HtM) gene, exon 5 and complete	*H. tuberculata*	Brown sea urchin
X05739	actin genomic DNA	*Strongylocentrotus purpuratus*	Purple sea urchin
J01168	actin 2 protein genomic DNA	*S. purpuratus*	Purple sea urchin
J01202	actin mRNA (5' and 3' ends putative);	*S. purpuratus*	Purple sea urchin
X03076	actin gene Sfa 15B	*S. franciscanus*	Red sea urchin
M35323	cytoskeletal actin CyIIb gene, complete cds	*S. purpuratus*	Purple sea urchin
X03075	actin gene Sfa 15A	*S. franciscanus*	Red sea urchin
U12271	cytoplasmic actin (HeCyI) gene, exon 4 and	*H. erythrogramma*	Purple sea urchin
U12272	CyI cytoplasmic actin genomic DNA	*H. tuberculata*	Brown sea urchin
U22507	cytoplasmic actin type III mRNA	*H. tuberculata*	Brown sea urchin
U82663	cytoplasmic actin CyII	*H. erythrogramma*	Purple sea urchin
U82661	cytoplasmic actin CyII	*H. erythrogramma*	Purple sea urchin
U82659	cytoplasmic actin CyII (HtCyII) gene, exon 4 and	*H. tuberculata*	Brown sea urchin
U09651	cytoskeletal actin mRNA	*Lytechinus pictus*	White sea urchin
U09652	cytoskeletal actin mRNA	*L. pictus*	White sea urchin
S74059	embryo actin	*Tripneustes gratilla*	Collector urchin
M35324	cytoskeletal actin CyIIIb gene, genomic DNA	*S. purpuratus*	Purple sea urchin
M35324	cytoskeletal actin CyIIIb gene, complete cds	*S. purpuratus*	Purple sea urchin

Table A0.8. Basic physical properties for the successful actin degenerate primer pair.

Primer Name	Sequence	Length	GC%	T_m°C	Degeneracy
ACTINFWD	TTCAAYDCVCCCGNCATGTAC	21	52.4	59.8	72
ACTINRVS	TCRTTDGCRATRGTGATRACCTG	23	44.9	59.5	48

1.20. Calculation of a primer 3'end stability

One of the characteristics used for the design of optimal species-specific primers for the QPCR assays was the stability of the primers' 3'-ends (see section 3.2.1) An approximate indication of a primer's 3'-end stability can be calculated as the ΔG or Gibbs free energy of the 5 bases at 3'-end (Rychlik, 2000)[9]. It is calculated from the thermodynamic relationship:

$$\Delta G = \Delta H - T\Delta S$$

Where,

ΔH = primer enthalpy as calculated by the nearest neighbour method of Breslauer (1986)

ΔS = primer entropy as calculated by the nearest neighbour method of Breslauer (1986)

T = °K, at 25°C = 298.15 °K

For example:

The 3'-end stability for the first primer listed in Table A0.9 (next page) is calculated:

$\Delta G(TCTCG) = \Delta H(TCTCG) - T\Delta S(TCTCG)$

$\Delta G(TCTCG)$ = -30900 cal/mol + (298.15 * -90.7 cal/mol) = -8.36 kcal/mol

Where,

$\Delta H(TCTCG) = \Delta H(TC) + \Delta H(CT) + \Delta H(TC) + \Delta H(CG)$

$\Delta H(TCTCG)$=5600+7800+5600+11900 =-30900 cal/mol

$\Delta S(TCTCG = \Delta S(TC) + \Delta S(CT) + \Delta S(TC) + \Delta S(CG)$

$\Delta S(TCTCG$ =13.5+20.8+13.5+27.8 = -90.7 cal/mol

The nearest neighbour entropy and enthalpy values are provided in Breslauer (1986)[10]

[9] Rychlik, W., 2000. Primer Selection and Design for Polymerase Chain Reaction. The Nucleic Acid Protocols Handbook, pp. 581-588.

[10] Breslauer, K.J., Frank, R., Blöcker, H., Marky, L.A., 1986. Predicting DNA duplex stability from the base sequence. Proceedings of the National Academy of Sciences of the United States of America 83 (11), 3746-3750.

1.21. Species-specific qPCR primers

Table A0.9. Complete list of species-specific qPCR primers, and their physical parameters, designed from the sequenced fragments of the three genes of interest for *Psammechinus miliaris* and *Brissopsis lyrifera*. Primers selected for use in the final qPCR assays are in bold. The NetPrimer score is derived from the analysis of primer properties by NetPrimer, and is calculated as 100 + (ΔG (Dimer) * 1.8 + ΔG (Hairpin) * 1.4).

Species/ Gene/ Primer Name	Primer nucleotide sequence 5' to 3'	Length (bp)	GC%	Tm (°C)	3' end stability (ΔG kcal/mol)	Homodimer stability (ΔG kcal/mol)	Net Primer Score
P. miliaris							
Citrate synthase							
PMCQPF1	**TCTCTCAGATCCTTACCTCTCG**	**22**	**50**	**60.3**	**-8.36**	**-4.62**	**91**
PMCQPF2	CAACGTCAGTTTGCTCTGAAGC	22	50	60.3	-8.26	-6.30	86
PMCQPF3	CGATGACCCCATGTTCCAG	19	58	58.8	-8.20	-5.38	90
PMCQPR1	**CACTTCCTGGTTAGCAAGTCC**	**21**	**52**	**59.8**	**-7.58**	**-5.88**	**87**
PMCQPR2	CTGGAACATGGGGTCATCG	19	58	58.8	-8.61	-5.38	90
PMCQPR3	CCTGCTCTAGGAGGATGTC	19	58	58.8	-6.35	-4.16	91
Heat shock protein 70							
PMHQPF1	AACGACCAAGGGAACAGAACC	21	52	59.8	-7.93	none formed	100
PMHQPF2	**AGTACCTCGGAGAAAAGAAGACG**	**23**	**48**	**60.6**	**-8.13**	**-3.65**	**93**
PMHQPF3	CTTGACCAAAATGAAAGAGACAGC	24	42	59.3	-8.03	none formed	100
PMHQPR1	AACCTTTCAGTGTCCGTGAAGC	22	50	60.3	-8.26	-6.47	85
PMHQPR2	**CGGCTGTCTCTTTCATTTTGGTC**	**23**	**48**	**60.6**	**-7.94**	**none formed**	**100**
PMHQPR3	GGCATCGGTGACCTTCTG	18	61	58.2	-7.07	none formed	100
Ubiquitin							
PMUQPF1	AGCCCAGTGACACCATTGAG	20	55	59.4	-7.07	none formed	100
PMUQPF2	**AAGATCCAAGACAAAGAAGGTATCC**	**25**	**40**	**59.7**	**-7.08**	**-4.62**	**91**
PMUQPF3	TCTGATCTTCGCTGGCAAGC	20	55	59.4	-8.64	-5.74	87
PMUQPR1	AGGGATACCTTCTTTGTCTTGG	22	46	58.4	-8.57	none formed	99

PMUQPR2	TTGCCAGCGAAGATCAGACG	20	55	59.4	-8.13	-4.62	91
PMUQPR3	**GATGTTGTAGTCTGACAGAGTGC**	**23**	**48**	**60.6**	**-8.03**	**-5.13**	**90**
B. lyrifera							
Citrate synthase							
BLCQPF1	CAGATCCCTACCTTTCGTTTGC	22	50	60.3	-8.98	-4.62	91
BLCQPF2	**CGTTTGCAGCTGGTATGAACG**	**21**	**50**	**59.8**	**-8.47**	**-10.24**	**81**
BLCQPF3	AGGGTGGACAGGTTGTGC	18	61	58.2	-8.39	-4.30	92
BLCQPR1	CTGGTTAGCAAGTCCATGAAGC	22	50	60.3	-8.26	-5.38	89
BLCQPR2	**ACAAGCACCTCCTGGTTAGC**	**20**	**55**	**59.4**	**-7.64**	**none formed**	**100**
BLCQPR3	GAACTCTCGCTGGCAAGTG	19	58	58.8	-6.84	-3.94	92
Heat shock protein 70							
BLHQPF1	AGTCCGACATGAAGCACTGG	20	55	59.4	-7.96	-3.94	92
BLHQPF2	TACATGGGGGAGACAAAGACG	21	52	59.8	-8.13	-5.38	90
BLHQPF3	GGGAGACAAAGACGCTTGC	19	58	58.8	-8.64	-4.9	90
BLHQPF4	**GGTTCAGTCCGACATGAAGC**	**20**	**55**	**59.4**	**-8.26**	**-6.47**	**85**
BLHQPF5	ATTACATGGGGGAGACAAAGACG	23	48	60.6	-8.13	-5.38	90
BLHQPR1	**ATGTAATCGGCCTGTAGCATCG**	**22**	**50**	**60.3**	**-8.61**	**-4.43**	**92**
BLHQPR2	CTGCTGTCTCTTTCATCTTGGTC	23	48	60.6	-7.94	none formed	100
BLHQPR3	CCAGGTATGCTTCTGCTGTC	20	55	59.4	-6.47	-4.55	91
BLHQPR4	GCCTGTAGCATCGGCTTGC	19	63	61.0	-8.64	-6.09	86
BLHQPR5	TTGACCCAGGTATGCTTCTGC	21	52	59.8	-8.27	-4.55	91
Ubiquitin							
BLUQPF1	TTAAGACCCTCACAGGCAAGAC	22	50	60.3	-6.85	-4.85	91
BLUQPF2	**CAAAGCCAAAATCCAGGACAAGG**	**23**	**48**	**60.6**	**-8.57**	**none formed**	**100**
BLUQPF3	ACGTCTGATCTTTGCTGGAAAGC	23	48	60.6	-8.63	-6.49	85
BLUQPR1	TGTCCTGGATTTTGGCTTTGAC	22	46	58.4	-6.82	-3.92	92
BLUQPR2	GCTTTCCAGCAAAGATCAGACG	22	50	60.3	-8.13	-5.49	88
BLUQPR3	**GATGTTGTAGTCTGACAGTGTGC**	**23**	**48**	**60.6**	**-8.39**	**-4.3**	**92**

Gene Sequence Results

1.22. Figure legend for the following five echinoid sequences

The following five appendices illustrate the nucleotide sequences for the *Brissopsis lyrifera* citrate synthase and heat shock protein 70 mRNA transcripts, and the *Psammechinus miliaris* citrate synthase, heat shock protein 70 and ubiquitin (fragment) mRNA transcripts. The nucleotide sequences are presented with the corresponding protein translations. Numbers on the left hand side of each sequence indicate the first nucleotide or amino acid number of that line. The following features of the sequences highlighted in boxes:

a) The 5'- and 3'- untranslated regions (UTRs; boxed)

b) Within the 5'-UTRs, putative TATA elements (in bold and in dotted boxes)

c) In the HSP70 5'-UTR sequences, putative heat shock elements (in bold, highlighted in grey and with the central 3 bp of the pentanucleotide repeats underlined)

d) Immediately after the end of the 5'-UTR regions, the initiation sequence 'ATG' at the start of the coding region.

e) The sites of degenerate PCR primers, qPCR primers, RACE gene specific primers and sequencing primers (boxed in solid or dashed lines), labelled with primer names in the HSP70 and CS sequences, numbered in the UBQL40 sequence.

f) The TAA 'STOP' codon prior to the 3'UTRs (asterisked).

g) Within the 3'-UTRs: putative polyadenylation signals (AATAAA; dashed boxes where present)

h) the poly-A tail (where present) at the end of the 3'UTRs

1.23. *Brissopsis lyrifera* citrate synthase

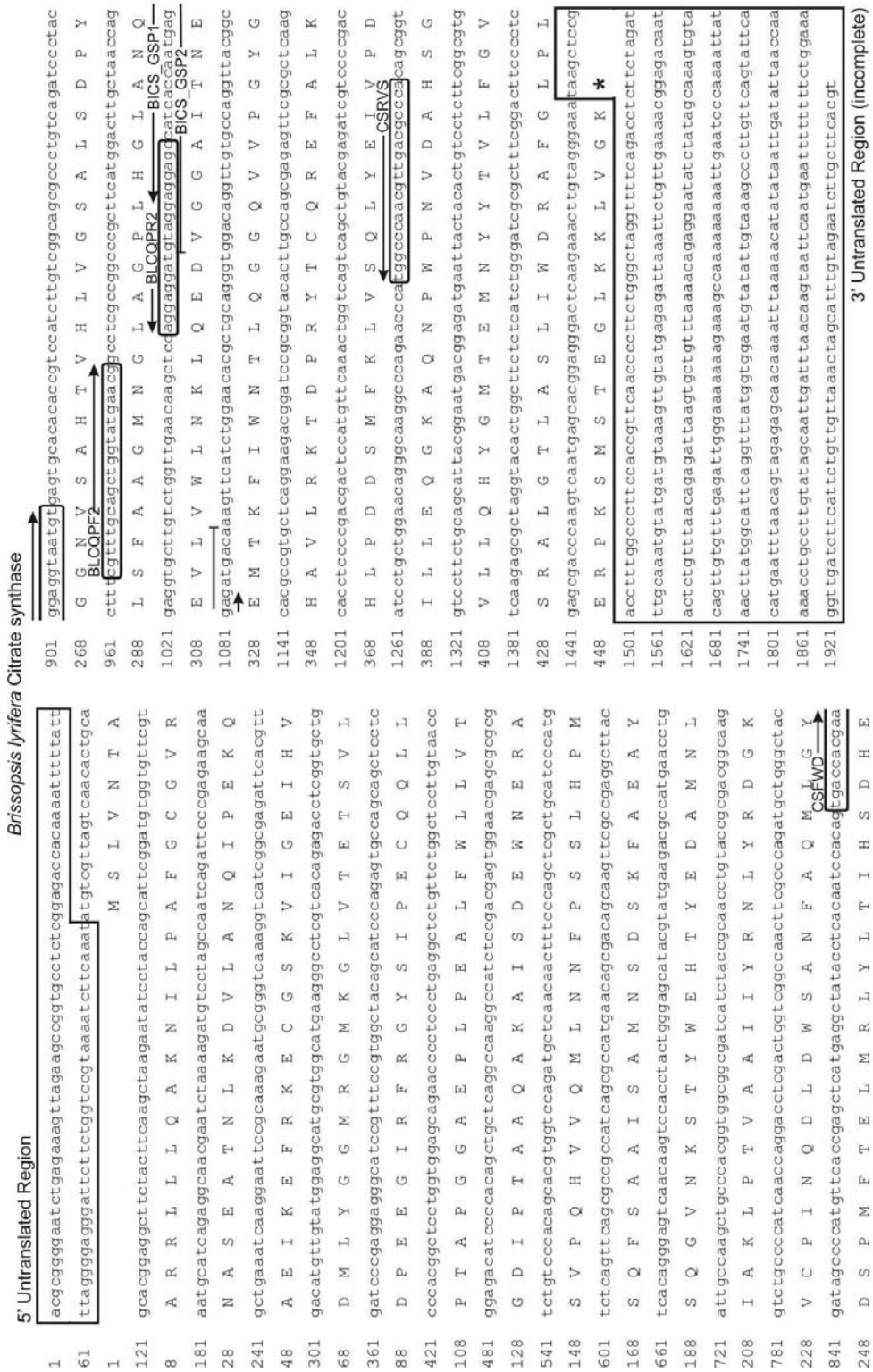

1.24. *Psammechinus miliaris* citrate synthase

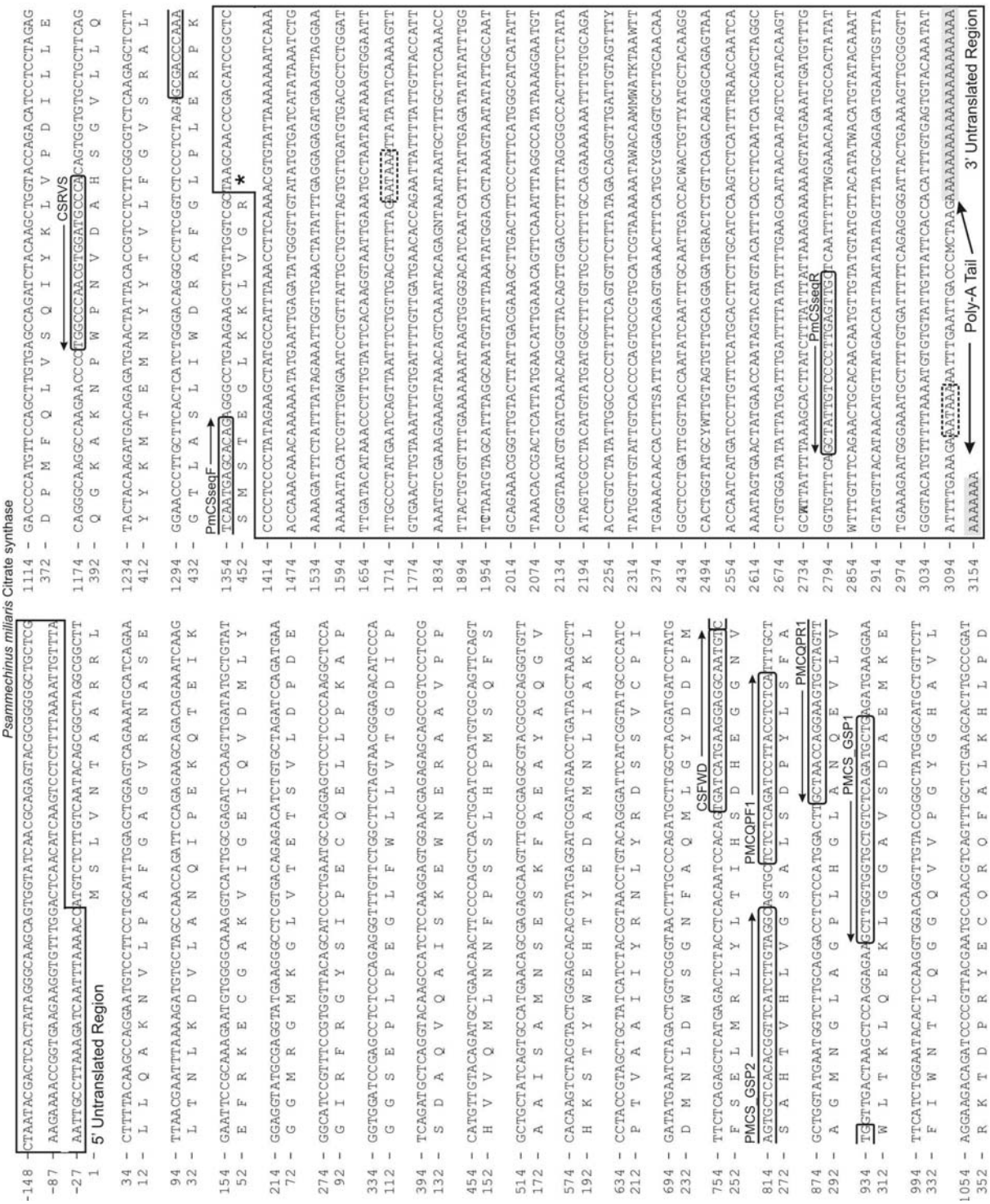

1.25. *Brissopsis lyrifera* putative heat shock protein 70

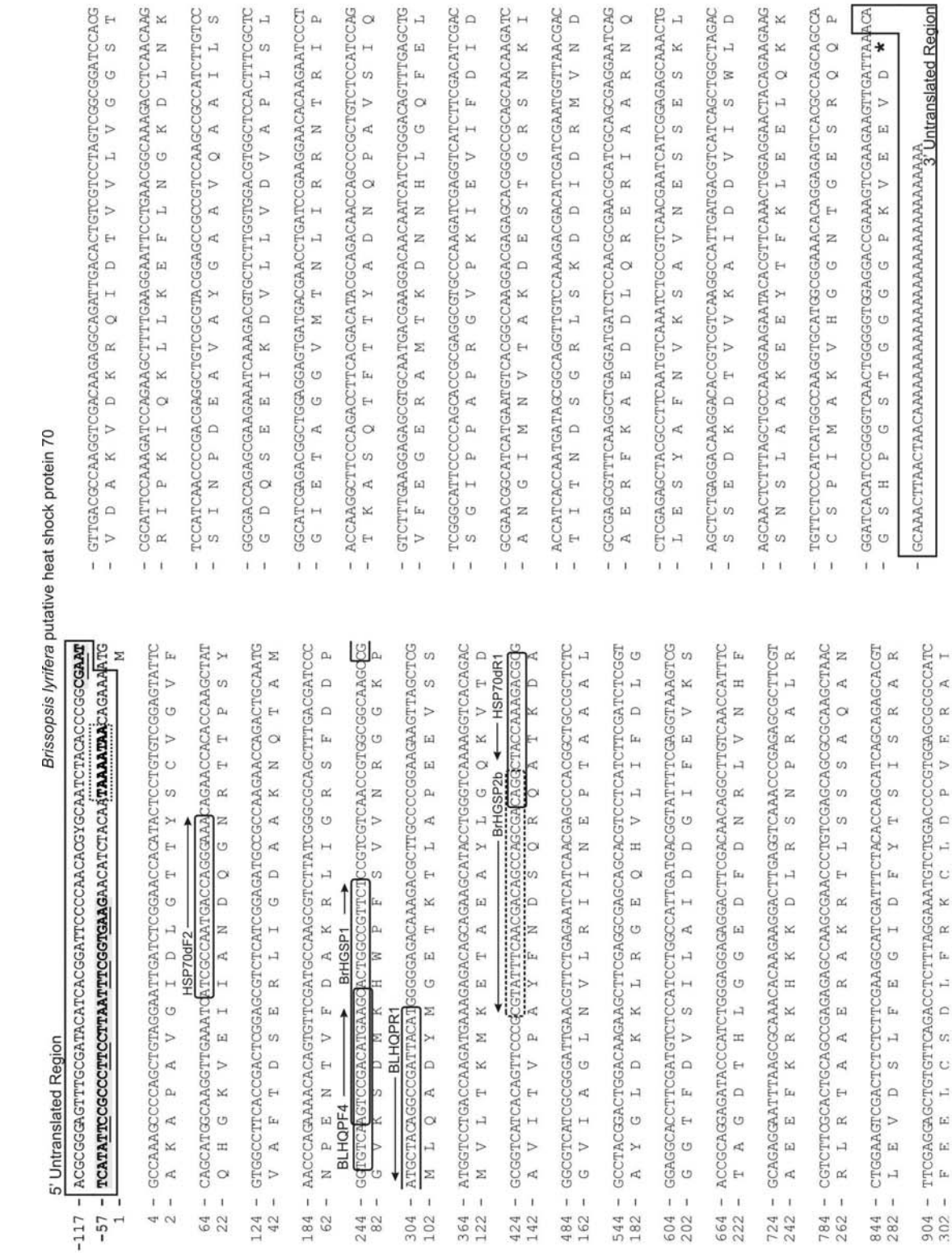

1.26. *Psammechinus miliaris* putative heat shock protein 70

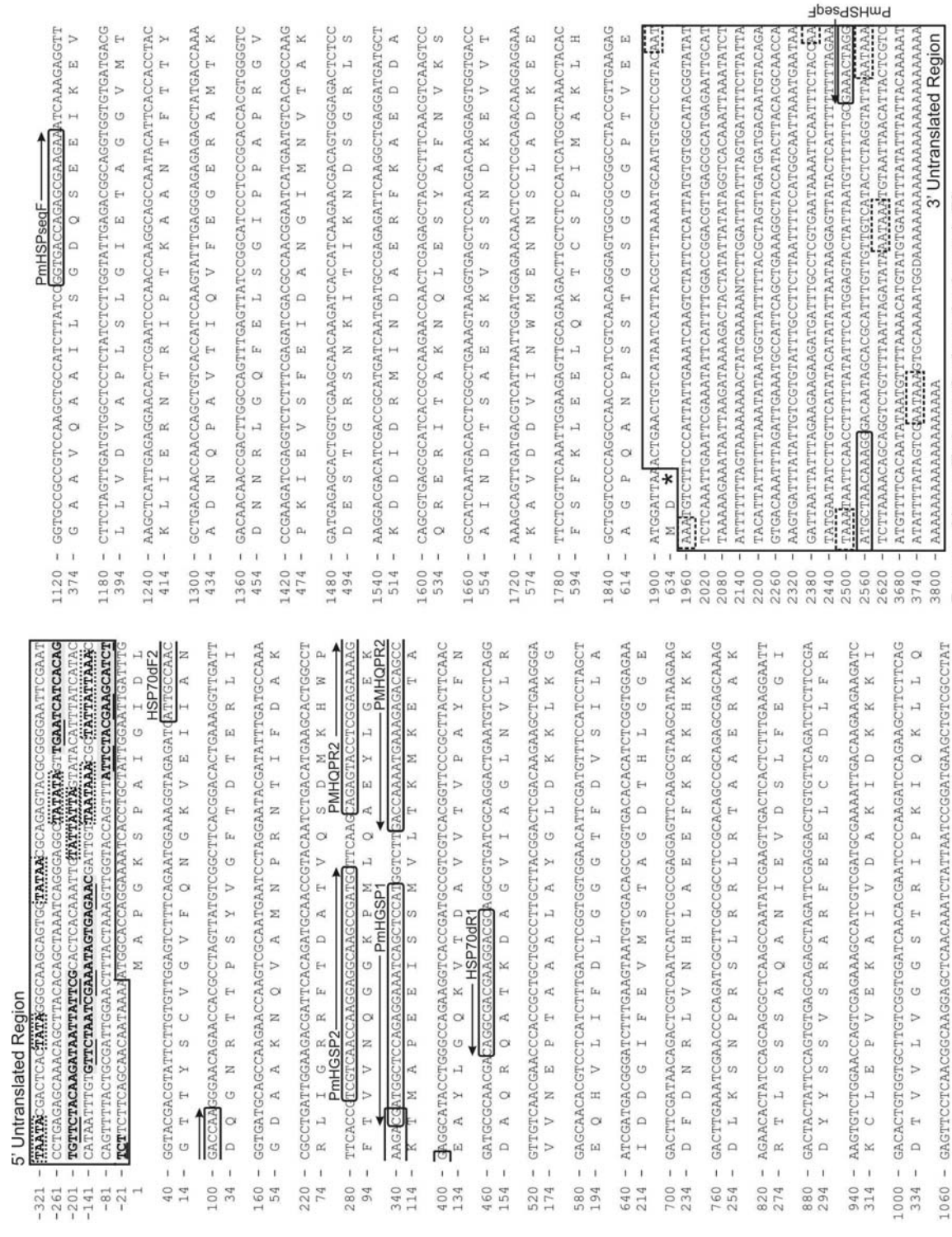

1.27. *Psammechinus miliaris* ubiquitin with 60S ribosomal protein L40

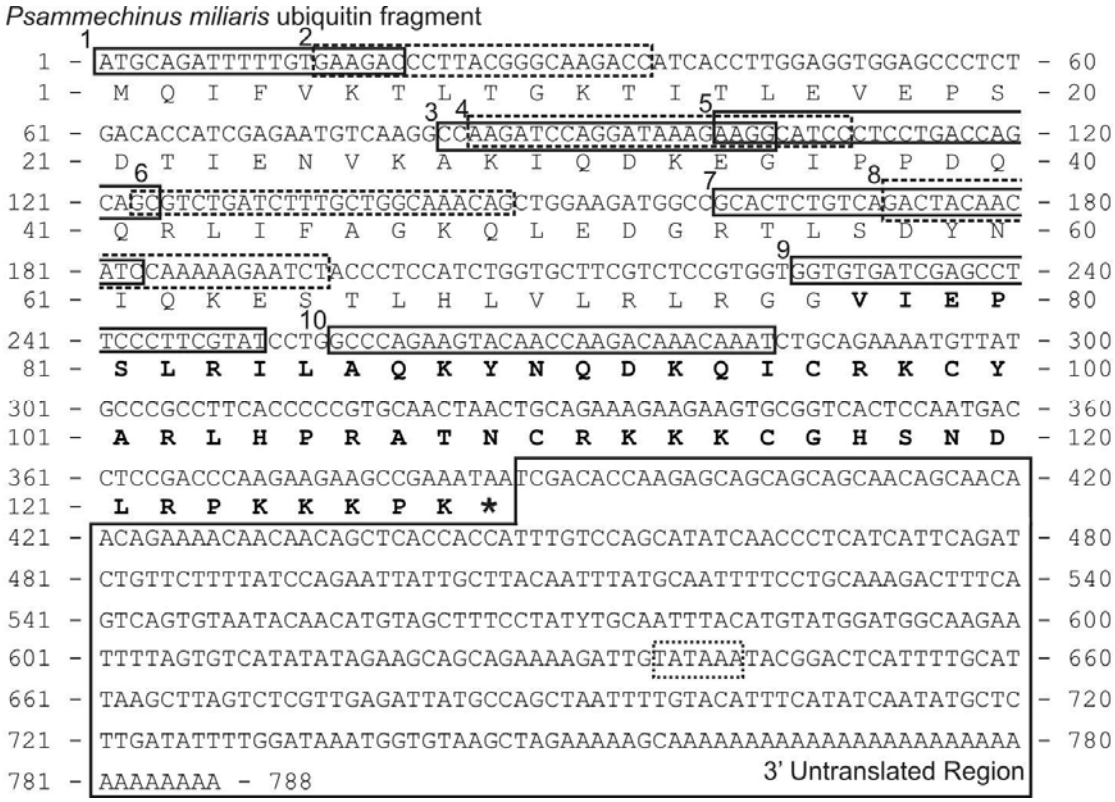

Bold amino acid residues indicate the L40 ribosomal protein sequence.

Primer identities associated with the numbers listed on the figure above:

1. UBQFWDe
2. PmUGSP2
3. UBQFWDb
4. PMUQPF2
5. PmUGSP2b
6. PmUGSP1
7. PMUQPR3
8. UBQRVSd
9. PmUGSP1d
10. PmUGSP1c

1.28. Accession numbers

The following lists of accession numbers refer to the proteins included in the alignments producing the phylogenetic trees included in Chapter 2 at the figures indicated. Accession numbers are listed in order from the top to the bottom of the tree.

Figure 2.13. (Citrate synthase). O24135, O80433, NP_850415, XP_001702983, XP_001386727, XP_367277, XP_001655738, Q7PV48, B4N2K9, B3NXS1, B4JNY9, B4M7X7, B4L2G7, CBK39083 (*P. miliaris*), CAR98205 (*B. lyrifera*), Q0GNE1, Q0GNEO, NP_004068, P0C1Z2, NP_080720, Q8VHF5, NP_001038186, NP_999441, NP_001080194, Q28DK1, NP_955892, Q659V6, Q6S9V5, Q4S5X1, Q6S9V7, Q6S9V8, Q6S9V9

Figure 2.17. (Stress-70): AAH41200, NP05338, BAD15288, BAD07713, CAA42685, CAA44620, AAP37760, BAB93214, AAO65876, AAA62445, AAB88009, AAP37770, ACJ54702, XP_780020, CBJ55211 (*B. lyrifera*), CBL53159 (*P. miliaris*), Q06428, CAA43653, NP_005518, AAN78092, AAA17441, AAH54782, CAA50749, BAA31697, XM_692958, Q91233, O73922, CAA37422, CAB02319, AF250996, AFI67352, AAC23392, AAN14526, AAN14525, ABA02165, AAQ05768, AAT46566, XP_802129, AAS17724, AAW52766, CAC83684, CAC83010, CAC83009, CAC83683, AAH77998, AAB21658, BAD05136, AAB03704, AAO43731, AAH46262, CAA74012, CAA68265, X53335, AAH66191, NM_006597.

Figure 2.20. (Ubiquitin): NP_012118, XP_001538414, XP_001700313, NP_565836, XP_002368400, XP_953703, XP_002141396, XP_789778, CBL53160 (*P. miliaris*), NP_001037372, XP_641020, XP_002130180, NP_001119684, XP_001120521, XP_968519, XP_002579964, XP_002735697, NP_001032190, NP_001117666, NP_001133215, XP_994469, XP_001135183, NP_003324, XP_001508987, XP_001115463.

Manuscripts submitted, in preparation and in press

1.29. Hughes et al. (submitted). Benthic abyssal research using a remotely operated vehicle (ROV): novel experimentation in the Nazaré Canyon.

Sarah J.M. Hughes[a*], Teresa Amaro[a,b], Jeroen Ingels[c], Ben Boorman[a], Lawrence E. Hawkins[a], Ann Vanreusel[c], Marina R. Cunha[b],

[a] DEEPSEAS Group, Ocean Biogeochemistry and Ecosystems, National Oceanography Centre, Southampton, University of Southampton, Waterfront Campus, European Way, Southampton, SO14 3ZH, UK.

[b] CESAM & Departmento de Biologia Universidad de Aveiro, Campus Universitário de Santiago, 3810-193 Aveiro, Portugal.

[c] Marine Biology Department, Ghent University, Krijgslaan 281 S8, 9000 Ghent, Belgium.

* Corresponding author Fax: +44 (0)23 8059 6247 Email: s.j.m.hughes@soton.ac.uk

Abstract

This paper describes the design, and ROV-facilitated deployment and manipulation, of equipment for three novel deep-sea *in situ* studies at abyssal depths in the submarine Nazaré Canyon (North East Atlantic). The first item of experimental equipment, the Benthic Incubation Chamber System 2 (BICS2) was an *in situ* respirometer and during three deployments at ca. 3500 m, the oxygen consumption rates of the ophiuroid *Ophiura irrorata concreta* (Koehler, 1901) were obtained. The second item of equipment, the Poo-Collector, enabled the collection of faeces from the holothurian *Molpadia musculus* (Risso, 1826) in order to gain further knowledge regarding the trophic ecology of these key abyssal deposit feeders. The third experiment, the Feedex ^{13}C pulse-chase experiment, investigated the selective uptake of two differently labelled food sources by the abyssal benthic nematode meiofauna. A brief review of each experimental design and its scientific motivation is discussed, together with a consideration of the experimental design success with respect to scientific operations carried with a ROV.

Key Words

ROV, Experimental ecology, Respirometer, Ophiuroid, Holothurian, Nematodes, North East Atlantic, Western Iberian Margin, Nazaré canyon

1.30. Hughes et al. (in prep). Abyssal echinoderm oxygen consumption and an interclass comparison of echinoderm metabolic rates

Hughes, S.J.M.[1]*, Ruhl, H. A.[2], Hawkins, L.E.[1], Hauton, C.[1], Boorman, B.[2], Billett, D.S.M.[2]

[1] School of Ocean and Earth Science, University of Southampton, National Oceanography Centre, European Way, Southampton, SO14 3HZ, UK

[2] National Oceanography Centre, Southampton, DEEPSEAS Group, European Way, Southampton, SO14 3ZH, UK

* Corresponding author: s.j.m.hughes@soton.ac.uk

Telephone number: +44(0)7811 378310, Fax number: +44(0)23 8059 3059 (c/o H. Ruhl)

Abstract

Despite the low metabolic rates of echinoderms, populations of deep-sea echinoderms can represent significant stores and users of energy in deep-sea benthic ecosystems. When present in large numbers and biomass, and by virtue of their functional role in sedimentary processes, the contribution of echinoderms to long-term deep-sea carbon sequestration could be substantial. Using novel deep-sea respirometry equipment, the oxygen consumption rates from four species of bathyal and abyssal echinoderms have been measured. This data is presented here together with collated metabolic rate data from a further 80 species of echinoderm from polar, temperature, tropical and deep-sea sites, and indicates that the metabolic rate of echinoderms apparently does not vary with depth. The determined allometric scaling relationships between metabolic rate and body mass for each echinoderm class represent updated values for the weight dependant deep-sea echinoderm respiration rates, which can be incorporated into deep-sea energy budget and carbon cycling models.

Key Words

Deep sea, ROV, Echinoderm, Oxygen consumption, Metabolism, Scaling

Journal of Experimental Marine Biology and Ecology 395 (2010) 37–47

Contents lists available at ScienceDirect

Journal of Experimental Marine Biology and Ecology

journal homepage: www.elsevier.com/locate/jembe

An assessment of drilling disturbance on *Echinus acutus* var. *norvegicus* based on *in-situ* observations and experiments using a remotely operated vehicle (ROV)

S.J.M. Hughes [a,*], D.O.B. Jones [b], C. Hauton [a], A.R. Gates [b], L.E. Hawkins [a]

[a] School of Ocean and Earth Science, University of Southampton, National Oceanography Centre, European Way, Southampton, SO14 3HZ, UK
[b] SERPENT Project, Ocean Biogeochemistry and Ecosystems, National Oceanography Centre, European Way, Southampton, SO14 3ZH, UK

ARTICLE INFO

Article history:
Received 18 April 2010
Received in revised form 3 August 2010
Accepted 5 August 2010

Keywords:
Disturbance
Echinoderm
qPCR
Remotely operated vehicle
Sedimentation
Stress-70

ABSTRACT

An industrial work-class remotely operated vehicle (ROV) carried out a video survey of epibenthic megafauna before and after physical disturbance caused by the drilling of a hydrocarbon exploration well in the North Sea, off Norway at 114 m water depth. Megafaunal density, in general, had declined one month after the drilling event. There were particular declines in the density of the numerically dominant echinoid, *Echinus acutus* var. *norvegicus*, in a 50 m zone around the drill site. The ROV was also used to carry out *in-situ* experiments to assay the effects of drilling disturbance (via sediment burial) on *E. acutus* and, in addition, to determine any consequence upon *E. acutus* of retrieval to the surface (due to decompression and temperature change). Changes in the expression of an inducible stress-70 protein in echinoid Aristotle's lantern muscle and intestine were evaluated using quantitative real-time PCR. Sediment burial caused a significant increase in the expression of a stress-70 gene from the echinoids' Aristotle's lantern muscle tissue. Repeated echinoid retrieval to the sea surface did not result in any significant alteration of stress-70 gene expression. These experiments show the utility of ROVs in linking ecological observations with real-time *in-situ* experimental manipulations, and that investigative gene expression techniques can be incorporated in the subsequent analysis of retrieved specimens.

1. Introduction

Industrial activities are expanding on the continental shelf and further into deeper water (Pinder, 2001; Davies et al., 2007; Eastwood et al., 2007). As industrial activity increases, physical disturbance will become more common in the deep sea, with many potential consequences for the deep-sea environment and associated communities (Bluhm, 2001). Anthropogenic causes of deep-sea physical disturbance include dumping of dredged material, deep-sea mining and drilling activities (Thiel, 2003).

The effects of anthropogenic disturbance, such as oil drilling activity, on the deep-sea benthic environment are conventionally assessed by sampling sediment (typically by grab) and then measuring chemical parameters (e.g. heavy metal content) and occasionally macrofauna (for diversity analyses) from the origin of the impact along four radiating transects at geometrically increasing distances (Gray et al., 1990; Kingston, 1992). The epifaunal megabenthic community can also be surveyed photographically, by towed camera platforms (Bluhm, 2001), submersibles or remotely operated vehicles (ROVs) (Jones et al., 2006), to evaluate the impacts of disturbance at the seafloor. Imaging studies allow fine scale survey of megabenthic fauna (Piepenburg and Schmid, 1997) over a much larger spatial extent than is usually possible with conventional macrofaunal sampling techniques. However, despite these investigative techniques, the mechanisms of the impact of physical disturbance on deep-sea animals are not understood and we currently lack the capacity to predict accurately the effects of anthropogenic physical disturbance upon deep-sea ecosystems (Gage, 1996; Ahnert and Borowski, 2000; Smith et al., 2008).

Terrestrial and shallow-water ecological investigations have progressed from simple observations of natural history and the description of organisms and populations, to planned investigations and experimental manipulations (Chapman, 2002). This progression is still ongoing within the field of deep-sea ecology, where ecological investigation is still primarily in the descriptive phase (Jones, 2009), and there is an incomplete understanding of deep-sea organisms, communities and processes (Gage, 1996; Smith et al., 2008). There is a need for well-planned experimental and manipulative work to investigate the mechanisms behind deep-sea ecological processes and change in deep-sea communities, such as that caused by anthropogenic disturbance (Ahnert and Borowski, 2000; Thiel, 2003).

Deep-water drilling activities cause physical changes to the seafloor as drill cuttings composed of drilling mud, chemicals, and fragments of rock are discharged to the seabed (Breuer et al., 2004).

* Corresponding author. Tel.: +44 7811 378310; fax: +44 23 8059 3059 (c/o C. Hauton).
E-mail addresses: sjmhughes@gmail.com (S.J.M. Hughes), djones@noc.soton.ac.uk (D.O.B. Jones), ch10@noc.soton.ac.uk (C. Hauton), arg3@noc.soton.ac.uk (A.R. Gates), leh@noc.soton.ac.uk (L.E. Hawkins).

0022-0981/$ – see front matter © 2010 Elsevier B.V. All rights reserved.
doi:10.1016/j.jembe.2010.08.012

Solid cuttings physically affect benthic fauna by burial, altering sediment particle size, generating anoxic conditions and changing chemical fluxes in the sediment–water interface (Neff et al., 2000; Trannum et al., 2010). Burial by sediment can have sublethal effects on affected organisms (Rogers, 1990), caused by changes in food supply, feeding inhibition, displacement to unsuitable habitats and physical injury (Hall, 1994), as well as directly causing mortality (Chandrasekara and Frid, 1998; Hinchey et al., 2006).

It is argued that to completely understand the impact of disturbance in the environment a 'systems biology' approach is required, one that incorporates investigative techniques throughout the hierarchy of biological organisation from the molecular to the population level (Moore et al., 2004; Connon et al., 2008). Modern biological investigations can detect changes at the molecular and cellular level of an organism in response to sublethal stressors (Sanders, 1993; Williams et al., 2003; Valavanidis et al., 2006). These changes can then be linked to physiological stress that may manifest itself at the population level (Menge et al., 2002; Dahlhoff, 2004). Up-regulated gene expression and activities of stress-inducible proteins have been used as molecular biomarkers of both environmental- and pollutant-induced stress for a number of years (Feder and Hofmann, 1999; Bierkens, 2000; Dahlhoff, 2004). The 70-kDa heat shock protein (HSP) family, also termed "stress-70 proteins" (Gething and Sambrook, 1992), have been widely used in aquatic biomonitoring and environmental toxicology (Feder and Hofmann, 1999; Lewis et al., 1999). HSPs are molecular chaperones that stabilize denaturing proteins and refold reversibly denatured proteins (Lindquist and Craig, 1988; Feder and Hofmann, 1999). These proteins are viewed as useful biomarkers because their expression is directly linked to cellular damage, and their induction is more sensitive to stress than traditional indices such as growth inhibition (Feder and Hofmann, 1999; Mukhopadhyay et al., 2003; Hamer et al., 2004).

Molecular-based investigations with deep-sea organisms are complicated by the physical environment that they inhabit. The deep sea is typically colder and always at a greater pressure than that found at the sea surface. Deep-sea organisms retrieved to the surface, unprotected from decompression and increasing temperature, may experience detrimental side effects ranging from molecular (Dixon et al., 2004) and physiological changes (Bailey et al., 1994) to paralysis (Macdonald, 1997) and death (Hessler, 1972; Treude et al., 2002). These side effects mean that experiments performed with organisms adversely affected by retrieval to the surface may generate results that are not representative of those that would have been found had the experiment been performed at the seafloor (Roer et al., 1984; Shirayama, 1995; Theron and Sebert, 2003). The validity of experiments performed with deep-sea organisms could be improved if they were carried out on the seafloor. *In-situ* deep-sea experiments, however, have historically been restricted by the technical difficulties associated with performing complex work at depths inaccessible to human divers.

The increasing use of modern robotic technology, such as ROVs, will make deep-sea experimentation easier and more frequent. ROVs are used extensively by the offshore drilling industry to support deep-water activities (Jones, 2009), and are now being increasingly used by the international scientific community for enhanced deep-sea observation, fine scale mapping and sampling (Bachmayer et al., 1998; Yoerger et al., 2007). Recent ROV activities show that these vehicles are not just useful as a platform for observational work (Laurenson et al., 2004; Benfield and Graham, 2010), but also make possible the interactive deployment and operation of equipment to carry out real-time *in-situ* research activities to test experimental hypotheses (Van Dover and Lutz, 2004; Jones, 2009). For example, ROVs have successfully been used in the deep sea to perform megafaunal exclusion caging experiments (Gallucci et al., 2008), elevated benthic CO_2 simulations (Thistle et al., 2007), megafauna isolation experiments (Hudson et al., 2004) and trophic selectivity manipulations (Andrews et al., 2008).

In this study, an industrial work-class ROV (Jones, 2009) was used to investigate the effects of physical disturbance caused by exploratory drilling on megabenthic organisms. ROV video surveys were used to assess the effect of disturbance on the megabenthic assemblage. To further explore observed patterns of megafaunal exclusion, and to test the potential of using a work-class ROV for manipulative *in-situ* experimentation, a novel experiment was undertaken to detect sublethal, molecular level effects of sediment burial in the numerically dominant species, the echinoid *Echinus acutus* var. *norvegicus* (Düben and Koren, 1846). Additionally, to assess possible artefacts within experimental results caused by post-experimental recovery to the surface from 114 m water depth, ROV-facilitated echinoid surface retrieval manipulations were also performed. The focus of the molecular investigations was the detection of changes in the expression of a stress-70 gene via quantitative real-time polymerase chain reactions (qPCR). To our knowledge, this is the first application of a sensitive molecular technique to detect the effects of drilling disturbance on a marine invertebrate via ROV-facilitated experimentation.

2. Materials and methods

2.1. Study site

The work was carried out in summer 2007 during two visits to the Ragnarokk hydrocarbon exploration area (Fig. 1), located west of Stavanger, Norway in the North Sea (058° 53 N, 002° 22 E). All work was carried out from the M.V. *West Epsilon*, a three-legged cantilever jack-up drilling unit, using a work-class Oceaneering Hydra Magnum 034 ROV. The ROV was equipped with 5-function and 7-function manipulator arms which were used for experimentation; a Kongsberg Colour Zoom video camera (model: OE14-366) used to make *in-situ* observations and record video transects, and a small Kongsberg colour video camera (model: OE14-110) mounted to the 7-function manipulator arm that allowed detailed inspection of the experimental chambers without disturbing the experiment.

The physical disturbance investigated during this study was drilling for a hydrocarbon exploration well, which occurred on 31 July 2007. The water depth at the drill site was 114 m and the water temperature recorded at the seabed with the ROV's parascientific temperature sensor was 8.4 °C. The sea surface temperature was not recorded during the time of deployment by the ROV, but CTD data collected previously at this location indicate a surface temperature of ~14 °C during July and August (BODC, 2009). Currents at 10 m above the seabed in the nearby PROVESS project (Howarth et al., 2002) study site (059°19.89′N, 001°00.06′E; 110 m water depth) were dominated by tidal motion (Knight et al., 2002). Currents were usually less than 0.20 m s^{-1} and never exceeded 0.30 m s^{-1} (Howarth et al., 2002; Jago et al., 2002).

2.2. In-situ video surveys

ROV video transects were used to quantify the distribution of megabenthic fauna around the source of the drilling disturbance. Video transects radiated outwards from a central conductor pipe, used to stabilize the well and to direct the drill bit. Transects were approximately 100 m in length and limited by the maximum safe extension of the ROV tether. Video transects were carried out before drilling (28/07/2007) and after drilling (01/09/2007). During both the pre- and post-drilling surveys eight video transects were taken on the following true bearings: 010, 055, 100, 145, 190, 235, 280 and 325°. The post-drilling 010° transect was of poor quality owing to low visibility and was excluded from subsequent analysis.

Before each transect the Kongsberg colour video camera was zoomed out to maximum extent and set to its most vertical angle (47° below horizontal). In all instances the ROV was run in a straight line

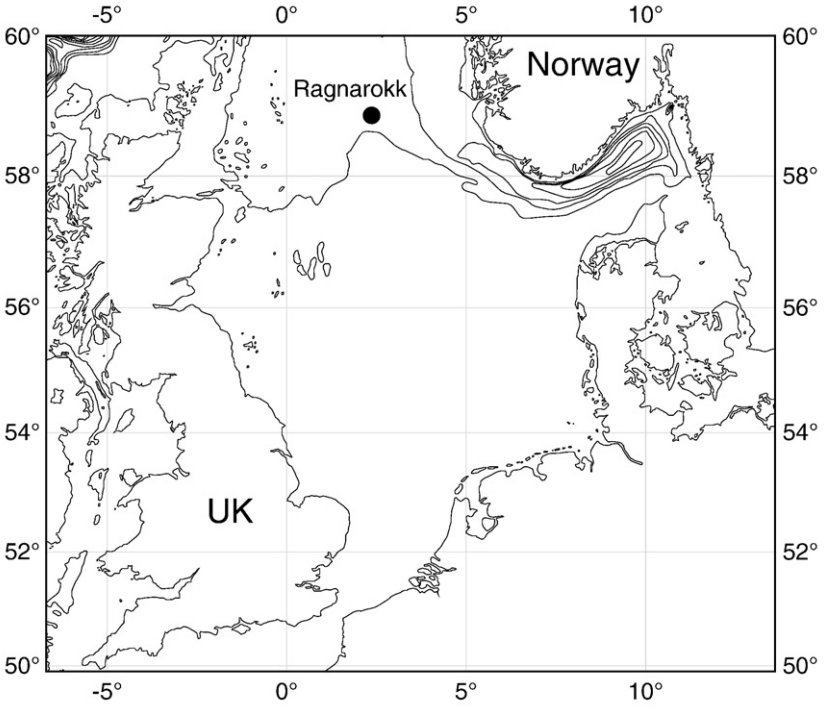

Fig. 1. Location of the Ragnarokk study site in the North Sea. 100 m isobaths are indicated.

away from the conductor pipe located at the source of drilling disturbance (Fig. 2), on a set bearing at a constant speed (0.3 m s^{-1}) and altitude (0.2 m). The width of the transect (0.91 m) was calculated from the camera acceptance angles and vehicle altitude (Jones et al., 2006); it was also verified by reference to objects of known size (e.g. the conductor pipe and ROV manipulator arms). This allowed the derivation of total surface area covered by each transect with a precision of ± 1 m^2. All megafaunal organisms observed during each transect were recorded, identified to the lowest taxonomic level possible from the video footage and megafaunal density along each transect calculated as the number of individuals per m^2 (indiv.m^{-2}).

The pre-drilling transects revealed the presence of large numbers of monospecific echinoids (Fig. 3), which were subsequently identified from samples collected for taxonomic analysis as *E. acutus* var. *norvegicus* (hereafter referred to as *E. acutus*). To further investigate the density changes of the numerically dominant *E. acutus*, each transect was divided into 10 m zones extending out from the conductor pipe. Mean echinoid densities were calculated for each zone from the results of all transects and expressed in indiv.m^{-2}.

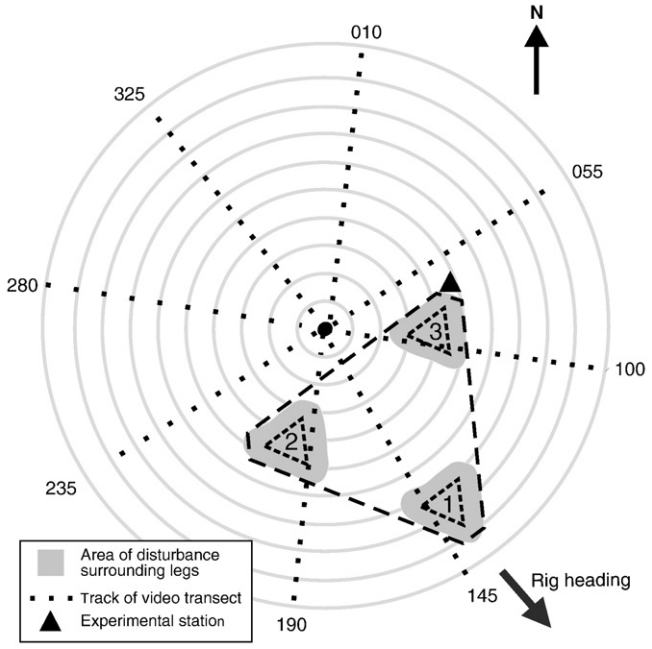

Fig. 2. Map of the seabed around the Ragnarokk drill site showing the position of the three rig legs (labelled small dashed triangles) and the estimated area of disturbance caused by the deployment of each leg. Each concentric ring around the central drill site (represented by the filled black circle, where the central conductor pipe was located) represents 10 m and illustrates the zones each transect was separated into for the calculation of echinoid densities. The eight tracks of the video transects are also shown. The filled triangle shows the site of experimental work. The position of the rig at the sea surface is shown by the large dashed triangle.

2.3. Sediment sampling

ROV push cores were used to collect sediment which was analysed for heavy metal content, total organic carbon and grain size before and after drilling. The push cores were of approximately 300 mm length and 58 mm internal diameter with a surface area of 2642 mm^2. Prior to drilling, the push core sites were located on a bearing of 145° and at distances of 0, 25, 50 and 120 m from the proposed drill site. Post-drill the push cores were taken on the same bearing at distances of 10, 25, 50 and 100 m from the drill site (owing to tether malfunction a push core at 120 m was not possible), and additionally at the site of echinoid experimentation (near leg 3). Two push cores were taken at each site; one for heavy metal analysis and the other for sediment property analysis (Table 1). At each site, once position was determined using ROV sonar fixes on the rig legs or central conductor pipe (precision ± 1 m), the ROV landed on the seabed as gently as possible and collected push core samples with the manipulator arms. The cores were pushed approximately 200 mm into the sediment, retrieved and stored on the ROV for < 1 h prior to processing on the rig. The top 50 mm of sediment was removed from each core and transferred into sample containers. Sediment samples were stored

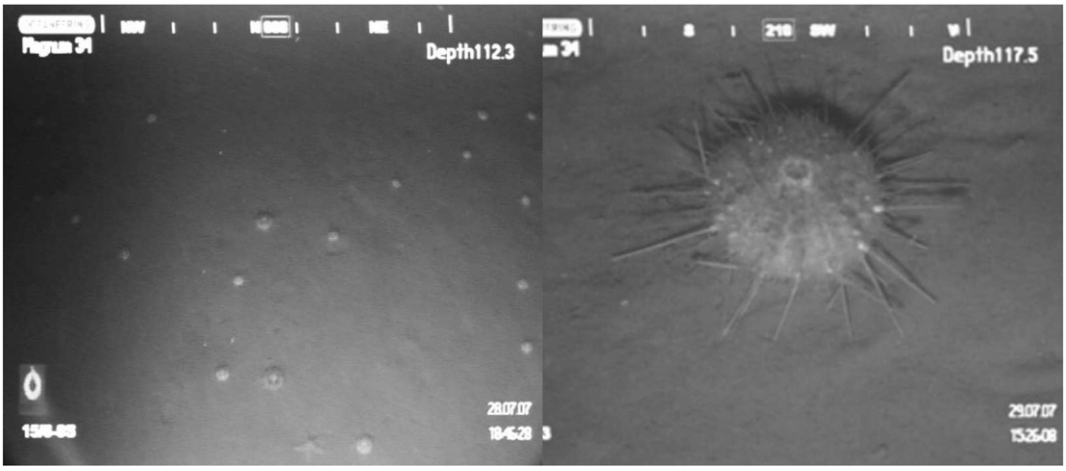

Fig. 3. *Echinus acutus* var. *norvegicus* were the most abundant organisms observed during the video transects at the Ragnarokk hydrocarbon exploration field in the North Sea. The image on the left is a video transect still photograph, and numerous *E. acutus* individuals can be seen as well as an asteroid at the bottom of the image. To the right is a close-up screen grab of an individual *E. acutus*.

frozen (−20 °C) until analysis by a commercial laboratory (Eurofins, Norway) using standard analysis protocols (Bett, 2001).

2.4. ROV experimentation

ROV-facilitated sediment burial and surface retrieval experiments were performed with *E. acutus* specimens during the second visit to the M.V. *West Epsilon* between 30/08/2007 and 05/09/2007.

2.4.1. Specimen collection

Specimens of the abundant echinoid *E. acutus* were collected near to leg 3 of the jack-up rig (Fig. 2) using a ROV operated push core held in the 7-function manipulator arm. Echinoids were scooped up into the push core with minimal disturbance and no damage. Once collected, the echinoids were transferred directly into experimental chambers or immediately brought to the surface in upturned push cores for further experimentation or preservation as detailed later. The time taken to transport the echinoids from the seabed to the deck of the rig was 14 min. Tissue samples dissected from the intestine and Aristotle's lantern musculature of the echinoids were immediately transferred into separate 2.5 ml sterile microcentrifuge tubes that contained 1.5 ml RNAlater® Solution (Ambion). The tissue samples were transferred to a freezer (−20 °C) within 1 h of dissection. Some additional whole specimens were retained in borax-buffered 10% formalin for later onshore taxonomic identification of the echinoid species.

2.4.2. Experiment 1: The effects of (in-situ) surface retrieval on stress-70 expression

On one dive, two echinoids were collected and immediately brought to the surface in a push core, dissected and preserved. From collection at the seafloor to final preservation took approximately 50 min. On the next ROV dive another two echinoids were collected in the core and brought up to a depth of 10 m. These two echinoids were then returned to the seabed and then immediately brought back up through the water column and recovered onto the deck of the rig. The echinoids were then dissected and preserved (within 70 min of collection at the seafloor). Temperature difference between the seafloor and sea surface was approximately 5.6 °C and the pressure change was approximately 1054 kPa.

2.4.3. Experiment 2 (in-situ): The effects of sedimentation on stress-70 expression

To investigate the impact of physical disturbance by sedimentary burial on stress-70 expression, an experiment was carried out subjecting *E. acutus* individuals to three treatments: a procedural control (C), a single sedimentation event (S) and multiple sedimentation events (MS), designed to simulate the discharge of sediment during the initial phases of a potential tophole drilling programme. Experimental chambers were constructed using 5 l plastic buckets weighted in the base with a large stainless steel washer. To improve their manoeuvrability whilst submerged, and to prevent the possible creation of an anoxic boundary layer in the bottom, 10 mm holes were drilled in the sides and base of each bucket. A polypropylene floating rope with a monkey's fist knot was attached to the bucket handle to

Table 1
Physical and chemical sediment measurements from ROV push cores collected on a bearing of 145° at the Ragnarokk hydrocarbon exploration area. Norwegian Continental Shelf (NCS) background levels are included (Frost et al., 2006). It is standard practice to report sediment contaminant levels per unit of dry weight; hence the sample dry weight % (of total wet weight) is listed. All metals are expressed in mg per kg sediment dry weight^{-1}.

Distance from drill site, m	Pre-drill				Post-drill					NCS
	0	25	50	120	10	25	50	100	Leg 3	Background
Dry weight, %	75.7	76.8	75.7	77.9	78.2	58.5	65.1	76.7	74.9	
Fraction <63 μm, %	6.2	6	6	6	54.9	50.1	11	6	7.3	
Total organic carbon, %	0.44	0.51	0.45	0.25	0.09	0.33	0.17	0.33	0.48	
Barium	39	80	58	45	6000	5200	760	150	260	4.6–554
Titanium	59	66	74	56	98	210	170	69	95	
Lead	4.8	4.5	4.1	4.2	6	15	5.3	3.8	4.8	1.92–46.5
Cadmium	0.018	0.018	0.023	0.019	0.041	0.096	0.036	0.013	0.02	0.003–0.13
Chromium	6.5	5.7	5.5	5.9	6.9	13	11	5.4	7.5	2.58–39.2
Copper	1.7	1.7	1.9	1.7	6.2	16	13	1.7	4.1	0.3–17.2
Zinc	9.8	9.3	9.3	8.3	18	40	18	7.3	12	0.42–83.7

facilitate ROV manipulation. A lid was placed on the bucket with an 87 mm diameter hole (20 mm larger than the push core tube) cut in it to allow for video inspection and the introduction of echinoid specimens and sediment.

Three clearly labelled experimental treatment chambers were deployed by the ROV next to each other on the seabed 5 m to the north of leg 3 of the rig (Fig. 2). Six echinoids were carefully added to each experimental chamber using the push core sampler. Immediately after echinoid introduction, approximately 1000 cm^3 of sediment was collected from the adjacent seabed using the push core sampler, and introduced to both the S and MS experimental chambers. No sediment was added to the control treatment chamber. A sediment volume of 1000 cm^3 represented an approximate sediment depth of 3 cm at the base of the experimental chambers. This treatment just covered the echinoids and produced a level sediment surface within the chamber. The echinoids were observed in all chambers without further disturbance using the small camera on the 7-function manipulator arm. One hour after the first sediment treatment, and after the echinoids had all repositioned themselves on the sediment surface, another ~1000 cm^3 of sediment was added to the MS treatment. Twenty-four hours after initial deployment another ~1000 cm^3 of sediment was added to the MS treatment. All experimental chambers were retrieved simultaneously 48 h after the start of the experiment. Three echinoids were found to remain in each of the experimental chambers (the missing echinoids were presumed to have escaped from the chambers via the lid observational hole); each remaining echinoid was processed and preserved within 80 min of leaving the seafloor.

2.4.4. Experiment 3 (ex-situ): Preliminary induction of a stress-70 HSP

To ensure the collection of tissue samples which contained sufficient numbers of stress-70 mRNA templates to allow the mRNA to be isolated with degenerate primers, individual echinoids were heat shocked. Heat shock treatment was chosen to stimulate stress-70 induction because previous studies have shown that echinoids express HSPs in response to thermal stress (Sconzo et al., 1995; Osovitz and Hofmann, 2005). Twenty echinoids were collected on the seafloor with a push core and brought immediately to the surface, where they were transferred to gently aerated aquaria maintained at 25 ± 1 °C on the rig. One echinoid was removed from the aquaria hourly from the start of the experiment, dissected and preserved immediately.

2.5. Gene expression analysis

2.5.1. Isolation of E. acutus-specific stress-70 mRNA fragments

Total RNA was extracted from the preserved Aristotle's lantern muscle tissue from a 10-hour heat shocked echinoid using TRI Reagent™ (Sigma-Aldrich) according to the manufacturer's protocol, and quantified by measuring the absorbance at 260 nm. Total RNA (~2 μg) was reverse transcripted into complementary DNA (cDNA) in a 20 μl reaction which included 200 units SuperScript II Reverse Transcriptase with accompanying First Strand Buffer and 0.1 M DTT (Invitrogen), 40 unit RNase Inhibitor (Sigma-Aldrich), random nonamers (2.5 μM final concentration; Sigma-Aldrich) and 10 mM dNTP mix (New England Biolabs). The cDNA obtained was used for conventional polymerase chain reaction (PCR) cycling with degenerate oligonucleotide primers.

The degenerate primers were designed against conserved regions identified from an alignment of a number of amino acid sequences for the inducible heat shock protein 70 (HSP70) from two decapod crustaceans, three Actinopterygii fish, two amphibians; and one galliform bird, lepidopteran insect, bivalve, demosponge, ascidian and anthozoan (respective GenBank accession nos. Q3S348, Q6GUA8, O93240, Q91233, Q6TDU0, P02827, Q91291, P08106, Q86GI6, Q53IQ6, Q24952, Q93147 and Q5FB18). The sequence of the forward primer was: 5′-ATHGCNAAYGANCARGGNAA-3′; and the sequence of the reverse primer was: 5′-GCRTCYTTNGKNGCYTG-3′. The primers were supplied by Eurofins MWG Operon (Ebersberg, Germany). PCR amplifications were carried out using a Primus 96 Legal PCR System Thermocycler (MWG Biotech). Cycling conditions consisted of 1 cycle of 94 °C for 3 min; 35 cycles of 94 °C for 30 s, 49 °C for 45 s, and 72 °C for 60 s and 1 cycle of 72 °C for 10 min. The PCR was performed with a 25 μl mixture containing 1 μl cDNA, 2.5 μl of 10× CoralLoad PCR buffer (QIAGEN), 0.5 μl of 10 mM dNTP mix (New England Biolabs), 2.5 U of *Taq* DNA polymerase (QIAGEN), 2 μM of each primer and nuclease-free water to 25 μl. A single band of approximately 400-bp was obtained.

The PCR fragment was gel-purified on a TAE 1% agarose gel, extracted using a QIAquick gel extraction kit (QIAGEN) and cloned using an Invitrogen TOPO TA Cloning® Kit for sequencing (pCR®4-TOPO® vector and One Shot® TOP10 *Escherichia coli*; Invitrogen). Positive *E. coli* transformants were identified by PCR using vector-specific (M13) primers. Selected colonies with the correct-sized insert were grown overnight in a LB broth with ampicillin (100 μg/ml). The plasmids were then extracted from the *E. coli* cultures using a QIAprep® Miniprep Kit (QIAGEN). The fragment was sequenced (three random clones; both strands) using M13 primers on a 3730xl DNA Analyzer (Applied Biosystems) by Geneservice Ltd. (Department of Biochemistry, University of Oxford). The obtained nucleotide sequences were aligned and translated using Geneious Basic trial software 4.8.3 (Drummond et al., 2010). A similarity analysis of the deduced protein sequence was carried out using BLAST 2.2.19+ at NCBI (Altschul et al., 1997).

2.5.2. Quantitative real-time PCR assay

Quantification of mRNA transcript abundance required a pair of species-specific primers to be designed for the stress-70 gene. Two qPCR primers, 5′-GAGTTCAAGGGAGAAACCAAGAC-3′ (forward) and 5′-GCAGTTTCTTTCATCTTGAGCAG-3′ (reverse) were designed targeting a 77-bp region of the sequenced *E. acutus* stress-70 gene fragment. The primers were designed manually and their features checked for qPCR suitability with NetPrimer (PREMIER Biosoft International; http://www.premierbiosoft.com/netprimer/index.html). The optimal primer concentration used in the qPCR was determined from a primer concentration matrix (Nolan et al., 2006), and the products from these optimisation tests were run out on an agarose gel and visualised to confirm that the product was the expected size. The efficiency and sensitivity of the qPCR assay were then tested using the standard curve method. A qPCR standard curve was produced from a dilution series of extracted pCR4-TOPO vectors, which contained a target amplicon specific to each qPCR primer. The plasmids were first linearised using the restriction enzyme Not I (Sigma-Aldrich), which cut the plasmid but not the cloned nucleotide sequences. The relationship between concentration and C_q (quantification cycle; Bustin et al., 2009) value was linear for seven orders of magnitude for the plasmid dilution series and calculated assay efficiency was 95% ($C_T = 31.525 - 3.447 \times \text{Log Dilution}$; $r^2 = 0.995$).

2.5.3. Reverse transcription and qPCR analysis of gene expression

The Aristotle's lantern muscle and intestine tissue samples taken from each experimentally treated echinoid were homogenized in TRI Reagent™ (Sigma-Aldrich) and total RNA isolated according to the manufacturer's protocol. To remove genomic DNA contamination, the total RNA samples were then treated with DNase Amplification Grade I (Sigma-Aldrich). Total RNA was then quantified with Quant-iT™ RiboGreen® RNA Quantitation Reagent (Invitrogen). For cDNA synthesis, 300 ng of DNase-treated total RNA was reverse transcripted using SuperScript Reverse Transcriptase III (Invitrogen) with random nonamer primers (Invitrogen). The qPCR assay was performed using a Rotorgene-3000 (Corbett Research Ltd.) using reactions containing 1 μl of cDNA, each qPCR primer (50 nM final concentration), 10 μl of 2× Precision Master mix with SYBRgreen (PrimerDesign Ltd.) and

nuclease-free water to a total volume of 20 µl. The qPCR was run with the following cycle parameters: 1 cycle of 95 °C for 10 min; 35 cycles of 95 °C for 10 s, 60 °C for 40 s, and 60 °C for 20 s. Each experimental cDNA sample was run in duplicate, three times (in order to control for qPCR reproducibility), together with "no template controls" and a cDNA calibrator sample. Melt curve analysis was performed following each qPCR to confirm that only a single product was amplified.

The number of mRNA transcript copies of the gene was determined using an absolute quantification approach (Bustin, 2000). To correct for inter-run variations, the C_q value of every sample was normalized to that of the corresponding cDNA calibrator sample included in each qPCR assay (Wong and Medrano, 2005). The mean C_q value of each duplicate sample was then compared to a standard curve produced from a serial dilution of the Not I linearised pCR4-TOPO vector according to an established protocol (Roche Diagnostics GmbH, 2003). The DNA concentration of the linearised plasmid was determined from optical fluorescence measurements using Quant-iT™ PicoGreen® dsDNA Quantitation Reagent (Invitrogen). The numbers of mRNA transcripts in each qPCR reaction were then calculated from the standard curve regression equation, and converted to transcript numbers per µg of starting total RNA.

2.6. Statistical analysis

Owing to the large numbers of echinoids around the drill site, statistical analysis was carried out separately on community density data (without echinoids) and on echinoid density data. This was performed to remove the dominant effect on community density data by the numerically dominant echinoids. Community density (indiv. m^{-2}) before and after drilling tested positive for normality and variance homogeneity and the Student's t-test was used to test significance using the total density of megafauna in each video transect as replicates ($n = 8$ prior to drilling and $n = 7$ post-drilling). Two-way analysis of variance on ranks was performed on the echinoid density data (which failed tests for normality and equal variance); with replicates composed of the echinoid density (indiv. m^{-2}) found within 10 m zones (i.e. 0–10 m, 10–20 m, etc.) along each transect (before and after drilling). *Post hoc* pairwise multiple comparison procedures to identify significant relationships followed the Holm–Sidak method.

For statistical analysis of the qPCR data the mean transcript copy number for each echinoid tissue sample (i.e. average transcript number derived from all runs of duplicate cDNA samples) was used as a replicate for statistical analysis. Therefore the sedimentation experiment consisted of three biological replicates per treatment and the surface retrieval experiment two biological replicates per treatment. As the two experiments were conducted independently of each other, the results of each experiment were analysed for statistical significance as separate tests but with the same methods. The results from the intestine and Aristotle's lantern muscle tissue were tested separately for each experiment. Prior to analysis, results were tested for homogeneity of variance and normality. Where these assumptions did not hold, data were $\log_{10}$ transformed prior to statistical analysis. Student's t-test or one-way analysis of variance was carried out on the mean transcript numbers. When $\log_{10}$ transformation did not achieve a normal distribution, the Kruskal–Wallis test was used to test for significance. Subsequent multiple comparison procedures to identify significant relationships followed the Student–Newman–Keuls method. All transformations and statistical analyses were conducted using the software package Sigmaplot Version 11.

3. Results

3.1. Megafaunal density

At the Ragnarokk hydrocarbon exploration area megabenthic organisms from 13 nominal taxa were recorded from the video transects in a total surveyed area of 664.3 m^2 for the pre-drilling survey (8 transects) and 564.2 m^2 for the post-drilling survey (7 transects). The megafaunal community included echinoderms (asteroids and echinoids), Porifera, anthozoans (actiniarians and pennatulids), molluscs, reptant decapods and demersal fish (Table 2). The megafaunal community around the drilling site was dominated numerically by the echinoid *E. acutus*, which was the most abundant organism observed during each transect. The other megafaunal species were of low abundance, both before (mean = 0.131 indiv. m^{-2}) and after drilling (mean = 0.037 indiv. m^{-2}). There was a statistically significant difference between community density (not including the numerically dominant echinoids) before and after drilling ($t = 4.27$, d.f. = 13, $p < 0.001$).

The numbers of motile organisms (hermit crabs and fish) observed after the drilling event were higher than those recorded pre-drilling. Conversely, the less motile asteroids (*Astropecten* sp.) and scallops (*Pecten* sp.) which were observed prior to drilling were not found during post-drilling surveys. Of the sessile fauna, the sea pen *Pennatula phosphorea*, which was found during the pre-drilling surveys, was absent post-drilling, whilst a second Pennatulid species was present both before and after drilling. The anthozoan *Calliactis parasitica* was only observed during the post-drilling surveys attached to a motile gastropod. Finally, a member of the Porifera was only observed during a post-drilling survey.

The distribution of the echinoids was patchy (Fig. 4) with mean pre-drilling densities ranging from 2.31 to 8.70 indiv. m^{-2} and post-drilling densities ranging between 0.28 and 7.85 indiv. m^{-2} (Table 3). In the 10 to 50 m concentric zones from the drilling site echinoid densities were lower post-drilling than pre-drilling (Fig. 5). In comparison, echinoid densities were higher in the 60 to 80 m concentric zones post-drilling but again fell below pre-drilling densities between 80 and 100 m. Two-way analysis of variance indicated that there was no significant interaction between drilling and distance upon echinoid densities (two-way ANOVA on ranks; $F = 0.801$, d.f. 4, 60, p = n.s.). A comparison of echinoid densities before and after the drilling event indicated that drilling did not have a significant effect on echinoid density (two-way ANOVA on ranks;

Table 2
Megafaunal density during pre- and post-drilling video surveys. Mean density figures have been standardised to number of individuals per m^2.

Phylum	Class	Species	Functional group	Density (indiv. m^{-2})	
				Pre-drill	Post-drill
Porifera	Demospongiae	Porifera sp.	Sessile	–	0.001
Cnidaria	Anthozoa	*Calliactis parasitica*	Parasitic	–	0.001
Cnidaria	Anthozoa	*Pennatula phosphorea*	Sessile	0.003	–
Cnidaria	Anthozoa	Pennatulid sp.	Sessile	0.006	0.007
Mollusca	Bivalvia	*Pecten* sp.	Hemisessile	0.001	–
Mollusca	Gastropoda	*Buccinum undatum*	Motile	0.005	0.005
Arthropoda	Malacostraca	*Pagurus* sp.	Motile	–	0.002
Echinodermata	Asteroidea	*Astropecten* sp.	Motile	0.089	–
Chordata	Myxini	*Myxine* sp.	Motile	0.005	0.007
Chordata	Elasmobranchii	Rajiformes sp.	Motile	–	0.002
Chordata	Actinopterygii	*Lophius piscatorius*	Motile	–	0.001
Chordata	Actinopterygii	Pleuronectidae sp.	Motile	0.021	0.011
			Sub Total	0.131	0.037
Echinodermata	Echinoidea	*Echinus acutus*	Motile	4.718	4.379
			Total	4.849	4.416

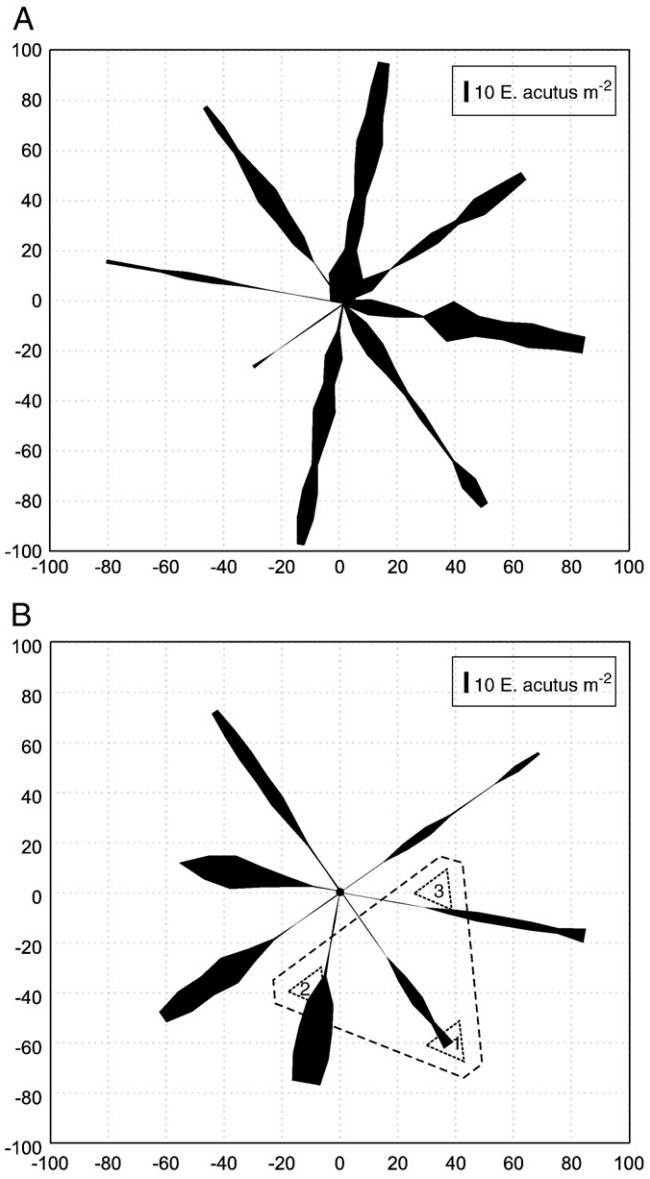

Fig. 4. *Echinus acutus* densities (individuals per m^2) on each ROV transect plotted as kite diagrams on a map of the surveyed area. Coordinates relative to the position of the well (0,0), in meters, are indicated on the axis. Line thickness indicates the density of *E. acutus* in each 10 m section of transect; the line thickness representing ten *E. acutus* m^{-2} is shown in a box. A, illustrates the *E. acutus* densities prior to drilling. On B, post-drilling, the central dark circle (0,0) represents the drilling position, and the rig outline and numbered leg positions are superimposed.

Table 3
Total densities of *Echinus acutus* (number of individuals per m^2) observed during each video transect within 10 m zones away from the drilling site during the pre- and post-drilling surveys.

Distance from drilling site (m)	Pre-drill (n = 8)	Post-drill (n = 7)
10	2.31	0.28
20	5.87	0.38
30	4.77	1.13
40	5.11	3.14
50	8.70	7.85
60	6.84	8.48
70	6.67	8.11
80	6.14	7.62
90	6.61	3.78
100	5.16	5.05

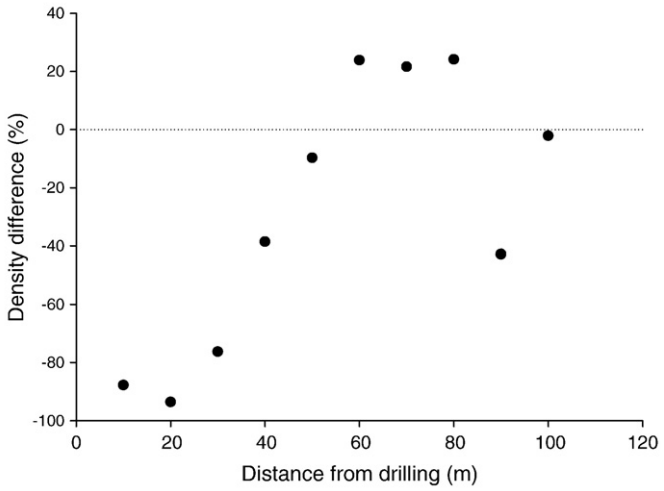

Fig. 5. Percentage differences in *Echinus acutus* mean densities within 10 m zones radiating away from the drilling site during the post-drilling (n = 7) survey in comparison to the pre-drilling survey (n = 8).

F = 2.210, d.f. 1, 117, p = n.s.). There was a significant effect of distance from the drill site on echinoid densities (two-way ANOVA on ranks; F = 3.808, d.f. 9, 117, $p < 0.001$). Multiple comparisons (Holm–Sidak) revealed significant differences in echinoid density comparing the 0–10 m zone with the 40–50 m, 50–60 m and 60–70 m zones.

3.2. Sediment analysis

In comparison with the samples taken prior to drilling the sediment concentrations of titanium, lead, chromium, copper and zinc at 10, 25 and 50 m distance from the drill site were all elevated post-drilling (Table 1), but still within typical background levels for the Norwegian Continental Shelf (NCS) where this was known (Frost et al., 2006). Concentrations of cadmium in the sediments were greater than NCS background levels both pre- and post-drilling, and were higher in the post-drilling samples. The change in sedimentary barium concentrations after drilling was of the greatest extent, with post-drilling concentrations 10–50 m from the drill site being greater than NCS background levels and one or two orders of magnitude higher than those found pre-drilling. The dry weight percentages of the sediment samples were lower at 25 and 50 m post-drilling. The % sediment size fraction <63 μm was greater, and the total organic carbon percentage (TOC%) lower, post-drilling at 10, 25 and 50 m. At leg 3, where the *in-situ E. acutus* experiments were performed, the concentration of all metals were within NCS background levels (where known). The chemical sediment properties at leg 3 were reflective of those found from push cores post-drilling.

3.3. E. acutus stress-70 protein sequence analysis

A 398-bp mRNA nucleotide fragment was obtained from the degenerate primer PCR from which a 129 amino acid peptide fragment was inferred (Fig. 6). One of the signature sequences of the stress-70 family, TVPAYFND (Rensing and Maier, 1994), was included in this peptide fragment indicating that it had been isolated from mRNA coding for a stress-70 protein. Also evident in the amino acid sequence was a conserved sequence found in proteins that bind ATP, such as the stress-70 proteins, the ATP/GTP-binding site motif A (also known as the P-loop); [AG]-x(4)-G-K-[ST] (prosite ID: ATP_GTP_A PS00017; Walker et al., 1982). A sequence homology search using BLASTP algorithms (Altschul et al., 1997) revealed that the amino acid sequence obtained was 93% identical to the predicted

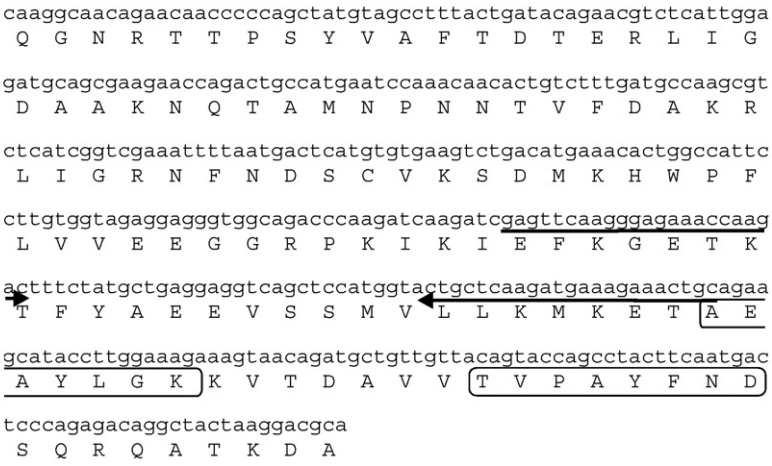

Fig. 6. Nucleotide and inferred amino acid sequence of the stress-70 sequence isolated from *Echinus acutus* (GenBank accession no. CAT00003). The characteristic stress-70 family motif TVPAYFND (Rensing and Maier, 1994) is boxed, as is the ATP/GTP-binding site motif A (P-loop) AEAYLGK (Walker et al., 1982). The qPCR primers are underlined.

71 kDa heat shock cognate (HSC) from the echinoid *Strongylocentrotus purpuratus* (GenBank accession no. XP_802129), and 83% identical to the 70 kDa heat shock cognate (HSC70) protein from *Homo sapiens* (GenBank accession no. NP_694881) and *Rattus norvegicus* (GenBank accession no. NP_077327). However, without a comprehensive analysis of the complete echinoid gene and protein sequence, the isolated mRNA fragment could not be conclusively identified as relating to a specific gene within the stress-70 family and is hence referred to hereafter as being derived from an inducible *stress-70* gene. This fragment was submitted to the EMBL online database (GenBank accession no. CAT00003), and was the first nucleotide sequence to be registered for this species.

3.4. Stress-70 gene expression results

The single surface retrieval manipulation resulted in a mean expression of 2251 (±343 S.D.) *stress-70* transcripts per μg total RNA in the intestine tissue and 330 (±105 S.D.) *stress-70* transcripts per μg total RNA in the Aristotle's lantern muscle tissue. The double surface retrieval manipulations resulted in the expression of a mean 1974 (±1002 S.D.) *stress-70* transcripts per μg total RNA in the intestine tissue and 319 (±50 S.D.) *stress-70* transcripts per μg total RNA in the Aristotle's lantern muscle tissue. There was no significant effect of repeated surface retrieval events on the expression of *stress-70* found in either the intestine ($H = 0.00$, d.f. = 1, p = n.s.) or the Aristotle's lantern muscle tissue ($H = 0.00$, d.f. = 1, p = n.s.) of *E. acutus*.

Of the six echinoids placed inside each experimental chamber for the sediment burial experiments, after recovery to deck only three echinoids remained in each chamber. The missing echinoids were presumed to have escaped from the chambers via the observation hole in the lids. The number of individual echinoids providing tissue samples for determination of the *stress-70* expression results was therefore only 3 per treatment (total 9 echinoids). The intestinal tissue of *E. acutus* showed no significant change in *stress-70* expression in response to the sediment burial treatments ($F = 1.85$, d.f. = 2, 8, p = n.s., Fig. 7). In comparison, a significant increase in *stress-70* expression following sediment burial treatment was found in the Aristotle's lantern muscle tissue ($F = 5.67$, d.f. = 2, 8, $p < 0.05$, Fig. 7). Pairwise tests revealed significant differences in the Aristotle's lantern muscle tissue *stress-70* expression between both the control and the S ($q = 4.532$, $p < 0.05$) and MS ($q = 3.527$, $p < 0.05$) treatments. Although the mean Aristotle's lantern muscle tissue *stress-70* expression was higher in the MS than the S treatment, the difference between these two sediment burial treatments was not significant ($q = 1.005$, p = n.s.).

4. Discussion

4.1. Effects of drilling disturbance on the megabenthic community

The disturbance caused by drilling a hydrocarbon exploratory well had a significant effect on the megabenthic community, with density one month after drilling being lower than that found prior to the drilling event. As well as numbers of individual organisms being altered post-drilling, the dominant functional groups of the megabenthos present after drilling reflected a typical post-physical disturbance pattern of increased motile predatory fauna and decreased sessile suspension feeding fauna, as found in other studies (Jones et al., 2006; Santos et al., 2009). These changes in the dominant lifestyles of megafauna found shortly after physical disturbance occur as sessile fauna, unable to escape direct physical burial or smothering of gill apparatus from suspended sediment, are killed and highly motile organisms, feeding on the resulting carrion, enter the area (Bluhm, 2001; Stronkhorst et al., 2003). In some situations, the smothering, burial and physical effects of solid drill cuttings are thought to be a more important determinant of community change than the potentially toxic action of the associated chemicals (Schaanning et al., 2008), although these physical effects are localised to the vicinity of the source of the drill spoil (Neff et al., 2000; Jones et al., 2007; Netto et al., 2009; Santos et al., 2009). However, a complete understanding of the interaction between drill cuttings and associated drilling muds is yet to be achieved. Other studies investigating the physical impact of cuttings have found evidence that factors other than burial primarily affect the benthic community (Trannum et al., 2010), and potential toxicological effects are highly dependent on the composition of the drilling fluids (Holdway, 2002; Dalmazzone et al., 2004; Neff, 2005).

One species, the echinoid *E. acutus* var. *norvegicus*, was present in sufficient numbers to permit a more detailed study of the change in density found before and after drilling. Although statistical analysis of the echinoid density data did not reveal a significant effect of drilling upon echinoids densities (i.e. a pre- and post-drilling comparison), a significant effect of distance from the drill site on post-drilling densities was found. It is possible that the increase in echinoid density within the 60–80 m region around the drill site (Fig. 5) was caused by echinoids moving away from the source of physical disturbance and hence depleting the number of echinoids found in the immediate vicinity of the drill site.

As it was not possible to visually determine the sea bed coverage of the drill cuttings and disturbed sediment from the video transect footage, the changes in echinoid density cannot be related visually to

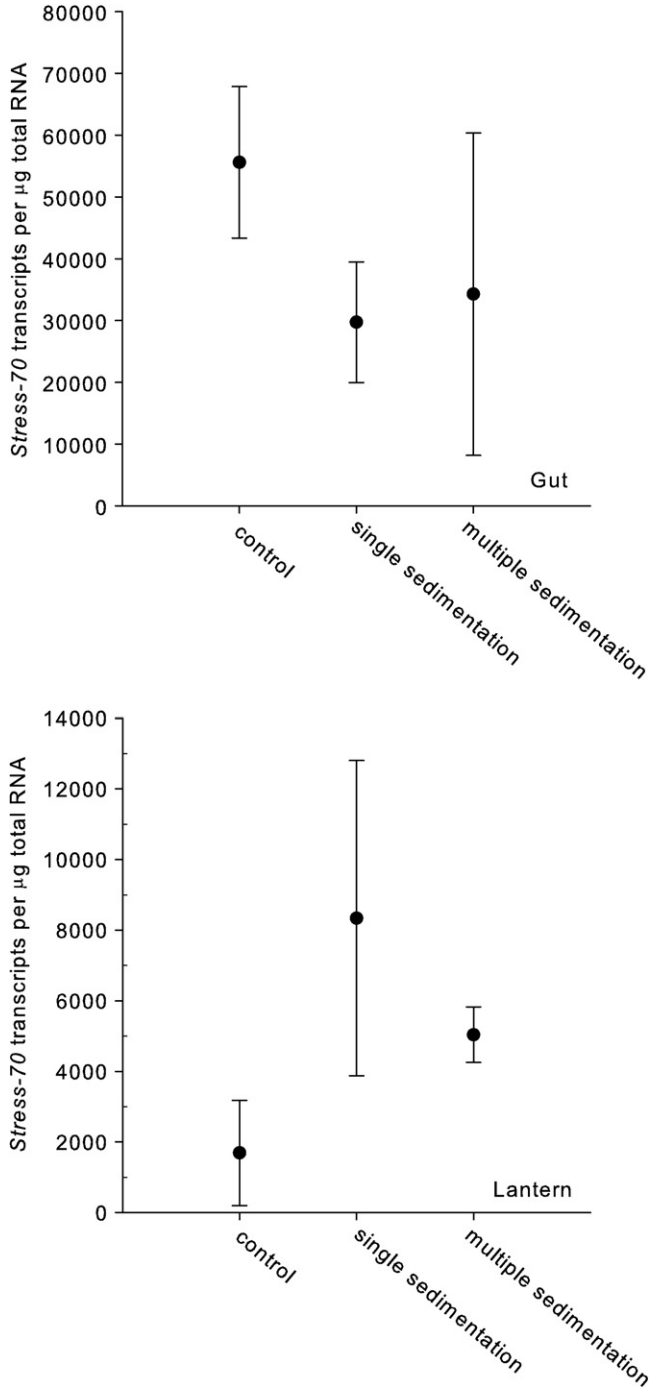

Fig. 7. The effects of sediment burial treatments on *stress-70* mRNA transcript expression in intestine tissue (top) and Aristotle's lantern muscle tissue (bottom) of *Echinus acutus*. Error bars represent ±1 standard deviation (n = 3). Note different y-axis scales.

drill cutting extent. However, the presence of high concentrations of barium in sediments has been suggested as tracer for drill cuttings in the environment because the mineral barite ($BaSO_4$) is one of the main constituents of drilling chemicals (Hartley, 1996; Breuer et al., 2004). Barium concentrations from the sediment samples collected at the Ragnarokk exploration area reflected a large increase in barium after drilling, with concentrations declining with distance from the central drilling site. The sediment barium concentrations at 10, 25 and 50 m from the drilling site were higher than both those found prior to drilling and typical background values for the Norwegian continental shelf. If the sediment barium concentrations are taken as indicative of drill cutting coverage, the decrease in echinoid density post-drilling within the 50 m zone around the drill site follows the presumed extent of drill cuttings coverage.

4.2. Stress-70 expression

Most studies investigating stress-70 expression in marine organisms have been carried out in laboratory-based experiments, with limited work carried out on *in-situ* induced stress in marine environments. This study was one of the first to combine ROV-facilitated experimentation with subsequent investigation of changes in *stress-70* expression. The surface retrieval manipulation experiment was performed to provide a preliminary indication of whether or not the retrieval of *E. acutus* individuals from the sea bed to deck could alter *stress-70* expression. Retrieval to the surface involved changes in two physical variables which have been shown to alter gene expression: pressure (via decompression) and temperature (an increase). Decompression causes a reduction in pressure which affects biological systems by altering molecular volume, which together with increased temperature, destabilizes the structure of proteins and membranes and their functioning (Somero, 1992; 1998). The echinoids' retrieval to the sea surface may therefore cause the induction of *stress-70* protein expression (Su et al., 2004; Ravaux et al., 2007) on account of deleterious effects on protein integrity (Mosholder et al., 1979; Dixon et al., 2004). Any such change may consequently mask alterations in *stress-70* expression caused by the stress of sedimentary burial at the sea floor. It is this unintended molecular artefact of retrieval to the surface which is a limiting factor in the successful performance of *in-situ* experiments which aim to investigate gene expression in deep-sea species.

The surface retrieval manipulations with *E. acutus* did not cause significant differences in *stress-70* expression between the single or double retrieval events in either of the two tissue types. It was not possible to include a control (i.e. no decompression) in this preliminary study as the echinoids had to be returned to the surface for processing. There is a limit to the conclusions that can be drawn from this result because of the low number of individual echinoid replicates used (two per manipulation), but there are four possible explanations for the result: 1) the echinoids' expression of *stress-70* was not affected by decompression from 114 m depth or temperature change during surface retrieval. 2) The echinoids were not decompressed from a depth, or experienced a temperature increase, sufficient to elicit the expression of *stress-70* during surface retrieval. 3) The time taken for recovery from the seafloor to final preservation of tissue samples was rapid (50–70 min), which was insufficient time for changes in *stress-70* expression owing to decompression and/or temperature change to become apparent in the transcriptomes. 4) As the relative change in pressure for each unit change in depth is greatest near the sea surface, and the echinoids subject to the two surface retrieval events were only brought to a depth of 10 m from the surface between dives, they were not sufficiently decompressed twice to cause a difference in *stress-70* expression compared to the echinoids subject to the single decompression event. If one of the first three explanations is correct, it can therefore be assumed that the surface retrieval of the echinoids did not cause any artefacts in changes to *stress-70* expression as a result of the sediment burial experiments.

In response to single and multiple sedimentation events, a significant increase in *stress-70* expression was found in the *E. acutus* Aristotle's lantern muscle tissue, but not in intestinal tissue. Tissue-specific *stress-70* expression patterns are known to occur. For example; in carp (*Cyprinus carpio*) Cd treatment resulted in enhanced induction of *hsc70* in the liver but not in other tissues (Ali et al., 2003), whilst elevated *hsc70* levels were found only in carp muscle tissue in response to cold shock (Ali et al., 2003) and in prawn (*Macrobrachium rosenbergii*) muscle tissue in response to heat shock (Liu et al., 2004).

In echinoids, the muscles of the lantern are isolated from direct contact with ingested sediment, which passes through the oesophagus before entering the digestive system (Hyman, 1955). The elevated expression of the stress-70 gene in the lantern muscle tissue may therefore reflect an overall level of stress the echinoids experienced as a result of sedimentary burial, rather than direct contact with sediment contaminated with drill cuttings. The differential expression of the *stress-70* gene found in *E. acutus* may reflect an elevated metabolic rate in the lantern muscle tissue in comparison to the intestinal tissue, but there is a paucity of published information on the metabolic rates of different echinoids tissues to support this theory further. With regard to the physical drilling disturbance at the Ragnarokk drilling site, whilst no direct correlation can be made between the reductions in echinoid numbers around the conductor pipe and the source of disturbance, this preliminary gene expression result does indicate that sediment burial causes sublethal stress that is detectable at the molecular level in these echinoids.

4.3. ROV-facilitated experimentation

The current study illustrates the advantages of working with a ROV at depths inaccessible to human divers. The industrial work-class ROV allowed the deployment and operation of experimental equipment both *in-situ* and in close proximity to the drilling rig, which would not have been feasible with traditional deep-sea research techniques and gear (e.g. trawls, grabs or free-fall landers). The ROV's manipulator arm allowed careful collection of individual echinoids for inclusion in the surface retrieval and sediment burial experiments. The repeated addition of sediment to the experimental bucket units used in the burial manipulations would also not have been possible without the use of a ROV, which enabled easy bucket relocation and controlled manipulation of sediment samples. The escape of the echinoids from the buckets does, however, demonstrate the necessity to employ equipment secure to the escape capabilities of target specimens. Improved caged experiment designs will contribute to future experiments with both horizontally and vertically mobile echinoderms.

The limited access to ROV equipment and the expense of ROV time limit the collection of replicate organisms and the deployment of multiple experimental units. Using ROV manipulators can be a slow process and manoeuvring a large ROV within a small area can be difficult and experiments can be damaged as a result (Thistle, 2003). However, many deep-sea research activities, including the experiments performed in this study, would not have been possible without ROV technology (Van Dover and Lutz, 2004). This study also demonstrates the novel opportunities available for molecular-related experimental investigation in deep water as facilitated by ROV activity.

5. Conclusions

No direct conclusions can be made from the results of this study with regard to a possible relationship between the increased expression of the *stress-70* gene in the individual echinoids subject to sediment burial activity and the observed changes to the densities of echinoid and other megabenthic populations found at the Ragnarokk site post-drilling. This study has, however, shown that it is possible to use an industrial work-class ROV for manipulative experimental work and that molecular techniques can be applied to ecological investigations in deep water. The inaccessibility of the deep-sea environment and the issue of decompression and temperature change altering the biochemical profiles, however, remain major obstacles to routine deep-sea ecological experimental research utilising modern techniques. With the current increase in the use of ROVs for deep-sea experimental work (Bachmayer et al., 1998; Van Dover and Lutz, 2004), the obstacle of accessing the deep sea to perform experimental work is gradually being removed. As new deep-sea experimental equipment to accompany ROV operations is designed the development of experimental devices which can eliminate the possible effects of decompression and temperature and permit modern molecular techniques to be used in deep-sea research is required.

Acknowledgments

The authors acknowledge Statoil and the crew of the drilling unit M.V. *West Epsilon*, Seadrill Ltd., Oceaneering International and their ROV team for supporting this project. We thank Nina Aas, Lars Petter Myhre, Ingunn Nilssen and Arne Myhrvold. We also thank the ROV pilots Terje Olsen, Trond Flæte, Bjørn Gundersen, Lars Grastveit, Øyvind Helgeneseth, Daniel Hesjedal, Jon Martin Holmøy, and Kåre Tjøstheim. This project was carried out as part of the SERPENT Project and DIEPS (Deepwater Industry, Environment, Policy and Science). S.J.M. Hughes was funded by NERC studentship NER/S/A/2005/13480 and D.O.B. Jones by NERC DIEPS grant NE/C508518/1. **[SS]**

References

Ahnert, A., Borowski, C., 2000. Environmental risk assessment of anthropogenic activity in the deep sea. J. Aquat. Ecosyst. Stress Recovery 7, 299–315.
Ali, K.S., Dorgai, L., Ábrahám, M., Hermesz, E., 2003. Tissue- and stressor-specific differential expression of two hsc70 genes in carp. Biochem. Biophys. Res. Commun. 307, 503–509.
Altschul, S.F., Madden, T.L., Schäffer, A.A., Zhang, J., Zhang, Z., Miller, W., Lipman, D.J., 1997. Gapped BLAST and PSI-BLAST: a new generation of protein database search programs. Nucleic Acids Res. 25, 3389–3402.
Andrews, G.O., Simpson, S.J., Pile, A.J., 2008. New method for presenting nutritionally defined food sources to marine organisms. Limnol. Oceanogr. Meth. 6, 299–306.
Bachmayer, R., Humphris, S., Fornari, D., Dover, C.V., Howland, J., Bowen, A., Elder, R., Crook, T., Gleason, D., Sellers, W., Lerner, S., 1998. Oceanographic research using remotely operated underwater robotic vehicles: exploration of hydrothermal vent sites on the Mid-Atlantic Ridge at 37°North 32°West. Mar. Technol. Soc. J. 32, 37–47.
Bailey, T.G., Torres, J.J., Youngbluth, M.J., Owen, G.P., 1994. Effect of decompression on mesopelagic gelatinous zooplankton — a comparison of in-situ and shipboard measurements of metabolism. Mar. Ecol. Prog. Ser. 113, 13–27.
Benfield, M.C., Graham, W.M., 2010. In situ observations of *Stygiomedusa gigantea* in the Gulf of Mexico with a review of its global distribution and habitat. Journal of the Marine Biological Association of the UK 90, 1079–1093.
Bett, B.J., 2001. UK Atlantic Margin Environmental Survey: introduction and overview of bathyal benthic ecology. Cont. Shelf Res. 21, 917–956.
Bierkens, J.G.E.A., 2000. Applications and pitfalls of stress-proteins in biomonitoring. Toxicology 153, 61–72.
Bluhm, H., 2001. Re-establishment of an abyssal megabenthic community after experimental physical disturbance of the seafloor. Deep Sea Res. II Top. Stud. Oceanogr. 48, 3841–3868.
BODC, 2009. British Oceanographic Data Centre. http://www.bodc.ac.uk/2009.
Breuer, E., Stevenson, A.G., Howe, J.A., Carroll, J., Shimmield, G.B., 2004. Drill cutting accumulations in the Northern and Central North Sea: a review of environmental interactions and chemical fate. Mar. Pollut. Bull. 48, 12–25.
Bustin, S.A., 2000. Absolute quantification of mRNA using real-time reverse transcription polymerase chain reaction assays. J. Mol. Endocrinol. 25, 169–193.
Bustin, S.A., Benes, V., Garson, J.A., Hellemans, J., Huggett, J., Kubista, M., Mueller, R., Nolan, T., Pfaffl, M.W., Shipley, G.L., Vandesompele, J., Wittwer, C.T., 2009. The MIQE guidelines: minimum information for publication of quantitative real-time PCR experiments. Clin. Chem. 55, 611–622.
Chandrasekara, W.U., Frid, C.L.J., 1998. A laboratory assessment of the survival and vertical movement of two epibenthic gastropod species, *Hydrobia ulvae* (Pennant) and *Littorina littorea* (Linnaeus), after burial in sediment. J. Exp. Mar. Biol. Ecol. 221, 191–207.
Chapman, P.M., 2002. Integrating toxicology and ecology: putting the "eco" into ecotoxicology. Mar. Pollut. Bull. 44, 7–15.
Connon, R., Hooper, H.L., Sibly, R.M., Lim, F.L., Heckmann, L.H., Moore, D.J., Watanabe, H., Soetaert, A., Cook, K., Maund, S.J., Hutchinson, T.H., Moggs, J., De Coen, W., Iguchi, T., Callaghan, A., 2008. Linking molecular and population stress responses in *Daphnia magna* exposed to cadmium. Environ. Sci. Technol. 42, 2181–2188.
Dahlhoff, E.P., 2004. Biochemical indicators of stress and metabolism: applications for marine ecological studies. Annu. Rev. Physiol. 66, 183–207.
Dalmazzone, C., Blanchet, D., Lamoureux, S., Dutrieux, E., Durrieu, J., Camps, R., Galgani, F., 2004. Impact of drilling activities in warm sea: recolonization capacities of seabed. Oil Gas Sci. Technol. 59, 625–647.
Davies, A.J., Roberts, J.M., Hall-Spencer, J., 2007. Preserving deep-sea natural heritage: emerging issues in offshore conservation and management. Biol. Conserv. 138, 299–312.
Dixon, D.R., Pruski, A.M., Dixon, L.R.J., 2004. The effects of hydrostatic pressure change on DNA integrity in the hydrothermal-vent mussel *Bathymodiolus azoricus*: implications for future deep-sea mutagenicity studies. Mutat. Res. Fundam. Mol. Mech. Mutagen. 552, 235–246.
Drummond, A.J., Ashton, B., Buxton, S., Cheung, M., Heled, J., Kearse, M., Moir, R., Stones-Havas, S., Thierer, T., Wilson, A., 2010. Geneious v4.8.

Düben, M.W.V., Koren, J., 1846. Öfversigt af Skandinaviens Echinodermer [Overview of Scandinavian Echinodermata]. Kungl. Svenska Vetenskapsakademiens Handlingar 1844.
Eastwood, P.D., Mills, C.M., Aldridge, J.N., Houghton, C.A., Rogers, S.I., 2007. Human activities in UK offshore waters: an assessment of direct, physical pressure on the seabed. ICES J. Mar. Sci. 64, 453–463.
Feder, M.E., Hofmann, G.E., 1999. Heat-shock proteins, molecular chaperones, and the stress response: evolutionary and ecological physiology. Annu. Rev. Physiol. 61, 243–282.
Frost, T.K., Nilssen, I., Neff, J.M., Altin, D., Lunde, K.E., 2006. Environmental Risk Management System Report 4: Toxicity of Drilling Discharges. SINTEF, Trondheim.
Gage, J.D., 1996. Why are there so many species in deep-sea sediments? J. Exp. Mar. Biol. Ecol. 200, 257–286.
Gallucci, F., Sauter, E., Sachs, O., Klages, M., Soltwedel, T., 2008. Caging experiment in the deep sea: efficiency and artefacts from a case study at the Arctic long-term observatory HAUSGARTEN. J. Exp. Mar. Biol. Ecol. 354, 39–55.
Gething, M.-J., Sambrook, J., 1992. Protein folding in the cell. Nature 355, 33–45.
Gray, J.S., Clarke, K.R., Warwick, R.M., Hobbs, G., 1990. Detection of initial effects of pollution on marine benthos: an example from the Ekofisk and Eldfisk oilfields, North Sea. Mar. Ecol. Prog. Ser. 66, 285–299.
Hall, S.J., 1994. Physical disturbance and marine benthic communities: life in unconsolidated sediments. Oceanogr. Mar. Biol. Annu. Rev. 32, 179–239.
Hamer, B., Hamer, D.P., Muller, W.E.G., Batel, R., 2004. Stress-70 proteins in marine mussel *Mytilus galloprovincialis* as biomarkers of environmental pollution: a field study. Environ. Int. 30, 873–882.
Hartley, J.P., 1996. Environmental monitoring of offshore oil and gas drilling discharges — a caution on the use of barium as a tracer. Mar. Pollut. Bull. 32, 727–733.
Hessler, R.R., 1972. Deep water organisms for high pressure aquarium studies. In: Brauer, R.W. (Ed.), Barobiology and the Experimental Biology of the Deep Sea. North Carolina Sea Grant Program, Chapel Hill, N.C., USA, pp. 151–163.
Hinchey, E.K., Schaffner, L.C., Hoar, C.C., Vogt, B.W., Batte, L.P., 2006. Responses of estuarine benthic invertebrates to sediment burial: the importance of mobility and adaptation. Hydrobiologia 556, 85–98.
Holdway, D.A., 2002. The acute and chronic effects of wastes associated with offshore oil and gas production on temperate and tropical marine ecological processes. Mar. Pollut. Bull. 44, 185–203.
Howarth, M.J., Simpson, J.H., Sündermann, J., van Haren, H., 2002. Processes of Vertical Exchange in Shelf Seas (PROVESS). J. Sea Res. 47, 199–208.
Hudson, I.R., Wigham, B.D., Tyler, P.A., 2004. The feeding behaviour of a deep-sea holothurian, *Stichopus tremulus* (Gunnerus) based on in situ observations and experiments using a remotely operated vehicle. J. Exp. Mar. Biol. Ecol. 301, 75–91.
Hyman, L.H., 1955. The Invertebrates: Echinodermata. McGraw-Hill Book Company, New York. 763 pp.
Jago, C.F., Jones, S.E., Latter, R.J., McCandliss, R.R., Hearn, M.R., Howarth, M.J., 2002. Resuspension of benthic fluff by tidal currents in deep stratified waters, northern North Sea. J. Sea Res. 48, 259–269.
Jones, D.O.B., 2009. Using existing industrial remotely operated vehicles for deep-sea science. Zool. Scr. 38, 41–47.
Jones, D.O.B., Hudson, I.R., Bett, B.J., 2006. Effects of physical disturbance on the cold-water megafaunal communities of the Faroe-Shetland Channel. Mar. Ecol. Prog. Ser. 319, 43–54.
Jones, D.O.B., Wigham, B.D., Hudson, I.R., Bett, B.J., 2007. Anthropogenic disturbance of deep-sea megabenthic assemblages: a study with remotely operated vehicles in the Faroe-Shetland Channel, NE Atlantic. Mar. Biol. 151, 1731–1741.
Kingston, P.F., 1992. Impact of offshore oil production installations on the benthos of the North Sea. ICES J. Mar. 49, 45–53.
Knight, P.J., Howarth, M.J., Rippeth, T.P., 2002. Intertidal currents in the northern North sea. J. Sea Res. 47, 269–284.
Laurenson, C.H., Hudson, I.R., Jones, D.O.B., Priede, I.G., 2004. Deep water observations of *Lophius piscatorius* in the north-eastern Atlantic Ocean by means of a remotely operated vehicle. J. Fish Biol. 65, 947–960.
Lewis, S., Handy, R.D., Cordi, B., Billinghurst, Z., Depledge, M.H., 1999. Stress proteins (HSPs): methods of detection and their use as an environmental biomarker. Ecotoxicology 8, 351–368.
Lindquist, S., Craig, E.A., 1988. The heat-shock proteins. Annu. Rev. Genet. 22, 631–677.
Liu, J., Yang, W.J., Zhu, X.J., Karouna-Renier, N.K., Rao, R.K., 2004. Molecular cloning and expression of two HSP70 genes in the prawn, *Macrobrachium rosenbergii*. Cell Stress Chaperones 9, 313–323.
Macdonald, A.G., 1997. Hydrostatic pressure as an environmental factor in life processes. Comp. Biochem. Physiol. A Physiol. 116, 291–297.
Menge, B.A., Olson, A.M., Dahlhoff, E.P., 2002. Environmental stress, bottom-up effects, and community dynamics: integrating molecular-physiological and ecological approaches. Integr. Comp. Biol. 42, 892–908.
Moore, M.N., Readman, J.W., Depledge, M.H., Paul Leonard, D.R., 2004. An integrated biomarker-based strategy for ecotoxicological evaluation of risk in environmental management. Mutat. Res. Fundam. Mol. Mech. Mutagen. 552, 247–268.
Mosholder, R., RV, J., Phleger, C., 1979. Swimbladder membrane protein of an abyssal fish, *Coryphaenoides acrolepis*. Physiol. Chem. Phys. 11, 37–47.
Mukhopadhyay, I., Nazir, A., Saxena, D.K., Kar Chowdhuri, D., 2003. Heat shock response: hsp70 in environmental monitoring. J. Biochem. Mol. Toxicol. 17, 249–254.
Neff, J.M., 2005. Composition, environmental fates, and biological effects of water based drilling muds and cuttings discharged to the marine environment: a synthesis and annotated bibliography. Prepared for the Petroleum Environmental Research Forum (PERF) and American Petroleum Institute, p. 73.
Neff, J.M., McKelvie, S., Ayers Jr., R.C., 2000. Environmental impacts of synthetic based drilling fluids. U.S. Department of the Interior Minerals Management Service Gulf of Mexico OCS Region New Orleans, LA, p. 118.
Netto, S.A., Gallucci, F., Fonseca, G., 2009. Deep-sea meiofauna response to synthetic-based drilling mud discharge off SE Brazil. Deep Sea Res. II Top. Stud. Oceanogr. 56, 41–49.
Nolan, T., Hands, R.E., Bustin, S.A., 2006. Quantification of mRNA using real-time RT-PCR. Nat. Protoc. 1, 1559–1582.
Osovitz, C.J., Hofmann, G.E., 2005. Thermal history-dependent expression of the hsp70 gene in purple sea urchins: biogeographic patterns and the effect of temperature acclimation. J. Exp. Mar. Biol. Ecol. 327, 134–143.
Piepenburg, D., Schmid, M.K., 1997. A photographic survey of the epibenthic megafauna of the Arctic Laptev Sea shelf: distribution, abundance and estimates of biomass and organic carbon demand. Mar. Ecol. Prog. Ser. 147, 63–75.
Pinder, D., 2001. Offshore oil and gas: global resource knowledge and technological change. Ocean Coast. Manage. 44, 579–600.
Ravaux, J., Toullec, J.Y., Léger, N., Lopez, P., Gaill, F., Shillito, B., 2007. First hsp70 from two hydrothermal vent shrimps, *Mirocaris fortunata* and *Rimicaris exoculata*: characterization and sequence analysis. Gene 386, 162–172.
Rensing, S.A., Maier, U.G., 1994. Phylogenetic analysis of the stress-70 protein family. J. Mol. Evol. 39, 80–86.
Roche Diagnostics GmbH, 2003. Absolute quantification with external standards. https://www.roche-applied-science.com/sis/rtpcr/lightcycler/lightcycler_docs/technical_notes/lc_11_updated.pdf2003.
Roer, R.D., Sidelyova, V.G., Brauer, R.W., Galazii, G.I., 1984. Effects of pressure on oxygen-consumption in cottid fish from Lake Baikal. Experientia 40, 771–773.
Rogers, C.S., 1990. Responses of coral reefs and reef organisms to sedimentation. Mar. Ecol. Prog. Ser. 62, 185–202.
Sanders, B.M., 1993. Stress proteins in aquatic organisms: an environmental perspective. Crit. Rev. Toxicol. 23, 49–75.
Santos, M.F.L., Lana, P.C., Silva, J., Fachel, J.G., Pulgati, F.H., 2009. Effects of non-aqueous fluids cuttings discharge from exploratory drilling activities on the deep-sea macrobenthic communities. Deep Sea Res. II Top. Stud. Oceanogr. 56, 32–40.
Schaanning, M.T., Trannum, H.C., Øxnevad, S., Carroll, J., Bakke, T., 2008. Effects of drill cuttings on biogeochemical fluxes and macrobenthos of marine sediments. J. Exp. Mar. Biol. Ecol. 361, 49–57.
Sconzo, G., Ferraro, M.G., Amore, G., Giudice, G., Cascino, D., Scardina, G., 1995. Activation by heat shock of hsp70 gene transcription in sea urchin embryos. Biochem. Biophys. Res. Commun. 217, 1032–1038.
Shirayama, Y., 1995. Current status of deep-sea biology in relation to the CO_2 disposal. In: Handa, N., Ohsumi, T. (Eds.), Direct Ocean Disposal of Carbon Dioxide. Terra Scientific Publishing, Tokyo, pp. 253–264.
Smith, C.R., Levin, L.A., Koslow, A., Tyler, P.A., Glover, A.G., 2008. The near future of the deep seafloor ecosystems. In: Polunin, N. (Ed.), Aquatic Ecosystems: Trends and Global Prospects. Cambridge University Press, pp. 334–351.
Somero, G.N., 1992. Adaptations to high hydrostatic pressure. Annu. Rev. Physiol. 54, 557–577.
Somero, G.N., 1998. Adaptation to cold and depth: contrasts between polar and deep-sea animals. In: Portner, H.O., Playle, R.C. (Eds.), Cold Ocean Physiology. Cambridge University Press, Cambridge, pp. 33–57.
Stronkhorst, J., Ariese, F., Van Hattum, B., Postma, J.F., De Kluijver, M., Den Besten, P.J., Bergman, M.J.N., Daan, R., Murk, A.J., Vethaak, A.D., 2003. Environmental impact and recovery at two dumping sites for dredged material in the North Sea. Environ. Pollut. 124, 17–31.
Su, C.-L., Wu, C.-P., Chen, S.-Y., Kang, B.-H., Huang, K.-L., Lin, Y.-C., 2004. Acclimatization to neurological decompression sickness in rabbits. Am. J. Physiol. Regul. Integr. Comp. Physiol. 287, R1214–R1218.
Theron, M., Sebert, P., 2003. Hydrostatic pressure and cellular respiration: are the values observed post-decompression representative of the reality under pressure? Mitochondrion 3, 75–81.
Thiel, H., 2003. Anthropogenic impacts on the deep sea. In: Tyler, P. (Ed.), Ecosystems of the Deep Oceans. Elsevier, Amsterdam, pp. 427–471.
Thistle, D., 2003. The deep-sea floor: an overview. In: Tyler, P. (Ed.), Ecosystems of the Deep Oceans. Elsevier, Amsterdam, pp. 5–37.
Thistle, D., Sedlacek, L., Carman, K.R., Fleeger, J.W., Brewer, P.G., Barry, J.P., 2007. Exposure to carbon dioxide-rich seawater is stressful for some deep-sea species: an in situ, behavioral study. Mar. Ecol. Prog. Ser. 340, 9–16.
Trannum, H.C., Nilsson, H.C., Schaanning, M.T., Øxnevad, S., 2010. Effects of sedimentation from water-based drill cuttings and natural sediment on benthic macrofaunal community structure and ecosystem processes. J. Exp. Mar. Biol. Ecol. 383, 111–121.
Treude, T., Janßen, F., Queisser, W., Witte, U., 2002. Metabolism and decompression tolerance of scavenging lysianassoid deep-sea amphipods. Deep Sea Res. I Oceanogr. Res. Pap. 49, 1281–1289.
Valavanidis, A., Vlahogianni, T., Dassenakis, M., Scoullos, M., 2006. Molecular biomarkers of oxidative stress in aquatic organisms in relation to toxic environmental pollutants. Ecotoxicol. Environ. Saf. 64, 178–189.
Van Dover, C.L., Lutz, R.A., 2004. Experimental ecology at deep-sea hydrothermal vents: a perspective. J. Exp. Mar. Biol. Ecol. 300, 273–307.
Walker, J.E., Saraste, M., Runswick, M.J., Gay, N.J., 1982. Distantly related sequences in the alpha- and beta-subunits of ATP synthase, myosin, kinases and other ATP-requiring enzymes and a common nucleotide binding fold. EMBO J. 1, 945–951.
Williams, T.D., Gensberg, K., Minchin, S.D., Chipman, J.K., 2003. A DNA expression array to detect toxic stress response in European flounder (*Platichthys flesus*). Aquat. Toxicol. 65, 141–157.
Wong, M.L., Medrano, J.F., 2005. Real-time PCR for mRNA quantitation. Biotechniques 39, 1–11.
Yoerger, D.R., Bradley, A.M., Jakuba, M., German, C.R., Shank, T., Tivey, M., 2007. Autonomous and remotely operated vehicle technology for hydrothermal vent discovery, exploration, and sampling. Oceanography 20, 152–161.